The Mineralogy and Petrology of Kimberlite and its Related Inclusions, with Special Reference to Premier Mine

by

Cornelis Frick

Submitted in partial fulfilment of the requirements for the degree Doctor of Science, in the Faculty of Science, University of Pretoria, Pretoria

January 1970

ABSTRACT

The structural and petrochemical relationships of the post-Waterberg alkaline intrusions north-east of Pretoria, were investigated. It was found that apart from being contemporaneous, these intrusions were influenced by the same tectonic pattern. The different magmas concerned, all belong to the alkaline basaltic rock series, but they appear to have formed as a consequence of separate differentiation sequences in the mantle of the earth. The alkaline intrusions simulates the normal alkaline differentiation trend, whereas the kimberlite and carbonatite intrusions formed individually, disconnected from the alkaline basalts and from one another.

The Premier Mine kimberlite was found to consist of at least four separate intrusions, starting off with the kimberlite of group-I which was highly explosive, succeeded by the kimberlites in the western and eastern portions of the mine, which were less explosive, and terminating with the unexplosive basaltic kimberlite veins. The latter rock-type, which was formerly described as carbonatite, compares favourably with the massive basaltic kimberlites of Benfontein, Wesselton, Dutoitspan and Jagersfontein. These rocks also show some correspondence to the melilite basalts, however, chemically they appear to be impoverished in magnesium, and enriched in calcium, phosphorous, sodium and potassium. Owing to the fact that their mineralogical constituents are not in equilibrium, the micaceous kimberlites differ from both the melilite basalts and the basaltic kimberlites, but in this respect they resemble the kimberlite breccias. The influence of the mode of emplacement on the various rock-types concerned has also been investigated. It was concluded that all the alkaline rocks originate in the eclogitic zone, which occurs at a depth of more than 100 km below the surface, and that, depending on the extent of crystallization of enstatite and olivine, a complete sequence of undersaturated alkaline rocks may result.

The comparison of the mineralogy of the constituents in eclogite, kimberlite and peridotite revealed that the minerals of kimberlite and peridotite show a remarkable

correspondence, whereas eclogitic minerals are absent in kimberlite. Petrologically it was found that the clinopyroxene in the eclogite modules are invariably in a stage of alteration, and this alteration product consists of a fine grained clinopyroxene. Some undevitrified clinopyroxene glass was also encountered in some of the eclogite nodules. The eclogite nodules often display metamorphic tentures, whereas the garnet peridotite nodules revealed the sequence of crystallization observed in the primary phenocrysts in kimberlite, and as predicted by O'Hara (1968) in the system diopside-pyrope at 30 kb to 20 kb, viz. pyrope, enstatite, clinopyroxene, olivine and spinel. Chemically the eclogite appears to be undifferentiated, whereas the ultramafic nodules are uniformly differentiated, corresponding to the first stages of the normal differentiation sequence for tholeiitic magmas. The paucity of K^+, Na^+, Al^{3+}, Ca^{2+} and Ti^{4+} in the ultramafic nodules, and their relatively high concentrations in all alkaline and kimberlitic magmas, suggest that the ultramafic nodules can hardly be the source material for these magmas. The eclogite, being enriched in these constituents, is a more likely parent material. The grospydites and kyanite eclogites, being poor in Mg^{2+} and Fe^{2+}, are considered to be the residue during the melting of eclogite and the crystallization of garnet peridotite. The depletion of Mg^{2+} and Fe^{2+} takes place during the crystallization above 30 kb, where both enstatite and forsterite are in the liquidus whereas both grossular and omphacite are in the solidus. Consequently a calcium-rich garnet and a jadeite-bearing clinopyroxene can crystallize. The excess of Al^{3+} may crystallize either as kyanite or as corundum.

From the mineralogical, petrological and chemical data of the rocks and minerals concerned, a model is proposed for the upper mantle of the earth (120 to 38 Km) and for the sequence and time of crystallization of the constituents in kimberlite.

Twenty new chemical analyses of eclogitic and ultramafic nodules and of their constituents and of kimberlite are reported.

The tholeiitic sill which is intrusive into the kimberlite at Premier Mine was also investigated, together with its metamorphic influence on the kimberlite. Three types of meta-kimberlite were observed, and the metamorphic facies established. The tholeiitic sill is differentiated into an olivine-orthopyroxene cumulate, a doleritic zone, and a granophyric zone. At the lower contact a fine-grained chilled margin could be identified.

Die Mineralogie en Petrologie van Kimberliet en die verwante insluitsels, met spesiale verwysing na Premiermyn.

Deur Cornelis Frick.

Opsomming.

Die petrochemiese en strukturele verwantskap tussen die na-waterbergse alkaliese gesteentes noord-oos van Pretoria is ondersoek, en daar is gevind dat die inplasing van hierdie gesteentes deur dieselfde tektoniese struktuur beheer is. Al die na-Waterbergse intrusies in die omgewing behoort tot die alkali-basaltiese reeks, maar dit wil voorkom asof hulle nie almal gevorm het as gevolg van 'n kontinue differensiasieproses nie. Die alkaliese gesteentes vorm een deurlopende reeks, terwyl die kimberliet en karbonatiet 'n afsonderlike reeks vorm. Gevolglik is die gevolgtrekking gemaak dat die kimberliet en karbonatiet gedurende dieselfde siklus van magmawerking, maar volgens 'n aparte differensiasieproses ontstaan het.

Die Premiermynkimberliet bestaan uit vier aparte fases van vulkanisme, waarvan die volgorde bepaal kon word. Die eerste fase bestaan uit die groep-I kimberliet, wat 'n hoogs eksplosiewe fase was. Hierdie fase is gevolg deur die inplasing van die Westelike en die Oostelike kimberliet, wat minder eksplosief was, en wat gevolg was deur die indringing van die gange van basaltiese kimberliet. Laasgenoemde gesteente is voorheen as 'n karbonatiet beskrywe, maar die vergelykende ondersoek van hierdie gesteente met soortgelyke gange in die kimberliet van Dutoitspan, Wesselton en Jagersfontein, dui daarop dat hierdie gange as basaltiese kimberliet geklassifiseer behoort te word. Hierdie gesteente vertoon ook dieselfde mineralogiese en petrologiese kenmerke as die kimberliet van Benfontein, en die melilietbasalt van Spiegelrivier. Die melilietbasalt en die basaltiese kimberliet kan egter op grond van die chemiese samestellings van mekaar onderskei word.

Die glimmeryke kimberliet en die kimberlietbreksies word ook gekenmerk deur die toestand van geen-ewewig tussen die mineraalbestanddele. Nog die massiewe basaltiese kimberliet, nog die melilietbasalt toon hierdie toestand van geen-ewewig. Die vorm van die intrusie het blykbaar 'n groot invloed op die mineraalsamestelling van die onderversadigde alkaliese gesteentes. Daar is ook

vasgestel dat die alkaliese gesteentes in die eklogietsone van die bo-mantel van die aarde ontstaan, en afhangende van die graad van kristalisasie van enstatiet en forsteriet, kan 'n hele reeks van onderversadigde gesteentes vorm.

'n Vergelyking van die mineralogie van eklogiet, kimberliet en peridotiet dui daarop dat die minerale in kimberliet en in granaatperidotiet dieselfde is, en dat die minerale in eklogietknolle baie selde in kimberliet voorkom. Die klinopirokseen in die eklogietknolle is ook meestal verander na 'n fynkorrelrige klinopirokseen, wat soms in gedevitrifiseerde glas oorgaan. Die orde waarin die minerale van die granaatperidotietknolle gekristaliseer het volg die reeks soos deur O'Hara (1968) voorspel is. Die reeks is soos volg: piroop, enstatiet, klinopirokseen, forsteriet en spinel.

Die chemiese analises van eklogiet dui daarop dat die gesteente ongedifferensieerd is, terwyl die peridotietknolle eenvormig gedifferensieerd is, en die eerste stadium van die differensiasiereeks van tholeiitiese magmas verteenwoordig. Die afwesigheid van K^{+}, Na^{+}, Al^{3+}, Ca^{2+} en Ti^{4+} in die ultramafiese knolle en hulle hoë konsentrasie in beide eklogiet en kimberliet dui daarop dat eklogiet eerder as die moedergesteente beskou behoort te word.

Beide kianieteklogiet en grospidiet vertoon lae konsentrasies van Mg^{2+} en Fe^{2+}, en word beskou as die residu tydens die opsmelting van eklogiet en die kristallisasie van granaatperidotiet. Die verarming in die Mg^{2+} en Fe^{2+} inhoud van die eklogiet vind plaas as gevolg van differensieële opsmelting van die eklogiet by ongeveer 30 kilobar druk, waar beide forsteriet en enstatiet in die magma oorgaan, terwyl grossulariet-draende granaat en jadeiet-draende klinopirokseen nog in die vaste toestand bestaan. Laasgenoemde fases kenmerk dan ook grospidiet en kianieteklogiet.

Die mineralogiese, petrologiese en chemiese gegewens van die minerale onder bespreking, is gebruik om 'n model van die bo-mantel van die aarde vas te stel. Die volgorde en die relatiewe tydsduur van die kristallisasie van die bestanddele in kimberliet is sodoende ook vasgestel. Twintig nuwe chemiese analises van eklogiet, peridotiet en kimberliet, en van die minerale in hierdie gesteente is gedoen, en word weergegee tesame met 'n volledige opgawe van alle soortgelyke analises wat versamel kon word.

Die plaatvormige intrusie wat diskordant oor die kimberliet van Premiermyn sny is ook ondersoek, en kon geklassifiseer word as 'n tholeiitiese intrusie. Die plaat is gedifferensieer om 'n sone van olivien-ortopirokseenkumulaat, 'n doleriet sone en 'n granofiriese sone te vorm, en aan die bodemkontak kon 'n fynkorrelrige kilfase onderskei word. Die intrusiewe plaat het die Premiermyn kimberliet in drie tipes meta-kimberliet verander, waarvan die metamorfe fasies ook vasgestel is.

CONTENTS

I. INTRODUCTION

During July and August, 1967, the samples were collected at Premier Mine. The unpublished maps by Rely (1962, mine plans) and the maps of Gerryts (1951) were used as base maps and the kimberlite was sampled according to the colour indices proposed by Gerryts. During 1968 a field investigation of the alkaline and kimberlitic intrusions north-east of Pretoria was carried out with the aid of the maps compiled by Jansen, (unpublished) and Visser, (1961). Samples were also collected from the kimberlite occurrences near Kimberley, Bothaville and at Pilanesberg.

The purpose of the present investigation was to obtain more information on the geology, petrology and mineralogy of the Premier Mine kimberlite and its related inclusions. According to Allsopp, Burger and Van Zyl (1967, p. 165) this kimberlite pipe is of pre-Cambrian age, whereas the other kimberlites are of post-Cretaceous age. Hence a comparison between these two generations of kimberlite was also made. Since very little information was available on the post-Cretaceous kimberlites, a mineralogical and petrological investigation of these kimberlites was necessary.

A comparative study was also undertaken of the ultramafic and eclogitic xenoliths found in kimberlites. The ultramafic nodules are considered by O'Hara and Mercy (1963, p. 296-304) to be fragments of the upper mantle of the earth, and by Schutte (1967, p. 2) as cumulates formed at various depths in the mantle. The present study includes a comparison of the mineralogy, petrology and petrochemistry of the nodules found in kimberlites and alkaline basalts.

The "carbonatite dykes" (Daly, 1925) which occur in the Premier Mine kimberlite, have also been investigated, and are compared to petrographically similar rocks from the Benfontein-, Wesselton-, Du Toitspan- and Jagersfontein-kimberlites.

The association of kimberlite and alkaline rocks is illustrated in the post-Waterberg volcanism north-east of Pretoria, and consequently the structural and petrochemical relationships between the various intrusions have also been investigated. The tholeiitic sill, which is

intrusive into the Premier Mine kimberlite has been studied both in the two bore-hole cores supplied by the C.S.I.R. and in samples collected in the mine. A study of the metamorphism of the kimberlite by this sill, has revealed much about the nature of the matrix of the kimberlite.

The laboratory work consisted mainly of the determinations of the optical, crystallographical and physical properties of the mineral constituents. The investigation of the clinopyroxenes necessitated the use of the techniques of single-crystal diffraction and of infra-red spectroscopy. The chemical analyses were done by the National Institute for Metallurgy.

The data obtained during the present investigation were used as a basis for the construction of a model of the mantle of the earth, and was also used to explain the genesis of kimberlites and the related, undersaturated alkaline magmas.

II. METHODS OF INVESTIGATION

The usual methods for studying the mineralogy and petrology of igneous rocks were used during the present investigation. Under special circumstances however, specialized techniques had to be adopted, and hence they will be described briefly.

A. Polished thin sections

Polished thin sections were found very useful during the investigation of small grains of opaque minerals which are embedded in larger grains of transparent minerals. This technique was mainly used during the investigation of the kelyphytic rims around the garnets.

B. Volumetric compositions

The usual techniques for point counting thin and polished sections were used. However, a new method had to be developed for the point-counting of the kimberlite breccias. The volumetric composition of the kimberlite was determined on rock slabs of at least 10 x 10 cm, and on at least 3 thin sections. The point-counting of the slabs was done by laying a grid over the polished surfaces and counting the proportions of matrix material (smaller than

2 mm), phenocrystal material, and wall-rock inclusions. The thin sections were then point-counted in terms of the same groups of constituents, and the values thus obtained were calculated as a fraction of the percentage matrix material. These fractions were then recombined to produce the volumetric compositions. eg.

Constituents	Slab	Thin section	Volumetric Composition
Matrix	x %	x_1 %	x_1 %
garnet	a "	x_2 "	a + x_2 %
olivine (first generation)	b "	x_3 "	b + x_3 %
wall-rock inclusions	c "	x_4 "	c + x_4 %
Total	100 %	x %	100 %

C. The optical properties

The optical axial angle was determined by means of a universal stage microscope, and conoscopic illumination. Hence the 2V was measured from one optical axis to the other, and was checked by measuring the angles from the optical axes to the acute bisectrix in the extinction position. At least 5 determinations were carried out on a single grain, and at least 4 grains were measured in every thin section. The average deviations found were always less than 1°, and hence a limit of accuracy of $\pm 1^{\circ}$ is accepted.

The refractive indices were determined by the immersion method, using methelene iodide and sulpher for refractive indices exceeding 1.720, and methelene iodide and phosphorous for indices exceeding 1.794. Successive measurements on the same garnet grain have indicated an accuracy of $\pm$ 0.003.

Unless stated otherwise, the limits of accuracy mentioned above, will always apply in the present discussion.

D. The Unit-Cell Dimensions and the d-Values

Depending on the amount of material available, and the nature of the material, either a AEG Guinier camera after Jagodzinski or a Debye Scherrer camera and Co Kα or Cu Kα radiation have been used. Silicon was used as an internal standard for the Guinier camera, and the usual "solution" pill method

was used for the Debye Scherrer camera.

The films were measured by means of a Hilger and Watts film viewer, and successive measurements of the same film indicated an accuracy of ± 0.005 mm. A calculation of the accuracy of the unit-cell dimensions, which is a function of this measurement error, as well as of the type of camera used, indicates that the following accuracies could be obtained:-

Guinier camera (± 0.002)Å
Debye Scherrer camera (± 0.005)Å.

Unless stated otherwise, these limits of accuracy will be applicable in the subsequent discussion.

More sophisticated X-ray techniques were used in certain special circumstances, but these techniques will be described in the relevant sections.

E. Other techniques which were used

Vickers hardness determinations, with the aid of a Leitz mini-load, using a steel standard, were carried out on the ilmenite in the kimberlite.

Differential thermal analyses were used to identify some clay and serpentine minerals, and the heated products were identified by means of X-rays.

Infra-red spectroscopy was applied to the clinopyroxenes in an attempt to determine the distribution of Al^{3+} between the tetrahedral and octahedral sites.

F. The Known Kimberlite Occurrences in Southern Africa

As has been stated in the introduction, kimberlites from several localities other than Premier Mine have also been investigated, in an attempt to obtain more data on kimberlite in general. Since some of the occurrences from which material has been studied are not widely known, a list of these occurrences and a description of their localities are reported in table 1. This list is by no means a complete catalogue on South African kimerlites, but it does include most of the known kimberlites in Southern Africa. For a complete list of the kimberlite occurrences in the Republic of South Africa, the reader is referred to the new 1/1,000,000 map of the Republic of South Africa (In Press).

Table 1. The distribution of kimberlites in Southern Africa.

1. Pretoria district

+Transpoort kimberlite
Beynespoort; 20 m. east of Pretoria
+Premier Mine; Cullinan near Pretoria; 25°40'20"S, 28°31'E
Zonderwater; 22 m. east of Pretoria; 25°41'S, 28°33'E
Pienaarspoort; 5 m from Hatherly station
Schuller-national mine; farm Rietfontein
Schuller-Kaalfontein mine;
Klein Zonderhout; 16 m south of Premier Mine
Montrose 1.)S.E of Premier Mine; 25°45'15"S,
Montrose 2.)28°32'E
+Derdepoort; east of Pretoria; 25°41'40"S, 28°17'20"E
Puntlyf;
Rietfontein No. 2
Elandshoek No. 1 and No. 2
Doornkloof.

2. Rustenburg district

Nooitgedacht dyke; Nooitgedacht 405
Winkelhaak dyke; Winkelhaak 280
Rustvoorby-Koornfontein dyke; Rustvoorby 895
Palmietfontein 567; 37 m N.W of Rustenburg
Stroom River 265; 25 m N.W of Rustenburg
Vaalboschlaagte 636; 30 m N of Rustenburg
Vlaklaagte 511; S.W. of Palmietfontein

3. Soutpansberg area

Seta mine; 60 m west of Messina

4. Potchefstroom area

Goedgevonden near Potchefstroom, 26°40'30"S, 26°46'20"E

5. Kroonstad area

Lace or Crown Mine; 18 m N.W Kroonstad; 27°27'S, 27°06'E
Voorspoed mine; 18 m N.W Kroonstad; 27°23'30"S, 27°12'E
Ruby; adjoins Crown mine.

Bester's kraal; 12 m N.W of Kroonstad
Baltimore; S.W of Crown Mine
Normandien; farm Normandien

6. Winburg area

Driekopjes; farm Welgegund 356
Byrne; farm Wynandsfontein
Deeldam; 5 m N.E of Theron siding
Driehoek mine; farm Driehoek 500
Ferreiras Rust; near Rietspruit
Kaal Valley; 8 m N.W Virginia siding; 28°02'S, 26°49'30"E
Lion Hill; farm Vergelegen
New Compound; farm Welgegund
+Monastery; 10 m S. Marquard 28°49'S, 27°25'E
New Thor; farm Vrederust
Monteleo; 1 m N.W of Lion Hill mine
Myforres; East of Theron's Kop
Phoenix; 1 m N.E Theron siding 28°19'S, 26°46'E
Sweetholme; adjoins New Thor
Theron; farm Wynandsfontein
+Wynandsfontein (Star Mine), 9.5 m N.E
Theunissen (28°18'30"S
(26°50'E
Braklaagte, 9 m N of Theunissen 28°16'S, 26°43'10"E
Outa, 6 m N.N.E of Virginia 28°02'30"S, 26°56'40"E
Lovedale , 8 m N.W Clocolan, 28°51'40"S, 27°27'E
Leeuwfontein, near Reddersburg, 29°46'S, 26°28'30"E

7. Boshof area

Biesjisdam; near Roberts Victor, 28°28'S, 25°38'E
Blaauwbosch; 15 m W of Boshof, 28°33'30"S, 25°27'E
Granaatplaats; between Roberts Victor and Blaauwbosch
Katdoorn Pan; 12 m S.W of Boshof
+New Elands; 3 m N of Blaauwbosch, 28°30'30"S, 25°29'E
Loxton's Dal; west of Boshof
Oliphant's mine; farm Oliphantsfontein
+Roberts Victor mine; farm Damplaats 319, 28°28'43"S, 25°33'44"E
Speculatie; adjoins farm Oliphansfontein 366

Tweelingsfontein; adjoining farm Damplaats 319
Vulcan; north of farm Bhauwbosch

8. Fauresmith district

Buffelhoutfontein; 11 m S.E of Jagersfontein
+Jagersfontein; in Jagersfontein 29°46'S, 25°25'30"E
Kalkfontein; East of Jagersfontein
Koppiesfontein; 250 yards from Buffelhoutfontein
Vogelfontein; 3 m N.W of Jagersfontein
Astoria mine; farm Twyfelhoek, 12 m N.E of Koffiefontein
Ebenhaezer; near Koffiefontein 29°24'30"S, 24°59'E
Klipfontein; near Koffiefontein
+Koffiefontein; 29°25'S, 24°59'30"E
Panfontein; adjoins Koffiefontein estate
Zwartrandsdam; near Koffiefontein; 29°20'S, 25°15'E
Poortje, near Koffiefontein; 29°26'30"S, 25°06'E
Brakdam; near road bridge over Modder River, N.E Jacobdal

9. East Griqualand area

Melkfontein; farm Melkfontein
Zeekoegat; farm Zeekoegat
Abbotsford; 30°27'40"S, 28°50'E
Sibi; Southern Pipe; 30°09'55"S, 28°47'45"E
Sibi; Northern Pipe; 30°10'S, 28°47'45"E
Robertsdale; 36°06'55"S, 38°49'45"E
Clarkton; farm Clarkton 30°00'30"S, 29°21'30"E
Bristol; farm Bristol
Mzongwani, near Mzongwani location
Rhamakakala, on farm Rhamakakala Run
Mooifontein; on farm Mooifontein
Mahlaki, near Mahlaki store (2 dykes)
Hlangwini location; 30°06'30"S, 29°01'E
Kingscote; farm Kingscote
Ezincuka; farm Ezincuka
Inyongo; farm Inyongo

10. Lesotho

+Kolo 1. 17 miles S.W of Maseru
Kolo 2. 17 miles S.W of Maseru

+Ngopetseu 29°33'S, 27°47'E
Berea Plateau (2 dykes), near Maseru
Sekhameng 28°48'S, 28°16'E
Koenaneng 1. 28°47'30"S, 28°12'30"E
Koenaneng 2. 28°47'30"S, 28°12'30'E
Marakabei (6 dykes) 8 miles west of Sekhameng
+Hololo 10 miles WNW of Sekhameng
+Kao 1 29°01'S, 28°38'E
Kao 2 29°01'S, 28°38'E
Kaunyane area (3 pipes)
Liqhobong (3 pipes) 28°59'20"S, 28°36'40"E
Solane 6 miles S.W of Sekhameng
+Thaba Putsoa 28°55'S, 28°39'E
+Qaqa 29°0'30"S, 28°52'E
Robert Makhotlong (4 dykes) 29°09'S, 29°01'E
Matsoku 29°05'S, 28°44'E
Khobos dyke 28°50'S, 28°16'E
Lemphane 28°57'S, 28°35'E
Letseng-La-Terai; 29°00'S, 28°40'E
Lipaleng, 28°46'12"S, 28°14'30"E
Malibamatso, 29°01'40"S, 28°33'E
Matai, 28°58'S, 28°48'E

11. Postmasburg district

Makganyene; 9 m. N.W of Postmansburg, farm Makganyene
Metseatsididi; farm Metseatsididi
Roscoe; farm Roscoe 52
West End Mine, 1 m NNE Postmansburg, 28°19'20"S, 23°04'30"E
Postmansburg Mine; 2¼ m E.N.E. Postmansburg (28°19'10"S (23°06'S
Blinkklip No. 1 on farm Blinkklip 69
Blinkklip No. 2 ditto
Blinkklip No. 3 ditto
Tigerkop on farm Tigerkop
Mahura Muthla, 35 m S.W of Vryburg
Makagene and Mamaghodi; 40 m N.W of Postmansburg
Victory; near Kuruman
Aarkop; near Van Drutens, Vlakfontein
De Bad; on Vaal River, 62 m west of Kimberley

Kouwater; 22 m from West End Mine, 4 m from Makanyene mine
Paardeberg east; 27 m S.W of Kimberley
Peisir Mine (Peiserton?); 19 m S.E of Postmansburg
Sanddrift; 18 m N.E. Prieska, 29°30'40"S, 22°56'E
Thakwaneng; 9 m E of Makanyene
Van Druten's; Vlakfontein M88
Waterstroom Vlei M63, 9 m S. Postmasburg

12. Victoria West area
Eende Kuil; 12 m S.E of Sutherland
Brandewyn's kuil; 600 yards north of Humansdam
Cordate's kuil; near Vosburg, 30°47'S, 22°52'E
Humansdam; near Vogelstruisfontein
Leijfontein; 32 m WNW of Victoria West
Witputs; farm Roode Draai
Balmoral; farm Ratelfontein, 20 m S.E. Frazerburg
Gansfontein, near Beaufort West, 31°46'S, 22°34'E
Melton Wold, 31°27'S, 22°47'E
Byersfontein, 31°02'S, 22°32'E
Hanover; Hanover 60, Hanover district
Governmentlaagte HV 32, Hanover district
Landover, farm Landover, Hanover district
Lushoff, 30°47'S, 22°58'E

13. Britstown area
Barends fontein; 30 m NNW of Britstown
Paarde Vallei; 10 m NE of Britstown; 30°34'20"S, 23°28'30"E
Brakkuilen; 8 m NE of Britstown
Vioolskraal; near Baren's fontein
Uitkyk; adjoins Baren's fontein
Blaauwboschput; 31 m W of Britstown, 30°38'20"S, 23°15'40"E
Britstown Commonage; W of Town, 30°35'35"S, 23°28'30"E

†Lovedale
14. Prieska area
Markt; 2.5 miles S.E of Markt Homestead
Middelwater; Middelwater farm
Uintjisberg; near Carnarvon, 30°49'S, 22°33'30"E
Du Plessisdam; 5 m N.E. De Aar, 30°38'S, 24°02'E

Vetlaagte; near Du Plessisdam
Witkop (Noeniput) 90 m N.W. of Upington 27°32'S, 20°11'E
Witberg; 40 m N.W. Prieska; 29°10'S, 22°21'E
Lekkerfontein; 30°21'S, 24°38'E
Koegas, farm Kwakwas, 29°12'S, 22°23'E
Kaffir's Kraal, 27 m E of Carnarvon 30°59'S, 22°21'30"E

15. Barkley West, Winserton area

Balmoral (Jubilee); 28°21'30"S, 24°39'30"E
Besters prospect; N.W of Barkley West
Borrell's Kopje; West of Barkley West
Cyprus; near Klipdam
+Frank Smith; Weltevreden, 28°15'S, 24°30'20"E
Harrisdale; 10 m N.W of Barkley West
Jubilee prospect mine; near Klipdam
Leicester; farm Klipdam; near Balmoral (Jubilee)
Llanover; near Klipdam
Russel; farm Good Hope
Victoria; farm Good Hope
Washington; farm Good Hope
Wringley's Kopje; near Klipdam
Newlands No. 1 28°21'S, 24°24'E
" No. 2 Close to No. 1
" No. 3 ditto
" No. 4 ditto
+Doornkloof; 28°12'50"S, 24°30'10"E
Excelsior; 28°12'20"S, 24°30'S"E
Mitchemanskraal; 28°14'40"S, 24°30'E
+Sovér; 28°20'S, 24°30'45"E
+Smiths Mine; 28°13'50"S, 24°29'45"E
+Bellsbank; 28°03'30"S, 24°23'E
Babbejaan Mine; 28°05'S, 24°24'E
Doornhoek; Doornhoek 84
Sydney-on-Vaal; 28°29'S, 24°17'E

16. Kimberley area

+Bultfontein Mine; 28°46'S; 24°48'E
+De Beers Mine; 28°44'10"S; 24°47'E
+Dutoitspan Mine; 28°45'30"S, 24°48'E

+Kimberley Mine; 28°44'15"S, 24°46'E
+Wesselton Mine; 28°46'S, 24°50'E
+Kamfersdam Mine 28°44'30"S, 24°46'E
Belgravia Mine; near Beit House, Kimberley
Doyle's Kopje; Kennilworth road, near Tram Shed
May Mine; farm Witpan
Otto's Kopje; W.N.W. of Kimberley
Pole Mine; farm Riverton
St Augustine Mine; West of Kimberley
Secretaris; 28°42'30"S, 24°30'30"E (3 occurrences)
Spytfontein; S. of Kimberley
Taylor's Kopje; 28°44'20"S, 24°44'E
Therons Mine; farm Roodepan
Thompson's Prospect; N.W. of Kimberley
Wimbledon Mine; 28°49'S, 24°43'E (2 pipes)
Southern fissures; 28°36'S; 25°0'E
+Riverton; farm Riverton
Phoenix Mine; farm Witpan
Kimberlite on farm Doorn Boom
Kimberlite on farm Vooruitzigt
Kimberlite on farm Alexanderfontein
Kimberlite on farm Holsdam
Kimberlite on farm Welgevonden
East Mine on Paardeberg East (+ 3 dykes)
+Benfontein; 9 m east of Kimberley

17. Other Occurrences

Gamoep 32 pipes
Kareeberge 17 pipes
Nuwefontein 2 pipes
Gibeon (S.W.A.) ± 40 pipes
Mt. Rupert (?)
Hager's Mine; Kruis River; Riversdale district
Botswana; West of Francis Town, several pipes
Tanzania; more than 200 occurrences are known

18. Rhodesia

Colossus Mine
Wessels Mine
Prospect 1
Prospect 2
Morwen Mine

19. Congo (Verhoogen)

Zefu	Pipe
Kashiaba	
Chilongo	
Lubanda	
M'Bo	Pipe
Golo	"
Gwena	"
Gondolo	"
Talala	"
Kambeli	"
Katipa	"
Mafwa	"
Tengo	"
Konzi	"
Luanza	"
Liasa	"
Kiando	"
Chimbwe	"
Congo	"
Chingululu	"
Mispashi	"
Fumbo	"
Mombwe	"
Gungwania	"
Lushipuka	"

+ The Kimberlites from which samples were investigated, during the present investigation

III. THE GENERAL GEOLOGY OF THE AREA SURROUNDING PREMIER MINE

A. The Country Rocks

Since kimberlite originates at a depth of more than 100 km below the surface of the earth, (Mercy, 1967, p. 421-441) it is clear that the vent along which the kimberlite intruded, cuts through all the formations existing at higher levels in the earth. In figure 1 a schematic section of the known formations presently cut by the Premier Mine kimberlite is represented.

According to figure 1 the granite basement is cut by the kimberlite vent at a depth of 8.5 km below the present surface. The granite is succeeded by the rocks of the Black Reef Series, which has a thickness of 176 m. The Dolomite Series overlies the Black Reef Series, and has a thickness of 1860 m, and is unconformably overlain by the sediments of the Pretoria Series. The Pretoria Series is complete up to the top of the Magaliesberg quartzite, and the succeeding sediments probably belong to the Smelterskop Stage. These sediments have been correlated with the Steenkampsberg quartzite and the associated carbonate-rocks in the Eastern Transvaal (Frick, 1967 p. 6). The kimberlite of Premier Mine is at present exposed at this horizon, but apparently it also intruded into the overlying Waterberg System, which is indicated by xenoliths of Waterberg quartzite and conglomerate in the kimberlite. The kimberlite has also intruded many diabase sills, which are intrusive into the Pretoria Series, and in the upper 600 meter of the profile a sheet-shaped body of felsite was transgressed.

According to map 1 it appears that Premier Mine is part of a volcanic phase consisting of 11 kimberlite diatrems and a number of alkaline intrusions. According to Shand (1922 p. 83) the alkaline intrusions of Franspoort, Leeuwfontein, Roodeplaat and Wallmannsthal, and the kimberlites of Franspoort (Franspoort J.R 332), and Pienaarspoort (Pienaarspoort JR 338) have intruded along the same north-north-west trending "Franspoort line". The kimberlites of Klein Zonder Hout JR 519, Beynespoort JR 335, Zonderwater JR 482, Montrose I and II, Schuller

(Rietfontein JR 214), Kaalfontein JR 513, and Premier Mine also intruded along a line, parallel to the "Franspoort line". The direction of these two lines coincides with that of the post-Waterberg syenite dykes. Since all these intrusions are of roughly the same age, and are apparently controlled by the same tectonics, it seems reasonable to group them into the same volcanic phase.

Since kimberlite is an explosive volcanic breccia, inclusions of the material through which the pipe has pierced can be expected in the breccia. The suite of xenoliths of wall-rock material which has been encountered, includes all the rock-types usually found in the formations shown in figure 1. However, some xenoliths of syenite, garnet peridotite, and eclogite are also occassionally found in the kimberlite. According to Visser (1961) the felsite sheet varies considerably in composition and even grades into syenite. This could account for the syenite xenoliths in the kimberlite. Many post-Waterberg syenite dykes are also known in this area, which may equally well be considered as the source of these xenoliths.

Apart from the ultramafic and eclogitic inclusions, all the other xenoliths were derived from the country rocks, and hence they will be termed inclusions of wall-rock. Since the eclogitic and ultramafic nodules cannot be explained in this way, they will be considered as "mantle inclusions". According to Mason (1958, p. 34) the Mohorovicic discontinuity is approximately 35 km deep in crustal areas, and as has been shown in figure 1, only the first 9 km could be accounted for, hence it is possible that these nodules may still be derived from some other source in the crust of the earth.

B. The Geology of Premier Mine

Premier Mine is the largest known kimberlite occurrence in the Republic of South Africa, and is situated 25 km east-north-east of Pretoria. It is well known for the discovery in 1905 of the Cullinan diamond (3,025 carats), the largest stone ever found.

In plan Premier Mine is oval-shaped with a constriction towards the east, thus creating the impression of two connected intrusions (figure 2). On surface the

A SCHEMATIC PROFILE ACROSS THE KNOWN FORMATIONS WHICH ARE TRAVERSED BY THE PREMIER MINE KIMBERLITE

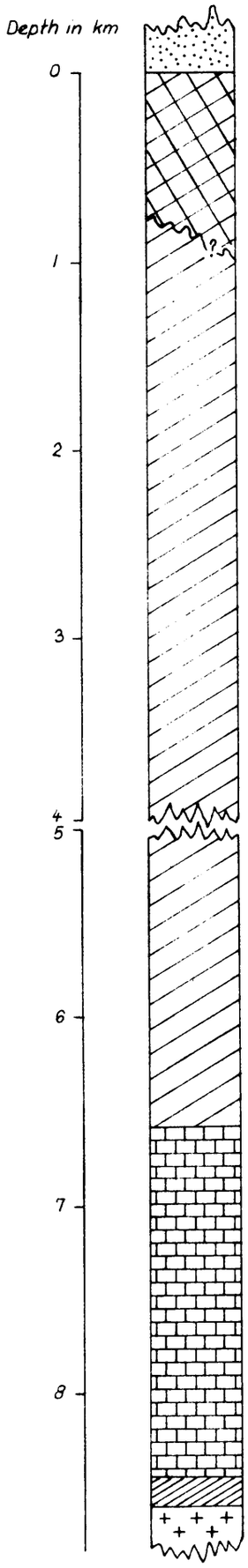

Waterberg System (Quartzite and Conglomerate)

PREMIER MINE felsite

Pretoria Series (Shale, Quartzite, Volconies, Limestone, Iron ore and Intrusive Diabase Sills

Dolomite Series (Dolomite, Shale and Chert)

Block Reef Series (Shale and Quartzite)

Granite Basement

FIG. .

THE PLAN OF PREMIER MINE AT SURFACE AND AT THE 520m LEVELS

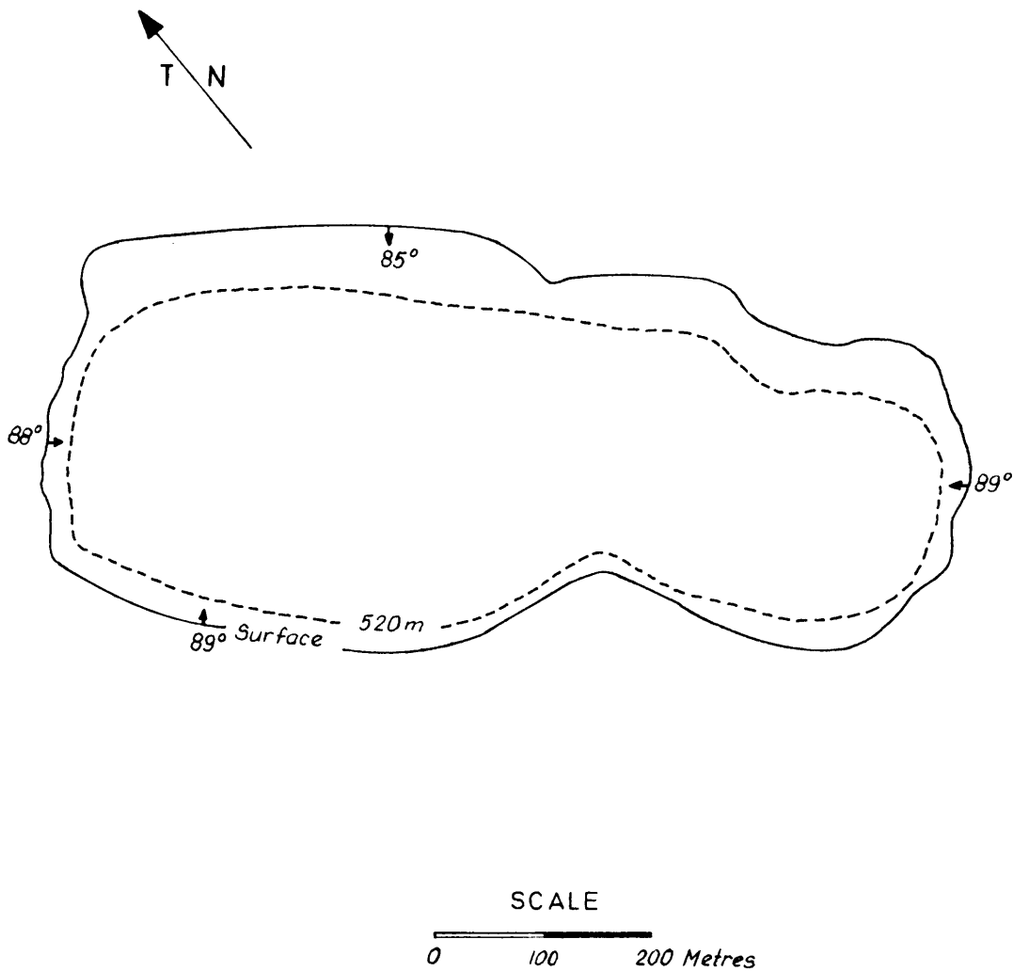

FIG. .

pipe has a length of 860 m and a width of 400 m, and on the 520 m level below the surface the dimensions are 810x300 m. According to figure 2 the dips of the sides of the pipe are steeper on the southern, eastern and western rims, and it appears that the pipe becomes a dyke-like body in depth, similar to the Kimberley Mine (Williams; 1932, p 115). Should the present dip of the walls persist, the pipe would change into a dyke at a depth of 2500 m. It is also noticeable that the direction of elongation of this diatrem coincides with the trend of the "Transpoort line".

The wall-rock which forms the sides of the diatrem consists of felsite, and is part of a large transgressive sheet-like intrusion. According to Visser (1961) this sheet-like body consists of a variety of rock-types including feldspathized quartzite, felsite, granophyre and syenite. The contact between felsite and kimberlite is sharp without any indications of brecciation or metasomatism. The contact is usually striated, irregular and varies considerably in dip over short distances.

The intrusive tholeiite sill also has sharp contacts with the kimberlite, and has caused intensive thermal metamorphism of the kimberlite. Olivine, garnet and pyroxene were found at the metamorphosed upper contact, and diopside, amphibole and serpentine at the bottom contact. The meta-kimberlite at the bottom contact decomposes easily and results in "bad ground". The sill has a thickness of 70 m, a N.E. dip of 15°, and displays a very irregular surface. It cuts through the kimberlite at a depth of 380 m on the southern rim and at 450 m on the northern rim.

At least six separate "carbonatite dykes" which are intrusive into and confined to the kimberlite body could be mapped. The contacts between the kimberlite and the carbonatite are sharp, without any indications of metasomatism. However, in some places near the contact with the carbonatite dykes the kimberlite is bleached. The carbonatite dykes vary in thickness from 0.5 m to several tens of meters, and have very steep dips (60° to 90°). As can be seen in map 2 the carbonatite does not follow any fixed structural pattern, and often cuts the boundaries between the different types of kimberlite.

The carbonatite dykes were also intruded by the tholeiitic sill, and have suffered metamorphic effects similar to the kimberlite.

Many small faults which have a strike distance of less than 10 m, and dips ranging from 7^{o} to 20^{o} towards the west, south-west and north-west are present in the kimberlite. Two larger faults have a strike distance of nearly 70 m, and occur in the eastern portion of the kimberlite. These faults have a dip of 75^{o} towards the east, and traverse the contacts between the various colours of kimberlite. According to Wagner (1911, p. 50) chrysotile asbestos could be identified on the fault planes.

Near the central portion of the pipe a large wedge-shaped, tilted mass, of red Waterberg quartzite and conglomerate is exposed. On the 270 m level the dimensions of the eastern and western lobes of the Waterberg quartzite inclusion are 180x70 m and 150x60 m respectively, whereas on the 520 m level the dimensions have shrunk to 70x20 m and 40x20 m respectively. The kimberlite in the immediate contact area of the Waterberg inclusion usually contains a large amount of small, rounded quartzite inclusions. This zone has been named the "boulder beds" by Gerryts (1951), and is indicated as such on map 2.

According to Wagner (1911, p. 50) four texturally different types of kimberlite could be discerned at Premier Mine. However, the subsequent mapping by Gerryts (1951) revealed 12 different colours of kimberlite. According to Haughton (1969, p. 231) three petrographically different types of kimberlite could be distinguished at Premier Mine. Taking these conflicting reports into account, the kimberlite has been treated as a homogeneous kimberlite breccia, which display some variations in colour.

C. <u>The Age-relationships and absolute ages</u>

Since the absolute ages of many of the alkaline and kimberlitic intrusions in the area north-east of Pretoria have been determined, the genetical relationship between the various intrusions is better understood.

The xenoliths of Waterberg quartzite give an indication of the maximum age of the Premier Mine kimberlite, and according to Oosthuyzen (1964) the Waterberg System is older than 1420 ± 70 million years (Leeuwfontein alkaline complex), possibly older than 1790 ± 70 m.y. (granite on Zaagkuil JR 204), but certainly younger than 1950 ± 50 m.y. (Nicolaysen et al., 1958). The tholeiitic sill, intrusive into the kimberlite, yields a minimum age of 1115 ± 15 m.y. by the Rb/Sr method, 1255 ± 50 m.y. by the K/Ar method and 1750 m.y. by the lead isotope method (Allsop et al., 1967).

Palaeomagnetic work by Jones and McElhinny (1966) on the tholeiitic sill indicates that it is of an age similar to the other post-Waterberg intrusions in Transvaal. Subsequent work by Jones (unpublished) on the Premier Mine kimberlite revealed a slight difference in age between the kimberlite and the tholeiitic sill. The palaeomagnetic work on the Montrose kimberlite by Jones (unpublished), yielded an age similar to that of the Premier Mine kimberlite. Considering all the available evidence it appears that the post-Waterberg alkaline intrusions and the kimberlites north-east of Pretoria are contemporaneous, and consequently the Premier Mine kimberlite is much older than the post-Cretaceous kimberlites from the type-locality (Williams; 1932).

The presence of yellowish-green to green diamonds in the Witwatersrand conglomerates (Raal; 1969, p 292) suggests that a third, and even older phase of kimberlite intrusion is present in South Africa. These diamonds are very small (0.08 to 1.6 carats), however, a stone of 8 carats has been recovered at Klerksdorp. At Modderfontein B Mine, and the highest production recorded was 194 carats per year (Mineral Resources of S. Africa; 1959, p. 48).

According to Holmes (1936) the He/U+0.27Th ratio indicates that the uncontaminated kimberlite from Bultfontein and the melilite basalts are of mid-Cretaceous age. Similar determinations revealed that neither eclogite nor garnet peridotite is co-magmatic with the kimberlite, but that they are older. The recent work by Allsop et al., (1969) indicates lower Rb/K and Sr^{87}/Sr^{86} ratios for the clino-pyroxenes derived from eclogite than for those derived from garnet peridotites, thus indicating a more primitive

age for the eclogite. Similar determinations on the garnets from these two rock-types revealed the same pattern.

D. The Structural Geology

As has been mentioned previously the alkaline intrusions and the kimberlite vents are arranged along the two north-north-west trending lines, viz the "Transpoort line" and the line through Premier Mine. According to Verwoerd, (1967) a line trending north-east, almost at right angles to the Transpoort line extends through the Premier Mine kimberlite and the Derdepoort carbonatite. Although no faults could be discerned along any of these directions it seems as if some structural control of these alkaline intrusions exists.

According to figure 3 it is clear that the post-Waterberg alkaline complexes in the Bushveld basin exhibit all very much the same distribution pattern with respect to the anticlinal fold axes. At the two localities where folding of the floor sediments is evident, the two large alkaline complexes are found, viz. at Pilanesberg and north-east of Pretoria. At the latter locality the series of alkaline intrusions show the pattern of the tectonics caused by the folding very well, however, at Pilanesberg the tectonic pattern is less clear. At both localities kimberlites are found associated with the alkaline intrusions.

According to the distribution of the forces during folding, the area at the nose of the fold is an area of tension, whereas the limbs are areas of compression. Consequently the alkaline intrusions, which are generally characteristic of fracture tectonics, would intrude into the areas of tension.

Figure 3 also indicates that the intrusions are arranged along zones which correspond to the directions of fracture in the resulting strain elipsoid. These directions of fracture also persist in the area of tension and were consequently more accessable for magmatic activity.

The structural map (map 1) of the area north-east of Pretoria indicates that this folding of the sediments of the Pretoria Series was a rather complicated process, because the directions in which the forces operated were continually changed as the process of folding proceeded.

THE RELATIONSHIP BETWEEN THE FLOOR OF THE BUSHVELD COMPLEX AND THE DISTRIBUTIONS OF ALKALINE INTRUSIONS

(Adapted from Hall 1928)

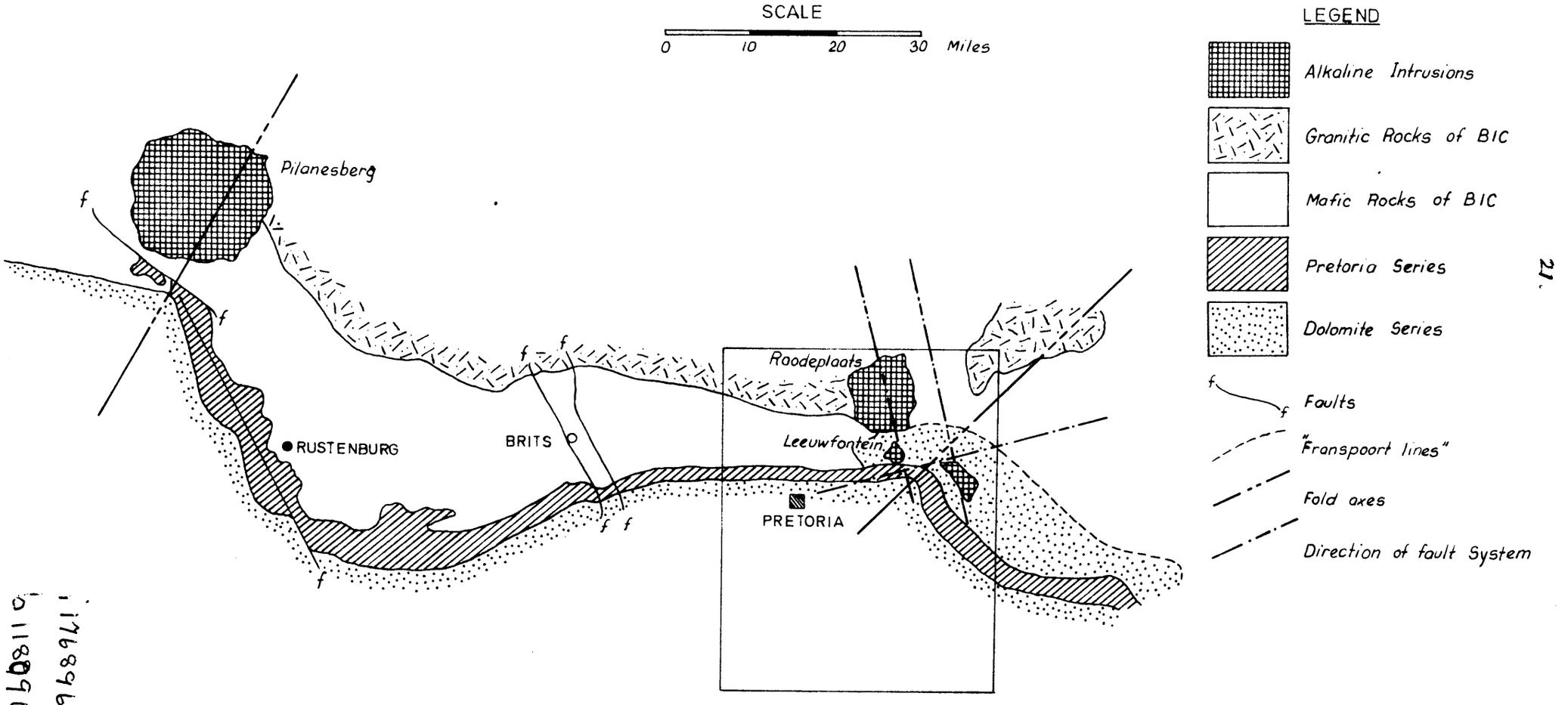

FIG. 3

The initial forces were the stress from the north, which was caused by the emplacement of the Bushveld Complex, and the counter stress from the south which was exherted by the Halfway House granite dome. Apparently the granite dome was sufficiently resistant, and consequently no folding could take place west of the present fold. However, to the east of the granite dome the counter force was not resistent enough, and consequently folding could take place. Since the granite dome has a circular eastern rim, the counter forces now acted from the south-west and the west, and the Bushveld Complex exherted pressure from the north-east and subsequently from the east.

It was these latter forces which resulted in the asymetrically-shaped fold north-east of Pretoria, and in the fault pattern, which consists of reverse faults (Truter, 1955) that are parallel to the south-west-north-east trending fracture zone of the strain elipsoid. All these faults are reverse faults with a downthrow on the southern side. Indicating intense pressure from the north-east (Truter, 1955).

This unequal distribution of forces thus caused the south-west trending fracture zone to be closed, and the south-east trending fracture zone to be open, and consequently accessable to magmatic activity. It was along this direction that the post-Waterberg syenite dykes, the alkaline complexes and the kimberlites intruded.

IV. THE PREMIER MINE FELSITE

According to Visser (1961) the Premier Mine felsite is part of a large transgressive sill, which has intruded into the Steenkampsberg quartzite. This sill varies in composition from syenite to felsite, and many hybrid rocks are developed.

In the felsite many xenoliths of quartzite were encountered, and inclusions of felsite were also recorded in the kimberlite. The felsite exposed in the northern rim tunnel on the 298 m level varies in colour from reddish to greyish. However, no difference between these two types could be observed microscopically.

A. The Petrography

In hand specimens the felsite is a greyish rock which consist of phenocrysts of clinopyroxene and many elongated needles of quartz in a cryptocrystalline matrix.

In a thin section the clinopyroxene phenocrysts show zonal textures with intense alteration of the cores of the grains (photo 1). The 2V and n_β of the clinopyroxene reveal that the cores consist of a more magnesium-rich clinopyroxene, whereas the rims are rich in iron.

The elongated needles (photo 2A & B) were described by Lombaard (1932, p 128) as pseudomorphs of quartz after biotite and feldspar. However, the measurement of the orientation of the individual quartz grains in the needles, has led Glatthaar (1956, p. 28) to conclude that these needles are inverted trydimite. The arrangement of the quartz grains in the needles also resembles the inverted trydimite described by Wager et al. (1954) from the granophyre at Coire Uaigneich, Skye.

The matrix consists largely of a granophyric intergrowth of quartz and orthoclase, with many small lath-shaped clinopyroxene grains, arranged in a trachytic texture. Very small lath-shaped grains, presumably plagioclase, could also be discerned in the matrix.

B. The Mineralogy

1. Clinopyroxene

Large phenocrysts (1.0 to 10.0 mm in length) of euhedral and zoned clinopyroxene occur in the matrix of the felsite. These phenocrysts are usually resorbed, and the cores of the grains are altered to a green chlorite. In the cores of the clinopyroxene the $2V_{\gamma} = 46^{\circ}$, and on the rims the $2V_{\gamma} = 48^{\circ}$.

2. Quartz

Pseudomorphs after trydimite occur as needles (1.0 to 15 mm in length) in the matrix of the felsite. These needles usually consist of several smaller quartz grains, which display a variation in optical orientation. According to Glatthaar (1956) the quartz which inverts from trydimite has an angle of $61^{\circ} \pm 5^{\circ}$ with the original c-axis of the trydimite phenocryst. Since his measurement yielded

this predicted value, it can be concluded that the quartz needles represent inverted trydimite.

C. The Chemical Analyses

In table 2 the chemical analyses of the Premier Mine felsite, Zonderwater syenite, Bushveld granite and Rooiberg felsite are compared. According to this table it appears that the Premier Mine felsite is a more differentiated portion of the syenite sill, and that it also differs from the Rooiberg felsite in being depleted in

Table 2. Chemical analyses of the Rooiberg and Premier Mine felsite, Bushveld granite and the Soda Syenite from Zonderwater

	A	B	C	D	E
SiO_2	75.13	77.78	74.35	75.60	55.81
TiO_2	0.20	0.52	0.09	0.24	3.12
Al_2O_3	9.96	8.81	11.23	11.54	13.58
Fe_2O_3	1.14	1.12	0.72	0.85	4.26
FeO	1.72	1.26	2.50	1.85	6.13
MnO	0.08	0.06	0.02	-	0.12
MgO	2.20	2.78	0.78	0.30	2.95
CaO	1.08	0.37	1.26	1.13	3.28
Na_2O	1.89	2.57	3.38	3.20	7.38
K_2O	3.57	3.48	4.40	4.50	0.91
H_2O^+	1.96	1.10	0.99)	1.08	1.34
H_2O^-	0.07	0.09	0.00)		0.09
P_2O_5	0.12	0.29	0.10	-	0.72
CO_2	1.22		-	-	0.13
Total	100.34	100.23	99.82	100.29	99.82

A + B. Premier Mine felsite; Lombaard (1932, p 186)
C. Rooiberg felsite; Visser (1964, p 128)
D. Bushveld granite; Visser (1964, p 17)
E. Zonderwater soda syenite; Lombaard (1932, p 186)

Na_2O and K_2O and enriched in MgO.

V. THE PETROGRAPHY OF THE UNMETAMORPHOSED KIMBERLITE

A. Introduction

The term kimberlite has been defined by several authors, however, the definition proposed by Dawson (1967, p 242) is the most widely applicable. He defines kimberlite as a serpentinized and carbonated mica peridotite which occurs in diatrems, dykes, veins and sills. The rock displays a porphyritic texture and may contain diamonds and inclusions of ultramafic rocks. The latter are characterized by the presence of high-pressure minerals such as pyrope and jadeite-bearing clinopyroxenes.

Wagner (1914) classified kimberlite on mineralogical and chemical grounds as basaltic or micaceous kimberlites. The average chemical and mineralogical compositions of the micaceous and basaltic kimberlites are compared in table 3.

A classification by Lewis (1887), based on the xenoliths in kimberlite, as amended by Rabhin et al., (1962) is as follows:-

(a) massive kimberlite
(b) kimberlite breccia
(c) kimberlite tuff.

The terms heterolithic and autolithic, which describe the type of inclusions in the kimberlite breccia, have also been introduced by Rabhin et al., (1962).

A combination of the classifications of Wagner and Rabhin et al., appears to be adequate to describe any kimberlite. The combination of any of these classifications with the shape of the kimberlite intrusion is not always applicable, since all transitions exist between pipes and dykes.

B. The Premier Mine Kimberlite

The classifications proposed by Gerryts (1951) and Wagner (1911, p 51) have no genetic significance, since neither is based on mineralogical or petrological data, but on variations in colour. Variations in colour may reflect petrographic differences, however, the succession of yellow ground by blue ground in depth due to secondary

Table 3. A comparison between the Chemical and Mineralogical compositions of the micaceous and basaltic kimerlites (Dawson; 1967, p 271)

	Micaceous kimberlite	Basaltic kimberlite
	1. Chemical analyses	
SiO_2	31.1	35.2
TiO_2	2.03	2.32
Al_2O_3	4.9	4.4
FeO	10.5	9.8
MnO	0.10	0.11
MgO	23.9	27.9
CaO	10.6	7.6
K_2O	2.1	0.98
Na_2O	0.31	0.32
H_2O^+	5.9	7.4
CO_2	7.1	3.3
P_2O_5	0.66	0.72
Mg /Fe	1.8	2.2
K /Na	7.5	3.4
	2. Mineralogical composition	
"Primary Phenocrysts" *1	Phlogopite; olivine; ilmenite; garnet; chromediopside; enstatite; diamond	olivine; chromediopside; ilmenite; garnet, enstatite; diamond
"Secondary Phenocrysts" *1	Sphene; perofskite; zircon; picotite	Sphene; perofskite; zircon; olivine (second generation); picotite
Matrix	phlogopite; calcite; magnetite; serpentine; apatite.	serpentine; chlorite; calcite, magnetite; hidrogrossular; amphibole; diopside.

*1 After Bobrievich et al., (1959).

alteration clearly invalidates the genetic significance of such a classification.

The Premier Mine kimberlite consists of "primary" and "secondary" phenocrystal phases which are set in a residua phase. Olivine (rounded grains; first generation), ilmenite, pyroxene and garnet usually constitute the primary phenocrystal phase, whereas the secondary phenocrystal phase consists of olivine (euhedral grains; second generation), sphene, perofskite, magnetite and apatite. The term phenocryst has been widely discussed, and the term xenocryst is often preferred (Schutte, 1967). However, in the present discussion the term phenocryst will be used, without implying any genetic significance. Calcite and serpentine are common constituents of the residua phase. Inclusions of different kinds of wall-rock are also present in varying proportions.

The volumetric composition of kimberlite reported in table 4 has been obtained by the point counting of at least 3 thin sections of each specimen, as has been outlined in chapter II. In figure 4 the amounts of primary phenocrysts, inclusions of wall-rock and matrix material (secondary phenocrysts plus residua phase) are represented for different kimberlites.

This figure clearly reveals four groups of kimberlite at Premier Mine, viz:-

(a) Group I:- The grey kimberlite of Gerryts (1951) falls into this group, and is marked by a high content of both wall-rock inclusions and primary phenocrysts. This kimberlite is also known to have a relatively low diamond content, probably due to the dilution of the kimberlite by wall-rock.

(b) Group II:- This kimberlite consists only of matrix material, and contains no diamonds. The carbonatite dykes at Premier Mine and the massive basaltic kimberlites of Benfontein, Du Toitspan, Wesselton and Jagersfontein fall into this group.

(c) Group III:- This kimberlite represents all the different colours of kimberlite from Premier Mine except the grey type and is shown in figure 5 as the eastern and the western kimberlites. This kimberlite contains the highest

THE DISTRIBUTION OF PRIMARY PHENOCRYSTS, INCLUSIONS OF WALL-ROCK AND MATRIX MATERIAL IN THE DIFFERENT TYPES OF KIMBERLITE FROM PREMIER MINE

(The names used in the legend are those that are used on the mine plans)

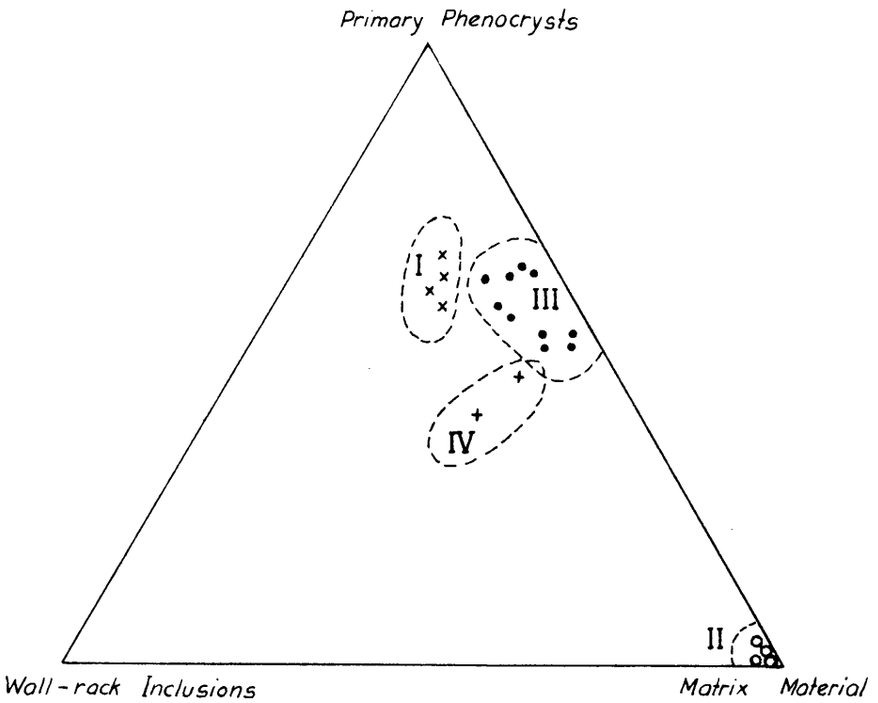

LEGEND

× "Grey" Kimberlite

• Different colours of Kimberlite

o "Carbonatite" dykes

\+ "Bleached" Kimberlite

FIG. .

Table 4. THE VOLUMETRIC COMPOSITION OF VARIOUS KIMBERLITES

Specimen	Primary phenocrysts Ol_1	Px	Ga	Il	Total	Wall-rock	Ol_2	Sph	Matrix material Pe	Mt	Oth	Total
1010-42	54.4	3.7	2.1	1.8	62.0	7.6	0.5		2.8		27.1	30.4
1010-12	53.4	1.3	1.7	2.4	58.8	10.8	2.4		1.5		26.5	30.5
1010-41	55.8	6.0		1.2	63.0	3.4	0.7		3.2		29.7	33.6
1010-38	44.2	4.8		6.2	55.2	10.1	0.5		3.0		31.0	34.5
1010-40	42.1	4.3		4.5	50.9	4.9	0.2		3.7		40.3	44.2
1010-3	57.4	4.2		1.1	62.7	16.4	0.8	2.0	0.6		17.5	30.1
1010-5					0.0	0.9			1.1	20.4	77.6*1	99.1
1010-8	47.2	2.6	1.6	0.4	51.8	7.9	2.9		4.1		33.4	40.4
1010-14	58.5	2.1		0.7	61.3	11.6	0.9		0.8		25.4	27.1
1010-15	54.9	5.1	2.3		62.3	5.0	1.2		0.2		31.3	32.7
1010-22	28.0	3.2	7.0	1.1	39.3	24.2	4.1	2.1			30.4	36.6
1010-20	38.7	5.1		2.5	46.3	14.6	7.5	0.9	2.8		28.1	39.3
1010-9	40.9	2.1	6.2	3.3	52.5	8.3	5.1		6.8		27.3	39.2
1010-12	40.6	2.8	1.2	8.5	53.1	3.2					39.8	43.7
Jag.12	60.9*5				N.D.	1.6					9.4*2	N.D.
Kof.1	59.7*5				N.D.					4.1	36.2*4	N.D.
Wes.3	48.5*5				N.D.	20.0			8.6	4.6	18.4	N.D.
Jag.13	59.5*5				N.D.					7.7	32.9	N.D.
Fs.1	47.5*5			0.5	N.D.				18.6*3	20.5	12.9	N.D.
Mon.	41.4*5			0.9	N.D.				17.5*3	17.7	22.5	N.D.
Benf. 2					0.0		36.2		11.5*2		52.3	100.0
Du P. 14					0.0	2.9	43.0		39.4*1	11.8	2.8	97.0
Sov.					0.0	32.1	37.2		13.6*1	3.3	13.8	67.9

Ol_1 = First generation olivine
Ol_2 = second generation olivine
Px = pyroxene
Ga = garnet
Il = ilmenite
Sph = sphene
Pe = perofskite
Mt = magnetite
Oth = others
*1 = Calcite and serpentine
*2 = Calcite
*3 = Calcite and phlogopite
*4 = Matrix, ilmenite, sphene and perofskite
*5 = total olivine

Samples:-

1010-42 to 1010-12 from Premier Mine
Jag 12 and 13 from Jagersfontein
Kof.1 from Koffiefontein
Wes.3 from Wesselton
Mon. from Monastry
Du P 14 from Dutoitspan
Fs.1 from Frank Smith
Benf.2 from Benfontein
Sov. from Sovér

THE DISTRIBUTION OF THE DIFFERENT PETROGRAPHICAL TYPES OF KIMBERLITE IN PREMIER MINE

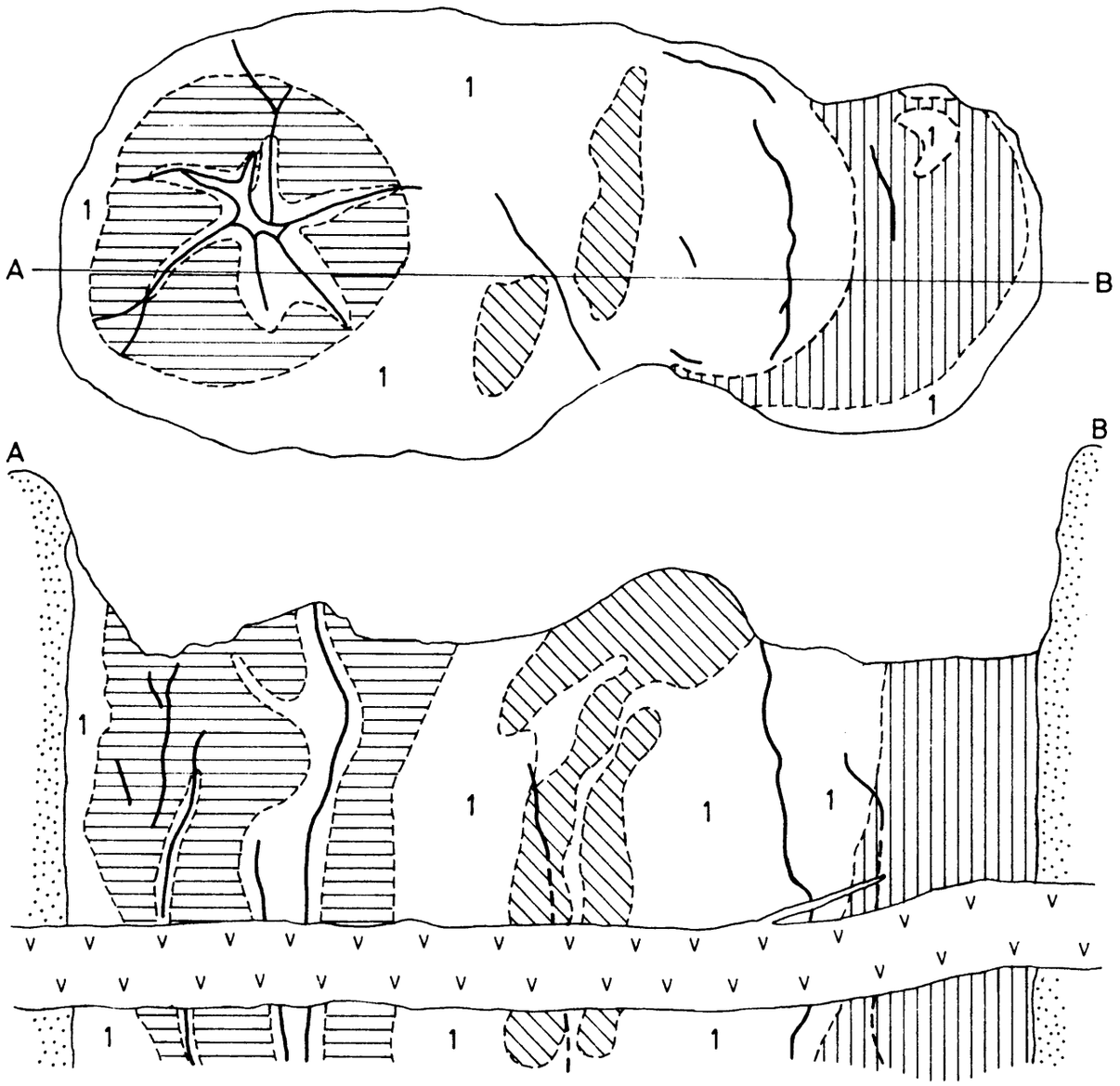

SCALE

0 100 200 Metres

LEGEND

- 1 — Kimberlite : Group I
- Kimberlite : Group II
- Kimberlite : Group III (Eastern Kimberlite)
- Kimberlite : Group III (Western Kimberlite)
- Kimberlite : Group IV
- Thoelitic Sill
- Waterberg Quartzite
- Felsite

FIG. .

amount of phenocrystal material, and is known to be the most profitable. Figure 5 also indicates that the eastern and the western kimberlites are not in any way connected; consequently they are considered to be two different types of kimberlite. The presence of ultramafic nodules in the western kimberlite and their absence in the eastern kimberlite also support this conclusion.

(d) Group IV:- This kimberlite contains a higher concentration of both wall-rock inclusions and matrix material. It occurs near the contact between the carbonatite dykes and the western kimberlite, and is known to contain some diamonds. According to its bleached nature and its method of occurrence, this kimberlite is considered to be a carbonated variety of the western kimberlite. It is conceivable that the influx of carbonates would destroy the phenocrystal material more readily than the xenoliths of wall-rock, hence resulting in a kimberlite enriched in both xenoliths of wall-rock and matrix material.

In table 4 the classification of the Premier Mine kimberlite is reported. This classification is based on the volumetric composition only, and will subsequently be verified by the mineralogical data.

C. The Petrography of Kimberlite Breccia

Table 5. The classification of the Premier Mine kimberlite

Group	Type of kimberlite	Classification after Williams and Nabhin
I	grey kimberlite	Heterolithic basaltic kimberlite breccia
II	carbonatite	massive basaltic kimberlite
III	eastern kimberlite	Autolithic basaltic kimberlite breccia
	western kimberlite	ditto
IV	carbonated western kimberlite	ditto

The petrology of the heterolithic and autolithic kimberlite breccias from Premier Mine does not differ much, and will therefore be described simultaneously.

1. The primary phenocrystal phase

This phase consists of the minerals which did not crystallize in situ from the kimberlite, and comprises the first generation olivine, ilmenite, garnet, pyroxene and chromite.

(a) First generation olivine

Although no fresh olivine was encountered in any of the samples from Premier Mine, the presence of primary olivine is revealed by the pseudomorphs of serpentine after olivine. The two generations of olivine in kimberlite have been mentioned by several authors, however no factual data on the two generations have been reported. The frequency distribution diagrams (figure 6) for the euhedral, subhedral and anhedral olivine grains in kimberlite indicate that an average of 18 per cent are euhedral, and 21 per cent subhedral, and thus 39 per cent second generation, and 60 per cent are of the first generation.

The grain size distribution of the olivine indicates that the grains smaller than 0.5 mm in diameter comprise also approximately 40 per cent of the olivine. Hence it is concluded that the smaller euhedral grains belong to a different generation than the larger anhedral grains. The massive basaltic kimberlite from Benfontein apparently only consists of second generation olivine (figure 6).

Since both generations are serpentinized these olivines cannot be distinguished on mineralogical grounds, however, the alteration products also reveal the differences between the two phases of olivine, and will be discussed subsequently.

The olivine grains occur in the fine-grained kimberlite matrix, and are surrounded by rims consisting of magnetite, sphene and perofskite, which are set in a matrix of either serpentine, diopside or hydrogrossular, depending on the prevailing stage of alteration or metamorphism (photo 3). The rims around the first generation olivine are more prominent than those surrounding the second generation olivine.

Many small grains of rutile and sphene are present in the serpentinized first generation olivine. The rutile occurs as small (0.01x0.1 mm), elongated needles (photo 4),

HISTOGRAMS SHOWING THE SHAPES OF THE PRIMARY AND SECONDARY PHENOCRYSTS OF OLIVINE IN KIMBERLITE

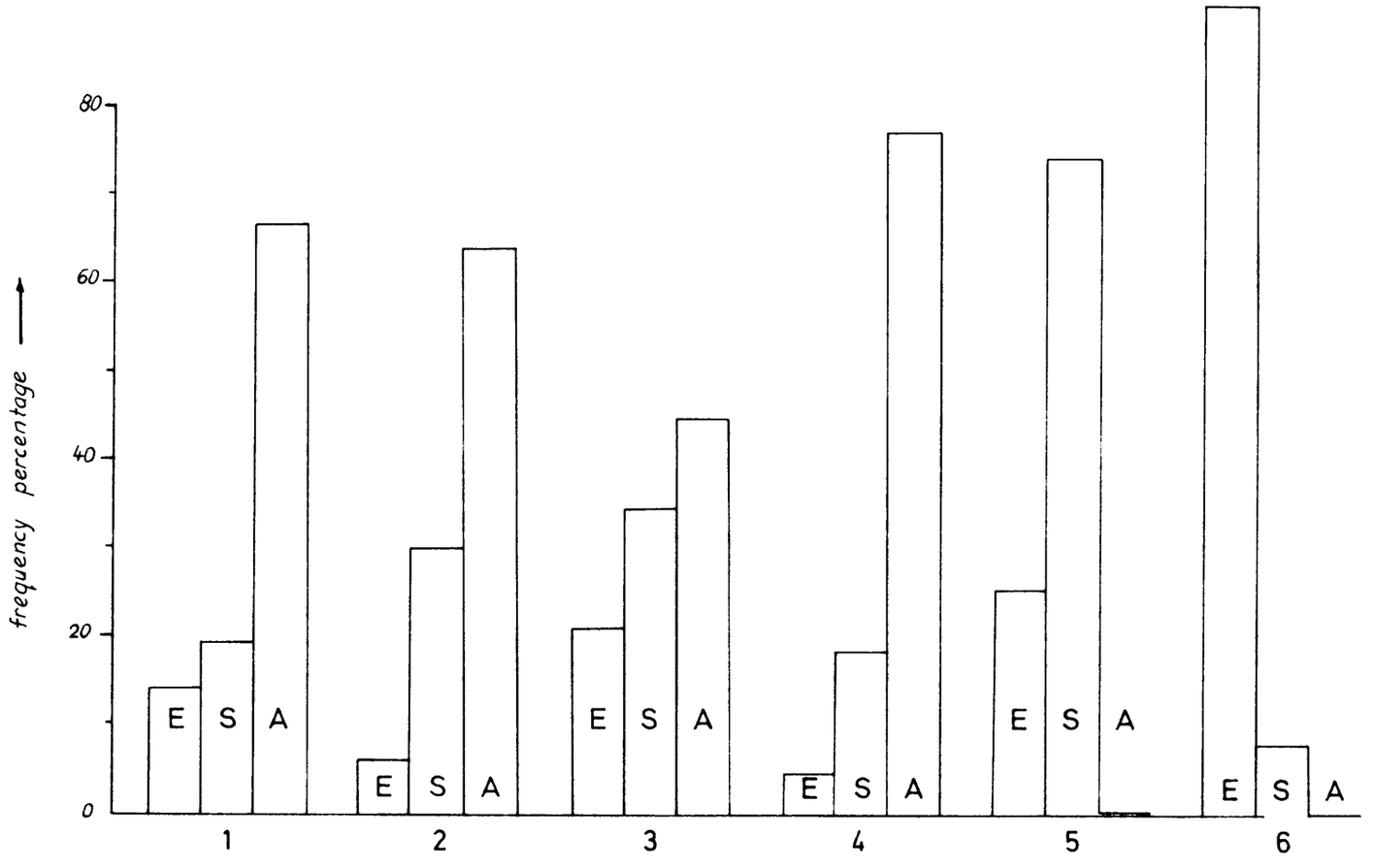

LEGEND

1 1010 - 9; Western Kimberlite ; 464 grains counted
2 1010 - 20; Carbonated Kimberlite ; 511 ditto
3 1010 - 22; ditto ; 349 ditto
4 1010 - 8; Western Kimberlite ; 604 ditto
5 1010 - 20; ditto ; 474 ditto
6 Be_2; Massive Kimberlite ; 391 ditto

E Euhedral
S Subhedral
A Anhedral

FIG. 6

whereas the sphene grains are subhedral to anhedral, and arranged in clusters in the altered olivine grains (photo 5). Gerryts (1951) identified these grains as zircon, however, the d-values shown in table 6 indicate that it is sphene. The needles of rutile are only present in the olivine grains which are altered to talc or bastite, whereas the sphene occurs in the more intensively altered olivine grains. It thus appears as if the sphene forms as a consequence of the reaction of rutile with Ca^{2+} and Si^{4+}-bearing liquids during the advanced stages of serpentinization.

Various stages of the alteration of olivine could be identified in the thin sections. At first the olivine alters to a greenish, highly birefringent mineral, which is pseudomorphous after olivine, and shows no exsolution phenomena of opaque minerals other than rutile. The optical properties of this mineral are $2V_{\alpha} = 20^{o}$, $n_{\alpha} = 1.542$; $n_{\beta} = 1.562$ and $n_{\gamma} = 1.570$, and the d-values, listed in table 7 also indicate that this mineral is saponite. However, larger grains of talc which replaces the olivine pseudomorphously, were also encountered.

At this stage of serpentinization or even at an earlier stage, colourless veins of serpentine may form along cracks in the olivine grains. This colourless serpentine has a low birefringence, and could be identified as antigorite.

Subsequent to this initial stage of alteration the talc alters pseudomorphously to a massive green serpentine which displays a moderately high birefringence. The more advanced stages of alteration, resulted in a variety of secondary minerals in almost any succession. This stage of serpentinization is marked by the formation of small exsolution bodies of hematite.

Euhedral grains of colourless calcite were often encountered in the green serpentine. The green serpentine alters to a fine-grained mass of either fibrous or flaky serpentine, the d-values of which are given in table 7. Many small needles of tremolite, which are arranged in a criss-cross texture, often forms in this fine-grained serpentine (photo 6) and may result from progressive metamorphism. In the more advanced stages of readjustment, these needles are enlarged (0.5 mm diameter) and may

Table 6. The d-values of the sphene in the primary olivine phenocrysts. (The d-values were obtained by means of a Debye-Scherrer camera using Cu Kα - radiation).

1010-8, Film No 401		1010-44, Film No 408		ASTM 11-142		
I/Io	d Å	I/Io	d Å	I/I_1	d Å	h k l
-	-	-	-	30	4.93	$\bar{1}11$
10	3.231	10	3.233	100	3.233	111,002
9	2.982	10	3.008	90	2.989	$\bar{2}02$
-	-	-	-	5	2.841	200
9	2.594	9	2.610	90	2.595	$\bar{2}21$,022
-	-	-	-	5	2.362	$\bar{1}13$,220
4	2.266	4	2.281	30	2.273	112,$\bar{1}32$
-	-	-	-	5	2.225	131
-	-	-	-	20	2.101	$\bar{3}12$
5	2.067	4	2.034	40	2.058	$\bar{3}11$
-	-	-	-	10	1.972	221
-	-	-	-	10	1.945	$\bar{3}13$
-	-	-	-	5	1.848	$\bar{2}04$,310
-	-	-	-	10	1.802	042,$\bar{2}41$
1	1.738	1	1.740	20	1.741	$\bar{3}32$
-	-	-	-	10	1.725	240
1	1.701	4	1.710	30	1.703	$\bar{2}24$
1	1.636	4	1.655	40	1.643	$\bar{3}33$
-	-	-	-	20	1.554	151,241
-	-	-	-	10	1.527	043,$\bar{1}34$
1	1.488	1	1.491	40	1.494	133
2	1.419	2	1.421	40	1.418 *1)	400

*1) plus 13 lines of low intensities

Table 7. The d-values of the alteration products of olivine in kimberlite. (The d-values were obtained by means of a Debye Scherrer camera, using Cu Kα radiation).

1010-41 Film no. 421		Saponite ASTM 6-0002			Blue chlorite 1010-20 Film no. 425		Penninite ASTM 10-422			Green-Serpentine 1010-22A Film no. 412	
I/Io	d Å	I/I_1	d Å	h k l	I/Io	d Å	I/I_1	d Å	h k l	I/Io	d Å
-	-	100	13.8	001			100	14.2	001	10	7.276
-	-	50	9.1	002			40	7.09	002	1	2.999
-	-	10	6.06	003			60	4.72	003	1	2.649
10	4.540	50	4.55	11.0.2,004	6	3.524	60	3.54	004	5	2.464
4	3.618	50	3.61	005	10	2.843	90	2.84	005	4	1.338
4	3.110	40	3.01	006	3	2.619	20	2.61	$131,20\bar{2}$	1	1.744
5	2.613	60	2.61	13.2.0			20	2.58	$13\bar{2},201$	1	1.695
5	2.471	30	2.48	-	2	2.476	30	2.46	$132,20\bar{3}$	1	1.661
-	-	20	2.26	22.0.4	2	2.281	30	2.27	$133,20\bar{4}$	2	1.610
-	-	10	2.00	009			20	2.01	$13\bar{5},204$	8	1.537
3	1.729	40	1.736	31.1.5	1	1.899	20	1.390	$13\bar{5},20\bar{6}$	2	1.503
6	1.532	70	1.536	33.0.6			30	1.720	$136,20\bar{7}$		
4	1.319	40	1.321	26.4.0	1	1.583	30	1.570	$137,20\bar{8}$		
-	-	20	1.271	0.0.14	2	1.548	30	1.552	$\overline{331}$ 060,$33\bar{1}$		
-	-				2	1.384	20	1.395	$13\bar{9},208$		

replace the entire olivine grain. In the metamorphosed kimberlites where tremolite becomes the major constituent, both hydrogrossular and diopside, which may also be fibrous, form from the tremolite. — an amphibole

In the secondarily weathered kimberlites this fine-grained serpentine alters to either a green chlorite or a blue penninite, ~~of which~~ the d-values of which are listed in table 7. An alkali amphibole showing pleochroism in blue, green and brown also occurs in places.

Some of the larger first generation olivine grains may exhibit a succession of zones of the monomineralic alteration products described previously (photo 7). Any combination of these zones may occur, although the complete succession is not always developed. However, the consistency with which these zones alternate is remarkable and the inversion of zones was never observed. The succession of these zones from the rim towards the centre is as follows:-

i. hydrogrossular
ii. diopside
iii. tremolite
iv. fine-grained serpentine
v. massive, green serpentine
vi. chlorite, penninite and calcite

All the zones may be dissected by veins of colourless serpentine.

Aggregates of olivine were sporadically encountered in the Premier Mine kimberlite. In sample No. 1060-25, a large inclusion (0.5x1.5 cm) consisting of rounded olivine grains and of a myrmekitic intergrowth of chromite and clinopyroxene, were observed. Inclusions of garnet in first generation were also encountered.

b. Ilmenite

Ilmenite in the Premier Mine kimberlite occurs as rounded and elipsoidal grains in the matrix, and they vary in size from 0.10x0.05 mm to 6.0x4.0 cm, and are composed of either large, single anhedral crystals, or of aggregates of rounded and randomly orientated crystals. Along the rims and the grain boundaries of the ilmenite a zonal arrangement of alteration products is evident. The zone nearest to the

ilmenite usually consists of highly reflecting leucoxene, succeeded by a zone of brown perofskite. The latter is mostly discontinuous and of varying thickness. The outer zone of sphene follows the perofskite zone and appears to be a reaction product between the perofskite and the matrix. The leucoxene replaces the ilmenite pseudomorphously, whereas the sphene and perofskite grains are euhedral to subhedral in shape.

In the carbonated western kimberlite, these reaction rims are more pronounced than in the other kimberlite breccias, and the ilmenite in the massive basaltic kimberlites ~~are~~ is in places entirely altered to sphene and perofskite.

In areas where only leucoxene was formed the presence of a black material, containing minute grains of highly reflecting rutile could be discerned. Willemse (1969) described similar black oxides from the ilmenites from the Bushveld Complex, and Bailey et al. (1956) identified similar material as a mixture of Fe^{2+} and Fe^{3+} oxides.

In the ilmenite from 1010-19 and from a sample of the Elandsdrif kimberlite, supplied by Dr. C.P. Snyman, a mineral with a low reflectivity and red to brown internal reflections was observed. Both the optical properties and the d-values of this material indicate that it is pseudobrookite. Pseudobrookite was also identified by Ramdohr (1960) in the kimberlite from the Kimberley mines.

The ilmenite from 1010-22 also shows a reaction rim of schorlomite, which replaces the sphene rim. The d-values of this brownish garnet are reported in table 8.

The unit-cell dimensions of the ilmenite are reported in table 9. These values have been calculated from the diffraction patterns obtained by means of a Guinier camera. Zoned ilmenites can be recognized quite readily by the doubling of lines on the X-ray photographs. Table 9 indicates that only the ilmenites from the group I-kimberlite are zoned, and that the ilmenite from the eastern kimberlite has higher a_o and c_o values than those from the western kimberlite. The exact location of sample 1060-7 is uncertain and it may ~~be derived from~~ represent either the eastern or ~~from~~ the group I-kimberlite. The a_o and the c_o values of the ilmenites of the group IV-kimberlite compare favourably

Table 8. The d-values of schorlomite from the Premier Mine kimberlite. (The d-values were obtained by means of a Debye Scherrer camera, Cu Kα radiation.)

Film no. 417 1010-22		Schorlomite ASTM 7-390		
I/Io	d Å	I/I_1	d Å	h k l
		10	4.31	220
4	3.002	50	3.026	400
7	2.701	80	2.702	420
		10	2.584	332
7	2.467	60	2.468	422
		10	2.366	431
3	2.210	10	2.205	521
1	1.981	20	1.964	611,532
		10	1.909	620
		10	1.845	541
1	1.786	20	1.781	631
1	1.734	10	1.743	444
6	1.676	70	1.679	640
10	1.611	100	1.614	642
3	1.493	30	1.512*1)	800
a_o = 11.98		a_o = 12.09		

*1) plus 4 lines

with those of the western kimberlite, except for sample 1060-28. The latter, however, occurs close to the contact between kimberlite and carbonatite, and consequently these anomalous high a_o and c_o values may be explained by the metamorphic influence of the carbonatite on the kimberlite.

From table 9 and figure 7 it appears that the group I-, eastern- and western-kimberlites are mineralogically different from one another. The carbonated kimberlite also compares favourably with the western kimberlite. The massive basaltic kimberlite does not contain any ilmenite.

c. Garnet

According to Wagner (1911, p. 52) the kimberlite from Premier Mine is very poor in garnet. However, this paucity in garnet can be ascribed to the alteration of the primary

Table 9. The a_o and c_o values of ilmenite in the different kimberlites from Premier Mine

Type of kimberlite	Sample	a_o (± 0.003)	c_o (± 0.005)
Group I	1010-3A	(5.067 (5.079	(13.926 (14.057
	1010-39	(5.072 (5.079	(13.992 (14.033
	1010-3B	(5.073 (5.088	(13.987 (13.989
	1060-10	5.069	13.960
Group III- (Eastern kimberlite)	1010-41	5.085	14.015
	1010-40	5.084	13.990
	1060-7	5.066	13.959
Group IV	1060-28	5.086	14.045
	1060-29	5.069	13.953
	1010-35	5.065	13.97
	1060-30	5.070	13.94
	1010-20	5.067	13.984
	1010-17	5.068	13.957
Group III- (Western kimberlite)	1010-42	5.070	13.972
	1010-42B	5.067	13.966
	1010-45	5.066	13.955
	Il_2	5.066	13.955
	1060-26	5.066	13.963
	1060-43	5.067	13.972
	1010-12	5.065	13.970
	1010-15A	5.067	13.976
	1010-15B	5.070	13.985
	1010-43	5.066	13.956
	1060-32	5.067	13.954
	1010-13	5.070	13.922
	1060-22	5.069	13.963

THE a_o/C_o RELATIONSHIP OF ILMENITE IN THE KIMBERLITE FROM PREMIER MINE

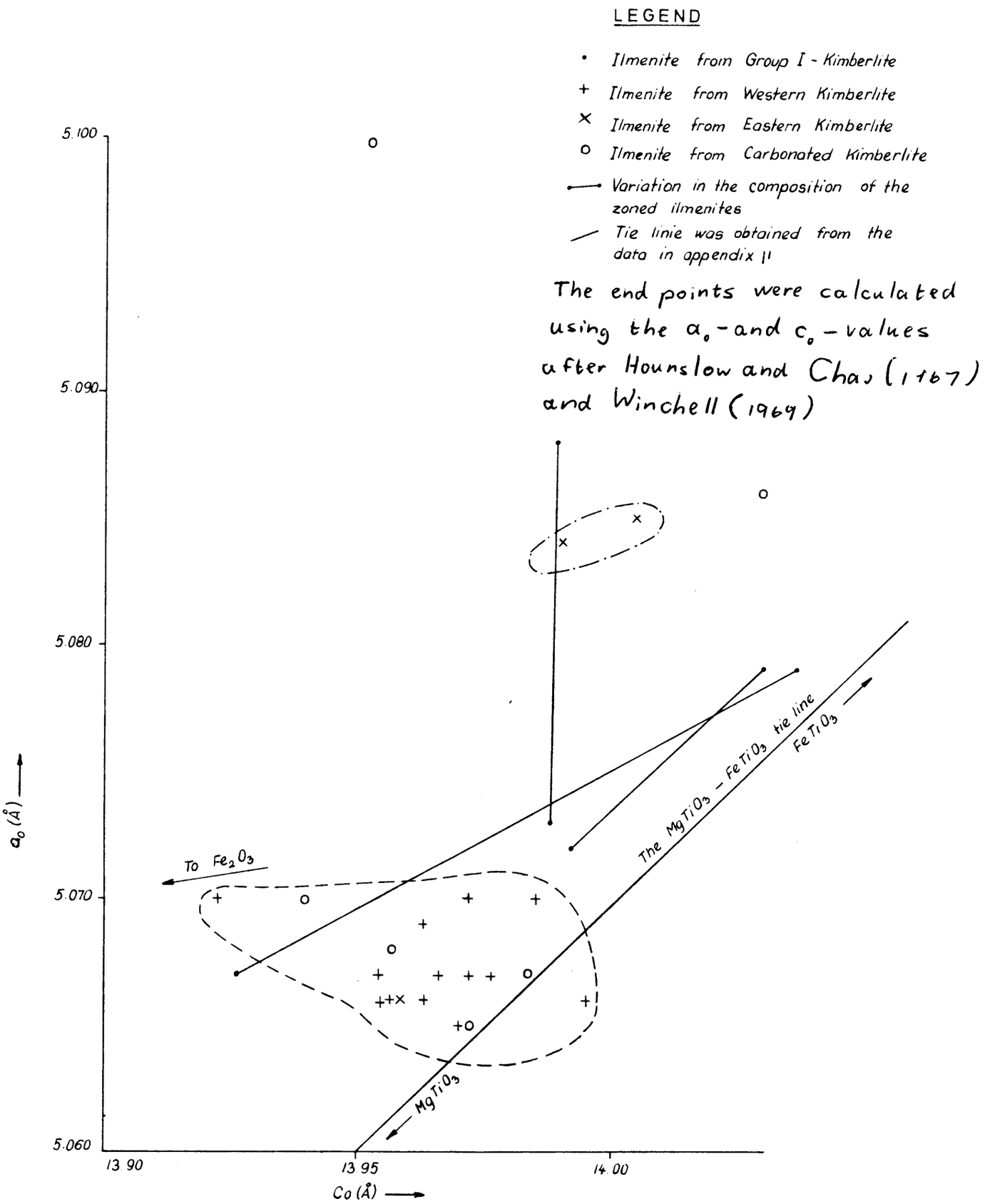

FIG. 7.

garnet to hydrogrossular and serpentine. Consequently the kimberlite is not inherently poor in garnet. Since only the primary garnets belong to the primary phenocrystal phase, only these garnets will be described here.

The grain size of the garnets ranges from 0.5x0.7 mm to 10.0 cm diameter, with an average diameter of 1.5 cm. The garnet grains are disseminated in the kimberlite, and are mostly rounded, however, angular fragments of garnet are also present. The fractured surfaces of these garnets do not show the development of any secondary kelyphyte-formation (photo 8). Small garnets surrounded by kelyphyte are of common occurrence as inclusions in first generation olivine (photo 9), however, the reverse has never been observed.

The kelyphyte consists of two succeeding zones of different mineral associations which replace the original garnet pseudomorphously. Depending on the conditions under which formation of kelyphyte occurred, both a primary kelyphyte and a secondary kelyphyte may result. The latter, however, formed as a consequence of the alteration of the pyrogenetic constituents of the primary kelyphyte, to hydatogenetic phases.

The primary kelyphyte consists of an outer zone of massive magnetite and hematite, and an inner zone of fibrous magnetite, chlorite and serpentine. The outer rim has an average width of 0.5 mm, and is usually marked by the absence of silicates. However, rims containing large grains of biotite, euhedral magnetite and spinel, hematite and serpentine, were also encountered. The fibres of the inner zone are radially orientated and contain wedge-shaped grains of serpentine and chlorite. Along the sharp contacts between kelyphyte and garnet, the garnet is usually altered to the same mineral association that forms along cracks and veins. Orthopyroxene, a greenish clinopyroxene, chrome spinel and magnetite usually comprise this mineral association. The pyroxenes are subhedral to anhedral, whereas the spinel is present as both euhedral and skeletal crystals.

The secondary alteration of these pyrogenetic minerals resulted in veins bearing spinel, serpentine, talc, biotite

and hydrogrossular. The secondary alteration of the original garnet also yields a zonal arrangement of alteration products, and consists of an outer rim (0.05 mm wide) of hydrogrossular. A broader zone (0.2 mm wide), composed of serpentine, chlorite and opaque oxides succeeds this outer rim, and a mass of yellow to green hydrogrossular with patches of opaque minerals, distributed at random, comprise the core of this garnet. The a_c values and refractive indices of the primary garnets and the secondary hydrogrossular are listed in tables 10 and 11 respectively.

Both table 10 and figure 8 after Deer, Howie and Zussman (1967) indicate that the garnets from the carbonated western kimberlite and the western kimberlite have a similar chemical composition, and that the composition differs from that of the garnet in the group I-kimberlite. The latter is enriched in almandine and pyrope, whereas the garnet in the western kimberlite is enriched in grossular. Both types of garnet, however, still fall into the field of the garnets from the ultramafic nodules (p. 97.).

(d) Orthopyroxene

No fresh orthopyroxene has been found in either the Premier Mine kimberlite or the tailings from the waste dumps. However, in the kimberlite from Monastry and Wesselton and on the dumps at De Beers, Bellsbank, Frank Smith, Lovedale and Brakfontein, occasional orthopyroxenes were found. In the garnet peridotite nodules from Premier Mine both fresh and altered orthopyroxenes were found of which the altered pyroxene is similar to the altered pyroxene in the kimberlite.

The altered orthopyroxene occurs as large (1.0x0.6 mm) euhedral grains in the matrix of the kimberlite and do not have any rims of magnetite and sphene. The grains consist of a green, highly birefringent mineral which exhibits parallel extinction and has the following optical properties, $2V_{\alpha} = 65^{\circ}$ to 68°; $n_{\alpha} = 1.554\text{-}1.557$; $n_{\beta} = 1.565\text{-}1.566$; $N_{\gamma} = 1.569\text{-}1.572$ from which it has been identified as bastite. Advanced alteration of this material resulted in a brownish, fibrous serpentine ($2V_{\alpha} = 47^{\circ}$; $\gamma \wedge c = 7.5^{\circ}$, $n_{\gamma} - n_{\alpha} = 0.008$) which is often replaced by euhedral calcite grains.

Table 10. The a_o values and refractive indices and the composition of the garnets from the different types of kimberlite from Premier Mine, after Deer, Howie and Zussman (1967, p 25). The a_o (Å)-values were obtained by means of a Guinier camera, using Cu Kα-radiation

Type of kimberlite	Specimen	a_o (Å)	n	% A*	% P*	% G*
Group I	CF302	11.521	1.751	29.5	63.5	7
	AC 1	11.522	1.751	29.0	63.0	8
Group III Western kimberlite	1060-43	11.537	1.745	23	64.5	12.5
	1060-26	11.545	1.758	34	55	11.0
Group IV	1060-29	11.533	1.750	28	60	12
	1060-22	11.580	1.749	27	58	15

*A = Almandine; P = pyrope; G = grossular.

Table 11. The a_o values and refractive indices of the hydrogrossular from the original garnet in kimberlite

Sample	Mode of Occurrence	n (± 0.005)	* a_o (± 0.005)
1010-12	Periphery of garnet		12.042
1010-12	Core of garnet		12.022
1010-12	ditto		11.988
1570-34	ditto		12.09
1060-27	ditto		12.043
1010-17	ditto	1.817	12.030
1010-9	ditto		12.023
1010-9	ditto		12.028
1010-8	Semi-opaque core of garnet		11.991
1010-3	Core of garnet	1.742	11.505
1010-3	ditto		11.540

* Obtained by means of a Debye Scherrer Camera.

THE COMPOSITION OF THE GARNETS FROM THE DIFFERENT TYPES OF KIMBERLITE FROM PREMIER MINE, ACCORDING TO THE PHYSICAL PROPERTIES AFTER DEER HOWIE AND ZUSSMANN (1967; P28)

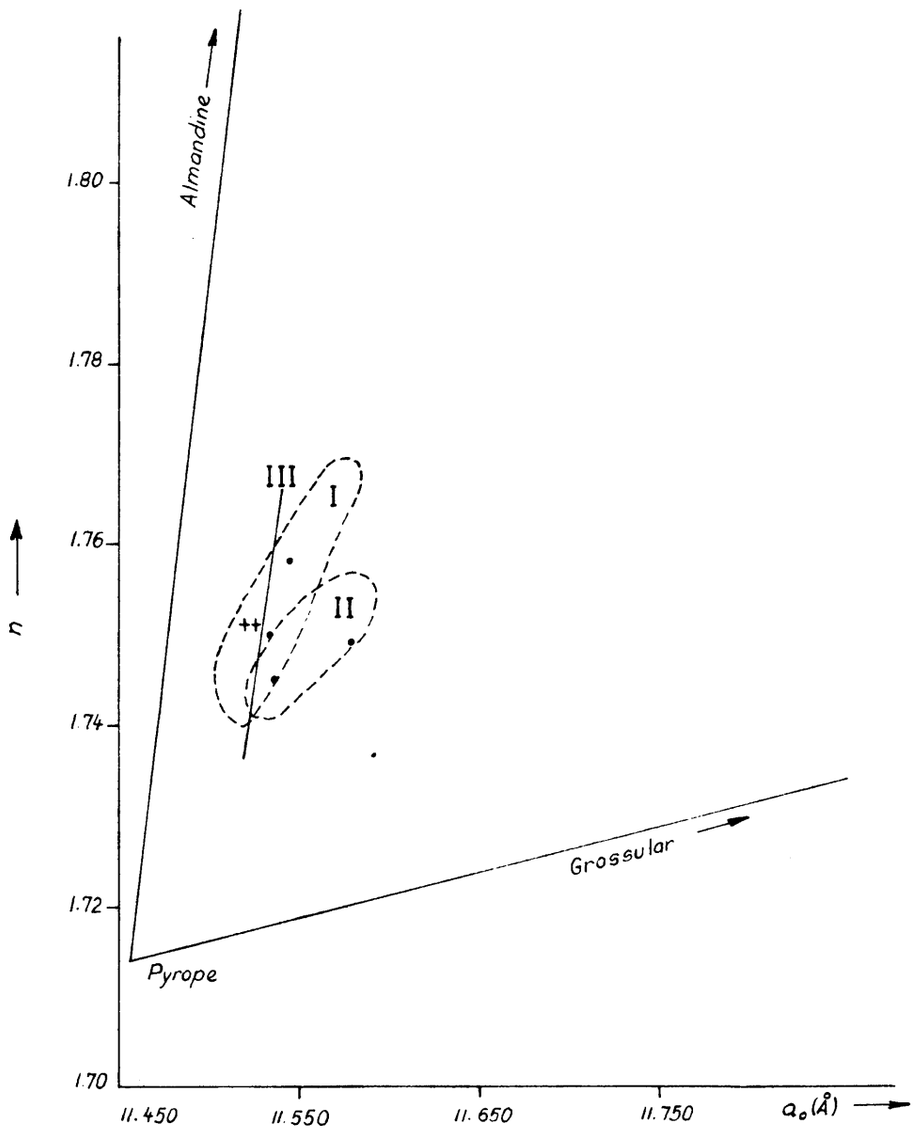

LEGEND

+	Group I Kimberlite
•	Carbonated Kimberlite + Western Kimberlite
I + II	Fields for the garnets from Ultramafic Nodules (P 97)
III	Line separating the garnets from the two types of Kimberlites

FIG. .

(e) Clinopyroxene

Clinopyroxene occurs in kimberlite both as disseminated grains and as a constituent of olivine - and/or garnet-bearing aggregates. The clinopyroxene is present as three morphological types which can readily be distinguished in hand specimens viz. a bright green, glassy type, a light green, soapy type and a dark brown, silky type. Despite the variation in the surface characteristics, these clinopyroxenes have the same mode of occurrence in the kimberlite.

The clinopyroxene phenocrysts in the fine-grained kimberlite matrix are subhedral and range in size from 0.26x0.13 mm to 4.0x3.0 cm. The absence of exsolution lamellae of orthopyroxene and the presence of zones are prominent features of the clinopyroxene. Exsolution lamellae of garnet parallel to (110) of the clinopyroxene were observed in the kimberlite of Monastry Mine (photo 10).

The clinopyroxene also reveals two types of intergrowths, viz. a myrmekitic intergrowth of clinopyroxene and spinel, and a myrmekitic intergrowth of clinopyroxene and ilmenite. The d-values obtained on the latter clinopyroxene correspond with those of the clinopyroxene from the kimberlite.

The clinopyroxene in the kimberlite is mostly altered to uralite, and the alteration is accompanied by the exsolution of rods and drops of magnetite. These rods and drops may produce a Schiller texture.

In table 12 the physical properties of the clinopyroxenes from the kimberlite from Premier Mine are listed, and in figure 9 the chemical composition as a function of the optical properties are represented after Hess (1949). Since the clinopyroxene in kimberlite contains an average of 2 per cent Al_2O_3 (Boyd, 1969), the variation diagram after Brown (1967, p. 120) could not be used. The data supplied by Sakata (1957, p. 165) indicate that a correction factor of at least 0.03 Å and 0.02 Å for b_o and c_o respectively is necessary for an alumina content of 2 per cent.

According to figure 9 the clinopyroxene from the western kimberlite contains less hedenbergite and more orthopyroxene in solid solution than the clinopyroxenes from the eastern kimberlite.

Table 12. The physical properties of the clinopyroxene from the different types of kimberlite from Premier Mine

Type of Kimberlite	Sample	n_β	$2V_\gamma$	a_o Å	b_o Å	C_o Å	β °	a Sin β
Group I	1060-22	1.680		9.457	8.893	5.185	75°37'	9.361
Group III (eastern kimberlite)	1010-40	1.694	57°					
Group III (western kimberlite)	1010-43A			9.490	8.858	5.188	74°58'	9.365
	1010-43B			9.489	8.876	5.198	75°5'	9.369
	1060-32	1.679		9.461	8.881	5.225	75°34'	9.362
	1010-8	1.694	50°					
	1060-26	1.679	54°					
	1010-9	1.681	59°					
	1010-44	1.670	60°					
	1060-29	1.680	53°					
	1060-22	1.680	54°					
	1010-8	1.697	53°	Augite inclusion.				
Group IV	1060-28	1.680		9.457	8.880	5.183	75°35'	9.359
	1060-30			9.456		5.011	75°20'	9.348
	1010-20	1.671						
	1010-22	1.694	58°					

The unit-cell dimensions were obtained by means of a Guinier Camera, CuKα radiation.

THE COMPOSITION OF THE CLINOPYROXENES FROM THE VARIOUS KIMBERLITES AFTER THE OPTICAL PROPERTIES

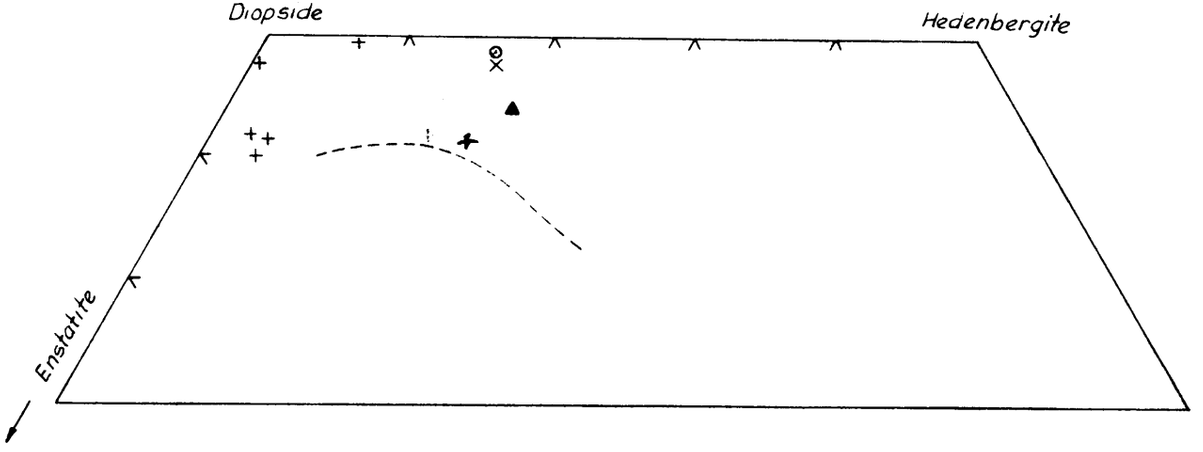

LEGEND

+ Clinopyroxene from the Western Kimberlite

× Clinopyroxene from the Eastern Kimberlite

⊙ Clinopyroxene from the Carbonated Western Kimberlite

▲ An Augite grain in the Western Kimberlite

---- Normal magmatic differentiation trend

FIG. 9

f. Chromite

Chromite is present in the kimberlite as a myrmekitic intergrowth of chromite and clinopyroxene, and as separate grains. The latter vary in colour from light to dark reddish-brown in transmitted light, and the colour depends on the amount of (Fe^{2+}, Mg^{2+}) and (Cr^{3+}, Al^{3+}) substitution Deer, Howie and Zussman (1967, p. 426). The individual grains are mostly rounded, and have an average diameter of 0.1 mm. Their rounded shape and manner of occurrence indicate that they belong to the primary phenocrystal phase.

2. The secondary phenocrystal phase

The minerals belonging to the secondary phenocrystal phase are disseminated in the residua phase and occur as idiomorphic grains with an average diameter of less than 0.3 mm. This phase crystallized rather late in the history of the kimberlite, but before the kimberlite was emplaced, because flow lines around these phenocrysts were observed in the massive basaltic kimberlites. Magnetite, sphene, perofskite, apatite, phlogopite and second generation olivine belong to this phase.

a. Magnetite

Many small, euhedral grains of disseminated magnetite (0.2 to 0.02 mm) occur in the residua phase of the kimberlite, and in places they are also concentrated along the periphery of olivine grains. Indistinct flow lines around magnetite are also evident in the massive kimberlites.

The magnetite is usually very fresh in polished sections, and exsolution lamellae of ulvite and hematite were not observed. Both the massive kimberlite and the micaceous kimberlite contain a larger percentage of magnetite than the kimberlite breccias, however, this may be due to the smaller amount of matrix material in the latter.

b. Perofskite

Small (0.1 to 0.5 mm), euhedral and subhedral phenocrysts of perofskite, of which many show complicated polysynthetic twinning, are disseminated in the residua phase of the kimberlite. Similar to the magnetite, the perofskite also constitutes an important part of the rims surrounding the olivine phenocrysts.

Some perofskite grains are rimmed by sphene, simulating the reaction rims around the ilmenite grains, and relicts of the latter often constitute the core of a perofskite grain. In all the kimberlites investigated the manner of occurrence of perofskite is identical. However, the perofskite content of the melilite basalts, massive kimberlites and micaceous kimberlites exceeds that in the kimberlite breccia.

c. Sphene

Sphene shows a variable mode of occurrence in the kimberlite, however, the only phenocrystal sphene is the euhedral and subhedral disseminations in the kimberlite, which are concentrated in the rims surrounding the olivine phenocrysts.

d. Apatite

Apatite is present in the kimberlite as large subhedral crystals, and as small euhedral grains. The former can be considered as a part of the phenocrystal phase, but the classification of the latter is doubtful.

However, the idiomorphism and the absence of inclusions in the apatite of the residua phase indicate that it should also be considered as phenocrystal material. The apatite is usually present as small, euhedral grains (0.08 mm), but larger subhedral grains (1.2x0.4 mm), which display a radial orientation have also been encountered.

The massive kimberlites are usually enriched in apatite, but in the kimberlite breccias apatite is very rare. The micaceous kimberlites have an apatite content between these extremes. The P_2O_5-content, which reflects the apatite content of the various types of kimberlites, is reported in table 13. This table shows a systematic increase in the P_2O_5-content from basaltic kimberlite, through micaceous kimberlite, melilite basalts, alnoiites and massive kimberlite to carbonatites.

e. Phlogopite

No fresh phlogopite was found in the Premier Mine kimberlite, but some hexagonal-shaped pseudomorphs of serpentine are present in the rims around olivine phenocrysts. These pseudomorphs may represent pre-existing phlogopite.

The subdivision by Williams (1932) into first - and second generation phlogopite can be applied to the kimberlites from Sovér and Monastry Mines. The first generation phlogopite probably belongs to the primary phenocrystal phase.

f. Zircon

According to Gerryts (1951) zircon is a prominent constituent of the Premier Mine kimberlite. However, only two zircon grains could be found in the 150 thin sections investigated, and both of them are considered to be derived from another source than the kimberlite. It appears as if Gerryts (1951) has mistaken sphene for zircon.

Table 13. The P_2O_5 content of the various kimberlites

Rock type	% P_2O_5	Reference
Basaltic kimberlite (P.M)	0.27	New analysis
Av. basaltic kimberlite[b]	0.72	Dawson (1967, p. 271)
Av. micaceous kimberlite[a]	0.66	ditto
Massive kimberlite (P.M)	1.14	New analysis
ditto (Benfontein)	3.66	Hawthorne (Personal communication)
Av. melilite basalt	1.69	Nockolds (Barth, 1962)
Av. alnoiite	2.38	ditto
Carbonatite (Malawi)	3.25	Garson (1965)
ditto	7.7	ditto

3. The residua phase of the kimberlite

a. Calcite

The petrological investigation of the calcite in the matrix of the kimberlite reveals the presence of primary and secondary calcite. Owing to the extensive alteration of the Premier Mine kimberlite the primary calcite cannot be recognized, but in the massive kimberlites the primary calcite is present as large anhedral grains which are intergranular to the serpentine. Optically this calcite is cloudy and is marked by the presence of many inclusions of phenocrystal material.

The secondary calcite occurs as euhedral and subhedral grains which formed in both the matrix and in the

phenocrystal phases. Optically this calcite is clear, and it seldom contains any inclusions of phenocrystal material.

b. Serpentine

A variety of serpentine minerals constitutes the largest portion of the Premier Mine kimberlite, whereas in the massive kimberlites serpentine is a less important constituent of the matrix. In a thin section of the Premier Mine kimberlite large fields of serpentine occupy the areas between the phenocrystal phases, and is often replaced by secondary calcite. The metamorphic minerals like amphibole, diopside and hydrogrossular were mainly formed in these serpentine masses.

In the micaceous kimberlites, the serpentine occurs as small (0.02 to 0.10 mm), rounded inclusions in the calcite, and has the habit of a former generation of olivine.

Both the flaky and fibrous serpentine and the massive green variety are present in the Premier Mine kimberlites. The flaky serpentine has the following optical properties, $n\alpha = 1.572$, $n\gamma = 1.576$ which compare favourably with antigorite. The fine-grained serpentine also alters to either a green chlorite, $n = 1.552$, or a bluish penninite $n\alpha = 1.559$; $n\gamma = 1.560$.

c. Diopside

The presence of diopside in the residua phase of kimberlite is only characteristic of Premier Mine, and its abundance increases with an increase in the grade of thermal metamorphism. In the melilite basalt from Spiegel River, diopside was also identified, but since the grains formed part of a trachytic texture, the diopside was considered as part of the phenocrystal phase. The diopside in the Premier Mine kimberlite occurs as porphyroblasts. The grains are small (0.01x0.04 mm), idioblastic and form aggregates of radially orientated grains surrounding cores of hydrogrossular. Diopside is also present as rims of radially orientated crystals surrounding the olivine phenocrysts. Along the edges of the masses of fibrous tremolite, small grains of diopside have formed, indicating that it formed at the expense of tremolite during metamorphism.

d. Biotite

Small anhedral grains (0.03 mm) of pleochroic biotite, which exhibit a decussate texture, occur in the matrix of the western kimberlite. The biotite occupies large fields between the primary phenocrysts, and in these fields secondary phenocrysts of magnetite, sphene and perofskite are embedded. The d-values of this biotite are listed in table 14.

In some areas it was observed that the biotite formed from a green chloritic material, remnants of which are still present, and occur as intergranular material with respect to some of the biotite grains. Gerryts (1951) identified the biotite as phlogopite, and consequently classified the rock as a micaceous kimberlite. However, this was evidently incorrect.

e. Hydrogrossular — garnet group $Ca_3Al_2(SiO_4)_3$

Hydrogrossular is one of the most prominent constituents in the Premier Mine kimberlite, and increases in abundance with an increase in the grade of thermal metamorphism. In the highly metamorphosed kimberlites the entire matrix is transformed into hydrogrossular. Apart from its presence in the Premier Mine kimberlites, this mineral was also encountered in the kimberlite breccias from Jagersfontein, Wesselton and Lesotho.

The hydrogrossular occurs as rims surrounding olivine phenocrysts, as cores around which diopside has formed, as individual grains in the serpentine matrix, and as an alteration product in inclusions of wall-rock material.

The grains of hydrogrossular are green in colour, xenomorphic, and slightly birefringent or isotropic. The grain size varies from 0.2 to 0.02 mm, and the physical properties are reported in table 15.

f. Amphibole

Amphibole was formed in the Premier Mine kimberlite as a consequence of thermal metamorphism, and depending on the grade of metamorphism it exhibits a variety of textures. In the zones of low grade metamorphism the amphibole is present as small idioblastic grains arranged in a decussate texture in the serpentine matrix. An increase in

Table 14. The d-values of biotite from Premier Mine, compared to those of phlogopite and biotite. (The d-values of the biotite from Premier Mine was obtained by means of a Debye Scherrer camera, using Cu Kα radiation.)

Biotite-1010-20 Film no. 419		Biotite ASTM 2-0045			Phlogopite ASTM 10-493		
I/I_c	d ^oA	I/I_1	d ^oA	h k l	I/I_1	d ^oA	h k l
		100	10.1	001	~100	10.13	002
					20	5.056	004
2	4.58	20	4.59	110,020	20	4.612	110,020
					8B	4.515	021
					6B	4.079	112
					20	3.814	023
					35	3.540	$11\bar{4}$
10	3.37	100	3.37	003	>100	3.362	006
					40	3.283	114
2	3.15	20	3.16	112	10	3.156	$11\bar{5}$
					40	3.040	025
1	2.91	20	2.92	$11\bar{3}$	10	2.926	115
					20	2.818	$11\bar{6}$
6	2.66	80	2.66	$20\bar{1}$,130	20B	2.651	$13\bar{1}$
					>100	2.624	116
3	2.51	40	2.52	004,113	30	2.522	008
6	2.45	80	2.45	201	40	2.439	133
					18B	2.361	117
					10B	2.304	220,040
		20	2.28	040,132	10B	2.270	$13\bar{5}$
6	2.18	80	2.18	-	45	2.180	135
					20	2.039	224
					65	2.017	0.0.10
8	2.00	80	2.00	-	20B	2.000	$13\bar{7}$
		20	1.91	-	6B	1.914	137
1	1.74	20	1.75	-	4B	1.751	139
					6B	1.737	227
6	1.68	80	1.67		45	1.677	153
6	1.54	80B	1.54*1)		50	1.538	330,060
					10B	1.521	062

*1) plus 5 lines.

the grade of metamorphism causes a mass of fibrous amphibole to form in the serpentine matrix. The optical properties of this amphibole are n_γ = 1.590-1.600; $\gamma \wedge c = 15^\circ$. In the zone where diopside becomes stable, large masses of coarse-grained porphyroblasts of amphibole are present.

Table 15. The physical properties of the hydrogrossular in the matrix of the Premier Mine kimberlite

Specimen	n (± 0.005)	a_o (± 0.005) *1)
1010-9	1.827	12.036
1010-43		11.950
1010-13		11.961

*1) The a_o value was obtained by means of a Debye Scherrer camera, using CuKα radiation

D. The Massive Basaltic Kimberlite at Premier Mine

1. Introduction

The carbonatite dykes comprise the group II-kimberlite from Premier Mine, and have been classified as massive basaltic kimberlites. Daly (1925) considered these rocks to be true magmatic carbonatites. However, both Gerryts (1951) and Verwoerd (1967) described them as veins of carbonated kimberlite.

Dykes which exhibit exactly the same mineralogy, petrology and manner of occurrence as the dykes in Premier Mine were encountered in the kimberlites of Jagersfontein, Wesselton and Dutoitspan. These dyke-rocks were very fresh, and hence a petrological investigation facilitated their classification. The Benfontein kimberlite is a similar rock, and has also been classified as massive basaltic kimberlite.

At least seven of these dykes have been mapped in the Premier Mine kimberlite. They vary considerably in dimensions, however, their manner of occurrence is remarkably consistent. The western kimberlite has been intruded by an extensive system of carbonatite veins which are all connected to a large north-south striking dyke.

The veins are variable in dimensions, and are arranged in a radial pattern. The individual veins occasionally traverse the contacts between the western and the group I-kimberlite, and peters out in the kimberlite both vertically and horizontally.

A zone of 15 m wide on both sides of the main dyke and of the veins exhibits the effects of metasomatism. This is especially evident in the black western kimberlite which has been bleached (group IV-kimberlite). The contact between the massive basaltic kimberlite and the bleached kimberlite is sharp. The strike and dip of both the main dyke and its branches vary considerably over short distances, but the dip is usually very close to 90°.

Two smaller dykes of massive basaltic kimberlite having a thickness of 1.0 to 1.5 m were encountered in the western kimberlite. The strike and dip of these veins also vary over short distances. These dykes, however, did not cause any metasomatic effects on the adjoining kimberlite. In the eastern kimberlite a very prominent dyke is present, which has a strike distance of over 200 m. It has an easterly dip which varies from 60° to 90°, but it changes considerably over short distances. This dyke has an average thickness of 2 m, and in the northern portion of the pipe it splits into two smaller dykes. The contact between the eastern kimberlite and the group I-kimberlite is cut by this dyke, which has not caused any metasomatic effects on the bordering kimberlite.

Several smaller dykes of massive basaltic kimberlite are also present in the Premier Mine kimberlite.

2. The Petrography of the massive basaltic kimberlites

The massive basaltic kimberlite from the dykes at Premier Mine varies considerably in colour, and black, blue, red, grey and khaki have been observed. However, mineralogically and petrologically they are very similar. They are composed of large, rounded blebs of serpentine, calcite and brucite in a matrix of calcite, sphene, perofskite, magnetite and serpentine. The massive basaltic kimberlite from Premier Mine is usually extensively altered, and consequently few of the original textures are evident.

In table 16 the volumetric composition of some of the massive kimberlites from Premier Mine are compared with that of some massive kimberlites mentioned earlier. The mineral assemblages depicted in table 16 show that the massive kimberlite from Premier Mine has been altered more extensively than the massive basaltic kimberlites from the Kimberley area, and that the sum of the serpentine and brucite of the former almost equals the olivine content of the latter. [illegible]

a. Calcite

In the massive kimberlite from Premier Mine calcite occurs as large rounded blebs, surrounded by rims of colourless serpentine which contains euhedral grains of magnetite, sphene and perofskite. These rims closely resemble those found around the olivine in the kimberlite breccias. Relicts of serpentine are often preserved in the calcite blebs, giving the impression that the calcite replaced the former serpentine grains.

In some of the less-altered material from Premier Mine large rounded blebs of serpentine, partly replaced by euhedral calcite, still persists. These serpentine grains are usually embedded in a fine-grained matrix of turbid calcite which contains inclusions of magnetite, sphene and perofskite. Hence it is clear that this fine-grained calcite is of primary origin, whereas the replacements are a secondary phase.

In the massive kimberlites from the Kimberley area, the olivine phenocrysts are embedded in a matrix of primary calcite. The latter also contains inclusions of sphene, magnetite and perofskite. In the melilite basalt from Spiegel River a calcite matrix similar to that of the massive kimberlites also contains abundant lath-shaped phenocrysts of melilite. Secondary veins, 0.2 to 3.0 mm wide, composed of euhedral, secondary calcite, have been encountered in most of the massive kimberlites.

Staining of the carbonate with Alizarine Red S (Holmes, 1930) revealed that the large blebs of carbonate, and the matrix of primary carbonate consist of a pure

Table 16. The Volumetric Composition of the Premier Mine massive kimberlite compared with that of other massive kimberlites

Specimen	1010-19	1010-21	Be_1	W5
Calcite	14.3	39.5	50.2	58.3
Serpentine	12.1	6.4		
Opaque minerals	47.6	10.9	15.7	23.9
Sphene and perofskite	4.0	11.0		
brucite	22.0	32.2		
olivine	-	-	34.1	17.8
Total	100.0	100.0	100.0	100.0

1010-19 and 1010-21 - Massive kimberlite from Premier Mine
Be 1 - Massive kimberlite from Benfontein
W5 - ditto from Wesselton

Table 17. The refractive indices of calcite from the massive kimberlite from Premier Mine

Sample	Mode of occurrence		n_ω	% Calcite*1)	% Dolomite*)
		(± 0.002)	(± 0.002)	± 2%	± 2%
1010-21	Rounded blebs	[illegible]	1.661	99	1
1010-19	ditto	[illegible]	1.659	100	0
1010-19	secondary vein	[illegible]	1.667	93	7

*1)
After Kennedy (1947, p. 561)

calcite, whereas the veins consist of a magnesium-bearing calcite. The refractive indices of these different types of calcites and their chemical compositions after Kennedy (1947) are given in table 17. In table 18 the d-values of the primary calcite of the matrix of 1010-19 are compared with the values for dolomite and calcite after Berry and Thompson (1962).

b. Olivine

No fresh olivine was found in the massive kimberlite from Premier Mine, however, the presence of serpentine and brucite suggests that olivine was originally present. The massive kimberlites from the Kimberley area contain appreciable quantities of euhedral phenocrysts of fresh olivine. Along the rims and in cracks of some of these olivine grains serpentine is developed, but the serpentinization has not destroyed the original euhedral shape of the olivine grains. A yellow to brownish, highly birefringent alteration product formed around some of the olivine grains, and was identified as iddingsite. In the massive kimberlite of Dutoitspan the resorbed outlines of some of the olivine grains, and the fine-grained olivine which constitutes a single phenocryst (photo 11) suggest that the olivine was recrystallized. Some olivine phenocrysts from this kimberlite were apparently melted and small xenomorphic olivine grains, which crystallized from the melt, occur in a brownish glass (photo 12).

In both the massive kimberlites from Wesselton and Benfontein the olivine phenocrysts are arranged in flow lines, indicating that these intratelluric phases were orientated during the intrusion of the magma. The physical properties of the olivine from both the massive kimberlites and the melilite basalt from Spiegel River are compared in table 19. The forsterite content has been determined according to Tröger (1959, p. 37) and Yoder and Sahama (1957, p. 666), from the optical properties and the d-values respectively.

e. Brucite

Brucite only occurs in the massive kimberlite from Premier Mine, and probably formed as a consequence of the decomposition of

Table 18. The d-values of calcite from 1010-19, compared to those of calcite and dolomite, after Berry and Thompson (1962, p 217 and 218) respectively. The d-values were obtained by means of a Guinier Camera, using Cu Kα radiation).

1010-19 Film no. 423		Calcite			Dolomite	
I/Io	d°A	h k l	I/Io	d°A	I/Io	d°A
		101			1	4.02
4	3.845	012	3	3.85	2	3.69
10	3.024	104	10	3.05	10	2.88
		006	2	2.85	3	2.67
		015			2	2.54
5	2.487	110	4	2.51	3	2.40
5	2.277	113	5	2.29	5	2.19
		021			1	2.07
6	2.091	202	5	2.10	4	2.01
6	1.924	024	7	1.922	1	1.845
1	1.908	018			6	1.801
7	1.872	116	6	1.877	6	1.784
1	1.620	211	1	1.631	1	1.568
4	1.599	122	4	1.608	3	1.544
		10.10	½	1.590	1	1.497
3	1.522	214	3	1.528	2	1.465
		208)	1	1.514	(1	1.441
		119)			(1	1.429
		125	1	1.480	0.5	1.410
3	1.437	300	3	1.447*1)	3	1.389*2)

*1) plus 29 lines
*2) plus 24 lines

olivine. The brucite is present as small (0.08 to 0.50 mm), subhedral to rounded grains in the rims of serpentine, surrounding the large blebs of calcite. Some of the grains have a hexagonal outline and display a zonal arrangement of inclusions, consisting of a core rich in magnetite and perofskite and an outer rim which is clouded by small inclusions of opaque minerals. The brucite has an anomalous low birefringence, n = 1.590 (± 0.010) and exhibits the following colours when stained. The brucite stains violet to purple with alizarine red, green with malachite green and brown with $AgNO_3$ (Holmes, 1930). According to Holmes (1930) these stains are diagnostic for brucite. The d-values of an impure sample of brucite are listed in table 20. These values indicate that this material is brucite, and not colloidal magnesiumhydroxide as was suggested by Gerryts (1951).

(d) Serpentine

Serpentine occurs in the massive kimberlite as anhedral to rounded grains, which are partly replaced by euhedral calcite. These serpentine grains resemble the original olivine phenocrysts which were encountered in the unaltered massive kimberlites. The individual, rounded grains are often zoned, and may also display an hour-glass texture. The intergranular serpentine which forms the rims around the calcite blebs is usually clouded with inclusions of magnetite, sphene and perofskite.

The serpentine is light green to colourless in thin section and massive; the flaky and fibrous types were never encountered.

e. Magnetite

The magnetite, being more resistant than any of the other constituents, has survived the alteration process, and exhibits the same textural features in the massive kimberlite from Premier Mine as in the massive kimberlite from the Kimberley area. The magnetite occurs as small euhedral phenocrysts in the residua phase of these massive kimberlites, and are arranged to show a flow-line texture.

The magnetite grains are zoned and have a core with a lower reflectivity than the outer rim. This increase in

Table 19. The ~~physical properties~~ d_{130} and optical values and the composition of the olivine from the massive kimberlite and melilite basalts, after Tröger (1959) and Yoder and Sahama (1957) respectively

Sample	Optical data					x-ray data	
	2V(± 1°)	n_α	n_β	n_γ	% Fo	d130	% Fo
Benfontein No. 1	+ 89°	1.653	1.672	1.681	90	2.770	94
Benfontein No. 2	+ 89°	-	-	-	90		
Dutoitspan No. 2	90°	-	-	-	88		
Wesselton No. 5	+ 87°	1.650	1.672	1.681	93	2.770	94
Melilite basalt	- 85°	-	-	-	79		
Alkaline basalt	- 89°				89		

Table 20. The d-values of brucite from the massive kimberlite from Premier Mine. (The d-values were obtained by means of a Guinier camera, using Cu Kα radiation)

1010-19 Film no. 415		Brucite ASTM 7-239		
I/Io	d °A	I/I_1	d °A	h k l
10	4.751	90	4.77	001
		6	2.725	100
10	2.364	100	2.365	101
5	1.787	55	1.794	102
4	1.569	35	1.573	110
2	1.490	18	1.494	111
2	1.376	16	1.373	103
		2	1.363	200
1	1.312	12	1.310*1)	201

*1) plus 17 lines.

reflectivity is probably due to an increase in the Fe^{2+}-content of the magnetite which suggests that the magma became increasingly enriched in iron during crystallization of olivine and magnetite.

Exsolution lamellae of ilmenite and ulvite are absent in this magnetite, and consequently the TiO_2 in the magnetite ~~must~~ is assumed to be in solid solution. According to the chemical analyses after Verwoerd (1967) and Smirnov (1959) the TiO_2 content in the magnetites from kimberlite and carbonatite is not very high (less than 5 per cent). According to Marmo (1959) the TiO_2 content of the magnetite can be used as a geothermometer.

The a_o values and the ulvite contents of the magnetites, after Lindsley (1965) for the magnetites from the massive-basaltic kimberlites and carbonatites are listed in table 21.

f. Sphene and Perofskite

Sphene and perofskite are abundant in the massive kimberlites and in the melilite basalt from Spiegel River. They are present as small (0.05 to 0.21 mm) euhedral to subhedral grains in the primary calcite matrix as well as in the serpentine rims in the altered massive kimberlite from Premier Mine. A reaction relationship between sphene and perofskite was observed, and perofskite is often included in the sphene grains. Ilmenite is absent in these kimberlites. However, in the massive kimberlite from Dutoitspan, grains of ilmenite which are intensively altered along the periphery to perofskite have been observed (photo 13). The absence of ilmenite in these rocks can thus be explained by the abundance of sphene and perofskite.

g. Apatite

Apatite occurs as euhedral grains in the matrix of primary calcite. It is of rare occurrence in the massive kimberlite from Premier Mine. However, approximately 30 per cent of the matrix of the massive kimberlite of Benfontein is composed of apatite.

Table 21. The a_o values of magnetite from various rock types and the content of ulvite in solid solution after Lindsley (1965). The a_o-values were determined by means of a Guinier Camera, using Cu Kα radiation

Section	a_o (°A)	% Ulvite $_{ss}$	Rock-type
1210-1	8.372	1%	Massive kimberlite . P.M.
1210-16	8.393	5	ditto
1010-19	8.380	2	ditto
1010-45	8.379	2	ditto
Der 1	8.388	3	Carbonatite Derdepoort
Twe 1	8.379	2	" Twee Rivier
Salt 1	8.376	1	" Saltpan

h. Melilite.

Melilite is very susceptible to alteration, consequently its presence in the massive kimberlite from Premier Mine is unlikely. In the Benfontein kimberlite many lath-shaped pseudomorphs of calcite after melilite are arranged in a "criss cross" texture (photo 14) very similar to the textures described by Watson (1967, p. 315) for the kimberlites from Canada. The melilite phenocrysts in the melilite basalt from Spiegel River are also lath-shaped, and display the same texture (photo 15).

According to Von Eckermann (1967, p. 305) the Swedish kimberlites also contain lath-shaped phenocrysts of melilite, which display the same textural features as those described from Benfontein.

From the discussion presented on the kimberlite breccia and the massive basaltic kimberlite it is clear that these two rock types differ only in the presence of primary phenocrystal material in the kimberlite breccia. Hence, it is evident that the massive kimberlite represents the matrix phase of the kimberlite breccia, as was defined on page 27., and should be considered as the solidified equivalent of the kimberlite magma, after the volatile constituents have escaped.

3. Inclusions of wall-rock in the massive kimberlites

None of the massive kimberlites contains significant amounts of wall-rock xenoliths. About 30 per cent of the thin sections show the presence of small inclusions of serpentinized wall-rock, and in the massive kimberlite from Premier Mine the inclusions of wall-rock are even less abundant.

An inclusion resembling a possible pre-existing garnet grain was observed in 1010-19. This xenolith consists of an outer rim of magnetite and calcite, and is succeeded by successive rims consisting of serpentine and calcite, serpentine, magnetite and finally a core of calcite, veined by serpentine. Although fresh garnet is absent in this kimberlite, this inclusion exhibits the textural phenomena of an original garnet inclusion.

4. The metamorphism of the massive kimberlites

The massive kimberlite dykes have been metamorphosed by the tholeiitic sill which is intrusive into the Premier Mine kimberlite. The metamorphosed basaltic kimberlite consists of large porphyroblasts of amphibole and diopside which are embedded in a matrix of serpentine and amphibole. The sphene and magnetite have survived the effects of thermal metamorphism and occur as idiomorphic grains in both the amphibole and diopside.

The original porphyritic texture of the massive kimberlite is destroyed by the metamorphism, but the kimberlite breccia, which has been metamorphosed in the same facies, still reveals the original kimberlitic texture. A thin section cut across the contact (photo 16) indicates that although the kimberlite has been carbonated, the contact between the massive kimberlite and the kimberlite breccia is sharp.

VI. THE PETROLOGY OF THE INCLUSIONS OF WALL-ROCK IN THE PREMIER MINE KIMBERLITE

A. Inclusions of Carbonate

From figure 1 it is clear that the Premier Mine kimberlite must have cut through the Dolomite Series, and consequently it is likely that the carbonate inclusions have been derived from this source. The inclusions are

usually metamorphosed, and those in the meta-kimberlite have been subjected to polymetamorphism, hence the metamorphic influences of the kimberlite are obliterated. Since the metamorphic effects of the kimberlite on the wall-rock inclusions are important geothermometers, only the inclusions in unmetamorphosed kimberlites have been studied, in order to determine the temperature of intrusion of the kimberlite.

Two types of nodules, viz. a diopside-fels and a garnet-diopside-fels could be identified. All the xenoliths are rounded to elipsoidal in shape and vary in size from 0.51x0.30 mm to 10.0x4.0 cm. The carbonate inclusions are evenly distributed throughout the kimberlite, but it appears as if the western kimberlite is enriched in these nodules relative to the other types. This may be due to the fact that they would be more conspicuous in the black kimberlite.

(1) The Inclusions of diopside-fels have a granulitic texture and consist of small (0.13x0.07), xenoblastic grains of diopside and sporadic garnet in a matrix of colourless serpentine. The mineralogy indicates that these xenoliths represent a silica-bearing dolomite which has been metamorphosed in the hornblende-hornfels facies. According to Winkler (1967, p 46) the lower boundary of this facies is 535°C at 1 kb pressure and 520°C at 0.5 kb.

2. The Inclusions of garnet-diopside-fels

These inclusions are zoned and show a remarkable consistency in the succession of monomineralic zones, viz.; from the periphery to the centre of the inclusions they consist of the following minerals; hydrogrossular, diopside, grossular, tremolite and serpentine.

The hydrogrossular zone which forms an outer rim approximately 0.1 mm wide, consists of green xenoblastic hydrogrossular, crowded with small inclusions of opaque minerals, whereas the grossular of the inner zone is coarser-grained, colourless, idioblastic and free from inclusions. The unit-cell dimensions of these two types of garnet are given in table 22.

In the diopside zone, the clinopyroxene grains are small, idioblastic, and are radially orientated towards the

centre of the inclusion. The diopside is colourless with $\wedge c = 40^{\circ}$. The d-values are reported in table 34, No. 1010 - 22 B_2

The brownish tremolite, which alters to diopside along the outer periphery constitutes the tremolite zone, and displays the same radial texture, described for the diopside zone. The core of these inclusions consists of a massive green variety of serpentine and of the flaky antigorite, described previously. The presence of small xenoblastic grains of magnetite, chalcopyrite and chalcosite and of large idioblastic grains of calcite which replace the massive serpentine, is characteristic of this zone.

The data presented indicate that no equilibrium exists in these nodules, and hence the facies classification is inapplicable. Since the petrological data indicate that the kimberlite pipes formed within a short time-interval, this lack of equilibrium can be explained quite readily. The coescistance of diopside and grossular in these inclusions, can be considered to represent the highest temperature at which they have been metamorphosed. According to Winkler (1967, p. 64-79) this indicates a temperature of 520°C to 540°C for a pressure of 0.5 to 2.0 kb respectively.

B. Inclusions of Kimberlite

Inclusions of an older kimberlite have been observed in all the different types of kimberlite from Premier Mine. The inclusions are rounded to elipsoidal in shape, and vary from 5.0x3.0 mm to 1.0 cm x 6.0 mm in size. In thin section these inclusions could be distinguished owing to differences in colour and texture compared to the host kimberlite. The mineralogy of these inclusions is identical to that of the host kimberlite, except that the latter is less altered.

First- and second generation olivine, as well as ilmenite, clinopyroxene and garnet surrounded by kelyphyte occur in these inclusions, and the matrix also contains secondary phenocrysts of sphene, perofskite and magnetite in a residua phase of serpentine, talc, chlorite, calcite, amphibole and diopside. Carbonate, shale, and syenite inclusions have also been observed in these xenoliths of older kimberlite.

Table 22. The a_o(Å) values of the garnets in the carbonate inclusions. The a_o-values were determined by means of a Debye Scherrer Camera, using Cu Kα radiation

Specimen	a_o(Å) (± 0.005)	Type of garnet
1010-12	12.028	hydrogrossular
1010-14	12.010	ditto
1010-8	11.981	grossular

Since the eastern and western kimberlites have intruded into the group I-kimberlite, the presence of inclusions of older kimberlite in this case can be explained. However it is difficult to explain the presence of kimberlite inclusions in the group I-kimberlite. These xenoliths may have been derived from a pre-existing phase of kimberlite, which did not reach the surface or they may represent ejected fragments of kimberlite which were re-enclosed in the kimberlite magma. The latter explanation requires a semi-solid "magma" of kimberlite which contains an active gaseous phase. The presence of xenoliths derived from the wall-rock near the surface in these inclusions of kimberlite indicates that they could not have been derived from a pre-existing kimberlite phase, and consequently they have to be considered as ejected fragments of kimberlite which became re-enclosed in the semi-solid "magma".

c. Diabase Inclusions

The diabase inclusions are rounded to elipsoidal in shape, and of variable dimensions. The cumulus orthopyroxene is altered to uralite or talc, and the intercumulus feldspar is altered to epidote and a brownish serpentine (n = 1.579) with d-values similar to those of amesite. Small euhedral grains of apatite as well as magnetite, which is extensively altered to hematite and which contains exsolution lamellae of ilmenite, occur in this brownish amesite. Both the cumulus and intercumulus clinopyroxene have the following optical properties,

$2V_{\alpha}$ = 58°, $\gamma \wedge c$ = 37°, n_{α} = 1.662, n_{β} = 1.670 and n_{γ} = 1.687. The clinopyroxene is altered to uralite, biotite and garnet. The garnet in the core of the pre-existing clinopyroxene belongs to the andradite-grossularite series (n = 1.861; a_o = 12.04 °A) whereas the garnet which formed along the rims consists of hydrogrossular.

Sporadic grains of idiomorphic calcite were formed in these inclusions, and porphyroblasts of amphibole, epidote, hydrogrossular and diopside have been encountered. The mineralogy thus indicates that these inclusions are in a state of disequilibrium, but the presence of uralite, diopside, amphibole, epidote and amesite indicates that the hornblende-hornfels facies prevailed.

D. Syenite Inlcusions

The syenite inclusions vary in size from 0.5x0.4 mm to several meters in diameter, and consist mainly of clinopyroxene, alkali-amphibole, sphene, apatite, serpentine and opaque oxides. The volumetric compositions of some of these inclusions are compared in table 23.

The clinopyroxene occurs as small (0.19x0.04 to 1.28x0.14 mm) subhedral grains, which are often altered to biotite. The optical properties of the clinopyroxene are: $2V_{\gamma}$ = 54° to 58°; $\gamma \wedge c$ = 43°; n_{α} = 1.675; n_{β} = 1.687 and n_{γ} = 1.696. The original [illegible] texture is still very evident in these inclusions. Biotite which formed from the clinopyroxene occurs as small (0.14 mm), xenoblastic porphyroblasts, and have the following optical properties: $2V_{\alpha}$ = 20°; n_{α} = 1.594; n_{β} = 1.644; n_{γ} = 1.646. The alkali-amphibole has a grain size of 0.6x0.4 mm, and is present in both the serpentine, and around the edges of the clinopyroxene grains. The amphibole is pleochroic from blueish-green to yellowish green, [illegible]

The euhedral sphene varies in size from 0.64x0.38 mm to 0.05x0.02 mm, has $2V_{\gamma}$ = 28° and occurs as inclusions in the serpentine. The euhedral apatite crystals (0.06 mm) are embedded in the biotite and the serpentine, and are present in large concentrations in the syenite

inclusions. The magnetite grains range in size from 0.03x0.01 to 0.90x0.38 mm and display alteration rims of hematite and exsolution lamellae of ilmenite parallel to (111) of magnetite. Exsolution lamellae of ilmenite parallel to (100) of magnetite which represents pseudomorphs after ulvite (Willemse, 1969) have also been encountered.

The fine-grained serpentine in the matrix of the inclusion has n max = 1.535, n min = 1.528 and the same d-values as amesite. The amesite still shows the original subophitic intergrowth which usually characterizes the unaltered syenite. The origin of these inclusions can be ascribed to either the post-Waterberg syenite dykes or to the syenite which constitutes the lower portion of the felsite sheet (Visser 1961). Since no syenite dyke is known from the immediate vicinity of the kimberlite intrusion, the latter explanation is more likely.

E. Inclusions of Shale

Many angular and rounded inclusions of metamorphosed shale are present in the Premier Mine kimberlite. They consist of small, anhedral porphyroblasts of biotite, diopside, magnetite, chlorite, calcite, tremolite and hydrogrossular. These xenoliths are often zoned, and show succeeding zones of hydrogrossular, diopside and tremolite from the rims to the cores. In some cases the original sedimentary layering is preserved and may even be accentuated by the thermal metamorphism, by the development of monomineralic layers.

The source of these inclusions appears to be the shale horizons of the Pretoria Series, and the metamorphism belongs to the hornblende-hornfels facies.

F. The Inclusions of Waterberg Quartzite

The inclusions of Waterberg quartzite and Waterberg conglomerate are the most abundant wall-rock xenoliths, and are confined to the group I-kimberlite. These inclusions have been observed on the 520 m level, which indicates that they have sunk for at least 520 meters in the kimberlitic magma.

Table 23. The volumetric composition of syenite inclusions in the western kimberlite

Sample	1010-44	Ti 1	1010 IN_4
Clinopyroxene	34.7	45.0	36.2
Amesite	30.1	15.7	26.9
Opaque minerals	5.9	11.0	24.3
Biotite	11.7*1	9.8	9.7
Apatite	3.8	3.4	0.6
Alkali amphibole	-	0.5	-
Sphene	13.8	14.6	2.3
Total	100.0	100.0	100.0

*1 Including alkali-amphibole

Quartz, feldspar and clay minerals are the principal constituents of these nodules (table 24). The quartz grains are rounded and vary in size from 0.5 mm to 1.50 mm. The feldspar grains are also rounded and have an average diameter of 1.0 mm, and are usually altered to sericite, chlorite and kaolinite. Roundish areas in which optically continuous quartz grains are embedded in a fine grained clay matrix, which may represent fragments of former granophyre, have also been encountered in these inclusions.

VII. THE PETROLOGY OF ULTRAMAFIC NODULES IN KIMBERLITE

A. Introduction

Basically two distinct rock-types occur as inclusions in kimberlite, and both types are found at Premier Mine. These nodules consist of ultramafic rocks of which olivine and orthopyroxene are the major constituents, and eclogite which is composed of garnet and clinopyroxene. At Premier Mine the former is very abundant, whereas only one nodule of eclogite has been recorded by Wagner (1911). The ratio of ultramafic to eclogite xenoliths is variable in other kimberlites, e.g. at Roberts Victor, Lovedale and Brakfontein, eclogite predominates, and in the kimberlites of Kimberley, Lesotho and Pretoria the ultramafic inclusions predominate.

Table 24. The volumetric composition of the inclusions of Waterberg quartzite in the Premier Mine kimberlite

Sample	1010-32	1060-19
Quartz	59.1	47.0
Feldspar	10.7	14.3
Matrix	30.2	38.7
Total	100.0	100.0

Similar ultramafic and eclogitic xenoliths are known from alkaline basalts. Eclogite has also been recorded in the nephelinite series at Hawaii (Yoder and Tilley, 1962), in the alkaline lavas in Tanzania and Uganda (Saggerson, 1968), and in the kimberlite breccias in Australia (Mason, 1968); New Zealand (Dicky, 1968) and Arizona (Watson and Morton, 1969). Ultramafic nodules are more abundant in alkaline lavas and have been found in the nephelinites at Hawaii (Jackson, 1968), the alkaline basalts from Japan (Kuno, 1967), the alkaline basalts from France and Germany (Frechen 1963; Ernst, 1935) and from many other occurences. Petrologically similar ultramafic rocks are known from Norway, Germany, South Africa and Rhodesia, but these ultramafic rocks occur as lenses in highly folded basement gneisses. The "alpino-type" peridotites from Turkey, Cuba and Cyprus also consist of ultramafic rocks which are petrographically similar to the nodules in kimberlite.

B. The ultramafic Nodules

1 Introduction

Three types of ultramafic nodules are present in kimberlite and at Premier Mine representatives of each have been encountered, viz. garnet peridotite, spinel peridotite and pyroxenite. In hand specimens the garnet peridotite consists of large orthopyroxene and garnet grains in a dense olivine matrix. The spinel peridotites are identical except for the absence of garnet and the presence of spinel. The pyroxenite nodules consist of cumulus orthopyroxene and often garnet in an intercumulus matrix of olivine and clinopyroxene.

These nodules vary in size from less than 1 cm to over 40 cm in diameter; they are rounded to ellipsoidal in shape, and often flattened into disc-shaped nodules. The outer surfaces are smooth and polished when found in situ, however, they display rough surfaces when found on the waste dumps, owing to differential weathering of the components.

Nodules occur only in the western kimberlite at Premier Mine, and according to Gerryts (1951) the levels closer to the surface contained more nodules than the levels exposed at present. During the present investigation it was observed that there is an abundance of nodules on the 298 m level, some on the 353 m level and only occassional ones on the 487 m level. The nodules occur as a heap of unorientated boulders which display neither grading nor flow lines. They are concentrated in the northern rim of the western kimberlite, and only isolated nodules were found in the southern rim of this kimberlite.

2. The petrology of the ultramafic xenoliths

A section through an ultramafic nodule found in situ reveals a zone of alteration, which varies in thickness from 4.5 cm to 0.5 cm, with an average of 3.0 cm. For obvious reasons the nodules collected from the waste dumps did not have any alteration rims.

Although the olivine and orthopyroxene have suffered alteration, the original texture of the ultramafic nodules is still preserved in these alteration rims. The garnet and the sporadical clinopyroxene grains have resisted the alteration.

The original, large subhedral grains of orthopyroxene are replaced pseudomorphously by a green talc which has a high birefringence, straight extinction and the optical properties reported in table 25. This talc yielded a very poor X-ray diffraction pattern. However, in table 26 the d-values recorded both with a Debye Scherrer camera and with a diffractometer are listed. The diffractometer charts of 893 In_5 and 893 In_6 also revealed prominent calcite lines, indicating the effect of the replacement of talc by secondary calcite. A D.T.A. recording of this material also yielded the peaks which are characteristic for talc.

Table 25. The optical properties of the talc, replacing the orthopyroxene in the alteration rims of the ultramafic nodules

Sample	2V	$n_{\alpha'}$	n_{β}	n_{γ}
893 I	12°	1.550	1.562	1.571
893 I		1.549	1.560	1.571
893 I	17-21°	1.542	1.562	1.570
893 I		1.546	1.565	1.570
893 I	48°	1.551	1.565	1.570
893 I		1.548	1.561	1.570
893 I	22°	1.538		1.566

The kink banding, undulatory extinction, and recrystallization phenomena which characterize the original orthopyroxene grains, are preserved. Relicts of orthopyroxene are present in the replacements, which are also traversed by veins of colourless serpentine. Euhedral calcite grains are also prominent in these talc pseudomorphs.

Although the olivine has been transformed into a variety of alteration products in the zones of alteration around the ultramafic nodules, the original textures, which were observed in the unaltered portions of these nodules, are still preserved. The meshwork of colourless serpentine is also mostly still preserved in these rims of alteration. The alteration products which formed as a consequence of the alteration of the olivine include a greenish talc with the following optical properties, $2V_{\alpha} = 33°$, n max = 1.565; n min 1.539 and $n_{\gamma} - n_{\alpha} = 0.016$. The grains close to the surface are more extensively altered, and a dark coloured fibrous serpentine replaces the talc. The optical properties of this fibrous serpentine are $n'_{\alpha} = 1.546$, and $n_{\gamma} = 1.551$, and it was identified as antigorite.

According to the d-values, the meshwork serpentine between the olivine grains consists of a mixture of antigorite and lizardite (table 27). The refractive

Table 26. The d-values of talc, compared to those of the talc, which replaces the orthopyroxene in the alteration rims of the ultramafic nodules. (The d-values of sample 893 In_2 have been obtained by means of a Guinier camera, using Cu Kα radiation, and the d-values of 893 In_5 and $_6$ have been obtained by means of a diffractometer, using Co K radiation.)

Co K_α +

893 In_2 Film no. 430		893 In_5 431		893 In_6 432		Talc ASTM 13.558		
I/Io	d ^oA	I/Io	d ^oA	I/Io	d ^oA	I/I_1	d ^oA	h k l
						100	9.34	002
10	4.65	6	4.62	6	4.60	90	4.66	004
10	4.547					30	4.55	020,11$\bar{1}$
						4	3.510	11$\bar{4}$
						1	3.430	113
8	3.148	10	3.14	10	3.13	100	3.116	006
						1	2.892	025
						12	2.629	20$\bar{2}$
4	2.601					30	2.595	13$\bar{2}$
10	2.504	5	2.49	4	2.50	65	2.476	132,20$\bar{4}$
						16	2.335	008
						20	2.212	134
½	2.196					10	2.196	20$\bar{6}$
½	2.127					8	2.122	204
½	1.996					20	2.103	13$\bar{6}$
½	1.916					6B	1.930	136
						40	1.870	0.0.10
½	1.731					-	1.725	24$\bar{2}$
2	1.667					20B	1.682	24$\bar{4}$,138
3	1.559					20	1.557	0.0.12
8	1.532					40	1.527*	060,33$\bar{2}$

* plus 9 lines.

Table 27. The d-values of the meshwork serpentine in the ultramafic inclusions, and those of antigorite and lizardite. (The d-values of the serpentine have been obtained by means of a Guinier camera using Cu Kα radiation

1010 In Film no. 434		Antigorite ASTM 7.417			lizardite *1)	
I/Io	d °A	I/I_1	d °A	h k l	I/Io	d °A
7	4.596	8	4.62*2)	020	15	4.55
		4	4.27	910		
3	3.879	6	4.01	$81\bar{1}$	5	3.91
10	3.648	300	3.63	$102,10\bar{2}$	60	3.65
		25	3.51	202,302		
1	2.965	2	2.88	$14.\bar{0}.1$		
4	2.654	4	2.59	930		
		8	2.57	17.0.0		
8	2.525	70	2.52	16.0.1		
4	2.492				35	2.499
2	2.454	10	2.46	$93\bar{1}$	20	2.447
2	2.425	40	2.42	18.0.0,003		
		10	2.39	17.0.1		
		6	2.35	403?		
		6	2.237	15.0.2		
		8	2.208	$16.0.\bar{2}$		
		20	2.167	$83\bar{2}$		
4	2.146	20	2.150	16.0.2	15	2.145
2	2.095	4	2.126	$93\bar{2}$		
		4	2.035	$11.3.\bar{2}$		
		4	1.886	$15.0.\bar{3}$		
		12	1.830	15.0.3		
		25	1.815	004		
3	1.791	14	1.781	$93\bar{3}$	5	1.789
1	1.748	4	1.755	$10.3.\bar{3}$		
2	1.738	10	1.736	17.0.3		
1	1.711	2	1.688	21.3.1		
1	1.614	2	1.640	22.3.1		
		4	1.584*3)	$14.0.\bar{4}$		

*1) d-values after Montoya, J.W. and G.S. Baur, (Amer. Min. 1963; p 1232)
*2) plus 7 more lines
*3) plus 14 more lines

indices of three specimens of this serpentine are compared to those of antigorite and lizardite, after Deer, Howie and Zussman (1967, p. 242), in table 28. The correspondence of the determined refractive indices with those of antigorite and lizardite shows that these two minerals constitutes the meshwork serpentine.

On the outer surface of the nodules the mixture of antigorite and lizardite is altered to a blue chlorite having $n = 1.566$, showing d-values similar to those of penninite. In these outer rims of the ultramafic nodules biotite is also present which has $2V_{\alpha} = 13^{\circ}$ to 25°, $n_{\alpha} = 1.578$, $n_{\beta} = 1.610$ and $n_{\gamma} = 1.611$. The peridotite nodules from Riverton consisted almost entirely of a similar biotite.

Close to the fresh portions of the nodules, the relicts of olivine are surrounded by a brown, highly birefringent alteration product, which was identified as iddingsite.

The presence of the meshwork serpentine accompanied by fresh olivine, and of the alteration zones around the outer rims of the ultramafic inclusions, indicates that two phases of alteration have been induced on the ultramafic nodules, namely the primary phase which caused the meshwork serpentine to form, and a secondary phase during which talc, serpentine and penninite were developed. The presence of alteration rims around the nodules found in situ and their absence in the specimens collected on the waste dumps invalidates the idea of weathering as an agent of alteration.

Regarding the stability regions of the minerals under consideration, the experimental work by Bowen and Tuttle (1949, p. 439), Roy and Roy (1957, p. 574) and Pistorius (1963) indicates that the transformation of serpentine to olivine takes place at 500°C, whereas the transformation of talc to forsterite and enstatite takes place at 700°C and 800°C respectively, depending on the prevailing pressure. Since the meshwork of serpentine is never altered to either olivine or talc, it is clear that these nodules were not metamorphosed at temperatures exceeding 500°C in an environment enriched in water. According to the phase diagrams mentioned talc would form as

Table 28. The refractive indices of the meshwork serpentine, antigorite and lizardite after Deer, Howie and Zussman (1967, p. 242)

Specimen	n_α (± 0.003)	n_γ (± 0.003)
1010 In_5	1.567	1.571
1010 In_4	1.559	1.568
Antigorite	(1.558	1.562
	(1.567	1.574
Lizardite	(1.538	1.546
	(1.554	1.560
1010 In_5	1.539	1.546

a stable phase at or below this temperature from both olivine and enstatite. Serpentine would also be stable at this temperature and would form at the expense of olivine. Hence these alteration rims could have formed in an environment enriched in water at or below 500°C, from would represent the conditions in the kimberlite magma during intrusion fairly closely.

According to Roy and Roy (1957, p. 574) the temperature at which serpentine transforms to forsterite, talc and vapour is not affected by pressure, however, Pistorius (1963) indicates that the temperature increases with an increase in pressure. Consequently the meshwork serpentine could have formed at even higher temperatures and pressures.

In table 29 the volumetric composition of the three types of ultramafic nodules found at Premier Mine is compared with the volumetric composition of some eclogite nodules. Since the former are coarse-grained, these determinations have been carried out on at least 5 thin sections for each nodule.

According to the volumetric compositions of the ultramafic nodules it is evident and table 29 that these nodules consist of orthopyroxene, clinopyroxene, olivine, garnet and a clinopyroxene chrome-spinel intergrowth. Table 29 indicates that the clinopyroxene content in the

Table 29. The volumetric composition of eclogite and ultramafic nodules from kimberlite and kimberlitic-breccias[1].

Specimen		Ol	Opx	Cpx	Ga.	Sp.[2]	He.	Se.	Ky.	Plag.	Oth.	Total
				A. Ultramafic Nodules.								
Bultfontein[3]	Bu.1.	62.5	31.9		5.2	0.4						100.0
	Bu.6.	56.4	33.0		6.9	3.7						100.0
	Bu.7.	74.5	19.9		1.5	4.1						100.0
	Bu.8.	85.2	7.4		7.4							100.0
	Bu.9.	84.2	15.8									100.0
Frank Smith	FS 2	55.8	38.3		5.8	0.1						100.0
	FS 4	76.0	22.5		1.1	0.4						100.0
Dutoitspan Du.P.2		67.7	21.0			0.8	10.5					100.0
Premier Mine $893In_1$		54.5	11.6	15.4	4.3	0.5	7.1	6.6				100.0
Premier Mine $893In_2$		68.6	26.5		2.3		2.7					100.1
Premier Mine $893In_4$		54.2	14.0	14.7	8.5		8.6					100.0
Premier Mine $893In_5$		58.5	16.5		0.4	13.3	11.0					100.0
Premier Mine $893In_6$		59.9	14.7		2.9	12.3	10.2					100.0
Premier Mine $893In_7$		63.5	19.6	5.4	5.9	5.6						100.0
Premier Mine $893In_8$		60.1	27.9		1.8	0.8	9.4					100.0
Premier Mine $893In_{13}$		60.9	29.2		2.1	7.8						100.0
Premier Mine 893_{14}		61.9	38.1									100.0
Premier Mine $893In_{15}$		71.8	24.4		1.3	2.5						100.0
Premier Mine $893In_{17}$		42.7	56.4		0.6	0.3						100.0
Premier Mine $893In_{18}$		73.6	24.0		2.4							100.0
Premier Mine $893In_{19}$		66.0	26.7		5.8	1.5						100.0
Premier Mine $893In_{21}$		84.9	13.6		1.5							100.0
Premier Mine $893In_{22}$		75.3	18.1		2.6	4.0						100.0

Specimen	Ol	Opx	Cpx	Ga.	Sp.*2)	He.	Se.	Ky.	Plag.	Oth.	Total
Premier Mine $893In_{23}$	82.9	12.2		3.1	1.8						100.0
Premier Mine $1010In_{3}$	39.5				1.9	5.7	52.9				100.0
Premier Mine $1010In_{5}$	63.5	14.0		9.8	4.4	6.1	2.2				100.0
Premier Mine $1010In_{6}$	40.3	54.7	2.9		2.1						100.0
Premier Mine $1010In_{7}$	66.5	23.3	2.5	4.7	2.5						100.0
Premier Mine $1010In_{8}$	80.5	12.5		4.3	2.7						100.0
Premier Mine $1010In_{10}$	71.8	13.6		8.7	5.9						100.0
Premier Mine $1010In_{2}$	70.7	26.8			2.5						100.0
Jagersfontein Ja 1.	41.6	44.8			13.5						99.9
Jagersfontein Ja 5.	78.7	16.5		2.1	2.7						100.0
De Beers DB4	68.4	30.2		1.4							100.0
DB5	64.0	29.7			6.3						100.0
Kimberley Ki 1.	62.8	29.3		7.5	0.4						100.0
Matsoku (LBM_{36})*4	34	-	34	26							
Excelsior (CSE_x1)	63	6	9	2							
Kamfersdam (AAB 1053)	77		7	16							
30/351 Jagersfontein	86	9	20.5	5							
Bultfontein 16/172	98	-	2	-							
Bultfontein 27/172	99	-	1	-							
Matsoku LBM_{24}*5	100										100.0
LBM_{27}	75	24.4	0.5		0.1						100.0
LBM_{25}	73	25.0	1.6		0.4						100.0
LBM_{19}	71	25.8	0.7	1.7	0.3					0.5	100.0
LBM_{28}	69.9	29.6	0.3		0.2						100.0
LBM_{13}	69.5	25.3	2.3	1.7	1.2						100.0
LBM_{21}	67.7	31.7			0.6						100.0
LBM_{10}	66.8	28.3	2.5	1.7	0.4					0.3	100.0
LBM_{30}	65.6	12.0	20.8	0.8	0.7					0.1	100.0
LBM_{39}	65.3	29.1	1.8	3.1	0.3					0.3	100.0
LBM_{29}	65.1	31.9	1.0		0.6					1.5	100.0

Specimen	Ol	Opx	Cpx	Ga.	Sp.*2)	He.	Se.	Ky.	Plag.	Oth.	Total
Matsoku LBM_1	64.7	26.0	2.9	5.0	1.1					0.3	100.0
LBM_{26}	62.6	37.4									100.0
LBM_2	61.6	33.2	0.5	2.4	1.5					0.8	100.0
LBM_{14}	61.3	28.6		8.6	0.3					1.2	100.0
LBM_{31}	60.9	37.7	0.5		0.9						100.0
LBM_{16}	60.7	33.8	1.8	0.7	1.1					1.9	100.0
LBM_3	58.5	31.7	2.1	5.1	2.1					0.5	100.0
LBM_{34}	58.0	39.2	2.0		0.2					0.6	100.0
LBM_7	55.8	31.9	0.3	9.4	2.2					0.4	100.0
LBM_{15}	55.8	36.5	2.2	3.9	0.8					0.8	100.0
LBM_5	55.2	26.4	4.2	9.5	4.7						100.0
LBM_{22}	52.2	37.1	5.6	1.4	2.5					1.2	100.0
LBM_4	50.3	44.7	1.0	3.5	0.4						100.0
LBM_8	42.3	52.7	0.1	4.3	0.5						100.0
LBM_{17}	42.1	50.5		6.7	0.5					0.2	100.0
LBM_{11}	40.5	54.4		4.1	1.0						100.0
LBM_{12}	34.1	31.6	15.8	15.6	2.9						100.0
" 32	31.8	38.5	8.0	12.6	7.7					1.4	100.0
"23	28.3	60.8	5.1	3.7	0.4					1.7	100.0
"41	21.3	60.2	14.9		0.1					3.5	100.0
"6	17.3	69.3	5.5	6.5	0.8					0.7	100.0
"44	16.2	33.2	18.1	1.9	29.2					1.4	100.0
"33	15.7	45.3	27.8	9.0	2.2						100.0
"38	14.7	57.2	16.4	5.5	6.2						100.0
"37	8.0	56.0	33.4	1.5	1.1						100.0
"40	2.6	83.8	-	10.7	2.9						100.0
"18	-	64.3	18.3	13.9	3.5						100.0
"36	34.1		34.0	26.1	5.8						100.0
Dunite 66ULUP-25 *6)	95.6	-	1.3	-	-	3.1					100.0
66KAP 1	97.7	0.1	0.8	-	-	1.4					100.0
Lherzolite 68SAL-3	76.1	17.5	5.5	-	-	0.9					100.0
66PAL-3	57.9	29.9	11.2	-	-	0.9					100.0
G Lherzolite 66 SAL-1	28.7	12.1	33.5	22.1	-	3.6					100.0
G Pyroxenite 68 SAL-11	-	-	62.1	36.9	-	0.5				0.5	100.0
G Pyroxenite 68 SAL 7	-	8.7	53.2	34.4	-	3.0				0.2	100.0
G Pyroxenite 68 SAL-26	-	16.2	65.6	16.2	-	1.4				0.3	100.0

Specimen	Ol	Opx	Cpx	Ga.	Sp. *2)	He.	Se.	Ky.	Plag.	Oth.	Total
G Pyroxenite SAL 24	-	20.0	63.5	11.2	-	0.2				0.1	100.0
G Pyroxenite SAL 6	-	22.0	70.5	7.3	-	tr				0.2	100.0
			B.	Eclogite Nodules.							
Roberts Victor *3 RV_1			38.2	55.4	6.4						100.0
Roberts Victor RV_5			23.1	75.3	1.6						100.0
Roberts Victor RV_6			10.1	81.3	8.6						100.0
Roberts Victor F_1			25.7	49.5	19.9					4.9	100.0
F_2			59.4	15.6			2.2	22.8			100.0
F_3			38.2	56.9				4.9			100.0
Jagersfontein Ja.			42.1	42.9	15.0						100.0
Lovedale B_2B			60.9	38.7	0.4						100.0
B_2B_1			55.6	34.4							100.0
B_2B_2			65.0	25.2	9.8						100.0
Garnet Ridge 1 *7 Arizona			48.2	43.2						8.6	100.0
2			88.3	9.8						1.9	100.0
3			92.9	5.0						2.1	100.0
4			78	20						2	100.0
5			46	36						18	100.0
6			51	29						20	100.0
7			54	35						11	100.0
8			59	33						8	100.0
9			62	33						5	100.0

*1) Described by Watson, (1967) from Arizona.

*2) Includes, chromite, spinel, kelyphyte and myrmekite. When garnet is present it implies kelyphyte, and when garnet is absent it is myrmekite.

Ol = olivine; Opx = orthopyroxene; Cpx = clinopyroxene; Ga = garnet; Sp = kelyphyte/myrmekite; He = hematite; Se = serpentine; Ky = kyanite; Plag = plagioclase; Oth = other minerals.

*3 Own determinations.

*4 Siebert, (1968).

*5 Rickwood et al., (1968).

*6 Jackson et al., (1969).

*7 Watson et al., (1969).

ultramafic nodules rarely exceed 10 per cent, and that the high contents observed in the nodules from Hawaii (Jackson and Wright, 1969) are seldom found. Since too little data are known as yet, it is not possible to produce an accurate comparison between the ultramafic nodules in kimberlite and those found in alkaline basalts. An attempt has nevertheless been made by using the data provided in table 29, and by representing it on the diagram after Jackson (1968) (figure 10).

The volumetric compositions determined during the present study have revealed that:

1. garnet and chrome spinel do not coexist other than in a kelyphyte relationship.

2. ilmenite is always absent in these nodules, and that the opaque minerals recorded in table 29 are hematite. The latter apparently formed as a consequence of the secondary alteration of olivine and pyroxene.

3. two types of spinel-bearing ultramafic nodules occur, ~~which are~~ viz the kelyphyte-bearing nodules and the myrmekite bearing nodules. Since the former ones often reveal the presence of very small relicts of garnet, they will be described henceforth as garnet peridotites. The myrmekite-bearing nodules do not show any relicts of garnet, and will be termed spinel peridotites.

4. At least two types of garnet peridotites were found which display completely different textures. The cumulate type which contains more than 50 per cent of pyroxene and which will be termed pyroxenites, whereas the other nodules will be described as garnet peridotites.

The pyroxenite nodules consist of orthopyroxene, clinopyroxene, olivine and either spinel or garnet. However, pyroxenite nodules in which garnet and spinel coexist other than in a kelyphyte relationship have not been found.

In figure 10 the volumetric composition of some of the ultramafic and eclogitic nodules has been plotted on a variation diagram showing olivine, orthopyroxene, clinopyroxene and garnet. This figure indicates that garnet-harzburgite predominates among the peridotitic nodules and that garnet lherzolite also occurs. The pyroxenite

THE VARIATION IN THE GARNET, OLIVINE, ORTHOPYROXENE AND CLINOPYROXENE CONTENT OF THE NODULES IN KIMBERLITE (VOLUME PERCENTAGES)

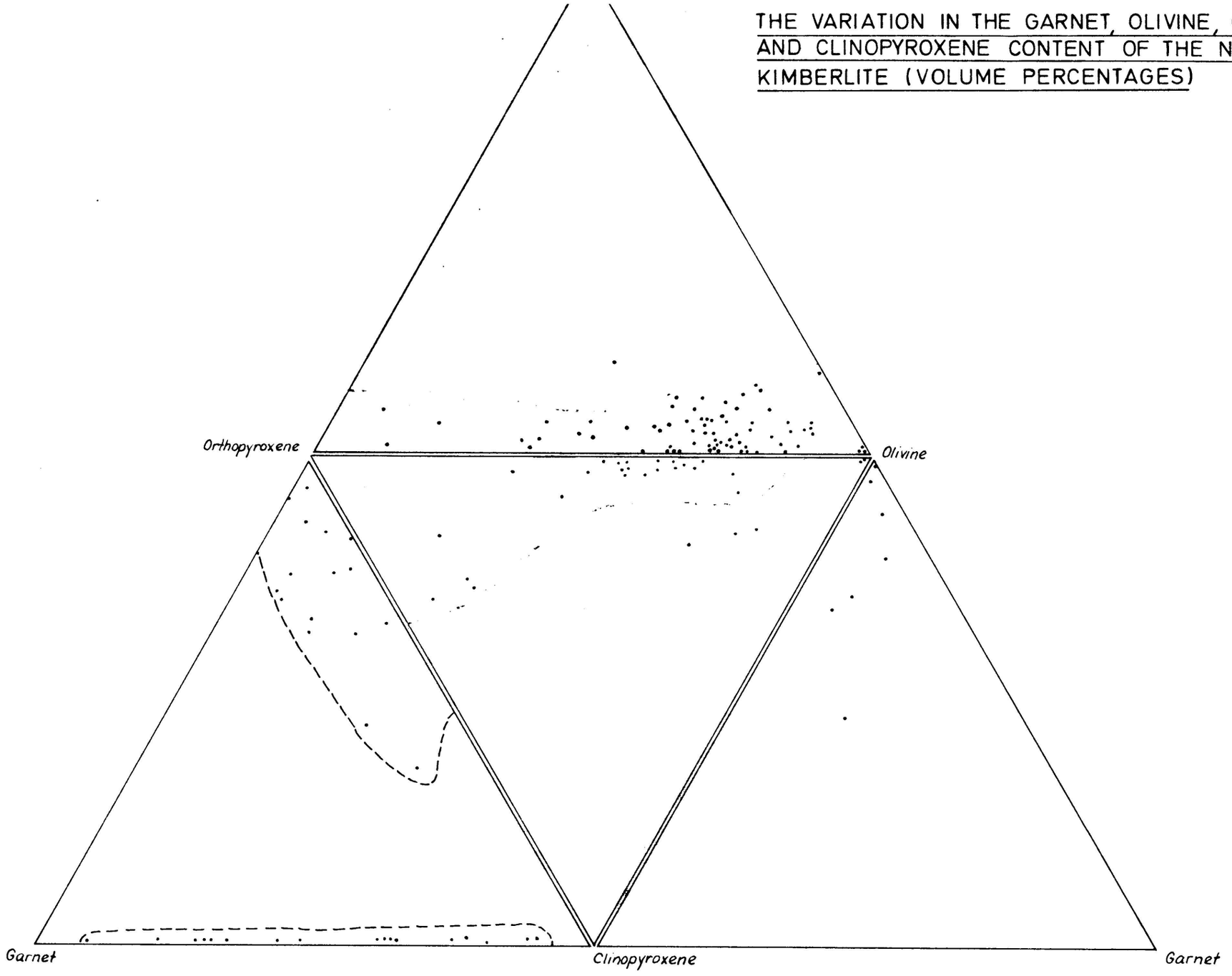

FIG.10

nodules are all lherzolites. According to Jackson, (1968) the nodules in the nephelinite series at Hawaii are predominantly harzburgite, lherzolite and garnet wehrlite. However, in the ultramafic nodules from kimberlite as well as from the nephelinites, a complete gradation occurs between all these rock-types.

Petrographically the garnet- and spinel peridotites are similar to the alpino-type peridotites from Turkey (Van der Kaaden, personal communication). These rocks consist of large (4.0 mm) euhedral and subhedral and often lenticular orthopyroxene grains in a fine-grained matrix of olivine. The orthopyroxene rarely contains inclusions of olivine, but garnet grains are frequently present in the orthopyroxene. Around the periphery of the large orthopyroxene grains, and often extending into the grains, a fine-grained, granular, orthopyroxene of exactly the same composition as the host grains, was observed. This texture (photo 17) is only present in the peridotite nodules in which the olivine grains are also granulated.

The large orthopyroxene crystals exhibit a type of translation twinning which simulates the kink bands described by Ernst, (1967) from the nodules in the Eifel region in Germany. The undulatory extinction of these orthopyroxenes (photo 18) also corresponds to that described by Ernst, (1967), and according to Raleigh (1967, p.199) both the undulatory extinction and translational-twinning indicate deformation under high stress.

The fine-grained orthopyroxene does not show any of these stress phenomena, nor any exsolution lamellae of clinopyroxene, hence this granulation took place due to recrystallization at reduced pressures of orthopyroxene strained previously at elevated pressures where complete solid-solution of clinopyroxene was possible in the orthopyroxene.

Olivine is the major constituent of these ultramafic nodules and occurs as large anhedral grains which ranges from 4.75x2.85 mm to 1.66x0.90 mm in size. In the nodules where granulation of orthopyroxene is evident, the olivine is equigranular, rounded and varies from 0.45x0.70

mm to 0.40x0.25 mm in size. In one peridotite nodule (893 In_5) the formation of fine-grained, equigranular olivine along the periphery of these large olivine crystals has been observed (photo 19). The large olivine grains also exhibit kink bands and undulatory extinction simulating the textures observed in the orthopyroxene, whereas the granular olivine does not show any of these phenomena. According to Raleigh (Jackson et al., 1969) the original large olivine was deformed under a considerable stress, whereas the granular olivine formed as a consequence of the recrystallization of the former. Since nodules containing either garnet or spinel were found associated with the recrystallized olivine, it is obvious that this recrystallization must have occurred at pressures close to 20 kb and at a temperature of approximately 1,000°C (O'Hara, 1968).

Rounded grains of pink, purple, red or orange garnets are included in the olivine and orthopyroxene grains in the ultramafic nodules. These grains vary in size from 4.75x2.90 mm to 0.25x0.2 mm, and are characterized by kelyphytic rims of a variable thickness. Most of the garnets are extensively cracked and along these cracks the development of the mineral phases which are present in the kelyphytic rims, took place.

The kelyphytic rims consist of an outer zone of coarse-grained material ($\geq$ 0.6 mm) and an inner zone of fine-grained fibrous material (0.02 to 0.06 mm in size) (photo 20). The coarse-grained material consist of a reddish brown spinel (picotite), a colourless clinopyroxene and a dark brown clinopyroxene. The latter has the following optical properties, $2V_{\gamma} = 60^{\circ}$, $n_{\alpha} = 1.670$, and shows the same d-values as those of diopside. The picotite occurs as small euhedral grains of 0.2 mm diameter, and also as skeleton crystals. Both varieties of clinopyroxene are present as small (0.03 mm) xenomorphic grains which display a high birefringence and a typical pyroxene cleavage. Apart from the primary constituents the following alteration products were also identified; hematite, magnetite, talc, serpentine and

biotite. The electron-microscope photograph of a nodule from Lesotho taken by Nixon, Von Knorring and Rooke (1963) revealed the presence of spinel, pyroxene and talc.

In the spinel-peridotite nodules, garnet is absent and spinel-pyroxene symplectites are abundant. The latter had been described by Holmes (1936) as an eutectic crystallization of spinel and pyroxene, or as a replacement of the one mineral by the other.

The symplectites consist of an orthopyroxene grain rimmed by a brownish clinopyroxene, and veined by "worm-like" lamellae of spinel (picotite). The latter form a continuous network which even extends into the clinopyroxene rims (photo 21). These symplectitic intergrowths usually display a rounded shape, and are enclosed in either olivine or orthopyroxene. The physical properties of the spinel and the clinopyroxene are very similar to those of the primary phases in the kelyphytic rims (chapter VII). The orthopyroxene in these nodules also has the same Al_2O_3 content as the orthopyroxene in the garnet peridotites (appendix 16). Consequently it is clear that these symplectites also resulted as a consequence of the equilibration of garnet at pressures below 20 kb and at a temperature of approximately 1000°C (O'Hara, 1967).

Spinel-bearing peridotites, in which the spinel phase is present as subhedral intergranular grains, and where neither symplectites nor kelyphyte is present, have also been observed. These nodules do not contain any garnet, and the orthopyroxenes are also marked by an increased content of Al_2O_3. Clinopyroxene is also a more prominent constituent of these nodules, and these clinopyroxenes are Cr^{3+}-bearing and resemble the clinopyroxene in the symplectites closely. It appears that the spinel phases in these nodules crystallized directly as such, and consequently it is apparent that these nodules crystallized well below 20 kb pressure and 1000°C.

Clinopyroxene is very rare in the garnet peridotite nodules, but more abundant in the spinel peridotite, due to the equilibration of garnet. In the clinopyroxene-bearing peridotites the clinopyroxene occurs as large

(7.10x2.40 to 0.50x0.40) subhedral to lens-shaped grains in the olivine matrix. Although the clinopyroxene does not exhibit the stress features described for olivine and orthopyroxene, it shows similar recrystallization phenomena.

The pyroxenite nodules consist of orthopyroxene, clinopyroxene, olivine and either garnet or spinel. Although the mineral constituents of these nodules are the same as those of the peridotites both the mineral proportions and the textures vary. The orthopyroxene cumulus crystals exhibit a fine-grained exsolution of clinopyroxene along the (100) direction of the orthopyroxene, simulating the Bushveld-type of orthopyroxene (Hess, 1952). The subhedral to anhedral intercumulus-clinopyroxene is polysynthetically twinned, and is accompanied by olivine and spinel. The cumulus garnets are euhedral to rounded, and are altered to kelyphyte in the same way as the garnets in the peridotite nodules.

3. The petrogenesis of the ultramafic xenoliths

The orthopyroxene of the peridotite nodules does not show exsolution lamellae of clinopyroxene, whereas the orthopyroxene in the pyroxenite nodules does show this phenomenon. Consequently, the pyroxenite nodules formed at lower temperatures, whereas the peridotite nodules formed at more elevated temperatures. [illegible] The pyroxenite nodules were not derived from ultramafic cumulates in the crust of the earth, because they contain pyrope garnet and show no reaction relationship between olivine and enstatite. The stability field for pyrope garnet indicate that these nodules formed at pressures exceeding 20 kb. The spinel-pyroxenites however formed at pressures below 20 kb, but must have crystallized above 5 kb, because there is no reaction relationship between olivine and pyroxene.

The garnet peridotite nodules show the coexistence of garnet, enstatite and olivine without any exsolution phenomena in the enstatite, and they also show signs of deformation at high pressures. Consequently it is concluded that these nodules formed at high pressures.

According to the system diopside-pyrope, O'Hara (1968, p 84) it is obvious that enstatite and garnet would crystallize before olivine at 30 kb pressure. At this pressure the olivine liquidus falls below the enstatite liquidus, and hence garnet-enstatolites would crystallize. At 27 kb the olivine liquidus enters the crystallization surface, and olivine would start to crystallize, resulting in garnet-harzburgites. At a subsequent release of pressure from 27 to 20 kb, the diopside solidus curve enters the crystallization surface, and the four-phase lherzolites would be able to crystallize. During this stage the garnet pyroxenites can also crystallize depending on the composition of the liquid. At 20 kb the spinel solidus enters the crystallization sequence, and garnet disappears. From this stage the spinel peridotites and spinel pyroxenites can crystallize. The spinel which forms below 20 kb would crystallize as individual, euhedral grains, similar to that of the regional peridotites (photo 22) (CF_{298}) + (1010 In_6) and not as symplectite, which is an equilibration phenomenon at decreasing pressures. The spinel-peridotites (CF_{298}) and spinel-pyroxenites (1010 In_6) thus represent material which formed below 20 kb, whereas the symplectite bearing spinel-peridotites formed at higher pressures.

The thin sections of the alpinotype peridotites, kindly supplied by the late Prof. J. Willemse, and of the regional peridotites from the Pafuri-area suggest that these rocks have crystallized below 20 kb, because the orthopyroxene contains exsolved lamellae of clinopyroxene, and the spinel grains are euhedral.

The recrystallization phenomena observed in the olivine and orthopyroxene grains are also present in the alpinotype-, and regional peridotites, and indicate that the recrystallization took place during an increase in temperature and a decrease in pressure. Since these nodules were transported from the upper mantle to the surface of the earth, it may be that the adaptation occurred during the ascent of the nodules.

C. The Eclogite Nodules

1. Introduction

The term eclogite is used for a large variety of rock-types, ranging from the garnet-pyroxene-bearing xenoliths in kimberlite and alkaline basalt to the high-pressure rocks in metamorphic complexes (regional areas). Haüy (1822) originally described eclogite as a rock consisting of diallage (omphacite) and garnet, accompanied by kyanite, zoisite, amphibole, quartz and pyrrhotite. According to Eskola (1921) the pyroxene is jadeite-bearing and the garnet contains appreciable amounts of almandine and pyrope.

Both the varied occurrence and the difference in the composition of the clinopyroxene and the garnet have led Smulikowski (1968, p 89) to classify the eclogites into three types, viz:

1. Regional eclogites
2. Alpino-type eclogites
3. Eclogites from kimberlitic and alkaline basaltic lavas.

Becke (Smulikowski, 1968) uses the term eclogite only for the garnet-pyroxene-rocks found in high-grade metamorphic terrains, and applies the term griquaiite to the garnet-pyroxene rocks found in kimberlites. However, since the minerals mentioned in Haüy's definition for eclogite have been found in the eclogites from the three different types of occurrences, the use of a new term seems hardly justified. Since the origin of these three types of eclogites is completely different, the term eclogite should only be used as a descriptive name, without implying any genetic significance.

2. The petrology of the eclogite nodules

Eclogitic nodules from the following kimberlite occurrences in South Africa have been investigated: Roberts Victor, Brakfontein, Lovedale and Jagersfontein. These four occurrences are by no means the only ones from which eclogite is known in the Republic of South Africa.

In the hand specimens the eelogite nodules consist of large grains of honey brown to red garnet and pale green clinopyroxene. No distinct layering simulating the*1) cumulates from layered intrusions could be discerned. The nodules are usually round to elipsoidal in shape, and show no alteration rims like the ultramafic nodules. These eclogite nodules consist largely of garnet and clinopyroxene, and the following accessory minerals have been identified by different researchers: kyanite, corundum, plagioclase, spinel, diamond, phlogopite (?), zeolites, quartz, glass, pyrite and second generation clinopyroxene, Rickwood et al. (1969).

The volumetric composition of 10 eelogite and kyanite eclogite nodules determined according to the technique described for the ultramafic nodules, are reported in table 29 and are plotted in figure 10. The garnet content varies from 15.6 to 81.3 per cent and gives a wider variation than that observed by Rickwood et al, (1968). They found a variation in the garnet content from 28 to 83 per cent. However, the nodule F_2 which has a garnet content of 15.6 per cent, shows an extensive alteration of garnet to kelyphyte, and may thus have contained a much higher percentage of fresh garnet. If the kelyphyte is recalculated as original garnet, the garnet content ranges from 34.4 to 90.0 per cent, with an average of 56.5 per cent, which compares well with the 50.5 per cent observed by Rickwood et al., (1968). Unfortunately these authors did not mention whether kelyphyte was included.

No two-pyroxene-garnet-rock has been observed among the eclogites from the kimberlites, however, an eclogite nodule from the nephelinite series at Hawaii, which consisted of two pyroxenes and garnet has been described (Yoder and Tilley, 1962).

According to the system diopside-pyrope (O'Hara, 1968) the association garnet clinopyroxene crystallizes in the temperature-pressure range of 30 to 40 kb, and 1650 to 1700°C. The ratio of clinopyroxene to garnet given by Rickwood et al. (1968) indicates eutectic crystallization

*1) Subsequent research has led to the discovery of layered eclogite nodules from Roberts Victor.

at 37 kb. The two-pyroxene-eclogite nodule from Salt Lake crater, Hawaii (Yoder and Tilley, 1962) indicates crystallization at somewhat reduced pressures, where the enstatite solidus exists, and probably formed in the 35 to 30 kb region. Assuming the effect of other constituents to be negligible, it appears as if the eclogite nodules, found in kimberlites, crystallized at pressures exceeding 32 kb, and at a depth exceeding 100 km.

The garnet grains vary in size from 0.2 to 10.0 mm, and are xenomorphic to rounded in shape. The colours vary from a dull brown to a dark red, and inclusions of clinopyroxene in garnet and vice versa are common. Around the uneven outlines of the garnet grains, rims of kelyphyte are often present. A large variety of mineral phases have developed in some of these kelyphytic rims, however each mineral assemblage usually forms a distinctly separate rim.

The following two mineral assemblages are the usual ones; an outer one which consists of spinel, a colourless clinopyroxene, a brownish clinopyroxene and pyrite (photo 23) and the inner one which consists of plagioclase, quartz and pyroxene (photo 24). Both these rims have suffered extensive secondary alteration resulting in biotite, talc, chlorite and zeolites.

The spinel grains occur both as small (0.1 mm) euhedral grains, and as skeleton crystals in the kelyphytic rims. The manner of occurrence of these grains simulates that of the spinel in the ultramafic nodules, however the grains are light brown in colour and more hercynitic in composition.

Plagioclase was only encountered in the kelyphytic rims of the kyanite eclogite nodules, and it was present as small (0.1x0.01 mm) lath-shaped grains, which are polysinthetically twinned. Associated with the plagioclase, small anhedral grains of quartz are often encountered. Both the method of occurrence and the stability fields for plagioclase indicate that these rims formed at pressures below 10 kb (O'Hara; 1968, p 13).

The kelyphytic rims in the eclogite nodules from Lovedale and Brakfontein also contained small euhedral

grains of pyrite. They are usually present in the spinel-clinopyroxene rims. The clinopyroxene in these rims closely simulates the clinopyroxenes in the rims around the garnets of the ultramafic nodules, and both the brownish and colourless varieties were found. Zeolite ($2V_{\alpha}$ = 25°), chlorite, talc and phlogopite (table 30) are associated with the primary kelyphyte minerals.

The eclogitic clinopyroxene is present as subhedral to anhedral grains with a grain size of 1.0 mm. These clinopyroxene grains are surrounded, and often partly replaced, by an extremely fine-grained material (< 0.005 mm) (photo 25). In places where this material is coarser-grained, it yields almost the same birefringence, refractive indices and extinction angles as the large eclogitic clinopyroxene. The d-values of a sample of this fine-grained material, which was hand-sorted, correspond exactly with those of the host-clinopyroxene, except for the broader lines, due to effects of particle size (table 34).

In some of the eclogite nodules the alteration products of clinopyroxene become very fine-grained so that aggregate polarization is no longer evident, and globulites and margarites (photo 26) could be identified. In nodule B_2B_2 from Brakfontein a dark-brown isotropic substance, which contains very small crystallites (photo 27) was observed, and was identified as glass. Consequently it was concluded that this fine-grained clinopyroxene represents the crystallization product of an original clinopyroxene which was re-melted. According to the system diopside-pyrope at 40-30 kb (O'Hara 1968), clinopyroxene is the first phase to enter the liquidus on a relief of pressure.

Kyanite is present as large, euhedral grains in the alteration products of the eclogite nodules, but it is never associated with either the spinel - or plagioclase-bearing kelyphyte, but with the fine-grained clinopyroxene.

3. The petrogenesis of the eclogite nodules

The phase experiments done by O'Hara and Yoder (1967), O'Hara and Schairer (1963), Kushiro (1965) and Davis (1964) on the system diopside-pyrope indicate that these two

Table 30. The d-values of phlogopite which formed in the secondary kelyphytic rims. (The d-values were obtained by means of a Guinier camera, using Cu Kα-radiation

RV$_1$ Film no. 411		ASTM 10-493		
I/I$_o$	d ^{o}A	I/I$_1$	d ^{o}A	h k l
10	10.23	100	10.13	002
1	5.063	20	5.056	004
		20	4.612	110,020
		8B	4.515	021
		6B	4.079	112
1	3.910	20	3.814	023
2	3.582	35	3.540	$11\bar{4}$
10	3.362	100	3.362	006
4	3.224	40	3.283	114
		10	3.156	$11\bar{5}$
4	3.024	40	3.040	025
1	2.9125	10	2.926	115
		20	2.818	$11\bar{6}$
1	2.647	20B	2.651	$13\bar{1}$
10	2.620	100	2.624	116
3	2.516	30	2.522	008
5	2.433	40	2.439	133
		18B	2.361	117
		10B	2.304	220,040
1	2.277	10B	2.270	$13\bar{5}$
7	2.174	45	2.180	135
		20	2.039	224
7	2.013	65	2.017	0.0.10
1	1.995	20B	2.000*1)	$13\bar{7}$

*1) plus 6 lines

minerals alone coexist at pressures exceeding 30 kb. The eutecticum for this system becomes increasingly rich in clinopyroxene with an increase in pressure. O'Hara and Yoder (1967) have shown that at 30 kb enstatite enters the solidus phase, resulting in the crystallization of a two-pyroxene-eclogite. In the 25-27 kb region olivine is stable, causing garnet-peridotite and garnet harzburgite to form, and hence eclogite cannot crystallize. The eclogite thus crystallized above 30 kb, where the volumetric proportions of garnet and clinopyroxene varied according to the pressure. This variation necessarily resulted in the systematic chemical variation observed by Yoder and Tilley (1962, p. 518).

Yoder and Tilley (1962, p. 470 to 518) explained the presence of kyanite in eclogite, but they only investigated regional eclogites, consequently their results may not necessarily apply to kimberlitic eclogites. The potential source of Al_2O_3 in both garnet and clinopyroxene, and the presence of kyanite in altered pyroxene indicate that the reactions:

1. Clinopyroxene + Ca-tschermak molecule ⟶ kyanite + diopside + grossular + liquid (Fo + En)
2. (grossular + pyrope) garnet ⟶ kyanite + Ca-tschermak molecule bearing diopside + liquid (Fo + En)

may have caused the formation of kyanite. Both these reactions are chemically valid and the minerals on the right hand side of the equations are stable above 30 kb (O'Hara, 1968). The melting of clinopyroxene observed in some nodules would cause the formation of kyanite at pressures exceeding 30 kb, and olivine and enstatite would still be in the liquidus (O'Hara, 1968).

VIII. THE MINERALOGY OF KIMBERLITE AND OF THE INCLUSIONS OF ECLOGITE AND ULTRAMAFIC NODULES

A. Garnet

1. Occurrence

Several types of garnet are present in the Premier Mine and other kimberlites. Since many of these garnets are of secondary origin, very little work has been done on

them apart from determining their physical properties. The primary garnets which occur in the ultramafic and eclogitic nodules, and as primary phenocrysts in the kimberlite, are extensively cracked and altered to kelyphyte. The mineral phases in the kelyphyte vary considerably from one rim to another.

The garnets from kimberlite and the ultramafic nodules vary from orange to purple in colour, and the eclogitic garnets are usually honey brown to dull brownish red in colour.

In the Premier Mine kimberlite fresh garnets are very scarce, owing to the extensive alteration of the primary garnet to a light green hydrogrossular. The hydrogrossular as well as an almandine-rich grossular are the main secondary garnets in the Premier Mine kimberlite, and they form large masses in the kimberlite matrix. The formation of these secondary garnets can be ascribed to the metamorphic influences of the tholeiitic sill.

2. The mineralogy of the garnets

The different reflections of a garnet powder, obtained by means of a Guinier Camera, using silicon as an internal standard and Cu Kα radiation, have been indexed according to the method after Klug and Alexander (1954, p. 344.) The indices thus obtained correspond to the indices supplied by ASTM 2-1008 and Bobrievich et al., (1959). By using the refractive index and the unit-cell dimension the molecular proportions of pyrope, almandine and grossular were determined after Deer, Howie and Zussman (1967, p. 98).

In appendices 1, 2 and 3 the physical properties and the composition of the garnets in mol. percentages of the garnets from kimberlite, garnet peridotite and eclogite respectively are given. According to figure 11A the grossular content of the kimberlitic garnets remains fairly constant, but a Mg^{2+}/Fe^{2+} substitution is present. The variation in the pyrope, almandine and grossular content in the garnets from the different South African kimberlites overlaps completely, and shows almost the same average values (figure 11B).

THE VARIATION IN THE PYROPE, GROSSUL[AR] CONTENT AS A FUNCTION OF THE a_o AND n-VALUES AFT[ER] ND ZUSSMAN (1967) FOR:

(A) The Garnets from Kimberlite

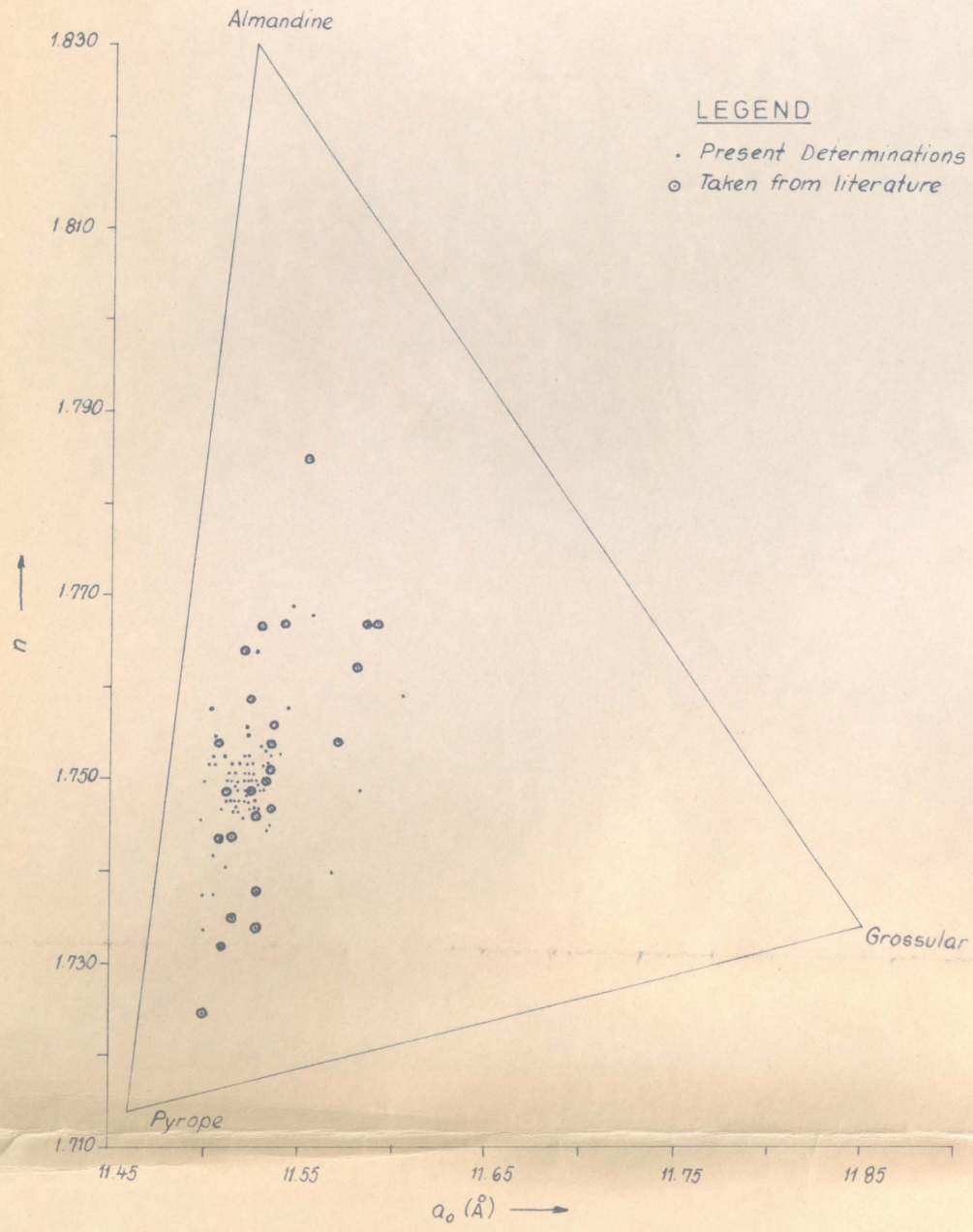

(B) The Garnets from some South African Kimberlites

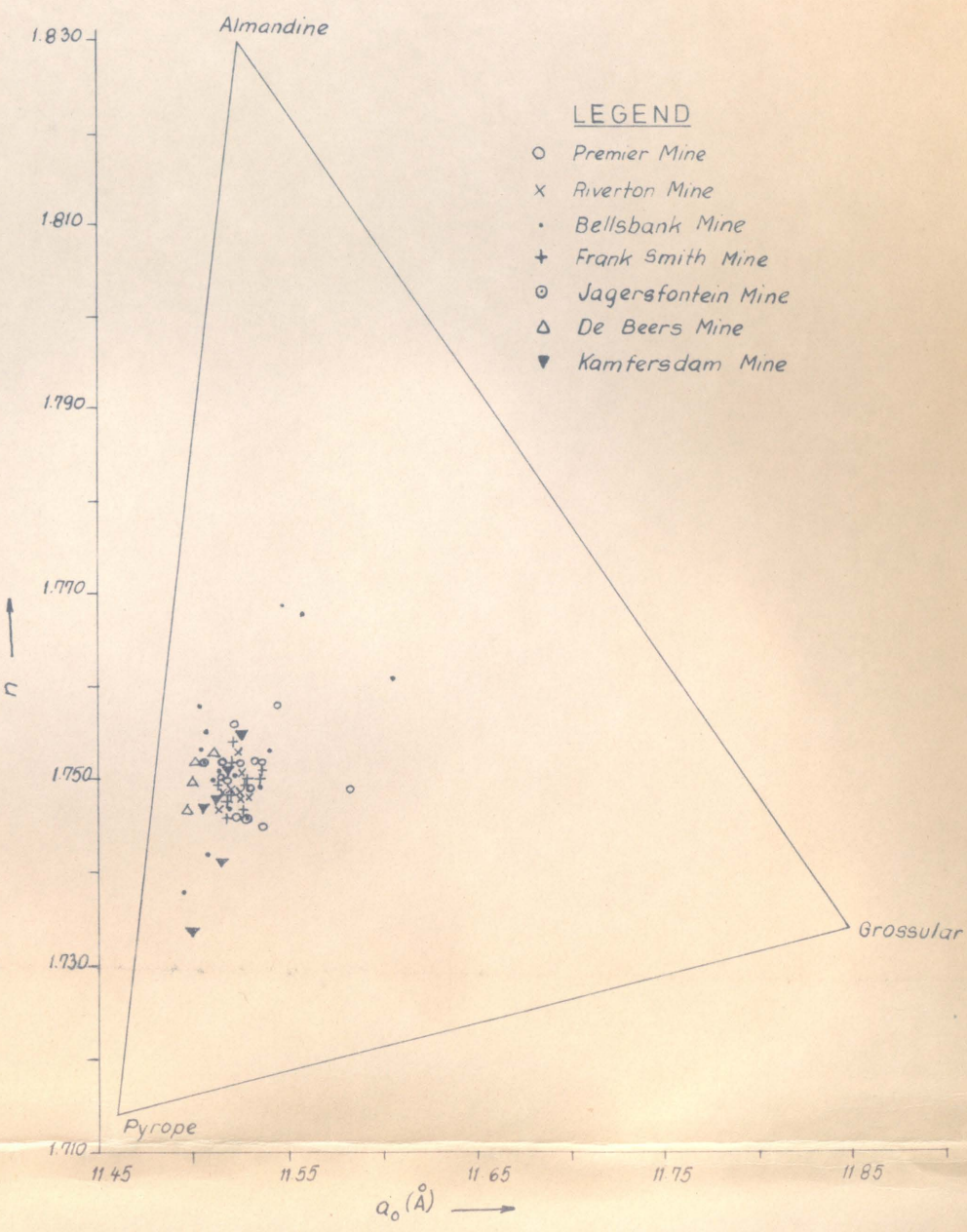

(C) The Garnets from Ultramafic Nodules

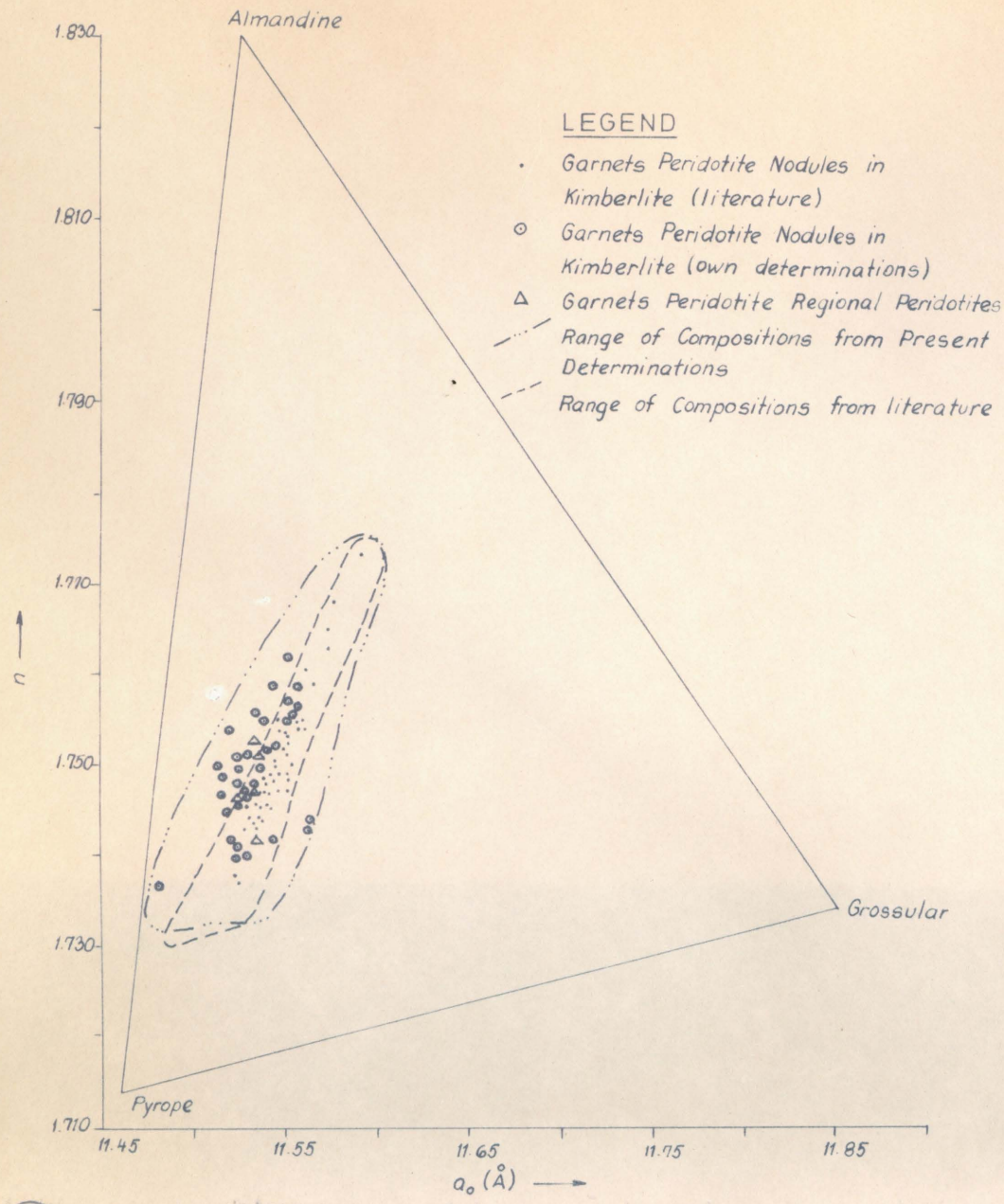

(D) The Garnets from Eclogitic Nodules

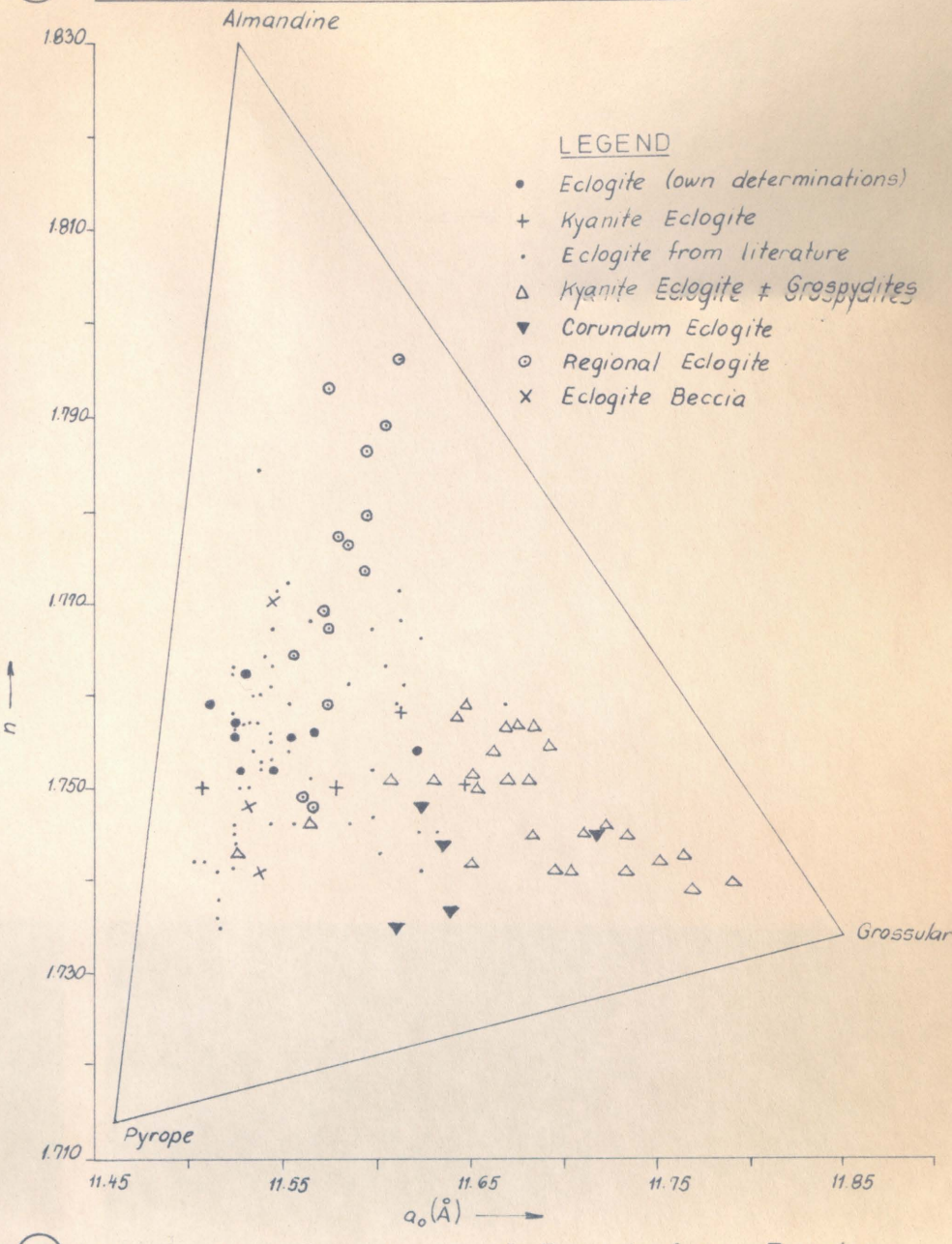

(E) The various Parentages of Garnets from Jagersfontein Kimberlite

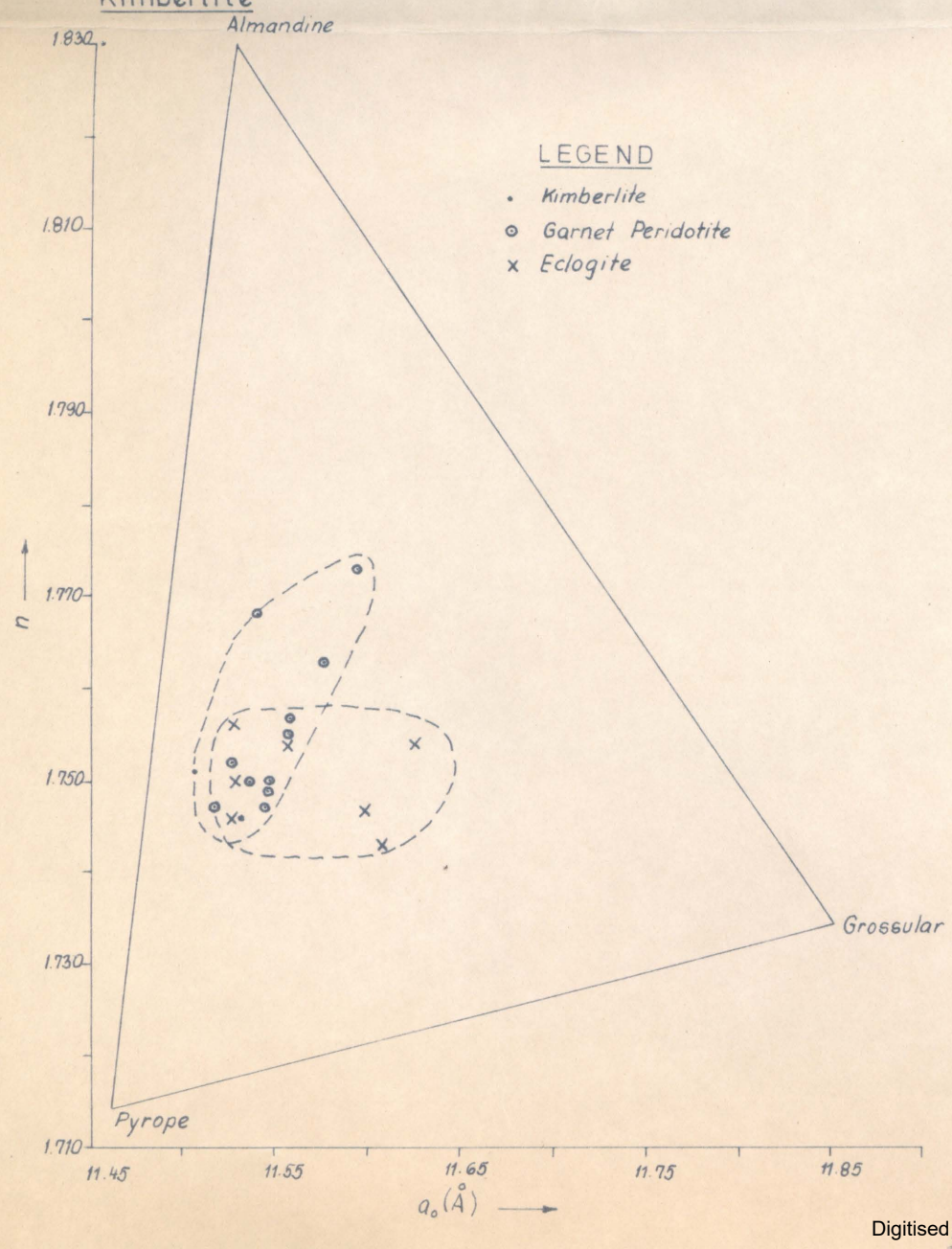

(F) The various Parentages of Garnets from Premier Mine

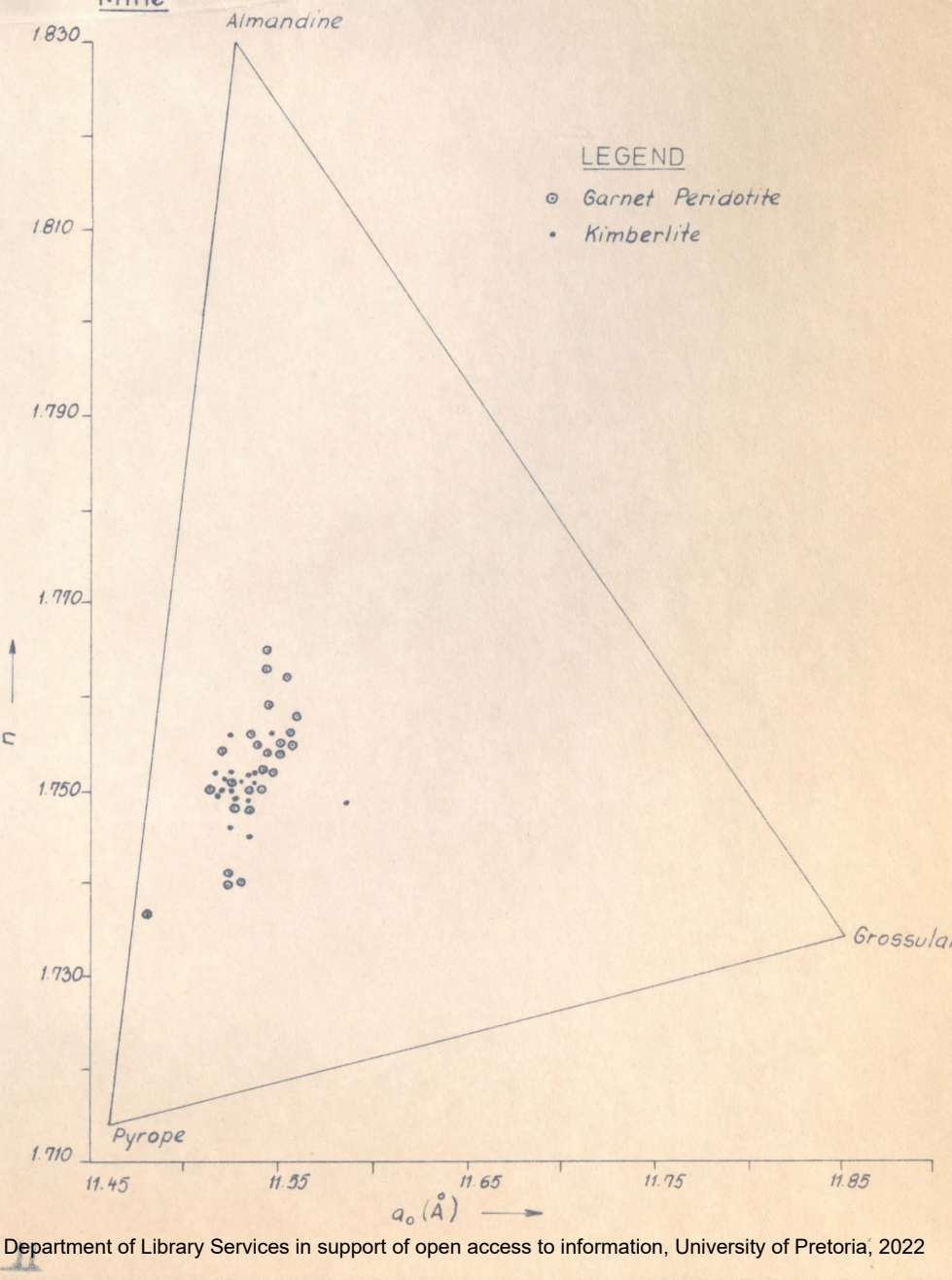

Figure 11C indicates that the garnets from garnet peridotite nodules show a distribution similar to the kimberlitic garnets for the mol. percentages of pyrope, almandine and grossular. The Mg^{2+}/Fe^{2+} substitution recorded in the kimberlitic garnets is also present in the garnets from the garnet peridotites, however, the latter appear to have a more restricted variation.

In figure 11D the distribution of these three components in the eclogitic garnets is represented and the pronounced scatter is evident. The eclogitic garnets show essentially the same distribution as the garnets from garnet peridotite, but some are more enriched in grossular, and have a more extensive Mg^{2+}/Fe^{2+} substitution. The garnets from kyanite eclogites, corundum eclogites and grospydites are more enriched in grossular. Hence, two definite variation trends are apparent in the eclogitic garnets, viz. an enrichment of almandine, and an enrichment of grossular.

According to figure 11E the garnets from kimberlite and from garnet peridotite have the same pyrope, grossular, and almandine contents, whereas the eclogitic garnets are more enriched in grossular. The garnets from the Premier Mine kimberlite have a composition similar to the garnet from the garnet peridotites (figure 11F).

3. The chemistry of the garnets

The chemical analyses and the molecular percentages of garnet end-member molecules of the garnets from kimberlite, garnet peridotite, eclogite and grospydyte are reported in appendix 4. The main garnet molecules have been calculated after the method proposed by Rickwood (1968), in the following sequence, pyrope, uvarovite, grossular, andradite and almandine. The Mn^{2+} and Ti^{4+} cations have been added to Fe^{2+} and Si^{4+} respectively before the calculation of the molecular percentages. The presence of excess SiO_2, Al_2O_3 in the molecular norms should be ascribed to the presence of kelyphyte in the analysed garnets. The frequency distribution diagrams for the CaO, Cr_2O_3 and TiO_2 contents of the garnets from the different percentages are presented in figures 12A, 12B, 12C and 12D respectively.

THE FREQUENCY DISTRIBUTION OF THE WEIGHT PER CENT CaO, Cr_2O_3 AND TiO_2 IN KIMBERLITIC GROSPYDITIC ECLOGITIC AND GARNET-PERIDOTITIC GARNETS

I The distribution of the wt per cent CaO
II The distribution of the wt per cent Cr_2O_3
III The distribution of the wt per cent TiO_2

I

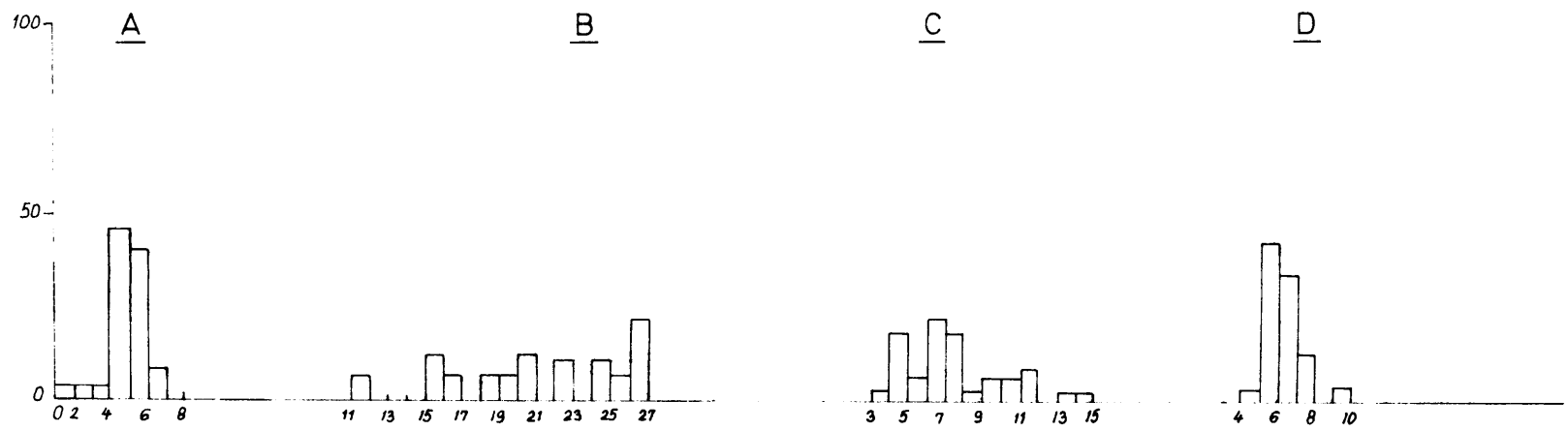

II

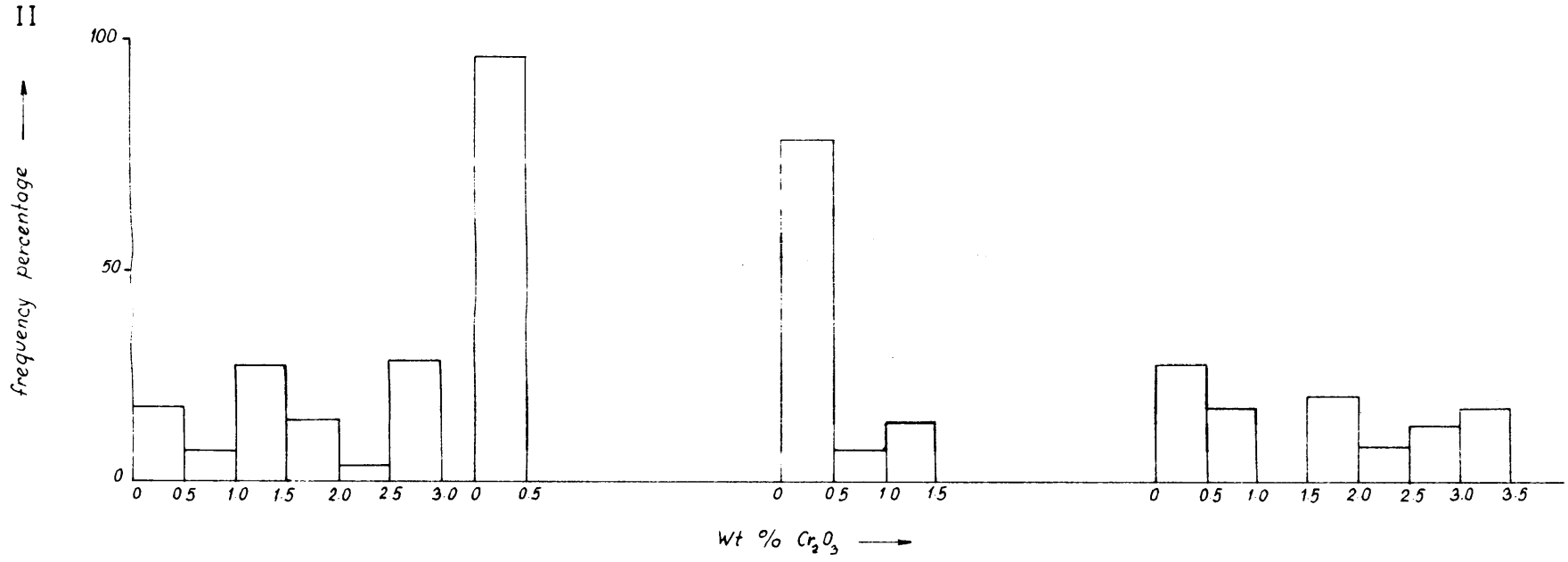

III

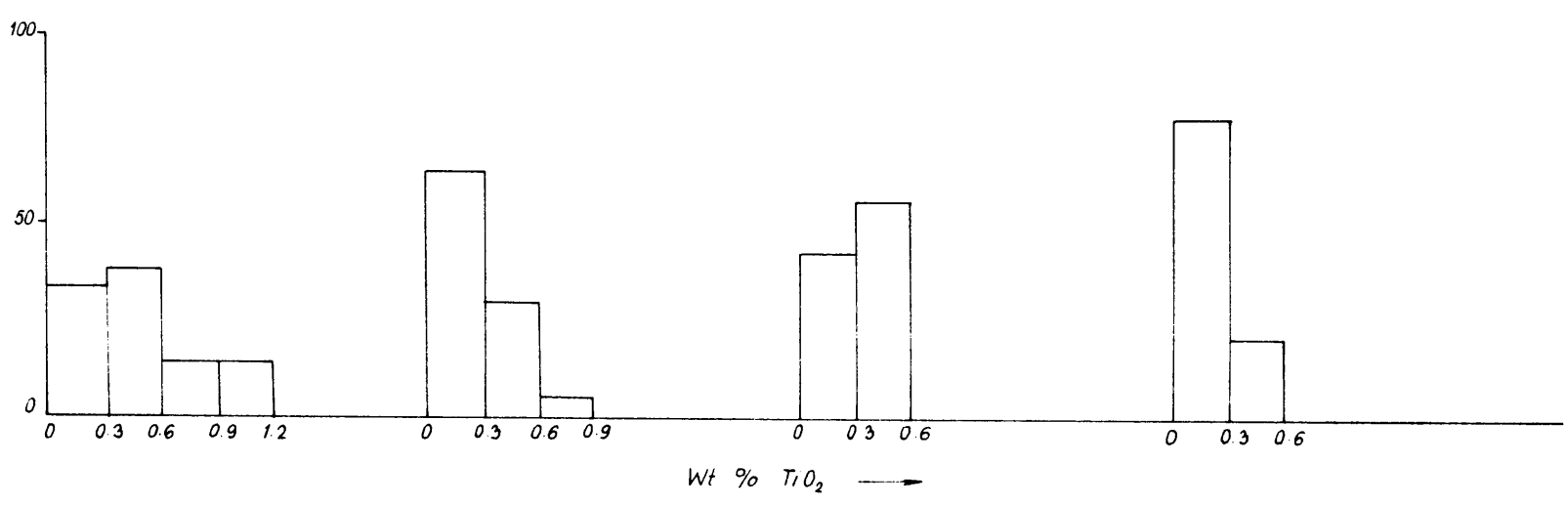

A Garnets from Kimberlite (38 analyses considered)

B Garnets from Grospydites (12 analyses considered)

C Garnets from Eclogite (23 analyses considered)

D Garnets from Garnet Peridotite (31 analyses considered)

FIG.

These diagrams yielded the following median values:

	% CaO	% Cr_2O_3	% TiO_2
kimberlitic garnets	5.3	1.5	0.5
garnet peridotitic garnets	4.5	1.6	0.2
eclogitic garnets	5.7	0.3	0.4
grospydite garnets	19.0	0.2	0.2

These median values indicate that the garnets from eclogite and grospydite, are characterized by a high grossular and a low uvarovite content compared with garnet from kimberlite and garnet peridotite. The TiO_2 content indicates that, according to the phase diagrams by McGreggor (1965, p.138), the garnet peridotites and grospydites formed under the same pressure conditions, and that the higher TiO_2 content of kimberlite garnets should be ascribed to its formation under reduced pressures. The intermediate position of the eclogitic garnets with respect to the CaO and Cr_2O_3 contents, and the higher TiO_2 content, indicate that this material can be considered to be the source material of the kimberlite magma, and the grospydites and garnet peridotites should then be viewed as the residue and cumulate phases respectively of the kimberlite magma.

The variation in the molecular proportions of pyrope, almandine and ugrandite (uvarovite, grossular and andradite) for the various parentages of garnets is given in figure 13. The complete overlap in the composition for the garnets from kimberlite and garnet peridotite as well as the variable Mg^{2+}/Fe^{2+} ratio, and the increased grossular content of the eclogitic garnets are also evident in this diagram. Two trends of enrichment can be distinguished in the garnet compositions, viz a pyrope-almandine and a pyrope-grossular trend.

4. Conclusions

1. The garnets from kimberlite are very similar to those in the garnet peridotites, except that the latter are low in TiO_2.
2. The eclogitic garnets are more enriched in Fe^{2+} and

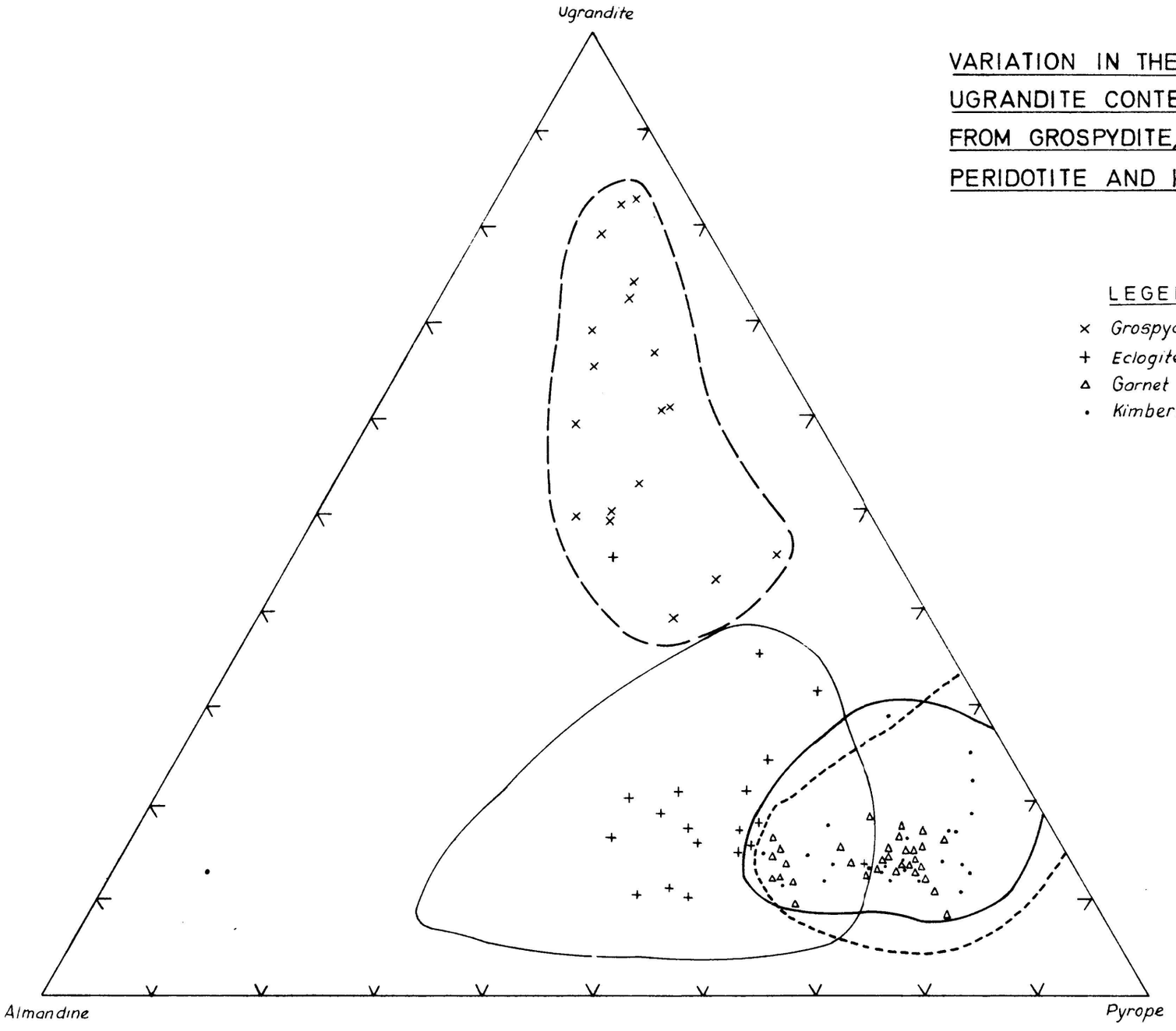

VARIATION IN THE ALMANDINE, PYROPE, UGRANDITE CONTENT IN THE GARNETS FROM GROSPYDITE, ECLOGITE, GARNET PERIDOTITE AND KIMBERLITE

LEGEND

× Grospydite
\+ Eclogite
△ Garnet peridotite
• Kimberlite

FIG.13

Ca^{2+} than the garnets from kimberlite or garnet peridotite.

3. Two variation trends could be discerned in the garnets, viz. (a) pyrope-almandine variation trend
(b) pyrope-grossular variation trend.

4. According to the stability fields for pyrope and almandine above 20 kb pressure (Boyd and England (1959), Yoder (1955) and Yoder and Chinner (1960, p. 81-83), a decrease in temperature at a constant pressure would cause a garnet on the join almandine-pyrope, to become enriched in almandine content. However, this only applies when the Mg^{2+}/Fe^{2+} ratio in the system remains constant, when no new mineral phases form, and when the distribution coefficients do not change with the change in pressure and temperature. Within the sequence of ultramafic rocks and eclogitic rocks the first and second conditions are constant, but the third may change. But should the distribution coefficients remain constant, a variation in Mg^{2+}/Fe^{2+} substitution is possible for a decrease in temperature at a constant pressure during crystallization of the magma. This process would then be able to account for the variation in Mg^{2+}/Fe^{2+} ratio of the garnets from the ultramafic nodules.

The grossular enrichment in the grospydite garnets can be explained by the extraction of Mg^{2+} and Fe^{2+}, due to the partial melting of eclogite at 30 kb pressure, and the formation of a garnet enriched in grossular. The Mg^{2+}/Fe^{2+} variation in the eclogitic garnets, could also be ascribed to crystallization during the slow decrease in temperature, at a constant pressure.

B. Olivine

1. Occurrence

Olivine occurs in both kimberlite and the ultramafic inclusions. In the kimberlite a first generation

(primary phenocrysts) and a second generation (secondary phenocrysts) could be distinguished. The former phase is present as large rounded inclusions, which are generally altered, in the residua phase, whereas the latter phase is present as small, fresh, euhedral phenocrysts. In the massive basaltic kimberlites the latter phase predominates, whereas the basaltic kimberlites consist mainly of first generation olivines.

The olivine in the ultramafic nodules comprises the intergranular material, having crystallized after the orthopyroxene. This olivine displays kink banding, undulatory extinction and recrystallization phenomena.

2. The mineralogy of olivine

In appendix 5 the indexed d-values of olivine from garnet peridotite, peridotite and second generation olivine from kimberlite are compared to the data supplied by Eliseiv (1955), and Yoder and Sahama (1957, p. 476). The indices of the latter authors have been accepted to calculate the a_o and c_o values and subsequently the indices were checked by comparing the experimentally determined $Sin^2\theta$ values and the values calculated according to equation (1).

$$Sin^2\theta = \lambda^2h^2/a_o^2 + \lambda^2k^2/b_o^2 + \lambda^2l^2/c_o^2 \text{-------} (1)$$

It was found that the h k l values supplied by Yoder and Sahama are correct and that the 030 reflection of Heckroodt, (1958) and Elesiev, (1957) should be 120. The unit-cell dimensions and the d_{130} values for the olivines are listed in appendix 6, together with the forsterite contents after Jambor and Smith (1964, p. 739) and Yoder and Sahama (1957) respectively. The curves by Heckroodt and Elesiev were not used, owing to the wrong indices, and the curves after Johanbagloo (1969, p. 247) were also not used owing to the fact that the composition calculated from the chemical analysed specimen from Premier Mine differed from the composition obtained by means of his curves.

The frequency distribution of the forsterite content of the olivine in kimberlite after the d_{130} values shows a bimodal distribution at forsterite 98 and forsterite 91, and a modal value of forsterite 96 for the ultramafic

nodules (figure 14A). Appendix 6 shows that the forsterite content of the second generation olivine corresponds to that of the olivine of the massive basaltic kimberlite, which has a forsterite content of 90 per cent.

The optical properties and the forsterite content of the olivine after Tröger (1959, p. 37) are given in appendices 7 and 8 for kimberlite and ultramafic nodules respectively. The frequency distribution of forsterite in the olivines from these percentages gives the following modal values: Kimberlitic olivines 91, regional peridotites 91, and ultramafic nodules 90 per cent Fo. Appendix 8 also shows that the first generation olivines are more enriched in forsterite than the second generation olivine, and also more enriched in forsterite than the olivine from the massive basaltic kimberlites.

3. The chemistry of the olivine

The chemical analyses and molecular percentages of the end member molecules are supplied in appendix 9. The molecular proportions of Ca_2SiO_4, Mg_2SiO_4, and Fe_2SiO_4; and Ni_2SiO_4, Mg_2SiO_4 and Fe_2SiO_4 are shown in figures 15A and 15B. These diagrams indicate that the olivine from the garnet peridotite nodules are the most enriched in forsterite, and that the olivine from the peridotite nodules plot in a line becoming increasingly enriched in fayalite. Neither Ca_2SiO_4 nor Ni_2SiO_4 are present in significant quantities in these olivines.

From the analyses it was established that no systematic relationship exists between the molecular percentages of forsterite and the weight percentages of CaO, TiO_2, Cr_2O_3, MnO and NiO, and that these ratios are of no use in distinguishing olivines from different parentages.

The chemical analyses of the olivines from kimberlite also show a bimodal distribution of forsterite content, viz. forsterite 95 for the first generation olivines and forsterite 89 for the second generation olivines from kimberlite.

4. Conclusions

1. The olivine from the garnet peridotite nodules is

THE FREQUENCY DISTRIBUTION OF THE FORSTERITE CONTENT IN THE OLIVINE FROM KIMBERLITE ULTRAMAFIC NODULES AND REGIONAL PERIDOTITES

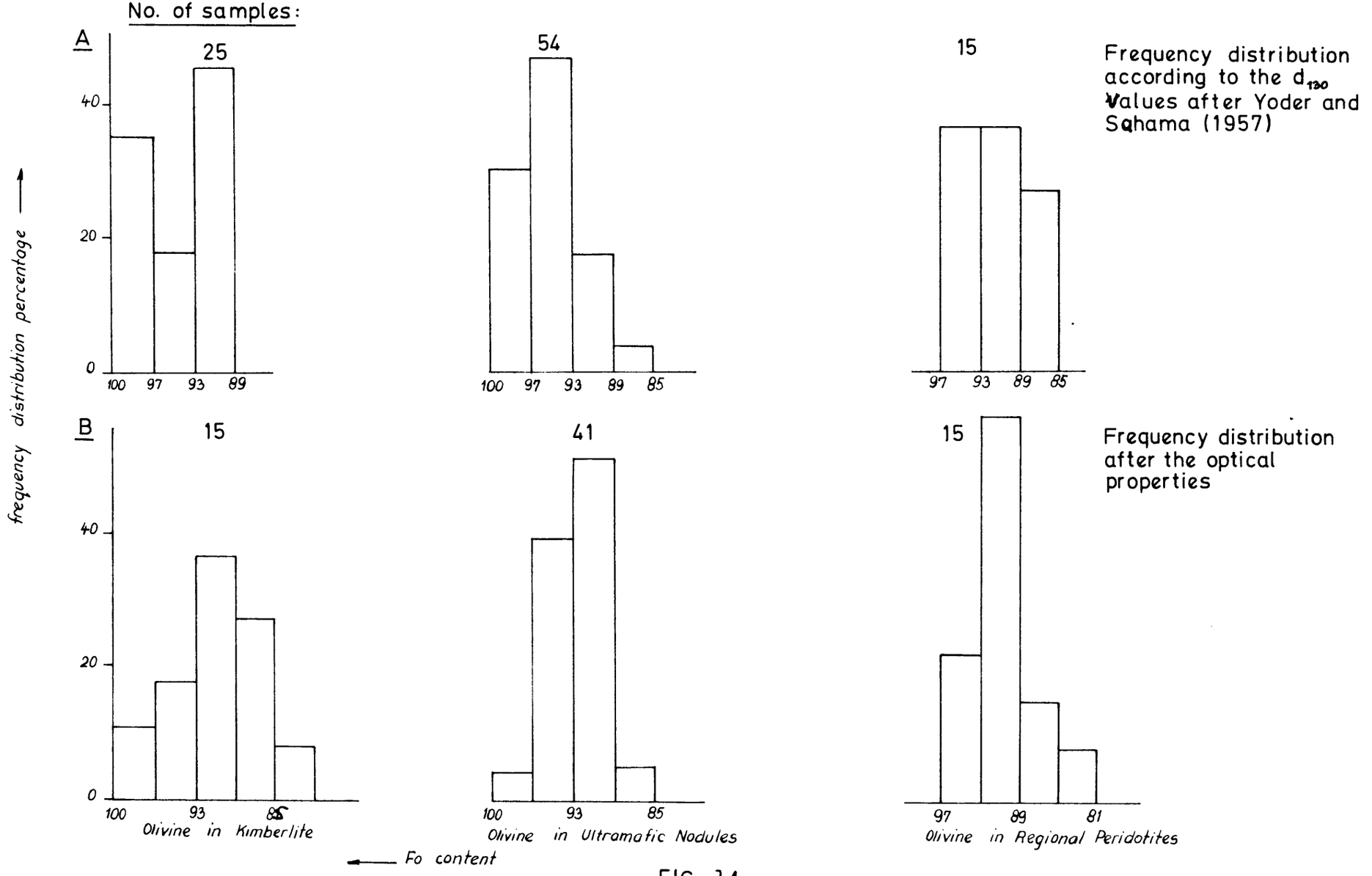

FIG. 14

LEGEND

+ Garnet Peridotite in Kimberlite
• Kimberlite
● Peridotite in Alkaline basalt
▲ Layered Intrusions
△ Regional Peridotites

Variation in Mg_2SiO_4, Fe_2SiO_4 and Ca_2SiO_4 contents of the olivine from various rock-types

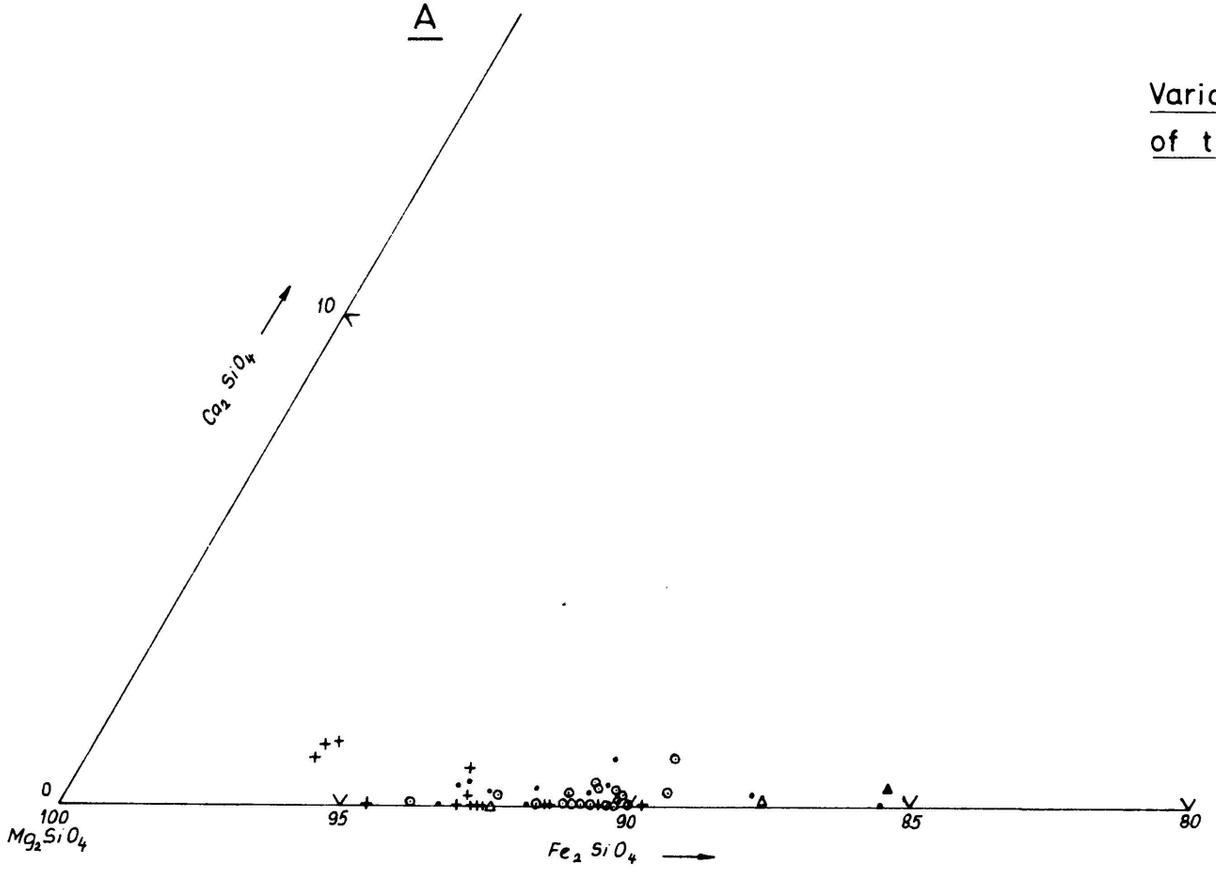

Variation in Mg_2SiO_4 Fe_2SiO_4 and Ni_2SiO_4 contents of the olivine from various rock-types

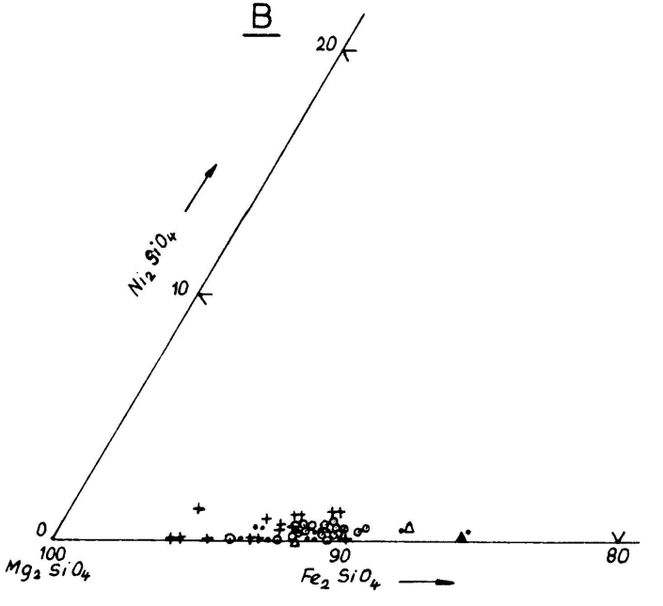

FIG. 1?

more forsterite-rich than those from the regional peridotites and from the peridotite nodules in alkaline basalts.

2. The first generation olivines compare ~~favourably to~~ well with the olivine from garnet peridotite nodules, whereas the second generation olivines are enriched in fayalite, and resemble the olivine in the massive basaltic kimberlites and in the peridotite nodules from alkaline basalts.

3. The first generation olivine probably formed simultaneously with the olivine in the garnet peridotite nodules [illegible], whereas the second generation olivine, and the olivine from peridotite nodules in alkaline basalts, formed during a later phase at lower temperatures, [illegible].

C. Ilmenite

1. Occurrence

The ilmenite occurs as rounded and elipsoidal grains or as aggregates of anhedral crystals. The amount varies from 0.1 to 8.0 per cent by volume.

The ilmenite is usually zoned in the group I-kimberlite from Premier Mine, and always surrounded by rims of alteration products. The alteration products consist of an outer rim of sphene succeeded by a zone of perofskite and terminated by a rim of leucoxene. The latter is the usual alteration product of ilmenite, and also forms along cracks in the ilmenite. The sphene and perofskite formed as a consequence of the reaction of ilmenite and the residua phase of the kimberlite, probably according to the reactions outlined below:-

$$(MgFe)TiO_3 + CaCO_3 \longrightarrow (MgFe)O + CaTiO_3 + CO_2$$
$$CaTiO_3 + SiO_2 \longrightarrow CaTiSiO_5$$

Exsolution lamellae of hematite in ilmenite were only observed in the metamorphosed kimberlite from Premier Mine, where they occur as small lenses parallel to (0001) of the ilmenite. Ilmenite grains which have been heated to 1000°C in a reducing atmosphere and subsequently quenched in mercury, yield worm-like and dendritic exsolution bodies of hematite parallel to (0001) of ilmenite (photo 28). The d-values of the heated ilmenite are compared with those of the untreated ilmenite in table 31. The former

revealed both ilmenite and hematite lines, whereas the latter only revealed ilmenite lines.

In the ilmenite from the Monastry and Kamfersdam kimberlites, myrmekitic intergrowths of clinopyroxene and ilmenite have been encountered. These intergrowths occur as large phenocrysts in the residua phase, and the d-values of the respective phases resemble those of the individual clinopyroxene and ilmenite phenocrysts in kimberlite. A sample consisting of an identical intergrowth from Hololo was also investigated. However, this sample also contained garnet and rutile, which indicate that the ilmenite replaces the pre-existing mineral phases. Texturally the evidence of replacement is also very clear (photo 29).

2. The Mineralogy of ilmenite

The X-ray powder data on the ilmenite were obtained by means of a Guinier Camera, using CuK radiation and silicon as an internal standard. The pattern was indexed because a line of low intensity with d = 1.612 ^{o}A was consistently recorded, but was not mentioned by Berry and Thompson (1962), Hounslow and Chao (1967) or the ASTM cards for geikielite. The ilmenite was indexed by comparing the $Sin^2\theta$ (Exp) values with the $Sin^2\theta$ (calc) values, and by subsequently checking the indeces by the extinction law - h + k + l = 3n where n = 1, 2 etc., for the R$\bar{3}$ space group. Hence this reflection was indexed as d_{122} (appendix 10).

The physical properties of the ilmenites are compared with the physical properties of some of the chemical analysed ilmenites in appendix 11. A diagram using the a_o and c_o-values of ilmenite as a function of the $FeTiO_3$, $MgTiO_3$ and Fe_2O_3 content has been constructed by using the a_o and c_o values of Winchell (1954) for Fe_2O_3, and $FeTiO_3$, and of Hounslow & Chao (1967) for $MgTiO_3$. This curve indicates a hematite content which varies from 0 to 25 per cent, and $FeTiO_3$ content which ranges from 35.0 to 52.0 per cent for ilmenite from kimberlite. The zoned ilmenites from the group I-kimberlite becomes enriched in $FeTiO_3$, up to 75.0 per cent.

Table 31. The d-values of natural and of heated ilmenite, both from the same crystal, Ti80. Guinier Camera, CuKα radiation

Sample Ti80 Film no. 432		Sample Ti80, heated Film no. 433		Mineral
I/I_o	d Å	I/I_o	d Å	
20	4.655			ilmenite
-		30	3.4962	hematite
-		20	3.1046	"
100	2.7301	100	2.7370	ilmenite
-		0.5	2.7008	hematite
-		40	2.5604	"
90	2.5317	60	2.5341	ilmenite
60	2.2230	40	2.2273	"
-		10	2.1195	hematite
-		10	2.0247	"
60	1.8560	80	1.8595	ilmenite
-		10	1.7320	hematite
70	1.7153	90	1.7160	ilmenite
20	1.6201	20	1.6239	"
10	1.6130		-	"
		10	1.5478	hematite
-		10	1.5344	"
50	1.4975	70	1.4992	ilmenite
50	1.4624	70	1.4638	ilmenite

A diagram constructed for the density as a function of the chemical composition of the ilmenite showed that the density is a more linear function of the composition than the c_o value. Consequently a diagram using the a_o values and the density as a function of the composition of the ilmenites has been constructed. This diagram has been checked by the a_o values and densities of analysed specimens, and it appears to be accurate within 2 per cent for the various end members.

The a_o-values and densities of the ilmenites which are reported in appendix 11 were plotted on this variation diagram in order to determine the variation in the composition of kimberlitic ilmenites. This diagram (figure 16) shows that the ilmenite/geikielite ratio varies from 72/28 to 53/47, and the hematite content from 2 to 20 per cent for kimberlitic ilmenites. This figure also reveals that an increase in the content of hematite in solid solution causes the unit-cell dimensions to decrease, and the density to increase. Hence an increase in pressure would favour hematite to enter into solid solution, whereas an increase in temperature at constant pressure would cause hematite to exsolve.

3. The chemistry of ilmenite

The chemical analyses, molecular percentages of the end member molecules, and the crystal-chemical formulas of ilmenite are given in appendix 12. In the calculation of the crystal chemical formulas the hematite in solid solution was not taken into account. The $FeTiO_3$, $MgTiO_2$ and $MnTiO_3$ variation diagram (figure 17A) indicates that the ilmenite from igneous rocks falls close to the $FeTiO_3$ end-point, and that the ilmenite from Skaergaard shows a differentiation sequence becoming enriched in $FeTiO_3$ and also in $MnTiO_3$ in the last stages of differentiation. The ilmenite from pegmatites are even more enriched in $MnTiO_3$, whereas the metamorphic ilmenites have any composition along the $MgTiO_3$, $FeTiO_3$ tie line. The composition of the metamorphic ilmenites depends on the chemical environment of crystallization. The ilmenite from anorthosites is only slightly more enriched in $FeTiO_3$ than that from kimberlites. The ilmenite in kimberlite has the highest content of $MgTiO_3$ of the ilmenites found in igneous rocks and contain 30.0 to 50.0 per cent of $MgTiO_3$.

On the $MgTiO_3$, $FeTiO_3$, Fe_2O_3 variation diagram (figure 17B) a line representing the maximum solid solution of hematite in ilmenite in subvolcanic rocks is shown, according to Edwards (1965). This diagram indicates that the ilmenite from Skaergaard and the metamorphic ilmenites plot below this line of maximum solid solution, whereas

DIAGRAM SHOWING THE COMPOSITION OF ILMENITE IN PERCENTAGE BY WEIGHT AS A FUNCTION OF THE a_o AND DENSITY VALUES

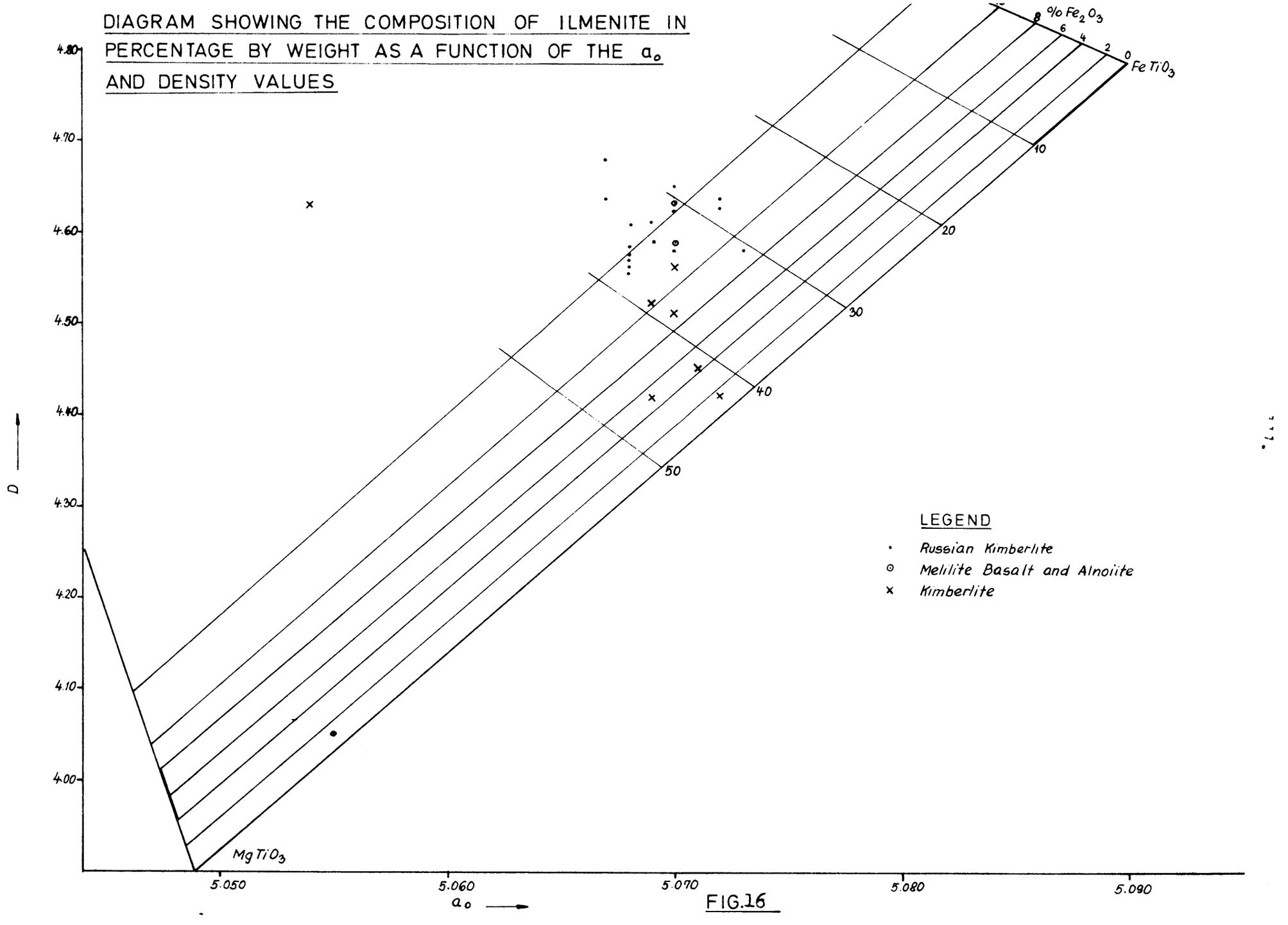

FIG.16

(A) THE VARIATION IN THE $MgTiO_3$, $FeTiO_3$ AND $MnTiO_3$ CONTENT OF SOME ILMENITES FROM VARIOUS ROCK TYPES LISTED IN APPENDIX 13

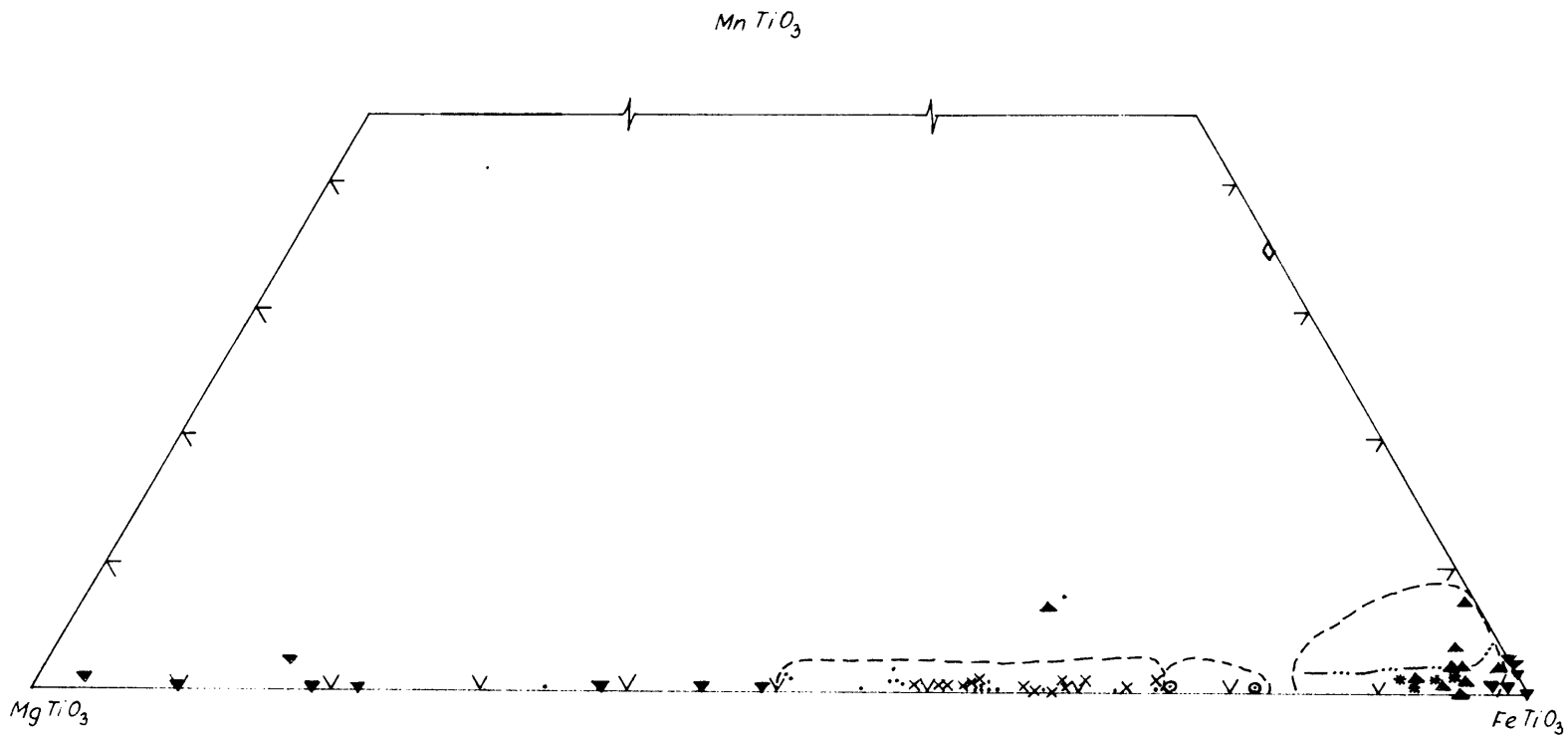

(B) THE VARIATION IN THE $MgTiO_3$, $FeTiO_3$ AND Fe_2O_3 CONTENT OF SOME OF THE ILMENITES LISTED IN APPENDIX 13

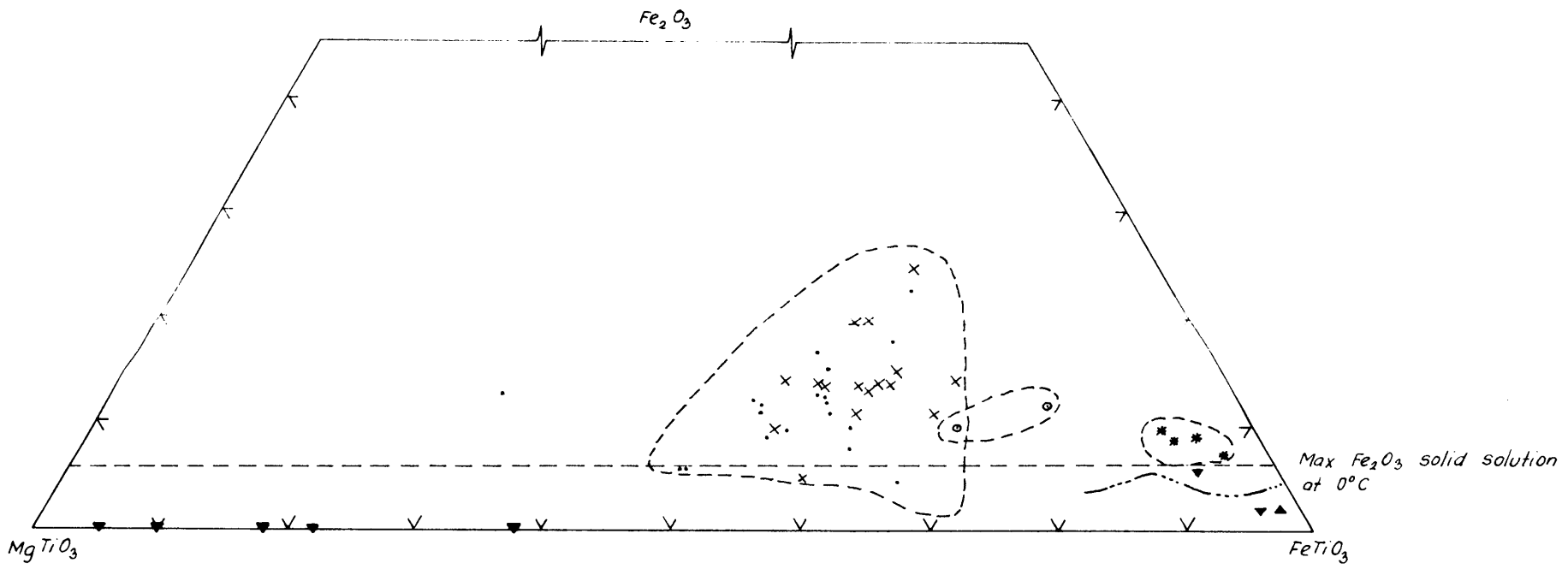

(C) THE VARIATION IN THE Fe_2O_3 AND $MgTiO_3$ CONTENT IN SOME IGNEOUS ILMENITES

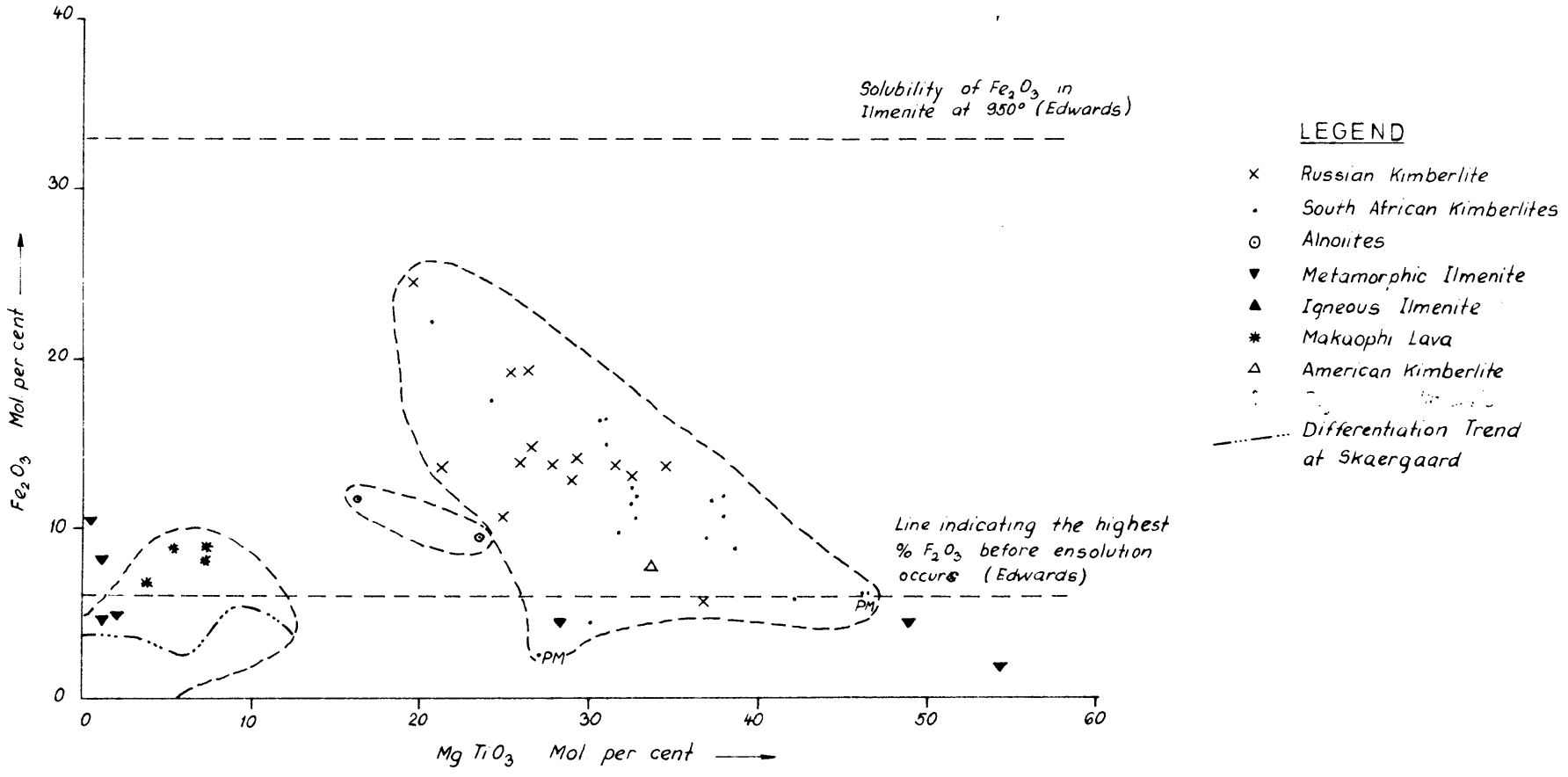

FIG. 17

the ilmenite from alnoiites, basaltic lavas and most of the kimberlite fall above this line. The ilmenite from kimberlite are by far the most enriched in Fe_2O_3, ranging from 6 to 25 per cent, showing an average of 14 per cent.

The variation in the molecular percentages Fe_2O_3 and $MgTiO_3$ for the different ilmenites (figure 17C) indicates that an increase in both constituents occurs in the sequence basalt, alnoiite and kimberlite. The NiO, MnO and Cr_2O_3 contents of the kimberlitic ilmenites do not show any variation trend with respect to either the $MgTiO_3$ or Fe_2O_3 contents.

The TiO_2 content in kimberlite varies from 1.0 to 5.0 per cent, and according to Dawson (1967, p 270) shows a modal value of 2.03 to 2.32 per cent, which is higher than the average of tholeiitic rocks but similar and even lower than that of some alkaline basaltic rocks. According to Chayes (1965) the Cenozoic oceanic basalts can be grouped into the TiO_2-rich alkaline basalts, and the TiO_2-poor tholeiitic basalts, hence it is clear that TiO_2 enrichment is a characteristic of alkaline basalts. According to McGreggor (1965) the system MgO, TiO_2, SiO_2 has revealed that at pressures increasing from 10 to 20 kb, and probably also at higher pressures, TiO_2 goes into the melt. Hence the magmas which generate at high pressures (alkaline basalts according to Yoder and Tilley, 1962) would be enriched in TiO_2 whereas the residue and cumulates which formed at this pressure would be depleted in TiO_2. The frequency distribution diagram for TiO_2 in eclogite and garnet peridotite is represented in figure 18, and indicates that the garnet peridotites are depleted in TiO_2, whereas the eclogites are more enriched in TiO_2. Hence it is concluded that the eclogites are the source material of the TiO_2 in the mantle, and that the garnet peridotites are the cumulus phase which formed at high pressures (more than 20 kb), whereas the kimberlite being enriched in TiO_2 represents the residual magma.

4. <u>The genesis of ilmenite</u>

1. The Mg/Fe ratio of the ilmenite in kimberlite is the highest of all igneous rocks known, and it corresponds to the Mg/Fe ratio of ilmenite in alnoiite.

THE FREQUENCY DISTRIBUTION OF TiO_2 IN ECLOGITE AND GARNET PERIDOTITE

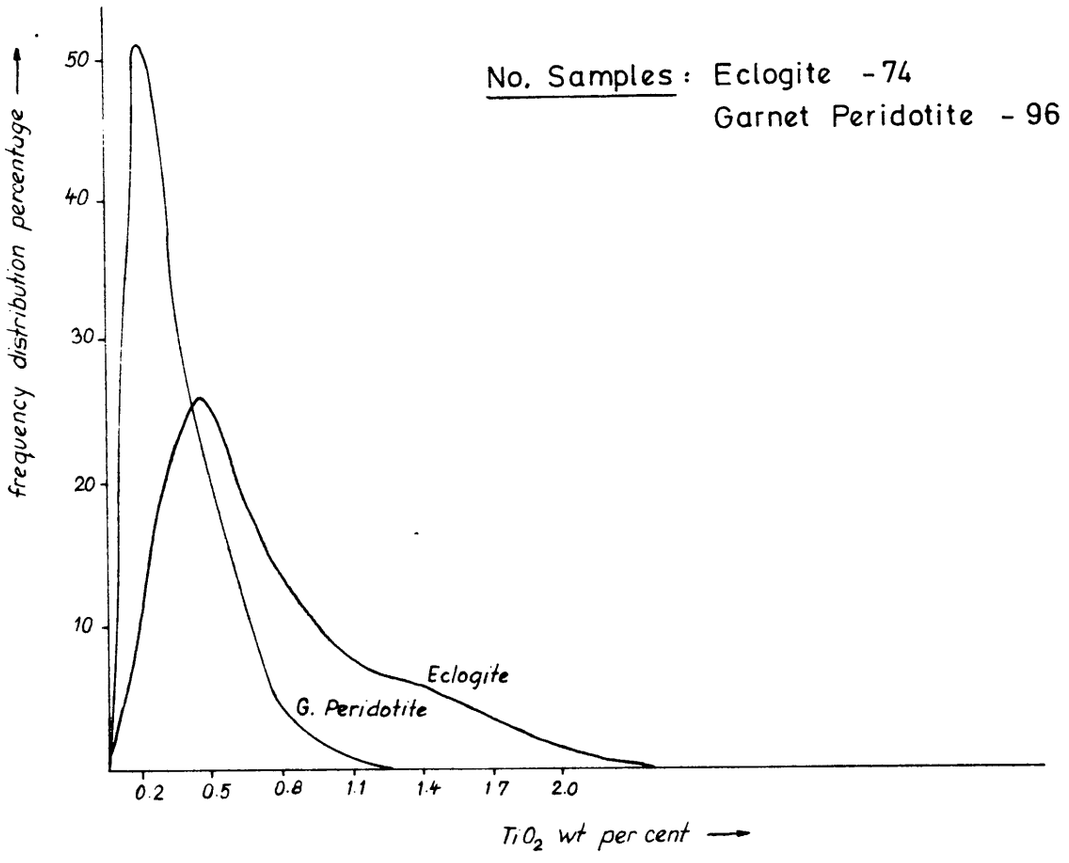

FIG18

2. The kimberlitic ilmenite must have crystallized above 950°C in order to be able to contain up to 25 per cent of Fe_2O_3 in solid solution, and must have been quenched during emplacement.

3. The increase in density and decrease in the unit-cell volume with an increase in Fe_2O_3 solid solution indicate that the kimberlitic ilmenite formed at elevated pressures. The positive relationship between $MgTiO_3$ and Fe_2O_3 found in ilmenite also substantiates this conclusion, since $MgTiO_3$ is believed to form at elevated pressures (Besson, 1967).

4. According to McGreggor (1965, p. 138) the TiO_2 goes into the melt in the region above 15 kb, thus it is clear that the ilmenite crystallized below 15 kb. The myrmekitic intergrowths of chrome-diopside and ilmenite, coexisting with garnet, indicate that the ilmenite probably formed close to 15 kb pressure. The absence of feldspar in kimberlite, and the presence of the myrmekitic intergrowths of chrome-diopside and chrome-spinel in kimberlite indicate that the association ilmenite and chrome-diopside formed at pressures of 12 to 15 kb.

5. The source of the TiO_2 for the kimberlite is the eclogite zone in the mantle of the earth, and both the residue and cumulus phases, viz. the grospydites and garnet peridotites, are depleted in TiO_2.

D. Chromite

Chromite occurs in the kimberlite matrix as euhedral to subhedral grains and as a myrmekitic intergrowth with clino-pyroxene. In the ultramafic and eclogite nodules the chromite is present as small euhedral grains in the kelyphytic rims surrounding the garnets. In the spinel peridotites and spinel pyroxenites the chromite is present as euhedral grains and as a myrmekitic intergrowth with clinopyroxene.

The d-values of all the chromites from Premier Mine correspond more closely to those of picotite and magnesio-chromite than to those of chromite (table 32.) The a_o-values and the refractive indices of the chromites from Premier Mine compare well with the values of the chromite from the Mir kimberlite and from the Twin Sisters dunite (ophiolitic intrusion) (table 33).

Table 32. The d-values of the chromite, magnesiochromite and the spinel phases from the Premier Mine kimberlite. The d-values obtained by means of a Debye Scherrer Camera, using CuK$_\alpha$ radiation

PM 893 In_{21} Film No. 484		Magnesiochromite			chromite	
Kelyphyte		Berry & Thompson (1962, p. 195)				
I/I_o	d (Å)	I	d (Å)	h k l	I	d (Å)
		2	4.76	111	4	4.80
6	2.908	2	2.92	220	2	2.95
10	2.477	10	2.49	311	10	2.51
8	2.053	5	2.07	400	5	2.08
		½	1.687	422	½	1.704
8	1.579	6	1.593	333,511	6	1.602
9	1.451	7	1.466	440	8	1.473
2	1.253	1	1.265	533	1	1.271
		½	1.249	622	½	1.254
1	1.187	½	1.197	444	1	1.201
				551,711	½	1.166
		½	1.108	642	1	1.112
4	1.068	5	1.081	553,731	9	1.084
1	1.028	2	1.038	800	4	1.041
a_o = 8.215		a_o = 8.277			a_o = 8.326	

Table 33. The physical properties of the various types of chromite. The unit-cell dimensions were obtained by means of a Debye Scherrer Camera, using CuKα radiation

Sample	Type of chromite	a_o Å	n
1060-25	inclusion in kimberlite	8.142	1.810
1570-9	myrmekyte	8.212	1.935
893 In_{21}	kelyphyte	8.215	1.936
893 In_4	myrmekyte	8.311	2.091
1010 In_2	"	8.228	1.803
893 In_3	"	8.315	2.105
893 In_8	kelyphyte	8.170	1.860
1010-38	kimberlite	8.180	1.880
Twin Sisters	serpentinite	8.311	-
Mir	kimberlite	8.183	1.90

Since the amount of chromite was insufficient for chemical analyses, the chemical composition of the chromite was determined by means of the a_o-value, which is a function of the chemical composition (McGregor and Smith, 1963). According to McGreggor and Smith (1963, p. 410) the weight percentages of the constituents obtained by their curves, are by no means absolute. However they maintain that their method is suitable to indicate major chemical trends. The reliability of the curves are also improved when it is known that the chromites crystallized at the same temperatures.

In appendix 13 the chemical compositions of the chromites thus determined, are compared to the compositions of chromites from stratiform intrusions, ophiolitic intrusions and kimberlites.

Since the compositions of the chromites from Premier Mine were determined by means of the method after McGregor and Smith (1963), the conclusions based on these results should be regarded as being tentative. Nevertheless, the compositions listed in appendix 13 suggest that:

1. The chromite from stratiform intrusions is marked by a higher FeO/MgO and a lower Al_2O_3/Cr_2O_3 ratios than the chromites from the ophiolitic peridotites. The kimberlitic chromites also follow the same trend as that of the ophiolitic chromite, and display a sequence from kelyphitic to symplectitic chromite becoming increasingly enriched in FeO and Cr_2O_3. Thus the chromite which formed as a consequence of the equilibration of garnet (kelyphyte) contains increased amounts of Al_2O_3, and coexists with chrome diopside, whereas the chromite which crystallized from garnet during the melting and crystallization sequence is enriched in Cr_2O_3 and coexists with aluminous enstatite.

E. Orthopyroxene

1. Occurrence

Orthopyroxene occurs in the peridotite and pyroxenite nodules, and is also present as phenocrysts in the kimberlite. Although the orthopyroxene from kimberlites is extensively altered to talc, fresh material was obtained from some heavy concentrates. The heavy medium concentrates from Brakfontein, kindly supplied by Dr. C.P. Snyman, contained a dark-brown, "glassy" orthopyroxene, which has the same physical properties as the other phenocrysts of orthopyroxene. A thin section of this "glassy" orthopyroxene, however, also displays the presence of a fine-grained glassy orthopyroxene, simulating the material described from the eclogitic clinopyroxenes.

2. The mineralogy of orthopyroxene

The unit-cell dimensions of orthopyroxene were calculated by using the 060, 1400, 004, 1200, 002 and 040 reflections. These indices were checked for one sample of orthopyroxene, by determining the a_o, b_o, c_o dimensions

by means of a Weissenberg Single Crystal Camera, and subsequently calculating the $Sin^2\theta$(Calc.) values. These latter values were compared to the $Sin^2\theta$ (Exp) values, obtained by means of a Guinier Camera, for the 6 reflections mentioned previously, and revealed a difference of less than 0.00027, which is close to the error of measurement.

The unit-cell dimensions thus determined, the molecular percentage enstatite and the Al^{VI} content after Brown (1967) are reported in appendix 14. The optical properties and the molecular percentage of enstatite after Tröger (1959) for the different orthopyroxenes are also supplied in appendix 14.

The frequency distributions of the molecular percentages of enstatite in the orthopyroxenes as determined from the optical properties are depicted in figure 19, for the various rock-types. This diagram indicates that the orthopyroxenes from garnet peridotites are more enriched in enstatite than those from peridotites, and that the kimberlitic orthopyroxene appears to have a bimodal distribution, corresponding with the garnet peridotites and peridotites. However, this apparent bimodal distribution may also be due to insufficient samples.

The molecular percentage of Al^{3+} in the orthopyroxenes was determined from a combination of the molecular percentage enstatite after Hess, and the Δ d (10.3.1) - (0.6.0.) and $\Delta\alpha$ (21.1) qz - (060) values according to the method described by Zwaan (1954, p 206-209). The molecular distribution Ca^{2+} was determined from the enstatite content after Hess, and from the Δ d(20.3) qz - (060) according to Zwaan (1954). These values are reported in appendix 15.

The frequency distributions of the mol. per cent Al^{3+} after Zwaan, and the Al^{VI} content in the same orthopyroxenes after Brown are compared in figure 20. This figure indicates a modal value of 0.027 per cent Al^{3+} in the orthopyroxenes, and of 0.022 per cent Al^{VI}, which indicates that the alumina in the orthopyroxene mostly enters the Y position. The chemical analyses of the orthopyroxenes in the ultramafic nodules indicate that the modal Al^{3+} content in the orthopyroxenes in these nodules is 0.05,

THE FREQUENCY DISTRIBUTION OF ENSTATITE IN THE ORTHOPYROXENE FROM KIMBERLITES, GARNET PERIDOTITES AND PERIDOTITES ACCORDING TO THE OPTICAL PROPERTIES

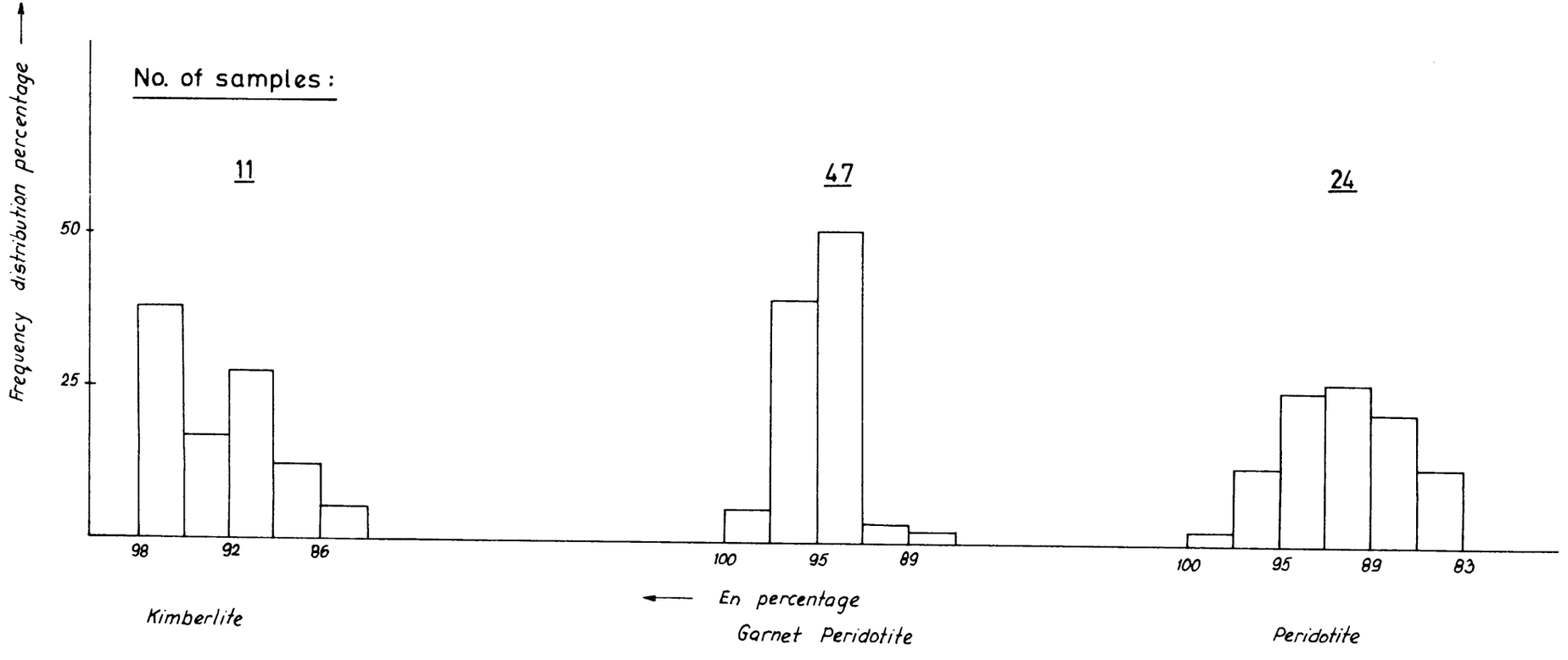

FIG.19

THE Al^{3+} IN THE ORTHOPYROXENE FROM GARNET PERIDOTITE AFTER ZWAAN, AND Al^{3+} CONTENT IN THE OCTAHEDRAL POSITION AFTER BROWN (1967)

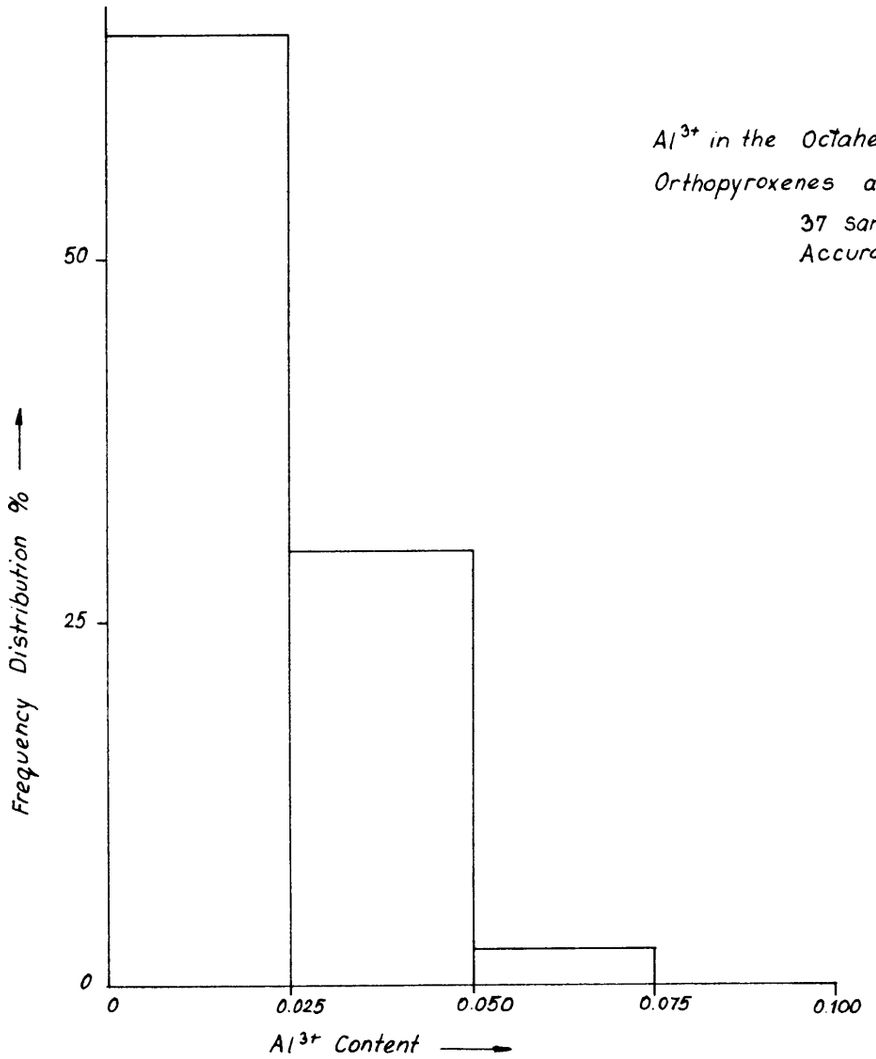

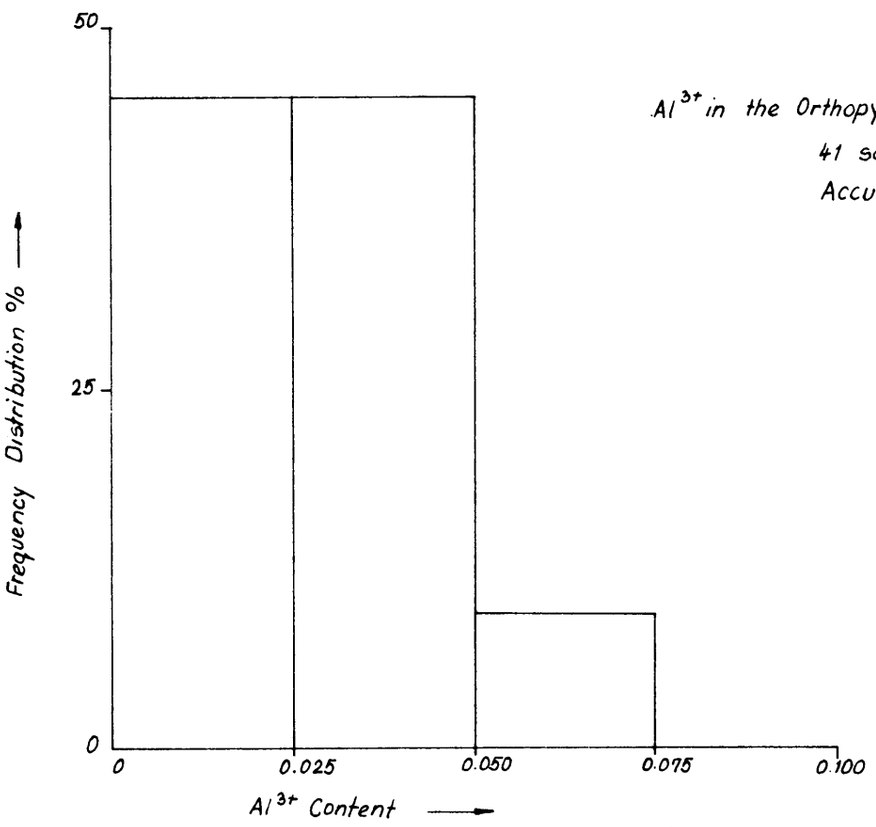

FIG. 0.

which is much higher than the value observed by means of the curves after Zwaan (1954). However the Al_2O_3 content in the orthopyroxenes in peridotite nodules exceeds that of the orthopyroxenes in garnet peridotites, consequently the value of 0.05 may again be too high. The analyses of orthopyroxenes from the garnet peridotites from Premier Mine indicate an even higher Al^{3+} content, viz. 0.09. Hence the conclusion regarding the Al^{VI}/Al^{IV} distribution in the orthopyroxenes as was determined by means of X-rays, should be applied with caution.

3. The chemistry of the orthopyroxenes

The chemical analyses and the molecular norms of the orthopyroxenes from the garnet peridotite nodules and from kimberlites are listed in appendix 16. The molecular norms of the orthopyroxenes were calculated according to the method proposed by Kushiro (1962). This method of calculation facilitates the constant distribution of Na^+ between acmite and jadeite, and consequently it results in a molecular norm in which the acmite and jadeite values are comparable. The structural formulas were calculated from these molecular norms according to the method suggested by Hess (1949). Because the molecular norms were calculated according to the method described above, the resulting structural formulas have comparable Al^{VI}/Al^{IV} ratios, but the structural formulas do not correspond exactly to the ideal pyroxene formula. Although several factors may influence the Al^{VI}/Al^{IV} ratios obtained in this way, they can be used on a comparative basis.

The variation in the composition of the orthopyroxene is shown on figure 25, which indicates that the orthopyroxene from the peridotite nodules in alkaline basalts generally contain more $FeSiO_3$ and diopside in solid solution than the orthopyroxenes from the garnet peridotite nodules. The latter, however, compares favourably with the garnet peridotites in gneiss masses (eg. Almklovdalen), Du Rietz (1935), whereas the orthopyroxenes from kimberlite overlaps with the orthopyroxenes in peridotites and garnet peridotites.

THE VARIATION IN THE $CaSiO_3$, $MgSiO_3$, $FeSiO_3$ CONTENT FOR THE ORTHOPYROXENES FROM VARIOUS ULTRAMAFIC PARENTAGES

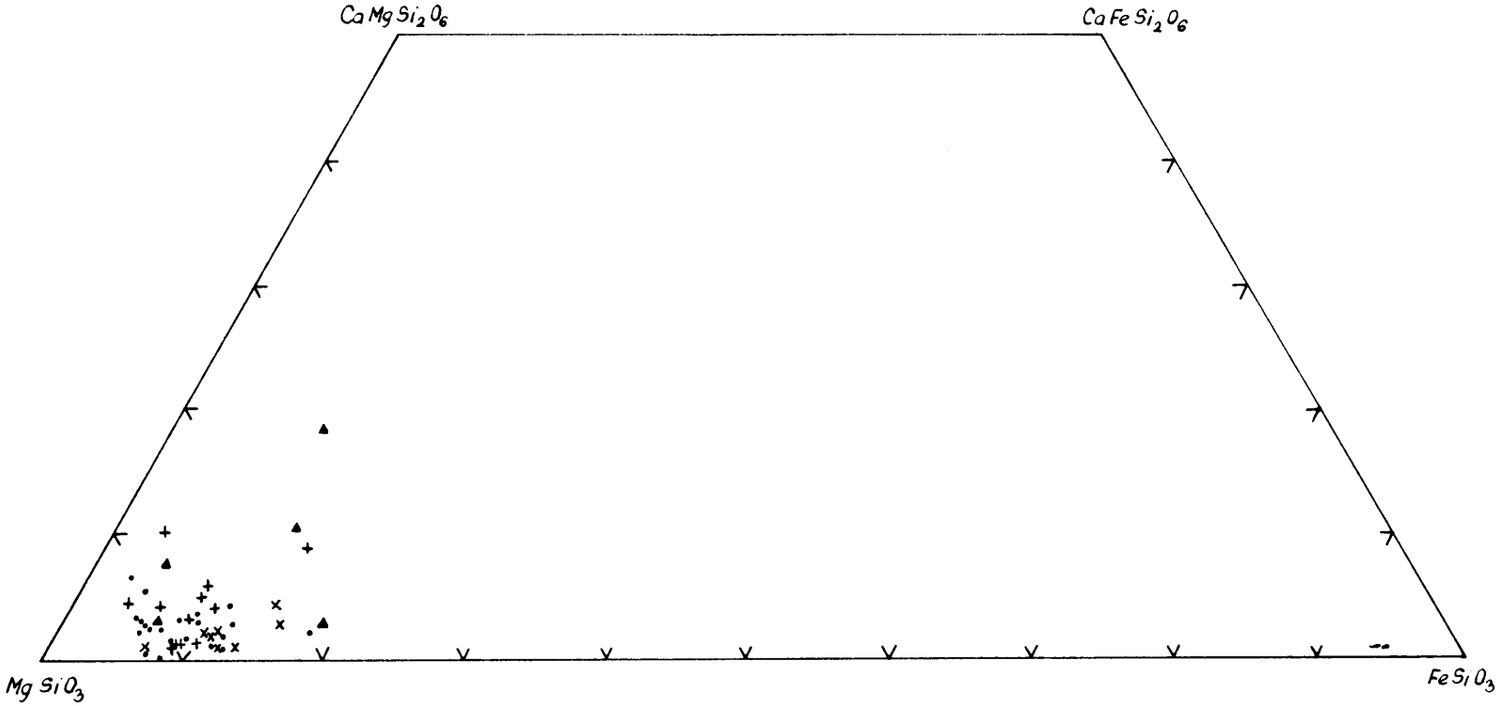

LEGEND

- • Orthopyroxene from Garnet Peridotite in Kimberlite
- ▲ Orthopyroxene from Peridotite in Alkaline basalts
- \+ Orthopyroxene in Kimberlite
- × Orthopyroxene in Regional Garnet Peridotites

FIG. 21

The weight percentage of Al_2O_3 as a function of the diopside content in solid solution (figure 23) shows the same distribution for the orthopyroxenes from both types of garnet peridotites, whereas the orthopyroxenes from the peridotite nodules from alkaline basalts are enriched in Al_2O_3. The kimberlitic orthopyroxenes overlap with those from peridotites, and are even more enriched in both Al_2O_3 and diopside.

The distribution of Al^{3+} between the X and Y positions of the orthopyroxenes (appendix 16) indicates that both the peridotitic and kimberlitic orthopyroxenes are enriched in Al^{IV}, whereas the orthopyroxenes from garnet peridotite show a variable ration of Al^{VI}/Al^{IV} but are generally more enriched in Al^{VI}. The results obtained by means of X-rays also yielded the same increase in the Al^{VI} content of the orthopyroxenes in the sequence kimberlite, peridotite, garnet peridotite.

The distribution of Al_2O_3 and Cr_2O_3 as a function of the Mg^{2+} content of the orthopyroxenes shows a much higher value for the kimberlitic orthopyroxenes than for the orthopyroxenes from the ultramafic nodules (figure 23). The Al_2O_3 content increases in the orthopyroxenes in the sequence garnet-peridotite, peridotite, kimberlite.

4. Conclusions

1. The orthopyroxene from kimberlite compares favourably with those in the peridotite nodules, but differs considerably from the orthopyroxenes in the garnet peridotites (figures 24-27).

2. The content of Cr_2O_3, Al_2O_3 and diopside in solid solution in the orthopyroxenes increases in the sequence garnet peridotite, peridotite, pyroxenite, kimberlite. The orthopyroxenes from the spinel peridotites and the garnet peridotites, however, are identical, which indicates that only the garnets from the garnet peridotites are equilibrated to form spinel and that the orthopyroxenes in these nodules are therefore still the same as in the original garnet peridotite nodules.

3. The decrease in Al^{IV} content of the orthopyroxenes in the sequence kimberlite, peridotite, garnet peridotite

THE VARIATION IN THE WT % Al_2O_3 / DIOPSIDE$_{ss}$ MOL. % IN THE ORTHOPYROXENES FROM VARIOUS ROCK - TYPES

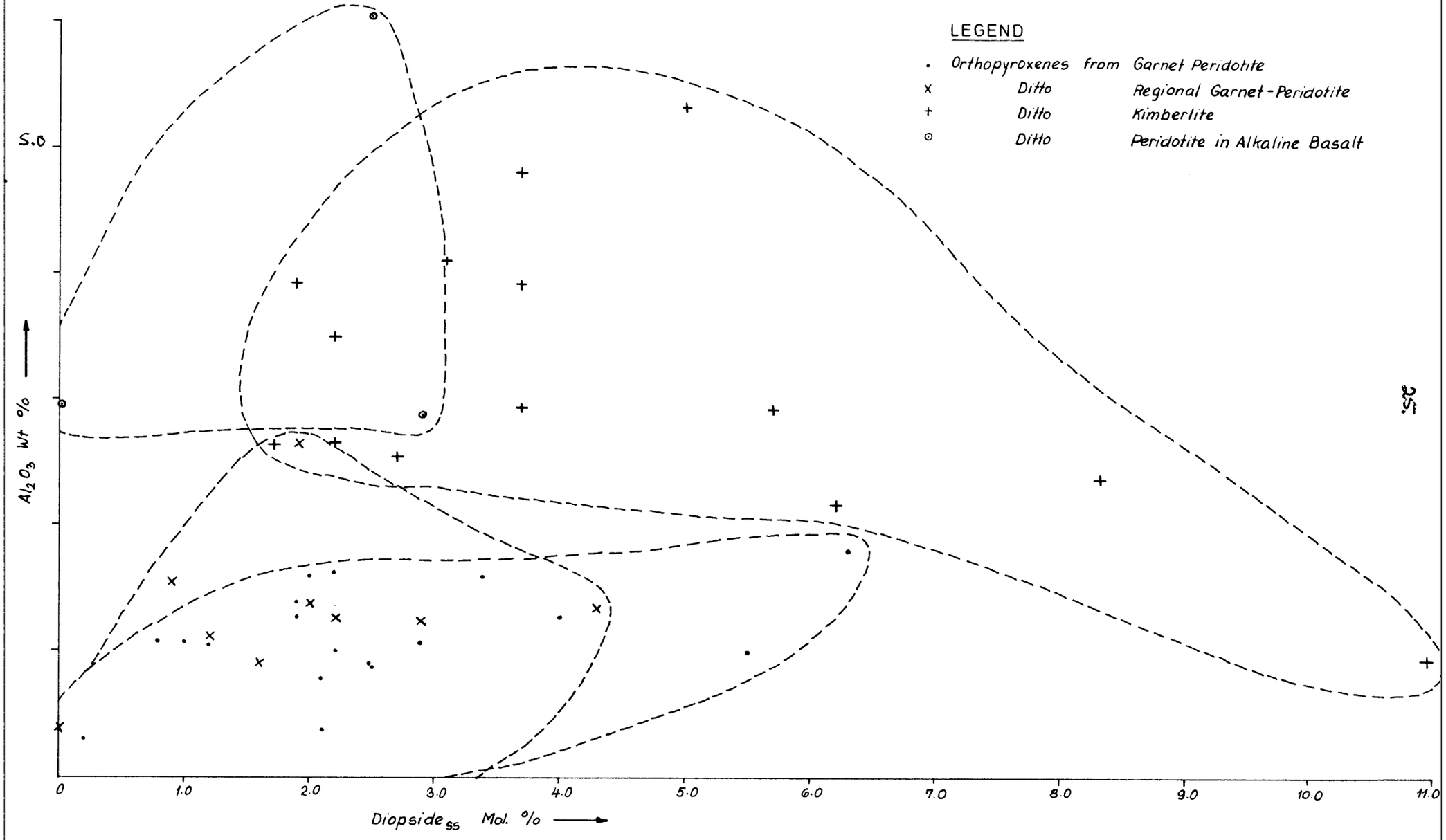

FIG. 2

THE VARIATION IN THE WEIGHT PERCENTAGES OF Cr_2O_3 AND Al_2O_3 FOR THE VARIOUS MOL. PERCENTAGES OF Mg^{2+} IN THE ORTHOPYROXENES FROM VARIOUS ULTRAMAFIC NODULES

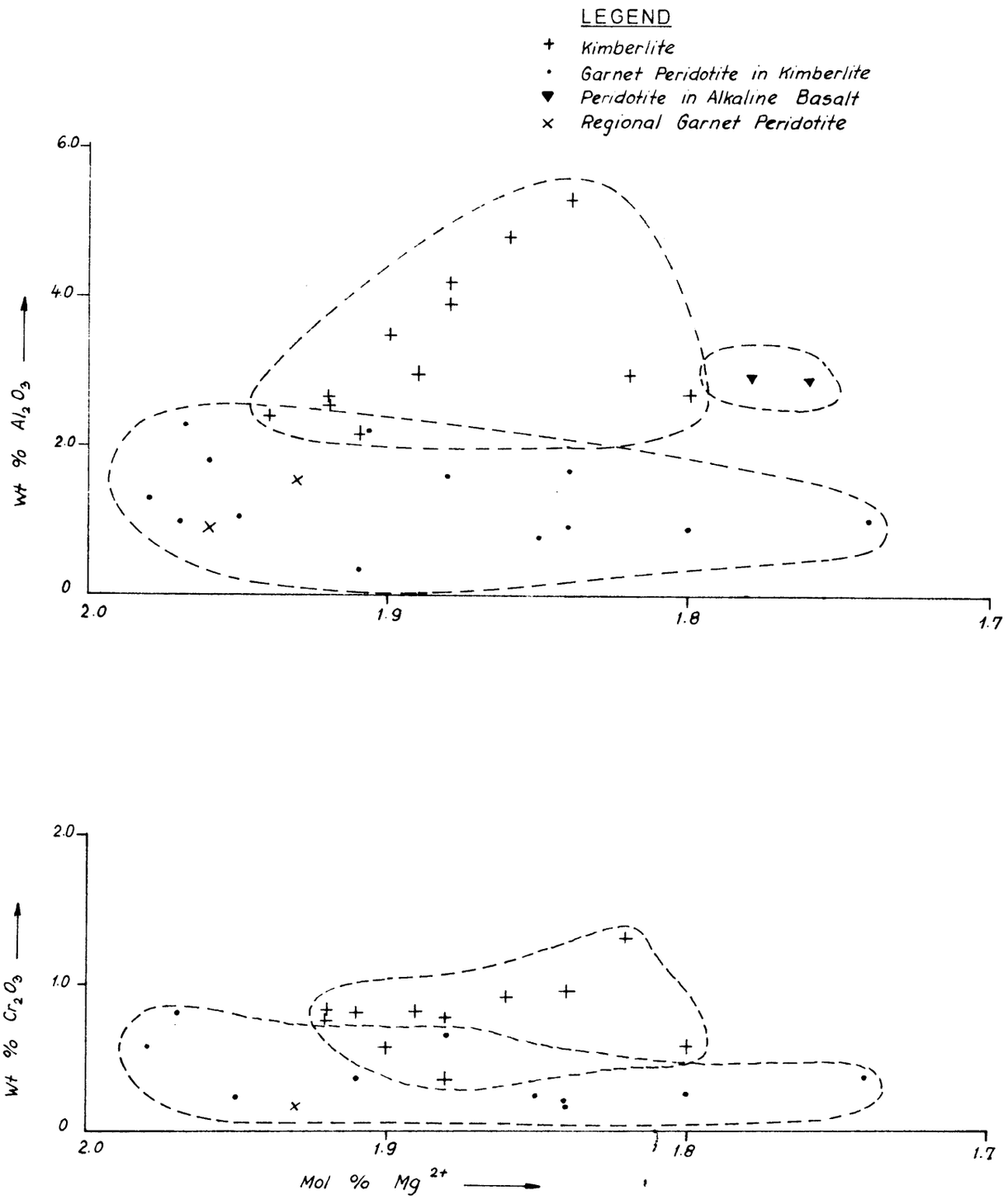

FIG. 23.

indicates an increase in the pressure of formation from kimberlite to garnet peridotite (Thompson, 1947).

4. The content of diopside in solid solution and of Al_2O_3 (appendix 16) can be used as indications of the temperature and pressure conditions in the earth at which the various orthopyroxenes crystallized. The following estimates were made by using the phase diagrams of Boyd and England (1964, p. 158) and MacGregor and Ringwood (1964, p. 162) to determine the pressure, and the diagrams after Boyd and Schairer (1964) and Davis and Boyd (1966, 3571) to determine the temperature. The phase diagram after Green and Ringwood (1967, p. 155) has been used to check the estimations and to correlate the depth in kilometer.

Type of Nodule	Pressure (Kb)	Temperature (^{o}C)	Depth (Km)
Garnet peridotite	32-30	1100	110
peridotite	29-24	1200 to 1300	70-100
pyroxenite	25-20	1300 to 1400	60-70
orthopyroxene in kimberlite	18-32	1100 to 1400	50-110

F. Clinopyroxene

1. Occurrence

Clinopyroxene occurs as phenocrysts in the Premier Mine kimberlite and as porphyroblasts in the meta-kimberlite. The eclogite and pyroxenite nodules invariably contain clinopyroxene, whereas the garnet peridotites often contain a small amount of clinopyroxene. In the kimberlite the clinopyroxene is present as primary phenocrysts or as a myrmekitic intergrowth with chromite. In the garnet peridotite the clinopyroxene occurs as large euhedral to subhedral grains in the olivine matrix, and in the pyroxenite nodules it is present in both the cumulus and intercumulus phases. Exsolution lamellae of orthopyroxene, kinkbanding and undulatory extinction do not occur in the clinopyroxene of either the kimberlite or the inclusions in kimberlite.*1) Texturally it appears as

*1) Recent investigation proved undulatory extinction in the eclogitic clinopyroxenes.

if the clinopyroxene crystallized after the garnet and orthopyroxene, but before the olivine.

The clinopyroxene in the eclogite nodules is altered to a fine-grained, micro-crystalline phase along the outer rims of the grains, and also in the central portions of the grains. The d-values of this fine-grained clinopyroxene phase are compared with the d-values of the unaltered clinopyroxene from the same eclogite nodule in table 34. This fine-grained clinopyroxene is also often transitional into a brownish glass, which indicates that the original eclogitic clinopyroxenes were partially melted at some stage.

A light greenish "glassy" clinopyroxene was also observed in the kimberlite from Lovedale, however, in thin section this material resembles the phenocrystal clinopyroxenes in kimberlite, by being completely crystalline. The d-values of this clinopyroxene are compared with the fine-grained, and eclogitic clinopyroxenes in table 34.

Three types of phenocrystal phase clinopyroxenes occur in the kimberlites, viz. a vivid green, glassy type, a dark-green silky type, and a light green soapy type. The d-values of each of these types of clinopyroxenes are compared with those of the clinopyroxenes from eclogite, kyanite eclogite, garnet peridotite, C2/c omphacite (Clarke & Papike, 1968), P2 omphacite (Coleman, 1959) and Ca-Tschermak-bearing clinopyroxene (Sakata, 1957) in appendix 17. This table indicates that the d-values of P2 omphacite differs slightly from those of the C2/c clinopyroxenes, and that the d-values of the different morphological types of clinopyroxenes also differ slightly.

The d-values of the various igneous and metamorphic clinopyroxenes in the Premier Mine kimberlite are compared in table 35, however, the d-values of these pyroxenes do not vary considerably.

2. The mineralogy of clinopyroxenes

The optical properties of the various clinopyroxenes are listed in appendix 18. The data indicate that the eclogitic clinopyroxenes have a $2V_{\gamma}$ ranging from 64° to 73°, but mostly exceed 70°. This high 2V is probably due

Table 34. The d-values of the clinopyroxene from Lovedale kimberlite, compared to the "glassy" clinopyroxene and the fine-grained clinopyroxene in the eclogite nodules. The d-values were obtained by means of a Guinier Camera, using CuKα radiation

Clinopyroxene Lovedale kimberlite Film no. 438		Glassy clinopyroxene Lovedale kimberlite Film no. 439		Fine-grained clinopyroxene in eclogite B_2B from Lovedale Film no. 440	
I/Io	d Å	I/Io	d Å	I/Io	d Å
4	4.397	2	4.458		
5	3.314	7	3.335	3*	3.324
3	3.184	7	3.222	3*	3.212
10	2.969	10	2.986	10	2.984
6	2.903	6	2.936	3	2.964
6	2.874	5	2.891	3*	2.890
1	2.578	5	2.558	4	2.550
4	2.538	2	2.532	9	2.521
5	2.512	7	2.518	3*	2.496
5	2.476	6	2.501	3	2.468
4	2.260	4	2.284	2	2.254
5	2.193	6	2.204	4*	2.204
5	2.183	6	2.190	6	2.192
-	-	2	2.146	3	2.180
1	2.122	3	2.127	1*	2.120
3	2.1112	3	2.1026	1*	2.1016
2	2.0859	3	2.0339		
4	2.0145	4	2.0153	2*	2.0115
4	2.0115	6	1.9933	2*	1.9923
3	1.9779	3	1.9644	2*	1.9624
2	1.9564	-	-		
4	1.8057	2	1.8050		
3	1.7929	3	1.7487		
1	1.6589	1	1.6579	7	1.6600
7	1.6210	9	1.6230	4*	1.6224
3	1.6056	1	1.6101		
1	1.5261	2	1.5445		
7	1.4950	6	1.5001	3*	1.4996
5	1.3959	4	1.4150	2*	1.4939
3	1.3726				

*Broad and often diffuse lines.

Table 35. The d-values of clinopyroxenes taken from kimberlite. The d-values were obtained by means of a Debye Scherrer Camera, using Cu Kα radiation

Film no.	44		447		445		448		467		531	
Sample	1010-3A		1010-3B		1010-22B$_1$		1010-22B$_2$		1010-20		1010 In$_1$	
	I/Io	d (Å)	I/Io	d (Å)	I/Io	d (Å)	I/Io	d (Å)	I/Io	d (Å)	I/Io	d (Å)
			1	3.266	1	3.332	2	3.336	6	3.525	8	3.344
			4	3.170	5	3.210	2	3.232	5	3.214		
			10	2.953	10	2.988	10	3.038	10	2.991	10	2.991
	10	2.873	1	2.861	5	2.887	2	2.891	4	2.865		
									1	2.554		
	10	2.480	10	2.494	9	2.521	9	2.529	9	2.523	8	2.531
			2	2.256	5	2.299	4	2.298	4	2.304		
	1	2.164	2	2.183	5	2.203	4	2.213	4	2.212	1	2.201
	3	2.100	4	2.103	5	2.129	4	2.139	4	2.140	1	2.117
	4	2.004	4	2.007	3	2.039	3	2.041	4	2.045	8	2.019
					3	2.009	3	2.009	4	2.010		
			2b	1.801	2	1.965	4	1.967	1	1.892	2	1.952
					2	1.824	1	1.837	1	1.832	2	1.815
	1b	1.739	6	1.726	6	1.748	2	1.7530	6	1.752	2	1.746
	1	1.653	3	1.647	2	1.669	2	1.678	3	1.669	3	1.669
	4	1.608	9	1.606	7	1.622	7	1.625	8	1.622	8	1.613
					4	1.522	1	1.537	3	1.531		
	4	1.487	1	1.485	4	1.496	2	1.500	3	1.506		
							3	1.439	3	1.490	1	1.496
	4	1.395	9	1.396	5	1.420						
							1	1.418	5	1.410		
					2	1.406					1	1.421
	2	1.339	1	1.364	5	1.327	2	1.330	4	1.331	2	1.370
			3	1.310								
	2	1.263	4	1.271	5	1.283	2	1.286	4	1.284	4	1.283
					3	1.264	1	1.256	1	1.263		
	2	1.230	4	1.231								
					3	1.249						
	1	1.			3	1.215						
					2	1.171						
	1	1.068			4	1.146						
					4	1.073						
	1	1.059							3	1.073		
					2	1.050						

EXPLANATION TO THE SAMPLES INVESTIGATED:

1010-3A	Clinopyroxene in kimberlite
1010 3B	" -ditto-
1010-22B$_1$	Clinopyroxene which formed in the meta-kimberlite
1010-22B$_2$	Diopside from the carbonate inclusion
	-ditto-
1010In$_1$	Augite from a diabase inclusion.

to the high Al^{3+} content in these clinopyroxenes (Hess, 1949). The optical properties of the various clinopyroxenes are plotted on the $MgSiO_3$, $FeSiO_3$ and $CaSiO_3$ variation diagram after Tröger (1959, p. 62). This diagram (figure 24) shows that the clinopyroxenes from the ultramafic nodules are more enriched in diopside that those from the kimberlite, however, the amount of enstatite in solid solution appears to be the approximately same in both types of clinopyroxenes. The composition of the clinopyroxenes from the different kimberlite occurrences shows a similar distribution as those from the Premier Mine kimberlite.

The frequency distributions for $FeSiO_3$ and $CaSiO_3$ contents in the kimberlitic and ultramafic clinopyroxenes, as determined from the optical properties, are shown in figure 30, and indicates the modal values of 5 per cent $FeSiO_3$ and 48 per cent $CaSiO_3$. Hence these clinopyroxenes would also have a modal value of 47 per cent $MgSiO_3$. According to figure 25 it is evident that the clinopyroxenes from the kimberlite and the ultramafic nodules have an orthopyroxene solid solution content ranging from 0 to 36 per cent.

The unit-cell dimensions of the clinopyroxenes were calculated from powder photographs by means of the 002,060 and 600 reflections, and the angle β was calculated according to the 531 and (53T) reflections, using the formulas:

$$\mathrm{Sin}^2\theta = n\lambda^2/d^2$$

$$i/d^2 = h^2/a_o^2\mathrm{Sin}^2\beta + k^2/b_o + l^2/c_o^2\mathrm{Sin}^2\beta - 2hl\mathrm{Cos}\beta/a_oc_o\mathrm{Sin}\beta$$

The indices 002, 060 and 600 after Sakata (1957) could be checked by means of a Weissenberg single-crystal camera, and were found to be correct. The unit-cell dimensions of the clinopyroxenes thus calculated are listed in appendix 19.

Since omphacite belongs to the P_2 space-group, and ordinary clinopyroxenes to the C^2/c space-group, the Weissenberg single-crystal photographs for the hk0, hkl and hk2 reflections of the "glassy" pyroxene, the eclogitic clynopyroxene, and the kimberlitic clinopyroxenes could be indexed. It was found that all these clinopyroxenes conform to the C^2/c space group, and hence they

THE VARIATION IN THE $MgSiO_3$, $FeSiO_3$ AND $CaSiO_3$ CONTENT OF THE CLINOPYROXENES FROM KIMBERLITE AND ULTRAMAFIC NODULES AFTER THE OPTICAL PROPERTIES, USING THE CURVE BY TROGER 1959

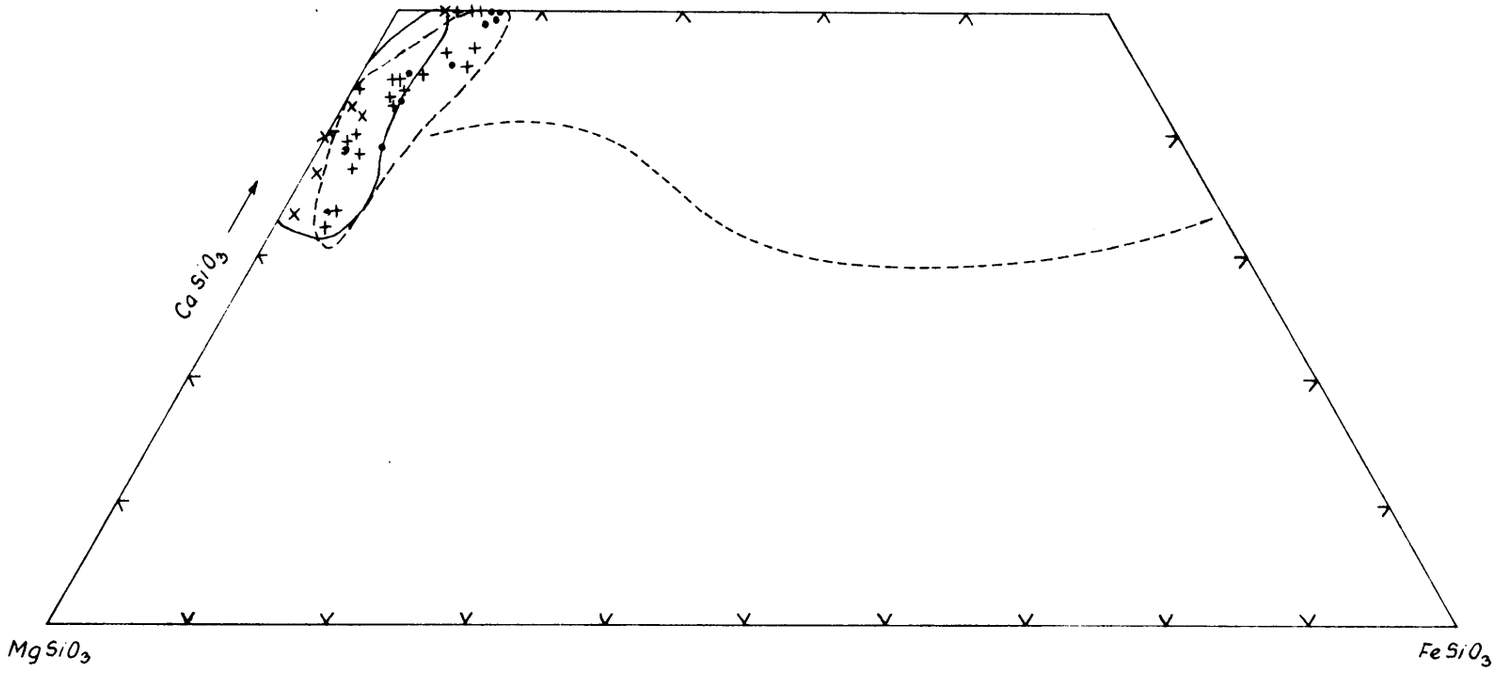

LEGEND

\+ Clinopyroxene Premier Mine

• Clinopyroxene Other Kimberlites

× Clinopyroxene from Ultramafic Nodules

------ Normal magmatic differentiation trends

FIG. 24

THE FREQUENCY DISTRIBUTION OF THE MOL. PER CENT FERROSILLITE, WOLLASTONITE AND THE WEIGHT PERCENTAGES $MgSiO_3$ AND Ca-TSCHERMAK'S MOLECULE IN THE CLINOPYROXENE IN KIMBERLITE

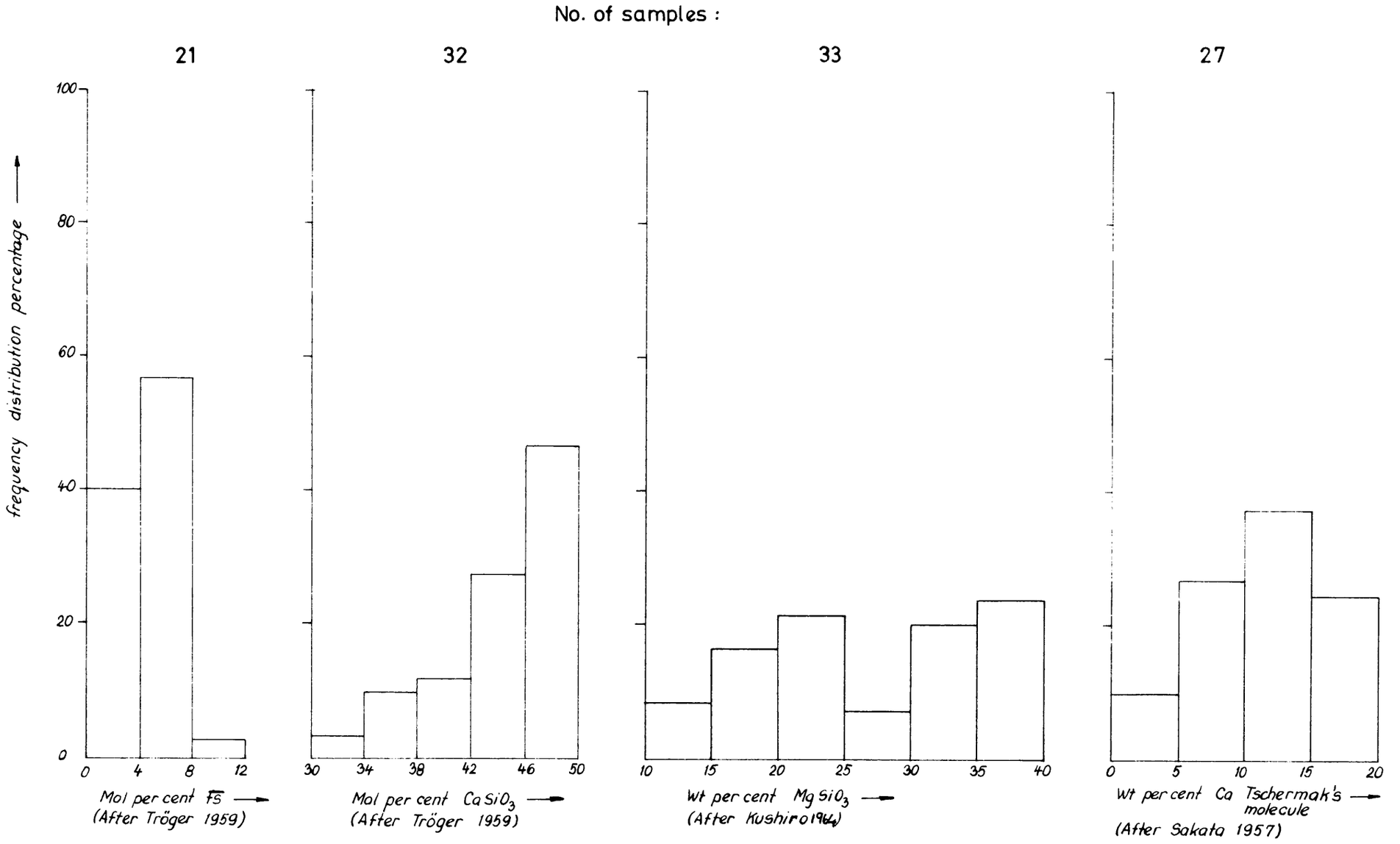

FIG. 35

are considered as diopsides rather than omphacites.

The Ca^{2+}, Mg^{2+} and Fe^{2+} variation diagram after Brown (1967) could not be used for the clinopyroxenes investigated, due to the fact that the Al_2O_3 content causes the b_o values to decrease (Brown 1967). The content of Ca-Tschermak molecules of the clinopyroxenes could, however, be estimated according to the diagram after Sakata (1957). However, since the curves provided by Sakata were constructed for pure diopside, a correction factor had to be introduced for the 5 per cent of $FeSiO_3$. This has been done by applying Vegard's law, and by using the unit-cell dimensions of diopside and hedenbergite after Strunz (1967).

The curves supplied by Sakata (1957) are not applicable to the eclogitic clinopyroxenes, owing to the presence of jadeite and acmite. The weight percentage of $CaAl_2SiO_6$ in the kimberlitic clinopyroxenes after Sakata (1957) are reported in appendix 19, and the frequency distribution diagram, depicted in figure 30, indicates a modal Ca-Tschermak molecule content of 11 per cent.

The mole per cent $CaMgSi_2O_6$ in the clinopyroxenes was determined by means of the 2θ(220) Cu K_α value after Davis and Boyd (1966; p.3572), and the weight percentage of $MgSiO_3$ by means of the $\Delta 2\theta\{(311)-(310)\}$ value after Kushiro (1964, p.101-108). These values, together with the percentages of $CaMgSi_2O_6$ and $MgSiO_3$, are reported in appendix 20. The frequency distribution for the $MgSiO_3$ values in the kimberlitic clinopyroxenes are depicted in figure 35 and yield the following modal values

$MgSiO_3$: 23 per cent.
38 per cent

The diagram constructed by Essene and Fyfe (1967, 7) figure 36, which shows the augite, jadeite and acmite contents of clinopyroxenes as a function of d_{221} (Å) and $n\beta$, indicates that the eclogitic clinopyroxenes are more enriched in jadeite and acmite than the clinopyroxenes from kimberlite or ultramafic nodules. The latter two types of clinopyroxenes overlap completely, and some of the kimberlitic clinopyroxenes also fall into the eclogite field.

THE VARIATION IN THE AUGITE, ACMITE, JADEITE CONTENT OF THE VARIOUS CLINOPYROXENES, AFTER ESSENE AND FYFE (1967), USING n_β AND d_{221} OF THE CLINOPYROXENE

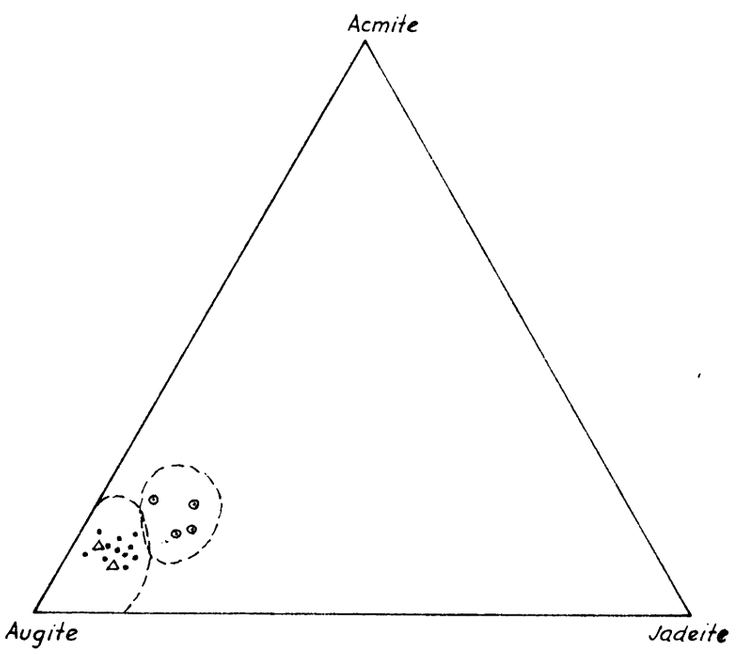

LEGEND

- · Clinopyroxenes from Kimberlite
- ⊙ Clinopyroxenes from Eclogite
- △ Clinopyroxene from Garnet-Peridotite Nodules

FIG. 2E.

In table 36 the infra-red absorption peaks of diopside, hedenbergite, jadeite and kimberlitic clinopyroxene are compared with the absorption peaks found by Moenke (1966). Inspection shows that jadeite, fassaite and augite exhibit some peaks different from those characteristic of the other clinopyroxenes. The consistancy of certain peaks at the wavenumbers cm^{-1}, 1080, 970, 930 and 510 in all silicates indicates that these absorption peaks are caused by the Si^{IV}- O vibrations. The Mg^{VI}- O, Fe^{VI}- O and CaO vibration peaks have also been established more or less clearly, therefore it is concluded that the peaks unaccounted for, should be ascribed to Al^{IV}- O, Al^{VI}- O or Na - O bonds. The predominance of the 440 and 790 absorption peaks in fassaite and the 720 and 740 peaks in jadeite indicates that the 720-740 peaks are due to Al^{VI}- O bonds, whereas the Al^{IV}- O bonds are represented by the 440 and 790 peaks.

3. The chemistry of the clinopyroxenes

In appendix 21 the chemical analyses and the molecular norms of the various clinopyroxenes are supplied. The molecular norms were calculated after the method suggested by Kushiro (1962), with the view to obtaining comparable values for the jadeite and Ca-Tchermak molecule contents. The Al^{3+} which was over after all the allocations had been made was distributed in equal proportions between the X and Y positions after the method suggested by Hess (1949). The amounts of cations in the pyroxene formula were subsequently calculated after the method by Hess (1949). Since the calculations were carried out in such a way that the molecular contents and the Al^{IV}/Al^{VI} ratio could be applied for the petrological interpretation of the analyses, the structural formulas in appendix 21 do not conform to the ideal pyroxene formula.

In figure 37 the frequency distribution of the contents of FeO, NaO + K_2O, jadeite (mol. per cent) and $MgSiO_3$ (mol. per cent) in solid solution in the clinopyroxenes in eclogite, kimberlite and ultramafic nodules is depicted. This diagram indicates that the FeO, Na_2O + K_2O, jadeite and enstatite contents of the kimberlitic and ultramafic clinopyroxenes are similar, whereas the eclogitic clinopyroxenes are enriched in Na_2O + K_2O and jadeite, but impoverished in FeO and enstatite.

The variation in the diopside, acmite, hedenbergite contents (figure 38), calculated from the chemical analyses, of the kimberlitic clinopyroxenes corresponds

Table 36. The infra-red absorption peaks in cm^{-1} for the various clinopyroxenes.
Values obtained by means of a Perkin Elmer infra-red spectrometer, using NaCl prisms and KBr discs.

XO_n Polyheder	$CaMgSi_2O_6$ *2	$CaFeSi_2O_6$ *2	$NaAlSi_2O_6$ *2	Augite *2	Fassaite *2	Ti450; U.S.A. Diopside	Ti475; U.S.A. Hedenbergite	N.E.1 New Zealand Jadeite	Ti200 P. Mine
Mg^{VI}–O Fe^{VI}–O	405	405	408	410	412		380	380	400
Al^{IV}–O			435		440		450	440	
CaO *1	475	472	470	465 477	475	460			
Si^{IV}–O	512	515		515	515	510	495	515	490
Na^{VIII}–O			590					575	
Na^{III}–O			615						
Mg^{VI}–O Fe^{VI}–O	635	630		637	640	630	630	640	620
Al^{VI}–O	672	672		676	670	670	670 690		670
Al^{VI}–O			718 748			710	715	720 740	
Al^{IV}–O					790			760 785	
Mg^{VI}–O Fe^{VI}–O	868	870	860	860 870	870	850	860	875	880
Si^{IV}–O	925	920	940	915	925	915	910		
Si^{IV}–O	970	970	995	970	970	960	950	950	955
Ca–O *1					1035				
Si^{IV}–O	1080	1078	1065	1070	1070	1070	1065	1030	1070

*1 Usually very weak

*2 Values after Manke (1966)

THE FREQUENCY DISTRIBUTION OF FeO, $Na_2O + K_2O$, PERCENTAGES JADEITE AND ENSTATITE (MOL. PERCENTAGES) IN CLINOPYROXENE FROM KIMBERLITE, ECLOGITE AND ULTRAMAFIC NODULES

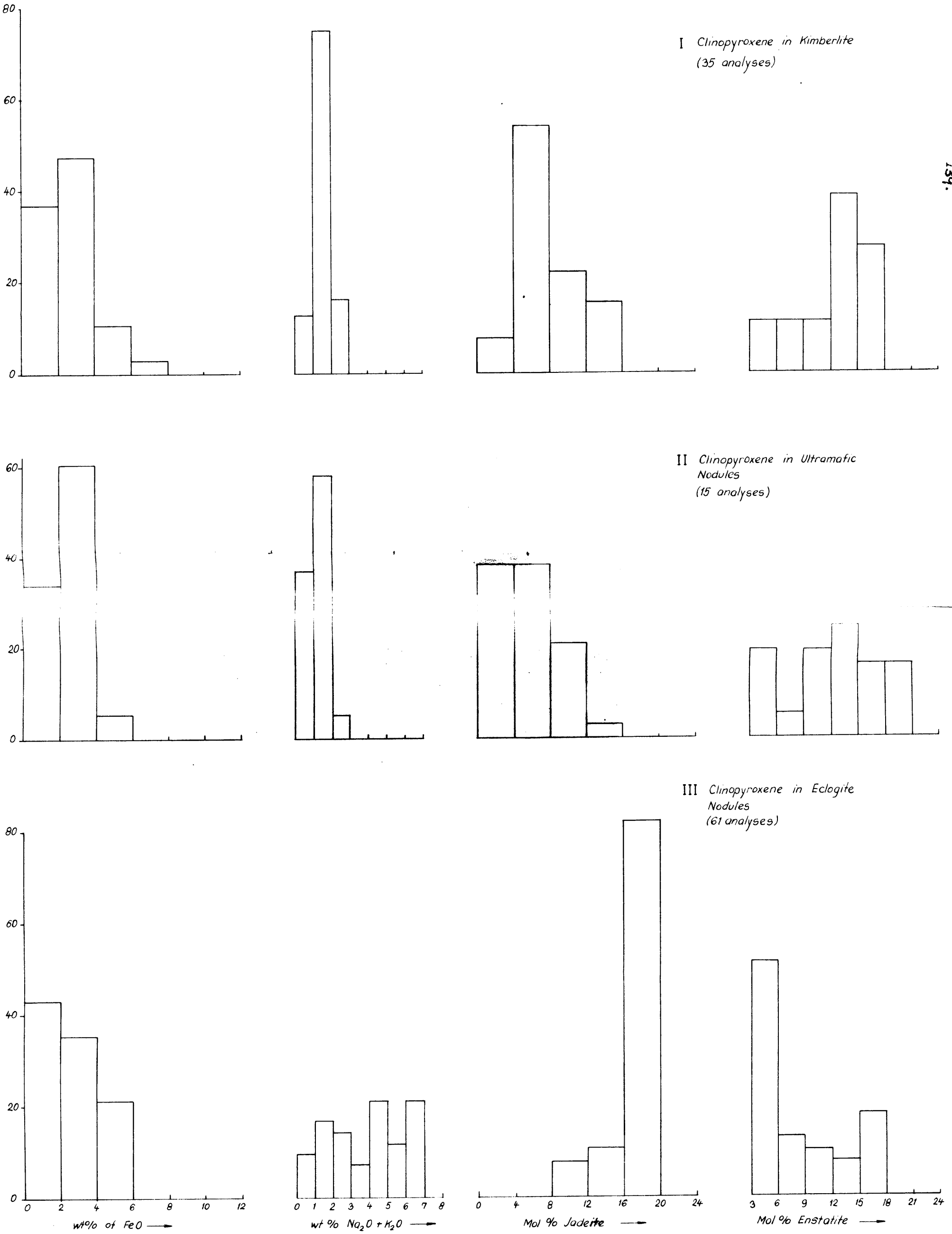

FIG 27

closely to the variation in the clinopyroxenes from the ultramafic nodules, However the latter have a more restricted variation. The eclogitic clinopyroxenes partly overlap with these clinopyroxenes, and then extend towards the hedenbergite corner of the diagram. This enrichment in hedenbergite contradicts the FeO distribution shown in figure 37 and may be due to the fact that an increase in Al_2O_3 and Na_2O in the eclogitic clinopyroxenes (appendix 21) results in a decrease in the FeO content. The clinopyroxenes from grospydites and kyanite eclogites, which were also taken into account in the compilation of figure 37, are marked by a low content of FeO. Hence it appears that the eclogitic clinopyroxenes are enriched in FeO, compared to the kimberlitic and ultramafic clinopyroxenes. The variation in the diopside, acmite and hedenbergite contents of clinopyroxenes from alkaline rocks after Tyler and King (1967) are also shown in figure 38.

The variation in the $Mg_2Si_2O_6$, $Fe_2Si_2O_6$ and $Ca_2Si_2O_6 + NaAlSi_2O_6$ contents of the various clinopyroxenes are depicted in figure 39. These values have been obtained from the chemical analyses in appendix 21. This diagram indicates that the clinopyroxenes from the ultramafic nodules and from the kimberlites fall in almost the same field, showing a low $Fe_2Si_2O_6$ content, a high content of diopside and a maximum solid solution content of 22 per cent of enstatite for the kimberlitic clinopyroxene and 32 per cent for those derived from the ultramafic nodules. The clinopyroxenes from the eclogite inclusions in kimberlite fall above the diopside-hedenbergite join, and are enriched in jadeite with respect to the clinopyroxenes from kimberlite and from the ultramafic xenoliths.

The variation in the $Mg_2Si_2O_6 + Fe_2Si_2O_6$ and $NaAlSi_2O_6$ contents of the various clinopyroxenes is shown in figure 30. This figure indicates that the clinopyroxenes from eclogite in kimberlite are more enriched in jadeite than the clinopyroxenes from kimberlite or from the ultramafic nodules found in kimberlite. The jadeite content of the clinopyroxenes from kimberlite and from the ultramafic nodules in kimberlite overlaps markedly.

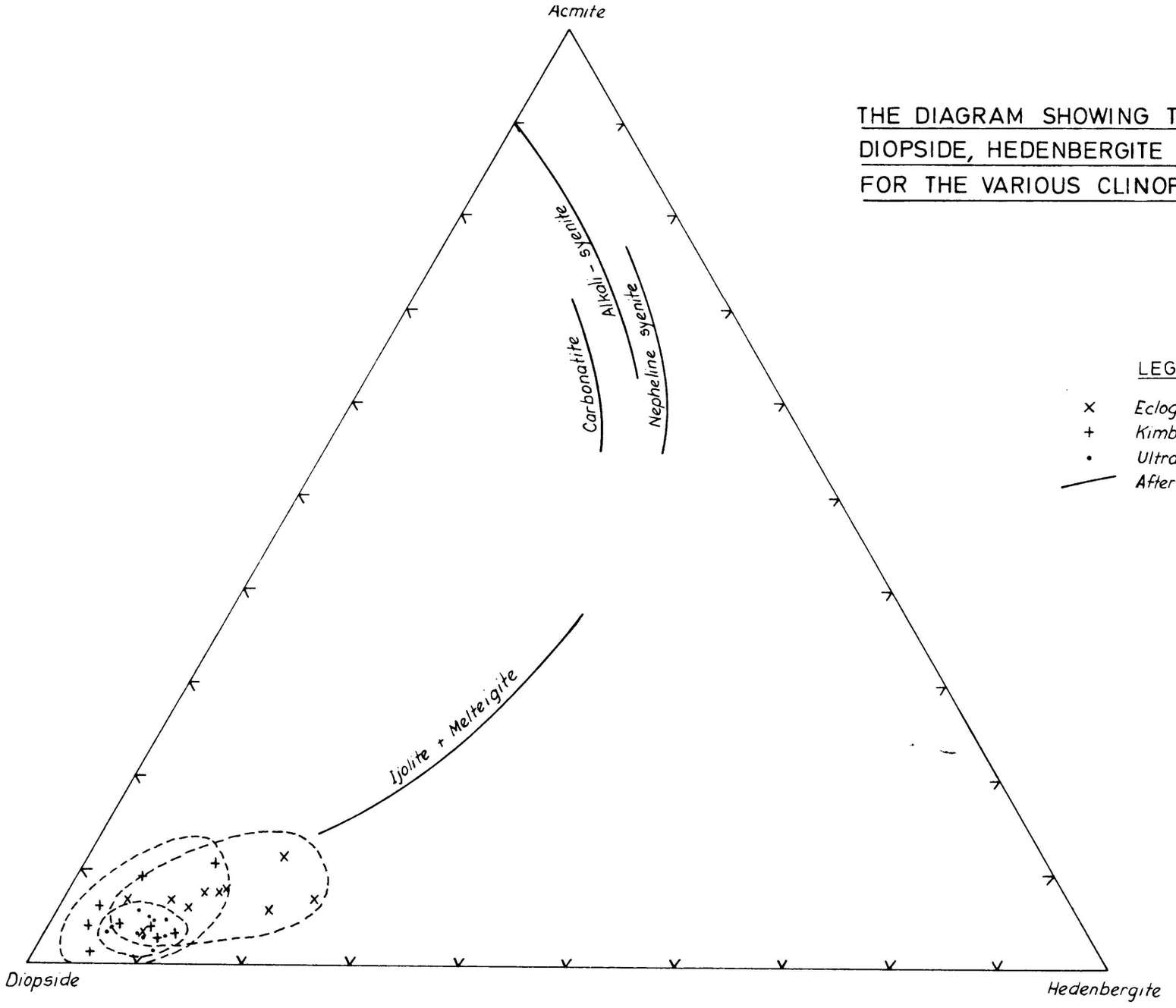

THE DIAGRAM SHOWING THE VARIATION IN THE DIOPSIDE, HEDENBERGITE AND ACMITE CONTENT FOR THE VARIOUS CLINOPYROXENES

LEGEND

× Eclogite
\+ Kimberlite
• Ultramafic Nodules
— After Tyler + King (1967; P 19)

FIG. 28

THE VARIATION IN THE ENSTATITE, FERROSILITE AND WOLLASTONITE AND JADEITE CONTENT OF THE VARIOUS CLINOPYROXENES

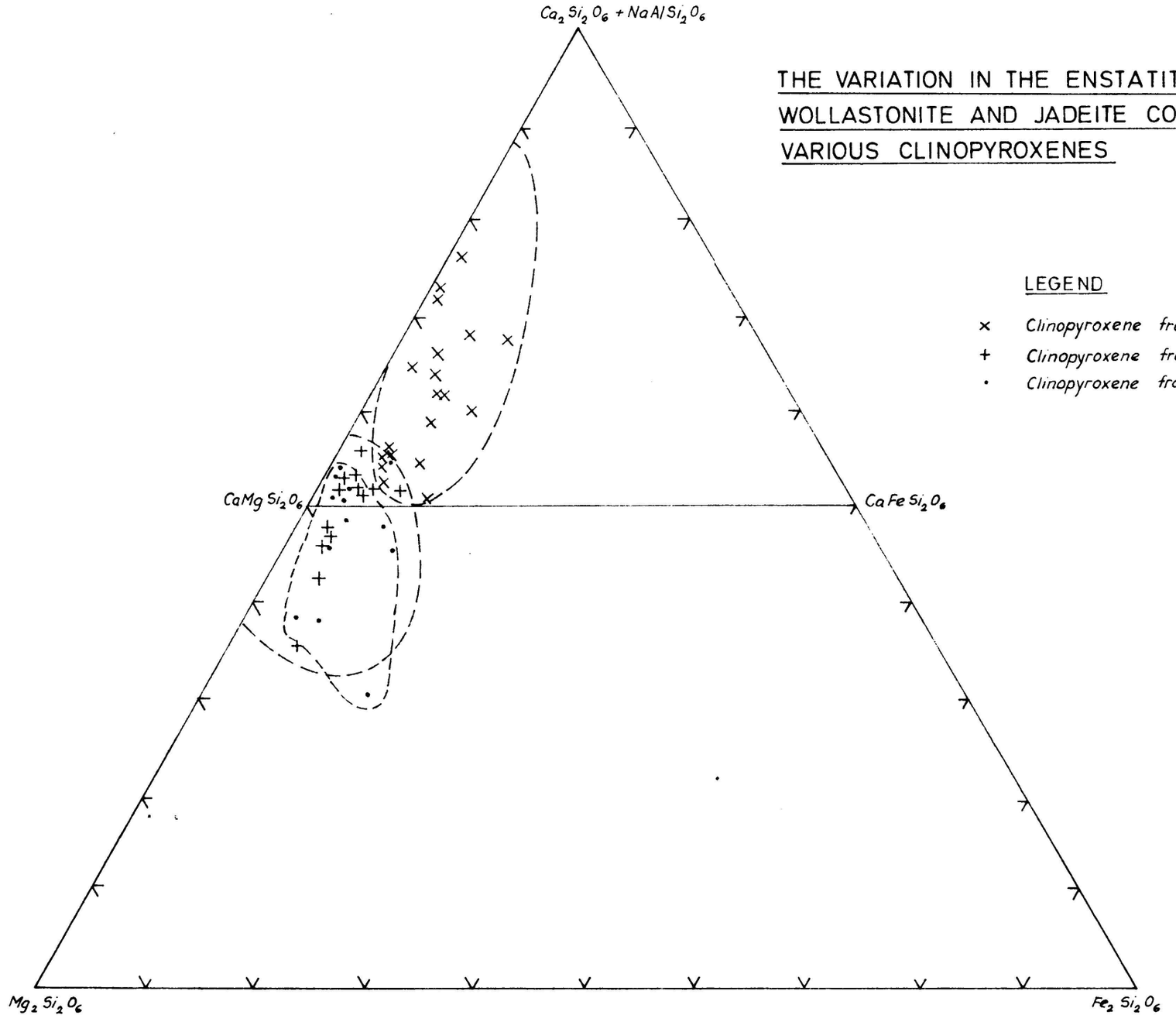

FIG. 29

THE VARIATION IN THE ENSTATITE, FERROSILITE, WOLLASTONITE AND JADEITE CONTENT OF THE VARIOUS CLINOPYROXENES

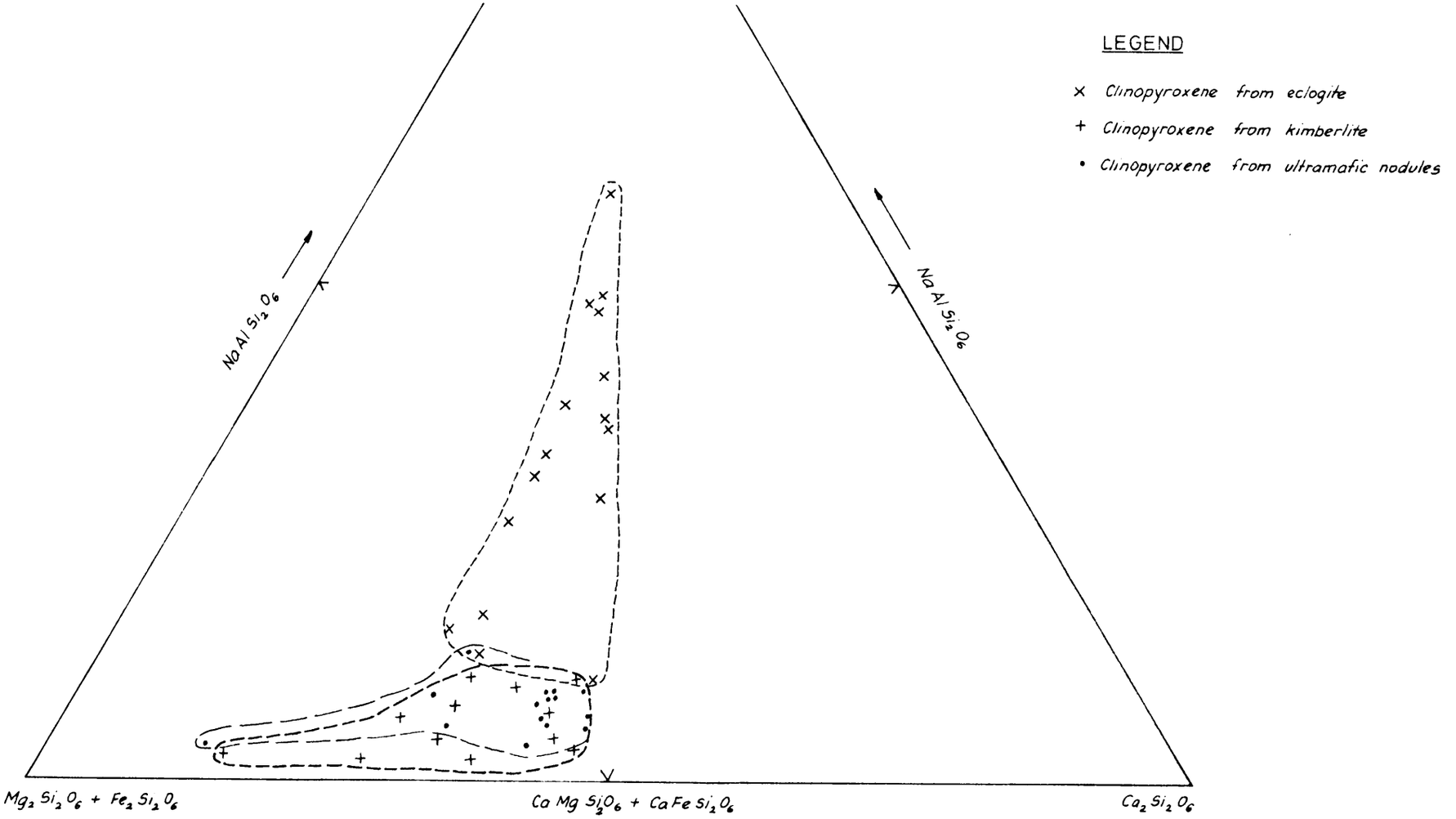

The Al^{IV}/Al^{VI} variation diagram after White (1964; p. 883) for the various clinopyroxenes listed in appendix 21 shows that Al^{VI} predominates in the clinopyroxenes from eclogite nodules (figure 31). This diagram also indicate an increase in the ratio Al^{VI}/Al^{IV} in the sequence from igneous to kimberlitic and ultramafic clinopyroxenes to those found in grospydite, kyanite eclogite and eclogite found in kimberlite. According to White (1964) this increase in the Al^{VI}/Al^{IV} ratio reflects an increase in the pressure of formation of the clinopyroxenes in this sequence of rock-types.

The diagram showing the weight percentages of SiO_2, and Al_2O_3 (figure 32) has been used by Le Bas (1962) to distinguish between tholeiitic and alkaline basaltic clinopyroxenes. This diagram indicates that the clinopyroxenes from ultramafic nodules and kimberlite resemble tholeiitic clinopyroxenes, whereas the eclogitic clinopyroxenes range from tholeiitic to per-alkaline in composition. The eclogitic clinopyroxenes are also marked by a much larger variation in SiO_2 and Al_2O_3 contents than the kimberlitic or ultramafic clinopyroxenes.

The ratio of Al_2O_3/Cr_2O_3 (expressed in percentages by weight of the clinopyroxenes (figure 33A) show a complete differentiation between the pyroxenes rich in Cr_2O_3 and poor in Al_2O_3 and vice versa. The clinopyroxenes from kimberlite and ultramafic nodules are rich in Cr_2O_3 and poor in Al_2O_3 (chrome-diopsides) and the eclogitic clinopyroxenes are poor in Cr_2O_3 and rich in Al_2O_3 (jadeite-bearing diopsides).

The atomic ratio Al^{3+}/Si^{4+} represented in figure 33B after Kushiro (1960) shows that all the clinopyroxenes concerned, constitutes a sequence which is characterized by a more rapid increase in Al^{3+} than is necessary for the Al^{IV}/Si^{IV} substitution and hence differs from the sequence usually evident for igneous clinopyroxenes (Kushiro, 1960). The variation trend for kimberlitic and ultramafic clinopyroxenes shows that Si^{4+} changes from 2.0 to 1.80, whereas the Al^{3+} content changes from 0.0. to 0.30. Hence a

THE Al^{VI} / Al^{IV} DISTRIBUTION IN THE VARIOUS CLINOPYROXENES

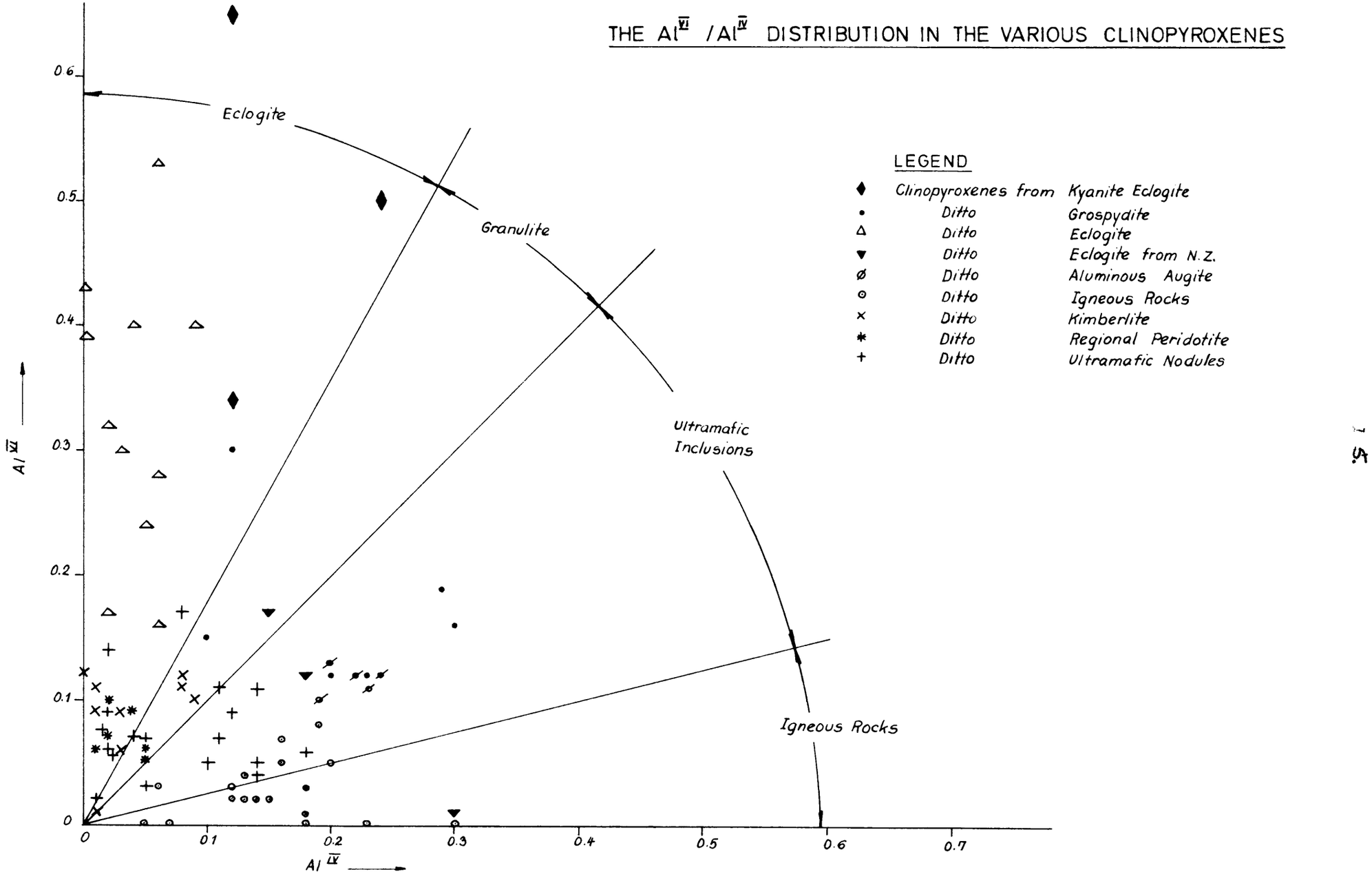

FIG. 31

THE VARIATION IN THE WEIGHT PERCENTAGES OF Al_2O_3 AND SiO_2 IN THE VARIOUS TYPES OF CLINOPYROXENES

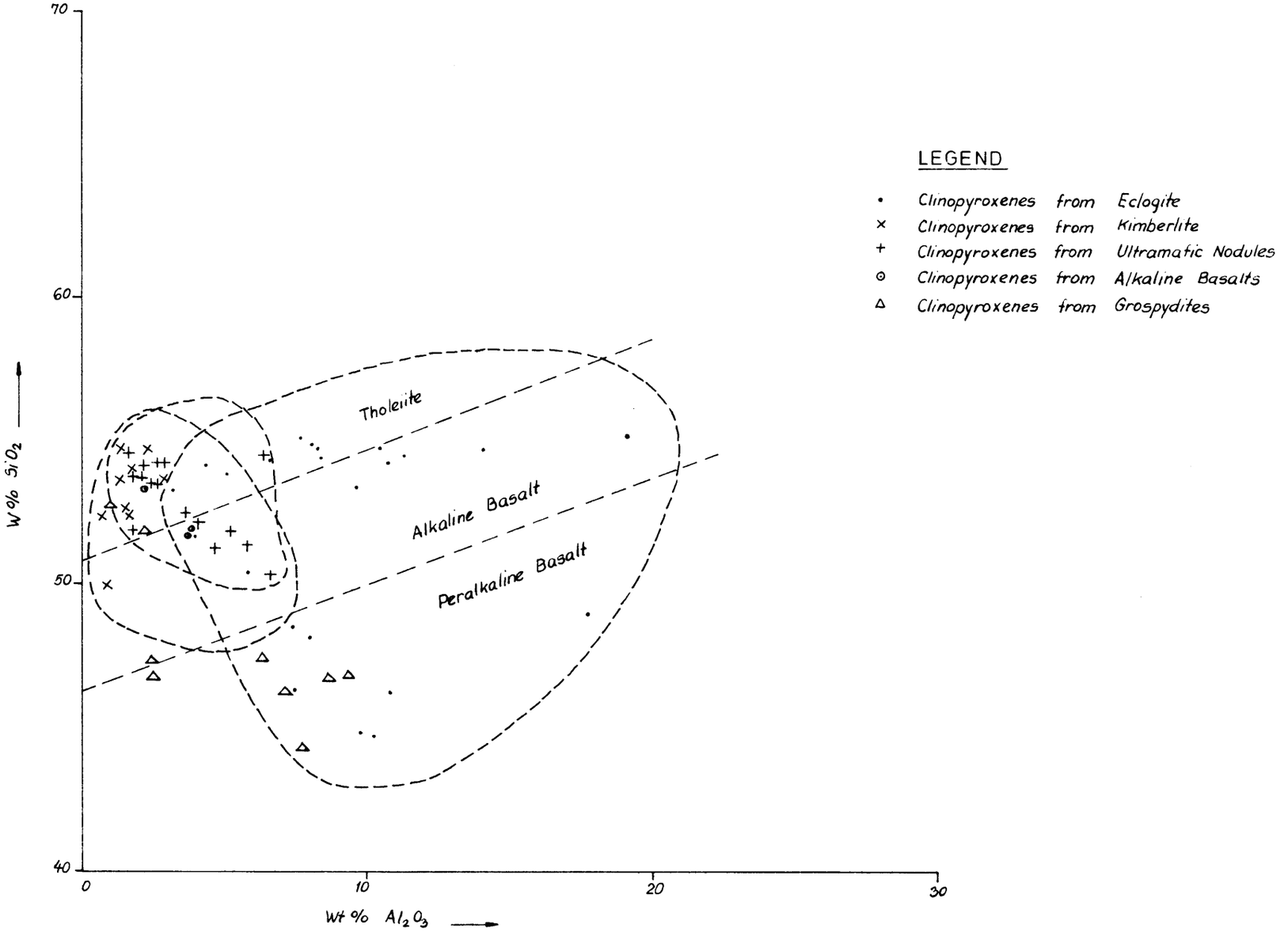

FIG. 38

(A) THE Cr_2O_3/Al_2O_3 DISTRIBUTION FOR THE VARIOUS CLINOPYROXENES

(B) THE Si^{4+}/Al^{3+} DISTRIBUTION FOR THE VARIOUS CLINOPYROXENES

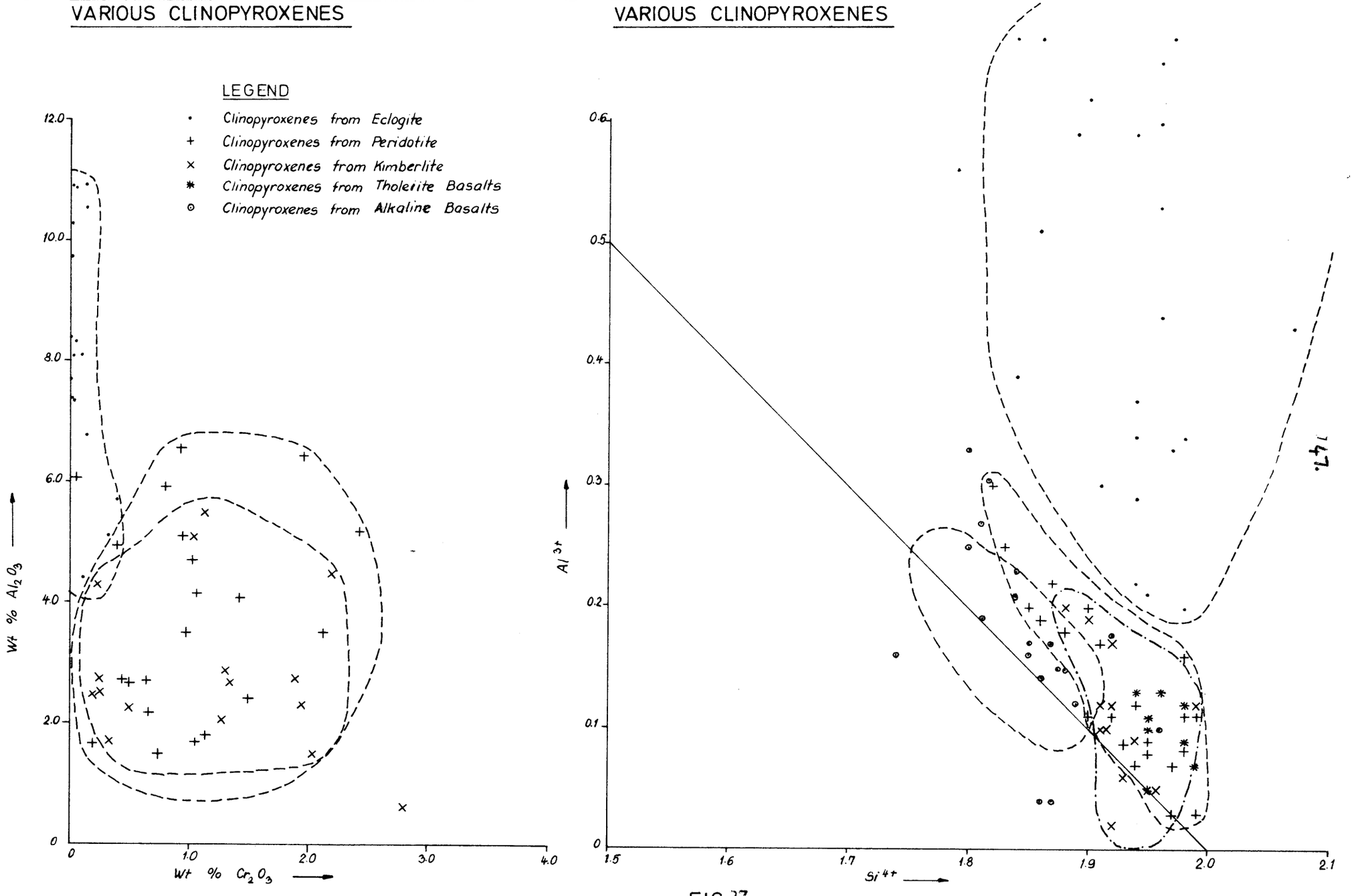

FIG. 33

systematic increase in Al^{VI} is evident in these clinopyroxenes. The eclogitic clinopyroxenes show a Si^{4+} variation from 2.0 to 1.80, and a Al^{3+} variation from 0.2 to more than 0.8, consequently the Al^{VI} and jadeite contents in these rocks are markedly increased. The igneous clinopyroxenes usually plot along the line indicated in figure 37B (Kushiro, 1960).

4. Conclusions.

1. The clinopyroxenes from ultramafic nodules and kimberlites are alike in almost all aspects, but the clinopyroxenes from the ultramafic nodules show a much larger variation in composition (appendix 21).

2. The clinopyroxenes from eclogites are different from the clinopyroxenes from kimberlite and ultramafic nodules in almost all respects. The higher Al^{VI}, jadeite, $FeSiO_3$, Al_2O_3, Na_2O and K_2O contents are very characteristic. The clinopyroxenes from grospydites and kyanite eclogites differ even more from the clinopyroxenes in kimberlite, ultramafic nodules and eclogite, by being very low in MgO, FeO and TiO_2 contents.

3. The variation diagrams thus indicate that the eclogitic clinopyroxene formed at the highest pressure, and is completely different from all the other pyroxenes. The clinopyroxenes from grospydites also formed at a high pressure, (However, lower than eclogite) and is marked by a lower content of MgO, FeO and TiO_2. The ultramafic and kimberlitic clinopyroxenes formed at an even lower pressure, and are marked by a variable content of orthopyroxene in solid solution.

4. According to Kushiro (1962) the amount of Ca-Tschermak's molecule in clinopyroxene can be used as an indication of the pressure of formation. The work done by Boyd and England (1963), O'Hara (1963), Bell (1964) and Yoder (1950) also support this contention of Kushiro. [illegible] According to the system diopside-enstatite by Davis and Boyd (1966) and Boyd and Schairer (1964) the amount of enstatite in solid solution in the clinopyroxene can be used to determine the temperature

of formation, because the diopside solvus is not influenced greatly with an increase in pressure. The estimates of the temperatures which are summarized below have been based on both the optical and chemical data for the kimberlitic and ultramafic clinopyroxenes, and only on the chemical data for the eclogitic clinopyroxenes.

	Temp (^{o}C)
Clinopyroxene from eclogite	1400
" " ultramafic nodules	1400 to 900
Clinopyroxene from kimberlite	1350 to 900

G. Apatite

1. Occurrence

Apatite occurs in the residua phase of kimberlite as small euhedral grains, and as large, radially orientated grains. The amount of apatite in the kimberlite breccias are much lower than in either the massive basaltic kimberlites or the micaceous kimberlites.

2. The mineralogy of apatite

Since either F^{-}, Cl^{-}, CO_3 or OH^{-} groups can replace one another in the structure of apatite, and because it crystallized as the last phase from the residua phase of kimberlites, it is an important indicator of the composition of the volatile phases in kimberlite magmas.

According to McConnell (1958, p. 110-111) the various anionic replacements in the apatite can be determined by the unit-cell dimensions and the d-values of the 11.2, 30.0 and 21.3 reflections. The n_ω and ($n_\omega - n_\varepsilon$) values for apatite can also be used as a criterion to distinguish between the various types of apatite (Deer, Howie and Zussman 1967, p. 507.

The apatite from the Premier Mine kimberlite (1010-43) has the following physical properties: $n_\omega = 1.636$; $n_\varepsilon = 1.632$; $a_o = 9.36$ Å; $co = 6.86$ Å and $c/a = 0.733$, which correspond very well with the physical properties of fluorine-apatite. According to Russel et al., (1954) the apatite from the Phalaborwa carbonatite is also enriched in fluorine.

The data presented thus indicate that the apatite, which was the last mineral to crystallize in the secondary phenocrystal phase, is enriched in fluorine. Consequently it may be concluded that the volatile phases of both the Premier Mine kimberlite and the Phalaborwa carbonatite were enriched in fluorine.

H. Pyrite

Large, euhedral grains of pyrite are present in most kimberlites. These pyrite grains vary in size from 0.5 mm to ± 2.0 cm. In the nodules of eclogite and garnet peridotite pyrite was also encountered. In the former it occurs as small euhedral grains in the kelyphytic rims, and in the latter it is present in the alteration products of olivine.

The unit-cell dimensions of the pyrite have been calculated from powder photographs by using the indexing after Berry and Thompson (1962, p. 87). According to Sutherland (1967, p. 81) an increase in the content of Ni^{2+} and Co^{2+} causes the a_o-value to increase significantly. The a_o-values reported in table 37 for the pyrite from Bellsbank and Premier Mine, indicate low Ni^{2+} and Co^{2+} values.

Apart from pyrite, other sulphides like chalcopyrite, pyrrhotite, chalcocite and bornite have been identified in the kimberlite and in the wall-rock xenoliths, these sulphides are also present as minute grains in the ultramafic nodules, but were never observed in the eclogite nodules.

According to Freedman (1959) pyrite can form as a consequence of the reaction of H_2S with iron-hydroxide gells and even with magnetite. The presence of magnetite in kelyphytic rims has already been described, consequently the penetration of H_2S into the eclogite nodules, could have caused the pyrite to form in the kelyphytic rims.

The pyrite in the kimberlite may thus have originated as a result of the activity of H_2S in the volcanic gasses, and consequently the pyrite should be considered as a fairly late product of the crystallization.

I. Phlogopite

In the micaceous kimberlites from Sovér, Bellsbank,

Table 37. The unit-cell dimensions for pyrite from kimberlite. Obtained by means of Guinier Camera, using Cu Kα radiation

Specimen	a_o (Å)	Reference
Nigadoo	5.4163	Sutherland (pyrite)
Backbay	5.4203	Sutherland (Ni + Co bearing pyrite)
Premier Mine Ti67	5.414 (± 0.002)	(pyrite)
" " Ti68	5.411 (± 0.002)	- ditto
" " Ti69	5.408 "	- ditto
" " Ti73	5.412 "	- ditto
" " Ti74	5.409 "	- ditto
" " Ti75	5.411 "	- ditto
" " Ti70	5.415 "	- ditto
" " Ti71	5.416 "	- ditto
" " Ti72	5.413 "	- ditto
Bellsbank Be 11	5.408 "	- ditto
" Be 12	5.413 "	- ditto
" Be 13	5.410 "	- ditto

Monastry and Swartruggens two generations of phlogopite are present. However, in the Premier Mine kimberlite no phlogopite was observed.

The first-generation phlogopite occurs as large, euhedral to rounded, primary phenocrysts in the kimberlite matrix. This phlogopite is usually pleochroic, with a $2V\alpha$ ranging from 15° to 25°.

The phlogopite in the matrix is present as small euhedral grains which constitute large percentages in the residua phase. This material is pale brown in colour, less pleochroic and has a $2V\alpha$ ranging from 15° to 25°.

In Table 22 the chemical analyses and structural formulas of 8 kimberlitic phlogopites, calculated on a basis of 16 oxygens per unit cell are compared to those of the phlogopites from carbonatites and metamorphic limestones. This table indicates that the metamorphic phlogopites are more enriched in Mg^{2+}, than those in kimberlites, and that no chemical difference exists between

the first- and second-generations of phlogopite in kimberlite. According to Aoki and Kushiro (1968) the phlogopite in eclogite nodules and in kimberlites may be derived from the mantle. However, the data presented on pages 51 and 93 have all indicated a secondary origin for the phlogopite in the eclogite nodules. The manner of occurrence of the first-generation phlogopite, however, suggests that this phase could have formed in the mantle.

J. Calcite

As has been mentioned previously, primary calcite is present in the residua phase of kimberlites, and the primary calcite from micaceous and massive basaltic kimberlites exhibits the same textural features as the calcite observed in the Glenover and Derdepoort carbonatites. The presence of secondary calcite in the matrix of primary calcite is a prominent feature of these kimberlites and therfore the original trace element distributions of the primary calcite may have been influenced.

The refractive indices of the calcite were mentioned and discussed on page 58, and indicated that the primary calcite is composed of $CaCO_3$. The D.T.A. curve for an impure sample of calcite from the massive basaltic kimberlite also corresponds to the curve for calcite. The chemical analyses of the calcite from kimberlite and carbonatite, listed in appendix 2B, have been plotted on the system calcite, dolomite and ankerite in figure 34 after Goldsmidt et al., (1962). This figure indicates that the calcite from the Premier Mine kimberlite has the same composition as that of the Russian kimberlites, and that they correspond to the carbonates from the sövitic carbonatites.

K. Magnetite

Magnetite occurs in the kimberlite breccias and in the massive basaltic kimberlites. In none of these rock-types could exsolution lamallae of ulvite or ilmenite ever be discerned in the magnetite. The magnetite is present as small euhedral to subhedral grains, which are disseminated through the residua phase. Euhedral magnetite as inclusions in the primary phenocrystal phase was never observed, but the presence of the magnetite along the outer peripheries

THE VARIATION IN THE COMPOSITION OF THE CALCITE FROM KIMBERLITE AND CARBONATITE

After Goldsmidt et al (1962)

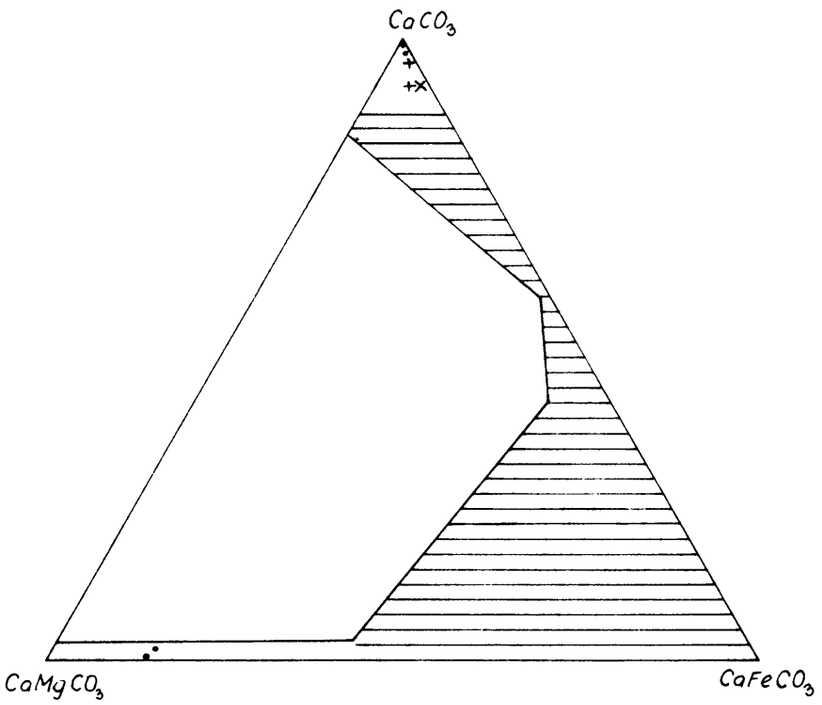

LEGEND

- • Calcite from Carbonatite
- \+ Calcite from the Russian Kimberlites
- × Calcite from Premier Mine Kimberlite
- Solid solution at 600°C

FIG. 24.

Table 38 The unit-cell dimensions and the densities of ilmenite from kimberlite and carbonatite

Sample	ao (^{o}A) ($\pm$ 0.002)	D	Reference
Kimberlite Mir.		4.67	Smirnov (1959)
" Zarnitsa		4.82	ditto
Hocheifel-basalt	8.465		Huckenholz (1966)
" -basalt	8.460		"
olivine gabbro. Skaergaerd	8.450^{+}		Deer, Howie, Zussman (1967)
massive kimb. 1210-1	8.372		Premier Mine
" " 1210-6	8.393		ditto
" " 1010-19	8.380		ditto
" " 1010-45	8.379		ditto
Der. 1	8.388		Derdepoort
Twe. 1	8.379		Tweefontein
Salt. 1	8.376		Saltpan

*Homogenized material.

of the primary phenocrystal phase is of common occurrence. The magnetite content of the massive kimberlite exceeds that of the kimberlite breccias, but this may be due to the difference in the amounts of residua phase material present in the two rock-types.

In table 38 the unit-cell dimensions and the densities of the magnetite in carbonatites, kimberlites, basalts and stratiform intrusions are compared. In Appendix 23 the chemical analyses of magnetite from carbonatite, kimberlite and tholeiite basalts are compared. According to the molecular norms calculated on a basis of 32 oxygen atoms per unit-cell (appendix 23) it is clear that the magnetites of carbonatites and kimberlites are more enriched in Mg^{2+}-spinel than the magnetite from the other rock-types. This increase in Mg^{2+}-spinel content of the magnetite in kimberlite and carbonatite is probably due to the more magnesium-rich environment from which the magnetite crystallized.

According to appendix 23 the magnetite from tholeiitic

rocks generally has a higher ilmenite content than the magnetite from kimberlite and carbonatite. The overlap between the ilmenite content of magnetite from the latter two rock types is also a very prominent feature. It thus appears that the initial temperature at which magnetite crystallized in kimberlite and carbonatite was lower than the temperatures of crystallization of the tholeiitic rocks, since only a limited amount of solid solution was possible. The presence of sphene, ilmenite and perofskite in the matrix of kimberlite and carbonatite clearly indicates that the lack of TiO_2 in the kimberlite magma was not responsible for the limited solid solution.

The absence of exsolution lamellae in the magnetite from kimberlite and carbonatite also indicates that cooling subsequent to crystallization was rapid. The presence of a low concentration of TiO_2 in these magnetites, however, also contributed to the absence of exsolution lamellae.

L. Conclusions

The mineralogical and chemical data presented in this chapter indicate that the minerals in the ultramafic nodules are similar to the primary phenocrystal minerals in kimberlite.

The minerals of the secondary phenocrystal phase differ from those of the primary phenocrystal phase in having crystallized at lower temperatures and pressures.

The eclogites are characterized by high-pressure mineral phases, which are completely different from the minerals in either kimberlite or garnet peridotite. The variation in the composition in the mineral phases in eclogite compared to the uniformity of the composition of the minerals in kimberlite is also a very characteristic feature.

In fig. 36 the paragenesis of the various minerals concerned is represented on an ordinary paragenesis diagram. The inferred depths and pressures at which the various mineral constituents formed are indicated on the Y-axis of this diagram. The mineral paragenesis diagram was then used to construct the model of the mantle (above 120 km) below the South African kimberlites, which is also represented in figure 40. The rock-types indicated in the model

was arrived at by considering the minerals in the paragenesis diagram. For example the presence of spinel at 15 kb. in the paragenesis diagram indicates that spinel peridotite should be present in the model of the mantle, which is proposed in the right hand side of this diagram. The succession of rock types depicted in the right hand side of this diagram corresponds exactly to the succession proposed by Jackson et al. for Hawaii. He derived his model from the investigation of the various rocks at Hawaii.

IX. THE PETROCHEMISTRY OF KIMBERLITE, UNDERSATURATED ALKALINE ROCKS AND THE COGNATE XENOLITHS FROM KIMBERLITE

A. Introduction

During the present investigation an attempt was made to collect all the available chemical analyses of kimberlite and rock-types associated with kimberlite. Although all the analyses have been calculated to their chemical norms, not all the chemical analyses have been plotted on the figures in this chapter. The analyses that have been plotted were sampled at random for each diagram.

The undersaturated alkaline basaltic rocks include the alnoiites, melilite basalts, carbonatites and the other calcite-olivine-phlogopite-bearing rocks, described from Sweden, South West Africa and the Congo. Since the mineralogy and the petrology of these rocks compare well to that of kimberlite (Von Eckerman, 1967), and since these rocks are mostly associated with kimberlite (Dawson, 1967) they will be referred to as rocks related to kimberlite.

The katamolecular norms of the kimberlite and the related rocks have been calculated on a cation basis, following the sequence that is usually followed in the equivalent norm (Burri, 1959). Hence calcite and dolomite are calculated before the silica allocations are made for the katamolecular norm.

B. The Petrochemistry of Kimberlite and Related Rocks.

A MODEL FOR THE COMPOSITION OF THE UPPER MANTLE AND THE FORMATION OF KIMBERLITES

(Depths and pressures correlated according to Green and Ringwood 1967)

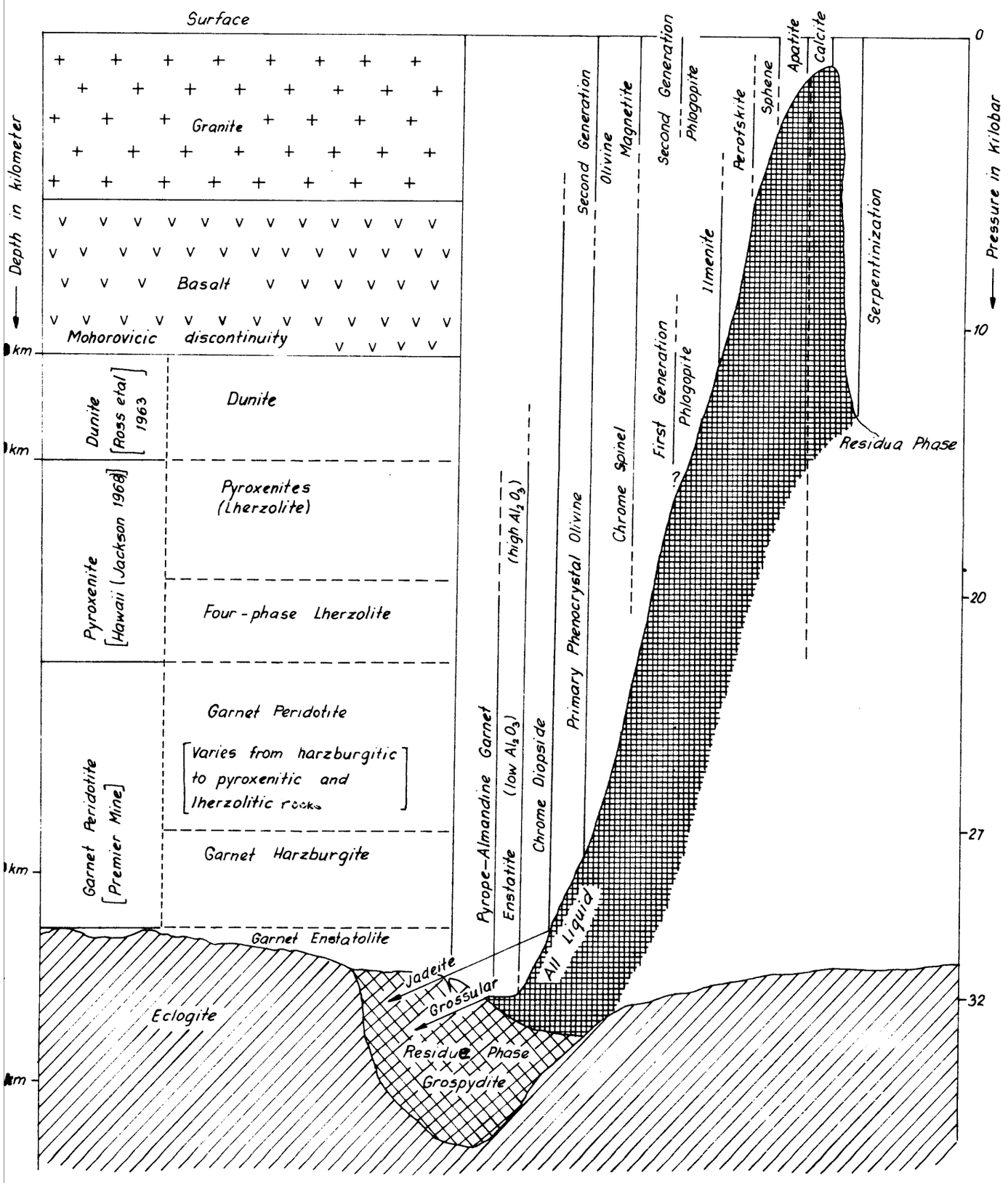

FIG. 36

The chemical analyses and katamolecular norms of all the available analyses of South African kimberlites are listed in appendix 24. The katamolecular norms indicate that most of the South African kimberlites are olivine and nepheline normative. The kimberlites which are enriched in CO_2 may contain normative feldspar and enstatite. Since kimberlite is a breccia consisting of various xenoliths which are not necessarily related, the presence of enstatite or nepheline in the norm does not reflect the original composition of the magma. The kimberlite dykes, however, which contain very few xenoliths of wall-rock generally also contain normative olivine and nepheline. Owing to the high CO_2 content of some kimberlites the ratio of $CaO+MgO/SiO_2$ decreases with the building of normative calcite and magnesite, which results in the presence of normative enstatite and feldspar, and this may not necessarily reflect the composition of the original kimberlitic magma, since secondary calcite is also present in some kimberlites.

According to Dawson (1967, p. 244) the micaceous and basaltic kimberlites on the average contain 0.3 per cent Na_2O, which is very similar to the sodium content of ultramafic rocks. However, the K_2O content of the micaceous kimberlites is much higher than that of basaltic kimberlite or ultramafic rocks. The CaO, $Na_2O + K_2O$, MgO + FeO variation diagram represented in figure 41, indicates that the micaceous kimberlites are relatively enriched in $Na_2O + K_2O$, the basaltic kimberlites in MgO + FeO and the massive kimberlites and alnoites in CaO.

According to Dawson (1967, p. 270) the CaO and CO_2 contents of the micaceous and basaltic kimberlites do not show single modal values on the frequency distribution diagrams, but usually show a large range of values between 0 and 40 per cent. However the micaceous kimberlites show more analyses in the high CO_2 content region than analyses of the basaltic kimberlites. The distribution of CaO in these rock-types also indicates a similar pattern. Microscopically the calcite content of the micaceous kimberlite also appears to exceed that of the kimberlite breccias, but is lower than that of the massive kimber-

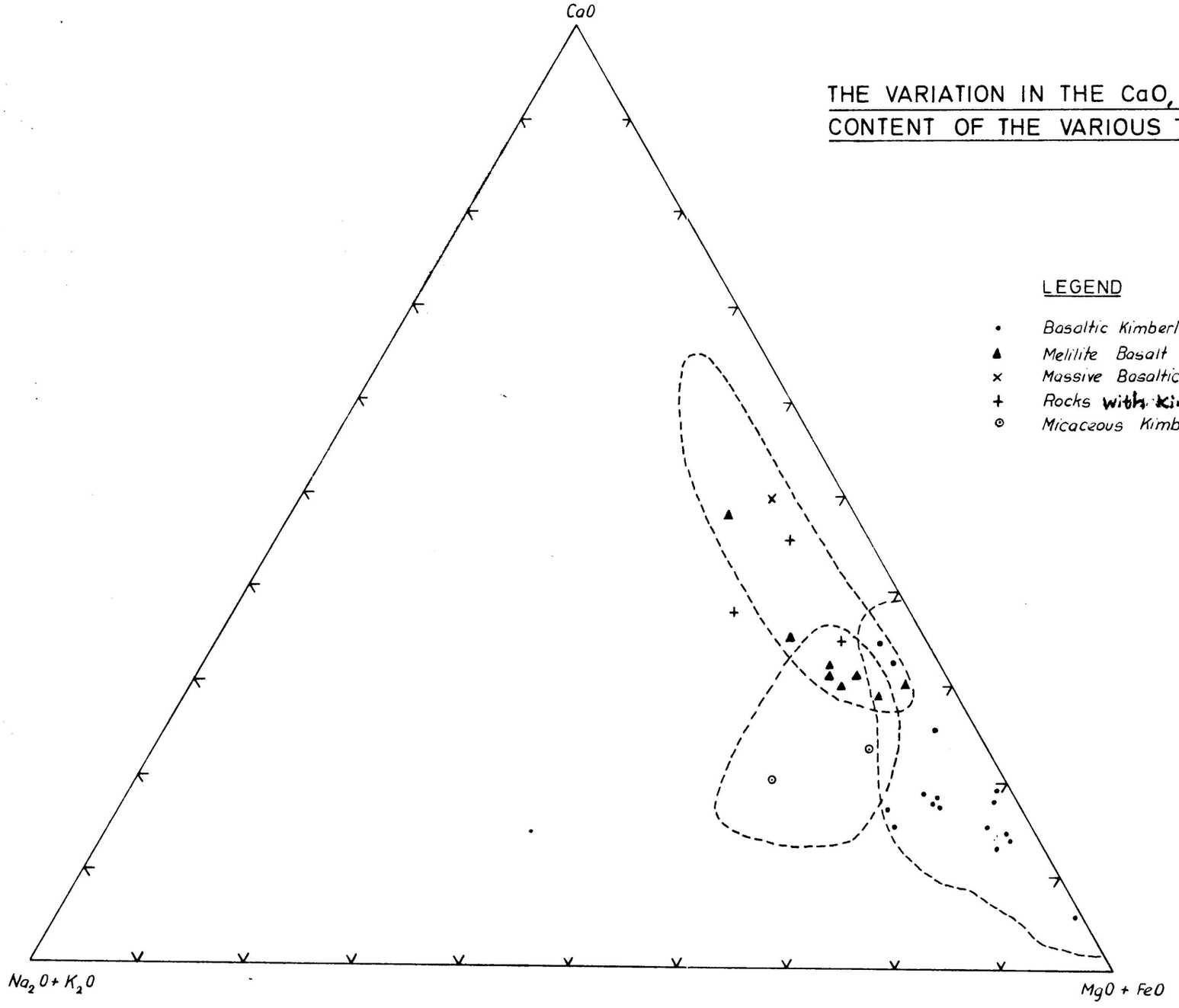

THE VARIATION IN THE CaO, $Na_2O + K_2O$, MgO + FeO CONTENT OF THE VARIOUS TYPES OF KIMBERLITE

LEGEND

- Basaltic Kimberlite
- Melilite Basalt
- Massive Basaltic Kimberlite
- \+ Rocks with kimberlitic affinities
- ⊙ Micaceous Kimberlite

FIG. 41

lites. The kimberlite breccias are usually more extensively replaced by secondary calcite, and consequently the distinction in CaO and CO_2 content of the basaltic and micaceous kimberlites is obliterated.

The chemical analyses and katamolecular norms of the kimberlites from outside Southern Africa are reported in appendix 25, and compare very well with the analyses of kimberlite from Southern Africa. Similar to the South African kimberlites, the analyses which contain appreciable amounts of CO_2 contain normative plagioclase and enstatite, whereas the other analyses contain normative Ca-olivine, nepheline and olivine. The chemical analyses and katamolecular norms of some undersaturated alkaline rocks related to kimberlite and which include melilite basalts, alnoiites and atlantites are supplied in appendix 26. The norms of these rocks contain nepheline, Ca-olivine and olivine, and display the same constituents as kimberlites. The chemical analyses closely resemble those of the massive basaltic kimberlites and the micaceous kimberlites. The chemical analyses and the katamolecular norms of the carbonatites and the massive kimberlites are given in appendix 27. This table shows that the carbonatites contain mostly normative enstatite and feldspar, whereas the massive kimberlites contain normative nepheline, Ca-olivine and olivine. However, owing to the high CO_2 content of the carbonatites, the norms contain enstatite and feldspar, and this does not necessarily reflect the original composition of the magma.

The chemical analyses reported in appendices 24 to 27 have been plotted in figures 42 to 45 according to the procedure outlined previously.

The AFM diagram figure 42 to 45 reveals that the kimberlites are enriched in MgO and that they mark the start of the normal differentiation trend of magmas in general. The melilite basalts partly overlap with the kimberlites, and then extend further away from the corner of the diagram, indicating that these rocks are more differentiated. The analyses of the massive- and micaceous kimberlites are mostly concentrated in the overlap-area. The carbonatites plot close to the F

THE AFM VARIATION FOR KIMBERLITE, CARBONATITE, MELILITE BASALT AND ALNOIITE

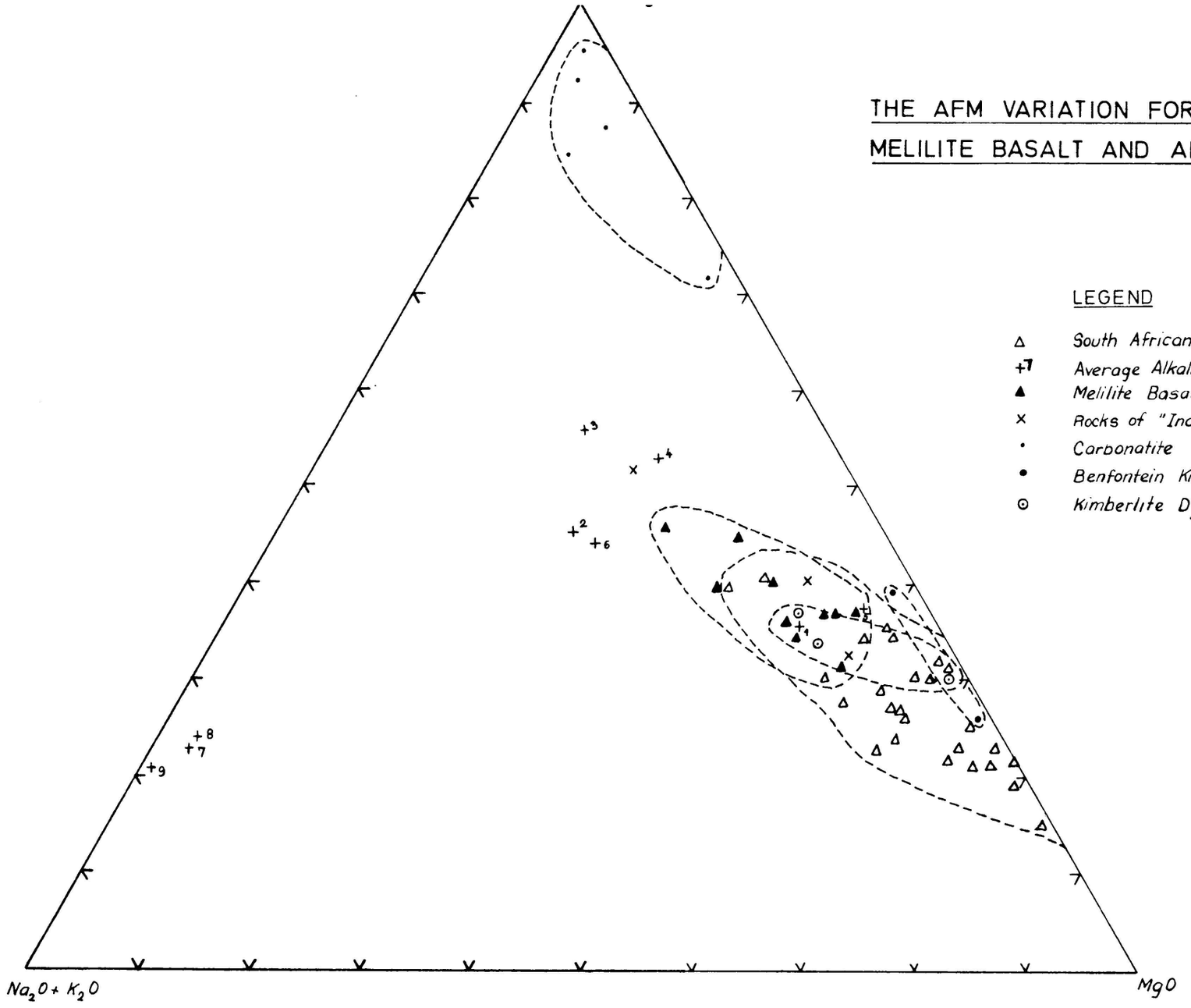

FIG. 42

corner, and extend along the F-M line, in the direction of the analysis of the massive kimberlites. Only the analyses of sövitic carbonatites have been used, because the primary carbonates were all found to be enriched in calcium in the kimberlites.

The C.F.M. variation diagram depicted in figure 43 shows a complete gradation from kimberlite through melilite basalt and massive kimberlite to the carbonatite field. This complete gradation of rock-types could also be discerned in the diagram showing the variation in volatile constituents, $SiO_2 + Al_2O_3 + Na_2O + K_2O$, and $CaO + MgO + FeO + Fe_2O_3 + TiO_2$ (Dawson 1967) depicted in figure 44. However in the latter diagram the sequence is reversed, showing a succession from melilite basalt, kimberlite, massive kimberlite and micaceous kimberlite to carbonatite.

The QLM and CLM variation diagrams, where C represents the normative amounts of calcite, magnesite, hematite and magnetite, represented in figure 45, show a trend of variation indicating a sequence from melilite basalt, through kimberlite and massive kimberlite to carbonatite at the C corner. The QLM diagram, however, produced no variation sequence with regard to these rocks.

C. The Petrochemistry of the Post-Waterberg Alkaline Province North-east of Pretoria

Since the petrology of the alkaline intrusions north-east of Pretoria has been described by Shand, (1922), Toens, (1952) and Verwoerd, (1967), only the petrochemical relations will be discussed.

The chemical analyses and katamolecular norms of the kimberlites and alkaline rocks from this area are given in appendix 29. The $Na_2O + K_2O/SiO_2$ diagram after McDonnald and Katsura, (1964) indicates that the massive kimberlites and the alkaline rocks fall into the alkaline basalt series (figure 46). The kimberlite breccias, however, fall into the tholeiitic rock series, but this may be due to the large amount of ultramafic phenocrysts, which cause the low alkali-content.

The AFM variation diagram (figure 47) reveals that the kimberlites form the initial portion of the normal differentiation curve, whereas the alkaline rocks form the

THE VARIATION IN THE CaO, MgO AND $FeO + Fe_2O_3 + MnO$ CONTENT IN KIMBERLITES AND RELATED ROCKS

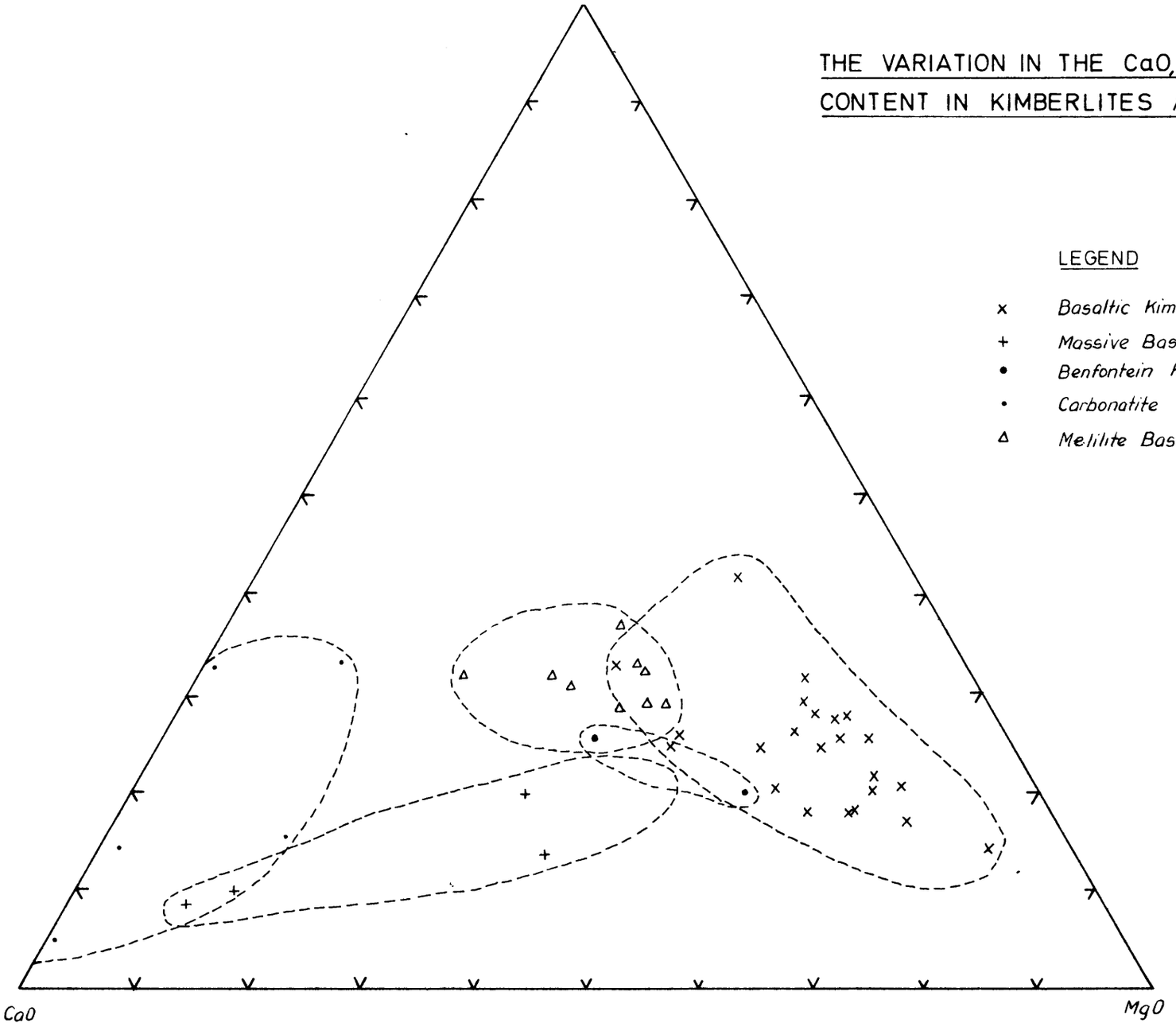

FIG.

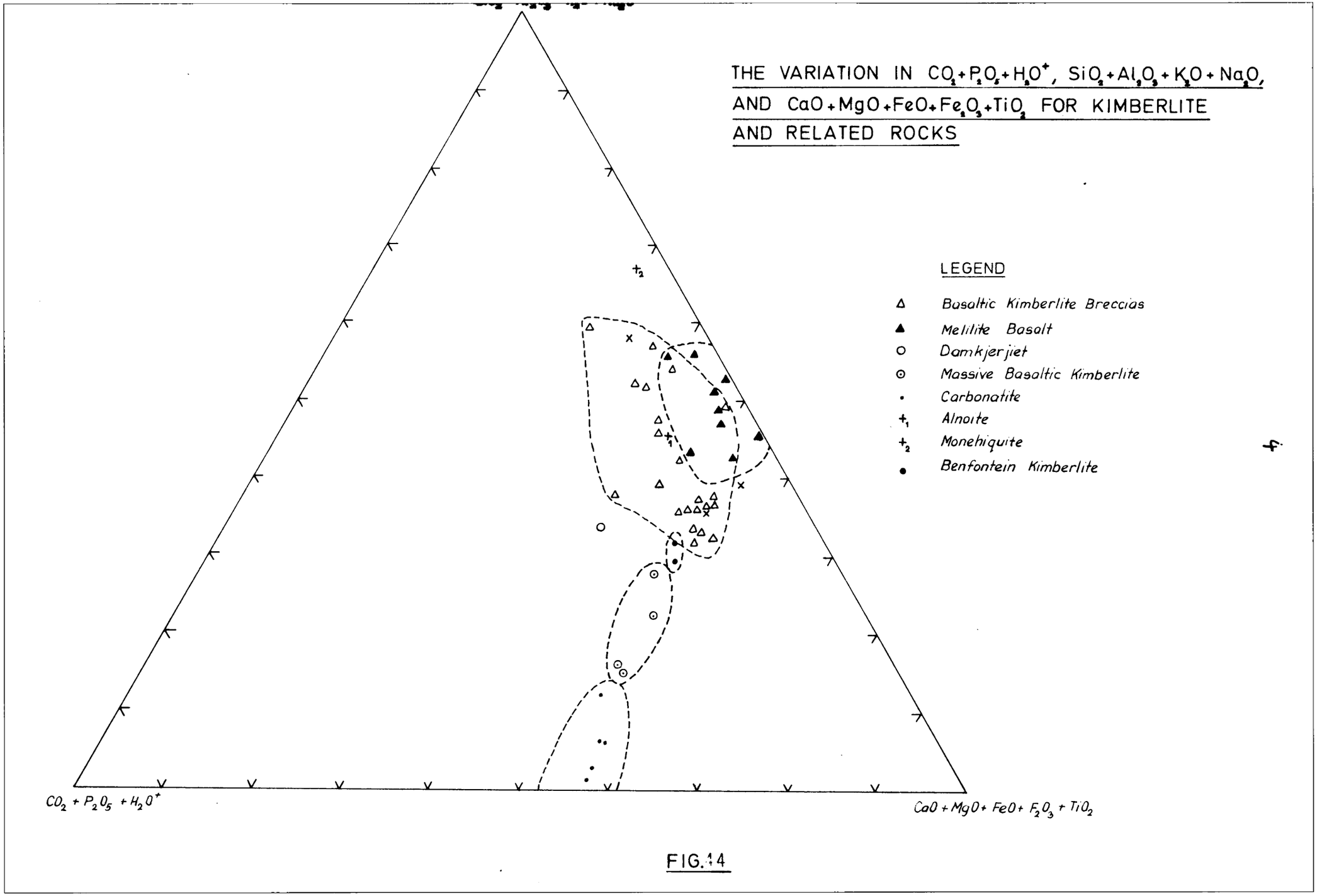

FIG. 14

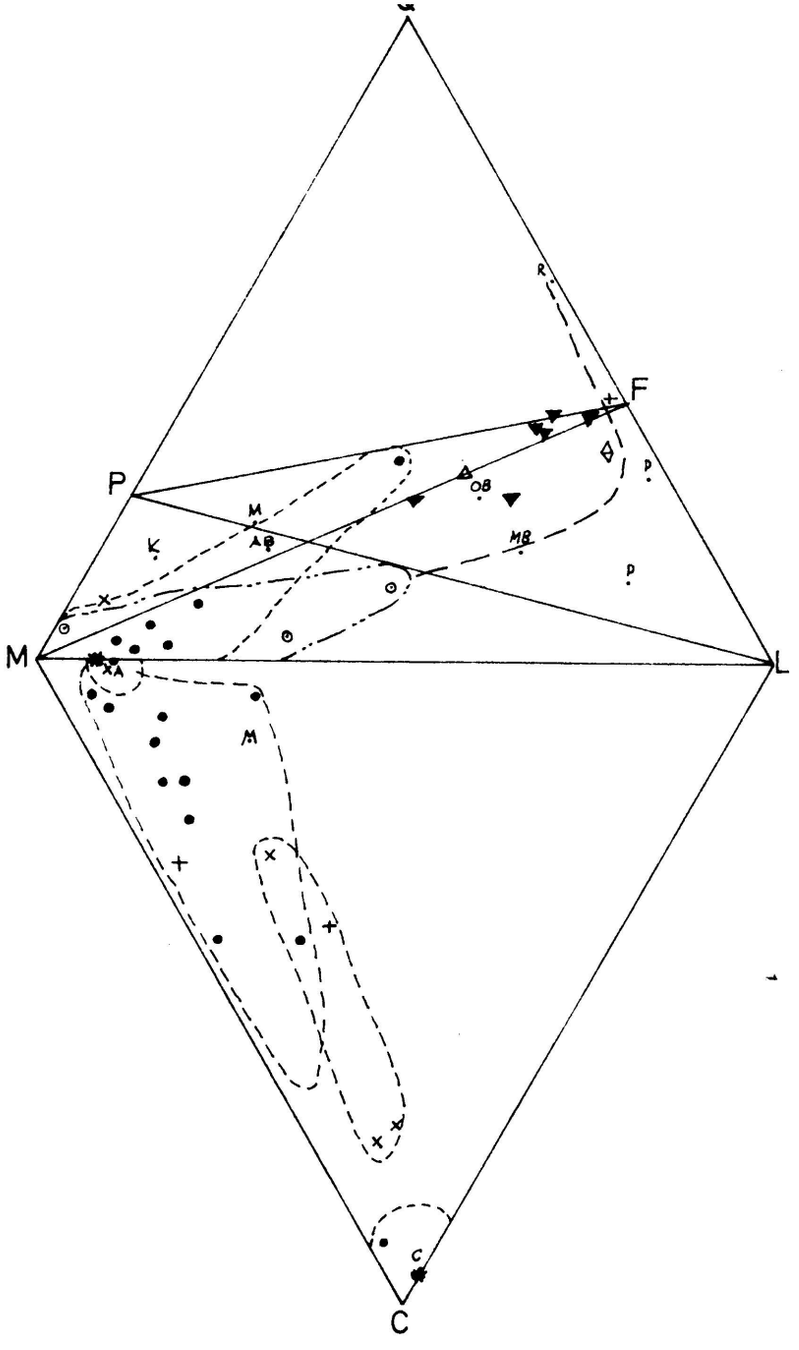

THE QLM AND CML VARIATION DIAGRAMS FOR VARIOUS UNDERSATECRATED ALKALINE ROCKS

LEGEND

- ⊙ Alnoite + Melilite Basalts
- • Basaltic Kimberlite Breccias
- ✱ Massive Basaltic Kimberlite
- × Carbonatite
- \+ Benfontein Kimberlite
- △ Atlantite
- ▼ Syenite
- ◈ Tinguaite

FIG. 45

THE $Na_2O + K_2O / SiO_2$ VARIATION DIAGRAM FOR THE ALKALINE IGNEOUS PROVINCE NORTH - EAST OF PRETORIA

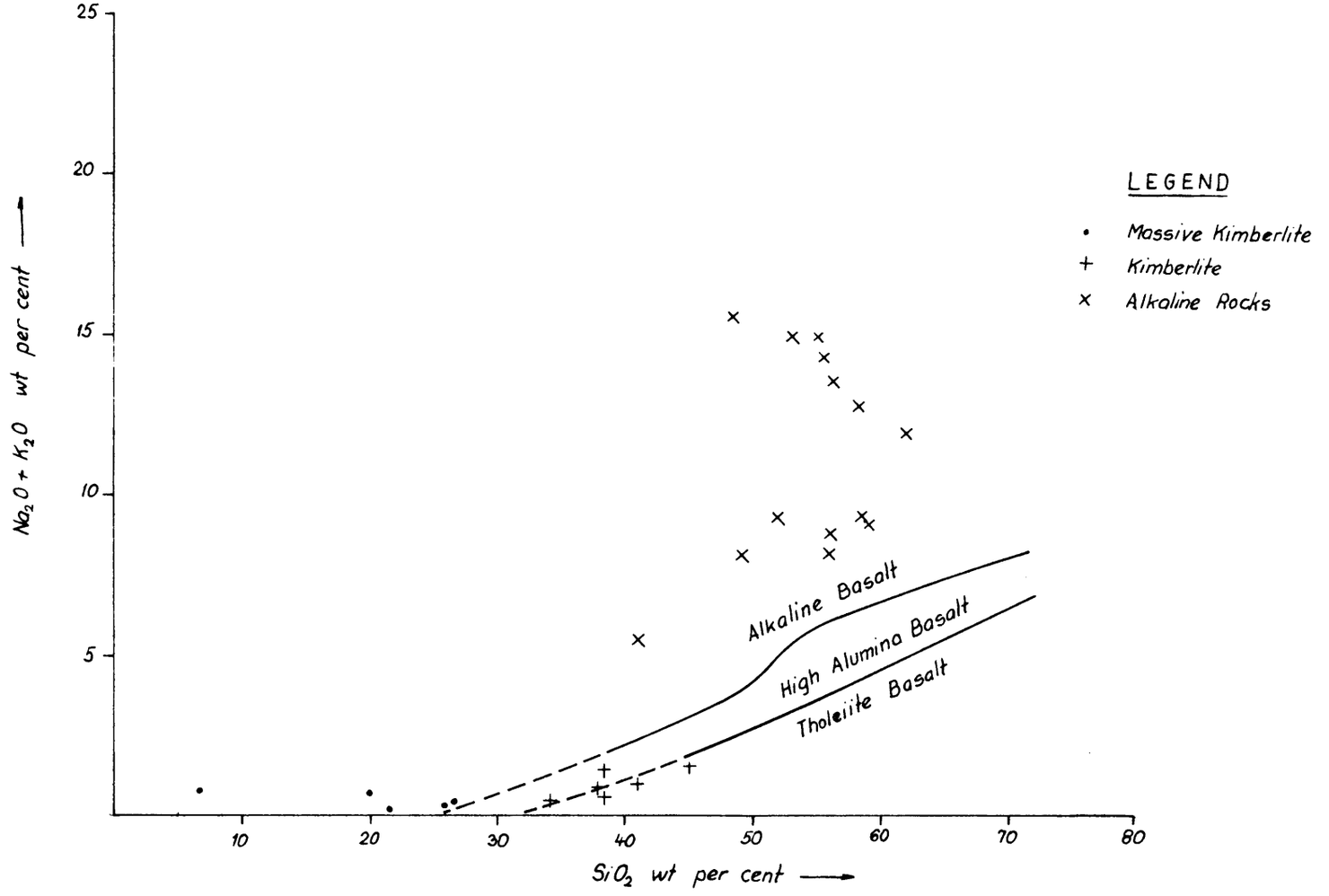

FIG. 46

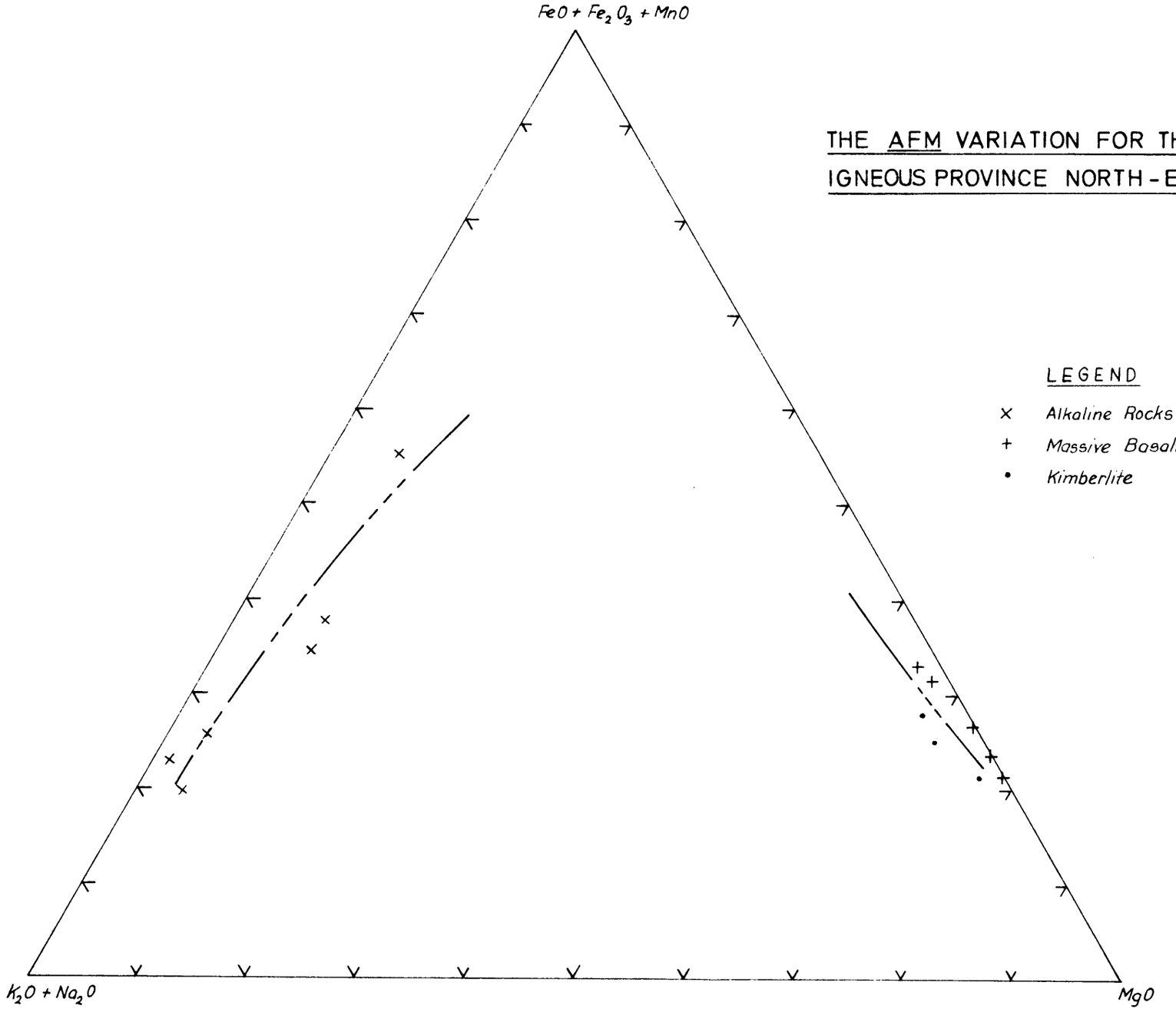

THE AFM VARIATION FOR THE ALKALINE IGNEOUS PROVINCE NORTH-EAST OF PRETORIA

LEGEND

× Alkaline Rocks

\+ Massive Basaltic Kimberlite

• Kimberlite

67

FIG. 47

end portion. The kimberlite and massive kimberlite also show the initial portion of the melilite basalt-carbonatite variation trend on the CFM variation diagram (figure 48).

According to these diagrams it appears that all the post-Waterberg intrusions in this area belong to the alkaline basalt series, and that a kimberlite-carbonatite, as well as a normal differentiation sequence for alkaline basalts could be established. This suggests that all the alkaline rocks north east of Pretoria were intruded during the same phase of magmatic activity, but that the kimberlites and carbonatites formed independently of the alkaline rocks in this province, and thus caused the two disconnected differentiation trends in figures 47 and 48.

D. The Chemistry of the Ultramafic and Eclogitic Nodules

It has been indicated on the preceeding pages that the ultramafic nodules in kimberlite are petrographically similar to the nodules in alkaline basalts and alpine peridotites. Chemically these rocks and the ultramafic differentiates of stratiform complexes are not widely different. The chemical analyses and katamolecular norms of ultramafic rocks derived from all these parentages are compared in appendix 39. The katamolecular norms of these analyses have been calculated in the same way as the katamoleculars of the kimberlites. According to the katamolecular norms presented in appendix 39 the nodules from the Russian kimberlites are mostly nepheline normative, and all the other nodules are enstatite normative. Consequently these latter nodules fall into the olivine tholeiite field according to Yoder and Tilley (1962). [illegible]. The katamolecular norms also indicate that these ultramafic nodules have a low content of diopside and feldspar.

The chemical analyses and katamolecular norms, calculated similarly to that of the kimberlites, of the different eclogite nodules are reported in appendix 30. The katamolecular norms indicate that some of the eclogite nodules are enstatite normative and others are nepheline normative. The diopside and feldspar content of the eclogite nodules are high, and range from 45.0 to 85.0

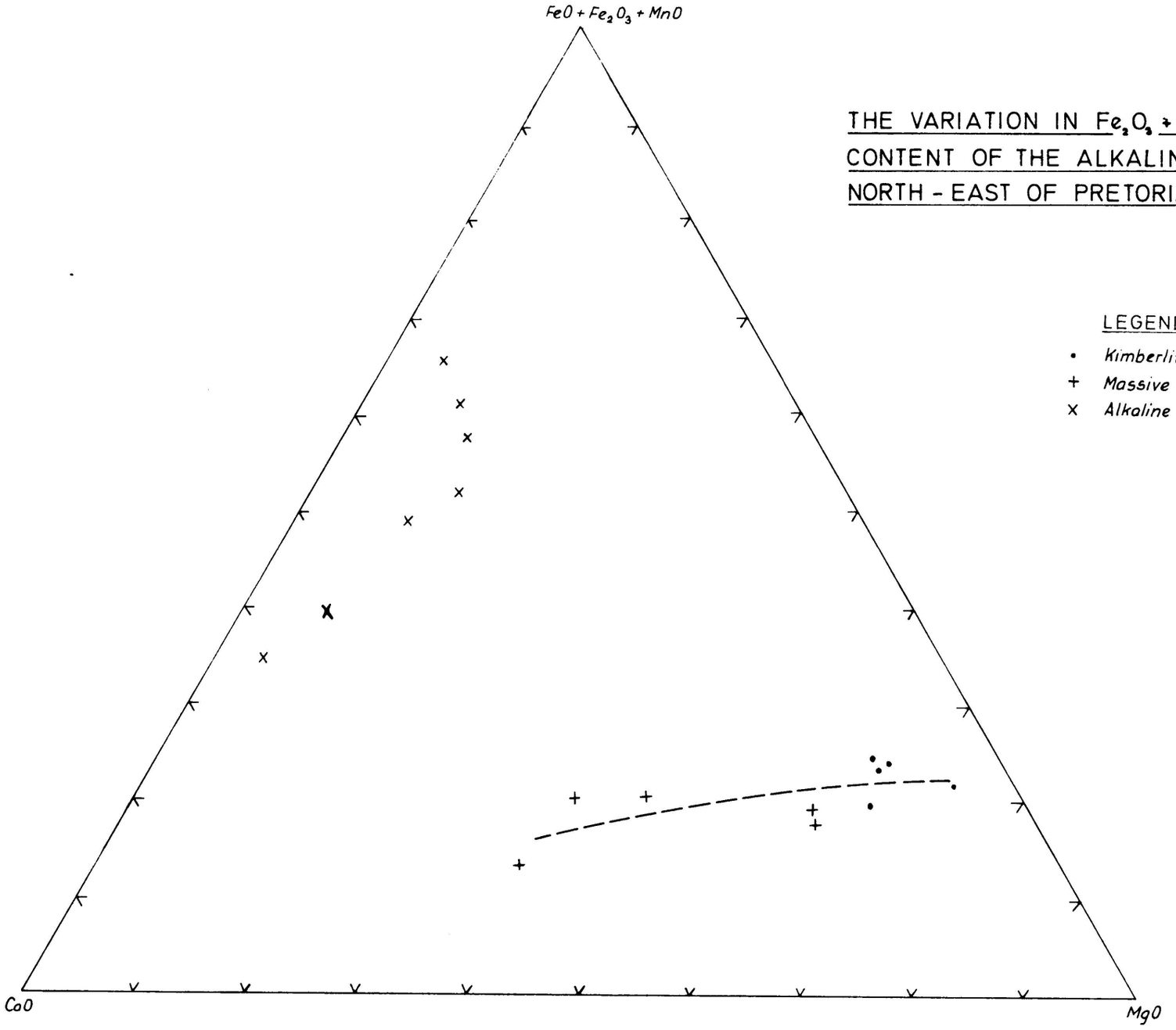

THE VARIATION IN Fe_2O_3 + FeO + MnO, MgO AND CaO CONTENT OF THE ALKALINE IGNEAS ROCKS NORTH - EAST OF PRETORIA

LEGEND

- Kimberlite
- \+ Massive Basaltic Kimberlite
- × Alkaline Rocks

FIG. 48

per cent. The kyanite eclogites are often kyanite normative, whereas the grospydites are invariably kyanite normative, and both types are depleted in enstatite and olivine although it has been stressed by O'Hara (1968), Mercy (1967), Green and Ringwood (1967) and others that eclogite is chemically similar to gabbro, but appendices 27 and 31 state that this is true for regional eclogites, but not for kimberlitic eclogites. The MgO/CaO ratio of eclogite is greater than 1.0 whereas that of gabbro or tholeiite basalts is less than 1.0. The grospydite and kyanite eclogite nodules have an Al_2O_3/ FeO + Fe_2O_3 ratio of 7 times that of either gabbro or tholeiite basalt. The chemical analyses of olivine basalts correspond better to the chemical analyses of the eclogite except that the MgO/Al_2O_3 ratio is different.

In figure 49, showing the Na_2O + K_2O/SiO_2 ratios after McDonnald and Katsura (1964), it is evident that the eclogite nodules are more enriched in SiO_2 than the ultramafic nodules. The ultramafic nodules of ~~all~~ the basalts and kimberlites ~~different parentages~~ appear to overlap completely, and fall mainly in the tholeiite field. Some garnet peridotites also plot in the high alumina basalt area. The kyanite eclogites and grospydites occur mostly in the alkaline basalt field, whereas the eclogites are concentrated in the high alumina basalt field. However, a large variation is evident in the latter rock-types.

The MgO/FeO ratios of the different parentages of ultramafic nodules are represented in fig. 50. Ninety two per cent of the ultramafic nodules in kimberlite fall below the line FeO = 0.1556 MgO, and 62 per cent below the line FeO = 0.1087 MgO+2.7, whereas ultramafic cumulates from stratiform complexes are more enriched in FeO, and plot above the line FeO = 0.1556 MgO+4. The MgO/FeO ratio of the ultramafic nodules in alkaline basalts and in alpine peridotites overlap with both the peridotites in kimberlite and the olivine cumulates in layered intrusions.

A comparison of the MgO/FeO ratios of eclogite and garnet peridotite nodules (figure 51), indicates a much lower value for eclogite than for garnet peridotite. Figure 51 also indicates that the MgO/FeO ratio in kyanite eclogite and grospydite is the same as that of eclogite,

THE $Na_2O + K_2O / SiO_2$ RATIO FOR THE VARIOUS ULTRAMAFIC AND ECLOGITIC ROCKS

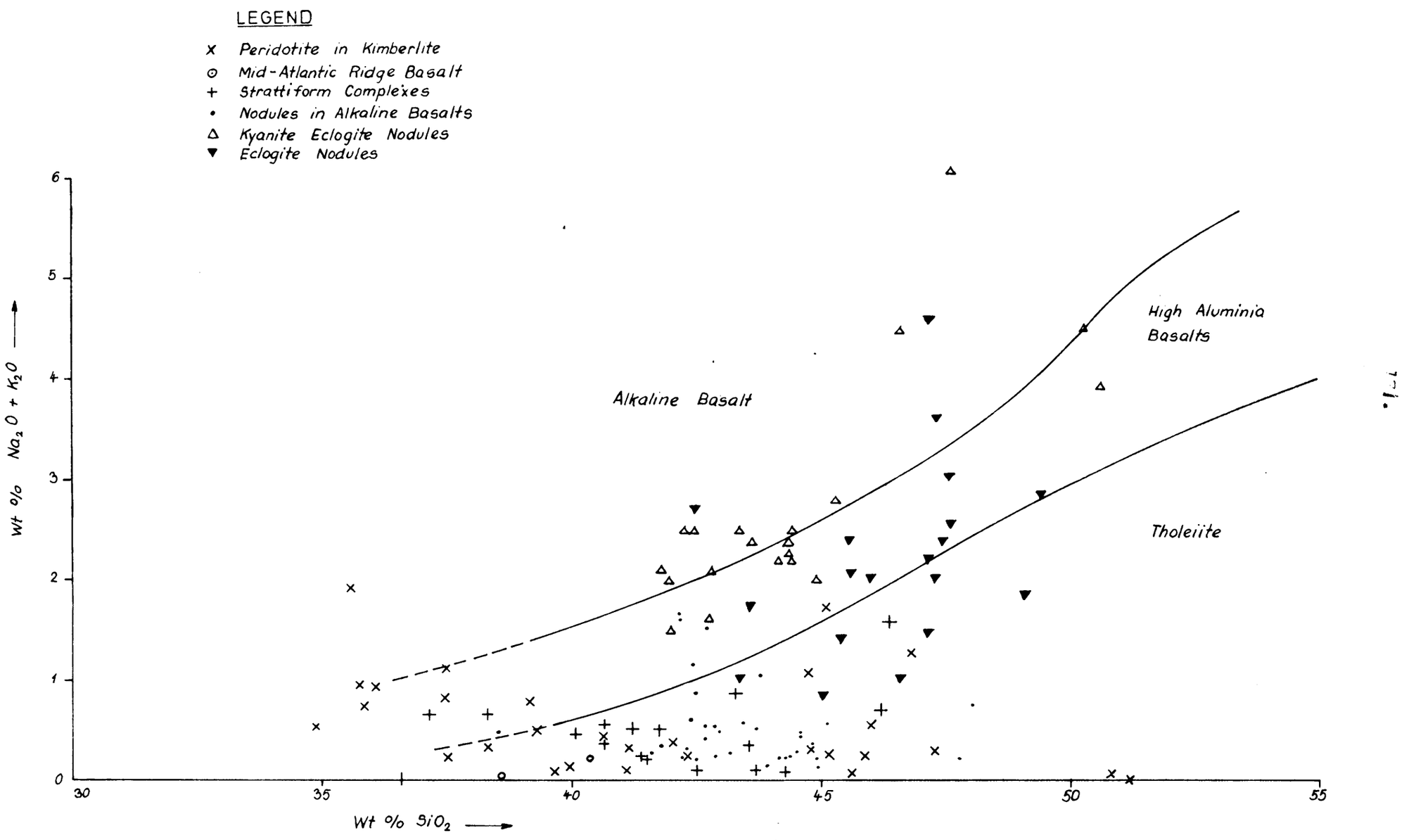

FIG. 49

THE MgO / FeO VARIATION FOR THE DIFFERENT PARENTAGES OF ULTRAMAFIC ROCKS

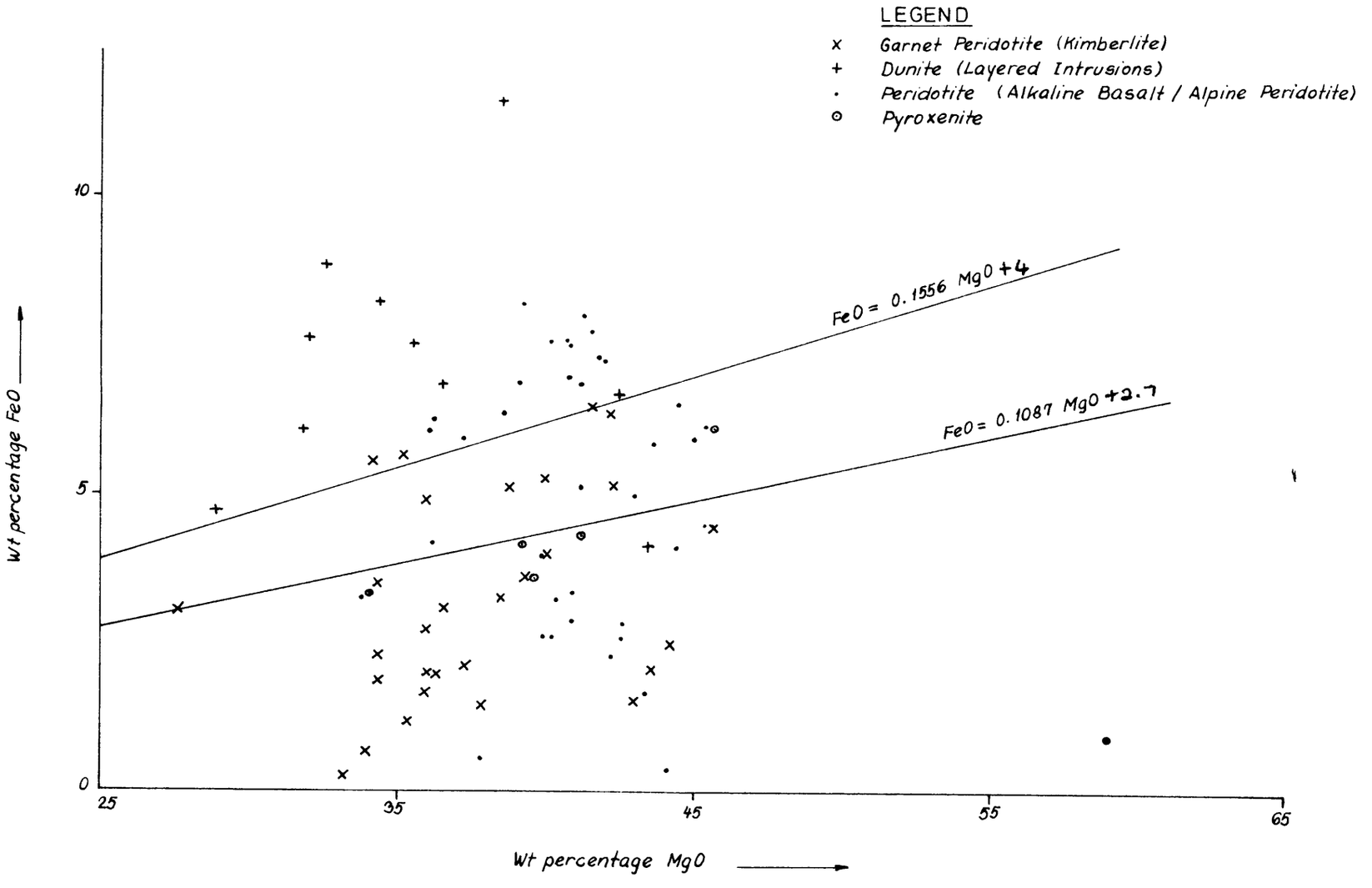

FIG. 50

THE VARIATION IN MgO/FeO IN ULTRAMAFIC AND ECLOGITIC NODULES IN KIMBERLITE

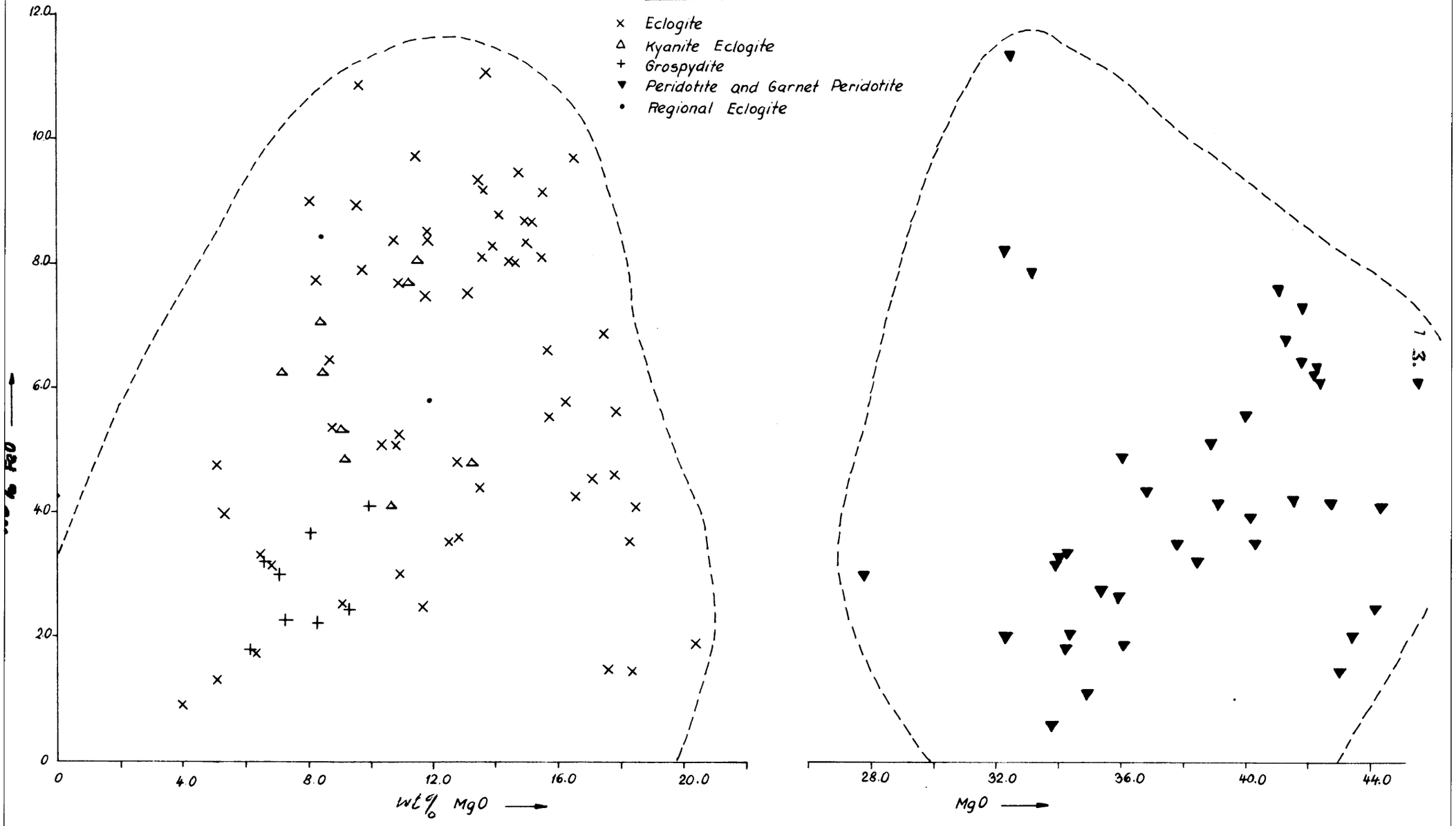

FIG.51

but that these rocks are impoverished in both constituents. Although fig. 51 shows a tremendous variation in the MgO/FeO ratio of eclogites, no systematic variation could be discerned. In table 39 the MgO/FeO ratios for the various rocks under discussion are compared. This table shows an increase in the FeO content in the sequence garnet peridotite, peridotite, pyroxenite, grosspydite, eclogite, kyanite eclogite.

Table 39. A comparison of the MgO/FeO ratio in ultramafic and eclogitic nodules

Type of Nodule	Host Rock	Av. MgO/FeO ratio
garnet peridotite	kimberlite	42.4
peridotite	"	40.5
pyroxenite	"	12.6
peridotite	alkaline basalt	25.9
eclogite	kimberlite	1.9
kyanite eclogite	"	1.7
grosspydite	"	2.8
stony meteorite	-	1.3
basalt of the mid-atlantic ridge	-	34.5

The FeO + Fe_2O_3, MgO, Na_2O + K_2O variation diagram (figure 52) shows a very limited distribution for the ultramafic nodules. The garnet peridotite nodules in kimberlite are more enriched in MgO than any of the other nodules, and the peridotite nodules from kimberlite compare well with the nodules in alkaline basalts, but the latter become slightly more enriched in FeO + Fe_2O_3. Of the sequence of nodules in kimberlite the pyroxenite nodules are the most enriched in iron and they correspond to the iron-enriched nodules in alkaline basalts. The alpine peridotites fall into the peridotite field for kimberlites, and the oceanic basalts from the mid-atlantic ridge plot in the peridotite field for alkaline basalts.

The eclogite, kyanite eclogite and grospydite nodules display a more random distribution in this diagram. The eclogite and some of the kyanite eclogite nodules plot

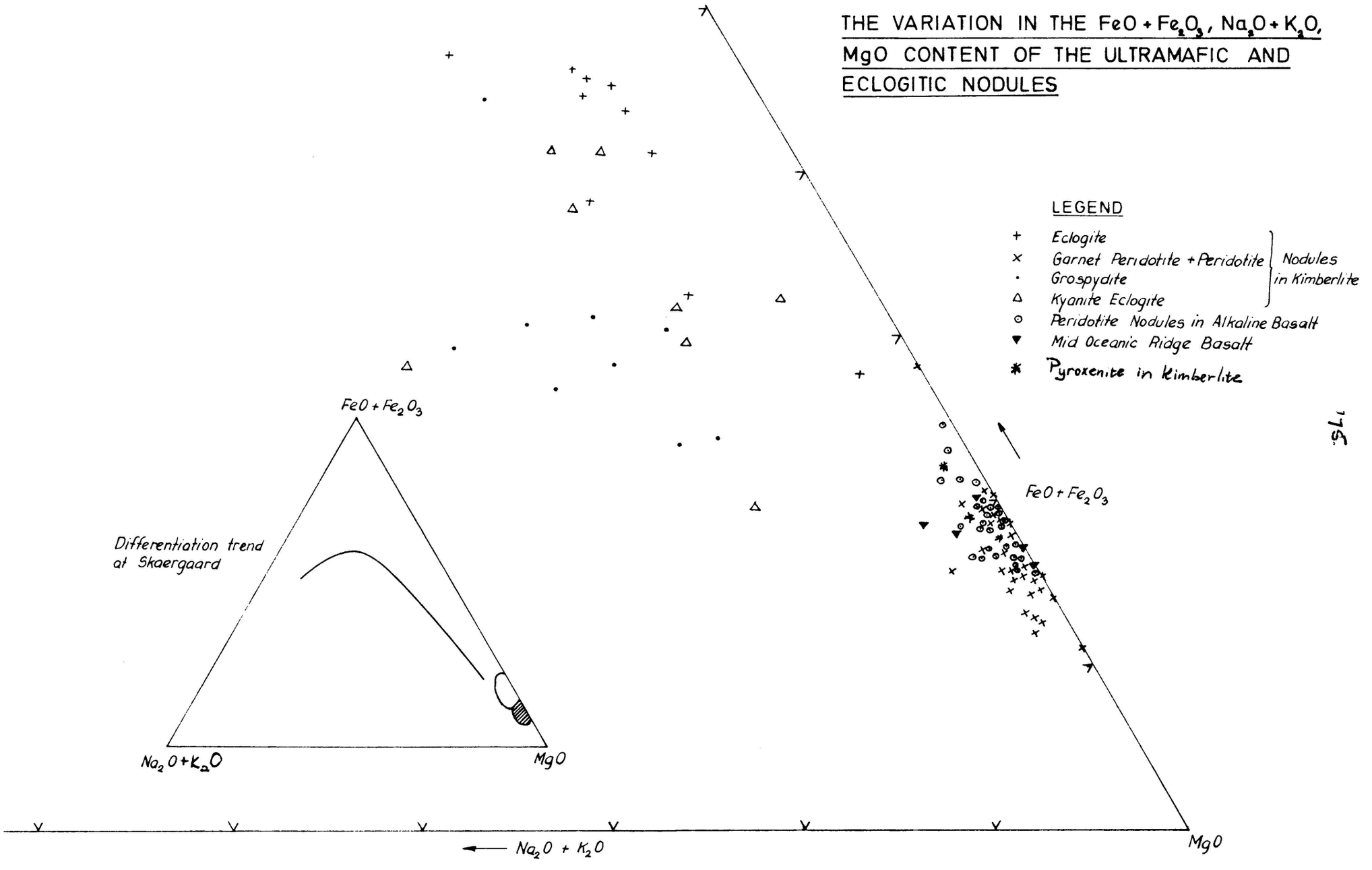

FIG. 2

along the normal differentiation trend for tholeiitic magmas, whereas other kyanite eclogites and the grospydites fall along the differentiation trend for alkaline basaltic magmas.

The MgO, Al_2O_3, CaO variation diagram (figure 53) indicates that the garnet peridotite nodules in kimberlite have a higher Al_2O_3 content than the peridotite nodules in alkaline basalts. The CaO content is very similar in these nodules, but is appreciably higher in the pyroxenite nodules from kimberlite. The Al_2O_3 content of the garnet peridotite nodules is very much the same as that in the pyroxenite nodules. The eclogite nodules form a sequence becoming increasingly enriched in Al_2O_3 in the sequence eclogite, kyanite eclogite and grospydite, but the CaO content remains fairly constant, corresponding to the CaO content of the pyroxenite nodules. This figure also shows that the kyanite eclogite and grospydite become increasingly impoverished in MgO, which indicates a decrease in the diopside content, and an increase in the grossularite and kyanite contents. The melting of clinopyroxene above 30 kb, according to the reaction on page 95., would thus be able to account for this sequence becoming enriched in Al_2O_3. According to this reaction the grospydite and kyanite eclogite should be considered as the residua on melting of the eclogite, and is characterized by a concentration of Al_2O_3 and CaO.

The variation in MgO, CaO and the $Al_2O_3 + Fe_2O_3 - (Na_2O + K_2O)$ contents of the different nodules are represented in figure 54. This diagram reveals that the eclogites, kyanite eclogites and grospydites contain a considerable amount of normative feldspar and that they plot further away from the alumina-alkali corner than in figure 53. The grospydite is still the most aluminous, succeeded by the kyanite eclogite and the eclogite. The peridotite nodules from the various parentages occupy the same position as in figure 53, indicating low percentages of normative feldspar.

In figure 55 the variation in the normative amounts of nepheline, quartz and olivine are depicted on the Q L M diagram after Niggli. The thermal divide after

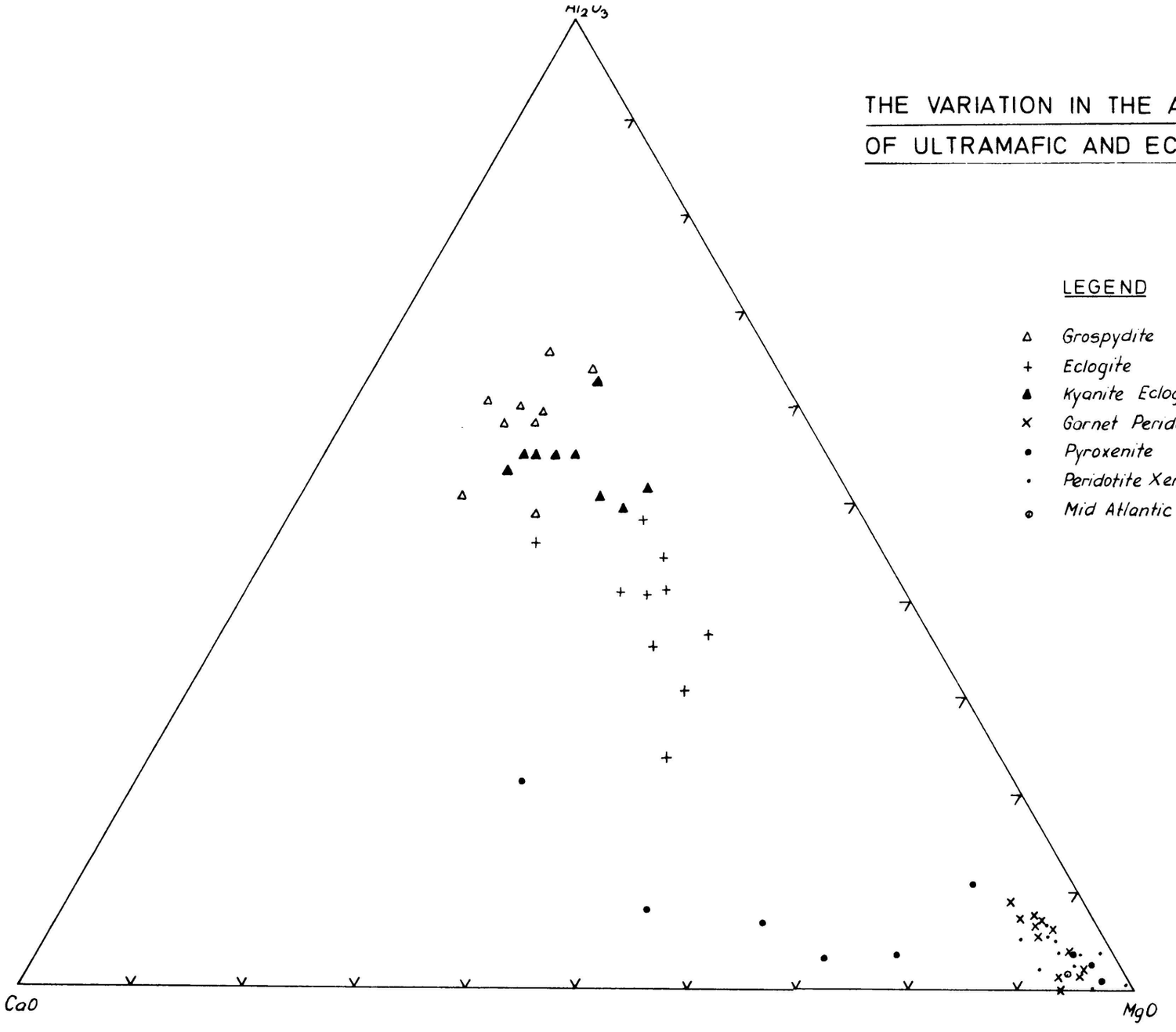

THE VARIATION IN THE Al_2O_3, MgO, CaO CONTENT OF ULTRAMAFIC AND ECLOGITIC NODULES

LEGEND

- △ Grospydite
- \+ Eclogite
- ▲ Kyanite Eclogite
- × Garnet Peridotite + Peridotite
- • Pyroxenite

} Nodules in Kimberlite

- · Peridotite Xenoliths from Alkaline Basalt
- ⊙ Mid Atlantic Ridge Basalt

77

FIG. 3

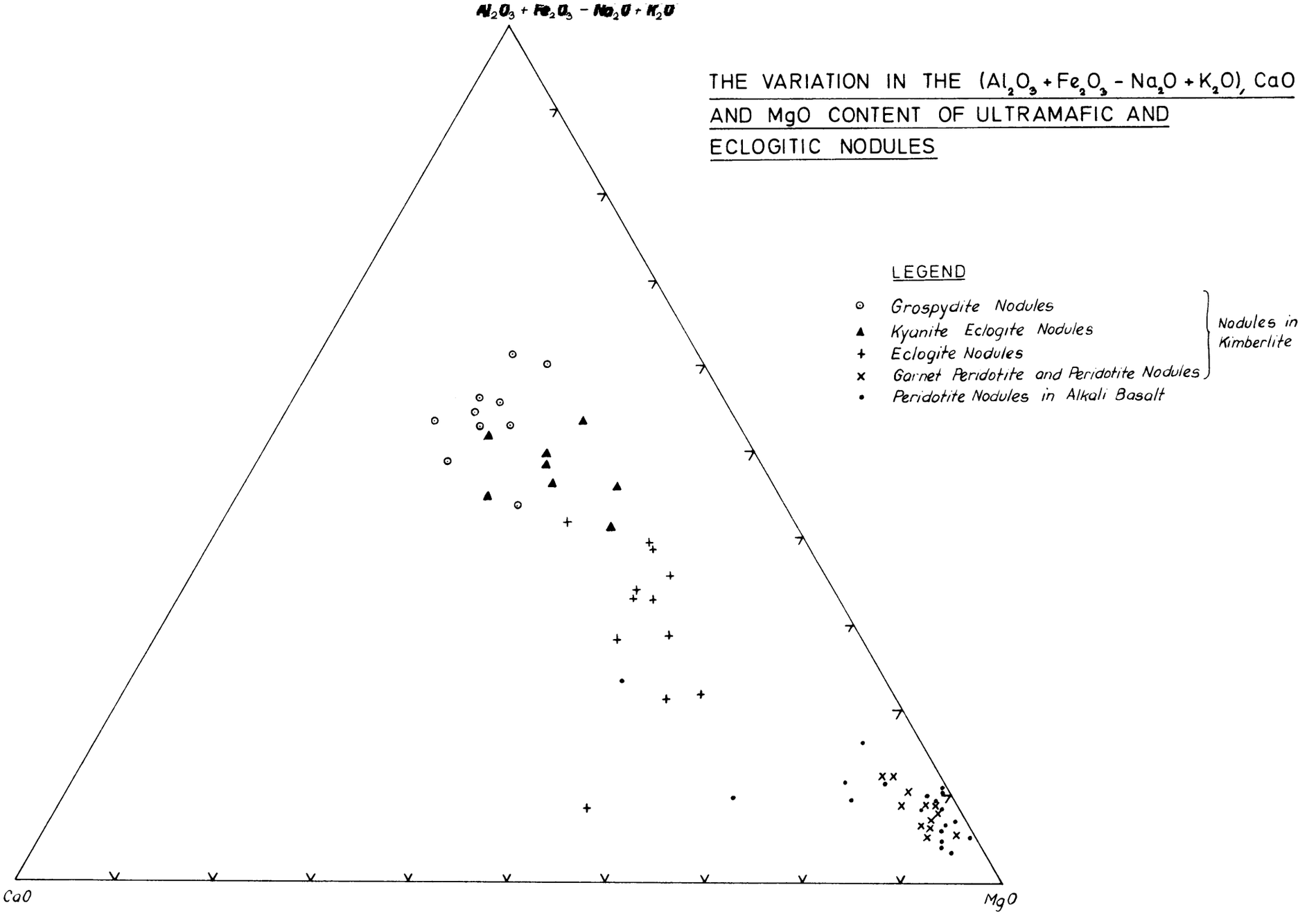

THE VARIATION IN THE $(Al_2O_3 + Fe_2O_3 - Na_2O + K_2O)$, CaO AND MgO CONTENT OF ULTRAMAFIC AND ECLOGITIC NODULES

LEGEND

- ⊙ Grospydite Nodules
- ▲ Kyanite Eclogite Nodules
- \+ Eclogite Nodules
- × Garnet Peridotite and Peridotite Nodules

} Nodules in Kimberlite

- • Peridotite Nodules in Alkali Basalt

FIG. 54

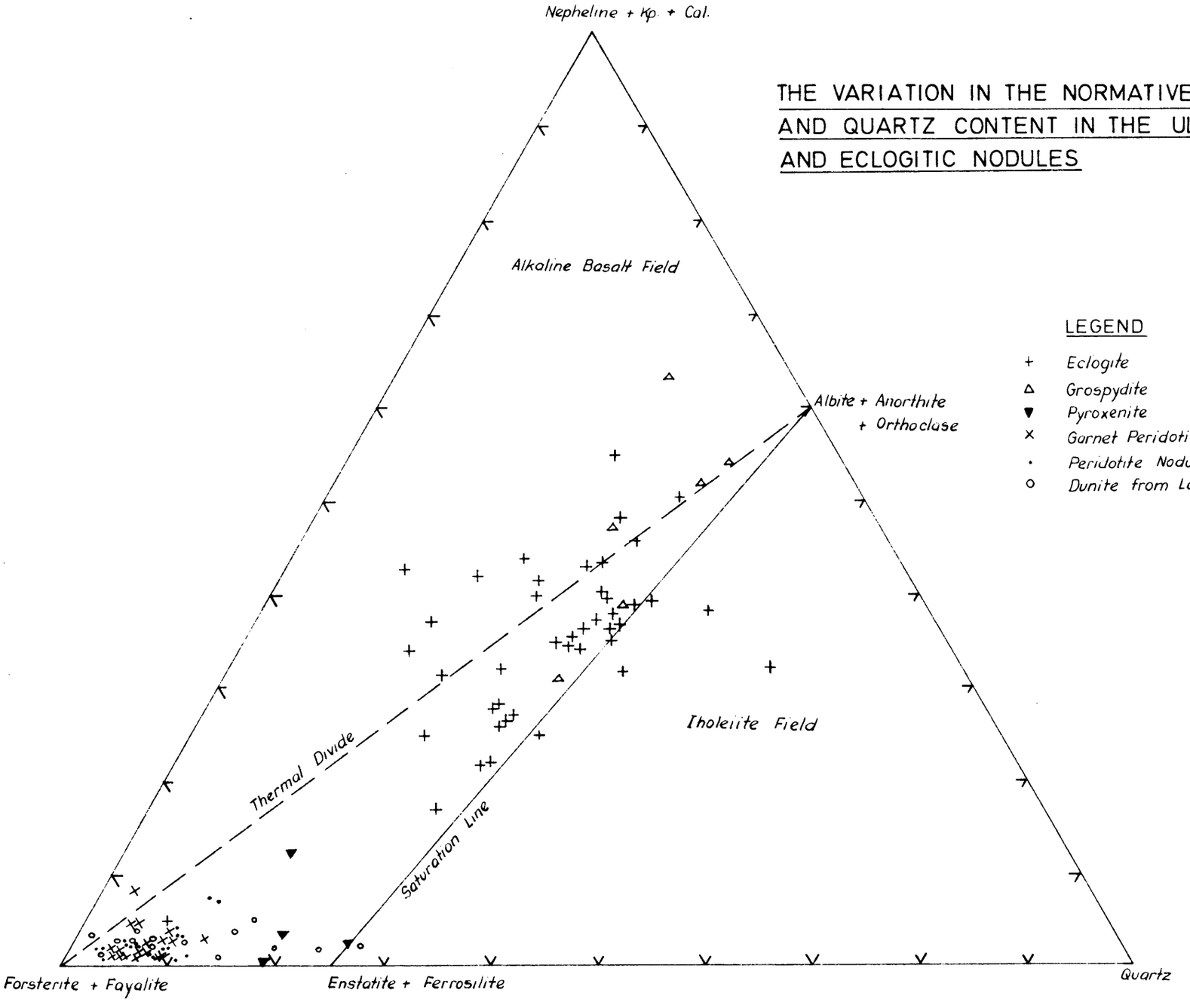

THE VARIATION IN THE NORMATIVE NEPHELINE, OLIVINE AND QUARTZ CONTENT IN THE ULTRAMAFIC AND ECLOGITIC NODULES

LEGEND

- \+ Eclogite
- △ Grospydite
- ▼ Pyroxenite
- × Garnet Peridotite and Peridotite

} Nodules in Kimberlite

- · Peridotite Nodules in Alkaline basalt
- ○ Dunite from Layered Intrusions

FIG. 55

Yoder and Tilley (1962) and the saturation line after Niggli are also shown. The peridotites from alkaline basalts and kimberlites fall in the olivine tholeiite field, and are thus not the likely source material for alkaline basalts. The eclogite, kyanite eclogite and grospydites fall into both the alkaline basalt and olivine tholeiite basalt fields, however, isolated analyses also occur in the tholeiite basalt field. Since the eclogites are mainly concentrated in the alkaline basalt field, they appear to be the most likely source material for the alkaline basalts.

The normative olivine, nepheline and diopside contents of the various nodules are shown in figure 56. This figure indicates that the ultramafic nodules occupy the area nearest to the olivine corner, and that the pyroxenite nodules are enriched in diopside. The eclogite analyses yield a complete scatter on the diagram and contain normative diopside and normative nepheline in appreciable quantities, but have a fairly constant [illegible] content. The kyanite eclogite and grospydite contain the highest amount of normative nepheline and the lowest percentages of olivine and diopside.

A comparison of the frequency distributions of Na_2O, K_2O, Cr_2O_3, TiO_2, CaO and FeO of the peridotite and eclogite nodules in kimberlite are shown in figure 57. This figure indicates the following modal distributions for the peridotite and eclogite nodules.

	Peridotite nodules	Eclogite nodules
Na_2O + [illegible]	0.5%	2.0
CaO	2.5	10.5
TiO_2	0.2	0.5
FeO	3.0	8.0
K_2O	<0.1	0.25

Since kimberlite contains a large amount of olivine, enstatite and pyrope garnet, the composition of which is similar to that of the corresponding constituents in the ultramafic nodules, it is to be expected that the MgO, Al_2O_3, Cr_2O_3 and SiO_2 contents of kimberlite would depend largely on the amount of inclusions of olivine, enstatite and pyrope garnet in the kimberlite. None of the elements

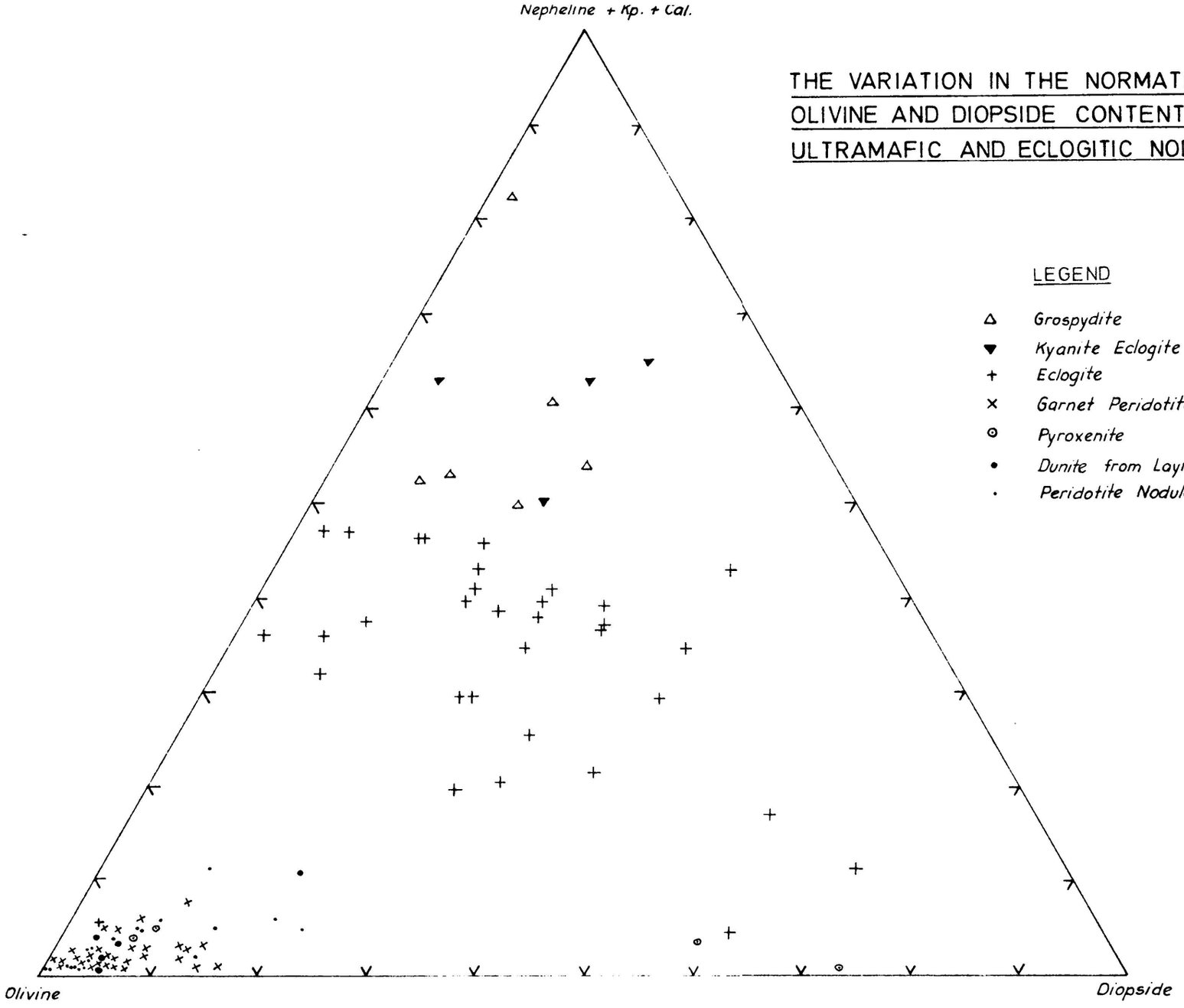

THE VARIATION IN THE NORMATIVE NEPHELINE, OLIVINE AND DIOPSIDE CONTENT OF THE ULTRAMAFIC AND ECLOGITIC NODULES

LEGEND

- △ Grospydite
- ▼ Kyanite Eclogite
- \+ Eclogite
- × Garnet Peridotite and Peridotite
- ⊙ Pyroxenite

} Nodules in Kimberlite

- • Dunite from Layred Intrusions
- · Peridotite Nodules in Alkaline basalt

FIG. 56

THE FREQUENCY DISTRIBUTION DIAGRAMS FOR CaO, TiO_2, Cr_2O_3, $FeO + Na_2O + K_2O$ IN THE ULTRAMAFIC AND ECLOGITIC NODULES IN KIMBERLITE

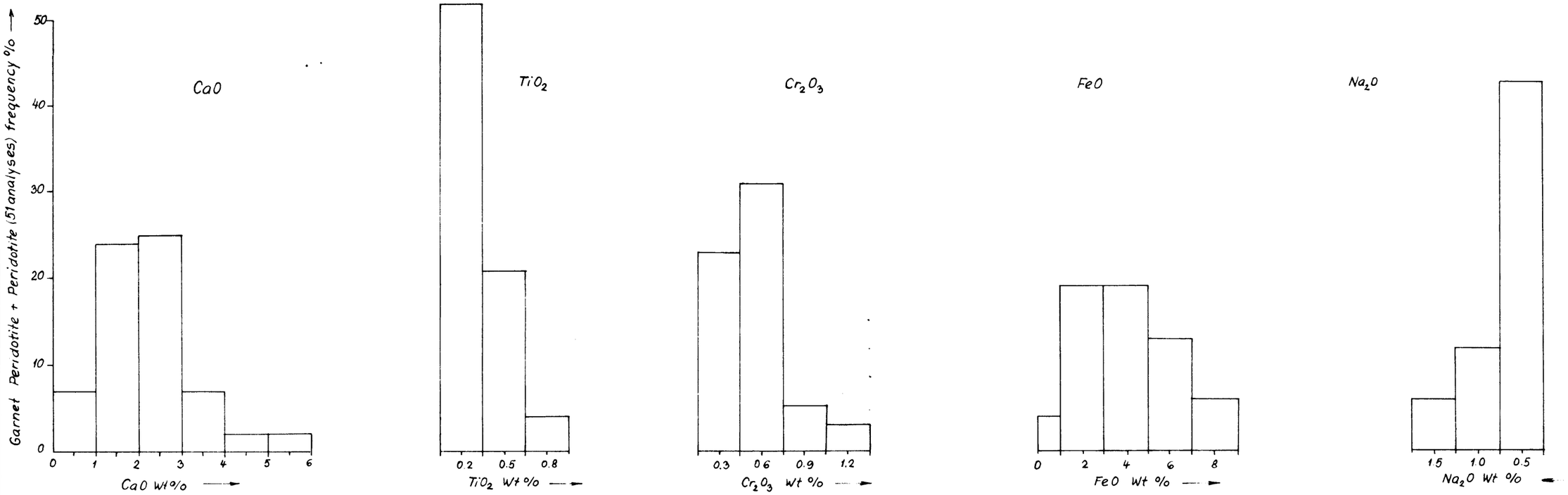

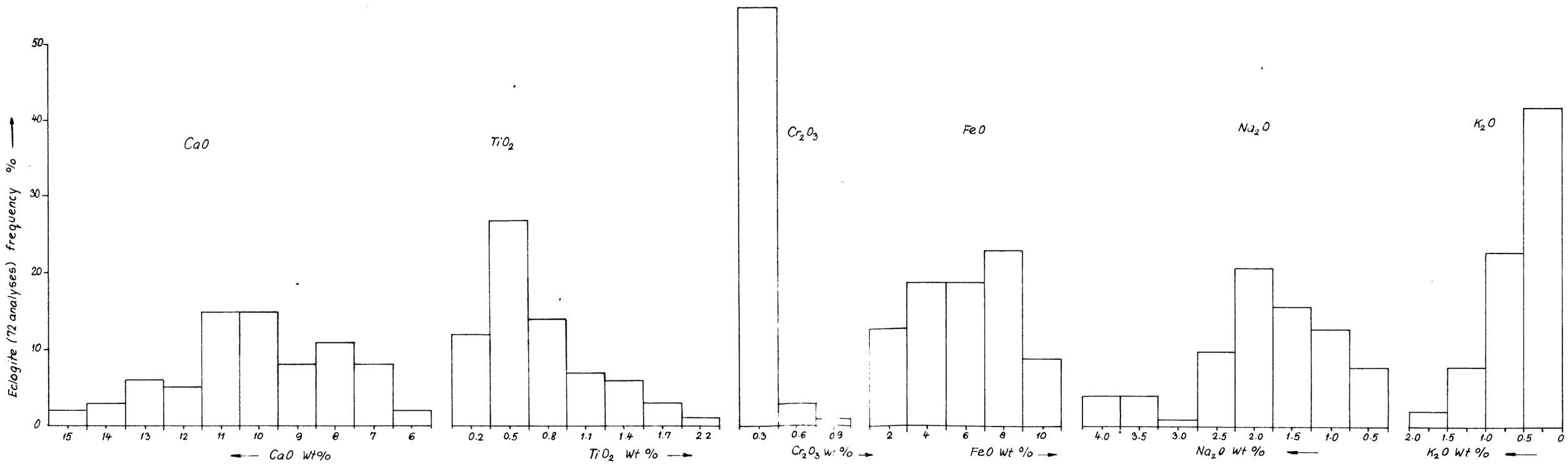

FIG. 57

listed above are present a large percentage in the included phases, therfore they can be used as to determine the source of the kimberlite magma.

The purer kimberlite magmas, like the massive basaltic kimberlites, are usually enriched in all the oxide fractions summarized above. The data presented show that an eclogite source material and the crystallization of peridotite would be able to yield a magma enriched in these oxides. The reverse, however, would certainly not be possible. Even the melting of a large volume of peridotite and the crystallization of a small proportion of eclogite would not be able to produce a kimberlite magma.

In figure 58 the projection from diopside onto the C_3A,M,S plane after O'Hara (1968), as well as the chemical analyses of ultramafic and eclogite nodules are represented. In this figure C = (mol. prop. CaO - $3\frac{1}{3}$ P_2O_5 + $2Na_2O$ + $2K_2O$) x 56.08; M = (mol. prop. FeO + MnO + MgO - TiO_2) x 40.31; A = (mol. prop. Al_2O_3 + Cr_2O_3 + Na_2O + K_2O + TiO_2) x 101.96; S = (mol. prop. SiO_2 - $2Na_2O$ - $2K_2O$) x 60.09. The figure reveals that all the analyses fall below the plane of silica saturation and that the analyses of pyroxenite, peridotite, eclogite, kyanite eclogite and grospydite form a zone stretching from olivine to grossular.

Considering the phase equilibria in the system CaO-MgO-Al_2O_3-SiO_2 after O'Hara (1968, p. 86-91) it appears to be impossible to consider garnet lherzolite as the source material and kimberlitic eclogite as the cumulus phase during the genesis of kimberlite magmas, under falling pressures. Note in figures 58, 59 and 60 that the melting of any rock in this system will start at B (in the figures), and that with a decrease in pressure this point would move into the garnet phase volume to A (at 20 kb.). Partial melting of a garnet lherzolite would thus yield a partial melt of composition B, and a residua on partial melting of dunite, which is depleted in Al_2O_3. The crystallization of this partial melt at reduced pressures must crystallize either olivine, or enstatite or both, and would not be able to produce kimberlitic eclogite. Conversely, the partial melting of eclogite would also result

in a liquid of composition B, and would yield a residua on partial melting which is depleted in normative olivine and enstatite, and enriched in normative anorthite and grossular. The grospydite and kyanite eclogite nodules in kimberlite closely resemble this rock-type. This partial melt at B would be able to crystallize enstatite and olvine or both, at reduced pressures, and would thus be able to produce garnet peridotites, garnet lherzolites and garnet pyroxenites.

It appears that the only way in which eclogite can be considered as a cumulus phase from the partial melting of a four-phase lherzolite, would be to start the crystallization of eclogite at exactly the pressure of partial melting. In order to crystallize eclogite at this point, the temparature must be raised "substantially" (O'Hara and Yoder 1967, p. 107), and the reaction of orthopyroxene with liquid to produce olivine, clinopyroxene and garnet (O'Hara 1967, p. 105) succeeded by the inferred reaction of olivine and liquid to produce clinopyroxene and garnet (O'Hara and Yoder 1967, p. 106) must take place. Should all this happen and "coincidence" places the composition of this liquid in the composition plane of the bimineralic eclogites (O'Hara and Yoder, 1967, p. 105) it is possible that eclogite would crystallize with falling pressure. However, the crystallization of the eclogite now requires that the pressure does not decrease significantly, because then the olivine and enstatite phase volumes would overrun the clinopyroxene phase volume. (Figures 58, 59 and 60). Crystallization of this melt must start to crystallize clinopyroxene first, resulting in a clinopyroxenite, and would then be able to produce bimineralic eclogite.

Apart from the speculative nature of the argument, the resulting eclogite and clinopyroxenite are inconsistent with the eclogite nodules found in kimberlite. Of the 514 eclogite nodules investigated only two instances were recorded where clinopyroxene was the "cumulus phase", and in both these cases the clinopyroxene "cumulus crystals" were concentrated in layers with a thickness of less than 2 cm., in layered eclogites. Among the 2000 odd nodules investigated no clinopyroxenite has been observed. It thus appears that eclogite should be considered as the source material, gros-

THE C_3A,M,S PROJECTION FROM THE DIOPSIDE POINT AFTER O'HARA (1968), SHOWING THE CHEMICAL ANALYSES OF ULTRAMAFIC AND ECLOGITIC XENOLITHS

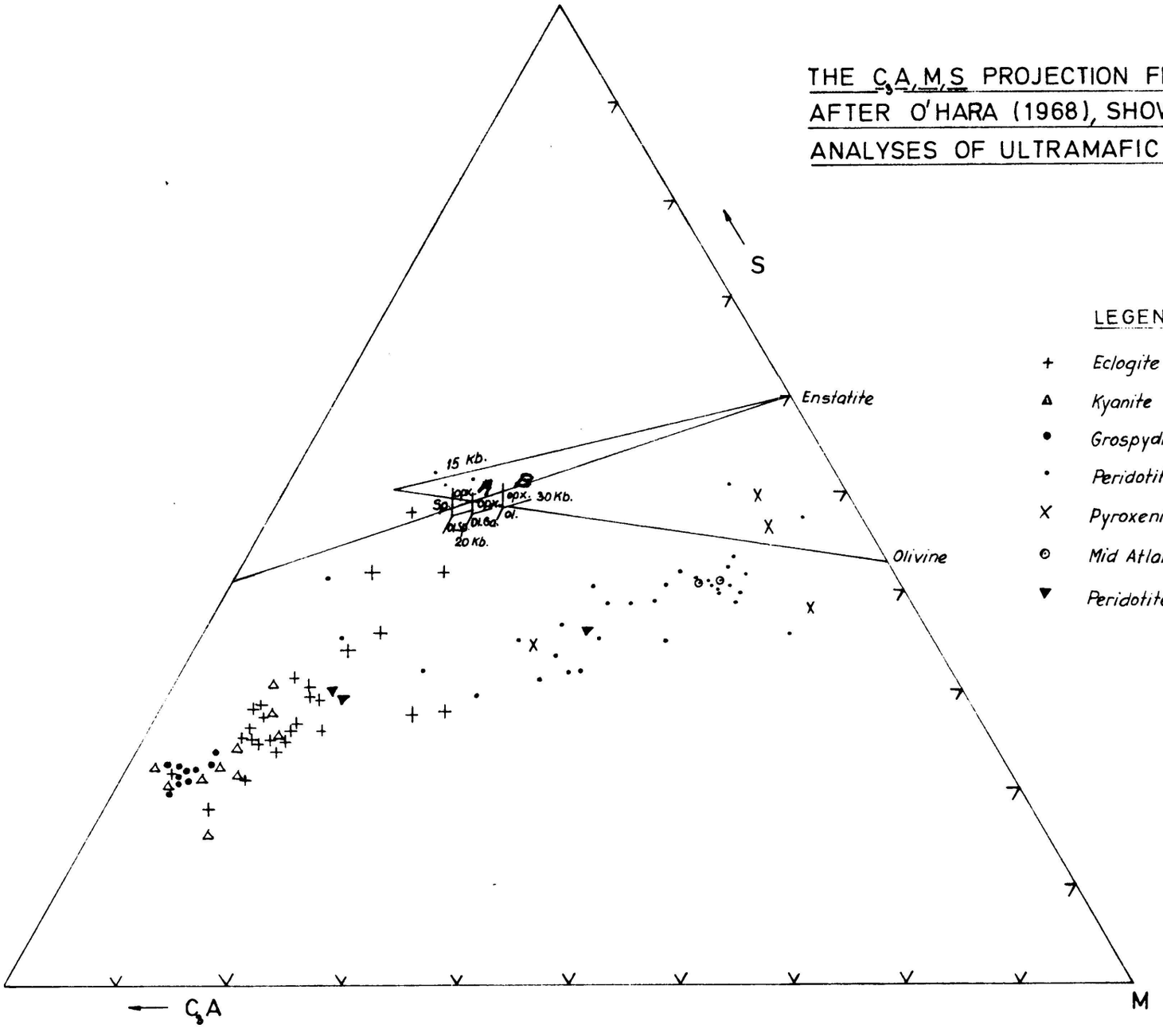

LEGEND

- + Eclogite
- △ Kyanite Eclogite
- ● Grospydite
- · Peridotite
- X Pyroxenite

} Nodules in Kimberlite

- ⊙ Mid Atlantic Ridge Basalt
- ▼ Peridotite Xenoliths in Alkaline Basalt

FIG.58

THE A, MS, CS SUBPROJECTION FROM THE OLIVINE POINT
(After O'Hara, 1968)

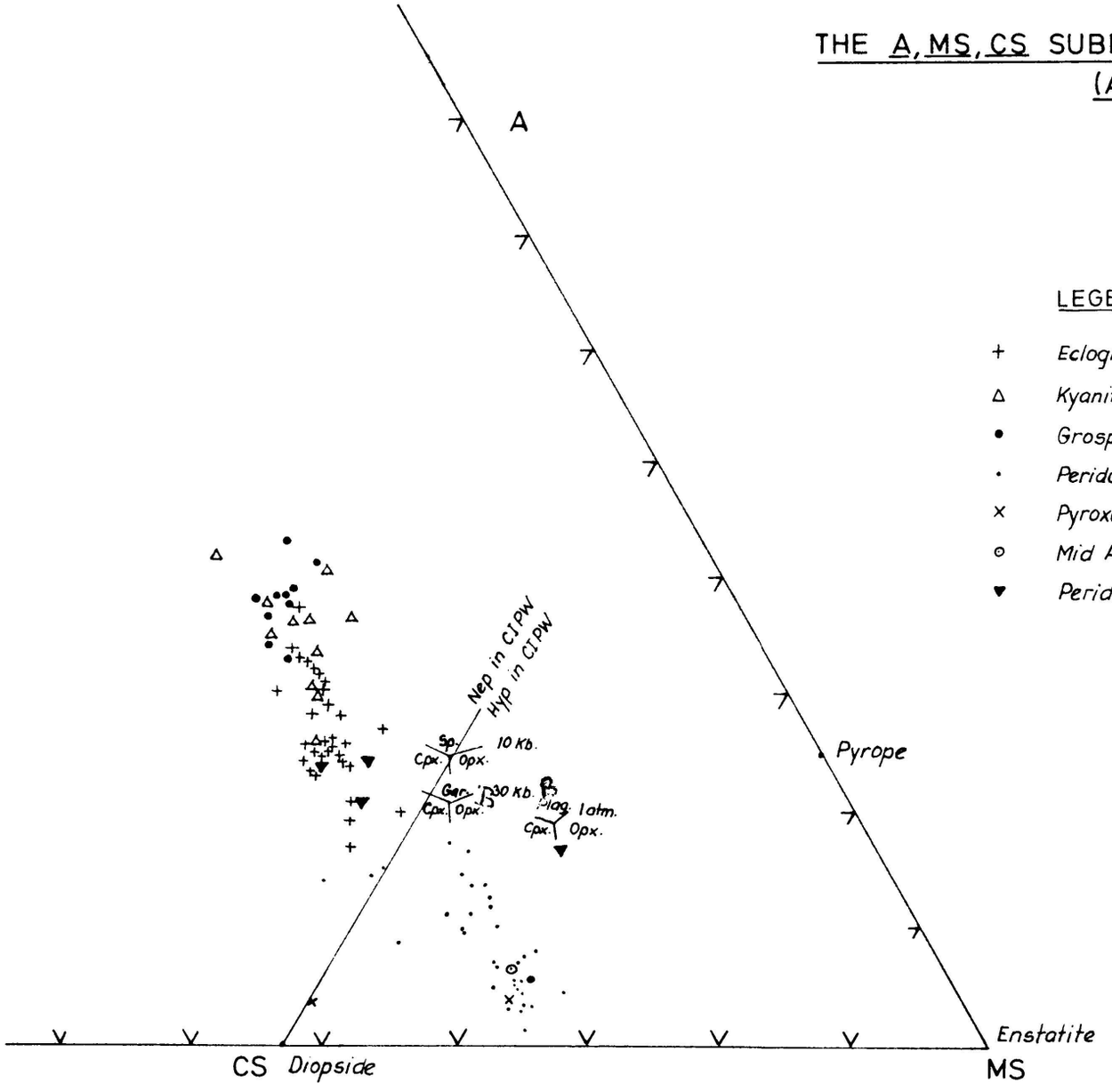

LEGEND

- + Eclogite
- △ Kyanite Eclogite
- ● Grospydite
- · Peridotite
- × Pyroxenite

} Nodules in Kimberlite

- ○ Mid Atlantic Ridge Basalt
- ▼ Peridotite Xenoliths in Alkali Basalts

FIG. 59

pydite and kyanite eclogite as the residua on partial melting and garnet peridotite as the cumulus phase during the formation of kimberlite magmas.

The distribution of diamonds between the eclogite and the ultramafic nodules and kimberlite also substantiates this conclusion. During the present investigation, diamonds were frequently encountered in eclogite nodules, and even more frequently in grospydite and kyanite eclogite nodules, but no diamond was found in the ultramafic nodules (1,500 nodules were investigated). This distribution pattern can easily be explained by considering the eclogite as the primary source material in the mantle of the earth. Both the residua of partial melting and the residual liquid would thus be diamondiferous and the ultramafic nodules would not necessarily be diamondiferous. The reverse, however, would imply that the diamonds crystallized subsequent to the partial melting of the ultramafic nodules and simultaneously with the crystallization of the eclogite. This argument will have to explain why the diamonds did not crystallize in the ultramafic nodules before partial melting, and would also have to explain the absence of either graphite or carbon in the garnet lherzolite nodules which (according to O'Hara and Yoder, 1967) represent the primary mantle material.

The data thus presented suggest that:

1. Eclogite is the only likely source material of kimberlite in the mantle of the earth.
2. The ultramafic rocks formed as cumulates in the process of differentiation at pressures lower than 30 kb.
3. That the mantle of the earth above 110 km is completely differentiated into a garnet-peridotite, peridotite, pyroxenite and dunite zones (figure 40), and that the eclogite below a depth of 110 km represents the primary differentiated mantle material. The differentiation trends present in the eclogites are:
   1. The tholeiite sequence
   2. The grospydite sequence (alkaline basaltic).

The tholeiite sequence is probably due to the differentiation process which caused the earth to form. This trend is only present in the eclogites, whereas the differentiation trend of the kyanite eclogites and grospydites is alkaline basaltic, and probably originated during the partial melting of the eclogite zone, and the rapid crystallization of ultramafic rocks.

4. The source of the alkalis and silica in the sialic crust, and the iron in the basaltic sima thus may have

THE A_2S_3, C_2S_3, M_2S PROJECTION FROM THE ENSTATITE POINT
(After O'Hara, 1968)

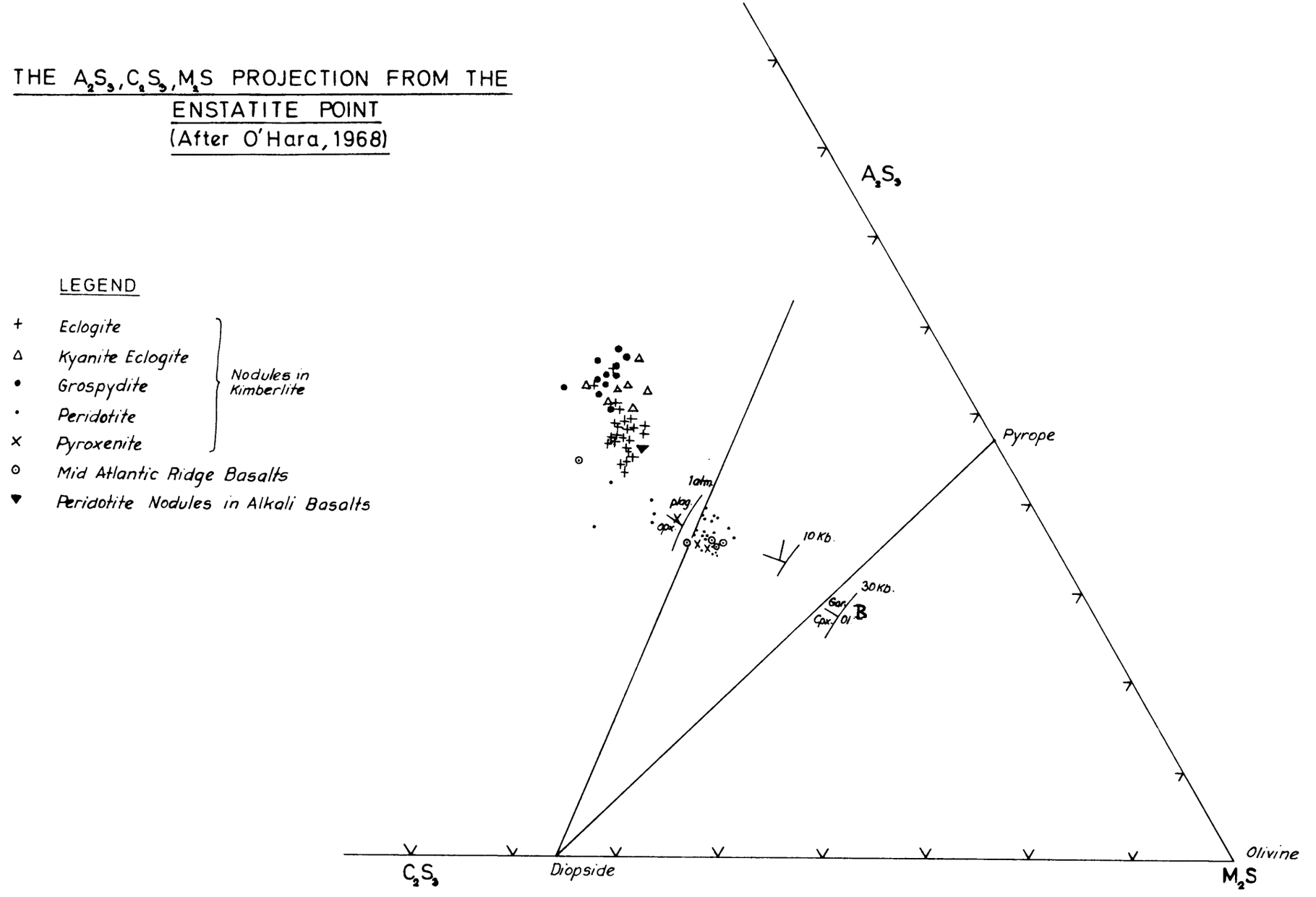

FIG. 6C

their origin in the less differentiated eclogite. The more magnesium bearing and silica undersaturated rocks in this differentiation sequence may then be represented by the ultramafic cumulates in the upper mantle (above 110 km). The ultramafic nodules in kimberlite and alkaline basalts are thus not necessarily cumulates which formed in the production of the respective magmas, but could have formed during the formation of the earth's crust.

X. THE PETROGENESIS OF KIMBERLITE WITH SPECIAL REFERENCE TO PREMIER MINE

A. The Emplacement of the Premier Mine Kimberlite

It was mentioned that the kimberlite pipe at Premier Mine consists of four petrographically distinct types of kimberlite; consequently it is assumed that ~~four stages of~~ intrusions took place in four stages. The intrusive nature of the eastern and the western kimberlites into the group I-kimberlite indicates that the intrusion of the group I - kimberlite was the initial phase of volcanism. The abundance of xenoliths derived from the wall-rock in this kimberlite also indicates that this phase of volcanism must have been highly explosive.

Subsequently the eastern and western kimberlites intruded into the pre-existing group I-kimberlite, and caused the "two-blow" pipe to be formed. The two bulges, shown on a plan of the Premier Mine pipe mark the positions of the eastern and western kimberlites. The sharpness of the contacts between the group I-kimberlite and the eastern and western kimberlites respectively, indicates that the group I-kimberlite was solidified at the time of their intrusion. Had the group I-kimberlite been in a "semi-plastic" state, the intrusion of the eastern and western kimberlites would have squeezed it out, and consequently the two bulges would not have formed.

The last phase of volcanism is characterized by the intrusion of dykes of massive basaltic kimberlite, which transgressed all the pre-existing phases of volcanism. These dykes were emplaced quietly, and caused carbonatization of the western kimberlite, giving rise to the bleached kimberlite.

B. The Petrogenesis of kimberlite

The mineralogy and petrology reveal that kimberlite is in disequilibrium, and that it consists of ~~an incompatable mineral associations~~ minerals which could not have formed simultaneously, like ilmenite, sphene and perofskite and also garnet and spinel. This indicates that the kimberlite was exposed to a variety of temperature and pressure conditions, and that these conditions did not last long enough to ensure equilibrium.

The rounding of most of the constituents in the kimberlite could have been caused either by physical abrasion or chemical corrosion. The rounded inclusions of wall-rock bears evidence of the former, whereas the perofskite rims around ilmenite are an indication of the latter.

Some of the minerals in the kimberlite are unstable in any magma which reaches the surface of the earth, eg. the pyrope garnet. Some mineral phases also consist of solid solutions which are unstable in any volcanic magma, eg. the high percentage of hematite in ilmenite, the garnet in clinopyroxene and the ulvite in magnetite. Hence it is concluded that these phases were formed at an elevated pressure, and were subsequently quenched. The fragments of garnet which did not suffer any formation of kelyphyte indicate that subsequent to the fracturing of the garnet, the magma intruded very rapidly and thus the formation of further kelyphyte was inhibited. The presence of feldspar in some kelyphytic rims indicate that this explosion took place at pressures sufficiently low to permit feldspar to crystallize in the place of spinel, viz. 8 kb (O'Hara, 1967).

The presence of both high and low pressure mineral assemblages in the kimberlite indicates that crystallization took place at several stages in the history of the kimberlite. The interrupted zoning of ilmenite and clinopyroxene also shows that the crystallization was a discontinuous process. It is thus concluded that both crystallization and remelting of mineral phases occurred in the kimberlitic magma during its ascent.

According to the mineral assemblages, which formed in the inclusions of wall-rock in the kimberlite the

temperature at the beginning of emplacement was certainly higher than 540°C, (amphibole-hornfels facies) and near the surface the temperature dropped to less than 250°C, (albite-epidote facies) and due to the volatile constituents, hydatogenetic minerals were formed in the Waterberg quartzite.

The presence of xenoliths of kimberlite in the group I-kimberlite at Premier Mine indicates that the kimberlitic magma was semi-solid during intrusions, and that the process itself was discontinuous. Since the kimberlite breccias contain more than 75 per cent of material that was crystalline before intrusion, it is to be expected that the kimberlite breccias were emplaced in a "semi-solid" state. The kimberlite magma can thus be visualized as a mixture of more than 75 per cent of solids in a fluid phase which consisted of a liquid which crystallized as the residua phase and an extremely active gaseous phase. The latter phase was probably responsible for the explosive nature of the kimberlite, and also for the fluidity of the magma. Due to the explosion the gaseous phase was released, and consequently sufficient free water and gasses were available to cause the autometasomatism in the kimberlite. The formation of volatile-bearing constituents were thus also prevented, because the gaseous phase could escape from the magma.

The micaceous and the massive basaltic kimberlites contain a much smaller amount of inclusions and phenocrysts and were thus probably more fluid during emplacement. Both these magmas also contained a larger percentage of the gaseous phase, but owing to the fact that these magmas were intruded slowly along fissures, the viscous constituents were not suddenly released, and consequently the viscosity of the magma was reduced, explosion and autometamorphism inhibited and the crystallization of volatile bearing constituents enhanced (apatite and second generation phlogopite).

C. The Model for the Formation of Kimberlite and Undersaturated Alkaline Rocks

In any petrogenetic explanation of the origin of kimberlite and the undersaturated alkaline basalts, the following facts must be considered.

1. Both kimberlites and carbonatites are usually associated with alkaline intrusions (Dawson, 1967).
2. Neither kimberlite, melilite basalt nor carbonatite intrusions shows differentiation to a diversity of rock types and they are very seldom an integral part of a differentiated complex. In most instances where carbonatite is a part of an alkaline complex it is associated with pyroxenite or dunite, and has an intrusive relationship to the other rock types of the complex. The kimberlites associated with alkaline intrusions also have an intrusive relationship to the alkaline rocks, and are not associated with ultramafic rocks. The kimberlite itself contains a large percentage of ultramafic xenoliths and phenocrysts.
3. Both kimberlite and carbonatite constitute a small percentage of all igneous rocks.
4. Both kimberlites and carbonatites have intruded into areas of fracture tectonics. The kimberlite occurs as diatrems, sills and dykes, the carbonatite occurs as diatrems and dykes, and the melilite basalts as sills and dykes.
5. A chemical relationship exists between all these rock-types which indicates that carbonatite is relatively enriched in iron, calcium and volatile constituents, kimberlite in magnesium, volatile constituents and often potassium, and melilite basalt only in magnesium (Figures 42-45.
6. Petrologically the kimberlite differs from melilite basalt and the massive basaltic kimberlite in that it contains primary phenocrysts, whereas the latter rock-types only contain the secondary phenocrysts and residua phase material, characteristic of kimberlite. The carbonatites also contain only secondary phenocrystal and residua phase material but the latter is significantly increased compared with kimberlites and melilite basalts. The sequence of crystallization of the secondary phenocrystal phase is olivine, magnetite, melilite, perofskite, sphene and phlogopite, and of the residua phase it is apatite, calcite and serpentine.

The presence of the primary phenocrystal phases in kimberlite, especially pyrope, forsterite and enstatite, gives the impression that kimberlite is an early dif-

ferentiate. The fact that these minerals are in disequilibrium, and not a part of the kimberlitic magma indicates that only the residua phase can be regarded as the kimberlite magma. Due to this fact, it is evident that the kimberlitic magma is more enriched in Ca^{2+}, Fe^{2+} and volatile phases, and hence not an early differentiate. The melilite basalt magma contains more Mg^{2+} than either the kimberlitic or carbonatite magmas, and hence represent either an equilibrated kimberlitic magma, of which the primary phenocrysts were completely remelted, or a less differentiated magma. The melilite basalts, massive kimberlites and alnoiites were completely equilibrated, and the ilmenites were mostly completely consumed to form sphene and perofskite, whereas the carbonatites are often also equilibrated. The kimberlite breccias differ from the micaceous kimberlites in having erupted more explosively, and hence lost all the free water and volatile constituents during emplacement. The presence of this active volatile and water bearing phase during intrusion was thus able to cause the serpentinization. The micaceous kimberlite, having intruded more slowly did not loose its volatile constituents, but retained them in the structures of the apatite and phlogopite grains, and hence did not suffer extensive serpentinization or brecciation.

The facts that the basaltic kimberlites erupted along vents and suffered more intense serpentination, indicate that the basaltic kimberlites might have contained a more active volatile phase prior to eruption than the micaceous kimberlites.

The data presented indicate that the melilite basalts represent a less differentiated magma than the kimberlites, but more differentiated than pyroxenites and peridotites. The carbonatites appear to be the most differentiated rocks in this series. This process of differentiation with respect to the depletion of Mg^{2+}, Al^{3+} and Si^{4+} in the magma, and the enrichment of Fe^{2+}, Na^{+}; K^{+}, Ca^{2+} and volatile phases could not have taken place in the crust of the earth at low pressures, because Al^{3+} and Si^{4+} depletion can only be explained by the early crystallization of pyrope and enstatite, (higher 27Kb) and not by the

crystallization of olivine (System pyrope - diopside; O'Hara 1968). The presence of pyrope, enstatite and jadeite-bearing clinopyroxene in kimberlite indicates that these rocks formed in the mantle of the earth.

It thus appears that the formation of alkaline basalt (eg. nepheline basalts, phonolites etc.), alkaline complexes (dunite-pyroxenite-carbonatite-complexes), melilite basalts, kimberlites, carbonatites and "maars" can be explained by an intricate interplay of the following factors.

1. Differentiation in depth.
2. Differentiation in place.
3. Assimilation of cumulus phases.
4. Time and degree of equilibration.
5. Method of emplacement.
6. The amount of residual material which formed in depth.

In this model, as has been stressed repeatedly, the eclogite is considered as the source material, the garnet harzburgites, garnet lherzolites, and dunites are considered as the cumulus phases, and the grospydites are the residua phase of partial melting.

In figure 61 the relationship between these undersaturated rocks is shown diagramatically. This diagram shows the influences of the factors mentioned above on the origin of the various alkaline basaltic magmas. According to figures 58, 59 and 60 the residua on partial melting of eclogite is grospydite and kyanite eclogite, and the partial melt is enriched in normative olivine and enstatite. This partial melt would be able to crystallize dunite and pyroxenite and during extreme fractional crystallization of olivine, pyrope and enstatite, carbonatite would be able to form. Should the melting of eclogite proceed to intermediate stages, the residue would become more olivine and enstatite normative with respect to grospydite and kyanite eclogite, and the partial melt would be enriched in normative anorthite and grossular. This partial melt would be able to crystallize dunite, pyroxenite and garnet peridotite, and

the residual liquid would be able to result in melilite basalt, alnoiite, kimberlite, carbonatite and even in gas explosions, depending on the degree of fractionation. However, it is not necessary that the whole range of rock-types indicated in the diagram need to form, but only one residual liquid may form during the fractional crystallization of dunite, pyroxenite and garnet peridotite. The data obtained from the present investigation on kimberlite suggest that kimberlite mostly forms during this discontinuous process. Should complete melting of the eclogite take place the melt would become even more enriched in normative anorthite and grossular. Crystallization of dunite, garnet peridotite and pyroxenite from this melt would yield a residual liquid that resembles alkaline basalts closely. The calculations by Jackson et al. have confirmed that this process is the only likely way of explaining the origin of the nephelinites at Hawaii. But it must be stressed that his calculations only take complete melting of eclogite into account, and that partial melting may be of consequence in the origin of the undersaturated alkaline basaltic magmas.

X. THE THOLEIITIC SILL

A. General Geology

The tholeiitic sill has a thickness of 71.0 meters, and strikes in an east west direction with a variable dip ranging from 25^{o} to 15^{o} to the north. Figure 5 and profiles 1 and 2 show that the sill appears to be curved into an anticlinal and synclinal shape in the southern

SHOWING THE RELATIONSHIPS BETWEEN THE VARIOUS UNDERSATURATED ALKALINE ROCKS

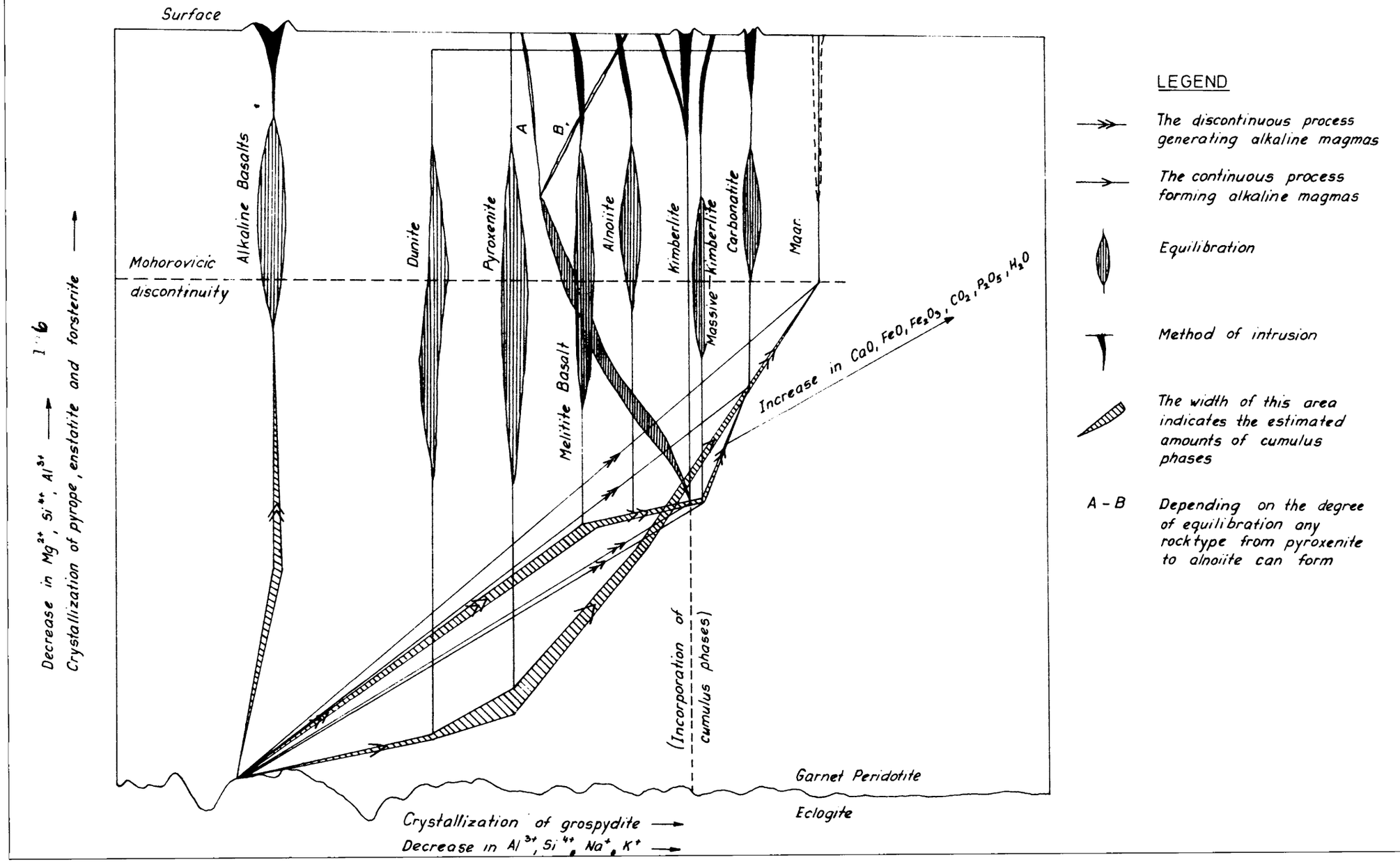

portion of the kimberlite vent. The sill also has many off-shoots into the kimberlite, which appear to end blindly, and enhance the irregular surface of the sill considerably.

The sill traverses the kimberlite without displacing the western or eastern kimberlites, the massive kimberlite veins or the xenoliths of Waterberg quartzite in any way. The sill has, however, caused a distinct thermal aureole in the kimberlite at both contacts. The meta-kimberlite at the floor contact appears to be metamorphosed to a lesser extent, and forms a zone 120 meter wide, of "bad ground", whereas the kimberlite at the roof-contact is highly metamorphosed, giving rise to a coarse-grained pyroxenite, which is very resistant to weathering.

The contact between the felsite and the tholeiitic sill is sharp, and metamorphic influences are negligible. The massive kimberlite veins appear to have resisted the alteration to bad ground at both contacts, and are largely transformed into amphibolites.

The age of this tholeiitic sill has been established by both palaeomagnetic and direct age determinations as post-Waterberg (1255 ± 50 m.y.) (Allsop et al 1967)

B. The Petrology of the Sill

In hand specimens it can be seen that this sill is a layered intrusion, showing the distinct characteristic of a differentiated intrusion. At the floor contact a zone of 7 meters of fine-grained gabbro characterizes the chilled zone. This portion is succeeded by 15 meters of olivine-orthopyroxene cumulate rocks, which show prominent igneous layering. The succeeding 49 meters of the intrusion consists of a dolerite, which becomes increasingly enriched in quartz, and the upper 20 meters can almost be described as a granophyre.

In thin sections it could be observed that the contact between the chilled gabbro and the kimberlite is sharp, whereas the contact between the chilled gabbro and the olivine-orthopyroxene cumulate is gradational. The chilled gabbro consists of subhedral to anhedral phenocrysts of clinopyroxene (1.0 mm diameter) in a matrix of clinopyroxene and plagioclase (0.1 x 0.25 mm dimensions).

The clinopyroxene phenocrysts are usually zoned, and often exhibit twinning, whereas the matrix shows a fine-grained ophitic intergrowth between clinopyroxene and feldspar. Sporadic orthopyroxene grains could also be identified in the matrix.

The olivine-orthopyroxene cumulates consist of idiomorphic to subhedral grains of olivine and orthopyroxene in an intercumulus matrix of plagioclase and clinopyroxene. Towards the top of this zone, cumulus crystals of clinopyroxene are also present. This zone passes gradually into a doleritic zone where the clinopyroxene and plagioclase are ophitically intergrown. The olivine occurs either as inclusions in the orthopyroxene cumulus crystals, or as euhedral cumulus crystals. The orthopyroxene grains are euhedral and display zoning. The outer rims of these primary orthopyroxene grains show exsolution lamellae parallel to (001) of the present orthopyroxene (photo 30), and are inverted pigeonite. Towards the top of this zone the amount of primary orthopyroxene decreases, and the inverted pigeonite increases markedly. The plagioclase constitutes the intercumulus phase in this zone.

In the last two meter of the cumulate zone the grains become subhedral to euhedral and are subophitically intergrown with the clinopyroxene. In the upper portion of the cumulate zone the clinopyroxene appears to be considerably altered to amphibole.

The doleritic portion of the sill is characterized by the ophitic intergrowths of plagioclase and clinopyroxene, and the presence of a granophyric intergrowth of quartz and orthoclase. Occasional orthopyroxene grains, rimmed by pigeonite, occur. However, the majority of orthopyroxene represents inverted pigeonite. Some original (uninverted) pigeonite ($2V_{\chi} = 20^{\circ}$), has also been encountered in some thin sections (B_1-6). In the topmost 10 meters of the sill, extensive alteration of the clinopyroxene and of the feldspar to amphibole and zoisite respectively is evident. In this area the amount of granophyric intergrowth and free quartz is high, and some euhedral apatite also occurs.

In the doleritic zone of the sill a dark glassy material (photo 31) occurs. This material is marked by skeletal crystals of magnetite, and in places this glass appears to have altered to biotite. In this biotite hexagonally arranged lamellae of magnetite is also evident. This glass may thus be considered as the last residual liquid which did not crystallize prior to the solidification of the rock.

C. The Mineralogy of the Sill

1. Olivine

Olivine occurs as cumulus crystals or as inclusions in orthopyroxene cumulus crystals in the cumulate zone of this tholeiitic sill. The olivine inclusions, which are mostly serpentinized, reveal the reaction relationship between the olivine and the magma to have produced the orthopyroxene. The olivine has a $2V_{\alpha} = 85^{\circ}$ and $d_{(130)} = 2.785\text{Å}$, which indicate Fo77 (Tröger, 1959) and Fo78 (Yoder and Sahama, 1957) respectively.

2. Orthopyroxene

In the cumulus zone of the tholeiitic sill the orthopyroxene has evidently formed as a consequence of the reaction of olivine, whereas the orthopyroxene in the upper portion of the cumulate zone and in the doleritic zone, is inverted pigeonite. The percentage by volume of orthopyroxene is high in the cumulate zone, and decreases rapidly towards the base of the doleritic zone. In the doleritic zone the amount of orthopyroxene again increases due to the inversion of pigeonite, and then remains fairly constant.

The orthopyroxene becomes gradually enriched in iron in the cumulate zone from En_{79} to En_{76}, and at the inversion point the orthopyroxene suddenly becomes more enriched in magnesium (En_{78}). From this point onwards the orthopyroxene again becomes enriched in iron.

The optical properties and relevant d values of the orthopyroxenes are represented in table 40. The curves after Zwaan (1954) indicate that above and below the pigeonite inversion the Al^{31+} content seems to be the same, and across the cumulate zone (B_{1-8} to B_{1-12}) the Al^{3+}

content also appears to be fairly constant. The constancy of the Al^{3+} content and the variation in the enstatite content of the orthopyroxene thus indicate that the orthopyroxenes formed at a constant pressure during a decrease in the temperature of the magma.

3. Clinopyroxene

The clinopyroxene occurs in all the rock types in the tholeiitic sill, and the amount decreases in the cumulate zone, and then increases again in the doleritic and the granophyre-bearing portions. According to the optical properties and the d-values of the clinopyroxene, very little differentiation is evident, compared to the trend observed in Skaergaard (Wager & Brown, 1968), (fig. 62). These properties of the clinopyroxenes are represented in table 41, and indicate a small variation in the ΔV across the section.

Table 40. The physical properties of the orthopyroxene from the tholeiitic sill

	Optical data		X-ray data (Zwaan 1954)			
	$2V_{\alpha}$ ($\pm 1^{o}$)	En% ($\pm$ 1%)	Δd [(10.3.1)-(0.6.0)] Å	Δd [$(21\bar{3}1)_{QZ}$-(060)] Å	Al^{3+}	En%
B_1-6	73^{o}	76	-	-	-	-
B1-7	74^{o}	77.5	0.014	Nd.	0.06	-
B1-8	72^{o}	75.5	0.014	0.070	0.06	77
B1-9	74^{o}	77.5	-	-	-	-
B1-11	75^{o}	78	-	-	-	-
B1-12	76^{o}	79	0.014	0.066	0.06	80

4. Plagioclase

Plagioclase is present in all the zones of this intrusion, however, its textural relationships vary considerably. In the chilled zone it is fine-grained and ophitically intergrown with clinopyroxene. In the doleritic zone this texture is repeated on a coarser scale. In the cumulate zone the plagioclase is intercumulus, and was evidently the last phase to crystallize. The amount of plagioclase varies inversely to that of the orthopyroxene in the section across the intrusion. The

THE VARIATION IN THE COMPOSITION OF THE PYROXENES IN A SECTION ACROSS THE GABBRO SILL
(After Hess 1949)

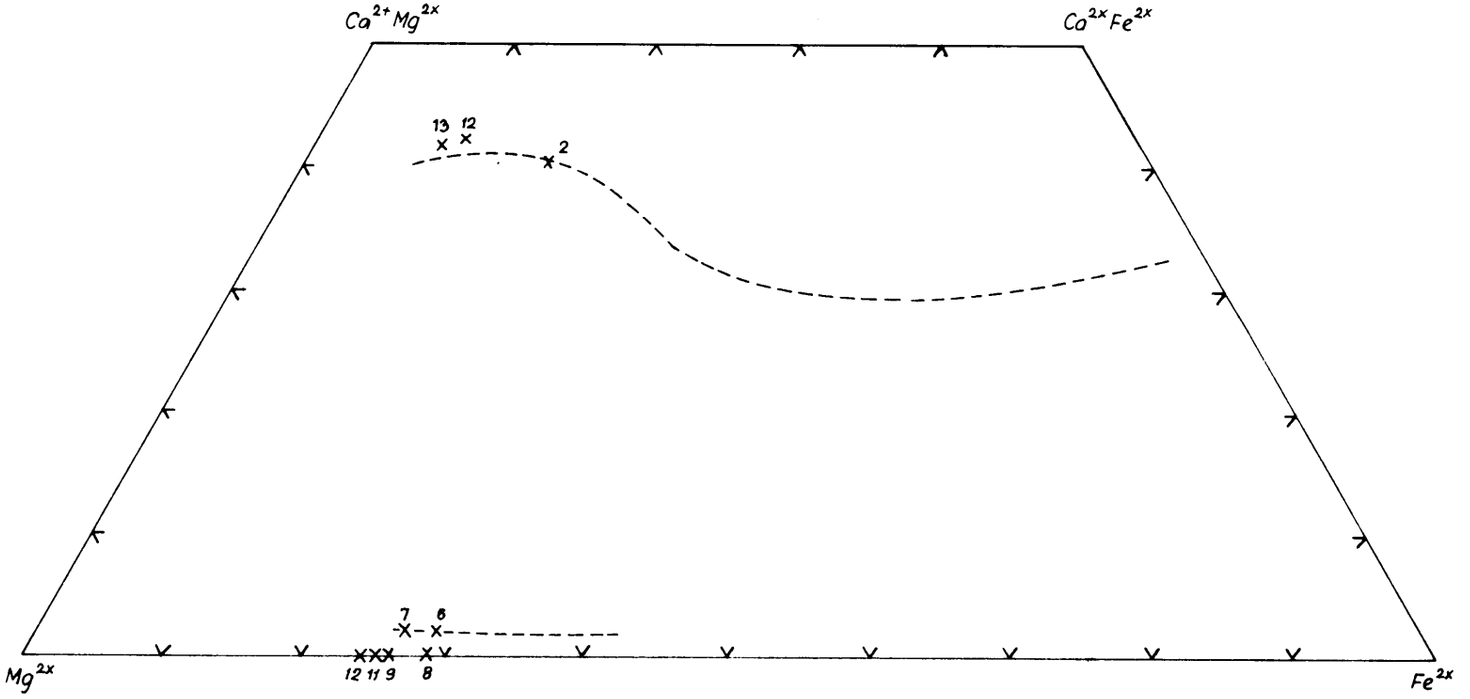

FIG.62

Table 41. The optical properties of the clinopyroxenes from the tholeiitic sill

Section	$2V_{\gamma}$ ($\pm 1^{o}$)	n_{γ} (± 0.003)
Bl-2	48^{o}	1.691
Bl-3	53^{o}	
Bl-4	55^{o}	
Bl-5	54^{o}	
Bl-6	56^{o}	
Bl-7	56^{o}	
Bl-8	53^{o}	
Bl-9	54^{o}	
Bl-10	53^{o}	
Bl-11	53^{o}	
Bl-12	53^{o}	1.688
Bl-13	51^{o}	1.687

variation in the chemical composition of the plagioclase in a vertical section across the sill is shown in figure 63, and indicates a break in the differentiation trend of the plagioclase. The sodium-rich plagioclase in the cumulate zone can evidently not be explained by either repeated intrusions or variations in pressure, because no evidence of these phenomena is present in the tholeiitic sill. Consequently this break in differentiation should be ascribed to the textural occurrence of the plagioclase. In the cumulate zone the plagioclase was the last phase to crystallize. Consequently the crystallization of the rims of pigeonite around the cumulus orthopyroxene, and the crystallization of the clinopyroxene, may have depleted the residua in Ca^{2+} and hence enriched it in sodium.

The plagioclase in the upper portion of the tholeiitic sill is largely altered to clinozoizite and prehenite, probably due to the effects of the volatile phases. The optical properties and the X-ray data after Tröger (1967) of the plagioclase are listed in table 42. The X-ray data of the plagioclase indicate that it represents the low temperature modification of plagioclase.

THE VARIATION IN THE PETROGRAPHICAL COMPOSITION (EXPRESSED AS A VOLUME PERCENTAGE), GRAIN-SIZE, AND COMPOSITION OF PLAGIOCLASE AND ORTHOPYROXENE IN A VERTICAL SECTION OF THE SILL

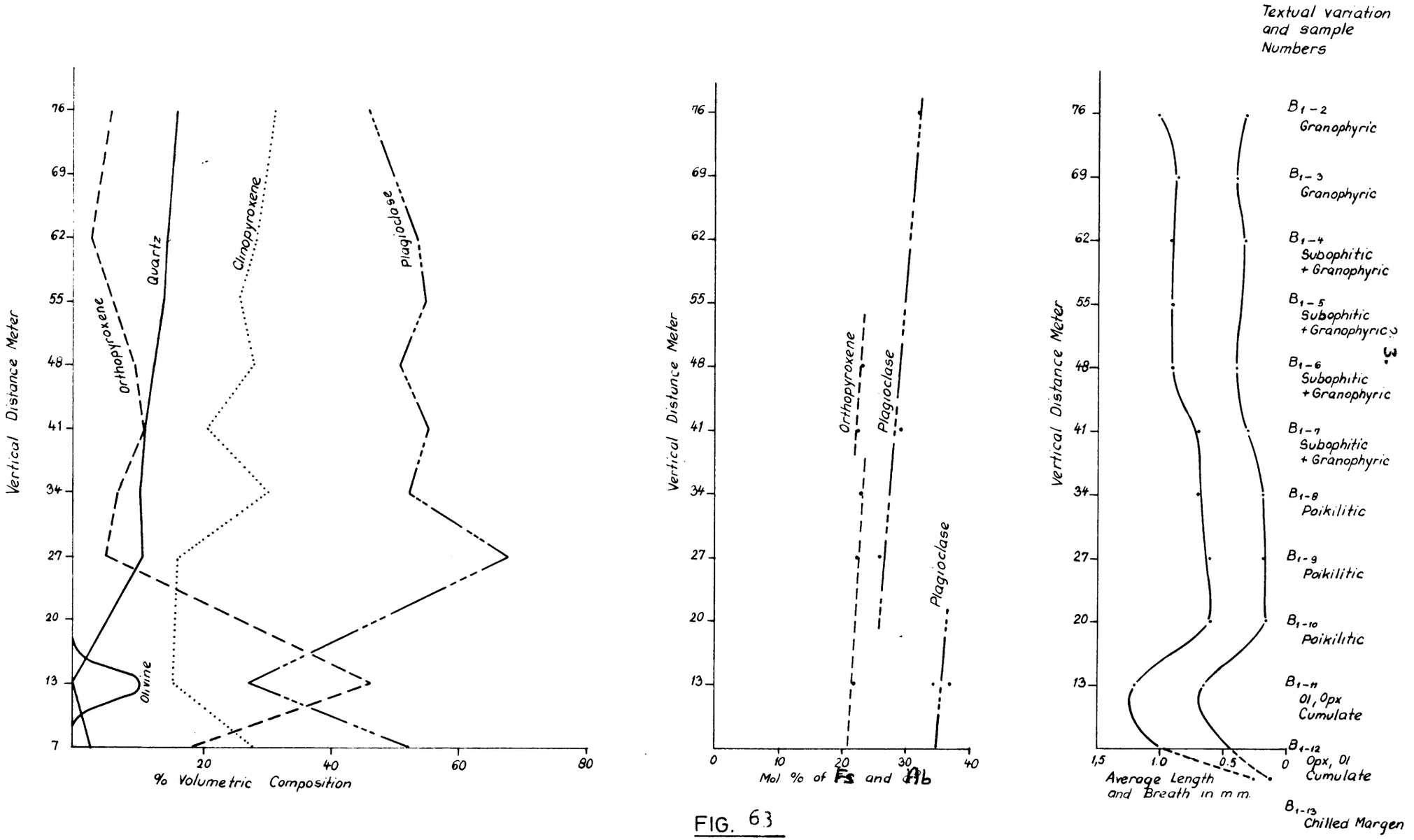

FIG. 63

Table 42. The Optical and the X-ray data after Tröger (1967) of the plagioclase from the tholeiitic sill

	Optical data		X-ray properties (Tröger, 1967)			
Section	2V (± 1°)	An%	Δ2θ (131)-($\bar{1}31$)	Δ2θ ($\bar{2}41$)-($\bar{2}\bar{4}1$)	Si/Al	An%
B1-2	-	-	1.995	0.205	1.40	68
B1-4	- 88°	69				
B1-5	+ 90°	70	The An-values were checked by means of			
B1-7	- 89°	71	x-rays.			
B1-9	- 84°	74				
B1-11	- 88°	67	1.905	0.240	1.46	63
B1-12	- 85°	66	1.940	0.240	1.50	64

The accessory constituents in the sill are magnetite, biotite, quartz, glass and granophyric intergrowths consisting of quartz and orthoclase.

D. The Petrogenesis of the Tholeiitic Sill

The chilled zone of the sill probably represents the original magma that was intruded and that was chilled against the wall-rock. The crystallization differentiation produced the three distinct zones in this intrusion. Apart from the textural and compositional indications of crystallization differentiation, each of the constituents also conforms to the usual differentiation trends.

According to the pigeonite geothermometer after Hess (1960, p. 40), which is applicable in the present circumstance, owing to the low pressure during intrusion, indicates that the temperature of the magma was higher than 1100°C. According to the thermal effects observed in the kimberlite, it appears as if most of the heat escaped through the roof contact, during the cooling of the magma.

E. The Metamorphism of the Premier Mine Kimberlite

The tholeiitic sill which intruded into the Premier Mine kimberlite prcduced a metamorphic aureole of several hundreds of meters. Since the different types of

kimberlite have been affected in the same way by this influx of heat, they will be discussed simultaneously. Depending on the distance from the tholeiitic sill, three types of meta-kimberlite were formed, viz: an olivine-enstatite meta-kimberlite, a diopsode-amphibole and a serpentine-amphibole meta-kimberlite.

1. The olivine-enstatite kimberlite

This type of meta-kimberlite was only found within the first meter from the upper contact of the tholeiitic sill. The original kimberlitic texture is destroyed and a porphyroblastic texture developed.

Porphyroblasts of olivine, partly altered to serpentine, show a reaction relationship to the larger orthopyroxene grains in which they are included. As d_{130} = 2.779 Å the olivine is Fo_{85} (Yoder and Sahama 1957). The $2V_{\alpha}$ = 87° and n_{γ} = 1.682 indicate a composition of En_{85} after the diagram by Hess (1960, p.27) for the orthopyroxene.

Clinopyroxene which is xenomorphic with respect to the olivine and orthopyroxene, but idiomorphic with respect to the feldspar, is often replaced by a greenish garnet. The latter also formed in the intergranular feldspar matrix. This greenish garnet is also occasionally anisotropic, and has been identified as hydrogrossular, and probably formed as a consequence of retrograde metamorphism. Apart from the crystalline phases mentioned, a brownish isotropic glass (photo 32), which is occasionally devitrified, could be identified in the matrix.

According to the ACF diagram (figure 64), the chemical analyses of the Premier Mine kimberlite plot into the enstatite-anorthite-diopside field of the orthopyroxene subfacies, of the K-feldspar-cordierite-hornfels facies, which corresponds to the modal composition of the rock. According to Winkler (1967; p. 73) this implies a temperature of 650 to 760°C and a pressure of 0.5 to 1.0 kb.

2. The diopside-amphibole kimberlite

The kimberlite in which these minerals were developed as a consequence of thermal metamorphism, occurs 2 meter

ACF DIAGRAM FOR THE ORTHOPYROXENE SUBFACIES OF THE K-FELDSPAR, CORDIERITE, HORNFELS FACIES, ON WHICH THE ANALYSES OF THE PREMIER MINE KIMBERLITE HAVE BEEN PLOTTED

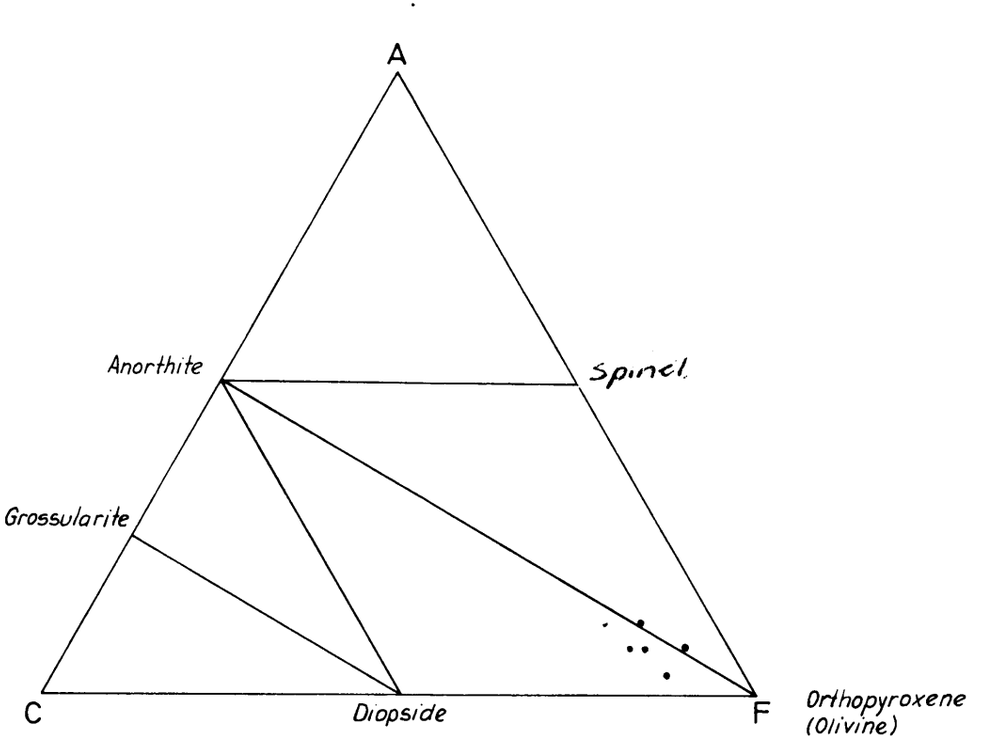

FIG. 54

away from the upper contact and also at the lower contact of the sill. The first 10 meters of this metamorphic zone show no kimberlitic textures, but further away the brecciated texture is indistinctly visible.

Apart from the ilmenite, none of the other primary constituents has survived the metamorphic effects, and in the ilmenite lamellae of hematite exsolved parallel to (0001) of the ilmenite. The d-values of the minerals constituting this metamorphic zone in the kimberlite are given in table 43. This table indicates that at least three types of amphibole, viz tremolite, actinolite and pargasite were formed in this meta-kimberlite. The presence of diopside and plagioclase is also evident from this table.

The amphibole ($2V_{\alpha}$ = 77° to 79°) occurs as large porphyroblasts and as small fibrous grains which are arranged in bundles parallel to one another. Both these euhedral to subhedral porphyroblasts and the composite fibrous grains are often arranged in a decusate texture in the meta-kimberlite. Magnetite and sphene are present in this meta-kimberlite, but perofskite is very rare.

The kimberlite further away from the contact of the tholeiitic sill exhibits the original kimberlitic texture, and is composed of round areas of pre-existing serpentine embedded in the matrix of fibrous amphibole and diopside. These sections also reveal that the increase in diopside content is accompanied by a decrease in the serpentine and perofskite content. This systematic increase in the diopside content reflects an increase in the grade of thermal metamorphism.

The ACF diagram represented in figure 65, on which the chemical analyses of the Premier Mine kimberlite have been plotted, indicates that this meta-kimberlite falls in the hornblende-hornfels facies, thus implying a temperature of 520 to 540°C for a pressure of 0.5 to 1.3 kb (Winkler, 1967 p. 79)

3. The serpentine-amphibole kimberlite

The mineralogy and petrology of this meta-kimberlite is essentially the same as for the unmetamorphosed Premier Mine kimberlite.

ACF DIAGRAM FOR THE HORNBLENDE HORNFELS FACIES SHOWING THE CHEMICAL ANALYSES OF THE PREMIER MINE KIMBERLITE

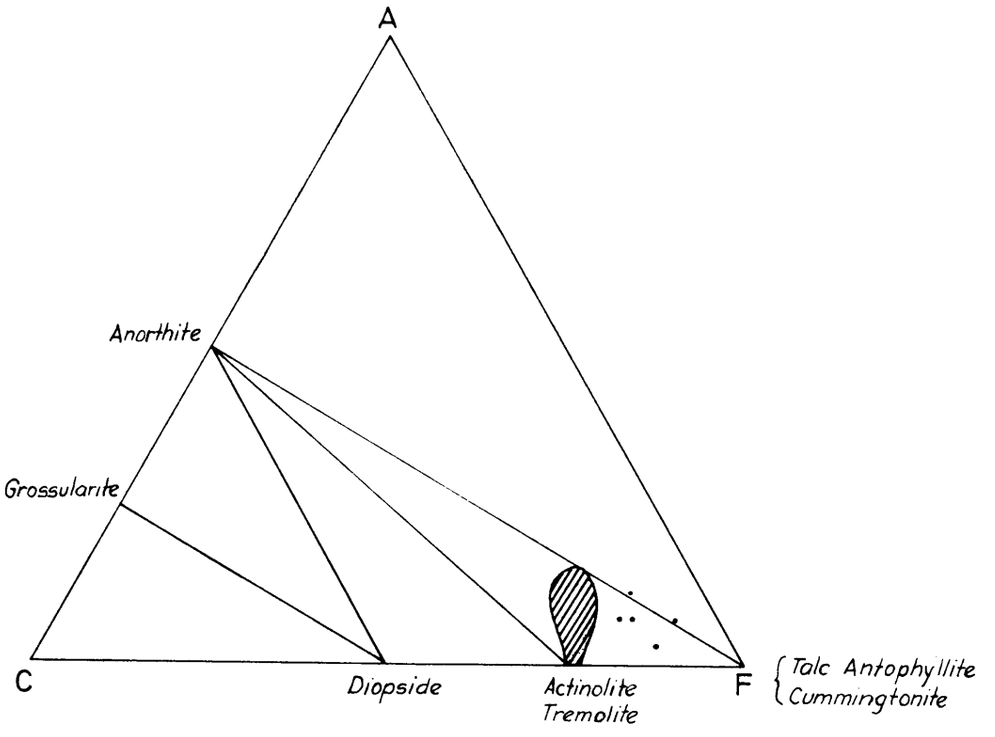

FIG. 65

Table 43. The d-values of the minerals in the meta-kimberlites

1410-6 Film no. 462			1410-13 463			1410-4 468			B1-15 470		
I/Io	d °A	Min.	I/Io	d °A	Min.	I/Io	d (Å)	Min.	I/Io	d °A	Min.
2	9.092	A	2	8.523	A	2	9.186	A	z	9.119	A
2	8.445	A	1	4.900	A	2	8.592	A	z	8.518	A
1	4.893	A	1	4.005	Pl	1	4.898	A	1	4.892	A
2	4.524	A	2	3.879	A	2	3.884	A	1.0	4.588	Pl
1	3.877	A	3	3.387	A	2	3.671	D	1	4.521	A
5	3.385	A	5	3.345	P	3	3.390	A	5.0	4.037	Pl
5	3.342	P	5	3.279	A&T	3	3.343	D	z	3.882	A
9	3.277	A	3	3.226	D	8	3.282	A	4	3.422	Pl
2	2.990	D	10	2.988	D	4	3.228	D	6	3.390	A
6	2.943	A	4	2.948	A&D	10	2.990	D	6	3.273	A
6	2.809	P	3	2.874	D	4	2.945	A	4	3.238	Pl
6	2.730	P	6	2.741	P	5	2.893	D	7	3.193	Pl
10	2.706	A	5	2.707	A&T	3	2.735	P	1	3.051	P
6	2.593	A	0.59	2.655	P?	10	2.703	P&A	8	2.943	A&Pl
8	2.556	P	0.5	2.625	?	4	2.655	P	4	2.802	T
9	2.531	A	5	2.588	A	0.5	2.622	?	1	2.725	T
6	2.333	P	1	2.560	D	2	2.589	A	10	2.703	A
2	2.319	T	5	2.536	A	2	2.560	D	5	2.592	A
3	2.295	P	4	2.524	D	8	2.536	A	0.5	2.554	P?
1	2.272	A	3	2.511	D	1	2.523	A	3	2.530	A
1	2.206	T	0.5	2.441	?	3	2.510	D	7	2.493	Pl
7	2.161	A	1	2.339	Am.	0.5	2.487	?	0.5	2.437	?
4	2.044	A&P	2	2.297	T	0.5	2.435	?	1	2.406	T
6	2.014	A	3	2.282	P	4	2.337	A	3	2.378	T
1	1.932	T	2	2.213	D	2	2.294	P	3	2.331	T
3	1.862	A	1	2.196	D	0.5	2.275	A	4	2.315	T
1	1.683	P	6	2.180	P	1	2.209	A	1	2.296	T
1	1.672	P	3	2.165	A	1	2.194	D	1	2.269	A
7	1.650	A	7	2.149	P	2	2.130	D	3	2.205	A
4	1.626	P	0.5	2.128	?	2	2.048	D	8	2.163	T
0.5	1.615	?	0.5	2.103	?	2	2.037	A	8	2.017	A
7	1.577	A	1	2.050	D	4	2.015	A	2	2.009	T
0.5	1.536	?	3	2.037	A	2	1.999	P	2	1.865	A
6	1.511	P	1	2.013	T	1	1.964	T	5	1.685	?

d-values obtained by means of a Guinier Camera, Cu Kα radiation.

A = Actinolite
Am = possibly hornblende
D = diopside
T = tremolite
P = pargasite
Pl = plagioclase

XII. SUMMARY AND CONCLUSIONS

The investigation of the structural and the petrochemical relationships of the post-Waterberg alkaline intrusions north-east of Pretoria indicates that these intrusions formed contemporaneously, were influenced by the same tectonic pattern, and originated by separate differentiation sequences in the mantle of the earth.

The Premier Mine kimberlite is composed of at least four separate kimberlite intrusions. The magmatic activity started with the intrusion of the highly explosive group I-kimberlite. This phase was succeeded by the intrusion of the less explosive eastern and western kimberlites respectively, and the activity terminated with the emplacement of the veins of massive basaltic kimberlite.

The petrochemical and the mineralogical investigation of the undersaturated alkaline intrusions, which are associated with kimberlites and carbonatites, suggested that a [illegible] petrochemical relationship exists between these rock types. The investigation also enabled the postulation of a model for explaining the genesis of these rock-types. It is concluded that these undersaturated alkaline rocks originate in the eclogite zone of the mantle (below 100 Km), and that depending on the amount of cumulates of garnet peridotite and peridotites that crystallize, and on the amount of residue material (grospydite and kyanite eclogite) that remain behind, various undersaturated alkaline magmas can originate.

The comparison of the mineralogy of the constituents in eclogite, kimberlite and garnet peridotite revealed that the minerals in kimberlite and garnet peridotite

show a remarkable correspondence, whereas eclogitic minerals are absent in kimberlite. The sequence of crystallization of the primary phenocrystal phases in kimberlite corresponds exactly to the sequence observed in the garnet peridotite nodules, and to the sequence predicted by O'Hara (1968) in the system diopside-pyrope at 20 to 30 kb, viz. pyrope, enstatite, clinopyroxene, olivine and spinel. Chemically the eclogite appears to be undifferentiated, whereas the ultramafic nodules are uniformly differentiated, corresponding to the first stages of the normal differentiation sequence for tholeiitic magmas. The paucity of K^{+}, Na^{+}, Al^{3+}, Ca^{2+} and Ti^{4+} in the ultramafic nodules, and their relatively high concentrations in all alkaline and kimberlitic magmas, suggest that the ultramafic nodules can hardly be the source material for these magmas. The eclogite being enriched in these constituents, is a more likely parent material. The grospydites and kyanite eclogites being poor in Mg^{2+} and Fe^{2+}, are considered to be the residue during the melting of the parent material (eclogite) and the crystallization of the cumulates (garnet peridotite), near 30 kb pressure.

From the mineralogical, petrological and chemical data of the rocks and minerals concerned, a model is proposed for the upper mantle of the earth (120 to 38 km) and for the sequence and time of the crystallization of the phenocrystal phases in kimberlite. Apart from some minor differences, the model thus constructed from the data on kimberlites, duplicates the model proposed by Jackson et al., (1969) for Hawaii.

XIII. APPENDICES

1. The physical properties and the composition of garnets from garnet peridotite nodules in kimberlite.
2. The physical properties and the composition of garnet in kimberlite.
3. The physical properties and the composition of garnets from eclogite.
4. The chemical analyses and the molecular norms of the

various parentages of garnet.

5. A comparison of the d-values and indices of olivine from kimberlite, to the d-values supplied by ASTM 7-79, Elesiev (1957) and Yoder and Sahama (1957).

6. The forsterite content of the various olivines according to d_{130}, a_o and c_o-values.

7. The forsterite content of the olivines from various types of ultramafic rocks according to the optical properties.

8. The forsterite content of the olivine from kimberlite, according to the optical properties.

9. The chemical analyses and the molecular norms of olivine from various olivine-bearing rocks.

10. The indexing of the reflections for ilmenite from kimberlite.

11. The physical properties and the molecular percentages of $MgTiO_3$, $FeTiO_3$ and Fe_2O_3 of the chemically analysed specimens of ilmenite, and the physical properties of the ilmenite in kimberlite.

12. The chemical analyses, molecular norms and the structural formulas of ilmenite.

13. The chemical compositions, molecular norms and structural formulas of chromite.

14. The physical properties and the enstatite and alumina contents of the orthopyroxene from kimberlite and garnet peridotite.

15. The Al^{3+} and Ca^{2+} contents of the orthopyroxenes from kimberlite and garnet peridotite nodules, after Zwaan (1954, p. 206-209).

16. The chemical analyses, molecular norms and structural formulas of orthopyroxenes from ultramafic rocks and from kimberlite.

17. The d-values of the clinopyroxene from eclogite, kyanite eclogite, garnet peridotite and kimberlite, compared with those of the P2 and C^2/c omphacite.

18. The optical properties of the clinopyroxenes and their $CaSiO_3$ and $FeSiO_3$ contents after Tröger (1959).

19. The unit-cell dimensions, the $a \sin\beta$ values, and the $CaAl_2SiO_6$ content of the various clinopyroxenes according to Sakata (1957).

20. The molecular per cent $CaMgSi_2O_6$, and the weight per cent $MgSiO_3$ in the clinopyroxenes, after the various d-value spacings.
21. The chemical analyses, molecular norms and structural formulas of the clinopyroxenes from various parentages.
22. The chemical analyses and structural formulas of phlogopite.
23. The chemical analyses, molecular norms and structural formulas of calcite from kimberlite and carbonatite.
24. The chemical analyses, molecular norms and structural formulas of magnetite.
25. The chemical analyses and katamolecular norms of kimberlite from South Africa.
26. The chemical analyses and katamolecular norms of the kimberlites from outside South Africa.
27. The chemical analyses and katamolecular norms of alkaline-basalts and undersaturated calcite bearing basalts.
28. The chemical analyses and the katamolecular norms of carbonatite and massive basaltic kimberlites.
29. The chemical composition and katamolecular norm of the alkaline-rocks north-east of Pretoria.
30. The chemical analyses and molecular norms of garnet peridotite, peridotite and dunite from various parentages.
31. The chemical analyses and molecular norms of eclogite.

XIV. ACKNOWLEDGEMENTS

The financial assistance supplied by the South African branch of the Upper Mantle Project is gratefully acknowledged for enabling the present research. Dr. Murray and Mr. B. Hawthorne of the Anglo American Corporation (Ltd.) are thanked for making the investigation possible by allowing me to collect material from Premier Mine. Mr. C.D. Hallam, Mr. D. du Toit and Messrs. P. Booth, D. White Cooper, R. Clement and H. van der Westhuizen are greatly thanked for their help and kindness during my visit to Kimberley.

The staff of Premier Diamond Mine, viz. Mr. Hodgen, Messrs. Kieser, Gennell, Oats and Sayer are also thanked for their help, during my stay at Premier Mine.

To the late Prof. J. Willemse, who suggested and guided this research, I wish to convey my sincerest gratitude. The guidance and never failing interest of Dr. C.P. Snyman and Dr. E.B. Förtsch during the last stages of this research are gratefully acknowledged. Prof. D.J.L. Visser, Mr. S. Zagt, Dr. W.J. Verwoerd, Dr. M.J. O'Hara, Dr. S. Haughton, Dr. E.D. Jackson and Dr. H.L. Allsop are also thanked for their many stimulating discussions.

Drs. O.R. van Eeden, C.B. Coetzee and H. Jansen, and Mr. W. Simpson, all of the Geological Survey of South Africa are thanked for allowing the new chemical analyses to be made and for the use of unpublished data in the structural map.

The assistance of Miss M. Uys with the considerable number of mathematical and chemical calculations is gratefully acknowledged. Miss Potgieter, Mrs. Barta and Mrs. Dicker are thanked for the final preparation of the thesis. To my family and friends, who always took an interest in my present research, I wish to express my sincerest thanks.

Mr. H. Auret kindly did the proof-reading of the manuscript, in its final form.

XV. REFERENCES

ALLEN, J.B. and T. DEANS, (1965), Ultrabasic eruptives with alnoiitic-kimberlitic affinities from Malaita, Solomon Islands. Min. Mag., 34. p. 16-34.

ALLSOPP, H.L., A.J. BURGER and C. VAN ZYL, (1967), A minimum age for the Premier Mine kimberlite pipe, yielded by biotite Rb/Sr measurements, with related galena isotopic data. Earth. Planet. Sci. Lett., 3. p. 161-166.

ALLSOPP, H.L., L.O. NICOLAYSEN and P. HAHN WEINHEIMER, (1969), Rb/Sr ratios and Sr isotopic composition of minerals in eclogitic and peridotitic rocks. Earth. Planet. Sci. Lett., 5. p. 231-244.

AOKI, K.I., (1964), Clinopyroxenes from alkaline rocks of Japan. Amer. Min., 49. p. 1199-1223.

BAILEY, S.W., E.N. CAMERON, H.R. SPEDDEN and R.J.J. WEEDGE, (1956), The alteration of ilmenite in beach sands. Econ. Geol., 57. p. 263-279.

BARTH, T.W.F., (1962), Theoretical Petrology, J. Wiley and Sons Inc., N.Y. 1962.

BELL, P.M., (1964), High pressure melting relations for jadeite composition. Carn. Inst. Yearb. Wash., 63. p. 171-174.

BERRY, L.G. and R.M. THOMPSON, (1962), X-ray powder data for ore minerals. Geol. Soc. of Amer., Memoir 85.

BESSON, M., (1967), La teneur de geikiélite des ilmenites des Kimberlites. Bull. Soc. fr. Minéral. Crystallogr., Vol. XC. p. 192-201.

BILGRAMI, S.A., (1969), Geology and chemical mineralogy of the Zhob Valley chromite deposits, West Pakistan. Amer. Min., 54. p. 134-148.

BOBRIEVICH, A.P., BONDARENKO M.N., GNEVEISHEV M.A., KRASOV, L.M., SMIRNOV G.I. and YURKEVICH R.K., (1959), The diamond deposits of Yakutia. Gasgeoltekhizdat, Moscow. (Russian).

BOESEN R.S., (1964), The clinopyroxene of a monzonitic complex at Mount Dromadary, New South Wales. Amer. Min., 49. p. 1435-1457.

BONATTI, E., (1968), Ultramafic Rocks from the Mid Atlantic Ridge. Nature, 219. p. 364.

BOWEN, N.L. and J.F. SCHAIRER, (1935), The system FeO-MgO-SiO_2. Am. Jour. Sci., 29. p. 151-217.

BOWEN, N.L. and O.F. TUTTLE, (1949), The system MgO-SiO_2-H_2O. Bull. Geol. Soc. Amer., 60. p. 439-460.

BOYD, F.R. and J.L. ENGLAND, (1960), Minerals of the mantle. Carn. Inst. Yearb. Wash., 59. p. 47-52.

BOYD, F.R. and J.L. ENGLAND, (1962), Mantle minerals. Carn. Inst. Yearb. Wash., 61. p. 107-112.

BOYD, F.R. and J.L. ENGLAND, (1964), The system enstatite-pyrope. Carn. Inst. Yearb. Wash., 63. p. 157-161.

BOYD, F.R. and J.F. SCHAIRER, (1964), The system $MgSiO_3$-$CaMgSi_2O_6$. Jour. Petrol., 5. p. 275-309.

BOYD, F.R. and J.L. ENGLAND, (1963), Effect of pressure on the melting of diopside and albite in the range up to 50 kb.. Jour. Geoph. Res., 68. p. 311-323.

BOYD, F.R. and J.L. ENGLAND., (1959), Pyrope. Carnegie. Inst. Yearb. Wash., 58. p. 83-87.

BOYD, F.R., (1969). Electron-probe study of diopside inclusions from kimberlite. Am. Jour. Sci., 267A. p. 50-62.

BROUSSE, R., (1968), La place des ultra-basites en France. Geol. Rdsch., 37. p. 621-655.

BROWN, G.M., (1967), Mineralogy of basaltic rocks, Basalts ed. by H.H. Hess and A. Poldervaart, Vol 1, p. 103-162, J Wylie and Sons Inc. N.Y. 1968.

BURRI, C., (1959), Petrochemische Berechmungsmethoden auf äquivalenter Grundlage (Methoden von Paul Niggli). Birkhäuser Verlag, Basel.

CAMERON, E.N., (1964), Chromite deposits of the eastern part of the Bushveld Complex. Geology of South African Ore Deposits, ed. S. Haughton. Geol. Soc. S. Afr., p. 131-168.

CAMERON, E.N., (1961), Ore microscopy, J. Wylie and Sons Inc. N.Y.

CARSWELL, D.A., (1968), Picritic magma, residual dunite relationships in garnet peridotite at Karlskaret near Tafjord, S. Norway. Contr. Mineral. Petrol., 19. p. 97-124.

CHAYES, F., (1965), Titanium and alumina content of oceanic and circumoceanic basalts. Min. Mag., 34. p. 126-131.

CLARK, I. and J.J. Papike, (1968), The crystal-chemical characterization of omphacites. Amer. Min., 53. p. 840-868.

COETZEE, C.B., (1957), Ilmeniethoudende sand langs die weskus, in die distrik van Van Rhynsdorp. Bull. Geol. Surv. S. Afr., 25.

COLEMAN, L.C., (1962), Effect of ionic substitution on the unit-cell dimensions of synthetic diopside. Bull. Geol. Soc. Amer., Buddington Volume, p. 429-446.

DALY, R.A., (1925), Carbonate dykes of the Premier Diamond Mine, Transvaal. Jour. Geol., 33. p. 659-684.

DANA, E.S., (1894), The System of Mineralogy of James Dwight Dana (1837-1868), Descriptive Mineralogy. Kegan Paul, Trench, Trübner and Co Ltd.

DAVIS, B.T.C. and F.R. BOYD, (1966), The join $Mg_2Si_2O_6$- at 30 kb pressure and its application to pyroxenes from kimberlite. Jour. Geoph. Res., 71. p. 3567-3576.

DAWSON, I.B., (1962), Basutoland Kimberlites. Bull. Geol. Soc. Amer., 73. p. 545-560.

DAWSON, I.B., (1967), A Review of the Geology of Kimberlite. Ultramafic and Related rocks. ed. P.J. Wyllie. J. Wiley and Sons. Inc., N.Y., 1967, p. 241-251.

DAWSON, I.B., (1967), Geochemistry and the Origin of Kimberlite. Ultramafic and Related rocks. ed. P.J. Wyllie. J. Wiley and Sons. Inc., N.Y., 1967, p. 269-278.

DEER, W.A. and D. ABBOT, (1965), Clinopyroxene of the gabbro cumulates of Kap Edvard Holm Complex, East Greenland. Min. Mag., 34. p. 177-193.

DEER, W.A., R.A. HOWIE and I. ZUSSMAN, (1967), An Introduction to the Rock forming minerals. Longmans, London.

DICKY, J.S., (1968), Eclogitic and other inclusions in the mineral breccia member of the Deborah Volcanic formation at Kakamui, New Zeeland. Amer. Miner., 52. p. 1304-1319.

DU RIETZ, T., (1935), Peridotites, serpentinites and soapstones of northern Sweden. Academic dissertation, Stockholm, 1935.

EDWARDS, A.B., (1965), Textures of the Ore Minerals. Australasian institute for Mining and Metallurgy, Melbourne, Australia.

ELISIEV, I.N., (1957), X-ray investigation on minerals of the isomorphous forsterite-fayalite series. Papers of Soviet Min. Soc. Vol. 86. No. 6.

ESKOLA, P., (1921), On the eclogites of Norway. Vidensk. Skr. I Nat. Kl. 8, p. 1-118.

ESSENE, E.J. and W.S. FYFE, (1967), Omphacite in Californian metamorphic rocks. Contr. Mineral. Petrol., 15. p. 1-23.

LAPHAM, J, (1964), A study of serpentine at A.M.S.O.C. bore-hole near Peuerto Rico. National Accad. Sci., p. 134-145.

LE BAS, M.J., (1962), The role of alumina in igneous clinopyroxenes with relation to their parentages. Am. Journ. Sci, 260. p. 267-288.

LEWIS, C. (1887), On a diamontiferous peridotite and the genesis of the diamond. Geol. Mag., 4. p. 22-24.

LINDSLEY, D.H., (1965), Iron-titanium oxides. Carn. Inst. Yearb. Wash., 64. p. 144-148.

LOMBAARD, B.V., (1932), The felsites and their relations to the Bushveld Complex. Trans. geol. Soc. S. Afr., 35. p. 125-189.

LIEBENBERG, C.J. (1960), The trace elements of the rocks of the Bushveld Igneous Complex. Publ. of Univ. of Pta. No. 12.

MacGREGGOR, R.I., (1964), A refractory chrome ore deposit in the Groot Marico district. Geology of South African Ore Deposits. ed. S. Haughton (1964). Geol. Soc. S. Afr., p. 203-208.

MacGREGOR I.D. and C.H. SMITH, (1963), The use of chrome spinels in petrographic studies of ultramafic intrusions. Can. Min., 7. p. 403-412.

MacGREGOR, I.D. and A.E. RINGWOOD, (1964), The natural system enstatite-pyrope. Carn. Inst. Yearb. Wash., 63. p. 161-163.

MacGREGOR, I.D., (1965), The effect of pressure on the minimum melting composition in the system MgO-SiO_2-TiO_2. Carn. Inst. Yearb. Wash., 64. p. 135-139.

MacKINLAY, A.C.M., (1955), Kimberlite intrusions cutting Karroo sediments in the Ruhuhu depression of South-western Tanganyika. Rec. Geol. Surv. Tanganyika, 5. p. 63-80.

MANTUR, S.M., (1962), Geology of the Parma diamond deposits. Rec. Geol. Surv. India, 87. p. 787-818.

ERNST, T., (1935), Olivienknollen der Basalte als Bruchstücke alter Olivienfelse. Nachr. Ges. Wiss. Göttingen. Mat. Phys. Gruppe IV Band I, p. 147-154.

ERNST. T., (1967), Olivine nodules and the composition of the earth's mantle. Mantles of the Earth and Terrestial Planets. ed. S.K. Runcorn, J. Wiley and Sons. Inc. N.Y., London.

EVANS, B.W. and J.G. MOORE, (1968), Mineralogy as a function of the depth in the prehistoric Makaopuhi tholeiitic lava lake, Hawaii. Contr. Mineral. Petrol., 17. p. 85-115.

FRANKEL, J.J., (1959), An inclusion bearing olivine melilitite from Mukarob, South West Africa. Trans. Roy. Soc. S. Afr., 35. p. 115-124.

FREEDMAN, J., (1959), The Samried Lake sulphide deposits Ontario, an example of a pyrite-pyrrholite iron formation. Econ. Geol., 54. p. 268-284.

FRECHEN, J., (1963), Kristallisation, Mineral-chemismus und Förderfolge der Mafitite vom Dreiser Weiher in der Eifel. Neues Jhb. Min. Mh., p. 205-225.

FRICK, C. (1967), The Margin of the Bushveld Complex in the Vicinity of De Berg, North of Dullstroom, Transvaal. MScthesis, (unpublished) University of Pretoria.

GARSON, M.S., (1965), Carbonatites and agglomeratic vents in Western Shire Valley. Geol. Surv. Malawi, Memoir 3.

GERRYTS, E., (1951), The Petrology of the kimberlites at Premier diamond mine, Transvaal, South Africa. Ph. D thesis, McGill University, (unpublished).

GIROD, M., (1967), Données petrographiques sur des pyroxenoliths a grenat en enclaves dans des basaltes du Hoggar. Bull. Soc. fr. Mineral. Cristallogr., Vol XC, p. 202-213.

GITTINS, J. and O.F. TUTTLE., (1966), Carbonatites. J. Wiley and Sons Inc. N.Y.

GLATTHAAR, C.W., (1956), Die verysterde piroklaste in 'n na-Waterbergse graniet, suid-oos van die dam Rust der Winter. MSc-thesis, University of Pretoria, (unpublished).

GOLDSMITH, J.R., D.L. GRAF, J. WITTERS and D. NORTHTROP., (1962), Studies in the system $CaCO_3$ - $MgCO_3$-$FeCO_3$. Jour. Geol., 70. p. 659-688.

GREEN, D.H. and A.E. RINGWOOD, (1967), An experimental investigation of gabbro to eclogite transformation and its petrological application. Geochem. et Cosmochem. Acta 31. p. 767-833.

GREEN, D.H., (1967), High temperature peridotite intrusions. Ultramafic and Related Rocks. p. 212-221. ed. P.J. Wyllie, J. Wiley and Sons Inc. N.Y.

GREEN, D.H. and A.E. RINGWOOD, (1967), The Stability fields of aluminous pyroxene peridotite and garnet peridotite and their relevance in the Upper Mantle structure. Earth. Planet. Sci. Lett., 3, p. 151-160.

HALL, A.L., (1932), The Bushveld Igneous Complex of the Central Transvaal. Geol. Survey of S. Afr., Memoir 28.

HALL, A.L., (1938), Analyses of Rocks, Ores, Coal, Soils and Waters. Geol. Surv. S. Afr., Memoir 32.

HAHN WEINHEIMER, P. and W. LUECKE, (1963), Garnets from eclogite of the Muenchberger gneiss massiv. Can. Mineral., 7. p. 764-795.

HAMAD, S. U D., (1962-1964), The Chemistry and mineralogy of the olivine nodules of Calton Hill Derbyshire. Min. Mag., 33 p. 483-497.

HOUNSLOW, A.W. and CHAO, K., (1967), Geikielite, a new Canadian occurrence. Can. Mineral., 9. p. 95-100.

HAUY, R.I., (1822), Traite dé Mineralogie II^{e} ed, 25. p. 613. Bachelier, Paris.

HAUGHTON, S.H., (1969), Geological History of Southern Africa. Geol. Soc. S. Afr., 1969.

HECKROODT, O.R., (1958), An X-ray method for the determination of olivine. Trans. Geol. Soc. S. Afr., LXI, p. 377-386.

HESS, H.H., (1949), Chemical composition and optical properties of common clinopyroxenes. Pt I, Amer. Miner., 34. p. 621-666.

HESS, H.H., (1952), Orthopyroxene of the Bushveld type, and ion substitution changes in unit cell dimensions. Am. Jour. Sci., Bowen volume. p. 173-187.

HESS, H.H., (1960), Stillwater Igneous Complex, Montana. Geol. Soc. Amer., Memoir 80.

HOLMES, A., (1930), Petrographic methods and calculations. Thomas Murby Co, London, 1930.

HOLMES, A., (1936), Petrology of kimberlite and its inclusions. Trans. Geol. Soc. S. Afr., 39. p. 379-427.

HUCKENHOLZ, H.G., (1965a, 1965b, 1966), Der Petrogenetische werdegang der Klinopiroksene in den Tertiären Vulkaniten der Hocheifel. Contr. Mineral. Petrol., Volumes 3 & 4.

IRWINE, T.N., (1967), The Duke Island Ultramafic Complex south-east Alaska. p. 84-97. Ultramafic and Related Rocks, ed. P.J. Wyllie. J. Wiley and Sons Inc. N.Y.

JACKSON, E.D., (1960), X-ray determination curve for natural olivine of composition Fo_{80-90}. U.S. Geol. Survey, Prof. Paper. 400B. p. 432-434.

JACKSON, E.D., (1968), The character of the lower crust and Upper mantle beneath the Hawaiian Islands. Intn. Geol. Congress, Vol 1. p. 135-150.

JACKSON, E.D., and T.L. WRIGHT, (1969), Xenoliths in the Honolulu Volcanic Series, Hawaii, In press.

JOHANBAGLOO, J.C., (1969), X-ray diffraction studies of olivine solid solution series. Amer. Miner., 54. p. 246-251.

JOHANNSEN, A., (1939), A descriptive petrography of Igneous rocks. Vol I to Vol IV. University of Chicago Press, Chicago.

JAMBOR, J.L. and SMITH, C.H., (1964), Olivine composition determination with small-diameter X-ray powder cameras. Min. Mag., 33. p. 730-741.

JONES, D.L., (1969), The Palaeomagnetism of the Premier Mine kimberlite, (in press).

JONES, D.L. and E. McELHINNY, (1966), Palaeomagnetic correlation of basic intrusions in the Pre Cambrian of S. Africa. Jour. Geoph. Res., 71. p. 543-552.

KENNEDY, G.C., (1947), Charts for correlation of optical properties with chemical composition of some rock forming minerals. Amer. Mineral., 32. p. 561-574.

KENNEDY, G.C. and B.E. NORDLIE, (1968), The genesis of diamond deposits. Econ. Geol., 63. p. 495-503.

KLUG, H.P. and L.E. ALEXANDER, (1954), X-ray diffraction procedures. J. Wiley and Sons Inc. N.Y.

KOPECKY, L. and V. SATTRAN, (1962), Ke genesi pyropu v. Cisken strudhori, Vestric U.U.C. roc., 37. p. 269-283.

KUNO, H., (1967), Mafic and ultramafic nodules from Itinome Gata, Japan. p. 337-342. Ultramafic and Related Rocks, ed. P.J. Wyllie. J. Wiley and Sons. Inc. N.Y.

KUSHIRO, I., (1960), Si-Al relations in clinopyroxenes from igneous rocks. Am. Jour. Sci. 258. p. 548-554.

KUSHIRO, I., (1962), Clinopyroxene solid solutions, the $CaAl_2SiO_6$ Component. Jap. Jour. Geol. and Geograp., 33. p. 213-220.

KUSHIRO, I., (1965), Clinopyroxene solid solutions at high pressures. Carn. Inst. Yearb. Wash., 64. p. 112-117.

KUSHIRO, I., (1964), The system diopside-forsterite-enstatite at 20 kb. Carn. Inst. Yearb., Wash., 63. p. 101-108.

KUSHIRO, I. and K.I. AOKI, (1968), Origin of some eclogite inclusions in kimberlite. Amer. Min., 53. p. 1347-1367.

MARMO, V., (1959), On the TiO_2-content of magnetites, a petrogenetic hints, Am. Jour. Sci., 257, p. 144.

MASON, B., (1958), Principles of Geochemistry. J. Wiley & Sons Inc, N.Y.

MASON, B., (1968), Eclogitic xenoliths from the volcanic breccia at Kakanui, New Zeeland. Contr. Mineral. and Petrol., 19. p. 316-326.

MATHIAS, M. and P.C. RICKWOOD, (1969), Ultramafic xenoliths in the Matsoku Kimberlite Pipe, Lesotho. (In press.)

McCONNELL, D, (1952), The problem of carbonate apatites IV, structural substitution involving CO_3 and OH. Bull. Soc. Franç. Min. Cryst., 75. p. 428.

McDONALD, G.A. and T. KATSURA, (1964), Chemical composition of Hawaiian lavas. Jour. Petrol., 5. p. 82-133.

MERCY, E.L.P., (1967), Geochemistry of the Mantle. p. 421-441. The Earth's Mantle. ed. T.F. Gaskel, Acad. Press, N.Y.

MILASHEV, V.A., (1965), Petrochemistry of the Kimberlites of Yakutia. Nedra. Leningrad. p. 160. (Russian)

MINERAL RESOURCES OF SOUTH AFRICA, (1959), Geological Survey S. Afr., 1959, p. 48.

MOENKE, H., (1962), Mineralspektrenn Tel II, Akademie Verlag, Berlin.

MONTOYA, J.W. and G.S. BAUR, (1963), Nickeliferous serpentines, chlorites and related minerals found in lateritic ores. Amer. Miner., 48. p. 1227-1238.

MUIR, I.D. and C.E. TILLEY, (1957 and 1963), Contributions to the petrology of Hawaiian basalts, parts I & II. Am. Jour. Sci., 255. 261. p. 241 and p. 253.

MURDOCH, J. and J.J. FAYLEY, (1949), Geikielite, a new find from California. Amer. Miner, 34. p. 835-838.

NICOLAYSEN, L.O., J.W.L. DE VILLIERS, A.J. BURGER and F.W.E. STRELOW, (1958), New measurements relating to the absolute age of the Transvaal System and of the Bushveld

Igneous Complex. Trans. Geol. Soc. S. Afr., 61. p. 137-163.

NIXON, P.H., O. VON KNORRING and J.M. ROOKE, (1963), Kimberlites and associated inclusions of Basutoland; a mineralogical and geochemical study. Amer. Miner., 48. p. 1090-1132.

O'HARA, M.J. and MERCY E.L.P., (1963)., Petrology and Petrogenesis of some garnetiferous Peridotites. Trans. Roy. Soc. of Edinburg, LXV, No 12, p. 251-314.

O'HARA, M.J., (1963), Melting of garnet peridotite at 30 kb. Carn. Inst. Yearb. Wash., 62. p. 71-76.

O'HARA, M.J., (1963), Melting of bimineralic eclogite at 30 kb. Carn. Inst. Yearb. Wash., 62. p. 76-77.

O'HARA, M.J., and J.F. SCHAIRER, (1963), The join diopside-pyrope at atmospheric pressure. Carn. Inst. Yearb. Wash., 62. p. 107-115.

O'HARA, M.J., (1967), Mineral paragenesis in Ultramafic Rocks. p. 393-403. Ultramafic and related rocks, ed. P.J. Wyllie, J. Wiley and Sons Inc. N.Y.

O'HARA, M.J. and E.L.P. MERCY, (1966), Exceptional calcic pyralspite from South African kyanite eclogite. Nature, 212, p. 68-69.

O'HARA, M.J. and H.S. YODER, (1967), Formation and fractionation of basic magmas at a high pressure. Scot. J. Geol., 3, p. 67-117.

O'HARA, M.J., (1968), The bearing of phase equilibria studies in synthetic and natural systems on the origin and evolution of basic and ultrabasic rocks. Earth Sci., Rev., 4. p. 69-133.

OOSTHUYZEN, E.J. and A.J. BURGER, (1964), Radiometric dating of intrusives associated with the Waterberg System. Ann. Geol. Surv. S. Afr., 3. p. 87-106.

PARK, C.F., and R.A. MacDIARMID, (1964), Ore Deposits. W.H. Freeman and Co. Ltd., San Francisco and London.

PEARRE, N.C., and A.V. HEYL, (1960), Chromite and other mineral deposits in serpentine rocks of Pietmont Upland, Maryland, Pennsylvania and Delaware. U.S.A. Geol. Surv. Bull., 1082-K.

PISTORIUS, C.W.F.T., (1967), Some phase relations in the system $MgO-SiO_2-H_2O$ to high pressures and temperatures. Neues Jhb. Min. Mh., 1967, p. 283.

RAAL, F.A., (1969), A study of some gold mine diamonds. Amer. Miner., 54. p. 292-295.

RABHIN, M.I, M.A. KRUTOYARSKI and V.A. MILASHEV, (1962), Classification and nomenclature of Yakutian kimberlites. Inst. Geol. Arktik., 121. p. 154-164.

RALEIGH, C.B., (1967), Experimental deformation of ultramafic rocks and minerals. p. 191-199. Ultramafic and related Rocks, ed P.J. Wyllie. J. Wiley and Sons. Inc.

RAMDOHR, P., (1960), Die Erzmineralien und ihre Verwachsungen, Akademie Verlag, Berlin.

REPORTS OF LEEDS UNIVERSITY, 1962-63, 1963-64, 1964-65, University of Leeds, Leeds.

RICKWOOD, P.C., (1968), On recasting analyses of garnet into end member molecules. Contr. Mineral. Petrol., 18. p. 175-198.

RICKWOOD, P.C., I.I. GURNEY and D.R. WHITE-COOPER, (1969), The nature and occurrence of eclogite xenoliths in the kimberlites of Southern Africa. (In Press).

RICKWOOD, P.C., M. MATHIAS, and J.C. SIEBERT, (1968), A study of garnets from eclogite and peridotite xenoliths in kimberlite. Contr. Mineral. Petrol., 19, p. 271-301.

RINGWOOD, A.E., McGREGOR I.D. and I.R. BOYD, (1964), Petrological composition of the upper mantle, Carn. Inst. Yearb. Wash., 63. p. 147-152.

RINGWOOD, A.E. and D.H. GREEN, (1966), An experimental investigation of the gabbro-eclogite transformation and some geophysical implications. Tectonophys., 3. p. 383-427.

ROSS, C.S., M.D. FORSTER and A.J. MYER, (1954), Origin of dunite and of olivine rich inclusions in basaltic rocks. Amer. Miner., 39. p. 693-737.

ROY, R. and D.M. ROY, (1957), A redistribution of equilibria in the system MgO-H_2O. Amer. Jour. Sci., 255. p. 574.

RUSSEL, H.D., S.A. HIEMSTRA and D. GROENEVELD, (1954), The mineralogy and petrology of the carbonatite at Loolekop Eastern Transvaal. Trans. Geol. Soc. S. Afr., 57. p. 197-208.

SOBOLEV, N.V., (1958), Rhombic pyroxenes from a garnet-peridotite and eclogite. Dokl. Akad. Nauk. SSR, 154. p. 395.

SAGGERSON, E.P., (1968), Eclogite nodules associated with alkaline olivine basalts, Kenya. Geol. Rdsch., 57. p. 890-904.

SAKATA, Y., (1957), Unitcell dimensions of synthetic aluminian diopsides. Japan. Journ. Geol and Geograp., 28. p. 161-168.

SAMPSON, T.G., (1953), The Volcanic hills at Igwisi. Rec. Geol. Surv. Tanganyika, 3. p. 48-53.

SCHAIRER, J.F. and H.S. YODER, (1960), The nature of residual liquids, from crystallization, with data on the system nepheline-diopside-silica, Am. Jour. Sci., 258A. p. 273-283.

SCHUTTE, F.J.F., (1967), Xenoliete en Xenokriste in Kimberliet van Barkley Wes. MSc thesis, University of Potchefstroom, (unpublished).

SHAND, S.J., (1921), The Igneous Complex of Leeuwfontein, Pretoria District. Trans. Geol. Soc. S. Afr., 24. p. 232-249.

SHAND, S.J., (1922), The alkaline rocks of the Franspoort line, Pretoria District. Trans. Geol. Soc. S. Afr., 25. p. 81-100.

SMIRNOV, G.I., (1959), Mineralogy of Siberian kimberlites. Int. Geol. Rev., 1. No 12. p. 21-39.

SMULIKOWSKI, K., (1968), Differentiation of eclogites and its possible causes. Lithos, 1. p. 89-102.

SOBOLEV, N.V., (1964), Rhombic pyroxenes from garnet peridotite and eclogite. Dokl. Akad. Nauk. SSSR, 1964. p. 110-111.

SOBOLEV, N.V., (1966), Mineralogy of diamond bearing eclogite. Dokl. Akad. Nauk. SSR, 167. p. 1365-1368.

SOBOLEV, N.V, KUZNETSOVA I.K., and N.I. ZYUZIN, (1968), The petrology of grospydite xenoliths from the Zagadachnaya kimberlite pipe in Yakutia. Jour. Petrol., 9. p. 253-280.

STRUNZ, H., (1966), Mineralogishe Tabellen. Akademische Verlagsgesellschaft, Leipzig.

SUTHERLAND I.K., (1967), The chemistry of some New Brunswick pyrites. Can. Mineral., 9. p. 71-84.

SVOBODA, I, (1966), The Regional Geology of Chechoslovakia, The Bohemian Massiv, Part I. The Chechoslovac Acad. Sci.

TALJAARD, M.S., (1936), South African melilite basalts and their relations. Trans. Geol. Soc. S. Afr., 37. p. 281-316.

TAYLOR, H.P., (1967), The zoned ultramafic complexes of southeast Alaska. p. 97-121. Ultramafic and related rocks. ed. P.J. Wylie, J. Wiley and Sons Inc., N.Y.

THOMPSON, J.B., (1947), The role of alumina in rock forming silicates. Bull. Geol. Soc. Amer., 58. p. 1232.

TOENS, D., (1952), The Geology of Leeuwfontein North East of Pretoria, MSc thesis, University of Pretoria (unpublished).

TRÖGER, W.E., (1959), Optische Bestimmung der gesteinsbildenden Minerale, Teil I. Bestimmungstabellen. Stuttgart, E. Schweizerbart'sche, Verlagsbuchhandlung.

TRÖGER, W.E., (1967), Optishce Bestimmung der gesteinsbildenden Minerale, Teil, II. Stuttgart, E. Schweizerbart'sche Verlagsbuchhandlung.

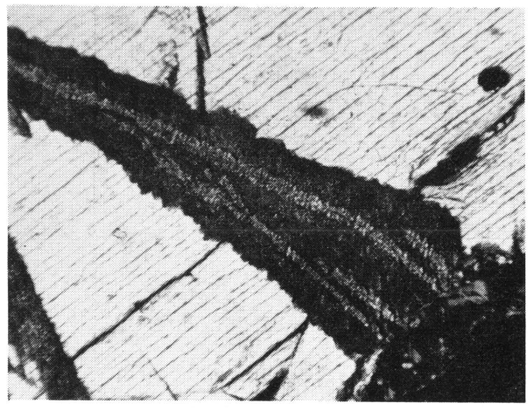

25

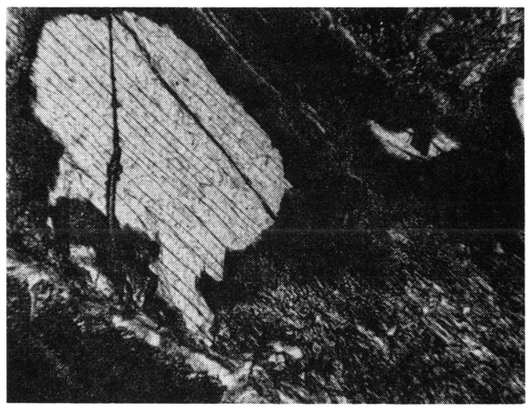

26

27

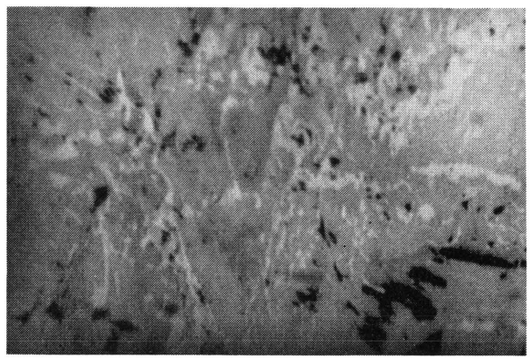

28

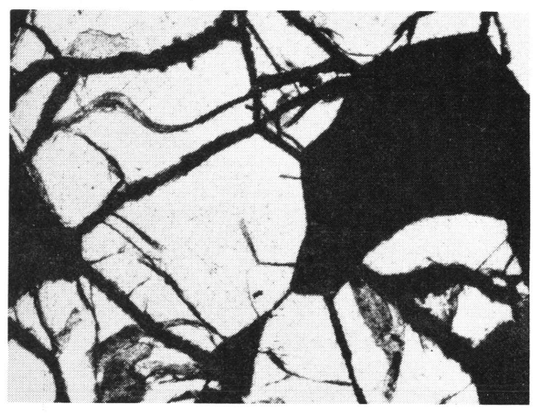

29

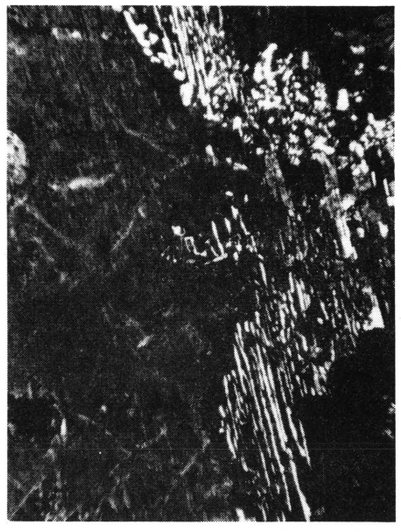

30

Photo 25 The clinopyroxene grains (light) of an eclogite nodule, which is replaced by a fine-grained, highly birefringent clinopyroxene (dark) section Ja. 2, Jagersfontein Mine, crossed nicols, x 50.

Photo 26 Fine-grained crystallites of secondary clinopyroxene (dark) passing into a brownish crypto-crystalline material. Section B_2B_2, Lovedale Kimberlite, transmittened light, x 250.

Photo 27 A rim of isotropic glass, traversing an area of fine-grained crystallites of clinopyroxene. Section B_2B-2, Lovedale Kimberlite, crossed nicols, x 250.

Photo 28 Unorientated exsolutions of hematite (white) from an ilmenite grain (grey) which was heated in an oxygen-free atmosphere, and subsequently quenched in Mercury. Sample Riv 27 from the Riverton Kimberlite occurrence, x 400, reflected light.

Photo 29 The replacement of garnet by ilmenite in an ilmenite-garnet-clinopyroxene nodule. Hololo 32, transmittened light, x 25.

Photo 30 A grain of primary orthopyroxene (Bushveld type), surrounded by a rim of pigeonite, which shows exsolution lamellae of clinopyroxene. Tholeiitic sill, section B_{1-10}, crossed nicols, x 25.

TRUTER, F.C., (1955), Modern concepts of the Bushveld Igneous Complex. First Meeting 8th. reg. Com. Geol., Salisbury. Publ. C.C.T.A., 1955, p. 71-79.

TYLER, R.C. and B.C. KING, (1967), The pyroxenes of the alkaline igneous complexes of eastern Uganda. Min. Mag., 36. p. 5-21.

VERHOOGEN, J., (1938), Les pipes du kimberlite de Katanga. Ann. Serv. Min. Com. Spec. Katanga., 9.

VERWOERD, W.J., (1967), The Carbonatites of South Africa and South West Africa. Geol. Surv. S. Afr., Handbook 6.

VINCENT, E.A. and R. PHILLIPS, (1954), Iron-titanium oxide minerals in the layered gabbros of Skaergaard Intrusion, Pt. I. Geochem. et Cosmochem. Acta., 6. p. 1-26.

VISSER, H.N., (1961), Die Geologie van die gebied tussen Middelburg en Cullinan, Transvaal. Explanation to Sheets 2528 D and 2529 D. Geol. Surv. S. Afr.

VISSER, J.N.J., (1964), Analyses of Rocks, Minerals and Ores. Geol. Surv. S. Afr., Handbook 5. 1964.

VON ECKERMANN, H., (1967), A Comparison of Swedish, South African and Russian Kimberlites. p. 302-312. Ultramafic and related Rocks, ed. P.J. Wyllie, J. Wiley and Sons Inc. N.Y.

WAGER L.R., D.S. WEEDON and E.A. VINCENT, (1954), A granophyre from Coire Uaigneich, Isle of Skye, containing pseudomorphs of tridymite. Min. Mag., 30. 263-276.

WAGER, L.R. and BROWN, G.M., (1968), Layered Igneous Rocks. Oliver and Boyd, Edinburgh.

WAGNER, P.A., (1911), Petrological notes on kimberlite in the Pretoria District. Trans. Geol. Soc. S. Afr., 14. p. 43-63.

WAGNER, P.A., (1914), Diamond fields of South Africa. The Transvaal Leader, Johannesburg.

WARNER, J., (1964), X-ray crystallography of omphacite. Amer. miner., 49. p. 1461-1467.

WATSON, K.D., (1967), Kimberlites of eastern North America. p. 312-323. Ultramafic and related rocks, ed. P.J. Wyllie, J. Wiley and Sons Inc., N.Y.

WATSON, K.D. and D.M. MORTON, (1969), Eclogite inclusions in kimberlite pipes of Garnet Ridge, Northern Arizona. Amer. Miner., 54. p. 267-286.

WHITE, A.J.R., (1964), Clinopyroxenes from eclogites and basic granulites., Amer., Miner., 49. p. 883-888.

WILLEMSE, J., (1969), The Vanadiferous Magnetic Iron Ore of the Bushveld Igneous Complex. Econ. Geol. Monograph 4, p. 187-208.

WILLIAMS, A.F., (1932), The Genesis of the Diamond. Ernest Benn Ltd. 1932.

WILLSHIRE, H.G. and BINNS R.A., (1961), Basic and ultrabasic xenoliths from volcanic rocks of New South Wales. Jour. Petrol., 2. p. 185-208.

WINCHELL, A.N. and H. WINCHELL, (1959), Elements of Optical Mineralogy, an introduction to microscopic petrography, part II. J. Wiley and Sons. Inc, N.Y.

WINCHELL, A.N., (1958), The composition and physical properties of garnet. Amer. Miner., 43. p. 595-600.

WINKLER, H.G.F., (1967), Petrogenesis of Metamorphic Rocks. Springer Verlag, Berlin.

WORST, B.G., (1964), Chromite in the Great Dyke of Southern Rhodesia. Geology of South African Ore Deposits. ed. S. Haughton (1964), Geol. Soc. S. Afr., p. 209-224.

YODER, H.S., (1955), Role of water in metamorphism. Geol. Soc. Amer. Spec. Paper 62, p. 505-524.

YODER, H.S. and Th. G. SAHAMA, (1957), Olivine X-ray determinative curve. Amer. Miner., 42. p. 475-491.

YODER, H.S., (1950), Stability relations of grossularite. Jour. Geol., 58. p. 221-253.

YODER, H.S. and G.A. CHINNER, (1960), Almandite-pyrope-water system at 10,000 bars. Carn. Inst. Yearb. Wash., 59. p. 81-84.

YODER, H.S. and C.E. TILLEY, (1962), Origin of basalt magmas: - an experimental study of natural and synthetic rock systems. Jour. Petrol., 3. p. 342-532.

ZWAAN, P.C., (1954), On the determination of pyroxene by X-ray powder diagrams. Leidse. Geol. Med., 19. p. 167-276.

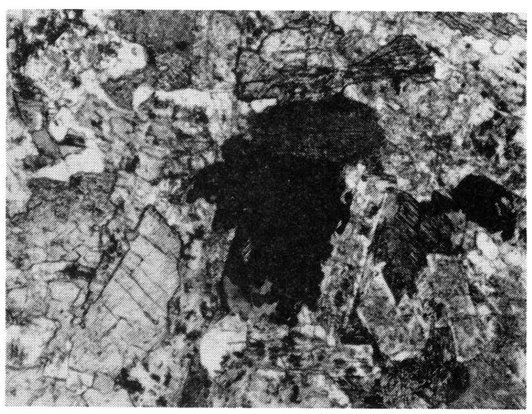

31

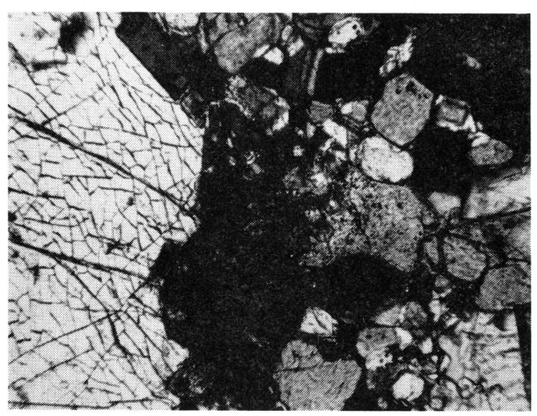

32

Photo 31 A skeleton crystal of magnetite in a glassy matrix. Tholeiitic sill, section B_{1-8}, Premier Mine, transmittened light, x 25.

Photo 32 The highly metamorphosed Kimberlite, consisting of olivine, enstatite, anorthite, and inter-granular glass (black material). Section B_{1-15}, Premier Mine, crossed nicols, x 25.

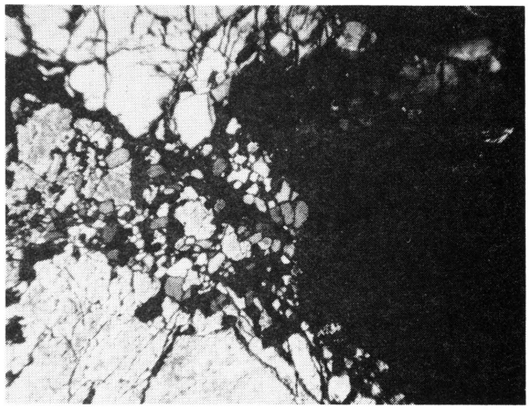

19

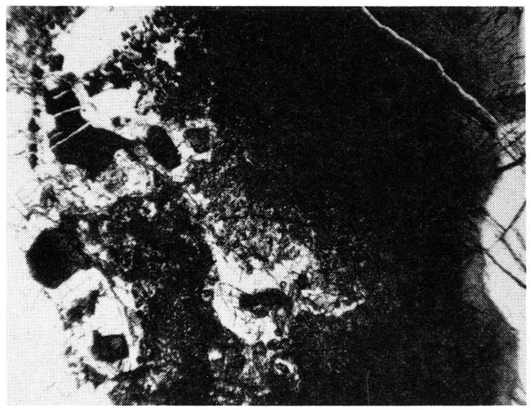

20

Photo 19 Recrystallization textures of an olivine grain, showing also kink-banding and undulatory extinction. Section Bu 7, Bultfontein Kimberlite, crossed nicols, x 50.

Photo 20 A garnet grain, showing an outer rim of kelyphyte, consisting of clinopyroxene and spinel, and an inner rim of fine-grained alternation products. Section $893In_{12}$, Premier Mine transmitted light, x 500.

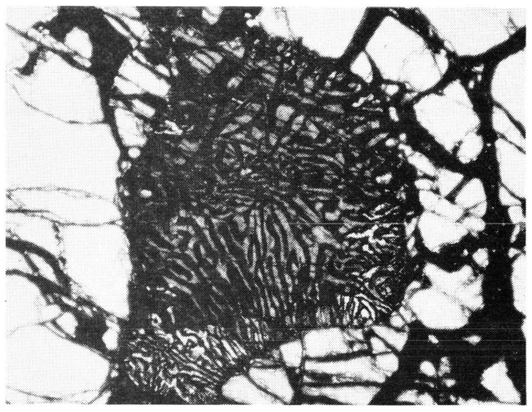

21

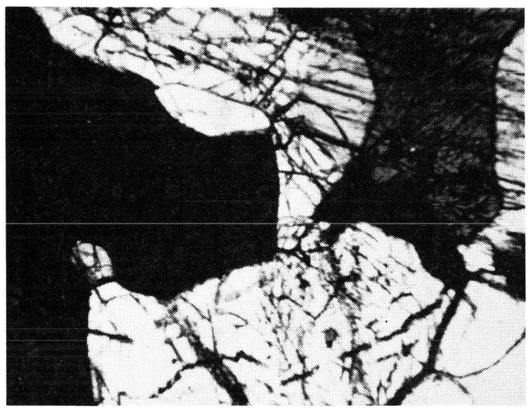

22

Photo 21 A symplectite consisting of worms of spinel in orthopyroxene surrounded by clinopyroxene. Section Dutoitspan 2, crossed nicols, x 100.

Photo 22 A large cumulus crystal consisting of the Bushveld type of orthopyroxene in an intercumulus phase of olivine and clinopyroxene, and some subhedral chromite grains. Section $1010In_6$, Premier Mine, crossed nicols, x 100.

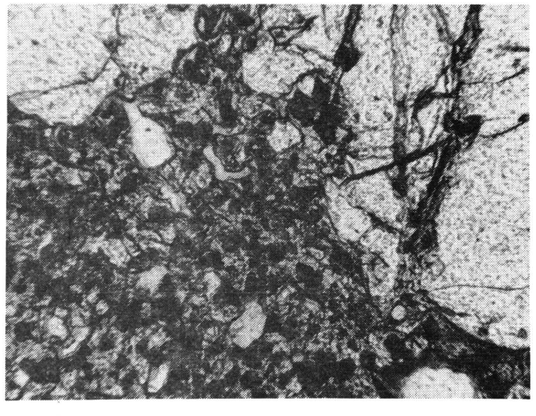

23

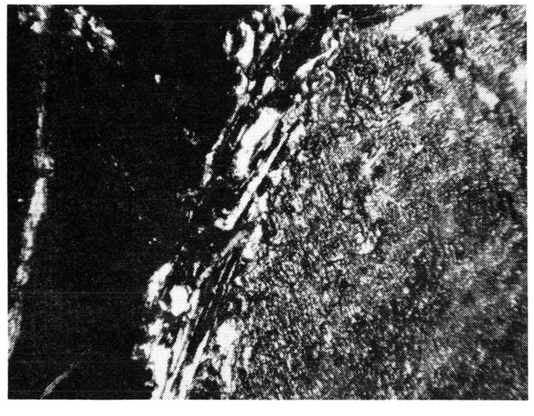

24

Photo 23 A kelyphytic rim consisting of spinel, pyrite and clinopyroxene, surrounding a garnet grain in an eclogite nodule. Section B_2B_2 Lovedale Kimberlite, transmittened light, x 500.

Photo 24 Plagioclase-bearing kelyphyte in an eclogite nodule, crossed nicols, Section $R.V.F._2$, Roberts Victor Mine, x 500.

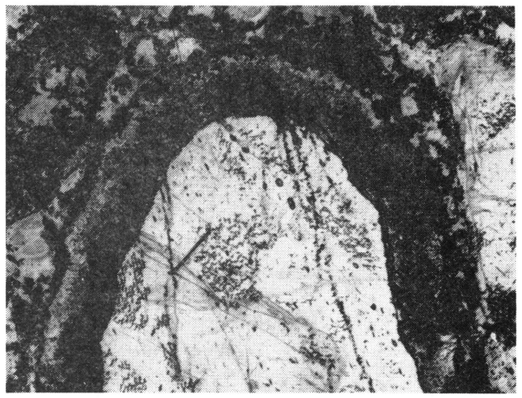

7

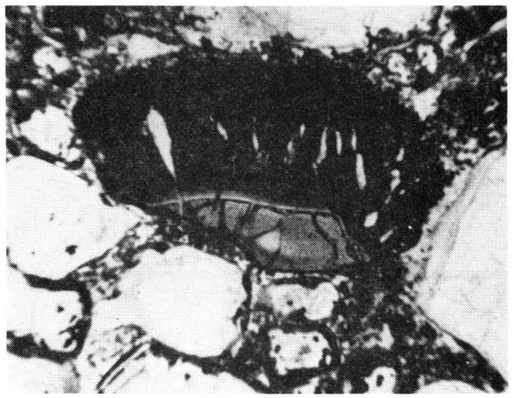

8

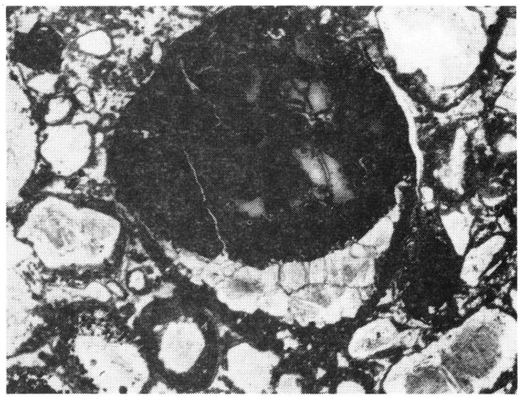

9

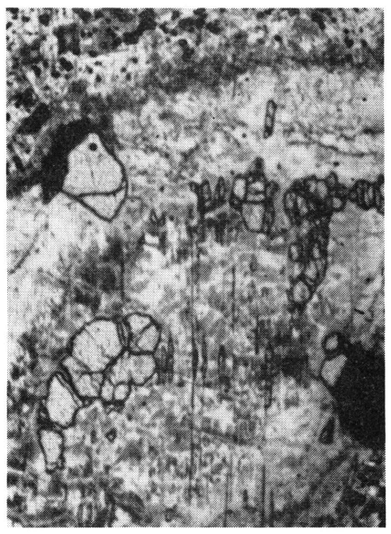

10

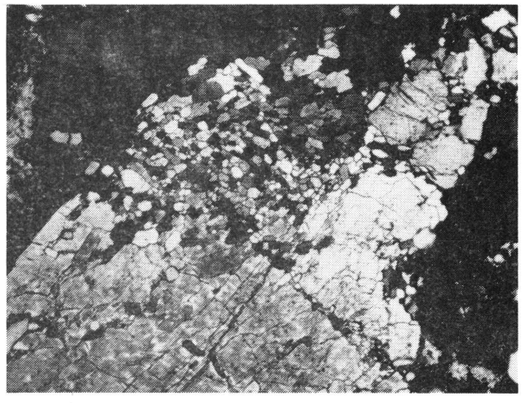

11

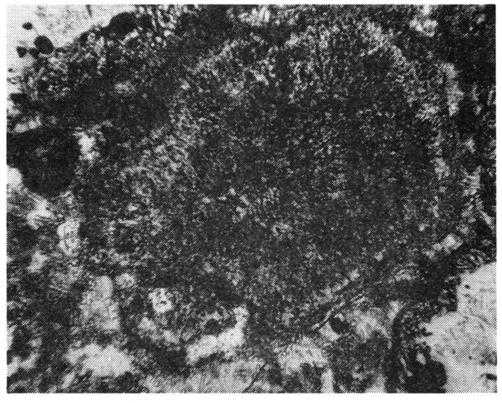

12

Photo 7 A first generation olivine grain, showing a zonal alteration to serpentine and tremolite, Premier Mine Kimberlite, section 1010-37, transmittened light, x 15.

Photo 8 A fractured garnet grain (grey), which did not develope a kelyphytic rim on the fractured surface. Premier Mine Kimberlite, section 1010-42, transmittened light, x 15.

Photo 9 A garnet grain (dark grey), surrounded by kelyphyte, as an inclusion in first generation olivine. Premier Mine Kimberlite, section 1010-40, transmittened light, x 15.

Photo 10 Exsolution bodies of garnet in an altered clinopyroxene along the (110) direction of the pyroxene. Monastry Mine Kimberlite, section Mon. 1, transmittened light, x 25.

Photo 11 A phenocryst of first-generation olivine showing original undulatory extinction and subsequent recrystallization. Crossed nicols, section Dutoitspan Kimberlite 2(A), x 25.

Photo 12 A completely melted primary olivine phenocryst, containing small crystallites of a second generation olivine. Transmittened light, section Dutoitspan Kimberlite 2(A), x 25.

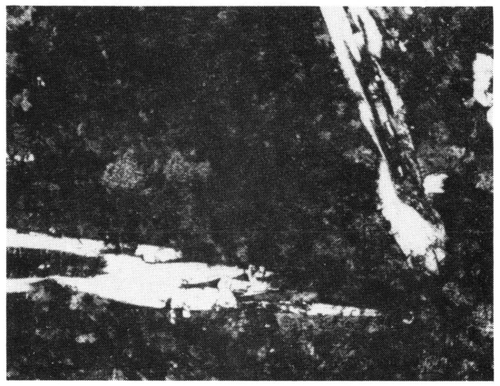

1

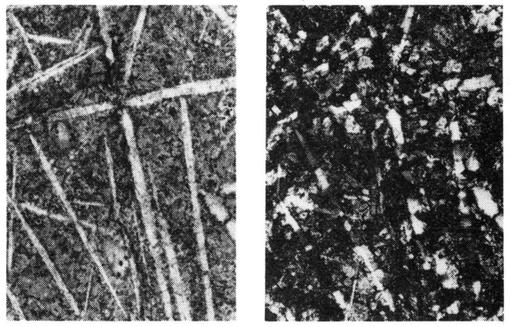

2

Photo 1 Clinopyroxene phenocrysts, which are zonally altered, due to the original zoned nature of the phenocrysts. Premier Mine Felsite, transmittened light, x 25.

Photo 2 Quartz needles, pseudomorphous after trydimite. Premier Mine Felsite. (A. Transmittened light, B. The quartz in the needles showing a random orientation, crossed nicols), x 15.

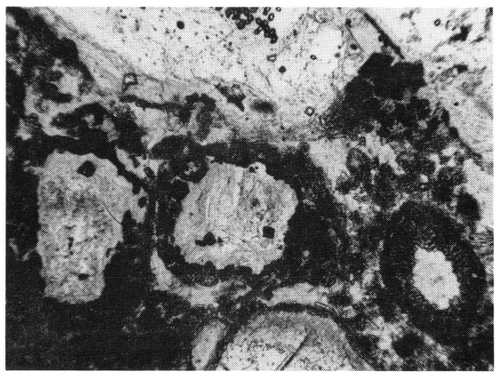

3

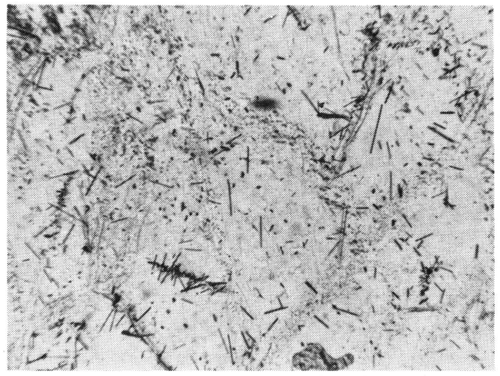

4

Photo 3 Rims of sphene and magnetite surrounding the altered first generation olivine. Section 1010-8, Premier Mine, Kimberlite transmittened light, x 15.

Photo 4 Needles of rutile in the serpentine pseudomorphous after first-generation olivine. Section 1310-10, Premier Mine, Kimberlite transmittened light, x 500.

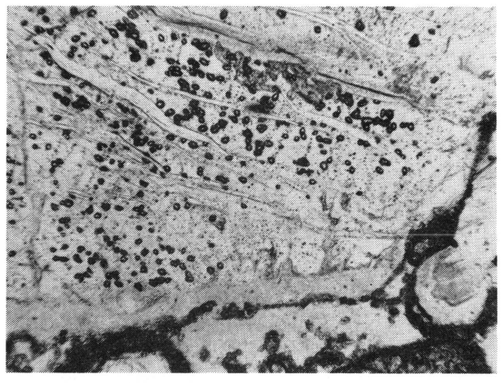

5

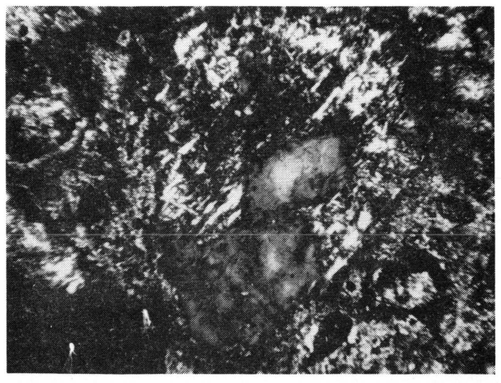

6

Photo 5 Small inclusions of sphene in altered first-generation olivine. Premier Mine Kimberlite, section 1010-42, transmittened light, x 500.

Photo 6 Fibrous tremolite forming in the serpentine pseudomorphous after olivine. Premier Mine Kimberlite, section 1310-8, crossed nicols, x 25.

APPENDIX 1 - The physical properties and the composition of garnets from garnet peridotite nodules in kimberlite

A. Present investigation

Locality & Sample No.	a_o Å ± 0.003	n ± 0.003	A	G	P
Kimberley Mine Ki 1.	11.534	1.750	29	13	58
Premier Mine P.M. 893 In 15	11.522	1.751	30	11	59
P.M. 893 In 17	11.553	1.762	39	16	45
P.M. 893 In 19	11.532	1.756	25	12	53
P.M. 893 In 11	11.519	1.754	32	10	58
P.M. 1010 In 7	11.511	1.750	30	8	62
P.M. 1010 In 10	11.524	1.748	26	12	62
P.M. 893 In 16	11.558	1.758	34	19	47
P.M. 893 In 16	11.557	1.755	32	19	49
P.M. 893 In 16	11.557	1.757	34	18	48
P.M. 893 In 1	11.542	1.759	35	15	50
" " "	11.539	1.755	33	14	53
P.M. 893 In 22	11.532	1.748	27	13	60
P.M. 893 In 23	11.537	1.750	29	15	56
P.M. 893 In 2	11.549	1.754	32	18	50
	11.550	1.755	32	18	50
P.M. 893 In 8	11.541	1.754	32	17	51
	11.540	1.752	30	17	53
P.M. 893 In 7	11.555	1.756	32	19	49
	11.542	1.752	30	16	54
P.M. 893 In 6	11.565	1.742	22	22	56
	11.563	1.741	20	22	58
P.M. 893 In 5	11.477	1.737	18	13	69
P.M. 893 In 4	11.528	1.740	20	13	67
	11.524	1.741	22	12	66
	11.524	1.740	22	12	66
P. M. 893 In 21	11.524	1.750	29	12	61
P. M. 1010 In 4	-	1.736	-	-	-
	-	1.737	-	-	-

Locality & Sample No.		a_o Å ± 0.003	n ± 0.003	A	G	P
Jagersfontein Mine	Jagersfontein 6	11.527	1.752	30	12	58
	" 5	11.533	1.751	29	14	57
	" 4	11.554	1.757	34	18	48
	" 3	11.516	1.747	26	10	64
Bultfontein Mine	Bultfontein 6	11.525	1.751	30	12	58
	" 7	11.517	1.748	28	10	62
	" 8	11.527	1.746	26	12	62
	" 1	(11.518	1.745	25	10	65
		(11.528	1.746	26	12	62
		(11.527	1.747	27	12	61
	Frank Smith 3	11.521	1.742	22	12	66
	" " 4	11.510	1.758	37	7	56
	" " 2	(	1.756	-	-	-
		(	1.755	-	-	-
		(	1.752	-	-	-
	Hololo Kimberlite	11.537	-	-	-	-
B. Values obtained from the literature						
Wesselton Mine +1		11.561	1.761	39	20	41
		11.558	1.754	32	20	48
		11.552	1.750	28	20	52
		11.528	1.746	26	13	61
		11.550	1.750	28	18	54
		11.555	1.756	33	19	68
		11.538	1.755	33	14	53
		11.544	1.747	26	18	56
		11.541	1.745	24	18	58
		11.554	1.752	29	20	51
		11.531	1.744	24	15	61
		11.540	1.747	27	17	56
		(11.507	1.737	19	9	72
		(11.513	1.741	24	10	66

Locality & Sample No.	a_o Å ± 0.003	n ± 0.003	A	G	P
Bultfontein Mine +1	11.522	1.741	22	13	65
	11.544	1.748	28	17	55
	11.543	1.748	27	17	56
	11.527	1.744	24	13	63
	11.541	1.748	27	17	56
	11.542	1.749	28	18	54
	11.545	1.748	27	17	56
	11.548	1.752	30	18	52
	11.531	1.748	27	14	59
	11.539	1.748	26	16	58
	11.553	1.752	30	19	51
	11.530	1.744	24	14	62
	11.545	1.748	26	1	73
	11.537	1.746	26	14	60
	11.556	1.755	32	19	39
	11.536	1.748	18	2	80
	11.533	1.744	24	15	61
	11.540	1.748	27	16	57
	11.555	1.753	31	20	49
	11.550	1.751	29	18	57
	11.572	1.765	41	22	37
	11.543	1.750	30	16	54
Russian kimberlites +2	-	1.754	-	-	-
	-	1.762	-	-	-
	-	1.737	-	-	-
	-	1.738	-	-	-
	-	1.754	-	-	-
	-	1.737	-	-	-
	-	1.738	-	-	-
	-	1.754	-	-	-

Locality & Sample No.	a_o Å ± 0.003	n ± 0.003	A	G	P
Jagersfontein Mine +1	11.590	1.773	47	26	27
	11.538	1.768	45	12	43
	11.555	1.755	33	19	48
	11.544	1.749	28	18	54
	11.577	1.763	38	22	40
	11.543	1.750	28	16	56
	11.544	1.747	26	17	57
	11.530	1.744	24	14	62
	11.547	1.755	33	17	50
	11.532	1.745	42	12	46
Frank Smith +1	11.553	1.755	32	18	50
	11.551	1.753	32	18	50
	11.549	1.752	30	18	52
	11.541	1.749	28	17	55
	11.533	1.743	24	15	61
	11.550	1.753	32	18	50
Roberts Victor +1	11.550	1.749	27	19	54
	11.539	1.747	27	15	58
Dutoitspan +1	11.550	1.749	28	19	53
	11.539	1.749	28	16	56
	11.534	1.747	26	15	59
	11.549	1.751	29	17	54
De Beers Mine +1	11.546	1.750	28	18	54
	11.576	1.768	43	22	35
	11.536	1.744	42	12	46
	11.547	1.747	26	17	57
	11.541	1.745	25	18	57
	11.558	1.755	33	20	47
	11.546	1.749	27	18	55
	11.537	1.745	25	15	60
Kimberley +1	11.542	1.746	25	17	58

Locality & Sample No.	a_o Å ± 0.003	n ± 0.003	A	G	P
Kamfersdam +1	11.540	1.749	28	16	56
	11.555	1.754	33	19	48
	11.550	1.749	28	19	53
	11.543	1.749	28	18	54
	11.546	1.749	28	18	54
	11.546	1.749	28	18	54
	11.549	1.752	30	18	52
+1 Monastry	11.542	1.749	28	18	54
+1 Koffiefontein	11.547	1.754	32	17	51
+1 Excelsior	11.537	1.747	27	15	58
Matsoku Kimberlite	11.564	1.756	33	18	49
	11.549	1.750	28	16	56
	11.549	1.751	29	16	55
	11.540	1.747	25	16	59
	11.545	1.750	29	11	60
	11.544	1.747	26	14	60
	11.542	1.747	25	15	60
	11.552	1.749	27	20	53
	11.548	1.748	26	16	58
	11.541	1.746	25	15	60
	11.537	1.747	26	13	61
	11.541	1.749	28	14	58
	11.548	1.750	27	18	55
	11.540	1.746	24	16	60
	11.540	1.747	25	16	59
	11.556	1.756	32	20	48
	11.541	1.750	28	15	57
	11.538	1.747	27	12	61
	11.536	1.744	23	14	63
	11.535	1.752	30	15	55
	11.524	1.746	26	12	62

Locality & Sample No.	ao Å ± 0.003	n ± 0.003	A	G	P
Matsoku Kimberlite	11.541	1.753	30	15	55
	11.538	1.748	28	14	58
	11.542	1.751	29	13	58
	11.535	1.750	28	13	59
	11.568	1.758	35	23	42
	11.540	1.750	28	15	57
	11.528	1.746	26	12	62
	11.553	1.753	29	20	51
	11.555	1.753	29	20	51
	11.553	1.752	29	20	51
	11.557	1.764	39	21	40

C. Garnets from Various Localities

Locality & Sample No.	ao Å ± 0.003	n ± 0.003	D	A	G	P
+4 Peridotite Kaalvalei	11.545	1.753		32	17	51
" " Kao	11.548	1.749	3.692	27	18	55
" " Malibe Matso	11.546	1.748	3.681	28	18	54
" " Thaba Putsoa	11.537	1.747	3.680	26	15	59
" " " "	11.538	1.749	3.679	28	15	57
" " " "	11.553	1.749	-	28	20	52
" " Sekhameng	11.565	1.758	3.715	35	22	43
" " Lauwrencia	11.528	1.743	3.712	25	13	62
" " Dutoitspan	11.531	1.746	-	23	15	62
" " USSR	11.522	1.738	-	18	13	69
" " "	11.485	1.732	-	15	5	80
" " Lesotho	-	1.742-46	-	-	-	-
+5 A_3 Garnet Lherzolite	11.534	1.744		24	15	61
A_4 " Harzburgite	11.559	1.756		34	19	47
A_6 " "	11.524	1.737		18	13	69
A_2 " Peridotite	11.537	1.735		15	18	67
A_5 " Harzburgite	11.567	1.759		36	21	43
A_g " "	-	1.763	-	-	-	-
A_{17} " Websterite	-	1.745		-	-	-

D. Garnets from Regional Peridotites from Norway

Locality & Sample No.	a_o Å ± 0.003	n ± 0.003	D	A	G	P
+5						
N_{23} Garnet peridotites	11.532	1.753		32	13	55
N_{26} " "	11.532	1.747		27	13	60
N_{69} " "	11.534	1.742		22	16	62
N_{70} " "	11.530	1.749		28	13	59
N_{71} " "	11.528	1.746		26	13	61
N_{67} " "	-	1.741		-	-	-
N_{68} " "	-	1.752		-	-	-
N_{75} " "	-	1.752		-	-	-
N_{76} " "	-	1.740		-	-	-
N_{77} " "	-	1.744		-	-	-
Garnet "	-	1.758		-	-	-

****

Appendix 1:

The physical properties and the composition of garnets from garnet peridotite nodules in kimberlite.

A : percentage almandine.

G : percentage grossular.

P : percentage pyrope.

+1. After Rickwood et al., (1968).

+2. After Bobrievich et al., (1959).

+3. After Mathias & Rickwood, (1969).

+4. After Nixon et al., (1963).

+5. After O'Hara & Mercy, (1963).

A. PRESENT INVESTIGATION

Locality & Sample No.	a_o (Å) ± 0.003	n ± 0.003	A	G	P
P. M. Ti 100	11.522	1.752	31	10	59
P. M. Ti 101	11.529	1.749	28	12	60
P. M. Ti 102	11.515	1.752	32	8	60
P. M. Ti 103	11.518	1.750	29	10	61
P. M. Ti 105	11.524	1.751	30	12	58
P. M. Ti 106	-	1.750	-	-	-
P. M. Ti 107	11.521	1.746	26	11	63
P. M. Ti 108	11.516	1.750	30	9	61
P. M. Ti 109	11.521	1.756	35	10	55
P. M. Ti 110	11.533	1.752	30	14	56
P. M. Ti 50	11.533	1.752	30	14	56
P. M. Ti 52	11.525	1.749	28	12	60
P. M. C. F. 302	11.521	1.751	30	11	59
P. M. A. C. 1	11.522	1.751	31	11	58
P. M. 1060 - 43	11.537	1.745	24	15	61
P. M. 1060 - 26	11.545	1.758	36	26	38
P. M. 1060 - 29	11.533	1.750	28	13	59
P. M. 1060 - 22	11.583	1.749	26	28	46
P. M. Concentrate	11.522	-	-	-	-
Riverton 1	11.524	1.747	27	12	61
" 2	11.524	1.750	29	12	59
" 3	11.523	1.753	32	11	57
" 4	11.528	1.749	28	12	60
" 5	11.515	1.748	28	9	63
" 6	11.515	1.747	27	9	64
" 7	11.522	1.748	28	12	60
" 8	11.518	1.749	28	10	62
" 9	11.520	1.749	28	11	61
" 25	11.521	1.748	27	11	62
" 26	11.520	-	-	-	-

APPENDIX 2 - (Continued)

Locality & Sample No.		a_o (Å) ± 0.003	n ± 0.003	A	G	P
Bellsbank	1	11.520	-	-	-	-
"	6	11.508	1.755	35	6	59
"	7	11.516	1.747	27	10	63
"	8	11.505	1.753	32	6	62
"	9	11.496	1.738	20	6	74
"	10	11.531	1.750	29	12	59
"	18	11.511	1.750	30	8	62
"	19	11.507	1.742	24	9	67
"	20	11.540	1.753	32	16	52
"	21	11.503	1.758	37	5	58
"	22	11.607	1.761	36	32	32
"	23	11.512	1.751	31	8	61
"	24	11.549	1.769	25	31	44
"	Concentrate	11.578	-	-	-	-
"	25	11.556	1.768	37	18	45
Frank Smith	4	11.535	1.751	30	14	56
"	5	11.519	1.752	29	6	65
"	6	11.517	1.748	28	9	63
"	1	11.522	1.750	30	9	61
"	2	11.523	1.750	30	9	61
"	3	11.513	1.749	29	9	62
"	7	11.525	1.747	27	12	61
"	8	11.532	1.750	29	13	58
"	9	11.520	1.754	33	10	57
"	10	11.519	1.746	26	10	64
"	12	11.517	1.748	28	10	62
"	13	11.512	1.750	30	9	61
Jagersfontein	10	11.505	1.752	32	7	61
"	11	11.231	1.746	26	14	60
De Beers	7	11.510	1.753	33	7	60
"	8	11.502	1.752	32	5	63
"	9	11.493	1.746	27	3	70
"	10	11.499	1.750	30	4	66

APPENDIX 2 (Continued)

Locality & Sample No.		a_o (Å) ± 0.003	n ± 0.003	A	G	P
Kamfersdam	15	11.497	1.734	16	7	77
"	16	11.508	1.747	28	8	64
"	18	11.515	1.748	28	10	62
"	19	11.512	1.741	22	10	68
"	17	11.518	1.751	31	9	60
"	20	11.522	1.755	34	10	56
Finch	1	11.505	1.738	20	9	71
Lovedale	1	11.528	1.747	27	13	60
Brakfontein	1	11.527	-	-	-	-
Carmel	R.4	11.529	1.764	42	10	48
"	R.6	11.521	1.750	29	10	61
"	R.7	11.512	1.753	33	8	59
"	V.6	11.533	1.753	32	13	55
"	V.7.	11.518	1.747	27	10	63
Hololo		11.552	-	-	-	-
Ngopetso		11.521	-	-	-	-
Kolo. 2.		11.515	-	-	-	-

B. Values obtained from the literature

Locality & Sample No.	a_o (Å) ± 0.003	n ± 0.003	D	A	G	P
+1 Russian Kimberlites	-	1.741	-	-	-	-
	-	1.750	-	-	-	-
	-	-	3.748	-	-	-
	-	-	3.737	-	-	-
	-	1.783-1.790	-	-	-	-
	-	1.790-1.802	-	-	-	-
	-	1.795-1.802	-	-	-	-
	-	1.795	-	-	-	-
	11.551	1.785	-	58	12	30

Locality & Sample No.	a_o (Å) ± 0.003	n ± 0.003	D	A	G	P
[+1] Russian Kimberlites	-	1.781	-	-	-	-
	11.496	1.725	-	8	8	84
	11.530	1.767	-	43	10	47
	11.456	1.734	-	18	0	82
	-	1.741	-	-	-	-
	11.535	1.747	-	26	15	59
	11.571	1.754	-	32	22	46
	11.580	1.762	-	38	24	38
	11.532	1.764	-	42	12	46
	11.588	1.767	-	42	25	33
	-	1.770	-	-	-	-
	-	1.741-1.754	-	-	-	-
	-	1.737-1.762	-	-	-	-
	-	1.740-1.754	-	-	-	-
	-	1.754	-	-	-	-
	-	1.748	-	-	-	-
	-	1.754	-	-	-	-
	-	1.740	-	-	-	-
[+2] Zarnitsa Kimberlite	11.510	1.749	3.68	29	8	63
" " 2	11.534	1.754	3.75	32	14	54
" " 3	11.522	1.759	3.72	37	10	53
" " 4	11.509	1.744	3.73	25	8	67
" " 5	11.527	1.749	3.65	28	15	57
" " 6	11.532	1.754	3.77	33	14	53
" " 7	11.516	1.754	3.74	33	9	58
" " 8	11.511	1.744	3.76	24	10	66
[+3] Russian Kimberlites	11.513	1.736	3.72	18	11	71
	11.513	1.736	3.72	18	11	71
	-	1.737-46	3.68	-	-	-
	-	1.737-46	3.68	-	-	-
	11.510	1.757-70	3.85	37	8	55
	11.510	1.757-70	3.85	37	8	55
[+4] Mir	11.542	1.767	-	43	13	44

Locality & Sample No.	a_o (Å) ± 0.003	n ± 0.003	D	A	G	P
+5 Thaba Putsoa	11.531	1.750	3.696	29	13	58
" Solane	11.535	1.751	3.726	30	14	56
" Liqhobong	11.535	1.750	3.711	30	14	56
" Kao	11.537	1.756	3.762	34	14	52
" Kimberley	11.528	1.748	-	28	12	60
Kao Concentrate	11.509	1.732	-	14	10	76
" "	11.525	1.734	-	15	13	72
" "	11.511	1.735	-	17	10	73
Kao Kimberlite	11.528	1.746	3.690	25	13	62
" "	11.528	1.738	-	19	14	67
" "	11.590	1.767	-	42	28	30
" "	11.659	1.799-1.807	3.756	-	-	-
" "	-	1.758	3.770	-	-	-
+6 Chechoslovak Kimb.	-	1.740-8	-	-	-	-
" "	-	1.748-52	-	-	-	-
" "	-	1.752-60	-	-	-	-
" "	-	1.760-8	-	-	-	-
-7 Belgium Congo	-	1.746-50	-	-	-	-
" "	-	1.735-40	-	-	-	-
+8 Lesotho Average	-	1.740-46	-	-	-	-

APPENDIX 2 - (Continued)

Locality & Sample No	ao (Å) ± 0.003	n ± 0.003	A	G	P
+ 9 Kimberley Region:					
Kimberley Pool	11.518	1.750	29	11	60
Olifants Kop	11.520	1.746	25	13	62
" "	11.529	1.742	22	13	65
Frank Smith	11.537	1.753	32	12	56
Bellsbank	11.532	1.757	33	12	55
Jagersfontein	11.532	1.747	25	13	62
Kamfersdam	11.534	1.747	25	13	62
"	11.522	1.738	18	13	69
Klipfontein	11.536	1.744	23	16	61
S. W. A.:					
Berseba Reserve	11.533	1.751	30	12	58
"	11.528	1.749	28	12	60
Lichtenfels	11.539	1.748	28	12	60
"	11.557	1.750	27	20	53
"	11.542	1.746	24	17	59
"	11.524	1.742	22	10	68
Colossus	11.544	1.755	33	15	52
Banonkero	11.546	1.763	40	12	48
Yengima	11.541	1.752	30	12	58
Mwadui	11.539	1.749	28	12	60
Mamungo	11.539	1.752	31	11	58
"	11.540	1.744	23	15	62
Mpuru	11.603	1.768	43	25	32
"	11.567	1.764	40	18	42
"	11.641	1.764	35	35	30
Itagata	11.554	1.761	37	18	45
"	11.545	1.754	32	15	53
"	11.542	1.751	29	15	56
"	11.542	1.748	28	14	58
Tambola	11.602	1.767	43	25	32
"	11.562	1.742	19	22	59
"	11.556	1.758	35	18	47

APPENDIX 2 - (Concluded)

Locality & Sample No	ao (Å) ± 0.003	n ± 0.003	A	G	P
Kimbelekise	11.545	1.752	30	15	55
"	11.515	1.738	19	9	72
Mingui	11.532	1.755	33	20	57
Gonambogo	11.535	1.753	31	11	58
Magoba	11.542	1.745	25	13	62
Daraja	11.541	1.747	26	14	60
"	11.516	1.745	23	9	68
Kitura	11.541	1.751	29	15	56
Mayaha	11.538	1.754	32	11	57
Mvelevele	11.548	1.752	29	16	55
"	11.537	1.748	27	13	60
Makilawa	11.537	1.746	25	13	62
Munu	11.533	1.749	29	11	60
Kolongo	11.533	1.743	21	13	66
"	11.531	1.745	25	11	64

****

Appendix 2:

The physical properties and the composition of garnet in kimberlite.

A : percentage almandine.

G : percentage grossular.

P : percentage pyrope.

+1. After Bobrievich et al., (1959).

+2. After Smirnov (1960).

+3. After Milashev (1965).

+4. After Min. abst., (1961-2, p. 289).

+5. After Nixon et al., (1963).

+6. After Kopecky (1963).

+7. After Verhoogen (1938).

+8. After Dawson (1962).

+9. After Gratton-Bellow (1966, p. 26) I.M.A. (Volume).

APPENDIX 3 - The physical properties and the Composition of garnets from Eclogite

Locality & Sample No.	a_o(Å) ± 0.003	n ± 0.003	D	A	G	P
1. Kyanite eclogite *1)						
Russia Z60	11.613	1.758		23	33	44
Z15	11.631	1.751		25	39	36
Z52	11.653	1.742		17	45	38
Z24	11.647	1.759		32	41	27
Z48	11.672	1.751		23	52	25
Z49	11.683	1.745		18	53	29
Roberts Victor RV_{15}	11.650	1.751		25	43	44
Bellsbank *2)	11.652	1.750		23	44	33
Roberts Victor	11.524	1.743		23	12	65
	11.691	1.755		28	52	20
	11.605	1.751		26	32	42
	11.647	1.758		32	40	28
	11.562	1.746		25	22	53
	11.669	1.757		28	49	23
2. Grospydite *1)						
Russia 1.	11.717	1.745		16	62	22
Z6	11.737	1.745		15	67	18
Z8	11.737	1.741		12	67	21
Z34	11.751	1.742		12	72	16
Z38	11.767	1.743		12	74	14
Z28	11.777	1.739		8	78	14
Z33	11.790	1.740		7	88	5
Z63	11.683	1.757		28	53	19
Z3	11.696	1.741		13	58	29
Z43	11.709	1.741		13	60	27
Z37	11.724	1.746		17	64	19
Roberts Victor *4)	11.680	1.751		23	52	25
Kao Eclogite *5)	11.585	1.761	3.835	37	27	36
Kao "	11.565	1.768	3.898	43	20	37
" "	11.539	1.784	3.995	59	10	31
Qaqa "	11.521	1.796	4.076	-	-	-

2/.....

APPENDIX 3 (Continued)

Locality & Sample No.	a_o (Å) ± 0.003	n ± 0.003	D	A	G	P
Collossus Eclogite *6)	-	-	3.64	-	-	-
" "	-	-	3.75	-	-	-
" "	-	-	3.72	-	-	-
Chechoslovakia " *7)	-	1.748	3.720	-	-	-
" "	-	1.746	3.705	-	-	-
" "	-	1.747	3.704	-	-	-
" "	-	1.748	3.698	-	-	-
" "	-	1.765	3.720	-	-	-
" "	-	1.748	3.718	-	-	-
" "	-	1.744	3.704	-	-	-
" "	-	1.740	3.688	-	-	-
U.S.S.R. " *8)	11.663	1.745	2.74	21	45	74
" "	11.841	1.753	3.627	-	-	-
" "	11.516	1.754	3.74	34	8	58
" "	-	1.741	-	-	-	-
" "	-	1.725	-	-	-	-
" "	-	1.734	-	-	-	-
" "	-	1.765	-	-	-	-
" "	-	1.765	-	-	-	-
Mitchemanskraal *2)	11.524	1.744	-	26	12	62
	11.523	1.741		22	13	65
Goedgevonden	11.581	1.745		22	28	50
Crown Lace	11.627	1.741		17	40	43
Wilsons (Tanzania)	11.614	1.768		41	32	27
	11.623	1.745		21	38	41
	11.597	1.752		27	31	42
	11.626	1.766		39	34	27
Roberts Victor	11.565	1.751		28	22	50
	11.539	1.764		42	12	46
	11.528	1.757		36	12	52
	11.516	1.738		19	11	70
	11.552	1.772		48	25	27
	11.543	1.755		32	16	52

3/.....

Locality & Sample No.	a_o (Å) ± 0.003	n ± 0.003	D	A	G	P
Roberts Victor	11.545	1.763		40	26	36
	11.501	1.742		23	7	70
	11.669	1.759		32	45	23
	11.677	1.757		37	48	15
	11.598	1.767		42	28	30
	11.585	1.746		23	27	50
	11.541	1.761		38	15	47
	11.531	1.763		40	12	48
	11.544	1.756		33	17	50
	11.532	1.762		39	12	49
	11.528	1.762		40	10	50
	11.531	1.757		35	12	53
	11.619	1.759		33	33	34
	11.614	1.761		35	32	33
	11.545	1.767		43	15	42
	11.516	1.736		17	12	71
	11.547	1.771		48	12	40
	11.538	1.753		32	15	53
	11.531	1.750		28	13	59
	11.534	1.754		32	12	56
	11.536	1.760		37	14	49
	11.607	1.763		35	32	33
	11.551	1.759		35	18	47
	11.537	1.752		30	15	55
	11.519	1.741		21	9	70
	11.553	1.746		23	20	57
	11.610	1.767		40	32	28
Jagersfontein	11.523	1.746		26	12	62
	11.596	1.747		24	31	45
	11.601	1.743		19	33	48
	11.553	1.754		32	18	50
	11.523	1.756		35	12	53
	11.526	1.750		29	12	59

4/.....

Locality & Sample No.	a_o (Å) ± 0.003	n ± 0.003	D	A	G	P
Frank Smith	11.523	1.745		26	12	62
	11.528	1.758		36	12	52
Excelsior	11.517	1.735		17	12	71
Bellsbank	11.508	1.742		23	12	65
New Zeeland *9)	11.531	1.748		28	12	60
	11.536	1.741		21	16	43
	11.545	1.770		48	12	40
U.S.A. *10)	11.556	1.797	-	70	12	18
	11.551	1.794	-	68	12	20
	11.551	1.794	-	68	12	20
4. Corundum eclogites						
Roberts Victor *2)	11.625	1.748		24	36	40
	11.637	1.744		18	41	41
	11.720	1.745		16	65	19
Jagersfontein	11.611	1.735		12	36	52
Regional eclogites *11)	11.580	1.777		45	23	32
	11.604	1.790		62	27	11
	11.585	1.760		35	26	39
	11.608	1.789		62	27	11
	11.561	1.749		27	19	54
	11.612	1.796		66	28	6
	11.594	1.786		58	25	17
	11.571	1.769		44	22	34
	11.591	1.773		47	27	26
	11.557	1.764		42	18	40
	11.575	1.767		42	22	36
	11.577	1.793		66	19	15
	11.561	1.748		26	21	53
	11.531	1.760		38	12	50
	11.572	1.757		33	24	43

5/.....

B. Present Investigation

Locality & Sample No.	a_o(Å) ± 0.003	n ± 0.003	D	A	G	P
"Eclogite" B_2B-1	11.544	1.752		30	16	54
B_2B-2	11.551	1.755		33	18	49
" Jag. 1	11.621	1.754		28	36	76
" (C.F. 300) RV 4	11.529	1.761		39	11	50
" RV6	-	1.755				
" RV5	11.565	1.756		33	22	45
" RV2	11.510	1.759		38	7	55
" RV1	11.527	1.757		36	12	52
"	11.527	1.752		31	12	57
"	11.526	1.755		36	12	52
Kyanite Eclogite F.1	11.506	1.750		30	5	65
" " F.2	11.579	1.751		28	27	45
" " F.3	11.649	1.752		26	42	32

****

Appendix 3:

The physical proportions and the composition of garnets from eclogite.

A percentage almandine

G percentage grossular

P percentage pyrope

*1 Sobolev, (1968).

*2 Rickwood et al., (1968).

*4 O'Hara, (1967).

*5 Nixon et al., (1963).

*6 Hall, (1928).

*7 Kopecky, (1960).

*8 Bobrievich et al., (1959).

*9 Dicky, (1968).

*10 Watson and Morton, (1968).

*11 Hahn Weinheimer et al., (1963).

APPENDIX 4 - THE CHEMICAL ANALYSES AND THE MOLECULAR NORMS OF THE VARIOUS PARENTAGES OF GARNET

A. Chemical analyses

	1	2	3	4	5	6	7	8	9	10	11	12	13	14	15	16	17
SiO_2	40.47	40.89	40.90	41.34	42.83	41.20	41.93	41.20	41.70	38.80	41.98	43.26	41.84	42.73	43.49	42.16	39.43
Al_2O_3	21.56	21.84	22.81	22.75	22.30	21.75	19.20	19.24	20.42	21.00	18.91	19.72	21.55	19.83	21.53	22.61	21.28
Fe_2O_3	3.83	1.87	-	-	1.03	2.21	3.00	3.22	1.42	2.25	0.62	2.24	1.80	0.81	0.80	0.70	2.08
FeO	7.84	9.06	13.34	12.12	6.72	9.31	8.08	7.40	7.27	5.70	7.18	5.61	12.30	7.01	6.38	6.63	20.40
MnO	0.27	0.30	0.38	0.36	-	-	0.33	0.22	0.21	0.44	0.24	0.20	0.31	0.33	0.36	0.39	0.42
MgO	19.92	19.17	16.43	16.20	21.30	19.32	20.03	18.70	20.86	20.60	20.98	20.27	15.88	21.54	19.28	19.49	11.33
CaO	5.09	4.93	4.70	5.17	4.06	4.74	4.93	6.84	5.94	6.72	5.21	4.73	5.99	4.69	4.87	5.26	5.13
Na_2O	N. D.	N. D.	N. D.	N. D.	-	-	-	-	-	-	-	-	-	-	0.10	-	-
K_2O	"	"	"	"	-	-	-	-	-	-	-	-	-	-	0.26	-	-
TiO_2	-	-	-	-	0.40	0.60	1.04	0.76	0.45	0.38	0.32	0.50	0.27	0.27	0.31	0.23	0.23
Cr_2O_3	1.15	1.79	1.48	2.96	0.70	0.33	0.65	1.56	1.91	3.82	4.02	2.70	0.07	2.92	2.34	2.53	0.06
H_2O							-	-	-	-							0.11
Other NiO					0.95	1.00	1.23	1.12	1.19	0.66	1.00	1.16					tr
Total	100.13	99.85	100.94	100.90	100.39	100.56	100.42	100.25	100.38	100.37	100.46	100.39	100.01	100.13	99.72	100.00	100.47
B. Molecular norms																	
Oxides *1)	-	-	-	4.9	-	-	-	-	-	-	-	3.4			5.1	3.4	-
Pyrope	70.5	68.6	59.8	58.9	57.8	71.8	71.4	67.5	71.3	71.7	72.7	73.2	58.3	74.4	68.8	69.1	42.6
Uvarovite	3.2	5.2	4.4	8.5	1.5	0.9	1.8	4.5	5.1	10.4	10.9	7.4	0.3	7.8	6.6	7.0	0.3
Andradite	10.1	5.2	-	-	2.8	6.8	8.0	8.5	3.7	6.2	1.7	4.5	5.2	2.1	2.2	2.0	5.8
Grossular	-	2.3	7.9	2.3	6.6	5.6	2.5	4.3	5.7	-	0.3	1.8 *2)	10.3	1.6	3.8	4.3	7.6
Almandine	16.2	18.7	27.9	25.4	13.3	14.9	16.3	15.2	14.2	11.7	14.4	9.7	25.9	14.1	13.5	14.2	43.7
Total	100.0	100.00	100.00	100.00	100.00	100.00	100.00	100.00	100.00	100.00	100.00	100.00	100.00	100.00	100.00	100.00	100.00

APPENDIX 4 - (Continued)

	18	19	20	21	22	23	24	25	26	27	28	29	30	31	32	33	34
SiO_2	46.16	41.34	40.90	40.89	40.47	39.43	38.98	42.25	42.13	40.29	40.79	40.60	39.46	42.86	42.04	39.00	40.58
Al_2O_3	20.17	22.75	22.81	21.84	21.56	22.00	21.52	21.10	20.56	20.97	12.81	24.95	21.94	23.00	21.84	22.74	21.86
Fe_2O_3	nd	0.00	-	1.87	3.83	1.50	0.91	1.00	1.70	2.75	4.35	1.44	1.92	-	1.92	4.76	3.40
FeO	8.17	12.12	13.34	9.06	7.84	27.00	28.68	6.86	8.10	7.02	7.39	8.06	6.91	7.71	7.47	9.40	4.86
MnO	0.18	0.36	-	0.30	0.27	0.78	1.80	0.37	0.32	0.43	-	0.17	0.09	0.30	0.24	0.31	1.27
MgO	20.30	16.20	16.43	19.17	19.92	7.95	3.99	20.19	19.95	20.97	17.89	20.44	20.44	20.15	20.51	14.04	18.72
CaO	4.90	5.17	4.70	4.93	5.09	1.70	3.57	5.05	5.30	4.60	5.46	0.42	5.18	5.20	4.37	6.44	4.62
Na_2O			0.38													0.31	
K_2O																1.42	
TiO_2	0.15							0.26	0.89				0.51	0.27	0.92	0.90	
Cr_2O_3	0.38	2.96	1.48	1.79	1.15	-	-	2.71	1.23	2.84	1.03		1.37	0.30	0.43		2.61
H_2O												0.90	1.53		0.17		
Other	0.10											0.08	0.29				
NiO																	0.14
Total	100.51	100.90	100.04	99.85	100.13	100.35	99.45	99.76	99.76	100.20	99.72	100.84	99.64	99.81	99.96	99.32	100.06
Oxides *1)	3.2					3.6	5.7	-	-			2.8				7.9	6.7
Pyrope	68.4	60.2	60.2	69.0	71.5	32.7	16.0	72.5	70.4	73.9	69.0	78.3	73.0	71.2	73.3	53.5	68.6
Uvarovite	1.1	8.6	4.4	5.3	-	-		7.8	3.4	8.1	3.0	-	3.7	0.8	1.3		7.5
Andradite				5.3	10.1	4.3	2.7	2.6	4.4	3.5	12.0	1.4	5.1	-	5.3	13.6	4.6
Grossular	10.9	5.2	7.9	2.3	2.6	0.5	7.4	2.6	5.4	4.2 *2	16.0 *2	3.2 *2	4.3	12.3	4.4	3.8	5.0 *2
Almandine	16.4	26.0	27.4	18.1	15.8	58.9	68.2	14.5	16.4	10.3		14.3	13.9	15.7	15.7	21.2	7.6
Total	100.0	100.0	100.0	100.0	100.0	100.0	100.0	100.0	100.0	100.0	100.0	100.0	100.0	100.0	100.0	100.0	100.0

	35	36	37	38	39	40	41	42	43	44	45	46	47	48	49	50
SiO_2	40.62	42.40	41.52	43.26	42.32	39.94	40.27	40.23	40.47	41.04	40.98	40.92	40.31	40.40	41.34	40.21
Al_2O_3	23.65	22.56	21.68	20.17	18.87	22.87	22.32	22.34	22.70	22.69	23.01	21.97	21.67	21.47	22.45	22.51
Fe_2O_3	1.57	1.46	2.35	2.36	1.38	0.49	0.98	2.44	4.66	0.61	0.70	1.10	1.22	1.68	1.09	1.57
FeO	15.26	14.43	6.44	6.05	6.79	19.09	11.08	11.43	10.37	12.64	13.23	15.02	17.66	16.57	13.01	17.01
MnO	0.46	0.43	0.50	0.44	0.29	0.81	0.14	0.21	0.33	0.24	0.43	0.45	0.58	0.99	0.54	0.32
MgO	13.47	13.64	18.92	19.04	19.93	12.60	7.40	7.25	14.88	14.58	15.50	15.33	14.02	14.56	17.54	11.67
CaO	4.49	4.15	5.65	5.00	5.65	4.55	17.24	15.95	6.34	7.77	5.63	5.01	3.91	3.64	3.39	6.58
Na_2O		0.10		0.26			nd	nd	nd							
K_2O		0.36		0.45			"	"	"							
TiO_2	0.17	0.16	0.04	0.22	0.80	0.11	0.51	0.35	0.15	0.38	0.35	0.47	0.57	0.46	0.42	-
Cr_2O_3	0.31	0.29	2.90	2.56	3.67		0.06	0.03	0.04	0.07	0.12	0.10	0.12	0.24	0.24	-
H_2O						0.04										
Other																-
NiO							0.005									
Total	100.00	100.01	100.00	99.81	99.70	100.50	100.00	100.13	99.94	100.02	99.95	100.31	100.06	100.01	100.02	99.87
Oxides *1)	6.2	7.8	4.1	5.2	4.0		2.4	5.9	6.7	-	-	-	-	-	-	2.9
Pyrope	49.4	50.3	67.4	68.7	66.0	46.7	29.5	27.1	54.1	53.9	57.0	55.7	51.7	53.8	63.6	43.2
Uvarovite	0.9	0.7	8.2	7.4	10.4	0.0	0.3	-	0.3	0.2	0.2	0.3	0.2	0.7	0.6	-
Andradite	4.4	4.4.	6.5	5.5	3.9	1.3	2.6	6.6	1.9	1.8	2.0	3.0	3.5	4.8	3.1	4.5
Grossular	6.6	5.9		0.9 *2)	0.3	10.7	40.5	36.1	5.3	18.6	12.7	9.5	6.8	4.2	5.1	13.2
Almandine	32.5	30.9	13.8	12.3	14.4	41.3	24.7	24.3	21.7	25.5	28.1	31.5	37.8	36.5	27.6	36.2
Total	100.0	100.0	100.0	100.0	100.0	100.0	100.0	100.0	100.0	100.0	100.0	100.0	100.0	100.0	100.0	100.0

	51	52	53	54	55	56	57	58	59	60	61	62	63	64	65	66
SiO_2	39.19	41.60	41.30	37.53	38.32	44.00	41.80	40.56	41.78	39.87	40.44	40.43	41.00	43.60	39.88	37.90
Al_2O_3	21.34	24.20	21.79	21.19	20.40	18.40	19.05	20.40	19.60	21.47	23.69	19.13	22.40	23.14	21.86	19.90
Fe_2O_3	1.26	0.63	1.79	3.07	5.00	6.00	4.40	2.00	3.62	4.95	6.51	4.94	4.40	0.55	4.02	4.24
FeO	25.66	15.19	13.86	18.92	9.90	11.88	14.40	8.28	5.98	8.10	11.38	8.66	6.84	9.93	22.43	0.86
MnO	0.43	0.21	0.44	0.33	-	-	-	-	0.42	0.23	0.60	0.12	[illegible]	nd	2.8	0.11
MgO	8.74	14.81	15.40	13.63	18.86	19.37	14.83	22.89	20.30	12.89	7.72	20.33	15.12	19.84	1.60	0.90
CaO	3.79	2.99	5.38	3.23	4.48		5.32	5.04	5.62	12.32	9.86	4.44	10.08	3.06	8.87	35.70
Na_2O															0.27	0.15
K_2O																[illegible]
TiO_2	-	0.25	0.18	-					0.27	-	-			0.09		0.38
Cr_2O_3	-	0.12	0.20	2.20		tr	tr		2.62	0.26	0.32	2.12	tr	nd		
H_2O					3.52											
Other									0.14						0.72	0.11
NiO																
Total	100.41	100.00	100.34	100.09	100.48	99.65	99.80	99.17	100.25	100.09	100.52	100.17	99.84	100.21	100.05	100.25
Oxides *1)	-	6.6	-	2.3		4.7	1.8			2.7	18.8		5.0	2.4	13.5	
Pyrope	33.4	54.0	56.4	50.0	68.2	70.6	54.9		72.0	47.6	29.2	72.5	54.8	70.2	6.3	3.2
Uvarovite	-	0.3	0.7	6.3	-				7.3	0.9	0.9	6.0	0.0	-		
Andradite	3.7	1.8	5.0	2.4	11.6		12.9		7.1	13.8	18.5	5.2	11.9	1.5	11.6	11.9
Grossular	6.8	5.7	8.3	6.3 *2	1.8 *2	16.4 *2	2.2		2.6 *2	17.7	7.3	8.1 *2	14.4	6.1	13.2	83.0
Almandine	56.1	31.6	29.6	32.7	18.4	8.3	28.2		11.0	17.3	25.3	8.2	13.9	19.7	55.4	1.9
Total	100.0	100.0	100.0	100.0	100.0	100.0	100.0	[illegible]	100.0	100.0	100.0	100.0	100.0	100.0	100.0	100.0

	67	68	69	70	71	72	73	74	75	76	77	78	79	80	81	82
SiO_2	40.70	42.20	39.00	41.12	40.24	40.46	40.52	41.48	43.70	40.43	41.58	37.84	39.04	39.90	41.82	39.57
Al_2O_3	20.41	19.30	22.74	21.69	22.04	21.20	22.39	21.60	23.36	22.32	21.87	22.82	22.41	28.40	21.60	22.94
Fe_2O_3	0.80	2.80	4.76	3.63	2.53	2.95	1.73	1.81	-	1.44	4.17	1.31	2.92	6.51	2.05	1.44
FeO	8.02	6.10	9.40	17.59	14.19	18.90	15.25	11.71	11.75	11.13	12.55	30.17	24.65	7.04	18.99	6.37
MnO	0.15		0.31			-	-	-	-	0.23	0.30	0.93	1.37	0.08	0.39	0.08
MgO	4.58	22.00	14.04	9.00	9.63	10.45	11.28	12.49	14.74	9.62	8.49	6.70	7.49	12.25	9.36	6.96
CaO	23.57	5.60	6.44	6.59	9.84	6.20	9.00	10.56	6.33	14.73	10.58	0.60	1.87	5.06	5.86	21.97
Na_2O														{ 0.20		
K_2O																
TiO_2	0.34		0.90	0.22	0.20	0.15	0.30	1.13	0.13	0.08	0.15			0.60	0.04	0.08
Cr_2O_3	tr	3.10		0.02	0.05	-	-	-	-	0.02	0.02			0.42	0.04	0.12
H_2O	0.73															
Other	1.02				0.76											
NiO																
Total	100.32	101.10	100.52	99.86	99.48	100.21	100.47	99.78	100.01	99.98	99.71	100.37	100.13	100.46	100.15	99.53
Oxides *1)			9.7	10.3	6.7	4.3			6.3		12.4	3.3	9.2	27.0	7.8	
Pyrope	17.6	74.7	52.5	34.2	36.4	39.1	42.8	46.8	53.2	36.3	32.0	26.2	29.1	44.6	35.3	25.9
Uvarovite		8.4	-	-	0.2	-	-							1.6		0.3
Andradite	2.2	5.2	13.6	10.2	7.3	8.6	5.3	7.6		4.1	11.7	1.8	5.2	12.2	5.9	4.1
Grossular	62.8	1.7 *2)	3.8	7.8	19.2	8.2	19.3	21.4	16.5	35.8	16.7	1.9 *2)	3.3 *2)	5.5 *2)	9.8	56.1
Almandine	17.4	10.0	20.4	37.5	30.2	39.8	32.6	24.2	24.0	23.8	27.2	66.8	53.2	9.1	41.2	13.6
Total	100.0	100.0	100.0	100.0	100.0	100.0	100.0	100.0	100.0	100.0	100.0	100.0	100.0	100.0	100.0	100.0

	83	84	85	86	87	88	89	90	91	92	93	94	95	96	97	98
SiO_2	41.45	40.70	39.68	41.69	39.95	40.09	40.04	39.68	41.95	40.76	39.19	41.60	41.42	39.95	42.53	42.24
Al_2O_3	21.71	20.41	23.16	22.72	21.78	22.26	22.06	22.88	22.20	22.76	22.85	22.28	21.59	21.96	22.32	21.44
Fe_2O_3	2.93	0.80	1.01	0.93	2.86	1.96	2.22	1.38	1.93	1.71	2.59	2.77	2.56	1.64	0.88	1.23
FeO	5.52	8.02	7.53	5.02	4.54	4.20	8.58	11.00	12.18	7.86	10.35	5.80	2.22	2.84	7.88	7.84
MnO	0.13	0.15	0.11	0.14	0.15	0.12	0.56	0.14	0.26	0.27	0.16	0.22	0.06	0.15	0.37	0.35
MgO	5.95	4.58	4.09	4.66	2.94	4.32	7.52	7.18	6.55	10.57	5.17	7.01	3.29	3.14	20.76	20.78
CaO	21.73	23.57	24.36	24.00	26.95	26.87	18.50	17.50	14.88	15.85	19.40	19.92	28.26	30.13	4.01	4.05
Na_2O																
K_2O																
TiO_2	0.22	0.34	0.35	0.19	0.62	0.10	0.34	0.38	0.19	0.30	0.44	0.10	0.11	0.17	0.61	0.66
Cr_2O_3	0.03	tr	0.02	0.04	0.03	0.03	0.06	0.04	0.02	tr	0.03	0.08	0.02	0.04	0.95	1.79
H_2O																
Other																
NiO																
Total	99.67	100.32	100.31	99.66	99.82	99.95	99.88	100.18	100.16	100.08	100.18	99.78	99.53	100.02	100.31	100.38
Oxides *1)	7.7		3.0	7.0	6.0		1.9	4.3	8.9		6.0	8.1	3.8	1.4		
Pyrope	22.7	17.7	15.4	17.7	11.1	16.6	27.9	26.7	24.5	39.7	19.2	26.1	12.6	11.8	73.3	73.6
Uvarovite	0.0	-	-	-			0.2	0.2	-		0.0	0.2	-	0.2	2.9	5.1
Andradite	8.5	2.2	3.2	2.7	8.2	5.9	6.5	6.8	5.5	4.8	7.4	7.7	7.4	4.5	2.3	3.1
Grossular	49.7	62.6	62.5	61.8	64.8	68.3	44.3	39.8	34.8	38.3	45.2	45.3	71.3	75.9	4.9	1.9
Almandine	11.4	17.4	15.9	10.8	9.9	9.2	19.2	23.2	26.3	17.2	22.2	12.6	4.9	6.2	16.6	16.2
Total	100.0	100.0	100.0	100.0	100.0	100.0	100.0	100.0	100.0	100.0	100.0	100.0	100.0	100.0	100.0	100.0

	99	100	101	102	103	104	105	106	107	108	109	110	111	112	113	114
SiO_2	42.47	41.47	42.15	42.50	42.23	42.29	39.11	41.45	41.30	44.76	41.98	38.59	43.15	42.35	41.20	40.50
Al_2O_3	22.74	18.41	21.61	21.58	21.84	22.34	22.47	23.50	22.00	21.27	21.19	23.40	26.78	20.26	19.47	21.13
Fe_2O_3	0.35	0.52	1.40	0.81	0.67	0.33	2.06	0.76	2.81	0.43	0.23	2.47	0.82	1.32	1.54	1.72
FeO	7.85	6.81	7.73	7.36	7.44	8.04	18.35	10.08	10.00	14.81	19.37	24.63	9.73	19.73	23.02	18.82
MnO	0.31	0.33	0.41	0.38	0.27	0.43	0.54	0.33	0.44	0.20	0.22	0.36	0.20	0.21	0.26	0.24
MgO	20.62	19.39	20.35	20.06	20.73	20.20	11.57	18.80	18.10	11.09	9.24	4.98	10.29	7.08	5.63	8.04
CaO	4.39	6.06	4.50	4.92	4.69	4.41	5.05	5.09	5.33	7.20	7.40	5.33	8.82	8.32	8.22	9.00
Na_2O							0.20	-								
K_2O							0.23	-								
TiO_2	0.43	0.28	0.57	0.53	0.52	0.43	0.25	0.51	0.28	0.19	0.37	0.24	0.06	0.72	0.65	0.52
Cr_2O_3	0.85	85	1.47	2.02	1.88	1.61	0.029	-	-	0.05	-	-	0.15	0.01	0.01	0.03
H_2O							0.68									
Other																
NiO																
Total	100.01	100.12	100.19	100.16	100.27	100.08	100.539	100.52	100.41	100.00	100.00	100.00	100.00	100.00	100.00	100.00
Ozides *1)							2.7			7.8	4.1	9.3	18.3	5.5	5.6	3.9
Pyrope	73.1	69.6	71.9	71.6	72.6	71.6	43.6	66.1	64.2	41.5	34.7	19.7	37.9	27.1	21.7	30.9
Uvarovite	2.4	15.6	4.2	5.5	5.6	4.6		0.0		0.3			0.4			
Andradite	1.1	3.9 *1)	3.8	2.1	1.7	0.9	5.9	2.1	7.5	1.1	0.7	7.8	2.2	3.8	4.6	4.9
Grossular	7.4	1.4 *2)	3.5	4.7	4.7	5.9	7.8	10.9	6.2	17.8	19.2	7.7	20.7	19.4	18.1	19.9
Almandine	16.1	9.4	16.6	16.1	15.4	17.0	40.0	20.9	21.1	31.5	41.3	55.5	20.5	44.2	50.0	40.3
Total	100.0	100.0	100.0	100.0	100.0	100.0	100.0	100.0	100.0	100.0	100.0	100.0	100.0	100.0	100.0	100.0

	115	116	117	118	119	120	121	122	123	124	125	126	127	128	129	130
SiO_2	40.03	43.23	40.11	38.92	43.83	40.31	40.45	41.52	37.67	41.06	42.11	42.77	41.90	42.44	41.71	41.50
Al_2O_3	21.43	19.94	19.57	20.96	21.78	19.10	23.22	23.01	20.61	22.54	22.10	21.91	16.92	22.24	21.55	21.53
Fe_2O_3	2.13	1.04	1.33	2.60	1.36	1.65	0.20	1.22	1.78	1.87	0.35	1.25	1.24	1.56	0.02	1.68
FeO	14.90	17.05	23.11	23.68	14.46	22.80	16.13	12.86	25.01	11.65	8.24	6.79	6.17	4.75	7.36	13.81
MnO	0.20	0.20	0.21	0.32	0.20	0.21	0.41	0.33	0.87	0.37	0.36	0.26	0.59	0.16	0.31	0.27
MgO	11.55	9.03	6.40	1.68	10.90	6.05	11.86	16.64	2.98	16.49	19.85	20.70	19.64	21.53	20.79	15.33
CaO	9.04	8.58	8.80	10.15	7.23	7.75	8.01	4.71	10.36	5.42	4.80	4.65	6.27	4.90	5.22	5.30
Na_2O							0.13			0.06						
K_2O							0.03			0.03						
TiO_2	0.67	0.92	0.45	1.69	0.23	2.13		tr	0.46	0.23	0.12	0.30	0.11	0.52	0.61	0.46
Cr_2O_3	0.05	0.01	0.02	-	0.01			0.22		0.63	1.91	1.90	7.52	1.98	2.97	0.12
H_2O								0.16			0.40					
Other																
NiO																
Total	100.00	100.00	100.00	100.00	100.00	100.00	100.44	100.67	100.22	100.42	100.24	100.53	100.36	100.08	100.54	100.00
Oxides *1)		6.8		11.3	7.6	6.6										7.6
Pyrope	43.8	33.8	25.1	6.7	41.4	23.7	44.2	60.3	11.9	59.5	70.2	73.8	71.2	75.5	72.1	57.9
Uvarovite	0.2	0.0						0.7		1.8	5.7	5.4	16.4	5.5	8.2	0.3
Andradite	6.4	3.0	4.3	7.7	4.1	5.0	0.6	3.3	5.5	5.2	1.0	3.4	5.5 *3)	4.2		4.9
Grossular	17.8	20.0	20.3	21.2	15.6	14.0	20.6	8.9	24.4	9.2	5.8	3.0	3.3 *2)	6.1	4.6	9.3
Almandine	31.8	36.4	50.3	53.1	31.3	50.7	34.6	26.8	58.2	24.3	17.3	14.4	3.6	8.7	15.2	20.0
Total	100.0	100.0	100.0	100.0	100.0	100.0	100.0	100.0	100.0	100.0	100.0	100.0	100.0	100.0	100.0	100.0

	131	132	133	134	135	136	137	138	139	140	141	142	143	144	145	146
SiO_2	42.49	42.20	41.20	40.86	36.94	39.13	44.38	41.19	42.58	40.61	41.30	41.06	41.78	41.42	42.07	41.54
Al_2O_3	23.20	19.30	21.75	23.11	17.86	19.68	23.63	23.69	22.60	21.84	21.67	23.45	22.26	19.97	22.62	21.72
Fe_2O_3	-	2.80	2.21	0.43	4.06	tr	0.76	1.66	0.95	3.99	3.26	1.80	1.91	1.31	0.67	0.68
FeO	8.36	6.10	9.31	7.05	30.52	26.50	5.59	10.15	4.86	13.83	11.84	5.02	7.08	5.61	5.63	8.98
MnO	0.19	-	nd	0.25	0.32	0.46	0.20	0.41	0.18	0.42	0.43	0.16	0.45	0.36	0.28	0.32
MgO	20.26	20.00	19.32	19.72	3.24	6.76	20.98	17.81	16.19	14.11	15.58	12.03	20.13	20.62	22.44	20.06
CaO	5.54	5.60	4.74	6.06	6.79	6.65	4.01	5.28	12.58	4.49	4.79	16.16	4.60	5.07	4.05	4.78
Na_2O			nd		0.25	tr						-	0.04	0.03	0.05	0.08
K_2O			nd		0.14	tr						-	tr	tr	tr	tr
TiO_2			0.60		tr	0.11	0.10	0.28	0.08	0.11	0.10	0.18	0.17	0.28	0.16	0.24
Cr_2O_3	0.49	5.10	0.33	1.83	0.019	0.06	0.24	-		0.25	0.84	0.05	2.32	5.20	2.10	1.70
H_2O			0.10	1.02	0.012	0.30						-	-	-	-	-
Other			1.00			0.60						-	-	-	-	-
NiO										$\geq$0.01	>0.01	-	0.02	0.02	0.02	0.03
Total	100.33	101.10	100.56	100.38	99.98	100.25	100.28	100.47	100.34	99.65	99.82	99.91	100.76	99.99	100.09	100.13
Oxides *1)						3.3	3.7	4.3		6.3	5.2	4.1	2.0	-	-	-
Pyrope	69.5	73.0	69.2	70.0	12.7	24.4	74.4	62.0	58.5	52.2	56.9	43.4	71.4	75.1	78.0	70.0
Uvarovite	1.3	14.6	1.0	5.1		0.3	0.7	-		0.9	2.4	-	6.4	14.8	5.9	4.6
Andradite			6.0	1.1	12.0	-	2.2	4.6	2.6	11.2	9.1	5.2	5.1	3.5 *2)	1.7	1.7
Grossular	12.5	7.6 *2)	5.3	9.2	7.1	17.2	7.3	9.1	30.2		1.2	36.7	-	-	3.0	5.8
Almandine	16.6	4.8	18.5	14.6	68.2	54.8	11.7	20.0	8.7	29.4	25.2	10.6	15.1	6.6	11.4	17.9
Total	100.0	100.0	100.0	100.0	100.0	100.0	100.0	100.0	100.0	100.0	100.0	100.0	100.0	100.0	100.0	100.0

	147	148	149	150	151	152	153	154	155	156	157	158	159	160	161	162
SiO_2	40.68	40.73	41.20	40.96	40.98	42.45	40.46	44.91	41.27	40.66	39.04	49.82	40.20	41.43	42.07	38.91
Al_2O_3	23.00	22.49	23.11	23.30	23.19	19.65	22.72	17.15	22.70	21.92	21.85	23.56	20.40	20.76	18.60	19.48
Fe_2O_3	2.67	0.64	1.59	0.40	2.40	0.61	0.49	1.68	3.90	-	0.13	0.70	4.00	1.74	0.97	1.87
FeO	12.94	13.28	10.40	11.17	11.11	5.80	13.12	6.45	4.37	15.73	18.42	10.70	5.04	14.89	5.25	7.30
MnO	0.42	0.47	0.41	0.42	0.42	0.28	0.62	-	-	0.45	0.47	0.30	-	0.50	0.29	0.31
MgO	15.79	17.23	17.96	18.12	17.08	20.74	16.28	14.27	17.20	17.43	9.04	19.04	21.89	13.78	24.33	21.95
CaO	4.44	4.46	4.55	4.58	4.52	5.21	6.42	11.28	8.57	5.60	10.63	4.70	4.20	5.36	4.55	5.20
Na_2O	0.07	0.06	0.05	0.04	0.04	0.03	> 0.02	1.01			0.06			0.45	0.09	0.14
K_2O	tr	tr	tr	tr	tr	0.01	> 0.02	0.89			0.03			0.13	0.05	0.43
TiO_2	0.17	0.19	0.19	0.19	0.15	0.13	0.23	0.46			0.21			0.54	0.59	1.00
Cr_2O_3	0.39	0.91	0.80	0.95	0.32	5.41	0.12	-	-	0.29	0.08	0.03	3.60	0.11	3.35	1.42
H_2O	-	-	-	-	-	nd	0.10	1.78	0.90							
Other	-	-	-	-	-	0.05	0.05									
NiO	0.01	0.02	0.03	0.05	0.03	-					0.01					
Total	100.67	100.49	100.29	100.19	100.25	100.37	100.61	99.88	98.91	102.80	99.97	99.85	99.33	99.69	100.14	98.01
Oxides *1)	3.1	-	2.1	-	2.7	-		4.2	6.8				2.0	2.2	1.7	-
Pyrope	58.0	61.6	64.4	64.8	61.9	74.4	56.9	50.1	62.0	57.0	33.1	66.8	77.5	51.5	77.7	73.2
Uvarovite	1.2	2.6	2.4	2.9	0.9	13.4	0.4	-	-	0.8	0.3		9.9	0.3	8.5	3.6
Andradite	7.5	1.7	4.3	1.1	6.6	2.0 *1	1.3	4.6	10.9		0.4	1.7	0.7	4.7	2.3	4.9
Grossular	2.9	7.0	4.9	7.8	4.3	1.7 *2	14.5	28.3	11.4	12.4	27.3	10.0	9.9 *2	9.0	-	4.0
Almandine	27.3	27.2	21.8	23.4	23.6	8.5	26.9	12.8	8.9	29.8	38.9	21.5		32.3	9.8	14.3
Total	100.0	100.0	100.0	100.0	100.0	100.0	100.0	100.0	100.0	100.0	100.0	100.0	100.0	100.0	100.0	100.0

****

Appendix 4:

The chemical analyses and the molecular norms of the various parentages of garnet.

*1)

The excess Al_2O_3 and SiO_2 in the calculation of the molecular norms.

*2)

$Fe_3Cr_2Si_3O_{12}$

*3)

$Fe_3Fe_2Si_3O_{12}$.

I. Garnets from Kimberlite.

1, 2 Garnet from Mukarob, S.W.A., Hall (1938, No. 1774, 1788).

3, 4 Garnet from Kimberley Mines, Hall (1938, No. 1787, 1786).

5-12 Garnet from Zarnitsa; Smirnov (1959).

13,14 Garnet from Kao; Visser (1964, 1937-1938).

15,16 Garnet from Russia; Milashev (1965).

17-24 Garnet from Russia; Bobrievich et al., (1959).

25,26 Garnet from Honaus and Amalia; Rep. Leeds. Univ, 1962-63.

27,28 Garnet from S.W.A. and Jagersfontein; Hall (1938, 1776-1777).

29,30 Garnet from Driekoppies; Hall (1938, 1790-1791).

31 Garnet from Kimberley Mine; Visser (1964).

32 Garnet from Thaba Putsoa; Nixon et al., (1963).

33,34 Garnet from Frank Smith and Postmasburg, Holmes (1936).

35-38 Garnet from Russia; Milashev (1965).

39-40 Garnet from Lichtfels and Luisenfelds. Rep. Leeds Univ., (1962-63).

II. Garnets from Eclogite.

41 Garnet from Roberts Victor; O'Hara (1966, p. 69).

42,43 Garnet from Roberts Victor, and Russia; Sobolev (1965).

44-49 Garnet from Roberts Victor; Aoki and Kushiro (1968).
50,51 Garnet from Kao; Visser (1964, No 1936, 1934).
52 Garnet from Roberts Victor; Hahn Weinheimer et al., (1963).
53-54 Garnet from S.W.A.; Rep. Leeds. Univ (1962-63); Hall (1938, No 1775).
55 Garnet from Roberts Victor; Hall (1938, 1782).
56-58; Garnets from Crown Mine, Jagersfontein and Roberts Victor, (Hall 1938).
59 Garnet Russia; Bobrievich et al., (1959).
60-62; Colossus Mine; Hall (1938, 4965-4967).
64-75 Garnets from Russia; Bobrievich et al., (1959).
76-77 Ditto ; Sobolev (1968).
78-79 Ditto ; Bobrievich et al., (1959).
80 Garnet from Sarsadskik; Kopecky (1962).
81 Garnet from Eclogite; Min abst., (1961, p. 19).
82-96 Garnet from Russia; Sobolev (1968).
97-104 Garnet from Chechoslovakia; Kopecky (1962).
105-107 Garnet from New Zealand; Dicky (1968).

III. Garnets from Regional Eclogites.

108-120 Garnets from Regional Eclogites, Hahn Weinheimer (1963).
121 Garnet from Saulpe, Austria. Contr. Min. & Petrol (1968, 340).
122 Garnet from eclogite; Deer, Howie and Zussman (1967, 24).
123 Average 11. Alpinotype eclogites Smulikowski (1968)
124 Average 12. Eclogites ditto

IV. Garnets from Garnet Peridotites in Kimberlite.

125 From Dutoitspan Mine, Visser (1964, No 1941).
126-131 From S.W.A. and Lesotho; Nixon et al. (1963).
132-133 From Kaalvallei and Kao; Visser (1964, No 1947, 1954).
134 From Postmasburg; Holmes, (1938).
135 From Russia; Bobrievich et al., (1959).
136 From Russia; Sobolev, (1964).

137-138 From Russia; Bobrievich et al., (1959).
139-140 From Russia and Hawaii; Sobolev, (1964).
141-142 From Regional Garnet Peridotites; Karlskaret; Carswell, (1968).
143 Corundum Eclogite from Russia; Sobolev, (1968).
144-146 Regional Peridotites; O'Hara and Mercy, (1963).
147-152 Garnet Peridotites; O'Hara and Mercy, (1963).
153 From Bultfontein; MacGreggor and Ringwood, (1964).
154 Min abst., (1964, 706).
155 From Premier Mine; Hall (1938).
156 From Frank Smith; Hall, (1938, No 1779).
157 From Garnet Peridotite; Bull. Geol. Soc. Franç. (1967, 206).
158 From Garnet Peridotite; Carnegie Inst. Yearb., (1963).

159 From Bultfontein, Holmes (1936).

V. New analyses.

160 CF 300; Eclogite; Roberts Victor.
161 CF 301; Garnet Peridotite; Premier Mine.
162 CF 303; Kimberlite; Frank Smith Mine.

Addendum to Appendix 4.

1. Garnet from Kimberley kimberlite.
2. Garnet from Mingui kimberlite.

	1	2
SiO_2	41.51	41.02
Al_2O_3	22.93	22.75
Fe_2O_3	1.00	1.05
FeO	10.84	10.19
CaO	3.62	4.51
MgO	19.31	18.80
Na_2O	0.09	0.08
K_2O	0.01	0.01
P_2O_5	0.20	0.19
TiO_2	0.48	0.78
MnO	0.38	0.38
Cr_2O_3	tr	tr
	100.37	99.76

Both after P.E. Gratten - Bellow, I.M.A. Volume, 1966, p 26).

APPENDIX 5 - A comparison of the d-values and indices of olivine from kimberlite to the d-values supplied by ASTM 7-79, Elesiev (1957), and Yoder and Sahama (1957)

Olivine from Peridotite (1010 In 10) Film 311			Olivine from garnet peridotite (893 In 14) Film 214		First generation olivine (DB 50) Film 214	
I/I_o	d(Å)	hkl	I/I_o	d(Å)	I/I_o	d(Å)
20	7.356	-	30	7.344	-	-
40	5.116	020	20	5.121	40	5.117
10	4.717	110	-	-	-	-
5	4.103	-	-	-	-	-
90	3.900	021	70	3.890	50	3.887
10	3.654	101	-	-	-	-
30	3.501	111	40	3.499	20	3.495
30	3.479	120	40	3.481	20	3.483
40	3.3030	-			80	3.3008
60	3.1486	121	20	3.0034	10	3.0064
30 b	2.9916	002	20	2.9936	30	2.9887
			10	2.9407(?)	40	2.9368
			5	2.8750(?)	40	2.8696
90	2.7666	130	90	2.7675	70	2.7675
50	2.5772	-	5	2.5836	-	-
			5	2.5348(?)	-	-
100	2.5101	131	100	2.5115	100	2.5115
20 b	2.4926	-	-	-	30	2.4912
100	2.4609	112	100	2.4609	80	2.4574
40	2.3468	041	30	2.3468	10	2.3441
30	2.3143	210	40	2.3166	20	2.3137
80	2.2684	122	50	2.2673	50	2.2667
70	2.2473	140	40	2.2482	40	2.2499
70	2.1582	211	40	2.1596	30	2.1572
40	2.1114	-	10	2.1119	20	2.1100
30	2.0535	-			10	2.0530
30	2.0311	132	20	2.0303	20	2.0292
5	1.9410	042	10	1.9481	10	1.9530
10	1.8761	150	-	-	-	-
10	1.8688	-	-	-	-	-

Olivine from Peridotite (1010 In 10)			Olivine from garnet peridotite (893 In 14)		First generation olivine (DB 50)	
I/I_o	d(Å)	hkl	I/I_o	d(Å)	I/I_o	d(Å)
10	1.7892	142	10	1.7893	-	-
100	1.7483	222	100	1.7483	100	1.7482
30	1.7380	123	40	1.7390	40	1.7376
40	1.6698	241	60	1.6831	30	1.6681
10	1.6620	-	-	-	-	-
10	1.6499	061			30	1.6470
30	1.6168	-	50	1.6168	20	1.6167
10 b	1.5878	-	10	1.5878		-
20 b	1.5700	-	20	1.5705	5	1.5701
20 b	1.5647	-	20	1.5652	5	1.5661
40	1.5393	-			30	1.5400
30	1.4951	004	40	1.4951	20	1.4841
30	1.4775	-	40	1.4780		
30 b	1.4696	-				
30 b	1.4367	-	20. b.	1.4359		
30	1.3952	-	30	1.3959		
30	1.3871	-				
50	1.3496	-	70	1.3500		

Second generation olivine (Be 2) Film 324		D. T. A. A *1) Film 215		D. T. A. B *1) Film 215		D. T. A. F *1) Film 215	
I/Io	d(Å)	I/Io	d(Å)	I/Io	d(Å)	I/Io	d(Å)
20	7.382						
40	5.132	20	5.116				
		10	4.265				
80	3.892	50	3.884	50	3.877	50	3.889
				10 b	3.722	10	3.679
40	3.502	20	3.494				
40	3.233			10 b	3.483	20 b	3.496
10	3.0024	60	3.0167	10	3.1617		
30	2.9887		-	10 b	2.9862	20	2.9916
-	-	-	-	20 b	2.8741	40 b	2.8703
100	2.7675	40	2.7668	30	2.7600	70	2.7712
		70	2.6969				
						10	2.6187
80	2.5111	90	2.5109	100	2.5050	9	2.5128
				10	2.4812		
80	2.4574	100	2.4578	100	2.4512	10 b	2.4557
20	2.3462	10	2.3468			10	2.3474
30	2.3143	10	2.3140			30	1.3109
60	2.2681	30	2.2681	20	2.2656	30	2.2667
60	2.2458	30	2.2463	20	2.2456	5 b	2.2469
50	2.1584	20 b	2.1559			10	2.1557
						10 b	2.1040
10	2.0283					10 b	2.0260
-	-	30	1.9564			10 b	1.9365
5	1.8788	20	1.9072				
-	-					30 b	1.8384
						70	1.7914
70	1.7498	30 b	1.7472	20 b	1.7447	30	1.7478
10	1.7311						
-	-	30 b	1.6723			30 b	1.6688

Second generation olivine (Be 2)		D. T. A. A*1)		D. T. A. B*1)		D. T. A F*1)	
$I/_{Io}$	d(Å)	$I/_{Io}$	d(Å)	$I/_{Io}$	d(Å)	$I/_{Io}$	d(Å)
20	1.6168	80	1.6101				
10	1.5706						
5	1.5657						
40	1.5397	40 b	1.5385				
				30	1.4925	50 b	1.4934
				30	1.4760	30	1.4763
						20	1.4705
		20	1.3469	30	1.3561	40	1.3467

A. S. T. M. 7-79, Fo 91%			Elesiev (1957)			Yoder & Sahama (1957)		
I	d(Å)	hkl	I	d(Å)	hkl	I	d(Å)	hkl
50	5.10	020	60	5.130	020	26	5.094	020
10	4.32	110				3	4.310	110
60	3.884	021	90	3.893	021	95	3.881	021
10	3.722	101	40	3.724	101	35	3.723	101
20	3.500	111	60	3.494	111	13	3.496	111
10	3.481	120	40	3.333	030	12	3.477	120
10	3.010	121						
10	2.994	002	30	2.985	002	41	2.989	002
100	2.770	130	100	2.772	130	51	2.766	130
100	2.514	131	100	2.508	131	100	2.510	131
80	2.460	112	100	2.455	112	100	2.456	112
20	2.350	041	20	2.326	041	18	2.345	041
10	2.318	210				8	2.315	210
50	2.271	122				50	2.267	122
30	2.251	140	80	2.263	140	48	2.247	140
10	2.162	220, 211	40	2.158	211	33	2.158	211
5	2.034	132				20	2.032	132
						8	1.940	042
10	1.879	150	20	1.880	150	10	1.874	150
			20	1.787	142			
40	1.751	222	100	1.747	222			
10	1.741	240						
10	1.733	123						
10	1.672	241	30	1.670*	241			
10	1.639	061	30	1.640	061			
-	-	-	10	1.633	232			
20	1.620	133	30	1.617	133			
5	1.591	152						
			20	1.568	043			
20	1.498	004						
20	1.481	062	60	1.479	004			

A. S. T. M. 7-79, Fo 91%			Elesiev (1957)			Yoder & Sahama (1957)		
I	d(Å)	hkl	I	d(Å)	hkl	I	d(Å)	hkl
			60	1.468	062			
10	1.396	170, 233	50	1.394	233			
5	1.390	312						
20	1.352	322	60	1.349	322			
10	1.317	134						

*1) d - values of olivine formed during the differential thermal analyses of serpentine

d - values of olivine obtained by means of Guinier Camera, and Cu Kα radiation

****

APPENDIX 6 - THE FORSTERITE CONTENT OF THE VARIOUS OLIVINES ACCORDING TO d_{130} AND a_o - AND c_o - VALUES

Specimen	d_{130} Å (± 0.002)	% Fo*3 (±0.2 %)	a_o Å (± 0.003)	c_o Å (± 0.003)	% Fo*2 (±2 %
Monastry	2.771	93		5.989	92
DB11 *1	2.768	98		5.973	98
Wes 6	2.768	98		5.979	97
Be 1	2.768	98	-	-	
Bel. 15 *1	2.763	100	4.749	5.977	97
Fs 14 *1	2.766	99	4.754	5.988	97
Ja 12	2.770	95	4.753	5.979	97
Nogopetso *1	2.768	98	4.753	5.982	97
Bel 14 *1	2.768	98	4.749	5.979	97
Bel 17 *1	2.768	98	4.749	5.979	97
W10 *1	2.768	98	4.750	5.978	97
Bel 16 *1	2.766	99	-	5.979	97
DTA-A	2.767	98		5.975	98
DTA-B	2.760	100		5.970	99
D. T. A. -F	2.770	95		5.974	98
OLIVINE FROM ULTRAMAFIC NODULES IN KIMBERLITE					
Jagersfontein 1.	2.763	100		5.976	97
" 3	2.770	95	4.750	5.981	97
" 4	1.769	97	4.749	5.977	97
" 6	2.770	95	4.750	5.982	97
Kimberley 1	2.767	99	4.753	5.981	97
Dutoitspan 2	2.766	99		5.980	97
Bultfontein 1	2.765	99		5.976	97
" 6	2.768	98	4.751	5.981	97
" 7	2.762	100	4.754	5.982	97
" 8	2.766	99	4.749	5.979	97
" 9	2.765	100	4.754	5.979	91
De Beers 5	2.764	100	4.749	5.975	98
Frank Smith 1	2.765	99		5.980	97
" 3	2.768	98	4.754	5.982	97
" 5	2.768	98	4.748	5.980	97

APPENDIX 6 (Continued)

Specimen	d_{130} Å (± 0.002	% Fo *3	a_o Å (± 0.003	c_o Å (±0.003	%Fo *2
Premier Mine 893 In_3	2.773	91	4.759	5.9[illegible]5	87
" " 893 In_{16}	2.768	98	4.753	5.981	97
" 1010 In_3	2.771	93			
" 893 In_8	2.769	97			
" 893 In_4	2.773	91			
" 893 In_5	2.768	98			
" 893 In_7	2.769	97	4.752	5.984	97
" 893 In_6	2.770	95	4.759	5.984	97
" 1010 In_2	2.770	95		5.981	97
" 893 In_1	2.771	93	4.750	5.981	97
" 1010 In_{10}	2.767	99		5.980	97
" 1010 In_6	2.770	95	4.751	5.982	97
" 1010 In_7	2.768	98	4.750	5.981	97
" 893 In_{14}	2.768	98	4.754	5.979	97
" 893 In_{13}	2.766	99	4.750	5.980	97
" 893 In_1	2.771	93			
" 893 In_{17}	2.766	99	-	5.981	97
" 893 In_{11}	2.767	99	4.751	5.981	97
" 893 In_{19}	2.768	98	4.751	5.979	97
" 1010 In_8	2.767	99	4.749	5.979	97
" 1010 In_3	2.766	99	4.750	5.979	97
" 893 In_{15}	2.766	99	4.748	5.978	97
" 893 In_{18}	2.770	95	4.750	5.978	97
" CF 314	2.766	99	4.749	5.972	98
" CF 313	2.769	97	4.751	5.986	98
" 893 In_{23}	2.765	99	4.752	5.981	97
" 893 In_{22}	2.768	98	4.749	5.975	98
VALUES AFTER O'HARA AND MERCY (1963)					
N_3	2.789	93			
N_6	2.845	92			
S_1	2.822	92			
N_{70}	2.883	90			
N_{69}	2.871	89			
N_{26}	2.956	85			

Specimen	d_{130} Å	% Fo *3
A_1	2.784	94
A_6	2.783	94
A_{15}	2.772	94
A_4	2.805	93
A_{10}	2.793	93
A_3	2.799	92
N_{67}	2.792	93
N_{196}	2.792	93
N_{197}	2.795	93
N_{135}	2.817	92
N_{21}	2.887	88
A_3	2.803	93
A_g	2.770	95

****

Appendix 6:

The forsterite content of the various olivines according to d_{130}, a_o and c_o-values.

*1

First generation olivine.

*2

Forsterite content after Jambor and Smith (1964, p. 739). The a_o-value usually gives a 5 per cent lower forsterite content than the co-value. The co-value has been used as far as possible.

* 3

Forsterite content after Yoder and Sahama (1957).

D.TA. Olivines which formed as a consequence of the differential thermal analyses of serpentine. A and B were taken from first generation olivine phenocrysts, and F was taken from second generation olivine.

APPENDIX 7 - The Forsterite Content of the olivines from various types of Ultramafic rocks according to the optical properties.

A. Present Investigation

1. Garnet peridotite nodules in kimberlite

Reference	$n\alpha$ (± 0.003)	$n\beta$ ± 0.003	$n\gamma$ ± (0.003)	2V (± 10)°	%Fo *1
Jagersfontein Ja 1	1.654	1.673	1.691	+78°	90
" Ja 1				+88°	92
" Ja 3	1.651	1.661	1.689	-	91
" Ja 5	1.648	1.662	1.684	+88°	93
" Ja 6	1.646	1.664	1.682	+87°	94
" Ja 4	1.645	1.664	1.681	-	95
Frank Smith Fs. 2	1.652	1.671	1.689	+88°	92
" "				+87°	96
" Fs. 3	1.649	1.667	1.685	+89°	93
" Fs. 4	1.649	-	1.686	+89°	93
P.M. 893 In_1	1.653	1.670	1.696	+89°	90
" 893 In_8				+87°	96
" 893 In_7	1.647	1.666	1.682	+87°	95
" 893 In_6	1.654	1.668	1.692	+88°	90
" 893 In_5	1.646	-	1.681	+85°	96
" 893 In_4	1.650	-	1.682	+87°	93
" 893 In_{16}	1.656	1.668	1.691		89
" 893 In_{11}	1.653	1.667	1.687	+89°	92
" 893 In_{14}	1.650	1.668	1.683	+86°	94
" 893 In_{13}	1.650	1.666	1.683		94
" 893 In_{19}	1.653	1.667	1.687	+87°	91
" 1010 In_3	1.642	1.661	1.680	+88°	96
" 1010 In_2	1.658	1.677	1.691	+90°	89
" 1010 In_8	1.650	1.665	1.683	+89°	94
" 1010 In_7	1.651	1.663	1.684	+87°	93
" 893 In_{15}	1.650	1.668	1.686	+89°	92
" 893 In_{17}	1.649	1.668	1.688	+89°	92
" 1010 In_6	1.654	-	1.687	+88°	91
" 893 In_{18}	1.646	1.662	1.683	+84°	94
" 1010 In_{10}	1.648	-	1.685	+87°	93

Reference		$n\alpha$ (± 0.003)	$n\beta$ ± 0.003	$n\gamma$ ± (0.003)	2V (± 10′)	%Fo *1
P. M. 893	In_{22}	1.650	1.667	1.686	+89°	92
" 893	In_{21}				+87	96
" 893	In_{23}	1.647	1.662	1.683	+85°	93
Dutoitspan	2	1.646	1.663	1.679	+87°	96
Bultfontein	No. 1	1.650	1.671	1.688	+87°	92
"	No. 8	1.645	1.664	1.680	+88°	95
"	No. 9	1.647	1.662	1.682	+89°	94
"	No. 6	1.642	1.664	1.678	+84°	97
"	No. 7	1.644	1.660	1.681	+86°	95
Hololo	33				+88°	92
De Beers	5	1.648	1.664	1.682	+89°	93
De Beers	4				+86°	98
Kimberley		1.642	1.666	1.678	+89°	97
B. "VALUES OBTAINED FROM LITERATURE						
1. Ultramafic nodules in kimberlite						
O' Hara, (1963) & Mercy	A_1	1.651	1.665	1.685	+80°	92
	A_{11}		1.669	1.690		91
	A_{13}		1.664	1.683		93
	A_{14}		1.665	1.692		90
	A_{15}		1.667	1.691		90
	A_{16}		1.668	-		91
	A_{10}		1.668	1.688	+87°	91
	A_4	1.646	1.665	1.686	+86°	93
	A_5	-	1.667	1.686	+90°	92
	A_6	1.648	1.666	1.687	+88°	92
	A_9	1.652	1.667	1.685	+89°	93
	A_3	1.648	1.666	1.686	+85°	93
	A_{17}	-	1.669			91
Nixon et al., (1963)	E_1	1.651	1.665	1.684	+87½°	92
	E_2	1.651	1.667	1.685	+87°	92
	E_3	1.651	1.668	1.686	+87½°	92

APPENDIX 7 (Continued)

Reference	$n\alpha$ (± 0.003)	$n\beta$ ± 0.003	$n\gamma$ ± (0.003)	2V (± 10)°	%Fo *1
Nixon et al., (1963) E_5	1.653	1.669	1.687	$+88\frac{1}{2}^{o}$	91
E_{11}	1.652	1.668	1.686	$+87\frac{1}{2}^{o}$	92
Bobrievich et al., (1959)	1.670		1.704	$+84^{o}$	85
" (1959)	1.690		1.728	$+86^{o}$	75
Bobrievich et al., (1959)		1.662	1.692	$+85^{o}$	88
	1.650		1.684	$+85^{o}$	92
		1.670	1.696	$+86^{o}$	85
		1.660	1.688	$+85\text{-}86^{o}$	89
		1.654	1.692	$+88^{o}$	90
		1.662	1.694	$+88^{o}$	88
	-		1.686	$+86^{o}$	92
	1.650		1.686	$+86^{o}$	92
		1.660	1.690	$+84^{o}$	89
	-		1.692	$+87^{o}$	89
2. ULTRAMAFIC BODIES IN REGIONAL AREAS					
O'Hara & Mercy (1963)					
N_1		1.665			93
N_3		1.667			92
N_6		1.667			92
N_7		1.662			94
N_{21}		1.678		-87^{o}	87
N_{23}		1.697			78
N_{26}	1.664	1.685	1.701	-86^{o}	84
N_{64}		1.671			90
N_{68}		1.669		$+88^{o}$	90
N_{67}	1.653	1.671	1.692	$+88^{o}$	89
N_{69}	1.656	1.671	1.694	$+88^{o}$	88
N_{70}	1.654	1.672	1.692	$+80^{o}$	89
N_{72}		1.665			93
N_{73}		1.668			91
N_{76}		1.673			89
S_1	1.654	1.671	1.691		89

Reference	$n\alpha$ (± 0.003)	$n\beta$ ± 0.003	$n\gamma$ ± (0.003	2V (± 10)	D	%Fo *1
Ross et al., (1954)					3.338	89
"					3.337	89
"					3.349	87
"					3.347	87
"					3.324	90
"					3.342	87
"					3.349	87
"					3.333	89
"					3.334	89
"					3.321	90
"					3.331	89
"					3.293	92
"					3.313	90

****

Appendix 7:

The forsterite content of the olivines from various types of ultramafic rocks according to the optical properties.

≠1)

The forsterite values have been determined by calculating the average values, determined by means of n_α, n_β and n_γ, after Tröger (1959, p.37)

Since the slope of the curve showing the 2V as a function of the composition is too small, these values have only been considered when refractive indices were not available.

APPENDIX 8 - THE FORSTERITE CONTENT OF THE OLIVINE FROM KIMBERLITE, ACCORDING TO THE OPTICAL PROPERTIES

A. Present Investigation

Rock and Locality	n_γ (± 0.003)	n_β (± 0.003)	n_α (± 0.003)	2V (± 1°)	%Fo	No.
Benfontein Kimberlite *1	1.685	1.672	1.653	+89°	90	Be 1
Benfontein *1				+89°	90	Be 2
Dutoitspan *1				+90°	88	DuP. 2
Dutoitspan				+87°	95	Du. Pan 14
Dutoitspan *1				+89°	90	Du. P. 11
"				+87°	95	Du P. 11
Belsbank Kimberlite	1.678	1.658	1.640	+87°	95	Bel. 14
"	1.677	-	1.641	+87°	95	Bel. 15
"	1.681	1.659	1.644	+87°	95	Bel. 16
"	1.683	1.662	1.646	+88°	92	Bel. 17
Monastry				+90°	88	Mon 1
Wesselton *1	1.681	1.672	1.650	+87°	94	We 5
" *1				+89°	90	We 3
"	1.683	1.666	1.650	-	93	We 10
De Beers				+86°	98	DB 11
" *1				+90°	88	DB 12
Frank Smith	1.682		1.646	+88°	94	Fs. 14
Kamfersdam	1.677	1.660	1.642	nd.	95	kd. 14
Jagersfontein *1	1.686	1.664	1.653	-	92	Ja 12
Jagersfontein *1)				+89°	90	Ja 13
Jagersfontein				+85°	99	Ja 13
Koffiefontein *1				+89°	90	Kof. 1
Koffiefontein				+88°	92	Kof. 1
Sovêr kimberlite				+87°	95	Sov. 1
Hololo *1				+89	90	
Hololo 135				+90	88	
Lesotho *1				+89°	90	
Hololo				+87°	95	
D_{66} Lesotho *1				+89°	90	
A_{28} " *1				+90°	88	
Melilite basalt				-85°	77	

APPENDIX 8 (Continued)

B. Values obtained from Literature

Rock and Locality	n_α (± 0.003)	n_β (± 0.003)	n_γ (± 0.003)	2V (± 10)°	D	%Fo	No.
Yakut Russia	1.684		1.647	90°	3.32	91	Sobolev, (1964)
" "	1.684		1.650	+88	3.30	93	
Dalnyaya "	1.690		1.652			90	
Molatoli Kimberlite	1.694	1.674	1.656	+90°	3.362	88	Nixon et al.,(1963)
Kauyane	1.690	1.674	1.656	+88½	3.340	90	
Liqhobong	1.697	1.678	1.660	-89½	3.378	87	
Siberia	1.682	1.663	1.642	+80-83°		98	
"	-	-	-	+86-87°	3.315	100	
"	1.690	-	1.652	-		90	
Tanzania				+88°		92	
Udachnaya	1.686		1.650		3.29	93	Bobrievich et al(1959)
Zarnitza	1.690		1.652		3.38	90	
Legkaya	1.690		1.654		nd	90	
Dalnaya	1.699		1.658		3.36	86	
Udachnaya	1.700		1.662		3.42	84	
S. A. Kimberley	1.704		1.668		3.44	84	
(Russian Kimberlite	1.696		1.658	+84-86°		88	
unspecified)	1.686		1.650	-		93	
	1.692		1.658	-86°		85	
	1.691		1.658	+83°		89	
	1.694		1.662	+88°		89	
	1.690		1.662	+84°		89	
	1.692		1.668	+86°		90	
	1.694		1.666	+88°		89	
	1.696		1.672	+86°		87	
	1.698		1.678	+88°		88	
	1.698		1.676	+88°		88	
	1.696		1.676	-87°		84	
	1.696		1.674	-86°		84	
	1.694		1.666	+85°		88	
	1.690		1.650	+84°		90	

APPENDIX 8 (Concluded)

Rock and Locality	n_γ (±0.003)	n_β (±0.003)	n_α (±0.003)	2V (± 1,0°)	D	%Fo	No.
(Russian Kimberlite unspecified)	1.692		1.662	+86°		88	
	1.692		1.660	+87-88°		88	
Olivinite	1.686	1.668	1.653	+88°		91	Doklady (1965; P 152

****

Appendix 8:

The forsterite content of the olivine from kimberlite, according to the optical properties.

*1)

Second generation olivine.

*2)

The forsterite content has been determined according to the procedure described in appendix 7.

APPENDIX 9 - The Chemical analyses and molecular norms of olivine from various olivine-bearing rocks

A. The Chemical analyses of olivine

	1	2	3	4	5	6	7	8	9	10	11
SiO_2	41.37	41.33	40.82	40.27	40.87	40.74	40.66	41.68	40.32	39.62	39.30
Al_2O_3	0.13	0.18	0.09	-	0.57	0.06	0.37	1.40	0.12	-	0.19
Fe_2O_3 *2)	1.14	1.04	1.14	2.21	-	0.38	0.66	0.07	0.24	0.87	1.12
FeO	6.24	6.34	8.06	7.14	6.77	7.45	7.41	7.76	8.55	11.23	13.43
MgO	49.61	49.70	49.10	48.61	50.84	50.46	50.08	48.29	49.44	47.42	45.32
CaO	0.15	0.15	0.70	-	-	0.13	0.14	0.02	0.23	0.15	0.02
MnO	0.11	0.12	0.06	tr	-	0.11	0.14	nd.	0.15	0.17	0.17
NiO	0.29	0.31	-	tr	-	0.32	0.28	nd	0.34	0.24	0.23
K_2O	0.15	0.15	-	-	-	-	-	-	-	-	-
Na_2O	0.17	0.19	-	-	-	-	-	-	-	-	-
TiO_2	0.07	0.07	-	-	-	-	-	0.08	-	-	-
Cr_2O_3	-	-	-	-	-	0.019	0.02	nd	0.038	0.007	0.011
H_2O	0.22	0.18	0.27	1.10	0.81	0.23	0.33	nd	0.28	0.33	0.54
Loss	0.72	0.81	-	-	-	-	-	nd	-	-	-
Other *1)	0.02	0.02	0.44	-	-	.009	0.017	-	0.013	0.006	0.016
Total	100.17	100.41	100.68	99.33	99.86	99.91	100.10	99.30	99.72	100.05	100.35

B. The Molecular norms of the olivine

Mg_2SiO_4	92.8	93.0	90.8	92.5	93.3	91.7	92.6	91.7	90.5	87.8	85.5
Fe_2SiO_4	6.5	6.4	8.3	7.5	6.7	7.7	6.9	8.3	8.7	11.6	14.2
Mn_2SiO_4	0.1	0.1	0.1	-	-	0.1	0.1	-	0.2	0.2	0.1
Ni_2SiO_4	0.3	0.3	-	-	-	0.3	0.2	-	0.3	0.2	0.2
Ca_2SiO_4	0.3	0.2	0.8	-	-	0.2	0.2	-	0.3	0.2	-
Total *2)	100.0	100.0	100.0	100.0	100.0	100.0	100.0	100.0	100.0	100.0	100.0

	12	13	14	15	16	17	18	19	20	21	22
SiO_2	39.42	39.64	42.30	39.87	40.80	40.91	40.81	40.65	40.61	40.93	40.30
Al_2O_3	0.00	0.00	0.65	-	-	0.13	0.10	0.24	-	0.19	0.25
Fe_2O_3 *2)	1.34	2.40	2.25	0.86	-	-	-	-	-	-	-
FeO	8.96	6.48	6.80	13.20	8.61	8.96	9.46	9.30	8.96	8.86	10.26
MgO	49.79	50.59	47.75	45.38	49.77	48.95	49.12	49.55	49.88	49.52	48.60
CaO	0.00	0.07	0.05	0.25	0.20	0.17	0.07	0.13	0.11	0.08	0.07
MnO	0.05	0.005	0.11	0.22	0.13	0.15	0.15	0.13	0.12	0.11	0.09
NiO	-	-	-	-	0.38	0.34	0.28	0.28	0.32	0.30	0.41
K_2O	0.09	-	-	0.01	-	-	-	-	-	0.03	0.03
Na_2O	0.04	-	-	0.04	-	0.02	0.01	0.02	0.01	0.03	0.04
TiO_2	0.13	-	0.05	0.03	0.04	0.01	0.035	0.01	0.01	0.15	0.15
Cr_2O_3	-	-	-	tr	0.04	0.03	0.03	0.04	0.04	0.05	0.03
H_2O	0.08	-	0.10	0.43	0.29	0.20	0.11	0.07	0.05	-	0.33
Loss	-	-	-	-	-	-	-	-	-	-	-
Other *1)	-	-	-	-	-	-	-	-	-	-	-
Total	99.90	99.185	100.06	100.80	100.28	99.88	100.19	100.43	101.11	100.25	100.56
Mg_2SiO_4	90.4	93.8	92.3	85.5	90.6	90.2	89.9	90.2	90.5	90.3	89.3
Fe_2SiO_4	9.6	6.2	7.5	13.9	8.8	9.3	9.7	9.3	9.2	9.3	10.2
Mn_2SiO_4	-	-	0.1	0.4	-	0.1	0.1	-	-	-	-
Ni_2SiO_4	-	-	-	-	0.3	0.3	0.3	0.3	0.3	0.3	0.3
Ca_2SiO_4	-	-	0.1	0.2	0.3	0.1	-	0.2	-	0.1	0.2
Total *2)	100.0	100.0	100.0	100.0	100.0	100.0	100.0	100.0	100.0	100.0	100.0

APPENDIX 9 (Continued)

	23	24	25	26	27	28	29	30	31	32	33
SiO_2	40.87	41.16	40.55	40.88	41.32	40.96	-	-	-	-	-
Al_2O_3	0.07	-	0.05	0.11	-	0.21	0.034	0.049	0.16	0.045	0.070
Fe_2O_3 *2)	-	-	-	-	0.03	-	6.98	7.06	8.04	7.71	6.98
FeO	8.72	8.89	7.99	8.28	7.49	7.86	-	-	-	-	-
MgO	49.78	49.56	50.57	50.10	49.56	50.45	51.61	51.29	50.44	50.71	51.31
CaO	0.07	0.07	0.06	0.03	0.15	0.13	0.095	0.098	0.106	0.095	0.084
MnO	0.15	0.15	0.12	0.15	0.29	0.15	0.02	0.08	0.07	0.09	0.06
NiO	0.34	0.30	0.28	0.32	0.31	0.25	0.38	0.34	0.41	0.35	0.35
K_2O	-	-	0.04	-	-	-	-	-	-	-	-
Na_2O	0.01	0.03	0.06	0.02	0.01	0.01	-	-	-	-	-
TiO_2	0.02	0.015	0.14	0.015	0.01	0.01	0.01	0.012	0.030	0.020	0.014
Cr_2O_3	0.02	0.02	0.06	0.02	0.04	0.02	0.004	0.016	0.025	0.006	0.024
H_2O	0.05	0.10	0.13	0.23	0.60	0.29	-	-	-	-	-
Loss	-	-	-	-	-	-	-	-	-	-	-
Other *1)	-	-	-	-	-	-	0.002	0.007	0.014	0.004	0.004
Total	100.11	100.30	100.05	100.17	100.09	100.35					
Mg_2SiO_4	90.9	90.5	91.6	91.2	91.7	91.5	92.6	92.6	91.3	91.4	92.5
Fe_2SiO_4	8.8	9.2	8.1	8.4	7.3	8.0	7.0	7.1	8.3	8.2	7.1
Mn_2SiO_4	-	-	-	0.1	0.1	0.1	-	-	-	-	-
Ni_2SiO_4	0.3	0.3	0.3	0.3	0.3	0.2	0.4	0.3	0.4	0.4	0.4
Ca_2SiO_4	-	-	-	-	0.3	0.2	-	-	-	-	-
Total *2)	100.0	100.0	100.0	100.0	100.0	100.0	100.0	100.0	100.0	100.0	100.0

APPENDIX 9 (Continued)

	34	35	36	37	38	39	40	41	42	43	44
SiO_2	-	-	41.03	40.94	40.30	41.10	39.68	39.90	40.49	42.20	-
Al_2O_3 *2)	0.044	0.10	-	0.06	-	1.00	0.80	1.20	0.86	1.31	0.01
Fe_2O_3	8.94	10.04	1.37	-	0.29	6.50	7.10	8.01	2.84	1.71	7.18
FeO	-	-	6.56	7.30	9.37	2.02	2.45	1.50	5.54	5.97	-
MgO	50.24	49.23	51.01	50.80	48.10	43.50	44.21	43.00	46.32	46.97	51.69
CaO	0.098	0.109	-	-	0.70	1.21	1.00	0.76	0.70	0.10	0.103
MnO	0.08	0.08	0.09	0.01	-	0.08	0.04	0.10	-	0.12	0.02
NiO	0.43	0.37	-	-	0.39	nd	nd	1.10	-	0.31	0.33
K_2O	-	-	0.08	-	-				0.10	0.04	-
Na_2O	-	-	0.18	0.03	-	0.10	0.08	0.12	0.70	0.08	-
TiO_2	0.029	0.082	-	-	-	0.01	tr	0.02	0.02	0.23	0.044
Cr_2O_3	0.08	0.023	-	-	-	0.65	tr	0.005	-	0.21	0.039
H_2O	-	-	-	0.38	1.04	0.50	1.00	1.64	0.05	1.58	-
Loss	-	-	-	-	0.019	-	-	-	-	-	-
Other *1)	0.076	0.015	-	-	-	3.50	4.00	3.50	2.88	-	0.09
Total			100.32	99.52	100.21	100.17	100.36	100.85	99.50	100.83	-
Mg_2SiO_4	90.5	89.7	93.0	94.5	89.1	95.6	95.5	95.7	93.1	93.8	
Fe_2SiO_4	9.1	10.3	6.9	5.5	9.7	2.5	3.0	1.8	6.0	6.6	
Mn_2SiO_4	-	-	0.1	-	-	0.1	-	0.1	-	-	
Ni_2SiO_4	0.4	-	-	-	0.3	-	-	1.2	-	0.3	
Ca_2SiO_4	-	-	-	-	0.9	1.8	1.5	1.1	0.9	0.3	
Total *2)	100.0	100.0	100.0	100.0	100.0	100.0	100.0	100.0	100.0	100.0	

APPENDIX 9 (Concluded)

	45	46	47	48	49	50	51	52	53	54	55	56
SiO_2	-	-	-	-	-	39.18	41.55	40.57	40.86	40.83	39.26	40.46
Al_2O_3	0.07	0.011	0.29	0.30	nil	0.44	0.01	-	-			0.39
Fe_2O_3 *2)	8.67	8.78	15.91	11.71	11.0	-	-	0.92	0.12		0.48	0.67
FeO	-	-	-	-	-	17.12	7.34	8.72	8.41	10.06	10.06	7.74
MgO	49.72	50.34	44.05	47.08	48.6	42.52	50.83	49.29	49.91	47.94	49.67	49.16
CaO	0.117	0.070	0.18	0.096	0.078	0.17	-	0.03	-	0.15	0.17	0.03
MnO	0.16	0.02	0.13	0.20	Nil	0.16	0.03	-	-	0.38	0.17	0.18
NiO	0.38	0.57	0.34	0.53	0.48	0.36	-	-	0.04			-
K_2O	-	-	-	-	-	-	-	0.05	0.14			0.12
Na_2O	-	-	-	-	-	-	-	0.27	0.30			0.66
TiO_2	0.021	0.049	0.14	0.082	0.063	0.06	-	-	-			0.06
Cr_2O_3	0.031	0.003	0.034	0.03	Nil	0.01	-	-	-			-
H_2O	-	-	-	-	-	-	0.24	0.19	0.05	0.79	0.64	0.06
Loss	-	-	-	-	-	-	-	-	-	-	-	0.86
Other *1)	0.07	0.03	0.02	0.08	0.09	-	-	0.03	0.01			0.15
Total						100.02	100.00	100.07	99.84	100.15	100.45	99.76
Mg_2SiO_4						87.7	92.5	90.8	91.2	89.0	89.3	91.6
Fe_2SiO_4						11.5	7.5	9.0	8.5	10.5	10.7	8.1
Mn_2SiO_4						0.2	-	-	-		-	-
Ni_2SiO_4						0.4	-	-	-	0.5	-	-
Ca_2SiO_4						0.2	-	0.2	0.3		-	0.3
Total *2)						100.0	100.0	100.0	100.0	100.0	100.0	100.0

****

Appendix 9:

The chemical analyses and the molecular norms of olivine from various olivine-bearing rocks.

I. Olivine from kimberlites.

1, 2, From Russian kimberlites, Milashev (1965).
3 From Dalnayaya kimberlite; Smirnov (1959).
4, 5 From De Beers and Klipfontein; Williams (1932).
6 From Udachnaya; Bobrievich et al., (1959).
7 From Zarnitsa; ditto
8 From Legkaya; ditto
9 From Dalnaya; ditto
10 From Udachnaya; ditto
11 From Kimberley; ditto

II. Olivine from nodules in basalts.

12-14 From France; Brousse (1968).
15 From Rhum; Wilshire and Binns (1961).
16-28 Ross et al., (1954).

III. Olivine from garnet peridotites in kimberlite.

29-35 Ultramafic nodules; O'Hara & Mercy, (1963).
36, 37 Garnet peridotite from Lesotho; Nixon et al., (1963).
38 Lherzolite; Sobolev, (1958).
39-42 From Russia; Bobrievich et al., (1959).
43 CF313; Premier Mine; New analysis.

IV. Olivine from regional Peridotites.

44-49 Regional garnet peridotites; O'Hara & Mercy (1963).
50-51 Regional garnet peridotite; Carswell, (1968).

V. Olivine from various Ultramafic Rocks.

52-53 Peridotite; Hamad, (1962-64).
54-55 Bushveld Complex; Heckroodt, (1958).
56 Olivine from olivinite; Dokl., (1965; p. 152).

*1) The other constituents have not been taken into consideration in the calculation of the molecular norm.

*2) Has been calculated as hematite, and was omitted from the molecular norm.

APPENDIX 10 - The indexing of the reflections for Ilmenite from Kimberlite. The d-values were obtained by means of a Guinier camera, using Cukα radiation

*1) Only the d-values in the range where the reflections were indexed, are quoted.

Sample:- P. M. -2, Premier Mine Film 301					ASTM-6-0494 *1)			Hounslow and Chao *1)		
I/Io	d Å	Sin $^2\theta$ cale	Sin $^2\theta$ Exp.	h kil	I/I_1	d(Å)	h kil	I	d(Å)	h kil
					30	4.64	003	10	4.64	003
					30	4.18	101	5	4.18	101
					45	3.703	012	35	3.705	102
10	2.7288	0.07968	0.07955	10.4	100	2.722	104	100	2.725	104
9	2.5334	0.09243	0.09259	11.0	55	2.527	110	40	2.528	110
7	2.2245	0.11990	0.11998	11.3	70	2.218	113	40	2.218	113
-		-	-	-	10	2.090	202			
5	1.8563	0.17216	0.17214	02.4	40	1.852	024	30	1.853	024
	-	-	-	-	4	1.809	107			
5	1.7134	0.20209	0.20214	11.6	55	1.708	116	60	1.709	116
					6	1.6434				
2	1.6190	0.22633	0.22652	01.8	12	1.6148	018	5	1.617	018
2	1.6121	0.22831	0.22821	12.2	-	-	-			
4	1.4964	0.26495	0.26473	21.4	30	1.4938	214	20	1.4958	214
					6	1.4708	027			
4	1.4614	0.27780	0.27777	03.0	40	1.4592	030	20	1.4610	030
					2	1.3919	303			
2	1.3643	0.31875	0.31850	20.8	2	1.3606	208			
3	1.3281	0.33556	0.33516	10.10	14	1.3247	1.0.10	10	1.3275	1.0.10
					8	1.3174	119	1	1.3198	119
					4	1.2708	217			
4	1.2657	0.37033	0.370356	22.0	10	1.2634	220	3	1.2655	220
4	1.2443	0.38316	0.38332	30.6	4	1.2191	223			
					2	1.2085	131			
					6	1.1978	128			
1	1.1767	0.42842	0.42861	02.10	6	1.1735	0.2.10			
3	1.1484	0.44990	0.44991	13.4	12	1.1462	134			
2	1.1122	0.47954	0.47990	22.6	10	1.1125	315			
					10	1.1093	226			
	ao =		5.067 (± 0.003)		ao = 5.054			ao = 5.055		
	co =		13.975(± 0.005)		co = 13.898			co = 13.907		
	co/ao =		2.758							

APPENDIX 11 - The physical properties and the molecular percentages of $MgTiO_3$, $FeTiO_3$ and Fe_2O_3 of the chemically analysed specimens of ilmenites in kimberlite

Specimen	ao (Å) (+ 0.003)	co (Å) (+ 0.005)	c/a	D	$MgTiO_3$	$FeTiO_3$	Fe_2O_3	Reference
A. Values obtained from the literature								
Geikielite	5.10	14.12	2.769	-	100	-	-	Strunz ~~Troger~~ (1966)
Ilmenite	5.09	14.07	2.764	-	-	100	-	ditto
Hematite	5.04	13.77	2.732	-	-	-	100	ditto
Wakefield (Canada)	5.055	13.907	2.751	4.05	79.5	15.4	4.4	Hounslow & Chao (1967)
Crichtonite	5.093	14.060	2.766	-	-	-	-	Berry and Thompson(1962)
Crestmore	5.058	13.929	2.754	-	96.9	2.4	0.0	Murdoch & Fahey (1953)
Mukarob (S.W.A.) 1.	-	-		4.556	32.6	56.2	10.5	Hall (1938)
Mukarob (S.W.A.) 2.	-	-	-	4.376	38.6	52.4	8.6	ditto
Mabuki Mine	-	-	-	4.56	24.1	59.4	17.5	Hall (1938)
Mabuki Mine	-	-	-	4.66	20.3	57.6	22.1	ditto
Kao	-	-	-	4.51 -(6)	32.3	56.3	11.4	Nixon et al., (1963)
Thaba Putsoa	-	-	-	4.557	30.7	54.0	14.8	Dawson (1962)
Kimberley Mines	-	-	-	4.51-(6)	42.1	52.1	5.8	Williams (1932)
Frank Smith	-	-	-	-	32.5	55.3	12.2	ditto
Mir U.S.S.R.	-	-	-	4.61	30.8	52.9	16.3	Smirnov (1959)
Bankoro	-	-	-	4.13	-	-	-	Besson (1967)
Bankoro	-	-	-	4.37	37.1	50.4	11.6	"
Bounoudou	-	-	-	4.54	36.9	53.2	9.5	"
Crichtonite(Winchell)	5.083	14.040	2.762	4.72	-	100	-	Winchell (1954)
Geikielite (Winchell)	5.086	14.093	2.771	4.02	100	-	-	
Malaita (Alnoiite)	5.07	13.97	2.755	4.63	23.3	67.2	9.5	Min.mag. (1965)
Fafo Ikafo(")	5.07	13.97	2.755	4.58	16.1	72.4	11.5	ditto
N_1 Russia Kimberlite	5.067	13.81	2.725	4.680	19.4	56.4	24.2	Bobnievich et al., (1959)
N_2	5.067	13.84	2.731	4.636	26.2	54.4	19.3	
N_3	5.072	13.84	2.729	4.625	25.1	55.3	19.1	
N_4	5.068	13.84	2.731	4.608	21.2	64.8	13.6	
N_5	5.069	13.82	2.726	4.590	25.6	60.3	13.6	
N_6	5.073	13.84	2.728	4.580	26.4	58.6	14.7	
N_7	5.068	13.82	2.727	4.575	28.8	58.3	12.9	
N_8	5.068	13.84	2.731	4.570	29.1	56.7	14.1	
N_9	5.070	13.84	2.730	4.650	-	-		
N_{10}	5.072	13.86	2.733	4.634	24.6	64.7	10.7	

Specimen	ao (Å)	co(Å)	c/a	D	$MgTiO_3$	$FeTiO_3$	Fe_2O_3
N_{10} Russia Kimberlite	5.072	13.86	2.733	4.634	24.6	64.7	10.7
N_{11}	5.070	13.84	2.730	4.622	27.7	58.6	13.7
N_{12}	5.069	13.85	2.732	4.610	31.4	54.3	13.8
N_{13}	-	-	-	-			
N_{14}	5.068	13.84	2.731	4.581	30.9	55.4	13.3
N_{15}	5.070	13.84	2.730	4.580	32.4	54.1	13.1
N_{16}	5.068	13.83	2.729	4.565	34.2	51.7	13.9
N_{17}	5.066	13.83	2.730	4.560	36.9	56.9	5.9
N_{18}	5.068	13.84	2.731	4.557	37.8	52.8	9.3
N_{19}	5.072	13.83	2.727	-	-	-	-
B. Present Investigation							
Isipingo (Coetzee)	5.083	14.086	2.771	-	3.3	86.1	8.9
Riverton No. 26	5.054	13.954	2.761	4.63			
27	5.054	13.954	2.761				
10	5.067	13.955	2.754	4.45			
11	5.068	13.953	2.753	-			
12	5.068	13.962	2.755	-			
13	5.072	13.966	2.754	4.42			
14	5.070	13.956	2.753	-			
15	5.071	13.960	2.753	-			
Hololo (32)	5.072	13.980	2.756	-			
Hololo	5.068	13.947	2.752	-			
Kolo No. 2	5.066	13.968	2.757	-			
Ngopetso	5.081	13.948	2.745	-			
Brakfontein	5.072	13.972	2.755	-			
Lovedale	5.071	13.973	2.755	-			
De Beers No. 30	5.070	13.956	2.753	-			
3	5.067	13.952	2.754	-			
17	5.066	14.000	2.764	-			
5	5.069	13.948	2.752	-			
Frank Smith CF317	5.070	13.956	2.753	-	37.8	50.0	11.8
Frank Smith 30	5.068	13.977	2.758	-			

APPENDIX 11 - (Continued)

Specimen	ao (Å) (± 0.003)	co(Å) (± 0.005)	c/a	D	$MgTiO_3$	$FeTiO_3$	Fe_2O_3
Kamfersdam No 4	5.067	13.962	2.755	-			
Kamfersdam No 5	5.071	13.961	2.753	-			
Kamfersdam No 6	5.066	13.954	2.754	-			
Kamfersdam No 78	5.069	13.983	2.759	-			
Kamfersdam No 3	5.069	13.960	2.754	-			
Dutoispan No 1	5.070	13.980	2.757	-			
Dutoitspan No 2	5.067	13.975	2.758	-			
Monastry No 2	5.069	13.956	2.753	4.42			
Monastry 13	5.072	13.979	2.756	4.42	31.7	58.6	9.7
CF 315	5.066	13.995	2.763	-	46.5	46.7	5.9
CF 316	5.066	13.955	2.755	-	46.2	47.0	5.9
Eastern Kimberlite							
1010-13	5.070	13.932	2.746	-			
1010-12	5.065	13.970	2.758	-			
1010-15	5.067	13.976	2.758	-			
1010-42	5.067	13.966	2.756	-			
1010-42	5.070	13.972	2.756	-			
1010-43	5.066	13.956	2.755	-			
1060-30	5.070	13.94	2.750	-			
1060-30	5.068	13.959	2.754	-			
1010-35	5.065	13.97	2.758	-			
1060-32	5.067	13.954	2.754	-			
1060-22	5.069	13.963	2.755	-			
1060-28	5.086	14.045	2.762	-			
Black Kimberlite							
1060-29	5.099	13.953	2.736	-			
1010-15	5.070	13.985	2.758	-			
1060-26	5.066	13.963	2.756	-			
1060-43	5.067	13.972	2.757	-			
1010-20	5.067	13.984	2.760	-			
1010-17	5.068	13.957	2.754	-			

Specimen	ao (Å) (± 0.003)	co(Å) (± 0.005)	c/a	D	$MgTiO_3$	$FeTiO_3$	Fe_2O_3
Group I Kimberlite							
K 1010-3	5.073	13.987	-				
	5.088	13.989	-				
" 1010-3	5.067	13.926	-				
	5.079	14.057	-				
" 1060-10	5.069	13.960	2.754				
" 1010-39	5.072	13.992	-				
	5.079	14.033	-				
Eastern Kimberlite							
1010-41	5.085	14.015	2.756				
1010-40	5.084	13.990	2.752				
1060-7	5.066	13.959	2.755				
Ti 58	5.085	14.08	2.773				
Ti 59	5.077	14.08	2.773				
Ti 61	5.085	14.063	2.766				
Ti 62	5.087	14.22	2.795				
Ti 63	5.089	14.08	2.767				
Ti 64	5.086	14.09	2.770				
Western Kimberlite							
Ti 65	5.066	13.98	2.760				
Ti 66	5.070	13.99	2.759				
Ti 67	5.068	13.976	2.758				
Ti 68	5.070	13.989	2.759				
Group I Kimberlite							
Ti 68	5.071	14.01	2.763				
Ti 60	5.085	14.09	2.771				

****

APPENDIX 12 - The chemical analyses, molecular norms and the structural formulas of ilmenite

A. Chemical analyses of Ilmenite

	1	2	3	4	5	6	7	8	9	10	11
Fe_2O_3	7.1	7.7	13.2	8.1	13.0	10.80	7.05	14.30	11.27	15.56	13.71
FeO	24.0	23.5	25.4	27.4	25.5	28.80	27.05	28.18	29.34	19.15	27.57
MgO	13.44	12.98	10.82	6.50	10.52	9.00	12.10	9.00	8.87	15.84	8.65
H_2O^+	0.36	0.44	0.30	0.48	0.28	-	-	-	-	-	-
TiO_2	53.90	53.4	49.6	53.0	50.7	50.00	53.79	49.32	49.27	45.80	49.35
Cr_2O_3	0.80	1.06	0.04	0.98	0.40	-	-	-	0.70	2.63	-
MnO	0.40	0.44	0.19	2.88	0.23	-	-	-	0.29	-	0.05
NiO	0.20	0.18	0.11	0.20	0.10	-	-	-	-	-	-
Other *1)						2.00			0.13	1.05	0.20
Total	100.20	99.70	99.72	100.54	100.73	100.60	99.99	100.80	99.80	100.03	99.86
B. The Molecular norm of the ilmenite *2)											
Geikielite	46.5	46.2	37.8	27.0	37.8	31.7	42.1	32.5	32.6	57.2	32.3
Ilmenite	46.7	47.0	50.0	64.0	51.2	58.6	52.1	55.3	56.2	30.3	56.3
Pyrophanite	0.9	0.9	0.4	6.9	0.4	-	-	-	0.7	-	-
Hematite	5.9	5.9	11.8	2.1	10.6	9.7	5.8	12.2	10.5	12.5	11.4
Total	100.0	100.0	100.0	100.0	100.0	100.0	100.0	100.0	100.0	100.0	100.0
C. The ~~Structural Formulas~~ Chemical composition of the ilmenite											
$Mg^{2+}TiO_3$	49.4	49.2	42.8	27.7	42.2	35.7	44.7	37.0	36.4	65.4	36.0
$Fe^{2+}TiO_3$	49.6	49.9	56.7	65.3	57.3	64.3	55.3	63.0	62.8	34.6	64.0
$Mn\ TiO_3$	1.0	0.9	0.5	7.0	0.5	0.0	0.0	0.0	0.8	0.0	0.0
Total	100.0	100.0	100.0	100.0	100.0	100.0	100.0	100.0	100.0	100.0	100.0

	12	13	14	15	16	17	18	19	20	21	22
Fe_2O_3	17.10	10.77	11.90	10.50	30.0	18.48	22.70	9.13	27.68	21.97	22.38
FeO	27.12	25.11	27.99	26.50	21.4	28.22	25.63	27.81	25.20	26.58	25.28
MgO	8.65	10.35	7.20	10.70	8.1	6.26	5.04	8.68	4.86	7.16	6.44
H_2O^+	-	-	-	-	-	-	-	-	0.18	0.14	0.19
TiO_2	48.26	50.30	53.21	51.00	39.2	43.87	38.58	49.32	41.40	43.90	44.20
Cr_2O_3	-	2.16	-	-	-	1.30	1.56	0.74	-	-	-
MnO	0.26	0.21	-	0.23	0.45	-	-	0.20	nd	0.10	0.18
NiO	-	-	-	-	-	-	-	-	-	-	-
Other *1)	0.26	0.19	-	0.40	0.50	2.32	7.60	0.23	0.28	0.11	0.09
Total	100.65	99.63	100.30	99.33	99.65	100.45	101.11	100.10	99.60	99.96	99.76
Geikielite	30.7	38.6	30.1	36.9	37.1	24.1	20.3	33.4	19.4	26.2	25.1
Ilmenite	54.0	52.4	65.6	53.2	50.4	59.4	57.6	58.5	56.4	54.4	55.3
Pyrophanite	0.5	0.4	-	0.4	1.1	0.0	-	0.4	-	0.1	0.5
Hematite	14.8	8.6	4.3	9.5	11.6	17.5	22.1	7.7	24.2	19.3	19.1
Total	100.0	100.0	100.0	100.0	100.0	100.0	100.0	100.0	100.0	100.0	100.0
$Mg^{2+}TiO_3$	36.0	42.2	31.5	40.8	42.0	28.0	26.0	36.2	24.1	31.3	31.0
$Fe^{2+}TiO_3$	63.4	57.4	68.5	58.8	56.7	72.0	74.0	63.4	75.9	66.7	68.5
$Mn\ TiO_3$	0.6	0.4	0.0	0.4	1.3	0.0	0.0	0.4	0.0	2.0	0.5
Total	100.0	100.0	100.0	100.0	100.0	100.0	100.0	100.0	100.0	100.0	100.0

/.....

APPENDIX 12 (Continued)

	23	24	25	26	27	28	29	30	31	32	33
Fe_2O_3	21.88	18.30	18.85	17.47	16.72	23.32	18.27	18.64	17.48	15.13	15.87
FeO	25.20	27.00	26.48	26.28	28.80	28.80	26.28	26.28	25.56	27.72	26.28
MgO	4.64	6.43	6.66	7.28	7.92	-	5.60	6.96	8.30	8.68	8.82
H_2O^+	0.15	0.16	0.18	0.16	-	-	0.33	-	0.13	0.05	0.12
TiO_2	47.58	47.65	47.12	48.40	46.40	43.12	48.90	47.95	48.32	48.50	48.86
Cr_2O_3	-	-	-	-	-	-	-	-	-	-	-
MnO	0.17	0.20	0.15	nd.	0.10	0.06	nd	nd	0.18	0.18	0.18
NiO	-	-	-	-	-	-	-	-	-	-	-
Other *1)	0.12	0.08	0.10	0.06	0.09	0.08	0.10	0.08	0.08	0.10	0.08
Total	99.74	99.82	99.54	99.65	100.03	100.38	99.48	99.91	100.05	100.36	100.21
Geikielite	21.2	25.6	26.4	28.8	29.1	-	24.6	27.7	31.4	30.9	32.4
Ilmenite	64.8	60.3	58.6	58.3	56.7	83.6	64.7	58.6	54.3	55.4	54.1
Pyrophanite	0.4	0.5	0.3	-	0.1	0.2	-	-	0.5	0.4	0.4
Hematite	13.6	13.6	14.7	12.9	14.1	16.2	10.7	13.7	13.8	13.3	13.1
Total	100.0	100.0	100.0	100.0	100.0	100.0	100.0	100.0	100.0	100.0	100.0
$Mg^{2+}TiO_3$	24.6	29.6	30.8	33.2	33.8		27.5	32.1	36.3	35.7	37.1
$Fe^{2+}TiO_3$	74.9	69.8	68.8	66.8	66.1	99.8	72.5	67.9	63.1	63.8	62.4
Mn TiO_3	0.5	0.6	0.4	-	0.1	0.2	-	-	0.6	0.5	0.5
Total	100.0	100.0	100.0	100.0	100.0	100.0	100.0	100.0	100.0	100.0	100.0

	34	35	36	37	38	39	40	41	42	43	44
Fe_2O_3	15.51	10.00	14.32	14.32	17.96	13.15	6.2	-	0.25	2.77	10.17
FeO	25.94	30.24	28.80	42.13	26.29	28.00	8.4	1.4	10.09	5.44	16.57
MgO	9.62	9.78	9.88	1.65	8.60	9.00	24.4	31.8	25.79	27.90	15.56
H_2O^+	0.05	-	-	0.16	-	-	-	-	-	-	-
TiO_2	48.12	49.52	47.10	45.56	46.33	47.95	60.7	64.9	63.94	64.41	57.64
Cr_2O_3	-	-	-	-	0.41	0.75	-	-	-	-	-
MnO	0.14	0.14	0.10	0.44	-	-	0.91	0.4	-	-	-
NiO	-	-	-	-	-	-	-	-	-	-	-
Other *1)	0.05	0.07	0.07	1.06	0.30	0.40	-	2.2	-	-	-
Total	99.43	99.75	100.27	100.47	99.89	99.58	100.6	100.7	100.07	100.52	99.94
Geikielite	34.2	36.9	37.8		30.8	32.6	79.5	96.9	82.0	90.5	61.4
Ilmenite	51.7	56.9	52.8		52.9	55.5	15.4	2.4	18.0	9.5	36.8
Pyrophanite	0.2	0.3	0.1		-	-	1.7	0.7	0.0		0.0
Hematite	13.9	5.9	9.3		16.3	11.9	3.4	0.0	0.0		1.8
Total	100.0	100.0	100.0		100.0	100.0	100.0	100.0	100.0	100.0	100.0
$Mg^{2+}TiO_3$	39.8	39.3	41.7		36.8	37.0	82.3	96.9	82.0	90.5	62.5
$Fe^{2+}TiO_3$	60.0	60.5	58.2		63.2	63.0	15.9	2.4	18.0	9.5	37.5
$Mn\ TiO_3$	0.2	0.2	0.1		0.0	0.0	1.8	0.7	0.0	0.0	0.0
Total	100.0	100.0	100.0			100.0	100.0	100.0	100.0	100.0	100.0

	45	46	47	48	49	50	51	52	53	54	55
Fe_2O_3	5.43	-	1.87	8.94	5.57	6.03	-	-	8.92	6.98	5.70
FeO	24.40	12.14	24.15	25.44	41.76	40.87	44.32	45.83	42.40	45.10	43.32
MgO	14.18	24.66	15.97	6.26	0.88	1.72	0.79	1.25	0.27	-	0.56
H_2O^+	-	-	-	-	0.15	0.12	-	-	-	0.31	-
TiO_2	56.08	64.03	57.29	48.88	48.64	50.02	52.50	52.73	47.70	47.2	48.90
Cr_2O_3	-	-	-	-	-	-	-	-	-	-	-
MnO	-	-	1.10	2.60	1.10	0.48	1.36	-	0.37	0.05	0.35
NiO	-	-	-	-	-	-	-	-	-	-	-
Other *1)	-	-	0.37	7.68	1.51	0.96	0.06	-	0.26	0.56	1.30
Total	100.09	100.83	100.75	99.80	99.61	100.20	99.03	99.81	99.90	100.20	100.13
Geikielite	48.7	78.3	54.3	28.1	3.3	6.6	3.1	4.7	1.0	-	2.0
Ilmenite	47.1	21.7	44.0	61.3	89.2	87.1	94.3	95.3	89.9	96.1	92.4
Pyrophanite	0.0	-	-	6.4	2.1	0.9	2.6	-	0.8	0.1	0.8
Hematite	4.2	-	1.7	4.2	5.4	5.4	0.0	-	8.3	3.8	4.8
Total	100.0	100.0	100.0	100.0	100.0	100.0	100.0	100.0	100.0	100.0	100.0
$Mg^{2+}TiO_3$	50.8	78.3	55.2	29.3	3.5	7.0	3.1	4.7	1.1	-	2.2
$Fe^{2+}TiO_3$	49.2	21.7	44.8	64.0	94.3	92.0	94.3	95.3	98.0	99.9	97.0
$Mn\ TiO_3$	0.0	-	-	6.7	2.2	1.0	2.6	-	0.9	0.1	0.8
Total	100.0	100.0	100.0	100.0	100.0	100.0	100.0	100.0	100.0	100.0	100.0

APPENDIX 12 (Continued)

	56	57	58	59	60	61	62	63	64	65
Fe_2O_3	9.96	9.11	13.82	10.7	9.3	7.3	8.8	4.25	6.26	2.58
FeO	33.84	39.51	33.87	39.1	40.0	41.9	39.8	39.64	40.39	42.72
MgO	1.04	-	0.76	1.9	1.3	1.06	1.9	3.27	2.27	1.48
H_2O^+	0.18	-	0.38	-	-	-	-	0.03	0.06	0.04
TiO_2	52.80	46.60	46.00	47.7	47.4	49.3	48.6	51.19	49.89	51.97
Cr_2O_3	-	0.10	-	0.06	0.00	0.01	0.05	0.00	nil	nil
MnO	0.28	0.77	0.85	0.41	0.44	0.48	0.44	0.47	0.41	0.62
NiO	-	-	0.06	-	-	-	-	-	-	-
Other *1)	2.04	4.00	4.85	1.77	0.66	0.41	0.22	0.95	0.68	0.71
Total	100.14	100.40	100.59	100.29	99.10	100.46	99.81	99.80	99.96	100.12
Geikielite		3.3	3.5	7.1	5.3	3.9	7.1	8.6	12.1	5.7
Ilmenite		86.1	85.3	83.1	85.1	87.6	83.8	84.5	83.9	91.1
Pyrophanite		1.7	2.1	0.8	0.7	1.6	0.8	0.9	1.1	1.4
Hematite		8.9	9.1	9.0	8.9	6.9	8.3	6.0	3.9	1.8
Total		100.0	100.0	100.0	100.0	100.0	100.0	100.0	100.0	100.0
$Mg^{2+}TiO_3$	5.2	3.6	3.9	7.8	5.8	4.2	7.7	9.2	12.6	5.8
$Fe^{2+}TiO_3$	94.0	94.5	93.8	91.3	93.4	94.1	91.4	89.8	86.3	92.8
Mn TiO_3	0.8	1.9	2.3	0.9	0.8	1.7	0.9	1.0	1.1	1.4
Total	100.0	100.0	100.0	100.0	100.0	100.0	100.0	100.0	100.0	100.0

	66	67	68	69	70	71	72	73	74	75
Fe_2O_3	3.92	4.19	8.0	9.4	10.9	28.63	10.86	11.33	15.68	13.44
FeO	43.30	42.18	39.7	36.7	33.0	22.37	35.39	26.95	32.11	29.95
MgO	0.62	0.46	-	-	-	Nil	0.24	0.10	4.03	5.88
H_2O^+	0.07	0.13	-	-	-	-	0.46	0.64	-	-
TiO_2	50.31	50.02	51.2	49.2	53.3	48.41	49.64	46.23	48.38	50.42
Cr_2O_3	Nil	Nd	-	-	-	-	-	-	0.016	0.001
MnO	0.65	1.44	0.6	0.9	0.6	0.67	2.70	13.80	0.01	0.18
NiO	-	-	-	-	-	-	-	-	-	-
Other *1)	1.03	1.22	0.8	1.8	2.1	-	0.43	0.32	0.29	0.20
Total	99.90	99.64	100.3	98.0	99.9	100.08	99.72	99.67	100.41	100.07
Geikielite	2.3	1.7	-	-	-	-	1.0	0.2	23.3	16.1
Ilmenite	92.8	91.8	96.6	95.2		87.5	87.5	58.5	67.2	72.4
Pyrophanite	1.4	3.0	1.4	2.3		2.0	6.9	30.6	-	-
Hematite	3.5	3.5	2.0	2.5		10.5	4.6	10.7	9.5	11.5
Total	100.0	100.0	100.0	100.0		100.0	100.0	100.0	100.0	100.0
$Mg^{2+}TiO_3$	2.4	1.8	-	-	-	97.8	91.7	65.5	25.8	18.2
$Fe^{2+}TiO_3$	96.2	95.0	98.6	97.6	98.3	-	1.1	0.2	74.2	81.8
Mn TiO_3	1.4	3.2	1.4	2.4	1.7	2.2	7.2	34.3	0.0	0.0
Total	100.0	100.0	100.0	100.0	100.0	100.0	100.0	100.0	100.0	100.0

****

Appendix 12:

The chemical analyses, molecular norms and the structural formulas of ilmenite.

1. Ilmenite from Kimberlite:

1. CF 315; Premier Mine (New analysis).
2. CF 316; Premier Mine (-ditto-).
3. CF 317; Frank Smith (-ditto-).
4. CF 318; Concentrate Premier Mine (ditto).
5. CF 319; Concentrate Riverton (ditto).
6. Monastry Mine; Williams (1932).
7. Kimberley Mines; ditto
8. Frank Smith; ditto
9. Mukarob; Wagner (1914).
10. Wesselton; Williams (1932).
11. Kao; Nixon et al. (1963).
12. Thaba Patsoa; Dawson (1962).
13. Mukarob; Visser (1964).
14. Zefu; Verhoogen (1938).
15-16. Congo; Besson (1967).
17-18. Mabuki Mine; Hall (1938).
19. Elliot Co., Kentucky; Daly (1925).
20-37. Russian Kimberlites; Bobrievich et al., (1959).
38. Mir ; Smirnov (1959).
39. Zarnitsa; Nixon et al. (1963).

2. Metamorphic Ilmenites.

40. Wakefield; Hounslow & Chao; (1967).
41. Crestmore; Murdoch & Fahey (1953).
42-46. Ceylon; Dana System of Mineralogy (1900).
47. Layton Farm; Warwick; ditto
48. Potatas; Brazil; ditto
49-50. Italy; ditto
51 Sunsvale; Sweden; ditto
52. Ruwenzori; Congo; ditto
53-54. Uganda & Norway; Min abst (vol. 17, p. 408).
55. India; Trans. Roy. Soc. Edinburgh, (1955, p. 725).

3. Ilmenites from basaltic rocks.

56. From Russia; Smirnov, (1959).
57-58. From Isipingo; Coetzee, (1957).
59-62. From Makaopuhi lava, Hawaii; Evans and Moore (1968).
62-67. From Skaergaard; Vincent et al., (1954).
68-70. From Madagascar; Min abst (1965, p. 307).
71. From Mongolia; Min abst (1959, 341).
72. From Japan; Jap. Journ. Ass. Min & Petr, (1958, 280).
73. From Iwazuini Tuin; Min abst (1956, p. 201).
74-75. From alnoiite, Malaita; Min Mag (1965, p. 16).

* For the excess Ti^{4+} an amount of Fe^{3+} was subtracted according to the reaction:- $4FeTiO_3 + O_2 \rightarrow 2Fe_2O_3 + 4TiO_2$ The hematite and rutile obtained in this way was not considered in the molecular norm.

*1) Other oxides, unspecified.

A. Chemical analyses and compositions

	1	2	3	4	5	6	7	8	9	10	11	12	13	14	15	16	17	18	19
Al_2O_3	31	23	27	2.10	35.41	37.58	23	13	27	21	12	11.0	48.5	10.28	6.30		3.6	10.7	6.4
Fe_2O_3	3	4	4		3.30	3.38	4	6	3	5	6			3.30		52.00	14.1	14.9	26.9
FeO	16	18	18	22.14	10.82	11.45	19	22	17	19	22	25.2	13.5	14.09	19.58		43.9	26.3	27.2
Cr_2O_3	36	43	39	52.90	26.52	28.59	43	52	39	45	52	54.5	15.5	59.40	55.39	43.00	15.5	36.6	35.3
MgO	13	11	12	6.90	16.03	15.91	11	7	13	10	7	8.6	22.2	12.62	15.68	5.00	2.8	7.0	3.5
TiO_2				15.30	2.79	2.90								0.14	1.56		18.4	4.3	0.42
NiO					-	-						< 1.0	< 1.0		-				
Other					1.16	4.51						< 2.0	< 2.0	0.40	1.12		0.44	0.47	0.64
Total	99.0	99	99	99.34	100.35	100.00	100	100	99	100	100	99.3	98.7	100.23	99.63	100.00	98.74	10.27	100.36
ao	8.142	8.212	8.189				8.215	8.311	8.170	8.228	8.315								
n	1.810	1.935	1.880				1.936	2.091	1.860	1.803	2.105								

B. The Structural formulas of chromite based on 3 cations per unit cell.

Al^{3+}	1.02	0.86	0.97	0.10	1.28	1.32	0.86	0.51	0.99	0.79	0.50	0.43	1.51	0.40	0.25		0.31	0.48	0.27
Fe^{3+}	0.04	0.10	0.08	-	0.08	-	0.11	0.10	0.08	0.10	0.12	0.13	0.17	0.06	0.29	0.80	0.78	0.43	0.72
Cr^{3+}	0.84	1.04	0.95	1.90	0.64	0.68	1.03	1.39	0.93	1.11	1.38	1.44	0.32	1.54	1.46	1.20	0.90	1.09	0.99
Fe^{2+}	0.41	0.48	0.55	0.71	0.27	0.29	0.49	0.63	0.57	0.51	0.64	0.57	0.13	0.61	0.22	0.26	0.30	0.40	0.19
Mg^{2+}	0.59	0.52	0.45	0.29	0.73	0.71	0.51	0.37	0.43	0.49	0.36	0.43	0.87	0.39	0.78	0.74	0.70	0.60	0.81

C. The molecular norms of chromite

$MgAl_2O_4$	55	43	48	4.4	62.7	63.3	43	25	50	39	25	21.7	75.2	19.4	12.2	-	9.4	22.3	13.5
$MgCr_2O_4$	5	10	7	18.8	9.2	4.5	7.	12	7	10	12	21.2	12.1	41.7	64.1	26.2	8.7	14.6	5.3
$FeCr_2O_4$	37	44	41	55.5	21.9	27.8	45	57	39	46	58	50.5	4.2	35.2	6.8	33.9	18.3	35.7	44.5
$FeAl_2O_4$	-	-	-	21.3 *1)	2.5 *2)	4.4 *2)						-	-	-	2.6 *1)		40.4 *1)	7.6 *1)	-
$FeFe_2O_4$	3	4	4		3.7		5	6	4	5	5	6.6	8.5	3.3	14.4	39.9	23.2	19.8	36.7
Total	100.0	100.0	100	100.0	100.0	100.0	100	100	100	100	100	100.0	100.0	100.0	100.0	100.0	100.0	100.0	100.0

****

Appendix 13:

The chemical compositions, molecular norms and structural formulas of chromite.

*1) ilmenite
*2) hematite and rutile.

A. Analyses and compositions of chromite from kimberlite.

1, 2, 3, from Premier Mine, samples P.M. 1060-25, 1570-9, 1010-38.
4, from Jagersfontein, Hall (1938, No. 1761).
5, 6 from Russia, Milashev (1965).

B. Analyses from ultramafic nodules.

7, 8, 9, 10, 11 from Premier Mine, samples P.M. $893In_{21}$, $893In_4$, $893In_8$, $1010In_2$, $893In_3$.
12, 13 from Mayagues Serpentinite; Lapham (1964).
14 from Twin Sister Mountains, Deer, Howie and Zussman (1967, p 427).
15, 16 from Great Dyke and Bushveld Complex respectively, Hall (1938, No. 4909, 1760).
17-19 from Makaophi lava, Evans & Moore (1968).

C. The analyses depicted in figures were derived from the following sources:-

1. Bilgrami (1969, 134).
2. Worst (1964, p 209).
3. Cameron (1964, 131).
4. Park and MacDairmid (1964).
5. MacGreggor (1964, 203).
6. Pearre and Heyl (1960).

APPENDIX 14 - The physical properties and the enstatite and alumina contents of the orthopyroxene from kimberlite and garnet peridotite

Sample		n_α ± 0.003	n_β ± 0.003	n_γ ± 0.003	$2V^o$ ± 2°	a_o(Å) ± 0.010	b_o(Å) ± 0.003	c_o(Å) ± 0.003	%En *1)	$\%Al_2O_3$ *2)	% En *3)	Al^{3+} *4)
A. Own Determinations												
1. Ultramafic nodules												
Jagersfontein	1	1.662		1.673	-67		8.811		94	0.9	-	0.05
	4	1.658		1.670		18.29	8.825	5.188	96	0	80	0.02
	5	1.658		1.666	+76	18.29	8.825	5.188	97	0	80	0.01
	6	1.660		1.669	+72	18.30	8.823	5.190	95	0.10	80	0.03
	3	1.661		1.670		18.30	8.825	5.190	96	0	80	0.02
Kimberley	1	1.657		1.666	+78	18.27	8.819	5.182	98	0.2	90	0.01
Bultfontein	6	1.659		1.671	+73	18.28	8.818	5.186	95	0.1	87	0.02
	7	1.658		1.668	+75	18.28	8.822	5.183	96	0.1	90	0.02
	8	1.656		1.667	+74	18.28	8.830	5.182	97	0	90	0
	9	1.658		1.669	+76	18.27	8.822	5.181	96	0	91	0.01
	1	1.655	1.658	1.666	+78		8.819		97	0.1		0.02
					+74				93			
De Beers	5	1.657		1.668	+79	18.29	8.829	5.186	96	0	87	0
	4				+74				93			
Frank Smith	3	1.660		1.669		18.30	8.829	5.190	97	0	80	0
	4	1.659		1.669	+81°	18.28	8.824	5.176	94	0	94	0.02
	2	1.661		1.670	+80°		8.820		93	0		0.03
Dutoitspan	2	1.662	1.668	1.673			8.818		95	0.10		0.02
Premier Mine:-												
P.M. 893 In_{22}		1.660	-	1.670	+64°	18.30	8.828	5.189	97	-	80	0.00
P.M. 893 In_{23}		1.659	-	1.671	+78°	18.28	8.825	5.193	95	-	79	0.03
P.M. 893 In_{14}		1.652	-	1.668	+75°	18.28	8.818	5.187	94	0.1	83	0.03
P.M. 1010 In_{10}					+77°	18.17	8.817	-	92	0.2	-	0.04
P.M. 893 In_{15}		1.659	1.661	1.669	+75°	18.30	8.825	5.184	96		89	0.02
P.M. 1010 In_7		1.653		1.666	+75°	18.27	8.816	5.185	97	0.2	88	0.02
P.M. 1010 In_6		1.653	-	1.667	+75°	18.32	8.829	5.188	97		80	0.00
P.M. 893 In_{19}		1.654	-	1.671	+79°	18.28	8.822	5.182	94		90	0.02
P.M. 893 In_1		1.658	-	1.667	+87°	18.31	8.832	5.193	92		79	0.03
P.M. 893 In_3					+81°	18.30	8.829	-	91		-	0.04
P.M. 893 In_{11}		1.653	-	1.662		18.28	8.816	5.183	100	0.2	89	0.00

APPENDIX 14 - (Continued)

Sample	$n\alpha'$ ± 0.003	n_β +0.003	n_γ +0.003	$2V^o$ ± 2°	a_o(Å) ± 0.010	b_o(Å) ± 0.003	c_o(Å) ± 0.003	%En *1)	$\%Al_2O_3$ *2)	%En *3)	Al^{3+} *4)
P. M. 893 In_{13}	1.652	-	1.667		18.29	8.824	5.186	98		87	0.00
P. M. 893 In_{16}	1.659	-	1.669		18.30	8.829	5.192	97		79	0.00
P. M. 893 In_7	1.662	1.665	1.673	+85°	18.28	8.828	5.184	94		89	0.01
	1.662	1.665	1.672	+83°	18.24	8.825	-	94		-	0.02
P. M. 893 In_6	1.664	1.669	1.676	+79°	-	8.821	-	92	0.10		0.040
	1.664	1.668	1.678	+80°	-	8.832	-	91	-		0.035
	1.664	1.668	1.675	+78°	18.29	8.825	5.179	92	-	91	0.030
P. M. 893 In_6	-	-	-	+78°	-	-	-	92			
P. M. 893 In_5	1.661	1.668	1.673	+80°	-	-	-	93			
P. M. 1010 In_2	1.664	1.667	1.673	+76°	-	-	-	92			
P. M. 1010 In_3		Not measureable									
P. M. 893 In_4	1.661	1.668	1.673	+81°	-	8.835	-	93	0.00		0.020
P. M. 893 In_{17}	1.660	-	1.668	+78°	18.29	8.957	5.189	94		80	0.00
P. M. 1010 In_8	1.654	-	1.668	+79°	18.29	8.822	5.188	93		80	0.03
P. M. 893 In_{18}	1.659	1.662	1.668	+77°	18.29	8.818	5.186	95	0.1	87	0.02
CF_{311}					18.26	8.859	5.177		0.00	93	0.00
CF310					18.31	8.825	5.188		0.00	80	0.07
2. From Kimberlite											
Dutoitspan 11				+75°	-	-	-	93			
Wesselton 3				+73°	-	-	-	94			
De Beers 12	1.662	-	1.670		18.27	8.806	5.180	96	1.20	91	0.05
Glas:-											
Brakfontein	1.668	-	1.679		18.30	8.831	5.180	88	0.00	91	0.02
1060 - 26					18.27	8.807	5.173		1.20	96	0.03
1060 - 29					18.28	8.820	5.184		0.10	89	0.05

APPENDIX 14 (Continued)

B. Determinations from Literature

Reference	n_α	n_β	n_γ	2V	%En *1)
1. Ultramafic nodules in kimberlite					
O'Hara & Mercy(1963) *1)	-	1.666	-	-	92
	-	1.664	1.670	$+74^o$	94
	1.661	1.664	1.668	$+78^o$	95
	-	1.663	1.670	$+75^o$	94
	1.658	1.661	1.667	$+71^o$	96
	1.655	1.662	1.667	$+71^o$	96
	1.662	1.666	1.671	$+78^o$	94
	-	1.669	1.672	-	93
Bobrievich et al.,(1959)	1.660	-	1.670	$+82^o$	91
	1.662	-	1.672	$+78^o$	93
	1.680	-	1.690	$+74^o$--+82	92
	1.700	-	1.712	-68^o	75
	1.700	-	1.708	-66^o	74
	1.700	-	1.714	-68^o	75
	1.698	-	1.712	-68^o	75
	1.700	-	1.710	-67^o	75
	1.706	-	1.718	-65^o	74
	1.702	-	1.714	-68^o	75
	1.706	-	1.718	-64^o	73
	1.698	-	1.703	-66^o	75
	1.700	-	1.712	-69^o	76
	1.714	-	1.724	-65^o	74
	1.702	-	1.712	-60^o	72
	1.706	-	1.718	-69^o	76
	1.667	-	1.679	-	90
	1.678	-	1.690	-74^o	79
	1.668	-	1.678	$+76^o$	92

APPENDIX 14 -(Continued)

Reference	n_α	n_β	n_γ	2V	%En *1)
Nixon et al, (1963)*3)	1.660	1.664	1.670	$+77^o$	95
	1.672	1.686	-	-	84
	1.661	1.665	1.672	$+79^o$	94
	1.660	1.665	1.671	$+79\frac{1}{2}$	95
	1.658	1.662	1.669	$+74^o$	96
	1.656	1.661	1.671	$+78\frac{1}{2}$	94
	1.661	1.665	1.672	$+79^o$	94
	1.662	1.667	1.672	$+79^o$	94
O'Hara + Mercy (1963)*1)	1.659	1.662	1.667	$+75^o$	95
	1.664	1.667	-	$+74^o$	93
	-	1.669	1.675	-	92
	-	1.662	1.667	-	95
	-	1.661	1.665	$+60^o$	98
2. From Kimberlite					
Nixon et al, (1963)*3)	1.660	1.665	1.671	$+77^o$	95
	1.660	1.664	1.670	$+75^o$	96
	1.657	1.662	1.669	$+70\frac{1}{2}$	97
	1.657	1.662	1.669	$+71\frac{1}{2}$	95
	1.664	1.669	1.676	+870	93
	1.666	1.672	1.678	-89^o	90
	1.669	1.675	1.680	$-86\frac{1}{2}$	87
	1.671	1.676	1.883	-83	84
	1.666	-	1.676	-	90
	1.655	-	1.666	-	97
	1.656	-	1.665	-	97

Reference	nα	nβ	nγ	D	2V	%En
Ross et al. (1954) *4)	-	-	-	3.302		87
	-	-	-	3.211		97
	-	-	-	3.302		87
				3.304		87
				3.305		87
				3.279		90
				3.312		85
				3.297		88
				3.298		89
				3.304		87
				3.278		91
4. From Regional garnet peridotite						
O'Hara & Mercy (1963)*1)	1.662	1.666	1.671		+79	96
	-	1.663	1.668		-	96
	-	-	1.666		-	98
	-	1.665	1.671		-	94
	-	-	1.671		-	94
	-	-	1.676		-	92
	1.673	1.678	1.684		-82^{o}	84
	1.670	1.674	1.677		+89	88
	-	-	1.673		-	93
	-	1.667	-		$+86^{o}$	91
	1.665	1.670	1.673		$+86^{o}$	92
	.663	1.667	1.673		$+81^{o}$	92
	1.664	1.668	1.673		$+87^{o}$	91
	-	-	1.672		$+71^{o}$	94
	-	-	1.671		-	95
	-	-	1.673		-	93
	1.660	1.664	1.670		-	96

****

Appendix 14:

The physical properties and the enstatite and alumina contents of the orthopyroxene from kimberlite and garnet peridotite.

The unit cell dimensions were determined by means of a Guinier Camera, using Cu K radiation.

*1) Enstatite percentage after Tröger (1959), using the refractive indices where possible.

*2) The percentage Al_2O_3 in the [illegible] orthopyroxene after Skinner + Boyd (Carn. Inst. Yearb. 63, 1964 p.163-16

*3) The En-value = 100 Mg/Mg+Fe^{2+} + Fe^{3+} + Mn, after Brown (1967), using the $c_0^{k_\alpha}$ value.

*4) The percentage Al^{3+} in the Y position in the orthopyroxene after Brown (1967).

APPENDIX 15 - The Al^{3+} and Ca^{2+} contents of the orthopyroxenes from kimberlite and garnet periodotite nodules, after Zwaan (1954 P_{-209}^{206})

Specimen	Δd (10.3.1-060) (±0.002 Å)	Al^{3+} (± 0.015)	Δd (21.1qz-060) (± 0.002 Å)	Al^{3+} (± 0.015)	d(20.3qz-11.3.1) (± 0.002Å)	Ca^{2+} (±0.015)
A. Kimberlite						
1060-26	0.0163	-	0.077	> 0.090	0.0126	< 0.010
1060-29	0.0160	-	0.078	> 0.100	-	-
DB -12	0.0158	0.020	0.074	0.030	0.0139	<0.010
"Glassy" type Brakfontein	0.0150	0.040	0.071	0.050	0.0160	< 0.010
B. Ultramafic Nodules:-						
Bu 1 Bultfontein	0.0140	< 0.010	0.073	0.010	0.0203	0.080
Bu 6	0.0150	0.020	0.074	0.035	0.0136	< 0.010
Bu 7	0.0148	0.020	0.073	0.035	0.0145	< 0.010
Bu 8	0.0136	< 0.010	0.071	< 0.010	0.0148	< 0.010
Bu 9	0.0144	0.010	0.073	0.025	0.0143	< 0.010
Fs. 2. Frank Smith	0.0238	> 0.090	0.081	> 0.090	-	-
Fs 3	0.0146	0.010	0.072	0.010	0.0150	< 0.010
Fs 5	0.0236	> 0.090	0.081	> 0.090	0.0213	0.100
P.M. 1010 In_6	0.0153	0.030	0.072	< 0.020	-	-
893 In_6 No.1	0.0156	0.030	0.073	0.040	-	-
893 In_6 No.2	0.0161	0.040	0.071	0.040	-	-
893 In_6 No. 3	0.0153	0.030	0.072	0.050	0.0156	< 0.010
893 In_7	0.0154	0.020	0.072	0.030	-	-
893 In_4	0.0150	0.030	0.071	0.030	0.0171	0.015
893 In_{16}	0.0156	0.030	0.074	0.045	0.0144	< 0.010
893 In_3	0.014	< 0.010	0.070	0.055	0.2019	0.070
893 In_1	-	-	-	-	0.0166	< 0.010
1010 In_{10}	0.0146	0.035	0.074	0.050	0.0206	0.080
893 In_{15}	0.0149	0.010	0.072	0.010	0.0152	< 0.010
893 In_{19}	0.0147	0.030	0.073	0.040	0.0146	< 0.010
1010 In_8	0.0154	0.030	0.073	0.045	0.0153	<0.010
1010 In_7	0.0180	0.055	0.076	0.055	-	-
893 In_{11}	0.0148	< 0.010	0.074	0.030	0.0143	< 0.010
893 In_{13}	0.0226	> 0.090	0.078	0.015	0.0144	< 0.010
893 In_{22}	0.0147	< 0.010	0.072	0.010	0.0159	< 0.010
893 In_{23}	0.0147	0.025	0.072	0.030	0.0158	< 0.010

APPENDIX 15 - (Concluded)

Specimen	Δd (10.3.1-060) ± 0.002 Å)	Al^{3+} (± 0.015	Δd (21.1qz-060) (± 0.002 Å)	Al^{3+} (± 0.015)	d(20.3qz-11.3.1) (± 0.002Å	Ca^{2+} (±0.015
P.M. 893 In_1	0.0161	0.050	0.071	0.040	0.0169	< 0.010
893 In_{18}	0.0154	0.045	0.073	0.050	0.0150	< 0.010
893 In_{17}	0.0151	0.020	0.072	0.030	0.0159	< 0.010
893 In_7	0.0049	0.020	0.072	0.030	-	-
C.F. 311	0.0154	-	0.076	-	0.0128	< 0.010
C.F. 310	0.0151	-	0.072	-	0.0153	< 0.010
893 In_{14}	0.0153	0.020	0.073	0.035	0.0139	< 0.010
Dutoitspan 2	0.0146	0.030	0.074	0.060	-	-
Kimberley 1	0.0148	< 0.010	0.073	0.010	0.0143	< 0.010
De Beers 5	0.0142	< 0.010	0.072	0.015	0.0155	< 0.010
Jagersfontein 1	0.0159	0.030	0.072	0.040	0.0199	0.080
3	0.0152	0.015	0.072	0.020	0.0153	< 0.010
4	0.0151	0.010	0.072	0.020	-	-
5	0.0158	0.015	0.072	0.010	0.0153	< 0.010
6	0.0163	0.040	0.073	0.045	0.0157	< 0.010

****

APPENDIX 16 - The chemical analyses, molecular norms and structural formulas, (calculated after Hess (1949)) of orthopyroxenes from ultramafic nodules and from kimberlites

A. The Chemical analyses of the Orthopyroxenes

	1	2	3	4	5	6	7	8	9	10	11	12	13	14
SiO_2	51.45	52.80	57.70	51.3	56.61	58.48	57.11	56.08	57.79	57.02	55.80	51.68	56.33	54.82
Al_2O_3	2.12	2.28	0.37	6.05	0.86	0.88	1.00	1.80	0.79	1.07	4.02	2.96	1.28	1.00
Fe_2O_3	1.33	0.13	1.18	-	1.35	0.72	1.82	1.47	-	0.72	0.76	2.45	0	0
FeO	4.56	4.10	3.79	12.8	3.73	3.93	3.61	2.41	3.96	3.76	4.85	2.77	7.75	5.28
MnO	0.14	0.14	0.09	-	0.10	0.02	0.12	0.10	0.10	0.11	-	0.10	0.12	0.09
MgO	36.05	38.45	35.55	29.9	35.90	34.71	34.02	36.80	36.36	35.86	34.70	34.58	32.74	35.62
CaO	1.72	0.35	0.55	0.70	0.70	0.50	1.50	1.76	0.53	0.82	none	1.57	1.03	0.60
Na_2O	0.24	0.06	0.24	-	0.09	0.23	0.35	-	-	0.09	-	0.60	0.02	-
K_2O	0.02	0.05	-	-	tr	0.08	0.03	-	-	0.01	-	0.33	-	-
H_2O	-	-	0.43	-	0.44	0.21	0.28	-	0.36	-	0.23	0.53	0.19	-
TiO_2	0.31	0.11	tr	0.36	0.00	tr	0.13	0.06	0.007	0.03	none	0.06	0.02	0.03
Cr_2O_3	0.38	0.26	0.34	0.32	0.17	0.25	0.35	-	0.23	0.23	0.20	1.30	0.58	0.80
NiO	0.16	0.11	-	-	-	-	-	-	-	-	-	0.12	0.04	0.05
Loss	-	-	-	-	-	-	-	-	-	-	-	2.09	-	-
Other	-	-	-	-	-	-	-	0.04	-	0.02	-	-	-	-
Total	98.48	98.84	100.24	101.43	99.95	100.01	100.32	100.52	100.117	99.74	100.56	100.61	100.10	98.29
B. Molecular norms														
Enstatite	89.5	92.1	91.0	80.0	90.9	88.8	85.2	90.1	91.6	90.1		83.8	83.2	89.1
Ferrosillite	5.4	5.7	5.4	12.1	5.2	5.5	4.8	3.1	5.6	5.5		4.0	11.2	7.6
Diopside	2.1	0.8	0.6	1.5	2.5	1.9	5.5	6.3	2.1	2.9		5.4	4.0	2.2
Acmite	1.6	0.4	1.6		0.8	0.4	2.7			0.6		5.2		
Jadeite	1.4 *1)	0.2	1.4 *2)		0.4 *2)		1.0 *2)							
$CaTiAl_2O_6$		0.4	-	1.1		-	0.2		0.0					
$Cr_2Al_2O_6$		0.4		0.4	0.2	0.4	0.5		0.3	0.3		1.7	0.8	1.1
$Fe^{3+}_2Al_2O_6$										0.6		0.4		
Al_2O_6				4.9		1.5 *1)	0.1	0.5	0.4	-			0.8	
Total	100.0	100.0	100.0	100.0	100.0	100.0	100.0	100.0	100.0	100.0		100.0	100.0	100.0

C. Structural formulas

	1	2	3	4	5	6	7	8	9	10	11	12	13	14
Si^{4+}		1.91	2.0	1.79	1.95	2.00	1.96	1.90	1.98	1.95		1.84	1.96	1.94
Al^{3+}		0.09		0.21	0.03	0.01	0.04	0.06	0.02	0.05		0.12	0.04	0.04
Al^{3+}		-	0.01	0.04	0.02	0.03	-	0.01	0.01	-			0.02	
Ti^{4+}		-	-	0.01	-	-	0.01	-	-					
Cr^{3+}		0.01	-	0.01	-	-	0.05	-	-	0.01		0.03	0.02	0.02
Fe^{3+}		-	0.03	-	0.02	0.02	-	0.04	-	0.02		0.06		
Mg^{2+}		2.04	1.91	1.56	1.84	1.80	1.74	1.96	1.85	1.82		1.84	1.64	1.84
Fe^{2+}		0.13	0.11	0.37	0.11	0.12	0.11	0.07	0.16	0.11		0.09	0.24	0.15
Ca^{2+}		0.01	0.02	0.02	0.02	0.02	0.06	0.06	0.02	0.03		0.06	0.04	0.02
Na^{+} & K^{+}		0.01	-		0.01	0.02	0.03	-	-	0.01		0.05		

	15	16	17	18	19	20	21	22	23	24	25	26	27
SiO_2	51.56	-								56.16	55.91		
Al_2O_3	1.60	1.39	0.30	1.03	1.60	1.08	1.28	1.09	0.38	-	0.90	2.65	1.09
Fe_2O_3	-	-	-					-	-	1.97	-	-	-
FeO	6.72	6.84	5.16	5.97	12.29	8.32	7.36	8.62	5.87	7.88	10.60	4.90	4.83
MnO	0.12	0.124	0.129	0.144	0.19	0.102	0.103	0.095	0.88	0.44	0.16	0.107	0.125
MgO	37.88	34.90	37.17	35.68	31.21	34.73	34.56	33.64	36.74	33.82	31.74	36.21	36.50
CaO	0.93	0.51	0.06	0.33	0.53	0.26	0.52	0.24	0.02		0.45	0.50	0.34
Na_2O	-	-	-	-	-	-	-	-	-		nd	-	-
K_2O	-	-	-	-	-	-	-	-	-		nd	-	-
H_2O	-	-	-	-	-	-	-	-	-	-	-	-	-
TiO_2	0.16	0.10	0.038	0.036	0.11	0.091	0.074	0.084	0.034		0.08	0.046	0.046
Cr_2O_3	0.63	0.12	0.023	0.081	0.028	0.081	0.062	0.044	0.033		0.08	0.58	0.41
NiO	0.15	0.08	0.06	0.11	0.082	0.10	0.086	0.085	0.087		0.08	0.10	0.090
Loss	-	-	-	-	-	-	-	-	-		-	-	-
Other	-	0.01	0.006	0.008	0.008	0.010	0.014	0.089	0.010		-	0.009	0.010
Total	99.75									100.27	100.00		
Enstatite	87.3	88.3	92.3	89.9	79.8	87.0	87.1	86.4	91.7	88.2	82.3	90.4	91.3
Ferrosillite	8.9	9.6	7.5	8.8	18.1	11.8	10.8	12.7	8.3	7.0	15.9	7.0	7.0
Diopside	2.6	1.9	0.2	1.2	2.0	1.0	1.9	0.8	-	-	1.6	1.8	1.2
Acmite	-	-	-	-	-	-	-	-	-	-	-	-	-
Jadeite	-	-	-	-	0.0	-	-	-	-	-	-	-	-
$CaTiAl_2O_6$	0.4	0.1			0.1	0.1	0.1	0.1			0.1	-	-
$Cr_2Al_2O_6$	0.8	0.1		0.1		0.1	0.1			0.3	0.1	0.8	0.5
$Fe^{3+}_2Al_2O_6$										0.5			
Al_2O_6										4.0			
Total	100.0	100.0	100.0	100.0	100.0	100.0	100.0	100.0	100.0	100.0	100.0	100.0	100.0

APPENDIX 16 (Continued)

	15	16	17	18	19	20	21	22	23	24	25	26	27
Si^{4+}	1.88									1.91	1.96		
Al^{3+}	0.12									0.09	0.04		
Al^{3+}										0.08			
Ti^{4+}	0.01												
Cr^{3+}	0.03									0.03			
Fe^{3+}													
Mg^{2+}	1.66									1.77	1.66		
Fe^{2+}	0.27									0.14	0.21		
Ca^{2+}	0.06										0.02		
Na^{+} & K^{+}													

	28	29	30	31	32	33	34	35	36	37	38	39	40
SiO_2				57.12		54.63	55.04	54.40	53.84	53.92	55.70	54.86	54.78
Al_2O_3	1.21	1.26	1.39	1.53	1.33	2.39	3.91	4.10	4.80	5.32	2.56	2.66	3.50
Fe_2O_3	-	-	-	0.06	-	1.71	-	-	0.16	-	-	-	-
FeO	4.86	4.74	4.28	5.00	6.48	7.07	5.93	6.83	6.21	6.10	5.77	6.32	6.86
MnO	0.112	0.110	0.097	0.114	0.145	0.14	0.15	0.13	0.12	0.12	0.10	0.12	0.13
MgO	35.90	36.35	36.40	36.22	34.58	30.30	33.56	32.84	32.48	32.45	33.86	34.14	33.28
CaO	0.83	0.58	0.54	0.24	1.18	2.20	1.02	0.84	1.00	1.36	0.75	0.60	0.62
Na_2O	-	-	-	-	-	0.45	-	0.04	0.15	0.08	0.11	-	0.07
K_2O	-	-	-	-	-	0.11	-	-	-	-	-	-	0.03
H_2O	-	-	-	-	-	1.01	0.20	0.15	-	0.08	0.10	-	0.13
TiO_2	0.059	0.060	0.049	0.074	0.055	0.36	0.10	0.003	0.03	0.007	0.02	0.28	0.15
Cr_2O_3	0.25	0.23	0.15	0.17	0.17	-	0.34	0.76	0.90	0.94	0.73	0.80	0.55
NiO	0.11	0.11	0.11	0.10	0.10	-	0.07	0.07	0.07	0.07	0.10	-	0.09
Loss	-	-	-	-	-	-	-	-	-	-	-	-	-
Other	0.015	0.015	0.015	0.014	0.026	0.12	0.02	-	-	-	-	0.01	0.01
Total	-	-	-	100.76	-	100.49	100.34	100.34	99.79	100.44	99.80	99.79	100.07
Enstatie	89.5	90.6	91.5	91.5	86.0	75.7	85.2	83.4	82.3	81.7	86.6	86.6	84.8
Ferrosillite	7.1	6.8	6.2	7.2	9.4	9.6	8.5	9.9	8.9	8.9	8.4	8.5	10.1
Diopside	2.9	2.2	2.0	0.9	4.3	8.3	3.7	3.1	3.7	5.0	2.7	2.2	2.2
Acmite	-	-	-	-	-	0.4	-	1.0	0.4	0.4			
Jadeite	-	-	-	-	-	3.6		0.2	0.6		0.6		0.6
$CaTiAl_2O_6$	0.1	0.1	0.1	0.2	0.1	0.4	0.2					0.4	0.2
$Cr_2Al_2O_6$	0.4	0.3	0.2	0.2	0.2		0.4		1.3	1.2	1.0	1.1	0.8
$Fe^{3+}_2Al_2O_6$													
Al_2O_6						2.0	2.0	2.4	2.8	2.8	0.7	1.3	1.3
Total	100.0	100.0	100.0	100.0	100.0	100.0	100.0	100.0	100.0	100.0	100.0	100.0	100.0

	28	29	30	31	32	33	34	35	36	37	38	39	40
Si^{4+}				1.93		1.94	1.88	1.88	1.86	1.84	1.92	1.92	1.90
Al^{3+}				0.07		0.06	0.12	0.12	0.14	0.16	0.08	0.08	0.10
Al^{3+}						0.03	0.04	0.06	0.06	0.06	0.02	0.02	0.02
Ti^{4+}						-						0.01	0.01
Cr^{3+}						-	0.01	0.02	0.03	0.02	0.02	0.02	0.02
Fe^{3+}						0.04							
Mg^{2+}				1.82		1.60	1.70	1.68	1.68	1.66	1.74	1.78	1.72
Fe^{2+}				0.16		0.20	0.17	0.20	0.18	0.17	0.17	0.18	0.20
Ca^{2+}				0.01		0.08	0.04	0.04	0.04	0.04	0.02	0.02	0.02
Na^{+} & K^{+}						0.04			0.01		0.01		0.01

APPENDIX 16 (Continued)

	41	42	43	44	45	46	47	48	49	50	51	52	53
SiO_2	55.38	54.85	56.00	53.46	55.60	57.34	55.91	55.20	54.96	52.36	54.13	51.78	52.84
Al_2O_3	2.97	2.18	2.50	0.95	-	3.91	2.64	2.95	2.89	6.17	1.62	6.22	0.44
Fe_2O_3	-	-	-	-	-	-	-	0.75	0.00	1.91	0.85	0.30	1.06
FeO	5.66	5.99	5.00	8.77	1.20	7.17	4.99	6.02	6.23	7.63	5.70	11.78	16.89
MnO	0.12	0.09	0.50	-	-	-	-	0.05	0.05	0.16	0.14	0.16	0.56
MgO	34.19	33.72	36.50	25.93	34.90	30.19	34.91	34.37	33.92	25.81	34.55	27.49	23.51
CaO	0.74	1.72	-	2.53	4.70	0.49	0.46	0.00	0.82	4.90	0.57	1.30	4.06
Na_2O	0.06	0.08	-	-	-	-	-	0.18	-	0.55	0.16	0.12	0.19
K_2O	-	0.07	-	-	-	-	-	0.11	-	0.02	0.16	-	-
H_2O	0.14	0.18	-	-	-	-	-	0.08	-	0.04	1.90	-	0.22
TiO_2	0.05	0.033	-	-	-	-	-	0.16	0.24	0.37	0.12	0.23	0.22
Cr_2O_3	0.80	0.80	0.60	-	-	-	0.54	-	-	0.25	0.21	0.01	-
NiO	0.07	0.08	-	-	-	-	-	-	-	-	0.08	-	-
Loss	-	-	-	8.36	-	0.44	-	-	-	-	-	-	-
Other	-	-	-	-	-	-	-	-	-	-	-	-	-
Total	100.18	99.79	101.10	100.0	96.40	99.54	99.45	99.87	99.11	100.17	199.19	99.74	99.99
Enstatite	85.4	83.7	91.9	73.0	81.1	79.7	89.3	87.7	86.3	59.7	87.1	71.2	60.2
Ferrosillite	8.2	8.5	2.8	13.9	1.5	10.1	6.3	8.7	9.1	10.8	8.4	17.3	22.7
Diopside	2.7	6.2		10.8	17.4	1.9	1.7		2.9	18.6	2.2	5.0	15.8
Acmite		0.5						1.6		3.9	1.7	0.6	1.3
Jadeite	0.4									0.6*2)	0.3*2)		
$CaTiAl_2O_6$	1.1							0.6	0.3	0.4		0.3	
$Cr_2Al_2O_6$		1.1	4.3				0.7			0.3	0.3		
$Fe_2^{3+}Al_2O_6$													
Al_2O_6	2.2			2.3*1		8.3*1	2.0	1.4	1.4	5.7		5.6	
Total	100.0	100.0	100.0	100.0	100.0	100.0	100.0	100.0	100.0	100.0	100.0	100.0	100.0

	41	42	43	44	45	46	47	48	49	50	51	52	53
Si^{4+}	1.89	1.91	1.90	2.00	1.92	2.00	1.93	1.90	1.91	1.87	1.94	1.85	1.96
Al^{3+}	0.11	0.09	0.10	-	0.08	-	0.07	0.10	0.09	0.13	0.06	0.15	0.02
Al^{3+}	0.05	0.01	-	0.04	-	0.16	0.04	0.04	0.03	0.11	-	0.11	
Ti^{4+}			0.01				0.01		0.01				
Cr^{3+}	0.02	0.02						0.01		0.01	0.0		
Fe^{3+}										0.05	0.02	0.01	0.03
Mg^{2+}	1.74	1.75	1.82	1.56	1.79	1.58	1.80	1.78	1.76	1.37	1.84	1.47	1.30
Fe^{2+}	0.17	0.18	0.17	0.29	0.04	0.21	0.13	0.18	0.18	0.23	0.18	0.35	0.53
Ca^{2+}	0.03	0.06	-	0.11	0.17	0.05	0.02		0.03	0.19	0.02	0.05	0.15
Na^{+} & K^{+}		0.01	-	-	-	-	-	0.02		0.04	0.02	0.01	0.01

****

Appendix 16:

The chemical analyses, molecular norms and structural formulas of orthopyroxenes from ultramafic rocks and from kimberlite.

I. Orthopyroxenes from ultramafic nodules in kimberlite.

1- CF 310; from garnet peridotite, Premier Mine (new analysis).
2 CF311; from peridotite, Premier Mine (ditto).
3 from Liqhobong; Nixon et. al., (1963).
4 from France; Bull. Soc. Franç, Crys. Min., (1967).
5- 7 from Thaba Putsoa; Nixon et. al., (1963).
8 from Mir; Sobolev, (1958).
9 from Kimberley, ditto.
10-11 from Bultfontein; MacGreggor and Ringwood, (1963).
12-15 from Russia; Bobrievich et. al., (1959).
16-23 from ultramafic nodules; O'Hara and Mercy, (1963).

II. Orthopyroxene from regional garnet peridotites.

24 from Norway.
25 from Karlskaret; Carswell, (1968).
26-32 from regional peridotites, O'Hara & Mercy, (1963).

III. Orthopyroxenes from kimberlites.

33-42 from Russian kimberlites; Bobrievich et. al., (1959).
43 from South Africa, Hall (1938).
44 from Kimberley Mines, (ditto).
45 from Jagersfontein, (ditto).
46 from Kimberley Mines, (ditto).
47 from Dutoitspan, (ditto).

IV. Orthopyroxene from nodules in alkaline basalts.

48-49 from Franç, Brousse (1968).
50-51 from Hawaii, Sobolev (1958).
52 Amer. Min. (53, 1968, 249).
53 Deer, Howie and Zussman, (1967, p 106).

*1) $Fe_2^{3+}Al_2^{3+}O_6$

*2) $Al_4^{3+}Si_3^{4+}O_{12}$

*3) $MgAl.AlSiO_6$

APPENDIX 17 - The d-values of the clinopyroxene from eclogite, Kyanite eclogite, garnet peridotite and kimberlite compared with those of the P2 and C2/c omphacite

P2 Omphacite Clark & Papike (1968)			C2/c C2/c Omphacite Coleman (1962)			20% $CaAl_2SiO_6$ Sa Kata (1957)		
I	d(Å)	hkl	hkl	d(Å)	I	I	d(Å)	hkl
10	4.371	020						
7	3.299	021	021	3.33	1	12	3.33	021
20	3.162	220	220	3.19	5	37	3.235	220
				3.12	1			
100	2.956	$\bar{2}21$	$22\bar{1}$	2.976	10	100	2.984	221
45	2.887	310	310	2.915	5	28	2.934	310
30	2.861	$31\bar{1}$	$31\bar{1}$	2.880	5	38	2.887	311
						7	2.862	$21\bar{1}$
						4	2.832	?
						3	2.769	?
						3	2.685	?
20	2.527	$\bar{1}31$	$13\bar{1}$	2.549	4	29	2.554	131
30	2.511	002	$20\bar{2}$	2.521	4	28	2.529	002
25	2.462	221	221	2.484	5	33	2.505	$22\bar{1}$
						5	2.378	131
10	2.247	311	311	2.268	3.5	14	2.291	311
7	2.186	112	$22\bar{2}$ 112	2.192	3	9	2.214	112
						10	2.197	022
			330	2.127	7	12	2.143	330
15	2.102	$\bar{3}31$	$33\bar{1}$	2.118	7	23	2.125	331
5b	2.074	$\bar{4}21$	$42\bar{1}$	2.088	2	12	2.100	421
			041	2.019	7	20	2.030	041
20	2.007	402				12	2.015	402
			240	1.987	1	7	2.003	240
			132	1.958	1	6	1.966	412
			$51\bar{1}$	1.879	1	-	-	
10	1.721	510	331 $42\bar{2}$	1.833	1	8	1.826	510
			510 $33\bar{2}$	1.810	2	-	-	

APPENDIX 17 - (Continued)

P2 Omphacite Clark & Papike (1968)			Calc c²/c Omphacite Coleman (1962)			20% $CaAl_2SiO_6$ Sakata (1957)		
I	d(Å)	hkl	hkl	d(Å)	I	I	d(Å)	hkl
			$24\bar{1}$	1.778	1	14	1.743	150
			421	1.749	1			
5b	1.655	$\bar{3}13$ 042	150	1.733	4	7	1.665	042
			$24\bar{2}$ 042	1.660	3		-	
7	1.622	$\bar{2}23$	$22\bar{3}$ $44\bar{1}$	1.624	2	13	1.626	223
10	1.597	$\bar{5}32$	531	1.609	3	14	1.619	531
7	1.582	440	440	1.597	2	7	1.602	?
			530	1.566	1	4	1.555	600
			600 113	1.545	1	5	1.540	350
			350	1.531	1			
5b	1.522	600 350	$60\bar{2}$	1.523	1			
			$53\bar{2}$ 402	1.502	2			
7	1.495	$\bar{1}33$				8	1.503	?
			060	1.472	2	7	1.478	060
			441 $62\bar{2}$	1.441	1			
10b	1.391	$\bar{3}52$ 531	422	1.421	1	13	1.415	$5\bar{3}1$
			061	1.412	1			
			531	1.402	8			

APPENDIX 17 - (Continued)

*1) F2 Kyanite Eclogite Film 491		*1) F1 Kyanite Eclogite 494		*1) Ja 3 Garnet Peridotite 492	
I/Io	d(Å)	I/Io	d(Å)	I/Io	d(Å)
7	4.040	1	4.4533	1	4.445
1	3.329	4	3.3334	6	3.328
9	3.207	4	3.2131	5	3.208
10	2.979	10	2.980	10	2.984
3	2.950	5	2.925	4	2.919
2	2.884	6	2.882	4	2.886
1	2.830				
8	2.549	3	2.569	5	2.552
		2	2.548	1	2.535
1	2.518	7	2.516	6	2.512
1	2.498	4	2.491	6	2.488
		1	2.4505		
2	2.2800	4	2.2772	5	2.2719
		1	2.2531		
2	2.2066	3	2.1984	5	2.1960
1	2.1882	3	2.1872	5	2.1851
1	2.1367	1	2.1479	1	2.1338
1	2.1185	2	2.1195	4	2.1228
		2	2.0970	3	2.0967
		3	2.0687	1	2.0549
1	2.0264	3	2.0111	5	2.0266
1	2.0098	2	1.9889	5	2.0153
				3	1.9831
1	1.9612	2	1.9600	3	1.9604
		2	1.8660		
2	1.8229	2	1.8178	1	1.8356
		2	1.8020	2	1.8151
1	1.7723			2	1.8099
1	1.7450	2	1.7415	4	1.7404
		1	1.7160	1	1.7175
1	1.6592			1	1.6904

APPENDIX 17 - (Continued)

*1) F2 Kyanite Eclogite		*1) F1 Kyanite Eclogite		*1) Ja 3 Garnet Peridotite	
I/I_o	d(Å)	I/I_o	d(Å)	I/I_o	d(Å)
4	1.6215	9	1.6210	5	1.6595
		1	1.6145	7	1.6224
		1	1.6034	2	1.6151
		4	1.5948	1	1.6022
		2	1.5368	1	1.5461
				2	1.5260
		5	1.5087	1	1.5026
		5	1.4977	5	1.4975
2	1.4986	1	1.4801	1	1.4848
				3	1.4765
				1	1.4448
1	1.4101	4	1.4083	1	1.4230
				1	1.4167
				4	1.4048

*1) Ti 6 cpx Film no. 496		*1) Ti 3 cpx 509		*1) Ti 200 521		*1) Ti 31 489	
I/Io	d(Å)	I/Io	d(Å)	I/Io	d(Å)	I/Io	d(Å)
3	4.504	7	4.1181	3	4.4401	2	4.445
2	3.648			1	3.7909		
7	3.343	5	3.317	7	3.3302	4	3.329
7	3.220	4	3.196	6	3.2109	5	3.219
10	2.980	10	2.988	10	2.9857	10	2.9865
8	2.933	3	2.915	8	2.9293	4	2.9284
8	2.888	3	2.880	8	2.889	7	2.888
7	2.555	4	2.551	8	2.554	6	2.557
1	2.538	1	2.537	1	2.534	10	2.520
7	2.518	8	2.508	9	2.516		
6	2.494	3	2.479	8	2.493	3	2.4966
1	2.379			1	2.374		
5	2.282	2	2.262	6	2.2772	4	2.2799
5	2.201			6	2.1999	6	2.2066
4	2.1872	3	2.188	6	2.1874	5	2.1887
3	2.1438	1	2.133	3	2.1382	1	2.1410
7	2.1247	3	2.125	7	2.1238	3	2.1256
3	2.1013	2	2.100	4	2.0983	2	2.0993
1	2.0639	4	2.024	1	2.0577	1	2.0597
4	2.0303			6	2.0290	4	2.0307
4	2.0142			6	2.0142	4	2.0128
4	1.9922	3	1.976	5	1.9887	4	1.9914
				5	1.9616	3	1.9624
3	1.9632	2	1.963				
1	1.9457	1	1.945				
2	1.9211						
2	1.8231	1	1.8712	1	1.8426	1	1.8443
2	1.8173	1	1.8127	2	1.8187	2	1.8215
1	1.8045	1	1.8045	2	1.8132	2	1.8161
8	1.7458	1	1.7947	2	1.7993	3	1.8023
1	1.7178	3	1.7418	4	1.7549	2	1.7440
1	1.7005	1	1.6862	1	1.7415		
3	1.6592	3	1.6625	1	1.7166		

*1) Ti 6 cpx		*1) Ti 3 cpx		*1) Ti 200		*1) Ti 31	
$I/_{Io}$	d(Å)	$I/_{Io}$	d(Å)	$I/_{Io}$	d(Å)	$I/_{Io}$	d(Å)
1	1.6353	5	1.6249	2	1.6955		
6	1.6217	4	1.6187	4	1.6621	2	1.6645
3	1.6184	1	1.6020	9	1.6574	4	1.6579
2	1.6065			1	1.6213	6	1.6225
1	1.5752	1	1.5414	3	1.6159	1	1.6065
1	1.5507			1	1.6032		
2	1.5410	1	1.5321	2	1.5747		
2	1.5270	1	1.5187	2	1.5483	1	1.5412
2	1.5106	1	1.5106	2	1.5387	3	1.5276
6	1.4996	3	1.4984	2	1.5258		
1	1.4818	1	1.4783	2	1.5174	2	1.5091
1	1.4664	1	1.4460	2	1.5065	5	1.4986
1	1.4498			7	1.4973		
1	1.4292			4	1.4781	2	1.4813
3	1.4114	2	1.4178	1	1.4473	1	1.4442
2	1.4053	4	1.4058	1	1.4417	2	1.4114
				1	1.4269	1	1.4044
				5	1.4082		

*1) Obtained by means of a Guinier Camera, using CuKα radiation and silicon as internal standard

Ti 6:- "glassy" type of clinopyroxene

Ti 3:- "Soapy" type of clinopyroxene

Ti 200:- "silky" type of clinopyroxene

Ti 31:- "silky" type of clinopyroxene

****

APPENDIX 18 - The optical properties of the clinopyroxenes and their $CaSiO_3$ and $FeSiO_3$ contents after Tröger (1959).

Specimen	$n\alpha$ (± 0.003)	$n\beta$ (± 0.003)	$n\gamma$ (± 0.003)	$2V_\gamma$ (± 1°)	$\%CaSiO_3$	$\%FeSiO_3$
1. Clinopyroxenes in kimberlite						
1010-14				63		
1010-12				60		
1010-41				57		
1010-38				53		
1010-38D				43		
1010-40	α'=1.689		1.694	57		
1010-40				65		
1010-3				63		
1010-13				61		
1010-8	1.674	1.679	1.694	50	36	4
1010-8	1.672	1.681	1.697	53	42	4
1010-8				64		
1010-8				57		
1410-6				55		
893-5				54		
1060-32		1.679				
1060-10		1.680				
1060-28		1.680				
1060-26		1.679				
1060-22		1.680				
1010-44				54		
1010-44 C	1.662	1.670		60	47	0
1010-9		1.681	1.702	59	49	7
1010-20 D		1.671				
1010-20				55		
1010-22	1.663	1.671	1.694	58	46	1
1570-31				53		
1060-25				59		
890-19				59		
890-19 D				55		
1060-25				61	Spinel - cpx intergrowth.	

APPENDIX 18 - (Continued)

2. Clinopyroxenes from Waste dumps

Specimen	n_α (± 0.003)	n_β (± 0.003)	n_γ (± 0.003)	$2V_z$ (± 1°)	$\%CaSiO_3$	$\%FeSiO_3$
Ti 12				53°	-	-
Ti 35	1.674	1.682	1.699	59°	50	9
Ti 111	1.673	1.680	1.694	-	-	-
Ti 112	1.671	1.681	1.693	-	-	-
Ti 36	1.672	1.683	1.698	55°	46	8
Ti 8	1.670	1.679	1.694	49°	37	3
Ti 4	1.675	1.682	1.701	49°	48	6
Ti 2	1.670	1.679	1.698	63°	50	6
Ti 3	1.673	1.683	1.703	55°	46	8
Ti 14	1.674	1.682	1.696	57°	49	8
Ti 76	-	1.696	-			
Kd 11	1.669	1.680	1.697	56°	45	5
Kd 12	1.614	1.628	1.632	not clinopyroxene		
Kd 13	1.672	1.680	1.694	52°	40	4
Kd 2	1.670	1.679	1.692	56°	44	4
Kd 8	1.669	1.679	1.694	61°	50	6
Kd 9	1.669	1.678	1.690		-	-
Kd 7	1.674	1.682	1.697	56°	45	8
Kd 10	1.674	1.682	1.697	59°	50	8
Kd 1	1.671	1.680	1.693	56°	45	5
DB 13	1.674	1.682	1.697	63°	50	6
DB 1	1.676	1.682	1.699	60°	50	7
DB 16	1.673	1.681	1.696	60°	50	7
DB 15	1.675	1.681	1.697	58°	50	7
Be 4	1.672	1.681	1.697	60°	50	7
Be 5	1.671	1.680	1.693	54°	43	4
Be 3				60°		
"Glassy" Lovedale	1.673	1.684	1.696			
1010-43A	1.671	1.682	1.692			
1010-43B	1.671	1.683	1.693			
Ti 51	1.673	1.682	1.697			
Hololo	1.675		65°			

Specimen	$n\alpha$ (± 0.003	$n\beta$ (± 0.003)	$n\gamma$ (± 0.003)	$2V_\gamma$ (±1°)	%$CaSiO_3$	%$FeSiO_3$
Ti 9	1.671	1.682	1.693	57°	49	8
Ti 22	1.672	1.680	1.695	60°	50	7
Ti 21	1.672	1.679	1.697	62°	50	6
Ti 23	1.673	1.685	1.701	55°	46	10
Ti 18	1.673	1.681	1.699	62°	50	7
Ti 19	1.670	1.680	1.694	56°	45	5
Ti 20	1.671	1.679	1.697	57°	49	7
Ti 31	1.671	1.679	1.693	55°	44	4
Ti 32	1.670	1.679	1.695	59°	50	7
Ti 33	1.671	1.680	1.695	58°	50	7
Ti 25	1.676	1.682	1.699	60°	50	8
Ti 27	1.670	1.680	1.693	59°	50	7
Ti 56	1.673	1.681	1.697		-	-
Ti 57	1.673	1.680	1.698			
Ti 26	1.672	1.680	1.694	59°	50	7
Ti 17	1.673	1.681	1.695	59°	50	8
Ti 16	1.671	1.680	1.694	55°	44	4
Ti 37	1.675	1.681	1.697	63°	-	-
Ti 38	1.672	1.680	1.693	54°	43	4
Wei 1	1.672	1.680	1.695		-	-
Ti 1	1.672	1.680	1.695	44°	35	5
Ti 4	1.669	1.677	1.693		-	-
Ti 28	1.670	1.678	1.693	58°	50	6
Ti 39	1.665	nd	1.687	54°	-	-
Ti 40	1.672	1.680	1.693	52°	40	4
Ti 30	1.670	1.678	1.692	53°	40	3
Ti 29	1.673	1.681	1.698	53°	42	4
Ti 34	1.669	1.678	1.691	56°	44	4
Ti 24	1.675	1.683	1.697	56°	45	8
Ti 15	1.669	1.678	1.692	61°	50	5
Ti 6	1.672	1.680	1.699	50°	37	3
Ti 7	1.669	1.679	1.693	43°	32	4
Ti 10	1.672	1.679	1.693	53°	40	3
Ti 11	1.672	1.676	1.697	56°	44	2
Ti 11				60°	-	-

Specimen	$n\alpha$ (± 0.003)	$n\beta$ (± 0.003)	$n\gamma$ (±0.003)	$2V_o$ (±1°)	%$CaSiO_3$	%$FeSiO_3$
3. Clinopyroxenes from eclogites						
RV_4	1.671	1.686	1.696	-		
B_2B - 2	1.675	1.688	1.697	72°		
B_2B_2-1	1.677	1.686	1.700	70°		
RV_1	1.673	1.682	1.697	66°		
B_2B_2-2	1.668	1.681	1.691	71°		
RV_5	1.667	1.681	1.689	73°		
RV_6				68°		
Ja. E.	1.670	-	1.693	70°		
Ja. E.				77°	in kelyphyte	
F_1		1.688		64°		
F_2		1.683		71°		
F_3		-		73°		
F_3		-		60°	in kelyphyte	
5. Clinopyroxenes from Ultramafic nodules						
Ja 3	1.668	1.676	1.691	-		
893 In_7	1.669	1.675	1.693	56°	43	2
				61°	in kelyphyte	
893 In_5				52°		
893 In_4	1.663	1.674		52°	36	0
	1.664	1.676	1.691	49°	32	1
893 In_7	1.661	1.667	1.686	61°	in kelyphyte	
1010 In_5	1.670	1.675	1.688	55°	38	0
1010 In_4				64°	25	0
893 In_3				66°		
F.S. 3				61°		
DB 5				65°		
Ki 1				55°		
Ja 6				61°		

C = Clinopyroxenes from Carbonate inclusions
D = Clinopyroxenes from diabase inclusions

****

APPENDIX 19 -The Unit -cell dimensions, the a Sin $\hat{\beta}$ values , and the $CaAl_2SiO_6$ content of the various Clinopyroxenes after bo (Sakata 1957).

Unit-cell dimonsions obtained by means of Guinier Camera, Cu Kα radiation

Specimen	a_o(Å) (±0.003)	b_o(Å) (±0.003)	c_o(Å) (±0.003)	$\hat{\beta}^o$ (± 10')	a Sin $\hat{\beta}$	$CaAl_2SiO_6$ wt% (± 2.0%)
1. Clinopyroxenes from Eclogites						
R. V_5	9.468	8.950	5.218	75°8'	9.1512	-
R V_2	9.457	8.966	5.182	75°34'	9.1585	-
F_1	9.544	8.880	5.207	75°3'	9.2209	16.0
F_3	9.258	-	5.190	76°19'	8.9953	-
RV_2	9.460	8.891	5.188	75°38'	9.1643	11.0
F_2		8.992				-
B_2B-2		8.963				-
2. Clinopyroxenes from Ultramafic Nodules						
Ja 3	9.445	8.859	5.183	75°47'	9.1558	20.0
1010-In_5	9.281	8.894	5.196	75°10'	8.9717	11.0
3. Clinopyroxenes collected on Dumps						
"Glassy" Lovedale	9.477	9.001	5.204	75°22'	9.1696	-
Lovedale	9.496	8.970	5.210	74°38'	9.1566	-
PM 2	9.342	-	5.173	75°22'	9.0389	-
Ti 3 P.M.	9.489	8.870	5.182	75°27'	9.1934	14.0
Ti 6	9.443	8.891	5.189	76°3'	9.1644	7.0
Ti 4	9.556	8.872	5.214	74°54'	9.2260	12.0
Ti 11	9.347	8.869	5.187	75°15'	9.0389	12.5
Pm 1	9.435	8.869	5.185	75°58'	9.1535	12.5
Ti 76	9.432	8.907	5.197	75°37'	9.1363	1.0
Jagersfontien	9.454	8.973	5.212	75°18'	9.1446	0.0
Ti 15 P.M.	9.498	8.887	5.220	74°42'	9.1614	6.0
Ti 41	9.472	8.880	5.202	75°14'	9.1592	8.0
Ti 40	9.373	8.856	5.178	75°13'	9.0627	10.0
Ti 26	9.382	8.861	5.185	75°12'	9.0707	20.0
Ti 37	9.412	8.874	5.204	75°13'	9.1004	17.0
Ti 18	9.468	8.869	5.210	75°8'	9.1512	13.0
Ti 19	9.293	8.864	5.190	75°9'	8.9826	13.5
Ti 20	9.282	8.859	5.181	75°20'	8.9797	21.0
Ti 23	9.460	8.861	5.190	75°33'	9.1725	20.0
Ti 32	9.444	8.896	5.191	75°50'	9.1570	17.0

APPENDIX 19 -(Continued)

Specimen	a_o(Å) (±0.003)	b_o(Å) (±0.003)	c_o(Å) (±0.003)	$\hat{\beta}^o$ (± 10')	a Sin $\hat{\beta}$	$CaAl_2SiO_6$ wt% (± 2.0%)
Ti 36	9.273	8.863	5.172	75°20'	8.9710	5.0
Ti 14	9.517	8.982	5.191	74°59'	9.1921	16.5
1010-43(1)	9.490	8.858	5.188	74°58'	9.1653	20.0
1010-43(2)	9.489	8.876	5.198	75°5'	9.1693	12.5
Ti 38	9.490	8.878	5.209	74°47'	9.1584	12.0
Ti 10	9.283	8.863	5.184	75°21	8.9812	16.5
Ti 9	9.424	8.882	5.185	76°6'	9.1134	11.0
Ti 31	9.478	8.888	5.213	75°15'	9.1656	8.0
Ti 21	9.482	8.889	5.210	75°12'	9.1674	7.5
Ti 22	9.485	8.889	5.211	75°11'	9.1696	7.5
1060-28	9.457	8.880	5.183	75°35'	9.1592	11.0
Ti 25	9.481	8.872	5.204	75°29'	9.1784	13.5
Ti 27	9.461	8.880	5.203	75°33'	9.1617	11.0
Ti 28	9.468	8.852	5.180	75°33'	9.1685	22.0
Ti 17	9.468	8.864	5.181	75°32'	9.1583	16.5
Ti 16	9.450	8.881	5.198	75°32'	9.1409	10.0
Ti 111	9.473	8.872	5.183	75°31'	9.1719	13.5
Ti 112	9.457	8.884	5.203	75°29'	9.1551	9.0
1060-22	9.457	8.893	5.185	75°37'	9.1605	6.0
1060-32	9.461	8.881	5.225	75°34'	9.1624	10.0
PM 3	9.462	8.874	5.216	75°12'	9.1481	13.0
Ti 56		8.886				8.5
Ti 8		8.867				15.5
Ti 7		8.858				19.5
Ti 254		8.864				18.0
1010-8		8.979				11.0
Ti 35		8.997				-
1010-15		8.913				0.0
1060 - 30	9.456	-	5.011	75°20'	9.1480	-
Ti 29	9.473	8.852	5.172	75°28'	9.1698	21.0
Ti 30	9.466	8.857	5.174	75°32'	9.1564	21.0
Ti 34	9.468	8.861	5.187	75°31'	9.1477	17.5
Ti 54	9.265	8.875	5.190	75°54'	8.9858	13.0
Ti 24	9.431	8.887	5.191	74°45'	9.0989	8.0

APPENDIX 19 (Continued)

Specimen	a_o (Å) (±0.003)	b_o (Å) (±0.003)	c_o (Å) (±0.003)	β° (± 10')	a Sin β	$CaAl_2SiO_6$ wt% (± 2.0%)
Ti 39	9.311	8.868	5.120	75° 1'	8.9944	-
Ti 57	9.510	8.872	5.162	76°10'	9.2349	13.5
Ti 55	9.640	8.884	5.222	74°52'	9.3056	9.0
Kamfersdam						
Kd 8	9.470	8.882	5.212	75°15'	9.1579	3.0
Kd 9	9.465	8.903	5.202	75°21'	9.1573	10.0
Kd 11	9.455	8.885	5.204	75°39'	9.1600	9.0
Kd 7	9.452	8.880	5.205	75°30'	9.1510	11.0
Kd 10	9.470	8.881	5.209	75°13'	9.1564	10.0
Kd 1	9.461	8.872	5.204	75°14'	9.1486	13.5
Kd 2	9.460	8.902	5.174	75°24'	9.1545	3.5
Kd 12		8.875				13.0
Kd 13		8.978				11.5
Bellsbank:-						
Be 5	9.413	8.896	5.179	75°22'	9.1067	5.0
Be 4	9.462	8.900	5.208	75°26'	9.1580	4.0
De Beers						
DB 15	9.460	8.900	5.205	75°25'	9.1552	4.0
DB 14	9.457	8.881	5.200	75°18'	9.1475	10.0
DB 16	9.467	8.893	5.210	75°20'	9.1567	3.0
DB 1	9.467	8.883	5.203	75°19'	9.1578	9.0

****

APPENDIX 20 - The Mol per cent $CaMgSi_2O_6$ and the Wt per cent $MgSiO_3$ in the clinopyroxenes, after the various d-value spacings

The values obtained by means of Guinier Camera, Cu Kα radiation.

Sample	$2\theta(220)^o$	Mol % Ca Mg Si_2O_6 (Davis & Boyd 1966)	$\Delta 2\theta(311-310)^o$ Cu Kα - radiation	Wt % $MgSiO_3$ (Kushiro 1964)
1. Clinopyroxene from Eclogite				
RV_6	27.79	52		
RV_5	27.80	50	0.276	33
Ja	27.66	72	0.430	24
RV_2	27.72	66	0.265	33
RV_4	28.015	-	0.485	16
RV_2	27.745	63	0.315	31
F_3	27.79	52	0.920	-
F_2	27.79	52	0.255	34
F_1	27.74	64	0.460	18
B_2B_2-1	27.75	63	0.406	24
2. Clinopyroxene from UltramaficNodules				
1010 In_5	27.815	40	0.270	33
893 In_7	27.92	33	0.256	34
893 In_3	27.188	100	-	-
1010 In_4	27.254	100	-	-
Ja 3	27.78	53	0.356	28
3. Metamorphic clinopyroxenes				
1010-20	27.530	100	-	-
1010-22	27.578	100	-	-
1010-22	27.580	100	-	-
4. Clinopyroxenes from Kimberlite				
1010-15	27.77	55	0.225	35
1060-32	27.775	54	0.370	27
1060-22	27.74	64	0.465	18
1060-28	27.815	48	0.380	27
1010-43	27.875	41	0.265	34
1010-43B	27.695	67	0.415	23
1060-30	27.62		0.440	21
Fawn K.	27.816	48	0.230	36

Sample	$2\theta(220)^{o}$	Mol % Ca Mg Si_2O_6 (Davis & Boyd 1966)	$\Delta 2\theta(311-310)^{o}$ Cu Kα radiation	Wt % $MgSiO_3$ (Kushiro 1964)
Frawn K. B.	27.796	51	0.210	36
1010-8	27.806	48		
1010-14	28.310	100		
1010-8	27.876	38	0.204	37
1010-8	27.79	52	0.406	24
5. Clinopyroxenes obtained from waste dumps				
Ti_{25}	27.83	46	0.245	35
Ti_{27}	27.72	66	0.460	18
Ti_{28}	27.755	58	0.260	34
Ti_{17}	27.82	48	0.285	33
Ti_{16}	27.735	64	0.445	21
Ti_{111}	27.765	56	0.360	29
Ti_{112}	27.72	66	0.450	20
A	27.76	56	0.446	21
B	27.69	68	0.515	14
Ti_{54}	27.735	64	0.445	21
Ti_{24}	27.860	42	0.180	37
Ti_{39}	27.745	59	0.305	32
Ti_{57}	27.805	50	0.420	23
Ti_{56}	27.875	41	0.200	37
Ti_{55}	27.690	68	0.445	21
Ti_{29}	27.86	42	0.175	37
Ti_{30}	27.865	41	0.205	37
Ti_{34}	27.78	53	0.240	35
Ti_{38}	27.765	56	0.410	23
Ti_{37}	27.730	65	0.905	0
Ti_{26}	27.820	48	0.230	36
Ti_{40}	27.865	42	0.170	37
Ti_{41}	27.770	55	0.950	0
Ti_{15}	27.70	68	0.390	24
Ti_{18}	27.765	56	0.420	23
Ti_{19}	27.875	41	0.235	35

Sample	$2\theta(220)^{o}$	Mol % $CaMgSi_2O_6$ (Davis & Boyd 1966)	$\Delta 2\theta(311-310)^{o}$ Cu Kα radiation	Wt% $MgSiO_3$ (Kushiro 1964)
Ti_{20}	27.87	41	0.180	37
Ti_{33}	27.84	46	0.270	33
Ti_{32}	27.725	65	0.435	22
Ti_{31}	27.69	68	0.440	21
Ti_{21}	27.745	63	0.475	18
Ti_{22}	27.74	64	0.455	19
Ti_{23}	27.72	66	0.120	40
Ti_{14}	27.82	48	0.196	37
Ti_{36}	27.87	41	0.136	39
Ti_{3}	27.89	40	0.285	33
Ti_{8}	27.905	38	0.195	37
Ti_{7}	27.80	48	0.265	34
Ti_{6}	27.68	68	0.485	16
Ti_{4}	27.72	66	0.34	29
Ti_{11}	27.806	48	0.38	27
Ti_{10}	27.830	46	0.260	33
Ti_{15}	27.745	63	0.465	18
Ti_{9}	27.750	63	0.470	18
PM. 1	27.875	41	0.185	37
Kamfersdam Kd_7	27.64	85	0.445	21
" Kd_2	27.62	90	0.485	16
" Kd_1	27.74	64	0.455	19
Kd_{10}	27.675	67	0.480	17
Kd_9	27.71	67	0.510	14
Kd_8	27.72	66	0.485	16
Kd_{11}	27.675	67	0.505	14
Kd_{12}	28.04	-	0.260	34
Kd_{13}	27.87	41	0.215	36
Lovedale 1	28.00	-	0.320	30
" 2	27.80	50	0.276	33

Sample	2θ (220)°	Mol % Ca Mg Si_2O_6 (Davis & Boyd 1966)	Δ2θ(311-310)° Cu Kα radiation	Wt% $MgSiO_3$ (Kushiro 1964)
"Glassy" type	27.66	72	0.243	35
Belsbank Be_4	27.69	68	0.590	3
" Be_5	27.71	67	0.505	14
De Beers DB_1	27.685	68	0.470	18
DB_{16}	27.735	64	0.520	13
DB_{13}	27.74	64	0.485	16
DB_{15}	27.675	67	0.525	13

****

APPENDIX 21 - The chemical analyses, molecular norms, and structural formulas of clinopyroxenes from various sources. The method of calculation is described on page 141.

I. Partial analyses of clinopyroxenes from kimberlites

No.	Locality	Ca	Mg	Fe	Al	Cr
75966-1	Bultfontein	16.0	10.2	3.1	0.1	0.4
-2	"	14.3	9.9	1.4	1.3	1.6
-4	"	14.2	10.2	2.5	1.0	0.8
75967-1	"	14.9	10.3	2.5	0.9	0.6
-3	"	14.6	9.9	2.6	1.0	0.7
75968-1	"	13.8	9.8	2.5	1.1	0.9
-2	"	14.8	10.0	2.4	0.9	0.7
75972-4	Wesselton	15.5	10.3	2.5	0.5	0.4
75973-1	"	14.2	10.0	2.5	1.0	0.7
-2	"	14.8	10.0	2.5	1.0	0.7
75974-1	"	13.8	9.8	2.7	1.2	0.8
75957-1	Kimberley	14.3	10.0	2.6	1.0	0.7
-2	"	13.8	9.8	2.7	1.2	0.9
-3	"	14.2	10.2	1.9	0.9	1.4
-4	"	15.4	10.3	2.4	0.7	0.5
75958-1	"	14.7	10.2	2.6	0.8	0.6
-2	"	14.2	9.9	2.8	1.0	0.7
-3	"	14.7	10.1	2.4	1.0	0.7
75959-1	"	14.5	10.2	2.4	0.9	0.8
-2	"	15.3	10.4	2.4	0.8	0.5
-3	"	15.1	10.2	2.4	0.9	0.7
75938-1	De Beers	15.5	10.3	2.4	0.7	0.5
-2	"	14.4	10.2	2.0	0.7	1.5
-3	"	14.9	10.2	2.3	0.8	0.9
-4	"	14.8	10.1	1.6	0.6	1.9
75936-1	"	14.2	10.0	2.2	0.9	1.3
-2	"	15.1	10.3	2.5	1.1	0.6
-3	"	15.3	10.3	2.5	0.7	0.6
73191-1	"	12.7	9.6	2.5	1.7	1.1
-2	"	15.9	10.6	2.4	0.4	0.4
-3	"	15.3	10.4	2.4	0.7	0.4
-4	"	14.9	10.3	2.5	0.8	0.6

No.	Locality	Ca	Mg′	Fe	Al	Cr
75937-1	De Beers	15.3	10.7	2.2	0.7	0.6
-2	"	15.0	10.4	2.4	0.8	0.6
-3	"	14.3	10.3	2.6	0.9	0.6
87703	"	15.1	10.2	2.5	0.7	0.8
DB_2 (Lherz).	"	14.7	11.0	-	-	-
L_3 "	Laurencia	15.0	10.5	-	-	-
K_{29} "	Kamfersdam	13.2	9.3	-	-	-
W_{46} "	Wesselton	13.8	9.2	-	-	-
D_{26} "	Dutoitspan	13.9	10.2	-	-	-

****

APPENDIX 21 - The chemical analyses, molecular norms, and structural formulas of clinopyroxenes from various sources. The method of calculation is described on page 141

II. Chemical analyses of clinopyroxenes

A. Chemical analyses

	1	2	3	4	5	6	7	8	9	10	11	12	13	14
SiO_2	54.47	54.10	54.61	54.52	54.09	53.53	54.52	36.00	50.06	54.25	45.04	57.33	54.06	53.47
Al_2O_3	8.33	2.74	2.23	0.01	1.57	1.30	3.58	6.48	0.96	1.40	10.08	16.73	2.05	2.70
Fe_2O_3	1.76	1.38	0.96	-	0.74		4.04	3.60	1.40	1.50	8.38	3.02	1.32	1.23
FeO	5.43	3.02	3,83	1.74	1.47	2.10	2.66	4.70	2.48	1.34	2.00	0.28	0.96	1.87
MnO	0.16	0.13	0.16	0.51	0.09		0.12	0.14	-	0.10	-	nd	0.06	0.08
MgO	11.90	20.01	20.51	17.44	16.96	17.88	23.04	27.28	16.24	16.70	10.21	7.20	16.81	16.61
CaO	13.63	16.02	15.30	25.34	21.10	22.96	18.48	8.12	19.68	21.60	21.08	11.42	21.92	20.33
Na_2O	2.76	1.64	1.29	0.27	1.37		tr	tr	1.44	-	1.68	3.16	1.54	1.96
K_2O	0.30	0.06	0.04	0.12	0.15		1.09	0.58	4.17	-	0.19	0.24	0.01	0.03
TiO_2	0.53	0.48	0.51	tr	0.28		0.50	0.50	-	1.07	0.78	tr	0.17	0.10
Cr_2O_3	0.13	0.42	0.50	-	2.03	1.96	0.12	0.40	1.12	1.82		nd.	1.29	1.33
H_2O^+	0.46	0.76	0.75	0.26	0.22		7.64	9.03	4.17	0.05	0.23	0.03	-	
H_2O^-	-			0.10	0.80		0.72	0.80				0.74		
NiO	-			-	0.03		-	-	-					
Other	-			-	0.26		14.11	3.30			0.61			
Total	99.86	100.76	100.69	100.31	100.64	99.73	100.62	100.93	99.45	100.33	100.28	100.15	100.19	99.71

B. Molecular norms

Ac	4.9	3.8	2.6	2.4	1.9		4.5	2.5	3.9		13.1	8.4	3.4	3.2
Jd	14.9	7.7	6.7		6.4				4.1			15.2	7.2	10.3
$CaTiAl_2O_6$	1.4	1.3	1.3		1.7 *6		1.2	1.3		3.4	2.3		0.4	0.2
$Cr_2Al_2O_6$	0.1	0.5	0.7		2.3	2.8	0.4	0.5	3.0 *6	2.8		1.8		1.8
$CaFe^{3+}_2SiO_6$					0.9		2.7	3.5		2.2	5.3			
$CaFe\ Si_2O_6$	16.9	9.3	11.4	4.3	5.5	7.8	7.5	14.0	7.6 *3	4.6	6.3	0.9	3.2	5.7
$CaMgSi_2O_6$	35.7	49.2	45.0	93.3	72.6	79.6	55.7	14.7	75.7	74.1	56.7	39.4	79.3	69.6
$(MgFe)SiO_3$	15.2	28.2	32.2		9.5	9.8	28.0	63.5	5.7	13.0		4.4 *1	4.7	8.2
$Al_4Si_3O_{12}$	7.4				-	-					14.2	21.2		
$Al_2Al_2O_6$	3.5 *8				-	-					2.1	10.5		
Total	100.0	100.0	100.0	100.0	100.0	100.0	100.0	100.0	100.0	100.0	100.0	100.0	100.0	100.0

C. Structural formules

	1	2	3	4	5	6	7	8	9	10	11	12	13	14
Na^{+}	0.25	0.11	0.09	0.02	0.10		0.05	0.03	0.19		0.13	0.18	0.11	0.14
Ca^{+}	0.63	0.60	0.58	0.98	0.81	0.92	0.67	0.40	0.76	0.83	0.85	0.35	0.83	0.81
Mg^{2+}	0.77	1.05	1.08	0.93	0.90	0.99	1.17	1.86	0.85	0.89	0.57	0.31	0.89	0.92
Fe^{2+}	0.20	0.09	0.59	0.04	0.05	0.07	0.08	0.18	0.08	0.04	0.06	0.01	0.03	0.06
Cr^{3+}	-	0.01	0.02		0.06	0.06		0.01	0.03	0.05			0.03	0.03
Ti^{4+}	0.02	0.01	0.01		0.01		0.01	0.02		0.03	0.02		0.00	
Fe^{3+}	0.06	0.04	0.03		0.02		0.10	0.12	0.04	0.04	0.23	0.07	0.03	0.03
Al^{3+}	0.43	0.07	0.06		0.06	0.06			0.04		0.13	0.56	0.01	0.11
Al^{3+}	-	0.04	0.03				0.14	0.35		0.04	0.31	0.37	0.01	0.01
Si^{4+}	2.38	1.90	1.94	1.96	1.93	2.00	1.86	1.65	1.81	1.96	1.69	1.63	1.92	1.99

	15	16	17	18	19	20	21	22	23	24	25	26	27	28
SiO_2	53.20	54.25	52.40	52.40	54.3	52.8	55.2	54.6	54.2	54.9	53.70	53.90	54.61	53.75
Al_2O_3	4.34	1.40	0.60	1.73	2.39	0.86	2.05	2.10	3.03	2.93	3.03	2.40	1.30	2.83
Fe_2O_3	0.19	1.50		3.68	-	-	-	-	-	-	0.82	1.34	1.14	1.27
FeO	1.52	1.34	6.50	4.25	4.04	5.89	3.34	2.13	2.59	2.14	1.91	1.28	3.02	1.62
MnO	0.02	0.10			0.14	0.71	0.12	0.09	0.09	0.08	0.06	0.08	0.10	0.07
MgO	15.90	16.70	15.50	21.61	20.9	16.1	21.1	16.1	17.3	16.6	17.22	16.39	20.88	16.19
CaO	22.16	21.60	20.50	13.30	15.4	20.9	16.1	19.9	19.5	20.1	17.91	20.57	16.20	20.64
Na_2O	1.57	tr			1.52	1.38	1.24	2.50	1.95	2.31	2.13	1.80	1.28	1.72
K_2O	0.04	tr			0.04	0.004	0.05	0.01	0.01	0.03	0.09	0.02	0.12	0.11
TiO_2	0.10	1.07		0.66	-	-	-	-	-	-	nd.	0.20	0.23	0.25
Cr_2O_3	0.21	1.82	2.80	0.31	-	-	-	-	-	-	-	1.55	0.92	1.30
H_2O^+			1.50	1.64	0.79	0.09	0.85	3.15	1.45	1.82	0.17	-	0.41	0.24
H_2O^-					0.13	0.43	0.16	0.15	0.41	0.003	3.03	-	0.07	0.10
NiO				0.26	-	-	-	-	-	-	nd	0.05	-	
Other		0.05		0.15	-	-	-	-	-	-	0.09	0.01	-	0.07
Total	99.92	100.33	99.80	100.12	99.7	99.2	100.4	100.7	100.6	101.0	100.15	99.59	100.28	100.16
Ac	0.7										2.1	3.8	2.8	3.4
Jd	10.6										12.4	8.8	5.3	9.1
$CaTiAl_2O_6$	0.2	3.2		2.0							0.4	0.6	0.6 *7	0.9
$Cr_2Al_2O_6$	0.4	2.7	3.7	0.4							4.1	2.2	2.4 *6	1.8
$CaFe^{3+}_2SiO_6$		0.4		5.2										
$CaFeSi_2O_6$	4.6	4.3	18.4	13.2							5.7	4.4	8.7	5.8
$CaMgSi_2O_6$	80.7	76.3	66.7	33.4							56.9	71.4	54.4	70.6
$(MgFe)SiO_3$	2.6	9.2	11.2	44.6							18.4	9.0	25.7	8.4
$Al_4Si_3O_{12}$														
$Al_2Al_2O_6$	0.2			1.2										
Total	100.0	100.0	100.0	100.0							100.0	100.0	100.0	100.0

APPENDIX 21 (Continued)

	15	16	17	18	19	20	21	22	23	24	25	26	27	28
Na^{+}	0.11				0.11	0.10	0.09	0.18	0.14	0.16	0.15	0.12	0.17	0.12
Ca^{+}	0.86	0.83	0.83	0.52	0.92	1.37	0.95	1.22	1.18	1.22	0.67	0.78	0.64	0.79
Mg^{2+}	0.86	0.89	0.87	1.19	1.73	1.36	1.74	1.38	1.45	1.40	0.90	0.87	1.14	0.87
Fe^{2+}	0.05	0.04	0.20	0.13	0.19	0.30	0.15	0.11	0.12	0.11	0.06	0.04	0.09	0.05
Cr^{3+}	0.01	0.05	0.09	0.01	0.02	-	0.02	0.09	0.04	0.05	0.08	0.05	0.02	0.04
Ti^{4+}		0.03		0.02	-	0.01	-	-	0.01	-		0.01		0.01
Fe^{3+}	0.01	0.04		0.10		-	-	-	-	-	0.02	0.04	0.02	0.03
Al^{3+}	0.11			0.02	0.07	0.02	0.06	0.06	0.09	0.09	0.12	0.09	0.05	0.09
Al^{3+}	0.08	0.06	0.03	0.06	0.04	0.03	0.03	0.03	0.05	0.03		0.01		0.03
Si^{4+}	1.92	1.94	1.97	1.94	1.96	1.97	1.97	1.97	1.95	1.97	1.88	1.91	2.00	1.92

	29	30	31	32	33	34	35	36	37	38	39	40	41	42
SiO_2	50.97	54.38	55.03	53.50	54.49	54.63	53.50	54.20	54.19	53.69	52.48	53.80	53.90	53.70
Al_2O_3	4.86	2.53	2.69	5.03	5.48	1.66	2.69	2.15	2.71	2.43	2.53	1.80	2.40	2.11
Fe_2O_3	0.92	1.13	1.20	1.62	1.77	0.57	0.90	0.98	0.31	0.86	0.53	1.11	1.34	-
FeO	1.41	3.57	3.48	2.03	1.77	1.54	1.65	1.55	3.05	2.83	2.14	1.81	1.28	2.92
MnO	0.10	0.09	0.09	0.07	0.07	0.04	0.05	0.05	0.07	0.06	0.07	0.10	0.08	nd
MgO	17.89	15.59	13.91	15.30	13.08	16.78	17.43	15.89		16.32	18.65	17.63	16.39	17.24
CaO	21.28	20.26	21.55	17.37	18.94	23.46	21.62	22.99	21.04	22.37	20.98	20.96	20.57	19.69
Na_2O	0.83	1.45	1.54	2.50	2.72	1.01	1.20	1.34	1.50	1.05	1.03	1.26	1.80	nd
K_2O	nd	0.10	0.10	0.11	0.12	0.01	0.01	0.01	0.01	0.01	0.02	0.04	0.02	nd
TiO_2	0.49	0.21	0.22	1.06	1.15	0.11	0.16	0.18	0.22	0.16	0.19	0.11	0.20	nd
Cr_2O_3	1.47	0.18	0.19	0.38	0.41	0.20	0.47	0.69	0.63	0.20	0.88	1.12	1.55	nd
H_2O^+	0.23													
H_2O^-	0.07	0.81		1.06										
NiO	nd	nd	nd	nd	-	0.05	0.08	0.08	0.05	0.06				nd
Other														
Total	100.52	100.30	100.00	100.03	100.00	100.06	99.76	100.11	100.10	100.04	99.50	99.74	99.53	95.66
Ac	2.4	3.1	3.3	4.4	4.8	1.5	2.4	2.8	0.8	2.4	1.5	3.0	3.8	
Jd	3.5	7.7	8.0	13.8	14.2	5.4	6.0	6.5	9.5	4.7	5.5	6.0	9.2	
$CaTiAl_2O_6$	1.3	0.7	0.7	1.1	1.1	0.4	0.6	0.6	0.8	0.7	0.6	0.4	0.7	
$Cr_2Al_2O_6$	2.1	0.4	0.4	1.6	1.6	0.3	0.6	0.9	0.9	0.4	1.7	1.5	2.3	
$CaFe^{3+}_2SiO_6$														
$CaFeSi_2O_6$	4.3	11.1	11.2	6.6	6.2	4.5	5.2	4.7	9.4	8.7	6.5	5.5	4.3	8.4
$CaMgSi_2O_6$	74.6	66.9	73.3	59.7	67.1	85.3	76.6	82.6	69.3	77.2	72.6	74.0	77.2	73.6
$(MgFe)SiO_3$	11.8	9.1	1.9	11.6	1.4	2.6	8.6	1.9	9.3	5.7	12.4	9.6	2.5	13.2
$Al_4Si_3O_{12}$		1.0	1.2		3.5									4.8
$Al_2Al_2O_6$				1.2						0.2				
Total	100.00	100.0	100.0	100.0	100.0	100.0	100.0	100.0	100.0	100.0	100.0	100.0	100.0	100.0

APPENDIX 21 (Continued)

	29	30	31	32	33	34	35	36	37	38	39	40	41	42
Na^{+}	0.06	0.11	0.11	0.18	0.20	0.07	0.09	0.09	0.12	0.07	0.07	0.09	0.13	
Ca^{+}	0.82	0.79	0.83	0.67	0.74	0.93	0.84	0.90	0.82	0.87	0.84	0.83	0.81	0.78
Mg^{2+}	0.96	0.85	0.75	0.83	0.71	0.92	0.95	0.86	0.89	0.88	1.03	0.97	0.90	0.96
Fe^{2+}	0.04	0.11	0.11	0.07	0.06	0.05	0.05	0.05	0.10	0.09	0.07	0.06	0.04	
Cr^{3+}	0.04	0.01	0.01	0.03	0.03	0.01	0.02	0.02	0.02	0.01	0.03	0.03	0.05	
Ti^{4+}	0.01	0.01	0.01	0.01	0.01	-	0.01	0.01	0.01	0.01	0.01	0.01	0.01	
Fe^{3+}	0.02	0.03	0.03	0.04	0.05	0.01	0.02	0.03	0.01	0.02	0.02	0.03	0.03	0.08
Al^{3+}	0.03	0.10	0.10	0.17	0.21	0.06	0.06	0.07	0.10	0.05	0.05	0.06	0.09	0.09
Al^{3+}	0.17	0.01	0.01	0.05	0.02	0.01	0.05	0.02	0.02	0.05	0.05	0.02	0.02	
Si^{4+}	1.83	1.99	1.99	1.95	1.98	1.99	1.95	1.98	1.98	1.95	1.95	1.98	1.98	2.00

	43	44	45	46	47	48	49	50	51	52	53	54
SiO_2	54.19	54.20	53.50	54.63	53.75	54.26	51.89	48.75	51.40	51.34	52.43	52.50
Al_2O_3	2.71	2.15	2.69	1.66	3.08	2.94	4.76	6.54	4.58	5.63	4.16	5.19
Fe_2O_3	0.31	0.98	0.90	0.57	1.39	2.22	-	2.58	4.50	3.63	2.66	-
FeO	3.05	1.55	1.65	1.54	2.46	2.58	4.40	4.21	0.05	0.07	3.53	2.31
MnO	0.065	0.049	0.051	0.039	0.06	0.06	0.54	-	0.03	0.03	0.12	-
MgO	16.32	15.89	17.43	16.78	15.91	15.23	15.47	14.45	16.85	15.29	18.19	18.01
CaO	21.04	22.99	21.62	23.46	20.82	20.40	19.73	19.78	20.02	19.62	16.56	19.52
Na_2O	1.50	1.34	1.20	1.01	1.84	2.15		1.14	1.31	1.91	0.90	
K_2O	0.01	<0.01	0.01	<0.01	0.02	0.01		0.01	-	-	0.07	
TiO_2	0.63	0.69	0.47	0.20	0.15	0.13		1.94	0.64	0.58	0.37	
Cr_2O_3	0.22	0.18	0.16	0.11	0.47	0.16	1.09	0.25	0.08	0.05	1.06	2.43
H_2O^+									0.82	0.88	0.20	
H_2O^-								0.16	0.16	0.44		
NiO	0.046	0.075	0.079	0.053	0.05	0.05					0.08	
Other	0.003	0.030	0.003	0.002							0.01	
Total	100.09	100.14	99.79	100.06	100.00	100.18	100.18	99.81	100.44	99.47	100.37	99.96
Ac	0.9	2.80	2.4	1.5	3.8	6.1		7.8	9.3	10.0	6.8	
Jd	9.4	6.6	6.0	5.4	8.8	9.0		0.9		3.5		
$CaTiAl_2O_6$	0.6	0.6	0.4	0.4	0.4	0.4		5.6	1.7	1.8	1.1	
$Cr_{2}^{3+}Al_2O_6$	0.8	0.9	0.6	0.3	0.7	0.4	1.6	0.5	0.1	0.2	1.6	3.6
$CaFe_2SiO_6$									1.4	0.0	0.3	
$CaFeSi_2O_6$	9.7	5.2	5.4	4.8	7.8	8.2	15.3	13.7	0.1	0.2	10.9	7.1
$CaMgSi_2O_6$	69.5	81.3	76.6	84.9	71.7	69.7	62.6	61.0	75.0	74.9	54.5	70.1
$(MgFe)SiO_3$	9.1	2.6	8.7	2.7	7.2	6.2	12.8	6.6	8.4	4.4	22.0	14.4
$Al_4Si_3O_{12}$							7.7			1.2		
$Al_2Al_2O_6$								3.9	4.0	3.8	3.8	4.8
Total	100.0	100.0	100.0	100.0	100.0	100.0	100.0	100.0	100.0	100.0	100.0	100.0

	43	44	45	46	47	48	49	50	51	52	53	54
Na^{+}	0.10	0.05	0.08	0.06	0.13	0.15		0.09	0.09	0.13	0.07	
Ca^{+}	0.81	0.89	0.83	0.90	0.80	0.79	0.80	0.82	0.79	0.77	0.64	0.75
Mg^{2+}	0.87	0.85	0.93	0.90	0.85	0.82	0.87	0.62	0.93	0.84	0.98	0.96
Fe^{2+}	0.10	0.05	0.05	0.05	0.08	0.08	0.15	0.14	-	-	0.11	0.07
Cr^{3+}	0.02	0.02	0.01	0.01	0.01	0.01	0.03	0.01			0.03	0.07
Ti^{4+}	0.01	0.01			0.00			0.06	0.02	0.02	0.01	
Fe^{3+}	0.01	0.03	0.02	0.02	0.04	0.06		0.07	0.12	0.09	0.10	
Al^{3+}	0.09	0.07	0.06	0.05	0.09	0.09	0.16	0.16	0.08	0.13	0.10	0.09
Al^{3+}	0.02	0.02	0.05	0.02	0.04	0.04	0.05	0.11	0.11	0.11	0.10	0.13
Si^{4+}	1.94	1.95	1.92	1.97	1.94	1.96	1.95	1.89	1.89	1.89	1.90	1.87

	55	56	57	58	59	60	61	62	63	64	65	66	67	68
SiO_2	52.37	51.86	50.24	53.88	53.89	53.44	49.87	54.50	51.78	51.42	50.36	52.48	51.41	52.12
Al_2O_3	6.11	1.56	4.57	0.68	0.72	3.74	5.44	6.47	5.14	5.97	6.58	3.56	4.69	4.08
Fe_2O_3	1.44	2.44	2.53	0.16	-	-	2.75	-	1.75	1.43	1.53	1.13	0.69	0.82
FeO	2.01	3.46	4.04	2.11	2.42	4.70	2.50	4.00	2.14	2.57	2.66	2.52	2.64	2.24
MnO	0.10	tr	0.13	2.07	0.12	0.31	-	0.70	0.12	0.15	0.09	0.15	0.11	0.09
MgO	16.72	17.40	16.53	18.84	17.84	16.19	16.26	14.58	16.04	16.17	16.59	17.03	16.32	16.48
CaO	20.88	22.15	19.96	22.38	23.56	19.90	20.74	17.87	20.32	19.95	18.78	19.00	21.63	19.34
Na_2O	-	0.12	0.58	0.78	0.52				1.06	1.36	1.41	-	0.72	2.14
K_2O	-		0.04	0.04	0.10				0.08	0.10	0.08	-	0.04	0.08
TiO_2	0.29	-	0.72	0.14	0.13				0.38	0.24	0.79	0.62	0.33	0.80
Cr_2O_3	0.05	0.73	1.22	0.87	0.69	0.75	1.76	1.98	0.95	0.80	0.92	2.12	1.03	1.44
H_2O^+	0.09			0.14	0.10		0.55						0.11	-
H_2O^-														
NiO				0.039	0.028				0.041	0.045	0.037	0.034	0.040	0.041
Other				0.02	0.01				0.04	0.03	0.03	0.04	0.05	0.03
Total	100.06	99.72	100.39	100.15	100.13	99.03	99.87	100.33	99.84	100.24	99.86	98.53	99.81	99.70
Ac			6.7	0.4	-	-	-	-	4.8	3.9	4.0	-	2.0	2.2
Jd			4.2	2.1	2.6	-	-	-	3.1	5.8	5.9	-	3.1	13.1
$CaTiAl_2O_6$	0.9		1.9	0.4	0.4	-	-	-	1.1	1.1	2.1	1.7	0.9	2.2
$Cr_{2}^{3+}Al_2O_6$	0.2	2.0	1.7	1.3	1.0	1.2	2.5	2.9	1.4	1.2	1.2	3.1	1.4	2.1
$CaFe_2^{3+}SiO_6$	2.1	3.3	-	-	-	-	3.8	-	-	-	-	1.5		
$CaFeSi_2O_6$	6.6	10.5	12.2	6.4	7.2	15.4	7.5	14.7	6.8	8.2	8.0	8.1	8.2	6.9
$CaMgSi_2O_6$	74.6	73.9	58.9	77.4	82.6	64.4	70.9	55.9	69.8	66.8	58.6	63.8	77.3	63.2
$(MgFe)SiO_3$	8.6	10.3	14.4	12.0	6.2	12.9	9.4	12.0	9.3	10.4	20.2	19.2	4.0	10.3
$Al4Si_3O_{12}$				-	-	7.1	2.8	10.0	-	-	-	-	-	-
$Al_2Al_2O_6$	5.0		-	-	-	-	3.1	4.5	3.7	2.6	-	2.6	3.1	-
Total	100.0	100.0	100.0	100.0	100.0	100.0	100.0	100.0	100.0	100.0	100.0	100.0	100.0	100.0

APPENDIX 21 (Continued)

	55	56	57	58	59	60	61	62	63	64	65	66	67	68
Na^{+}			0.12	0.06	0.04	-	-	-	0.08	0.09	0.10	-	0.05	0.16
Ca^{+}	0.80	0.88	0.79	0.88	0.93	0.79	0.86	0.70	0.79	0.77	0.73	0.74	0.85	0.78
Mg^{2+}	0.89	0.97	0.91	1.03	0.98	0.89	0.93	0.82	0.87	0.87	1.01	1.02	0.79	0.86
Fe^{2+}	0.06	0.11	0.13	0.06	0.08	0.15	0.08	0.15	0.07	0.08	0.08	0.08	0.08	0.07
Cr^{3+}	-	0.02	0.04	0.02	0.02	0.02	0.05	0.06	0.03	0.02	0.03	0.06	0.03	0.04
Ti^{4+}	0.01	-	0.02						0.01	0.01	0.02	0.02	0.01	0.02
Fe^{3+}	0.04	0.07	0.07				0.08		0.05	0.04	0.04	0.03	0.02	0.02
Al^{3+}	0.09	-	0.04	0.02	0.02	0.14	0.17	0.28	0.11	0.11	0.06	0.05	0.09	0.14
Al^{3+}	0.17	0.07	0.15	0.01		0.02	0.08		0.11	0.14	0.18	0.10	0.12	0.04
Si^{4+}	1.83	1.94	1.85	1.99	2.00	1.98	1.92	2.00	1.89	1.86	1.82	1.90	1.88	1.96

	69	70	71	72	73	74	75	76	77	78	79	80	81	82
SiO_2	51.87	48.57	48.05	50.43	54.15	46.13	44.89	46.20	51.72	44.62	51.52	50.87	51.17	41.78
Al_2O_3	1.72	7.38	8.02	5.76	10.83	10.84	10.23	7.38	3.87	9.83	4.47	5.92	6.46	10.86
Fe_2O_3	1.61	2.92	2.60	1.77	4.26	3.67	7.18	6.94	3.02	4.09	1.84	1.93	0.85	7.00
FeO	3.66	2.68	3.11	3.24	4.22	3.74	5.58	5.97	3.77	2.47	2.78	2.95	2.87	1.76
MnO	0.06	0.11	0.10	0.11	0.14	0.14	0.37	0.26	0.21	0.06	0.12	0.11	0.16	0.02
MgO	17.94	14.22	13.96	16.12	10.37	11.62	8.11	8.96	15.02	12.29	15.64	16.46	17.65	11.71
CaO	20.92	20.90	21.15	19.45	20.79	20.92	18.84	19.85	19.45	23.17	20.46	19.19	18.27	20.76
Na_2O	0.33	0.79	0.83	0.93	1.33	0.90	2.27	1.91	1.38	0.52	1.07	0.97	1.20	0.94
K_2O	0.02	0.03	0.04	0.02	0.03	0.03	0.05	0.06	0.11	0.02	0.01	0.04	0.08	-
TiO_2	0.65	0.45	0.40	0.34	0.48	0.54	0.54	0.67	0.58	-	0.43	-	0.14	1.92
Cr_3O_3	1.07													0.012
H_2O^+	0.08	1.48	1.76	0.88	2.09	1.32	1.97	1.70	0.70	3.36	0.98	0.86	0.28	-
H_2O^-		0.02	0.11	0.40	0.18	0.06	0.01	0.00	0.24	-	0.54	0.55	1.20	-
NiO	0.040													
Other	-												0.036 0.14	
Total	99.97	99.68	100.13	99.54	99.87	99.92	100.04	99.86	99.92	100.45	99.86	99.85	100.40	99.722
Ac	2.2	5.8	6.0	5.0	8.9	6.5	16.8	13.3	8.5	3.8	5.1	5.2	1.2	6.8
Jd				1.8					2.0		2.4	1.7	6.2	
$CaTiAl_2O_6$	1.8	4.2	4.9	2.5	5.4	3.6	5.7	4.5	2.0	9.4	2.9	2.4	0.9	5.5
$Cr_2Al_2O_6$	1.4			0.6	0.3	0.2			0.4		0.8	0.9	1.9	
$CaFe^{3+}_2SiO_6$	0.9	1.1	0.6		1.2	1.9	1.8	2.7		3.8				6.7
$CaFeSi_2O_6$	10.5	8.7	9.7	10.4	12.8	12.1	18.9	18.7	12.5	7.8	8.8	9.2	8.9	6.8
$CaMgSi_2O_6$	62.5	68.9	68.2	65.0	53.1	63.8	45.7	46.1	62.2	67.6	66.6	61.3	56.3	66.4
$(MgFe)SiO_3$	20.7	5.4	4.5	7.0	5.1 *1)	0.3	1.3 *6)	0.9	7.6		9.2	13.8	18.6	
$Al_4Si_3O_{12}$	-			5.2	12.8		9.8	13.8		7.6 *1)				
$Al_2Al_2O_6$	-	5.9	6.1	2.5		11.6			4.8		4.2	5.5	6.0	7.8
Total	100.0	100.0	100.0	100.0	100.0	100.0	100.0	100.0	100.0	100.0	100.0	100.0	100.0	100.0

APPENDIX 21 (Continued)

	69	70	71	72	73	74	75	76	77	78	79	80	81	82
Na^{+}	0.02	0.06	0.06	0.07	0.09	0.07	0.17	0.15	0.10	0.04	0.07	0.07	0.09	0.07
Ca^{+}	0.83	0.83	0.84	0.79	0.77	0.83	0.76	0.87	0.68	0.92	0.80	0.74	0.70	0.85
Mg^{2+}	1.15	0.78	0.77	0.90	0.53	0.64	0.46	0.45	0.68	0.68	0.85	0.89	0.94	0.67
Fe^{2+}	0.12	0.09	0.10	0.10	0.12	0.12	0.19	0.21	0.13	0.07	0.08	0.09	0.09	0.05
Cr^{3+}	0.03			0.01							0.01	0.02	0.03	
Ti^{4+}	0.02	0.04	0.05	0.02	0.05	0.04	0.06	0.05	0.02	0.09	0.02	0.02	0.01	0.05
Fe^{3+}	0.04	0.08	0.07	0.05	0.11	0.10	0.20	0.21	0.08	0.11	0.05	0.05	0.02	0.20
Al^{3+}	-	0.12	0.12	0.15	0.31	0.19	0.16	0.35	0.09	0.07	0.07	0.09	0.09	0.09
Al^{3+}	0.07	0.20	0.23	0.10	0.12	0.29	0.30	0.11	0.08	0.35	0.12	0.16	0.17	0.40
Si^{4+}	1.93	1.80	1.77	1.90	1.88	1.71	1.70	1.89	1.92	1.65	1.88	1.84	1.83	1.60

APPENDIX 21 (Continued)

	83	84	85	86	87	88	89	90	91	92	93	94	95	96
SiO_2	51.10	50.95	52.24	51.08	54.76	53.36	55.06	54.08	52.04	55.50	51.99	55.25	54.37	53.32
Al_2O_3	4.94	5.43	2.77	3.44	8.33	9.66	7.67	9.20	6.93	15.63	15.75	16.17	14.47	12.40
Fe_2O_3	0.45	0.09	3.54	4.12	1.29	1.69	1.68	0.83	2.59	1.94	1.55	1.64	2.38	1.48
FeO	2.70	2.73	0.47	0.18	2.70	5.68	4.01	2.18	4.10	0.96	0.58	1.36	0.95	1.40
MnO	0.04	0.03	0.02	0.02	0.04	tr	0.07	tr	0.09	0.02	tr	0.04	0.02	tr
MgO	17.29	14.05	16.93	17.04	11.59	9.50	11.97	11.51	11.65	7.17	10.72	7.23	8.95	10.40
CaO	20.19	22.45	19.62	19.05	16.35	12.18	14.22	17.50	19.49	10.52	14.75	12.34	13.35	14.67
Na_2O	1.65	1.32	1.66	1.47	4.63	6.82	4.70	4.20	2.22	7.61	4.22	6.36	5.21	4.79
K_2O	-	0.08	0.00	0.19	0.05	tr	0.08	0.04	-	0.08	0.22	0.07	0.13	0.16
TiO_2	0.55	0.40	0.00	0.57	0.44	0.34	0.51	0.14	0.54	0.18	0.28	0.23	0.13	0.23
Cr_3O_3	0.40	2.20	1.90	0.98	-	-	-	-	0.023	0.04	0.03	0.04	0.03	0.92
H_2O^+	-	0.42	0.06	1.62	-	1.05		0.46	-					
H_2O^-	0.08	0·14	0.36	0.86	-			-	-					
NiO		0.14												
Other														
Total	99.39	99.29	99.57	100.62	100.18	100.50	99.97	100.14	99.67	99.65	100.09	100.73	99.99	99.77
Ac	1.3	0.2	9.7	11.4	3.1	4.3	4.5	2.1	7.3	5.1	4.3	4.2	6.4	4.1
Jd	4.6	9.3	2.2		26.2	39.1	28.8	26.7	8.6	47.5	25.4	39.5	30.3	30.2
$CaTiAl_2O_6$	1.5	1.1		0.9	1.0	0.8	1.3	0.4	1.5	0.6	0.9	0.6	0.4	0.7
$Cr_2Al_2O_6$	0.6	3.2	2.7	2.9										1.3
$CaFe^{3+}_2SiO_6$														
$CaFeSi_2O_6$	8.4	9.6	2.3	0.7	7.4	16.4	12.1	6.6	13.1	3.0	1.7	4.0	3.0	5.5
$CaMgSi_2O_6$	68.6	74.3	71.8	71.8	58.5	30.0	41.4	61.0	62.3	36.2	53.7	39.5	47.2	49.9
$(MgFe)SiO_3$	13.1	2.3	11.3	11.5	3.8	9.4	11.8	1.1 *1	0.8	0.7	1.6			2.1
$Al_4Si_3O_{12}$							0.5		3.6	6.9	5.7	10.6	9.0	3.5
$Al_2Al_2O_6$	1.9			0.8				2.1	2.8		6.7	1.6	2.7	2.7
Total	100.0	100.0	100.0	100.0	100.0	100.0	100.0	100.0	100.0	100.0	100.0	100.0	100.0	100.0

APPENDIX 21 (Continued)

	83	84	85	86	87	88	89	90	91	92	93	94	95	96
Na^{+}	0.06	0.10	0.12	0.11	0.32	0.46	0.32	0.29	0.16	0.52	0.30	0.44	0.37	0.34
Ca^{+}	0.79	0.90	0.76	0.76	0.53	0.45	0.54	0.67	0.77	0.40	0.56	0.47	0.51	0.58
Mg^{2+}	0.94	0.78	0.92	0.96	0.61	0.49	0.64	0.61	0.64	0.38	0.57	0.38	0.48	0.57
Fe^{2+}	0.08	0.09	0.02	0.01	0.08	0.16	0.12	0.06	0.13	0.03	0.02	0.04	0.03	0.04
Cr^{3+}	0.01	0.07	0.06	0.03										0.03
Ti^{4+}	0.01	0.01	-	0.01	0.01	0.01	0.01			0.01	0.01	0.01	0.01	0.01
Fe^{3+}	0.01		0.09	0.11	0.03	0.04	0.05	0.02	0.07	0.05	0.04	0.04	0.06	0.04
Al^{3+}	0.08	0.09	0.03	0.01	0.28	0.39	0.30	0.31	0.21	0.61	0.51	0.64	0.75	0.49
Al^{3+}	0.12	0.10	0.09	0.09	0.06		0.03	0.06	0.09	0.04	0.16	0.03	0.06	0.04
Si^{4+}	1.88	1.90	1.91	1.91	1.94	1.84	1.97	1.94	1.91	1.96	1.84	1.97	1.94	1.96

	97	98	99	100	101	102	103	104	105	106	107	108	109	110
SiO_2	54.82	54.03	54.70	54.06	55.16	54.56	55.31	55.10	55.18	54.51	48.99	54.73	54.72	54.96
Al_2O_3	14.19	12.91	14.41	17.64	15.22	16.50	19.26	17.95	19.07	11.36	17.78	14.10	10.51	8.01
Fe_2O_3	1.63	1.53	1.53	1.56	1.01	1.56	0.82	1.08	0.66	2.68	0.72	1.17	1.69	1.92
FeO	0.64	0.75	0.61	0.83	1.00	0.40	1.10	0.58	0.76	0.75	0.74	1.74	2.56	3.13
MnO	0.03	0.05	tr	tr	0.02	0.01	tr	tr	tr	0.05	0.02	0.04	0.07	0.10
MgO	9.08	10.12	8.67	6.87	8.22	7.26	5.57	6.28	6.10	10.67	9.73	8.84	11.02	11.62
CaO	14.94	16.58	14.17	11.98	14.55	12.94	10.11	11.40	10.98	13.20	18.23	11.62	13.36	14.13
Na_2O	4.68	4.62	5.31	6.20	5.12	6.00	7.30	6.81	7.00	6.12	3.30	6.61	5.05	4.78
K_2O	0.07	0.12	0.05	0.12	0.16	0.07	0.11	0.06	0.06	0.06	0.06	0.24	0.17	0.18
TiO_2	0.12	0.04	0.18	0.42	0.10	0.10	0.38	0.03				0.41	0.41	0.42
Cr_2O_3	0.09	0.08	0.024	0.03	0.03	0.04	0.02	0.024				0.10	0.16	0.06
H_2O^+									0.05	0.25	0.13	0.38	nd	0.40
H_2O^-									0.08	0.06	0.05	0.17	nd	0.25
NiO														
Other														
Total	100.29	100.83	99.65	99.71	100.59	99.44	99.98	99.31	99.94	99.71	99.75	100.15	99.72	99.96
Ac	4.4	4.0	4.1	4.2	2.7	4.3	2.1	3.0	1.9	7.5	1.9	3.2	4.5	5.2
Jd	28.9	28.2	33.1	38.1	32.5	37.6	48.2	41.5	46.2	36.1	21.1	43.3	31.2	30.8
$CaTiAl_2O_6$	0.4	0.2	0.6	1.1	0.4	0.4	1.1		0.1	0.9	0.4	1.1	1.1	1.1
$Cr_2Al_2O_6$	0.2	0.2						0.0	0.1	0.2	0.2	0.2	0.4	0.2
$CaFe^{3+}_2SiO_6$														
$CaFeSi_2O_6$	2.0	2.5	1.7	1.9	2.9	1.3	3.2	1.7	2.3	2.6	2.2	5.1	7.9	9.5
$CaMgSi_2O_6$	50.0	53.4	46.4	36.4	44.1	38.5	29.4	33.7	32.0	47.7	52.1	37.6	42.3	43.13
$(MgFe)SiO_3$		6.4 *1	5.6	6.1 *1	8.7 *1	9.4 *1	4.7 *1	8.4 *1	7.2 *1	5.0	15.0	4.5	8.2	8.8
$Al_4Si_3O_{12}$	12.4	0.9	7.5	8.8	5.5	5.5	8.9	7.7	8.0					0.8
$Al_2Al_2O_6$	1.7	4.2	1.0	3.4 *8)	3.2 *8	3.0 *8	2.4 *8	4.0	2.2	-	7.1	4.0	4.4	-
Total	100.0	100.0	100.0	100.0	100.0	100.0	100.0	100.0	100.0	100.0	100.0	100.0	100.0	100.0

APPENDIX 21 (Continued)

	97	98	99	100	101	102	103	104	105	106	107	108	109	110
Na^{+}	0,33	0,31	0,36	0,42	0,35	0,40	0,50	0,45	0,46	0,41	0,23	0,47	0,38	0,34
Ca^{+}	0,57	0,61	0,52	0,45	0,54	0,47	0,38	0,41	0,40	0,49	0,70	0,44	0,51	0,54
Mg^{2+}	0,56	0,52	0,45	0,41	0,47	0,37	0,29	0,31	0,31	0,55	0,52	0,47	0,59	0,62
Fe^{2+}	0,02	0,02	0,02	0,02	0,03	0,01	0,03	0,02	0,02	0,02	0,02	0,05	0,08	0,10
Cr^{3+}														
Ti^{4+}				0,01	0,01					0,01		0,01	0,01	0,01
Fe^{3+}	0,04	0,04	0,04	0,04	0,03	0,04	0,02	0,03	0,02	0,07	0,02	0,03	0,05	0,05
Al^{3+}	0,56	0,37	0,48	0,64	0,52	0,53	0,73	0,57	0,65	0,34	0,50	0,53	0,40	0,32
Al^{3+}	0,04	0,14	0,11	0,08	0,10	0,14	0,06	0,14	0,12	0,12	0,25	0,06	0,04	0,02
Si^{4+}	1,96	1,86	1,89	1,92	1,90	1,86	1,94	1,86	1,88	1,88	1,75	1,94	1,96	1,98

APPENDIX 21 (Continued)

	111	112	113	114	115	116	117	118	119	120	121	122	123	124
SiO_2	54.21	54.29	53.74	54.74	54.3	51.80	50.47	49.8	50.73	50.69	52.53	53.93	51.71	50.78
Al_2O_3	6.76	4.40	5.06	5.61	10.0	1.84	4.36	6.98	7.86	7.68	4.23	9.64	4.53	7.24
Fe_2O_3	3.10	2.92	2.65	4.56	3.5	1.82	2.87	3.36	3.69	2.50	1.24	2.04	3.41	2.96
FeO	4.44	5.29	3.46	3.83	3.2	7.45	5.40	5.15	3.45	8.43	2.81	2.50	1.93	3.35
MnO	0.14	0.28	0.16	0.03	0.02	0.47	0.15	0.18	-	0.17	0.06	0.02	0.07	0.03
MgO	12.39	13.66	15.60	10.83	8.2	12.38	13.26	16.30	16.65	12.28	15.97	10.54	14.57	11.92
CaO	13.68	14.20	15.48	15.11	13.3	22.85	22.24	15.8	15.82	13.34	20.93	16.35	21.77	20.12
Na_2O	4.47	2.99	2.62	4.56	6.8	0.61	0.67	1.25	1.27	2.57	1.19	4.06	1.71	2.84
K_2O	0.21	0.20	0.17	0.01	0.02	0.03	0.03	tr	0.0	0.13	0.09	0.26	0.05	0.06
TiO_2	0.55	0.34	0.31	0.09	0.20	0.24	0.73	0.93	0.74	0.95	0.30	0.39	0.60	0.23
Cr_2O_3	0.15	0.11	0.34	0.01	-	0.01	0.01	-	-	0.076	0.26	0.03	-	-
H_2O^+	nd	0.77	0.41	0.50	0.12	0.26	0.14	-	0.04	0.74	0.54	0.25	-	0.66
H_2O^-	nd	0.25	0.14	0.20	0.06	-								
NiO				0.01	-	-								
Other				0.05	-	0.20	0.03			0.27				0.02
Total	100.10	99.70	100.14	100.23	99.72	99.96	100.36	99.97	100.25	99.95	100.15	100.01	100.35	100.21
Ac	8.5	8.1	7.4	10.2	9.5	4.3	4.7	8.8	10.1	7.2	3.3	5.8	9.3	8.1
Jd	23.7	14.7	11.8	16.0	37.7					12.4	5.7	24.2	2.8	12.1
$CaTiAl_1O_6$	1.5	0.9	0.9	0.2	0.6	0.7	2.2	2.4	2.4	2.8	0.9	1.1	1.7	0.7
$Cr_2Al_2O_6$	0.2	0.2	0.5							0.2	0.5	-		
$CaFe^{3+}_2SiO_6$						0.4	1.7	0.2	0.8					
$CaFeSi_2O_6$	13.5	17.5	10.8	9.5	9.7	25.0	17.3	16.7	12.9	27.3	8.8	8.0	6.2	10.2
$CaMgSi_2O_6$	37.9	38.2	48.7	57.9	41.3	66.1	67.8	42.8	59.5	24.4	72.0	45.4	76.3	63.9
$(MgFe)SiO_3$	14.7	18.9	17.9	4.8	1.2	2.0	3.7	23.0	12.6	22.9	7.6	7.2	1.0	2.8
$Al_4Si_3O_{12}$		1.5	-	0.7								8.3		
$Al_2Al_2O_6$			2.0	0.7		1.5	2.6	6.1	0.7	2.8	1.2		2.7	2.2
Total	100.0	100.0	100.0	100.0	100.0	100.0	100.0	100.0	100.0	100.0	100.0	100.0	100.0	100.0

	111	112	113	114	115	116	117	118	119	120	121	122	123	124
Na^{+}	0.32	0.23	0.19	0.32	0.47	0.04	0.05	0.09	0.08	0.19	0.09	0.30	0.12	0.20
Ca^{+}	0.53	0.56	0.60	0.59	0.51	0.92	0.88	0.62	0.57	0.52	0.82	0.52	0.85	0.80
Mg^{2+}	0.67	0.74	0.84	0.59	0.44	0.70	0.73	0.89	0.83	0.67	0.87	0.58	0.79	0.66
Fe^{2+}	0.14	0.17	0.11	0.12	0.10	0.25	0.17	0.17	0.10	0.07	0.09	0.08	0.06	0.10
Cr^{3+}			0.01								0.01			
Ti^{4+}	0.02	0.01	0.01		0.01	0.01	0.02	0.02	0.02	0.02	0.01	0.01	0.02	0.01
Fe^{3+}	0.08	0.07	0.07	0.12	0.10	0.05	0.08	0.09	0.09	0.06	0.03	0.06	0.09	0.08
Al^{3+}	0.24	0.17	0.16	0.23	0.28	0.03	0.05	0.12	0.01	0.17	0.08	0.39	0.07	0.20
Al^{3+}	0.05	0.02	0.06	0.02	0.05	0.05	0.14	0.18	0.30	0.16	0.09	0.02	0.11	0.12
Si^{4+}	1.95	1.98	1.94	1.98	1.95	1.95	1.86	1.82	1.70	1.84	1.91	1.98	1.88	1.88

	125	126	127	128	129	130	131	132	133	134	135	136	137	138
SiO_2	52.0	46.20	52.66	49.24	45.50	51.62	52.87	51.72	52.39	52.00	49.68	52.92	59.38	48.24
Al_2O_3	0.92	7.15	1.00	4.61	6.89	3.14	2.14	3.82	4.00	0.92	0.78	2.80	25.82	0.30
Fe_2O_3	2.64	3.68	9.06	0.68	3.24	1.25	1.10	0.90	1.55	2.64	3.29	0.85	0.45	1.50
FeO	3.89	2.98	5.60	6.00	3.88	5.63	12.59	5.77	8.59	3.89	18.15	5.57	tr	22.94
MnO	0.26	0.11	0.28	0.10	0.08	0.14	0.26	0.14	0.21	0.26	0.59	0.15	-	3.70
MgO	14.52	14.25	9.90	14.18	11.81	17.42	26.70	16.80	15.25	14.52	16.19	16.40	0.12	1.06
CaO	23.49	22.80	16.83	22.06	25.95	19.45	2.72	19.13	15.17	23.49	9.90	19.97	0.13	21.30
Na_2O	0.74	0.71	4.15	0.55	0.12	0.32	0.16	0.45	0.70	0.74	0.65	0.35	13.40	0.14
K_2O	0.06	0.20	0.06	0.04	0.04	0.01	0.04	0.05	0.21	0.06	0.15	0.01	0.02	0.03
TiO_2	0.04	1.72	0.57	2.05	2.47	0.72	1.12	0.92	1.43	1.68	0.56	0.50	0.04	0.08
Cr_2O_3	0.02	0.46	-	0.40	nd	0.49	0.11	0.52	0.54	-	-	0.88	0.01	-
H_2O^+			0.06	0.20	0.58	nd	0.03	-	-	0.04	0.10	0.17	0.38	0.46
H_2O^-	1.68		0.02		0.11					0.02				
NiO				-	-							0.10		
Other														
Total	100.26	100.26	100.19	100.11	100.67	100.19	99.84	100.22	100.04	100.26	100.04	100.67	99.75	99.85
Ac	5.5	6.4	25.2	2.0		2.2	1.3	2.2	3.3	5.3	5.3	2.4	1.3	1.0
Jd			4.9	2.2								0.2	90.0	
$CaTiAl_2O_6$	2.0	5.0	1.5	8.6		1.7	3.0	2.2	4.2	4.4	1.5	1.3		0.2
$Cr_2Al_2O_6$	2.6[*5]	0.7		0.6		1.2	0.2	1.2	0.8			1.3		
$CaFe^{3+}_2SiO_6$	0.9	2.0				0.5	0.8	0.4	0.5	0.9	3.7			1.9
$CaFeSi_2O_6$	12.5	10.2	18.1	18.6		15.6	19.4	16.5	28.7	12.2	28.4[*4]	18.0		94.1
$CaMgSi_2O_6$	75.5	69.8	46.4	58.4		60.4	7.2	61.1	30.7	71.1		59.5	0.6	
$(Mg,Fe)SiO_3$	3.0	2.0	3.9	9.6		17.4	68.1	16.4	25.7	5.1	44.3	15.5		2.3
$Al_4Si_3O_{12}$									3.5		16.8[*2]		8.1	0.5
$Al_2Al_2O_6$		4.9							2.6			1.8		
Total	100.0	100.0	100.0	100.0		100.0	100.0	100.0	100.0	100.0	100.0	100.0	100.0	100.0

APPENDIX 21 (Continued)

	125	126	127	128	129	130	131	132	133	134	135	136	137	138
Na^{+}	0.06	0.06	0.31	0.04	0.01	0.02	0.01	0.03	0.06	0.05	0.05	0.03	0.91	0.01
Ca^{+}	0.94	0.88	0.69	0.79	0.07	0.70	0.10	0.73	0.60	0.91	0.40	0.79	0.01	0.94
Mg^{2+}	0.81	0.83	0.56	0.70	0.68	0.88	1.44	0.89	0.78	0.91	0.90	0.90	0.01	0.06
Fe^{2+}	0.13	0.10	0.19	0.17	0.13	0.16	0.39	0.18	0.27	0.13	0.58	0.20		0.92
Cr^{3+}		0.01		0.01		0.02		0.02	0.02			0.03		
Ti^{4+}	0.05	0.05	0.02	0.08	0.08	0.02	0.03	0.02	0.04	0.05	0.02	0.01		0.01
Fe^{3+}	0.08	0.10	0.26	0.02	0.09	0.03	0.03	0.02	0.04	0.07	0.09	0.03	0.01	
Al^{3+}		0.12	0.05	0.02	0.06			0.01	0.09			0.04	1.07	0.01
Al^{3+}	0.04	0.18		0.16	0.25	0.13	0.09	0.15	0.08	0.04	0.04	0.06	-	-
Si^{4+}	1.96	1.82	2.00	1.84	1.75	1.74	1.91	1.85	1.92	1.87	1.86	1.96	2.04	2.00

	139	140	141	142	143	144	145	146	147	148	149	150	151	152	153
SiO_2	46.20	44.43	47.45	46.20	46.40	51.94	54.01	54.63	42.21	46.72	48.54	42.15	46.60	51.94	49.78
Al_2O_3	7.15	7.93	6.30	8.58	9.32	1.44	2.08	0.50	9.92	2.41	8.71	0.55	6.07	1.44	4.89
Fe_2O_3	3.68	4.30	2.38	2.68	2.13	1.98	1.24	0.16	5.28	17.29	2.81	17.40	4.85	1.98	1.41
FeO	2.98	3.28	4.29	5.47	5.10	6.10	6.52	1.39	1.96	10.57	0.96	17.80	3.72	6.10	8.64
MnO	0.11	0.13	0.12	0.18	0.13	0.17	0.14	0.05		1.31		0.50		0.17	0.19
MgO	14.25	13.71	15.12	11.66	10.89	13.56	31.98	18.08	13.90	2.57	14.42	1.10	12.21	13.56	14.11
CaO	22.80	22.10	20.92	20.10	20.91	23.95	2.22	25.04	22.28	13.51	24.56	14.10	23.88	23.95	19.45
Na_2O	0.71	0.70	0.90	0.91	0.92	0.40	0.21	tr	0.92	4.88		3.35	0.47	0.40	0.67
K_2O	0.20	0.22	0.15	0.20	0.26	0.17	0.13	tr	0.64	-		0.55	0.28	0.17	0.04
TiO_2	1.72	2.42	2.28	2.96	3.56	0.20	0.04	0.24	0.24	tr		0.41	1.59	0.20	1.09
Cr_2O_3	0.46	0.18	0.13	0.17	nd	-	0.33	-	0.08			-	-	-	
H_2O^+				0.80		0.32	0.71	0.33	0.30				0.26	0.32	0.04
H_2O^-															
NiO															
Other						0.08			2.50			1.90		0.08	
Total	100.26	99.40	100.04	99.91	99.62	100.31	99.61	100.42	100.23	99.74	100.00	99.81	99.93	100.31	100.31
Ac	6.0	6.1	6.6	7.8	6.3	3.6	1.7		9.9	39.3		27.3	4.7	3.8	4.0
Jd			0.4		1.6										1.1
$CaTiAl_2O_6$	4.6	6.7	6.3	8.5	10.5	0.7		0.5	0.7			1.0	4.5	0.7	3.1
$Cr_2Al_2O_6$	0.7	0.4	0.2	0.3			0.4		0.2					1.1	0.4
$CaFe^{3+}_2SiO_6$	1.7	3.1				1.0	0.7	0.2	2.5	5.7	7.7	22.6	9.0	1.1	
$CaFeSi_2O_6$	9.5	10.7	13.3	18.1	17.0	19.4		4.4	6.1	38.8	3.1	33.8	11.6	14.8	27.3
$CaMgSi_2O_6$	75.6	70.8	62.2	55.0	59.4	74.4	5.9	92.2	77.2	16.2	78.3		67.8	79.5	46.3
$(MgFe)SiO_3$	1.3	2.8	10.4	5.6	1.8	0.0	1.8	2.5	3.4 *1)			15.3		0.1	15.7
$Al_4Si_3O_{12}$							9.5 *4				7.0 *1		2.5 *1		
$Al_2Al_2O_6$	0.6		0.6	4.7	3.4						3.9				2.1
Total	100.0	100.0	100.0	100.0	100.0	100.0	100.0	100.0	100.0	100.0	100.0	100.0	100.0	100.0	100.0

	139	140	141	142	143	144	145	146	147	148	149	150	151	152	153
Na^{+}	0.06	0.06	0.07	0.07	0.08	0.04	0.02		0.10	0.37		0.50	0.04	0.04	0.05
Ca^{+}	0.90	0.88	0.83	0.80	0.81	0.95	0.08	0.99	0.90	0.57	0.93	0.57	0.91	0.95	0.77
Mg^{2+}	0.78	0.76	0.83	0.65	0.59	0.75	1.68	0.99	0.78	0.15	0.75	0.06	0.65	0.75	0.78
Fe^{2+}	0.10	0.11	0.13	0.18	0.16	0.20	0.19	0.04	0.06	0.39	0.03	0.58	0.11	0.20	0.20
Cr^{3+}	0.01	0.01					0.01								
Ti^{4+}	0.05	0.07	0.06	0.08	0.10	0.01		0.01	0.01			0.10	0.04	0.01	0.03
Fe^{3+}	0.10	0.12	0.06	0.08	0.06	0.05	0.03		0.15	0.51	0.07	0.50	0.13	0.06	0.04
Al^{3+}	0.03		0.02	0.09	0.08				0.02		0.07		0.02	-	0.05
Al^{3+}	0.30	0.35	0.26	0.29	0.31	0.06	0.08	0.02	0.41	0.11	0.29	0.02	0.23	0.07	0.16
Si^{4+}	1.70	1.65	1.74	1.71	1.69	1.94	1.92	1.98	1.59	1.82	1.71	1.60	1.66	1.93	1.84

APPENDIX 21 (Continued)

	154	155	156	157	158	159	160	161	162	163	164	165	166	167	168
SiO_2	50.51	48.17	48.84	44.22	49.69	50.25	50.56	50.61	50.89	49.20	49.65	49.78	48.74	47.46	48.42
Al_2O_3	3.41	6.10	5.40	6.46	3.95	3.83	3.40	4.01	3.06	5.56	4.34	7.66	6.76	8.19	7.49
Fe_2O_3	1.30	3.61	1.35	1.48	1.75	1.95	1.46	0.97	1.35	1.00	1.92	1.91	3.23	3.14	2.50
FeO	9.23	7.77	10.33	19.36	6.25	6.34	7.52	7.98	8.53	5.96	8.09	4.18	4.86	4.76	4.50
MnO	0.19	0.20	0.19	0.73	0.17	0.19	0.14	0.25	0.28	0.12	0.17	0.16	0.16	0.17	0.15
MgO	13.89	12.73	12.43	6.74	15.35	14.85	14.79	14.51	14.24	15.90	14.49	14.27	13.60	13.58	14.05
CaO	20.11	19.97	19.64	17.79	20.91	20.77	20.95	20.55	20.48	20.50	20.21	20.23	20.52	19.90	20.35
Na_2O	0.37	0.32	0.45	0.47	0.49	0.41	0.50	0.42	0.39	0.33	0.41	0.73	0.58	0.74	0.65
K_2O	0.03	0.02	0.07	0.08	0.01	0.01	0.03	0.01	0.01	0.01	0.01	0.07	0.02	0.03	0.05
TiO_2	0.76	1.01	1.46	2.27	1.05	1.41	0.83	0.93	1.10	0.89	0.91	0.19	1.41	1.67	1.33
Cr_2O_3					0.75	0.24	-	-	-	0.46	-	0.18	0.13	0.05	0.13
H_2O^+	0.21	0.21	0.08	0.41	0.03	-	0.13	-	-	0.15	0.11			0.21	0.31
H_2O^-															
NiO															
Other															
Total	100.01	100.11	100.27	100.01	100.40	100.25	100.31	100.24	100.33	100.08	100.31	100.36	100.01	99.90	99.93
Ac	2.9	2.5	3.4	3.4	3.6	2.8	3.6	2.7	2.9	2.4	2.8	5.3	4.2	5.4	4.8
Jd												0.2		3.3	2.0
$CaTiAl_2O_6$	2.2	2.9	4.2	5.8	3.1	4.3	2.2	2.7	3.2	2.4	2.4	3.3	4.0	2.4	0.4
$Cr_2Al_2O_6$	0.2				1.1	0.4				0.7		0.7	0.4	0.2	0.4
$CaFe^{3+}_2SiO_6$	0.4	3.8	0.5	0.4	0.7	1.4	0.4	0.2	0.6	0.2	1.2		4.9	4.7	1.8
$CaFeSi_2O_6$	29.3	25.1	33.0	56.6	15.5	20.6	23.4	25.6	27.6	18.6	25.4	13.1	15.7	15.2	14.4
$CaMgSi_2O_6$	49.1	52.6	41.2	1.2	64.8	55.2	56.6	53.7	51.5	59.5	55.6	63.6	56.6	60.3	63.9
$(MgFe)SiO_3$	14.2	9.3	14.2	32.6	10.2	13.6	13.0	13.1	14.0	13.8	12.0	6.8	9.2	7.4	6.8
$Al_4Si_3O_{12}$												0.8			
$Al_2Al_2O_6$	1.7	3.8	3.6	-	1.0	1.7	0.8	2.0	0.2	2.4	0.6	6.2	5.0	5.8	5.9
Total	100.0	100.0	100.0	100.0	100.0	100.0	100.0	100.0	100.0	100.0	100.0	100.0	100.0	100.0	100.0

	154	155	156	157	158	159	160	161	162	163	164	165	166	167	168
Na^{+}	0.03	0.03	0.03	0.04	0.04	0.03	0.04	0.03	0.03	0.02	0.03	0.06	0.04	0.06	0.05
Ca^{+}	0.80	0.81	0.79	0.73	0.83	0.83	0.83	0.81	0.83	0.81	0.79	0.78	0.81	0.79	0.84
Mg^{2+}	0.77	0.71	0.70	0.39	0.85	0.82	0.81	0.80	0.80	0.87	0.79	0.77	0.75	0.75	0.77
Fe^{2+}	0.30	0.25	0.33	0.65	0.15	0.20	0.24	0.26	0.28	0.19	0.25	0.13	0.16	0.15	0.14
Cr^{3+}					0.02	0.01				0.01		0.01	-		
Ti^{4+}	0.03	0.03	0.04	0.07	0.03	0.04	0.02	0.03	0.03	0.02	0.02	0.03	0.04	0.05	0.03
Fe^{3+}	0.04	0.10	0.04	0.04	0.05	0.06	0.04	0.03	0.04	0.03	0.05	0.06	0.09	0.09	0.07
Al^{3+}	0.03	0.08	0.07	-	0.02	0.04	0.02	0.04	0.02	0.05	0.01	0.13	0.10	0.12	0.12
Al^{3+}	0.12	0.19	0.16	0.30	0.15	0.13	0.14	0.13	0.12	0.20	0.18	0.20	0.19	0.24	0.22
Si^{4+}	1.88	1.81	1.84	1.70	1.85	1.87	1.86	1.87	1.88	1.80	1.82	1.80	1.81	1.76	1.78

	169	170	171	172	173	174	175	176	177	178	179	180	181	182	183
SiO_2	48.07	48.11	48.43	50.19	50.04	50.24	49.90	49.04	47.98	48.90	52.42	52.40	58.14	52.66	51.22
Al_2O_3	7.93	7.26	8.02	3.94	3.98	3.58	4.08	4.57	5.17	3.98	1.72	1.19	1.51	2.10	3.68
Fe_2O_3	2.66	3.13	2.68	3.33	3.60	3.66	3.60	4.48	4.15	3.76	1.91	2.56	2.16	2.40	2.24
FeO	4.51	4.86	4.78	5.62	2.51	2.73	2.87	2.44	3.09	2.73	2.16	2.41	2.73	2.87	2.87
MnO	0.15	0.11	0.15	0.21	0.11	0.15	0.13	0.10	0.13	0.14	0.09	0.10	0.10	0.12	0.14
MgO	14.22	14.04	13.60	13.78	15.39	15.53	14.10	14.15	14.51	15.17	17.22	17.46	15.30	14.98	16.07
CaO	20.15	20.46	20.46	21.10	23.62	22.89	23.45	23.28	22.66	23.11	23.89	22.94	24.33	23.69	23.41
Na_2O	0.61	0.66	0.84	0.32	0.36	0.49	0.53	0.59	0.50	0.42	0.69	0.52	0.52	0.61	0.35
K_2O	0.02	0.04	0.04	0.06											
TiO_2	1.48	1.14	1.15	1.30	0.40	0.34	0.48	0.47	0.55	0.37	0.15	0.19	0.19	0.25	0.30
Cr_2O_3	0.11	-	0.10	0.00	0.02	0.02	0.02	0.03	0.03	0.03	0.20	0.33	0.22	0.20	0.09
H_2O^+	-	0.43	-	-	0.44	0.65	0.61	0.38	0.73	0.57	0.20	0.64	0.78	0.76	0.14
H_2O^-															
NiO															
Other					0.02	0.03	0.02	0.04	0.02						
Total	99.91	100.24	100.25	99.94	100.49	100.31	99.79	99.57	99.52	99.72	100.85	100.77	100.78	100.64	100.54
Ac	4.5	5.1	6.2	2.6	2.7	3.5	3.8	4.3	4.3	3.5	4.9	3.4	3.6	4.2	2.5
Jd	3.1														
$CaTiAl_2O_6$		3.1	3.3	3.5	1.1	0.9	1.3	1.3	1.6	1.5	0.4	0.6	0.7	0.9	0.9
$Cr_2Al_2O_6$	0.2	1.0	0.2								0.6	0.9	0.7	0.7	0.2
$CaFe_2SiO_6$	2.1	1.8	0.7	3.4	3.6	3.3	3.2	4.2	4.1	4.0	0.2	1.7	1.2	1.5	1.7
$CaFeSi_2O_6$	14.5	15.4	15.2	15.2	8.0	8.9	9.4	7.8	10.1	9.8	6.7	7.5	8.6	9.1	9.2
$CaMgSi_2O_6$	61.9	62.3	62.1	66.8	83.7	80.4	80.6	81.2	77.4	77.8	83.1	78.8	85.2	82.2	81.3
$(Mg,Fe)SiO_3$	8.2	7.4	6.1	5.4	0.3	2.4	0.0	0.0	3.5	3.5	4.1	7.1	0.0	0.0	3.8
$Al_4Si_3O_{12}$				1.2											
$Al_2Al_2O_6$	5.5	4.9	6.2	1.9	0.6	0.6	1.8	1.3						1.4	1.2
Total	100.0	100.0	100.0	100.0	100.0	100.0	100.0	100.0	100.0	100.0	100.0	100.0	100.0	100.0	100.0

	169	170	171	172	173	174	175	176	177	178	179	180	181	182	183
Na^{+}	0.05	0.05	0.06	0.03	0.03	0.03	0.03	0.04	0.03	0.03	0.05	0.03	0.03	0.04	0.03
Ca^{+}	0.79	0.86	0.81	0.86	0.93	0.90	0.93	0.93	0.90	0.92	0.94	0.91	0.97	0.93	0.91
Mg^{2+}	0.78	0.77	0.74	0.78	0.85	0.85	0.78	0.80	0.85	0.84	0.94	0.97	0.85	0.82	0.87
Fe^{2+}	0.14	0.15	0.15	0.15	0.08	0.09	0.09	0.08	0.10	0.09	0.07	0.08	0.09	0.09	0.09
Cr^{3+}											0.01	0.01	0.01	0.01	-
Ti^{4+}	0.05	0.03	0.03	0.03	0.01	0.01	0.01	0.01	0.02	0.01	-	0.01	0.01	0.01	0.01
Fe^{3+}	0.08	0.09	0.07	0.10	0.10	0.10	0.10	0.12	0.12	0.11	0.05	0.07	0.06	0.07	0.06
Al^{3+}	0.11	0.10	0.12	0.06	0.01	0.01	0.04	0.03						0.03	0.02
Al^{3+}	0.23	0.22	0.16	0.11	0.16	0.15	0.14	0.18	0.23	0.18	0.07	0.05	0.06	0.06	0.13
Si^{4+}	1.77	1.78	1.84	1.89	1.84	1.85	1.86	1.82	1.77	1.82	1.93	1.95	1.94	1.94	1.87

****

Appendix 21:

The chemical analyses, molecular norms and structural formulas of the clinopyroxenes from various parentages.

I. Partial analyses of clinopyroxenes from kimberlite.

41 partial analyses of clinopyroxenes from various sources; Boyd (1969).

II. New chemical analyses.

1. CF_{304}; Eclogitic clinopyroxene; Roberts Victor.
2. CF_{305}; Clinopyroxene from garnet peridotite; Jagersfontein.
3. CF_{307}; Clinopyroxene from kimberlite; Premier Mine.

III. Clinopyroxene in kimberlite.

4 from Premier Mine; Hall (1938).
5 - 6 from Jagersfontein; Holmes (1936).
7 - 8 from Jagersfontein; Hall (1938).
9 -12 from Russia; Bobrievich et. al., (1959).
13 from Deutche Erde; Ann. Rep. Univ. Leeds (1962-63).
14 from Mukarob, S.W.A.; (ditto).
15 from Deutche Erde; (ditto).
16 from Zagodachnaya; Smirnov (1959).
17-18 from Kimberley; Holmes (1936).
19 from Tanzanian kimberlite; Boyd (1969).
20 diopside inclusion in a diamond; (ditto).

IV. Clinopyroxene in ultramafic nodules.

21 from Thaba Putsoa; Boyd (1969).
22 from Lauwrencia; (ditto).
23 from Monastry; (ditto).
24 from Malibe Matso; (ditto).
25 from Dutoitspan; MacGreggor et. al., (1963).
26 O'Hara and Mercy (1963).
27 from Thaba Putsoa; Nixon et al., (1963).
28 from Dutoitspan; (ditto).
29 from Peridotite nodule; Min. abst., (1963-64).
30-33 from Russia; Bobrievich et al., (1959).
34-39 from regional peridotites; O'Hara and Mercy, (1963).

40-48 nodules from kimberlite; O'Hara and Mercy, (1963).
49-50 regional garnet peridotite from Karlskaret; Carswell, (1968).

V. Clinopyroxene from ultramafic nodules in alkaline basalts.

51 from a nodule in basalt; Ross et. al., (1954).
52 from the alkaline basalt in France; Bull. Soc. Min. Cryst., (1967, p. 207).
53-54 from France; Brousse (1968).
55-71 from various alkaline basalts; Ross et. al., (1954, p 709).
72-83 from various nodules and lapili; Kuno (1967).
84-88 from France; Brousse (1968).

VI. Clinopyroxene from Eclogite nodules.

89 from Kao; Nixon et. al., (1963).
90 from Jagersfontein; (ditto).
91 from Kaalvalei; (ditto).
92-93 from Regional eclogites; Church & Edgar; Contr. Min & Petr., (1968; p 340).
94-109 from kyanite eclogite (6), grospydite (8) and corundum eclogite; Sobolev (1968).
110-115 from Roberts Victor; Kushiro and Aoki (1968).

VII. Clinopyroxene from Regional Eclogites.

116,117 Omphacite; Clark and Papike (1968).
118,119 Omphacite; Boesen, Amer. Min., (1964, 1447).
120,122 Breccia, New Zealand; Dicky (1968).
123 Average of eclogite nodules in kimberlite; Smulikowski (1968).
124 Average of regional eclogite; (ditto).
125 Clinopyroxene from nodule from Kaudus; Ann. Rep. Leeds. Univ. (1962).
126 Omphacite; Min. Abst. (1959, p 428).

VIII. Clinopyroxenes from various Igneous Rocks.

127 Melilitite matrix; Min. abst., (1963-4, 197).
128 Ankaratrite; Eifel; Huckenholz (1966).
129 Melteigite; Min. abst., (1959; 499).
130-131 From Mustang Sill; Min. abst., (1959, p 350) and (1961-2, p 219).

132-135 Kiluaea basalt; Muir and Tilly; (1963).
136 from melilitite; (Geol. Rundchau (1968, 911).
137-140 Deer, Howie and Zussman, (1967, p 106).
141-154 from various rock-types in South Africa; Hall (1938).
155-160 from Kap Edward Complex; Min. Mag. (1965, p 183).
167-174 aluminous augites; Amer. Min. (1968, 249).
175-183 from Urals; All. Union. Min. Soc., (1967, p 138).

*1) $CaAlSiAlO_6$
*2) $Ca_2Si_2O_6$
*3) $NaFe^{3+}Si_2O_6$
*4) $Fe_2Si_2O_6$
*5) $CaTiAl_2O_6$
*6) $NaCrSi_2O_6$
*7) $NaTiAlSiO_6$
*8) SiO_2
*9) Other oxides, not specified.

APPENDIX 22- The chemical analyses, molecular norms and Structural formulas of calcite from kimberlite and carbonatite

A. Chemical analyses

	1	2	3	4	5	6	7
SiO_2		2.56	0.03				3.18
Al_2O_3		0.51					1.52
Fe_2O_3		0.07					1.10
FeO		0.14		3.10	0.52	4.24	0.81
CaO	55.85	52.84	52.91	30.35	54.57	31.75	52.08
SrO		0.43	0.03	0.91	0.18	0.48	
BaO			0.12	tr	0.05	tr	
MgO		0.78	2.47	18.80	0.51	18.02	1.90
CO_2	44.06	42.62	44.37	46.84^{+}	44.17^{+}	45.51	38.61
Total	99.91	99.95	99.93	100.0	100.0	100.0	100.0^{+1}

B. Molecular norms

$CaCO_3$	100.0	97.5	93.8	51.2	98.0	52.5	93.3
$MgCO_3$		2.0	6.1	43.9	1.2	41.5	5.4
$FeCO_3$		0.2		4.1	0.7	5.5	1.3
$SrCO_3$		0.3		0.8	0.1	0.5	
$BaCO_3$			0.1				
Total	100.0	100.0	100.0	100.0	100.0	100.0	100.0

C. Structural formula based on one cation per unit cell

Ca^{2+}	1.00	0.98	0.94	0.51	0.98	0.53	0.94
Mg^{2+}		0.02	0.06	0.44	0.01	0.42	0.05
Fe^{2+}				0.04	0.01	0.06	0.01
Sr^{2+}				0.01		0.01	
Ba^{2+}						-	
CO_3^{2-}	1.00	0.99	1.0	1.0	1.0	1.0	0.88

****

Appendix 23:

The chemical analyses, molecular norms and structural formulas of calcite from kimberlite and carbonatite.

1 + calcite
2 + 3 calcite from Russian kimberlites) Bobrievich et al., (1959).
4 - 6 calcite from carbonatite; Gittins and Tuttle (1966).
7 calcite nodule from Premier Mine, Hall (1938, p 1827).

+ Determined by difference

$^{+}_{1}$ Includes 0.46% SO_3 and 0.40% H_2O.

A. Chemical Analyses

	1	2	3	4	5	6	7	8
SiO_2	1.56	0.20			0.52			0.10
Al_2O_3					2.39			1.39
Fe_2O_3	72.10	69.30	56.56	60.26	45.67	33.5	36.2	28.37
FeO	25.20	27.93	25.80	20.80	25.68	44.9	43.6	46.06
CaO					0.24			0.06
MgO		0.90	6.80	4.67	10.45	0.5	n.d.	2.29
H_2O					0.08			
TiO_2	0.40	0.80	11.54	14.71	13.80	19.4	17.3	19.42
P_2O_5					0.17			
MnO		0.23			0.10	1.2	0.9	0.33
Other						0.50	2.0	0.07
Total	99.26	99.36	100.70	100.44	99.88	100.0	100.0	100.06

B. Molecular norms

$MgAl_2O_4$	-		-	-	5.8	-	-	3.8
$MgFe_2O_4$	-	5.2	41.1	25.8	58.5	3.2		12.1
$MnFe_2O_4$	-	0.7	-	-		4.5	3.5	1.1
$Fe^{2+}TiO_3$	0.8	1.7	21.7	27.5	28.7	43.5	38.8	46.0
$FeFe_2O_4$	82.5	88.0	37.2	23.8	7.0	48.8	57.7	37.0
Fe_2O_3	16.7	4.4	-	22.9		-	-	-
Total	100.0	100.0	100.0	100.0	100.0	100.0	100.0	100.0

C. Structural formula based on 32 oxygens per unit cell

Mg^{2+}		0.4	3.0	2.7	4.9	0.2	-	1.0
Mn^{2+}		-	-		-	0.3	0.2	0.1
Fe^{2+}	8.0 23.9	7.6 24.0	6.3 24.1	6.8 24.1	6.9 27.0	10.4 22.9	11.2 24.0	11.3 23.5
Al^{3+}					0.9			0.5
Fe^{3+}	15.8	15.9	12.3	10.3	11.0	7.6	8.5	6.3
Ti^{4+}	0.1	0.1	2.5	4.3	3.3	4.4	4.1	4.3

Appendix 23:

The chemical analyses, molecular norms and structural formulas of magnetite.

A. Magnetite from kimberlite:-

1, 2 from Mir and Zarnitza; (Smirnov 1959).
3, 4 from Zefu, Verhoogen (1938).

B. Magnetite from other rock-types:-

5 from carbonatite, Sobolev (1958, p 152).
6, 7 from Hocheifel, Huckenholz (1966).
8 from Skaergaard, Deer, Howie and Zussman (1967).

	1	2	3	4	5	6	7	8	9	10	11	12	13	14
SiO_2	36.86	38.82	37.64	42.08	40.56	44.12	28.68	40.56	43.70	43.90	38.20	41.96	42.36	38.68
Al_2O_3	3.60	7.00	3.88	4.55	4.67	6.29	4.88	7.43	7.04	6.50	6.66	8.55	5.93	5.97
Fe_2O_3	6.57	5.93	6.73	5.94	6.25	5.05	7.04	4.16	5.60	5.30	5.13	4.17	7.05	5.57
FeO	4.17	4.03	4.03	4.74	4.46	3.74	5.18	4.53	3.59	3.88	4.39	4.16	4.46	3.45
MnO	0.05	0.02	0.06	0.02	0.02	0.06	0.09	0.04	-	0.04	0.04	0.02	0.04	0.07
MgO	25.92	23.76	26.06	20.16	21.85	19.44	15.12	20.88	19.87	19.80	23.40	21.38	19.80	24.91
CaO	6.46	5.60	6.16	5.88	6.44	5.18	15.96	6.30	4.92	4.34	4.90	3.92	5.60	3.64
Na_2O	1.77	0.68	0.66	2.54	2.68	2.57	0.77	0.72	1.64	2.72	2.11	1.92	1.12	1.83
K_2O	1.36	0.85	1.00	1.95	1.49	1.14	0.54	1.92	1.03	1.42	0.57	0.85	1.31	1.28
H_2O^+	8.26	6.18	9.36	5.66	5.65	5.10	4.41	2.82	4.62	4.42	4.96	5.34	5.76	4.96
H_2O^-	1.68	4.72	1.04	2.88	3.06	4.64	3.80	3.88	4.94	5.32	1.94	0.57	1.33	1.09
P_2O_5	0.71	0.29	0.80	0.44	0.49	0.32	0.59	0.45	0.34	0.32	0.30	0.28		
CO_2	1.12	1.50	0.79	2.26	1.30	1.01	9.33	2.13	-	1.38	6.09	5.70	4.41	7.83
TiO_2	1.34	0.65	1.30	1.11	0.86	0.77	1.03	1.48	1.54	0.64	0.68	0.99	1.03	0.68
Cr_2O_3	-	-	-	-	-	-	-	-	0.86	-	-	-	-	-
Other *2)	-	-	-	-	-	-	-	-	-	-	-	-	-	-
Total	99.87	100.03	99.51	100.21	99.78	99.43	99.46	99.32	99.75	99.98	99.37	99.82	100.20	100.16
B. The Katamolecular norms														
Ne	3.3				4.1									
Kp														
Cal														
Ab	9.4	6.5	6.2	23.9	18.4	24.5	16.7	7.0	16.0	26.3	18.9	17.2	9.8	16.3
Or	8.5	5.3	5.9	4.7	9.1	7.1	3.5	11.8	6.5	9.0	3.4	5.0	7.9	7.8
An		14.3	5.3			2.4	4.0	12.0	9.2	1.5	7.0	12.2	7.6	4.1
Ap	2.3	1.0	2.6	1.4	1.6	0.9	1.9	1.6	1.4	1.0	0.9	0.9		
Hm	4.8	4.4	4.9	4.3	4.4	3.8	5.2	3.1	4.2	4.0	3.6	2.9	5.0	3.8
Il	2.0	1.1	1.9	1.6	1.2	1.2	1.5	2.2		1.0	1.0	1.4	1.6	1.0
Ol	59.8	37.6	49.2	27.6	50.5	31.5	38.2		19.2	35.6	32.8	14.8	5.6	17.3
Di	7.0	0.7	6.9	0.3	7.3	5.9	4.1	28.3	0.4	3.4				
En		24.9	15.0	26.7		20.1	-	28.2	38.8	17.1	16.8	31.2	51.0	27.6
CC	2.9	4.2	2.1	9.5	3.4	2.7	24.9	5.8	4.2	3.9	5.6	1.6	8.2	5.5
MC										0.0	10.0	12.8	3.3	16.6
Ca-Ol														
Total	100.0	100.0	100.0	100.0	100.0	100.0	100.0	100.0	100.0	100.0	100.0	100.0	100.0	100.0

	15	16	17	18	19	20	21	22	23	24	25	26	27	28
SiO_2	37.84	37.96	30.66	34.52	26.16	25.12	29.12	31.78	36.00	27.56	29.56	38.77	21.00	36.58
Al_2O_3	5.94	6.23	2.86	2.32	3.79	6.37	3.44	2.18	0.69	3.63	2.47	14.63	2.05	7.15
Fe_2O_3	5.37	5.45	3.08	7.84	7.88	9.02	9.02	9.48	4.44	5.13	4.18	11.36	5.17	6.69
FeO	4.53	4.82	5.98	0.86	2.63	3.45	2.66	2.27	2.90	4.03	4.84		0.75	4.99
MnO	0.05	0.06	0.16	0.24	0.30	0.20	tr	0.10					0.04	0.34
MgO	24.84	24.84	31.24	29.95	23.40	22.32	31.00	25.77	39.70	33.12	37.47	12.14	20.52	22.55
CaO	5.04	5.88	10.92	7.14	14.70	14.42	7.56	10.64	3.58	8.96	7.19	4.51	24.64	6.05
Na_2O	1.22	1.48	0.17	tr	tr	tr	nil	0.28	0.11	nd	0.22	1.90		0.28
K_2O	1.67	1.79	1.23	0.23	0.78	1.74	nil	0.93	0.26	nd	0.33	2.60		0.47
H_2O^+	3.50	1.12	3.01	10.96	6.75	5.05	9.78	7.48	8.02	11.11	4.82		5.73	8.51
H_2O^-	0.95	0.56	0.93	0.24	0.16	nil	0.18	0.60	0.63	0.84	0.43		0.28	3.31
P_2O_5	0.38	0.29	1.64	0.54	0.86	1.58	0.63	0.94	0.64		0.43		0.91	0.38
CO_2	7.19	9.06	6.00	1.50	2.50	3.40	2.23	2.58	0.58	3.01	6.71	13.55	17.93	-
TiO_2	0.79	0.86	1.63	0.20	0.17	0.19	-	-		0.77	1.18		1.00	2.67
Cr_2O_3			0.10	3.10	9.94	7.26	3.68	4.92	2.74	-				
Other *2)			0.30	0.18	0.12	0.10	1.08	0.51			0.30		0.82	
Total	99.31	100.40	100.10	99.82	100.14	100.22	100.38	100.46	100.29	98.76	100.18	99.45	100.84	99.96
Ne			0.8								1.1			
Kp						4.4					1.1			
Cal										6.3	1.5			
Ab	10.9	12.1						5.8	1.4		0.0			3.1
Or	9.6	9.6	6.9	1.5	4.8	3.6		2.9	0.8		0.0			3.4
An	4.3	4.7	3.3	5.9	8.2	13.0	9.9	1.9	0.8		1.9		5.4	18.2
Ap	1.3	0.8	4.9	1.6	2.7	5.4	1.9	3.0	2.0		1.3		2.8	1.5
Hm	3.7	3.5	2.0	5.7	5.5	6.8	6.5	6.9	3.0	3.7	2.8		3.5	5.2
Il	1.1	1.1	2.1	2.2	3.5	5.1	3.2	3.8	0.9	1.2	1.6		1.4	4.2
Ol	31.1	30.6	65.4	40.8	39.6	47.8	61.4	42.6	67.5	76.0	72.8		27.4	37.2
Di				2.0				3.7		4.8				3.7
En	20.2	13.8		31.8	10.3		7.4	17.1	16.7				15.2	23.5
CC	6.0	7.5	11.9	8.2	22.0	10.9	8.9	13.0	3.4	8.0	9.7		41.4	
MC	11.8	13.3	2.6		3.2	2.7	0.8		3.5		6.2		2.9	
Ca-Ol			0.1 *1)	0.3 *1)	0.2 *1)	0.3 *1)								
Total	100.0	100.0	100.0	100.0	100.0	100.0	100.0	100.0	100.0	100.0	100.0		100.0	100.0

APPENDIX 25 (Continued)

	29	30	31	32	33	34	35	36	37	38	39	40	41	42
SiO_2	31.60	30.72	27.93	25.12	40.56	36.54	35.96	35.40	35.49	31.80	41.60	37.68	34.48	36.36
Al_2O_3	3.21	4.04	4.47	6.37	5.95	4.29	6.76	4.55	3.42	3.41	5.26	5.20	4.67	5.95
Fe_2O_3	6.33	6.65	7.04	9.02	5.36	5.84	5.60	5.44	6.37	5.19	4.80			4.96
FeO	3.37	4.57	5.12	3.45	4.45	3.38	3.64	4.10	3.02	3.48	4.32			4.17
MnO	0.30	0.16	0.23	0.20	0.026	0.055	0.041	0.04			-	-	-	0.05
MgO	29.45	32.40	25.42	22.32	25.84	28.47	27.97	28.58	30.98	24.69	34.13	23.40	26.71	29.05
CaO	8.07	6.30	10.01	14.42	5.18	4.90	4.90	7.14	5.12	10.04	3.78	4.34	7.28	6.30
Na_2O	0.16	0.17	0.21	tr	0.29	0.63	0.22	0.30	0.20	0.29	-	-	-	0.30
K_2O	0.34	1.00	1.18	1.74	1.63	0.81	1.49	2.72	2.61	4.32	-	-	-	1.49
H_2O^+	11.37	8.90	7.89	5.05	7.67	10.13	8.73	7.23	6.69	5.59	3.69	7.34	9.11	8.71
H_2O^-	0.87	0.57	0.68	-	2.14	2.16	2.68	0.64	0.47	0.63	1.00	5.80	1.76	0.80
P_2O_5	0.94	0.77	1.07	1.58	0.37	0.80	0.43	1.00	0.63	1.49	-	-	-	0.71
CO_2	1.96	2.01	5.61	7.26	0.38	0.49	0.55	1.59	3.03	7.65	0.19	1.06	1.33	0.56
TiO_2	2.02	1.81	2.73	3.40	0.86	0.86	0.77	1.11	1.65	1.40	0.34	0.60	0.60	1.29
Cr_2O_3														
Other*2)			0.89								0.89	3.73	4.95	-
Total	99.99	100.77	100.44	100.22	100.70	99.35	99.74	99.84	99.68	99.98	100.00	100.00	100.00	100.70
Ne		0.9	0.9	4.2			1.3	1.7		1.7				1.7
Kp		2.9					2.6	5.8		4.0				
Cal														
Ab	1.5		0.3	3.4	2.9	6.5			1.7	-				
Or	2.1	1.4	7.2		10.2	5.3	5.5	11.8	15.4	18.6				9.2
An	7.4	7.4	8.1	12.3	10.5	7.8	15.6		0.8	0.0	12.7	18.0	14.0	10.7
Ap	3.6	2.5	3.3	5.2	1.4	2.7	1.5	3.7	1.8	4.7	0.0			1.4
Hm	4.6	4.8	5.1	6.3	3.8	4.6	4.3	3.7	4.5	0.5	3.0			3.5
Il	2.9	2.6	3.9	4.8	1.3	1.4	1.2	1.6	2.4	2.0	0.4	1.1	1.0	1.8
Ol	51.9	72.4	56.5	45.4	45.9	44.7	65.9	63.3	65.8	49.0	54.0	11.3	57.1	65.3
Di	3.0				3.5	2.2	0.9	4.4			1.1	0.1	6.7	5.4
En	19.8				19.4	23.4					28.3	66.0	17.4	-
CC	5.2	5.1	12.5	16.1	1.1	1.4	1.6	4.0	7.2	13.0	0.5	3.5	3.8	1.1
MC			2.2	2.3					0.4	6.5				
Ca-Ol														
Total	100.0	100.0	100.0	100.0	100.0	100.0	100.0	100.0	100.0	100.0	100.0	100.0	100.0	100.0

	43	44	45	46	47	48	49	50	51	52	53	54
SiO_2	30.32	32.03	30.95	31.17	36.15	36.95	37.93	35.37	36.64	33.37	33.40	32.56
Al_2O_3	2.74	2.90	4.17	6.25	15.18	7.85	6.59	6.50	7.96	7.56	2.92	2.82
Fe_2O_3	4.50	6.12	6.16	3.22	4.87	4.78	6.81	7.23	6.19	5.33	7.85	9.28
FeO	4.09	3.40	2.66	9.64	9.11	8.70	4.37	5.00	5.59	6.39	5.18	3.17
MnO		-	-	-	0.33	0.20	0.18	0.24	0.17	0.20	0.22	0.11
MgO	29.60	33.43	32.30	19.90	13.63	15.87	14.54	14.08	18.15	12.50	25.20	27.00
CaO	10.40	7.60	8.92	17.76	11.40	13.60	15.23	16.79	15.11	20.25	9.52	8.82
Na_2O	0.45	0.35	0.35	2.03	1.42	2.32	0.88	1.32	2.85	2.03	tr	tr
K_2O	0.75	1.34	1.61	2.51	1.81	2.04	2.65	4.09	1.44	3.06	1.38	0.62
H_2O^+	6.56	6.31	6.81	2.05	1.95	1.64	3.38	2.78	1.56	3.06	6.98	8.97
H_2O^-	6.21	0.51	0.55	0.44	0.37	0.49	1.42	1.15	0.03	0.10	0.40	0.88
P_2O_5	1.34	1.45	-	1.69	0.26	0.83	1.03	0.74	0.91	1.50	0.39	0.68
CO_2	6.21	2.50	2.54	-	-	0.06	0.50	0.09	0.53	1.50	3.65	2.90
TiO_2	1.78	1.73	2.34	2.96	2.30	4.59	4.12	3.87	2.50	2.56	2.30	2.40
Cr_2O_3				-	0.10	0.03	0.05	0.01	-	0.08	0.17	0.19
Other*2)	0.04	0.06	-			0.09	0.30	0.25	0.05	0.32		
Total	99.97	99.73	99.36	99.62	100.43	100.25	100.51	100.36	99.81	100.76	100.32	100.40
Ne		2.0	1.9	10.1	13.2	12.7	5.6	8.6	15.1	11.7		
Kp		1.7	5.7	8.1	6.4	3.4		0.8	4.6	11.5		
Cal			4.9	13.6	1.0					1.5		
Ab	4.2											
Or	4.4	5.1				6.2	17.8	1.0	0.8		8.7	3.9
An	3.2	2.2			23.7	5.2	7.0	0.0	4.5		3.9	6.3
Ap	4.0	4.4		4.9	0.9	2.7	3.6	2.7	2.9	4.9	1.4	2.4
Hm	3.1	4.2	4.3	2.0	3.4	3.4	3.9	6.1	4.3	4.0	5.7	7.0
Il	2.5	2.4	3.3	3.8	3.3	6.5	6.5	6.7	3.4	3.8	3.4	3.6
Ol	60.1	70.6	66.7	44.9	36.9	38.6	35.4	37.6	40.9	32.4	49.0	51.0
Di				9.9	10.4	21.2	18.7	36.4	22.2	13.4	6.2	7.5
En	2.9										10.8	13.7
CC	13.2	6.2	6.4	2.7		0.1	1.4	0.1	1.3	4.0	9.6	5.2
MC	2.4									0.1	0.3*1)	0.4*1)
Ca-Ol		1.2	6.7		0.1*1)		0.1*1)			12.7		
Total	100.0	100.0	100.0	100.0	100.0	100.0	100.0	100.0	100.0	100.0	100.0	100.0

****

Appendix 24:

The chemical analyses and katamolecular norms of the kimberlites from South Africa.

Dutoitspan kimberlite: 1- 8; Hall (1938, No 240-247).
9; Holmes (1936).
10-16; Hall (1938, No. 341-347).
17; Holmes (1936).

Jagersfontein kimberlite: 18-20; Hall (1938, No. 222-224).
Frank Smith kimberlite: 21, 22; Hall (1938, No. 225, 227).
Klipfontein kimberlite: 23; Hall (1938, No. 261).
St. Augustine kimberlite: 24, 25; Hall (1938, No 230, 248.
Newlands kimberlite: 26, 27; Hall (1938, No 257; 258).
Kimberlite from Lesotho: 28-31; Dawson (1962).
Koffiefontein kimberlite: 32-36; Hall (1938).
Lion Hill kimberlite: 37-38; Hall (1938, 259-260).
De Beers kimberlite: 39-46; Hall (1938, 253-256, 227-229).
Kimberley kimberlite: 47-52; Hall (1938).
Koffiefontein kimberlite: 53-54; Hall (1938).

*1) Chromite.
*2) Other oxides, unspecified.

A. CHEMICAL ANALYSES

	1	2	3	4	5	6	7	8	9	10	11	12	13	14	15
SiO_2	26.31	31.77	32.31	28.82	30.22	25.96	29.94	18.0	30.30	25.06	45.85	45.65	38.60	39.75	47.79
Al_2O_3	3.85	7.99	9.50	4.92	3.93	3.42	5.40	11.7	2.54	4.72	10.82	13.20	12.86	8.31	11.79
Fe_2O_3	3.65	7.07	5.42	5.36	6.39	5.95	8.97	7.4	6.80	7.18	2.79	2.55	3.04	3.78	3.57
FeO	7.42	3.40	6.34	5.69	3.82	3.64	4.50	2.2	0.62	0.56	4.69	2.42	4.02	4.09	4.45
MnO	0.22			0.18	1.16	0.39	0.02	0.22	0.08	0.11	0.152	0.04	0.084	0.11	0.10
MgO	16.27	19.86	17.43	14.30	24.78	23.46	27.31	23.2	15.39	14.00	10.31	3.51	4.25	16.19	6.56
CaO	13.37	13.82	13.58	16.76	11.27	14.24	10.99	16.7	15.03	18.80	9.54	8.72	12.83	3.37	11.15
Na_2O	0.72	1.62	1.42	0.48	0.24	tr	0.74	-	0.46	0.31	2.14	3.02	0.75	0.78	0.20
K_2O	2.40	2.25	2.70	2.41	2.02	0.88	0.35	-	0.27	0.15	1.94	1.14	0.93	2.31	1.70
H_2O^+	1.82	0.52		4.34	6.18	7.86	3.55	12.1	5.76	5.88				6.05	
H_2O^-	1.30	0.21	3.15	2.35	0.48	0.40	0.62	0.14	8.64	8.47				9.70	
P_2O_5	0.64	0.95	2.38	0.78	1.14	0.82	0.42	-	0.58	0.53	0.225	0.761	0.486	0.31	0.20
Cr_2O_3	0.10							-	0.29	0.28					
TiO_2	4.88	1.98	1.41	1.80	3.37	2.88	2.55	3.65	4.16	3.80	1.72	3.98	2.29	1.00	2.13
CO_2	16.54	7.75	4.35	11.31	6.03	10.22	4.20	5.5	8.20	10.60				2.62	
Others	-	-	-	0.42	-	-	-	-	0.24	0.13					
Total	98.49	99.22	99.99	99.92	101.03	100.12	99.56	100.81	99.36	100.58	90.567	85.073	80.304	99.83	92.0

B. KATA MOLECULAR NORMS

Ne		5.4	7.4				4.0								
Kp							1.2								
Cal								20.2							
Ab	1.1	6.4		4.6	2.3				4.6	3.1	21.0	32.0	9.2	8.8	1.9
Or	0.3	14.2	15.6	14.8	11.9	5.1			1.5	0.9	12.3	8.0	7.4	16.6	11.4
An	3.3	8.0	10.6	4.2	3.9	11.7	10.3		2.7	12.4	15.4	22.6	38.4	14.8	39.2
Ap	1.1	3.3	7.4	2.5	3.7	2.4	2.0		2.0	1.8	0.7	2.9	2.1	1.1	0.8
Cc		13.5	10.8	28.1	15.6	21.5	10.4	14.6	22.8	30.2					
MC	0.1 *1)	6.3		0.7	-	3.8			0.4 *1)	0.4 *1)					
Il	0.5	2.9	2.0	2.6	4.8	3.9	3.5	5.3	6.3	6.0	2.5	6.6	4.3	1.7	3.4
Hm	5.1	5.2	3.7	3.9	4.5	4.0	6.2	5.4	5.2	5.5	2.2	2.1	2.8	3.2	2.9
Ol	69.6	39.8	41.5	27.4	52.0	38.0	58.2	49.3	2.0 *3)	8.8	14.2	9.3	11.4	20.4	25.2
Di	2.8				0.2		4.2		5.1	4.1	13.4	7.0	15.3	0.5	12.1
Ca-Ol	16.1 *4)			10.6 *4)	2.3 *4)	9.6 *4)	-	5.1	47.4 *4)	26.8 *4)	17.4 *4)	9.5 *4)	9.1 *4)	32.9 *4)	12.2 *4)
Total	100.0	100.0	100.0	100.0	100.0	100.0	100.0	100.0	100.0	100.0	100.0	100.0	100.0	100.0	100.0

	16	17	18	19	20	21	22	23	24	25	26	27	28	29	30
SiO_2	29.58	30.64	29.46	31.92	27.02	29.78	29.64	30.27	26.05	30.22	30.07	29.43	37.98	34.73	25.66
Al_2O_3	2.30	2.00	2.10	2.05	2.09	7.11	9.02	0.81	3.42	3.26	5.31	1.17	5.92	2.88	2.61
Fe_2O_3	7.53	8.29	9.25	3.94	4.08	4.21	5.21	14.14	6.68	4.52	9.39	13.18	8.72	6.10	9.23
FeO	1.24	1.06	0.74	1.35	1.50	1.14	0.82	0.39	0.94	0.24	0.35	0.26	0.32	3.13	1.71
MnO	0.10	0.08	0.11	0.12	0.04	0.03	0.08	0.23	0.13	0.08	0.11	0.22	0.09	-	0.20
MgO	32.09	32.23	32.42	28.47	29.27	17.86	17.09	30.02	25.02	26.33	26.63	24.03	30.87	31.41	25.4
CaO	6.04	5.62	8.58	11.12	15.04	16.51	15.27	7.67	15.18	13.04	7.64	11.60	1.86	5.79	13.28
Na_2O)	0.74	0.80	0.49	0.59	0.34	0.33	0.32	0.05	0.62	0.36	0.82	0.73	0.16	0.33)	0.07
K_2O)						1.43	1.03	0.58	0.28	0.55	0.52	0.61	1.97	1.13)	
H_2O^+	2.00	1.12	1.18	2.27	1.50	4.77	6.00								7.60
H_2O^-						2.46	1.48	1.16	0.80	2.81	2.98	2.13	1.43	2.58	0.40
P_2O_5	0.72	0.87	1.11	0.54	0.90	0.95	0.17	0.76	0.39	0.35	0.22	0.34	0.09	1.06	0.35
Cr_2O_3	0.40	0.30	0.34	0.29	0.30	0.09	0.13	0.12	0.38	0.064	0.053	0.039	0.13	-	0.20
TiO_2	1.71	1.66	1.93	1.47	1.45	0.12	0.61	1.74	1.21	0.88	1.12	1.60	1.56	1.62	2.77
CO_2 + Loss	14.60	15.00	12.68	16.10	16.00	12.97	12.00	12.45	19.07	16.89	14.72	15.14	8.75	9.20	10.20
Others	0.22	0.10	0.12	0.12	0.08	0.15	0.15		0.10						0.42
Total	99.27	99.77	100.51	100.35	99.61	99.91	100.22	100.39	100.27	99.59	99.93	100.48	99.58	100.00	100.19
Ne	3.0	2.4	1.3	2.5	1.3			0.4	3.4	2.3	4.9	4.6			
Kp								2.4	1.1	2.3	2.1	2.5			
Cal	2.2		2.7	2.6	3.1			0.1	3.7	3.9	2.5				
Ab		1.5				2.7	3.1						1.4	3.2	0.5
Or						7.5	5.9						11.8	7.1	
An	0.9	3.2				12.3	21.6				6.7		8.7	3.2	6.9
Ap	1.5	1.7	2.2	1.0	2.0	1.2	0.2	1.5	1.4	1.5	1.0	1.0	0.2	3.8	0.7
CC						22.8	21.4								23.2
MC						6.7	9.2						0.9 *5)		3.2
Il	2.7	2.6	2.9	2.5	2.5	0.1	0.9	2.0	1.3	1.0	1.3	1.9	1.7	1.8	4.0
Hm	5.9	6.5	7.0	3.1	3.1	2.7	3.6	10.8	5.1	3.6	7.4	10.6	6.3	4.5	6.5
Ol	73.8	73.0	71.2	66.2	67.3	16.1	20.4	68.2	56.4	63.1	62.6	57.0	55.4	71.1	37.9
Di	9.4	8.6	12.2	21.6	20.2	0.1 *1)	0.2 *1)	14.5	27.1	13.3	11.4	14.7	0.2 *1)	5.2	0.3 *4)
Ca-Ol	0.6 *1)	0.5 *1)	0.5 *1)	0.5 *1)	0.5 *1)	17.7 *4)	13.4 *4)	0.1 *1)	0.5 *1)	9.0	0.1 *1)	7.7	13.0 *4)		16.8 *1).
Total	100.0	100.0	100.0	100.0	100.0	100.0	100.0	100.0	100.0	100.0	100.0	100.0	100.0	100.0	100.0

APPENDIX 28 (Continued)

	31	32	33	34	35	36	37	38	39	40	41	42	43	44	45	46	47	48
SiO_2	29.72	29.94	25.64	27.20	30.56	28.47	27.59	32.23	34.73	32.95	30.50	34.46	38.42	30.10	33.60	29.09	36.61	35.40
Al_2O_3	6.51	6.20	8.88	4.98	1.20	3.70	3.66	2.77	2.88	3.02	4.27	2.97	3.50	3.76	4.12	3.84	2.91	3.08
Fe_2O_3	10.17	2.06	5.85	11.34	7.66	8.11	4.36	8.04	6.10	3.80	4.51	4.81	3.82	4.31	4.62	4.30	5.09	3.28
FeO	2.58	11.40	1.61	2.00	1.71	1.43	1.71	1.20	3.13	3.11	2.98	1.95	3.86	2.64	2.67	2.87	2.08	4.48
MnO	0.14	0.22	0.20	0.21	0.14	0.13	0.12	0.10	-	0.05	0.14	0.11	0.04	0.09	0.07	0.14	0.11	0.08
MgO	29.80	32.69	31.66	27.08	32.21	28.66	27.61	32.63	31.41	23.06	28.47	25.31	29.39	27.99	25.72	27.15	26.84	28.54
CaO	6.00	2.44	8.60	8.80	7.80	9.48	13.54	5.84	5.79	12.78	12.58	8.31	5.22	10.21	9.76	11.94	8.89	7.88
Na_2O	0.30	0.16	0.10		0.34	0.26	0.22	0.27	0.33	0.26	0.21	0.48	0.14	0.21	0.25	0.32	0.65	0.72
K_2O					0.17		0.09	0.07	1.17	0.49	0.30	0.31	0.33	0.48	0.38	0.31		
H_2O^+	10.80	12.76	15.20	8.31	9.82	15.57	19.19	14.02	9.20	15.47	13.53	20.16	13.11	16.50	14.18	17.69	15.63	14.75
H_2O^-	0.68	0.44	0.50	1.56	1.26	1.08	0.58	0.60	-	4.85	6.65	1.00	3.49	1.28	6.16	2.84	6.65	3.97
P_2O_5	0.32	N.D.	N.D.	0.12	0.20	0.75	0.06	0.34	1.06	0.94	0.75	0.23	0.57	0.32	0.27	0.67	0.24	0.20
Cr_2O_3	0.19	0.05	0.17	0.04	0.08	0.22	0.15	0.14	-	0.10	0.12	0.08	0.08	0.13	0.11	0.12	0.08	0.18
TiO_2	0.21	1.05	1.78	2.51	2.10	2.68	1.55	1.91	1.62	1.36	2.11	0.89	1.14	1.78	1.46	2.01	0.94	1.47
SO_2	2.96			6.03	5.31				2.58	H_2O^+	H_2O^+	H_2O^+	H_2O^+	H_2O^+	H_2O^+	H_2O^+	H_2O^+	H_2O^+
Others	0.08	0.26	0.25	0.31	0.26	0.23	0.21	0.25	-									0.29
Total	100.46	99.67	100.44	100.44	100.86	100.77	100.62	100.42	100.00	99.47	100.70	100.05	99.67	100.33	99.77	100.65	100.10	100.35
Ne	0.7	0.5	0.4				1.2	1.3		1.6	1.1			1.2	1.3	2.0		
Kp						0.9	0.4			1.2	1.1			2.1		1.2		
Cal	0.2	5.4	6.2			7.0	6.1				6.5			5.4		6.1		
Ab					3.4			0.3	3.2			4.9	1.2					
Or					0.9			0.6	6.8	1.3		2.0	2.9		2.5		5.0	5.1
An	17.5	4.3		14.3	1.3			6.6	3.2	5.0		6.0	12.1		10.2		6.9	7.5
Ap	0.7			0.2	0.2	1.5	0.3	0.7	1.9	1.6	1.5	0.3	1.3	0.5	0.5	1.4	0.3	0.3
Cc	4.3			12.3	13.7				6.7									
Mt	3.5	2.8 *5)		3.7	0.1 *1)						0.1 *1)	0.1 *1)	0.1 *1)	0.3 *1)	0.1 *1)	0.1 *1)	0.1 *1)	0.3 *1)
Il	0.3	1.7	2.6	3.6	3.0	4.2	2.6	2.9	2.3	2.2	6.2	1.4	2.3	3.0	2.4	3.4	1.5	2.6
Hm	7.5	1.5	4.4	8.3	5.5	6.3	3.5	6.1	4.4	3.2	3.4	3.8	4.0	3.5	3.6	3.7	4.0	2.8
Qz	65.0	82.8	70.9	52.0	63.5	65.3	66.5	72.5	66.4	58.3	66.0	58.7	67.5	68.2	62.2	70.3	53.4	59.6
Di			5.9	0.1 *1)	1.4	14.4	19.1	8.8	1.4	25.5	6.2	16.5	8.6	7.3	17.2	5.4	15.5	9.0
Ol-Cs	0.3 *1)		0.2 *1)	5.6 *4)	7.1 *4)	0.4 *1)	0.2 *1)	0.2 *1)	3.7 *4)	0.1	10.9	6.3 *4)		8.8		6.4	14.3 *4)	12.8 *4)
Total	100.0	100.0	100.0	100.0	100.0	100.0	100.0	100.0	100.0	100.0	100.0	100.00	100.0	100.0	100.0	100.0	100.0	100.0

	49	50	51	52	53	54	55	56	57	58	59	60	61	62	63	64	65	66
iO_2	32.71	35.62	32.57	35.36	38.32	33.47	33.21	34.73	27.60	27.88	29.26	27.72	26.91	27.98	32.07	29.67	30.36	28.95
$.1_2O_3$	2.95	3.05	2.96	3.29	3.20	3.20	3.54	2.88	1.41	3.08	3.12	2.08	2.86	3.83	2.32	4.10	2.86	3.06
$'e_2O_3$	2.25	3.58	4.53	3.54	3.03	4.63	3.40	6.10	7.63	3.17	2.95	3.44	5.72	7.69	9.29	6.65	8.16	9.34
'eO	5.25	3.42	3.48	4.42	4.49	3.66	2.76	3.13	1.64	2.05	4.57	1.90	1.49	0.41	1.45	0.85	2.27	2.14
fnO	0.05	0.05	0.08	0.04	0.08	0.08	0.09		0.18	0.13	0.08	0.08	0.14	0.15	0.13	0.13	0.14	0.16
fgO	27.07	27.32	29.61	29.23	27.82	29.51	26.73	31.41	26.67	27.98	23.40	27.79	22.76	24.84	21.90	23.30	31.11	31.04
aO	10.88	9.21	8.47	7.15	6.65	7.68	9.95	5.79	12.40	14.05	17.70	14.67	16.42	13.34	11.04	12.74	6.42	5.95
a_2O							0.27	0.33		0.40			1.20	1.14	0.82	1.60	0.45	0.21
$_2O$	1.04	0.92	0.76	1.13	1.55	0.88	0.36	1.17	0.10	0.88	0.24	1.30	0.33	0.41	0.41	0.47	0.10	0.05
$_2O^+$	16.07	14.49	16.05	13.84	12.37	14.62	16.83	9.20	8.52	9.68	17.86	19.10	8.70	6.73	8.60	9.41	11.32	15.30
$_2O^-$	2.79	3.21	1.68	2.64	3.08	1.61	4.10	-	1.20	0.88	0.44	0.65	1.18	1.66	1.94	1.37	2.36	1.20
$_2O_5$	0.29	0.26	0.27	0.26	0.35	0.21	0.49	1.06	0.46	-	-	0.33	0.27	0.19	0.24	0.20	-	0.212
r_2O_3	0.16	0.16	0.18	0.18	0.19	0.20	0.10	-	0.16	0.03	0.06	0.024	0.065	0.058	0.064	0.083	0.19	0.15
iO_2	1.37	1.63	1.29	1.45	1.56	1.63	1.46	1.62	2.29	0.79	0.69	0.81	1.28	1.04	0.75	0.68	2.85	1.65
$_2$									9.76	10.32	-	-	10.77	10.27	9.62	9.07	3.56	-
thers	0.14	0.10	0.20	0.16	0.08	0.16	-	-	0.34		0.21	0.18	0.14	0.15	0.17	0.19	0.19	0.45
otal	100.23	99.81	100.45	100.05	99.70	99.93	100.06	100.00	100.51	101.04	100.58	99.89	100.27	99.88	100.79	100.49	100.16	99.88
e	4.2		2.9	0.7		2.9	1.7	0.7			1.0		2.3	0.8		0.7		1.1
py							0.9											0.2
a	3.4		2.8								5.3							4.1
r		5.9		6.0	9.3	0.6		2.1		3.4		5.2	5.5	8.6	7.7	11.6	4.3	
							0.6	7.0	0.6	2.2			2.0	2.5	2.6	2.9	0.6	
n		6.3	2.6	6.1	5.6	6.8	8.2	3.2	3.6	5.7		1.2	1.5	4.1	1.3	2.6	4.1	1.4
p	0.5	0.4	0.5	0.5	0.7	0.5	1.0	1.8	0.9	0.0		0.8	0.7		0.5	0.2	0.2	0.3
C									22.7	25.0			28.3	23.4	21.3	24.0	9.3	9.5
[	0.3 *1)	0.1 *1)	0.3 *1)	0.3 *1)	0.3 *1)	0.3 *1)	0.1 *1)		2.9	1.2	0.1 *1)			2.3	3.5		0.3 *1)	0.3 *1)
n	2.2	2.5	2.0	2.3	2.2	2.6	2.4	2.3	3.3	1.1	1.2	1.2	1.8	1.4	1.1	1.0	4.1	2.6
i	1.8	2.8	3.4	2.6	2.1	3.5	2.7	4.5	5.5	2.2	2.4	2.7	4.1	5.3	6.6	4.9	5.7	7.3
	68.8	62.7	70.2	69.0	60.3	69.7	64.8	70.5	37.1	59.2	61.6	66.0	49.8	51.5	23.7	51.0	59.0	73.2
	9.5	17.1	15.3	12.5	10.1	13.1	17.6	7.9	0.2 *1)		2.4		3.9		0.1 *1)	1.0	2.2	
a	Ol 9.3	2.2 *4)			9.4 *4)				23.2 *4)		26.0	22.9	0.1 *1)	0.1 *1)	31.6 *4)	0.1 *1)	9.2 *4)	
otal	100.00	100.00	100.00	100.00	100.00	100.00	100.00	100.00	100.00	100.00	100.00	100.00	100.00	100.00	100.00	100.00	100.00	100.00

APPENDIX 26 (Continued)

	67	68	69	70	71	72	73	74	75	76	77	78	79	80	81	82	83	84	85
SiO_2	28.14	26.60	28.07	28.39	27.2	30.56	26.85	26.61	26.43	26.60	29.56	29.78	27.90	23.10	29.45	27.68	27.88	28.80	26.86
Al_2O_3	3.74	4.79	2.49	4.38	4.98	1.20	2.34	2.35	2.18	3.74	5.91	7.11	1.90	3.50	8.92	5.20	3.59	2.26	3.34
Fe_2O_3	8.94	8.69	9.21	8.93	11.34	7.66	4.77	7.08	6.19	5.72	9.36	4.21	6.14	5.78	4.58	1.55	5.08	4.73	3.57
FeO	1.74	1.87	2.04	1.76	2.00	1.71	2.34	1.80	2.00	2.11	1.76	1.14	1.48	2.95	1.17	2.66	1.24	1.47	2.22
MnO	0.15	0.22	0.14	0.13	0.21	1.14	0.12	0.10	0.10	0.13	0.12	0.03	0.06	0.08	0.04	0.08	0.08	0.06	0.06
MgO	30.14	29.33	28.33	30.03	27.08	32.21	22.82	25.32	24.95	24.07	23.01	16.51	26.54	22.58	13.65	26.88	27.82	27.52	24.92
CaO	7.10	7.08	8.74	7.81	8.80	7.80	17.37	14.60	15.20	15.31	10.11	17.86	14.54	17.32	17.42	12.54	12.05	13.02	16.76
Na_2O	0.12	0.13	0.15	0.17			0.24	0.26		0.51	0.46	1.89	0.33	0.30	0.85	0.26	0.56	0.20	0.10
K_2O		0.10	0.09	0.08						0.17	0.56	0.10			1.13		0.58		
H_2O^+	15.26	16.75	17.21	14.60	8.31	9.82	6.40	7.40	7.53	7.32	6.76	4.77	19.15	21.20	7.94	20.68	9.28	20.20	20.80
H_2O^-	1.47	1.35	1.83	1.31	1.56	1.26	1.35	1.17	1.27	2.00	2.84	2.46	0.70	1.60	1.43	0.36	1.14	0.08	0.46
P_2O_5	0.18	0.18	0.09	0.25	0.12	0.20	0.16	0.30	0.24			0.95			0.76				
Cr_2O_3	0.17	0.19	0.16	0.18	0.04	0.08	0.14	0.11	0.30	0.10	0.10	0.09	0.10	0.08	0.10	0.06	0.10	0.08	0.06
TiO_2	1.61	1.99	1.36	1.94	2.51	2.10	1.40	1.60	1.81	2.20	2.30	0.12	1.41	1.10	0.81	1.50	2.07	1.15	0.79
CO_2					6.03	5.31	13.80	11.60	11.40	11.52	7.20	12.97			11.95		8.44		
Others	0.40	0.47	0.33	0.39	0.17	0.22	0.07	0.08	0.16	0.34	0.58	0.15	0.17	0.37	0.11	0.23	0.11	0.19	0.27
Total	99.21	99.81	100.29	100.68	100.40	100.09	100.17	100.28	99.76	99.84	100.73	100.14	100.42	99.96	100.31	99.68	100.02	99.76	100.21
Ne	0.8	0.8	1.0	1.3									2.1			1.6	1.0	1.2	0.6
Ko		0.4	0.4	0.4															
Cal	1.6	1.9	4.1	7.2									2.5			9.2		1.6	6.2
Ab										4.3	4.6	19.6			7.8		2.7		
Or							2.2	2.2		0.8	3.5	0.7			6.8		3.7		
An					14.2	3.2	5.2	5.3	6.1	7.3	13.0	13.0			17.9		5.7	3.6	
Ap	0.3	0.3	0.2	0.5	0.2	0.2	0.2	0.5	0.2			1.9			2.4				
CC	8.5	9.6			12.5	13.8	31.7	26.4	27.9	26.3	15.6	34.2			24.4		21.8		
MC	4.0	2.6	0.2*1)	0.4*1)	3.3	0.1*1)	2.9	3.3	1.2	1.6	3.4	4.8	0.1*1)		6.8	0.1*1)	0.1*1)	0.1*1)	0.1*1)
Il	2.6	3.2	2.2	3.0	3.6	3.0	2.0	2.2	2.6	3.0	3.4	0.1	2.3		1.2	2.5	3.0	1.9	1.3
Hm	7.3	7.2	7.5	6.9	8.3	5.6	3.2	5.0	4.4	3.8	6.7	3.5	4.9		3.5	1.3	3.6	3.9	3.2
Ol	76.4	73.6	70.1	69.8	50.3	55.4	27.7	39.1	36.3	52.8	36.8	13.9	23.7		12.4	67.7	58.1	66.9	62.6
I			5.5	5.4		0.9	0.2*1)	0.1*1)	0.5*1)		0.1*1)	0.1*1)	64.4		0.1*1)		0.3	20.8	
Ca-Ol	0.3*1)	0.4*1)	8.8	5.1	7.6*4)	17.8*4)	23.7*4)	15.9*4)	20.8*8)	0.1*1)	12.9*4)	7.9*4)	23.7		16.4*4)	17.6			26.0
Total	100.00	100.00	100.00	100.00	100.00	100.00	100.00	100.00	100.00	100.00	100.00	100.00	100.00	100.00	100.00	100.00	100.00	100.00	100.00

- bad analysis
Not calculated

	86	87	88	89	90	91	92	93	94	95	96	97	98	99	100	101
SiO_2	25.93	25.62	33.02	31.12	26.48	27.43	24.66	25.64	26.99	24.18	28.00	27.52	25.09	27.64	29.38	25.24
Al_2O_3	2.90	2.79	3.00	3.21	2.69	4.23	2.35	2.61	3.61	2.07	3.60	2.43	2.30	3.33	3.17	3.77
Fe_2O_3	3.86	7.28	7.64	6.64	3.44	5.22	4.23	4.19	6.78	4.10	3.13	4.34	4.90	8.05	3.31	7.28
FeO	0.74	0.68	4.31	1.68	2.02	1.30	1.79	1.51	1.01	0.87	2.38	1.37	1.35	0.79	2.76	2.87
MnO	0.13	0.09	0.16	0.17	0.04	0.13	0.03	0.03	0.03	0.03	0.08	0.09	0.12	0.08	0.07	0.17
MgO	27.35	23.97	30.12	28.19	22.58	27.47	23.44	24.75	22.32	20.94	25.81	25.84	25.28	25.80	28.65	24.16
CaO	15.46	16.39	6.74	11.25	17.70	11.69	19.07	17.55	16.96	21.42	15.19	15.34	17.35	11.18	11.25	14.03
Na_2O	0.28	0.34	0.58	0.10	0.45	0.32	0.44	0.27	0.28	0.37	0.41	0.30	0.38	0.44	0.42	0.31
K_2O	0.08	0.21	0.10	0.14	0.35	0.65	0.47	0.33	0.47	0.46	0.39	0.14	0.41	0.43		
H_2O^+	20.88	20.34	10.06	14.03	21.99	19.02	21.78	21.11	18.42	23.45	19.98	19.72	20.89	18.85	18.25	18.09
H_2O^-	0.76	1.80	2.07	1.35	1.78	1.78	1.15	0.98	1.15	2.22	1.72	1.61	1.50	3.23	1.07	0.92
P_2O_5	0.14	0.43	0.14	0.22	0.24	0.19	0.13	0.32	0.37	0.50	0.20	0.73	0.32	0.38	0.30	0.77
Cr_2O_3	0.22	0.22	0.16	0.13	0.10	0.16	0.11	0.16	0.14	0.11	0.14	0.11	0.14	0.17	0.11	0.12
TiO_2	1.72	2.04	1.49	1.34	1.65	2.19	1.30	1.40	1.58	1.42	1.18	1.18	1.07	2.54	1.37	2.38
SO_2	H_2O^+	H_2O^+				Same as H_2O^+										
Others	0.16	0.23														
Total	100.61	100.63	99.90	99.82	99.31	100.17	99.97	100.12	100.28	100.02	100.60	99.23	99.73	99.89	99.17	99.42
	1.7	2.4	3.2	0.6	3.1	1.9	3.0	1.5	1.7	2.3	2.6	2.0	2.3	2.9	1.5	1.2
	0.4	0.8		0.6	1.5	2.7	1.8	1.3	1.9	1.7	1.6	0.6	1.5	1.8		
	4.4	3.8		5.9	3.5	5.7	2.4	3.5	2.4	1.7	5.0	3.5	2.3	4.0	5.2	6.7
			0.6													
			5.8													
	0.3	0.8	0.2	0.3	0.6	0.3	0.3	0.5	0.8	1.0	0.3	1.3	0.5	0.8	0.5	1.6
	0.4 *1)	0.4 *1)	0.2 *1)	0.3 *1)	0.1 *1)	0.2 *1)	0.1 *1)	0.3 *1)	0.3 *1)	0.1 *1)	0.3 *1)	0.1 *1)	0.1 *1)	0.3 *1)	0.1 *1)	0.2 *1)
	2.7	3.3	2.3	2.4	3.1	3.6	2.1	2.3	2.8	2.3	2.0	2.0	1.8	4.2	2.2	4.0
	3.2	5.3	5.7	5.8	3.1	4.2	3.5	3.4	5.9	3.3	2.6	3.6	3.9	6.6	2.6	6.0
	63.2	57.0	70.5	73.7	62.4	64.2	54.8	59.4	53.4	52.9	61.6	62.6	60.0	59.9	70.5	60.4
			11.5	10.4	5.5	1.2			5.0		1.2	1.5		3.8	4.3	1.1
Fa-Ol	23.7	26.2		10.0	17.1	16.0	32.0	27.8	25.8	34.7	22.8	22.8	27.7	14.7	13.1	18.8
Total	100.00	100.00	100.00	100.00	100.00	100.00	100.00	100.00	100.00	100.00	100.00	100.00	100.00	100.00	100.00	100.00

Addendum to Appendix 25.

	1.	2.	3.	4.
SiO_2	22.74	24.15	22.86	28.83
TiO_2	5.86	6.46	2.98	5.67
Al_2O_3	3.09	2.58	3.78	2.94
Fe_2O_3	8.47	7.67	4.79	3.60
Cr_2O_3	0.09	0.0	0.06	0.0
FeO	7.45	8.36	5.32	5.13
MnO	0.21	0.16	0.17	N.D.
NiO	0.0	0.02	-	N.D.
MgO	23.83	24.03	14.58	24.31
CaO	11.82	10.27	22.24	11.24
Na_2O	0.27	0.25	0.33	0.75
K_2O	0.94	1.02	1.52	1.31
H_2O^+	6.22	4.98	3.42	3.96
H_2O^-	0.76	0.90	1.65	0.83
P_2O_5	0.68	0.23	1.32	0.77
CO_2	7.24	9.02	14.84	11.64
S	0.0	0.0	0.0	N.D.
TOTAL	99.76	100.10	99.86	100.98

1, 2, 3. Bachelor Lake Kimberlite. Quebec (Watson, Amer. Min. 1955, p.573)

4. Mica Peridotite, Pennsylvania, (ditto).

Appendix 26:

The chemical analyses and katamolecular norms of the kimberlites from outside South Africa.

1. Micaceous kimberlite; $\ddot{A}lno$; Min. abst., (1963-64, p. 198).

2. Damkjernite; $\ddot{A}lno$) Verhoogen (1938)

3. Alnoiite; $\ddot{A}lno$)

4. Kimberlite dyke; $\ddot{A}lno$; Min. abst, (1961-62).

5. Gwena kimberlite; Congo; Verhoogen (1938).

6 & 7 Kimberlites; Tanzania; Mackinlay (1955).

8 Igwisi kimberlite, Sampson (1953).

9 & 10 Majhgwan kimberlite; Mantur (1962).

11 & 12 Lhimnorka Hill kimberlite; Svoboda (1966).

13 - 15 Nova Trubka; Svoboda (1966).

16 - 101 Russian kimberlites; Bobrievich et al (1959).

*1) Chromite

*2) Ca_2SiO_4

*3) Quartz

*4) Enstatite

*5) Spinel.

A. Chemical analyses

	1	2	3	4	5	6	7	8	9	10
SiO_2	32.31	45.17	39.07	46.77	43.69	56.90	61.95	74.57	36.95	37.78
Al_2O_3	9.50	14.78	12.82	14.65	9.06	20.17	18.03	12.58	7.85	8.03
Fe_2O_3	5.42	5.10	8.75	3.71	3.46	2.26	2.33	1.30	4.78	4.89
FeO	6.34	5.05	6.39	7.94	9.43	1.85	1.51	1.02	8.70	8.90
MnO	0.01	0.35	0.26	0.15	0.16	0.19	0.13	0.05	0.20	0.00
MgO	17.43	6.26	6.14	6.82	19.68	0.58	0.63	0.11	15.87	16.23
CaO	13.58	11.06	14.20	12.42	9.18	1.88	1.89	0.61	13.60	13.91
Na_2O	1.42	3.69	4.09	2.59	1.49	8.76	6.55	4.13	2.32	2.37
K_2O	2.70	2.73	2.07	1.07	0.69	5.42	5.53	4.73	2.04	2.09
H_2O	7.50	3.40	1.59	0.51	0.74	0.96	0.54	0.66	2.13	
P_2O_5	2.38	0.51	0.76	0.37	0.30	0.17	0.18	0.07	0.83	0.85
TiO_2	1.41	1.90	3.86	3.00	2.12	0.59	0.73	0.17	4.59	
CO_2	0.38								0.06	
Other									0.09	
Total									100.25	95.05

B. The Katamolecular norms

Ne	5.2		20.6	8.5		24.0	1.2		12.6	13.1
Kp									3.7	6.5
Cal										
Ab		13.2	4.4	11.0	13.3	35.3	66.5	37.5		
Or			10.5	6.4	4.1	31.0	32.6	28.5	5.9	2.0
An			11.0	25.8	15.8		1.9	1.1	5.1	5.1
Di	17.8	24.8	20.8	26.8	11.7	3.7	2.9	0.5	21.0	22.7
Ol	48.2		17.1	14.4	46.0	2.6	2.3		38.9	45.4
En	17.3 *1)	30.3			3.9			1.7		
Ap	8.7	2.3	2.6						2.7	2.7
Hm		18.4 *1)	6.4	2.7	2.4	1.6	1.6	0.9	3.4	3.5
Il	2.3	3.4	5.8	4.4	2.8	0.8	1.0	0.2	6.5	
CC		9.3 *2)							0.2	
C a-Ol										
Oxide	0.5	4.3						29.6 *2)		
Total	100.0	100.0	100.0	100.0	100.0	100.0	100.0	100.0	100.0	100.0

	11	12	13	14	15	16	17	18	19	20	21
SiO_2	37.13	30.54	33.41	34.45	36.15	31.17	38.30	40.76	42.96	31.16	28.0
Al_2O_3	10.58	10.23	5.35	8.99	15.18	6.25	11.56	12.03	14.95	5.63	3.8
Fe_2O_3	2.00	4.75	4.78	6.20	4.87	3.22	5.43	3.22	6.24	7.32	8.18
FeO	10.43	8.86	9.76	8.25	9.11	9.64	6.53	7.70	7.58	9.04	2.37
MnO	0.26	0.24	0.18	0.26	0.33		0.39			0.27	0.22
MgO	19.12	20.05	17.43	17.22	13.63	19.90	9.10	12.02	7.68	20.18	19.0
CaO	13.02	14.58	12.59	11.47	11.40	17.76	17.40	13.20	11.77	17.09	20.3
Na_2O	1.32	3.30	1.87	1.85	2.42	2.03	3.48	3.95	3.65	2.12	0.44
K_2O	0.51	0.75	1.00	1.31	1.81	2.51	1.53	1.05	1.43	1.52	2.71
H_2O	1.20	1.76	1.05	3.13	2.32	2.49	2.65	2.38	0.80	1.60	6.14
P_2O_5			1.84	0.97	0.26	1.69	0.54	0.86	1.00	0.28	
TiO_2	3.61	2.74	8.19	5.21	2.30	2.96	2.30	2.60	2.10	3.44	2.28
CO_2	0.47	1.78	0.42	0.33			0.08	-		0.62	8.12
Other		0.04			0.16						
Total	99.56	100.88	98.10	100.08	100.43	99.62	99.29	99.77	100.21	100.27	101.56
Ne	7.5	17.1	5.7	11.4	13.1	10.6	19.3	16.8	0.6	11.4	2.5
Kp	1.9	2.6		5.4	6.4	8.0	4.3			5.3	9.5
Cal	2.1	7.2		8.6	15.3	0.3				0.7	0.3
Ab			5.7					7.8	30.2		
Or			5.4				2.3	6.2	8.2		
An	19.0		3.3				11.7	11.8	19.2		
Di	11.1		12.9		11.2	14.0	28.3	17.4	10.2	22.6	14.9
Ol	50.4	47.7	46.9	46.2	37.0	46.9	25.2	31.4	21.6	48.0	39.9
En											
Ap			5.4	3.6	0.9	5.2	1.6	2.7	3.0	0.8	
Hm	1.5	3.2	3.1	5.0	3.4	2.1	3.9	2.2	4.2	5.0	5.7
Il	5.3	3.7	10.6	8.3	3.3	3.9	3.3	3.7	2.8	4.7	3.2
CC	1.2	4.4	0.9	0.9			0.1			1.5	20.5
Ca-Ol		14.1		10.6	9.3	9.0					3.5
Oxide					0.1 *3)						
Total	100.0	100.0	100.0	100.0	100.0	100.0	100.0	100.0	100.0	100.0	100.0

****

Appendix 2b:

The chemical analyses and katamolecular norms of alkaline-basalts and undersaturated calcite bearing basalts.

1.	Alnoiite, average	Barth (1962, p 58-59).
2.	Monchiquite, average	
3.	Nepheline basalt, average	
4.	Alkaline basalt, average	
5.	Olivine basalt, average	
6.	Phonolite, average	
7.	Alkaline trachyte, average	
8.	Alkaline rhyolite, average	
9, 10	Olivine melilitite, Spiegel River, Taljaard, (1936).	
11, 18	Melilite basalts from Sutherland (11-14), Spiegel River (15-18), Taljaard, (1936).	
19	Atlantite, Johannsen (1939).	
20-21	Undersaturated calcite bearing rocks from Brukaros, Ann. Rep. Univ. Leeds, 1963-64.	

Appendix 29:

The chemical analyses and the katamolecular norms of carbonatite and massive basaltic kimberlites.

1, 2, 3	Bastnaesite carbonatite; Garson (1965).	
4	Singwe carbonatite.	)
5	brown carbonatite; Tundulu center 1	)
6	Siderite Sovite; ditto	) Garson (1965).
7	Pale coloured Sovite; ditto	)
8	Aegerine magnetite Sovite; ditto	)
9-11	Massive kimberlite, Jagersfontein; Hall (1938, No 217-219).	
12-13	Benfontein kimberlite, Hawthorne (personal communication).	
14	Massive kimberlite, Wesselton Mine, (new analysis).	

*1) Rutile.

*2) Ca_2SiO_4.

APPENDIX 28 - The Chemical analyses and the katamolecular norms of Carbonatite and Massive basaltic kimberlites

A. Chemical Analyses

	1	2	3	4	5	6	7	8	9	10	11	12	13	14
SiO_2	4.34	6.44	6.01	0.92	4.29	3.99	0.88	4.65	11.00	11.12	12.24	25.19	18.66	32.56
Al_2O_3	0.77	1.93	2.67	0.77	1.32	0.57	0.37	1.42	3.05	7.25	2.08	2.27	6.17	1.36
Fe_2O_3	11.80	14.80	13.00	6.33	9.28	3.36	2.62	17.10	2.80	5.05	3.28	3.72	8.47	2.42
FeO								1.90	1.44	1.58	1.73	6.72	4.61	7.31
MnO	2.54	2.72	3.06	1.66	0.96	1.40	0.40	0.68	0.14	0.25	0.14	0.22	0.33	
MgO	0.53	2.19	5.76	0.59	0.25	1.35	0.31	0.50	6.98	6.84	7.20	29.69	20.11	35.97
CaO	39.64	33.32	25.53	46.45	45.62	48.54	53.60	40.06	40.74	37.94	39.20	13.59	19.21	8.58
Na_2O	0.53	0.35	0.40	0.50	0.06	0.21	0.09	1.00	0.34	tr	0.28	0.01	0.37	0.17
K_2O	0.18	0.93	0.20	0.36	0.22	0.13	0.03	0.16	1.24	0.24	1.34	0.15	0.33	1.08
H_2O^+	1.97	1.05	1.09	0.84	1.20			0.05	1.53	1.12	1.52	1.15	2.30	0.18
H_2O^-	0.42	0.53	0.28	0.17	0.35	0.09	0.06	0.11	-	0.56	-	-	-	0.83
P_2O_5	10.65	1.91	3.25	0.41	0.03	0.07	3.18	1.60	1.95	0.39	2.92	2.20	3.66	0.39
CO_2	20.56	27.96	26.99	37.58	34.88	40.22	38.38	28.43	26.95	26.62	26.67	12.89	10.44	5.06
TiO_2	0.56	0.50	0.10	0.10	0.23	0.06	0.18	0.59	1.60	1.20	1.60	1.89	4.20	2.18
Other	1.06	0.67	0.81	3.28	-	-	0.06	0.69	0.59	0.58	0.78	-	-	-
Total	95.55	95.20	89.15	100.26	98.69	99.99	100.16	98.94	100.35	100.74	100.65	99.62	98.86	98.09

B. Katamolecular Norms

Ne				2.6				5.8	1.7				0.3	0.8
Kp				1.1				0.5	2.5	0.8		0.4		3.7
Cal										3.2		2.1		
Ab	4.7	3.5	3.9		0.8	1.5	0.8				2.7		2.8	
Or	0.1	5.8	1.2		1.1	0.5	0.3		2.9		7.9		1.9	
An		0.9	5.3		2.6	0.5	0.4		3.0	12.8	0.3	1.5	14.3	
Ap	33.4	6.3	11.2	1.3	0.2	0.2	9.4	4.2	6.3	1.3	8.9	6.2	11.6	0.8
CC	28.5	59.8	36.6	86.4	86.1	87.7	85.8	69.8	64.5	62.3	62.1	13.9	3.8	11.2
MC	23.3	14.6	37.9	4.3	0.8	5.4	.3	5.8	0.0	1.6	3.4	15.1	22.5	
Il	0.8	0.7	0.1	4.3 *1	0.3	0.1	0.3	1.0	2.1	1.6	2.2	2.4	5.9	1.6
He	8.2	8.4	2.7		6.3	2.1	1.7	12.9	1.8	3.4	2.2	2.3	5.9	1.7
Di									1.3					2.7 *2)
Ol					1.8				13.9	13.0	9.7	60.1	25.7	77.5
En											2.6			
Qz			1.1			2.0								
Total	100.0	100.0	100.0	100.0	100.0	100.0	100.0	100.0	100.0	100.0	100.0	100.0	100.0	100.0

A. Chemical Analyses

	1	2	3	4	5	6	7	8	9	10	11	12
SiO_2	19.64	26.40	26.00	33.84	32.48	7.01	7.29	23.65	41.55	38.29	38.02	38.15
Al_2O_3	1.27	-	0.69	-	1.30	0.99	1.04	1.68	2.96	2.66	3.03	1.19
Fe_2O_3	9.00	2.79	13.52	6.65	5.74	8.06	2.23	7.01	3.30	5.77	8.13	6.55
FeO	2.70	3.64	0.79	1.22	4.03	3.84	1.58	3.62	4.55	2.93	2.21	3.24
MnO	0.47	0.51	0.28	0.16	tr	0.68	0.35	0.24	0.16	-	-	-
MgO	22.17	19.80	20.80	30.96	31.36	24.82	3.74	24.11	27.72	29.46	27.78	27.33
CaO	20.16	25.62	17.92	9.66	10.08	24.76	45.71	17.73	5.89	2.42	4.80	4.13
Na_2O	nd	nd	nd	nd	nd	0.39	nd	0.03	0.37	0.30	0.84	0.25
K_2O	nd	nd	nd	nd	nd	0.43	nd	0.03	0.54	1.03		0.56
H_2O^+	1.32	-		0.36		0.16	1.24	8.16	9.46	10.19	10.11	9.69
H_2O^-	4.64	7.54	6.62	10.27	4.68	9.61	0.54	0.17	0.40	3.13	2.60	3.52
TiO_2	1.72	1.05	1.80	0.60	1.30	1.53	0.86	1.53	2.11	2.00	2.30	1.72
Cr_2O_3	-	-	-	-	-			0.03	-	-	-	-
CO_2	15.84	12.94	2.18	6.75	7.92	16.93	34.88	11.60	0.13	0.20	0.28	1.41
P_2O_5	1.14	0.41	0.23	0.22	tr	1.22	0.67	1.03	0.27	1.44	0.41	2.15
Other	-	-	-	1.37	-		0.20	-	-	-	-	-
Total	100.07	100.70	100.83	100.69	100.26	100.43	100.33	100.62	99.41	99.82	100.51	99.89

B. Katamolecular norms

Ne						2.2						
Kp						1.5						
Cal												
Ab								0.3	3.5	3.0	8.1	2.4
Or								0.3	3.5	6.6		3.7
An	4.2		2.4				2.7	4.3	5.0	3.0	4.9	0.5
Ol	13.5	46.3	45.3	38.0	42.9	5.5		41.6	37.2	31.0	39.0	19.1
En	32.2 *1	7.5 *1	18.8 *1	37.4	29.9	26.3 *2	9.5	13.4	35.2	43.7	30.8	57.1
Di		7.0	10.6	1.0		0.4 *1)			8.6		5.4	
Ap	4.4	1.4	0.8	0.7	2.1	3.8	2.1	3.7	1.0	4.8	1.4	8.0
CC	35.2	34.3	7.1	17.3	19.5	42.6	83.0	29.4	0.7	0.6	0.8	0.9
Il	2.8	1.5	3.2	0.9	1.7	2.1	1.2	2.1	3.0	3.0	3.5	3.3
Hm	7.7	2.0	1.8	4.7	3.9	5.6	1.5	4.9	2.3	4.3	6.1	5.0
Total	100.0	100.0	100.0	100.0	100.0	100.0	100.0	100.0	100.0	100.0	100.0	100.0

APPENDIX 29 (Continued)

	13	14	15	16	17	18	19	20	21	22	23	24
SiO_2	46.83	41.00	49.20	55.76	53.94	58.05	58.72	56.80	60.24	48.35	56.12	55.45
Al_2O_3	3.71	10.05	9.23	19.93	20.70	18.62	18.49	17.81	18.54	23.10	19.62	17.80
Fe_2O_3	3.24	4.60	7.73	2.36	2.04	1.63	0.49	1.40	0.54	2.48	2.32	5.90
FeO	4.35	7.20	3.24	2.11	1.92	2.89	5.14	4.84	2.36	1.89	0.90	0.72
MnO	-	nd	nd	0.05	0.04	0.06	0.00	-	-	-	-	-
MgO	21.33	9.23	1.35	0.35	0.36	0.68	1.48	1.34	0.76	0.89	0.13	0.14
CaO	3.83	15.85	11.55	2.04	1.18	2.29	3.98	5.21	2.29	2.51	2.07	1.90
Na_2O	0.63	2.32	6.20	8.64	9.76	7.14	6.10	6.15	6.59	13.20	9.50	4.69
K_2O	0.70	3.20	1.96	6.45	5.24	5.79	3.37	2.81	5.44	3.58	4.17	9.71
K_2O^+	5.22			1.21	3.30	1.21	0.23	1.60	0.72	2.91	3.50	2.64
K_2O^-	7.95			0.34	0.29	0.30	0.30		0.50			
TiO_2	1.34	3.37	7.13	0.01	0.35	1.02						
Cr_2O_3												
CO_2												
P_2O_5	0.74			0.58	0.01	0.01	0.48		0.27			
Other				0.22	0.72	0.12	0.04		0.02	1.49	0.80	0.72
Total	99.87	96.82	97.59	100.0	99.85	99.81	99.93	100.02	99.21	100.85	99.59	100.80
Ne		5.7	4.4	20.6	64.8	-		4.2	2.4	56.0	22.4	14.2
Kp					23.7							
Cal												
Ab	6.2	0.5	22.8	33.3		47.2	52.8	50.5	51.8	8.9	39.4	8.9
Or	4.7	19.0	11.7	32.5		39.0	19.6	16.6	31.4	20.3	24.4	61.4
An	5.8	-	10.8	1.2		2.3	13.3	12.9	5.7		2.9	2.1
Ol		5.8				4.3		4.5	1.6	3.9	0.3 *1)	
En	71.0	53.5	18.0	5.9			9.8					
Di		4.8 *3)	10.2 *3)		9.7	4.3	1.3	10.3	5.8	10.3	3.5	8.6
Ap	4.7	8.5 *4)	22.1 *4)	5.7 *4)			1.5				6.4 *4)	
CC	4.0 *6)	2.2 *5)			0.5	1.6	1.5		1.3	0.6	0.7 *3)	1.7 *3)
Il	1.1			0.8	0.3	1.3		1.0				3.1
Hm	2.5						0.2					
Total	100.0	100.0	100.0	100.0	100.0	100.0	100.0	100.0	100.0	100.0	100.0	100.0

****

Appendix 28:

The chemical composition and katamolecular norm of the alkaline-rocks north-east of Pretoria.

1. Massive basaltic kimberlite from Premier Mine.

1. Serpentine calcite rock, Premier Mine; Hall (1938; No. 437).
2. Calciferous dyke.
3. Altered dyke.
4. Serpentine calcite dyke.
5. Serpentine calcite dyke.
6. Carbonated dyke.
7. Carbonated dyke.
8. CF 328 (New analysis).

2. Kimberlite from Premier Mine.

9. CF 329 (New analysis).
10-13 kimberlite; Shand (1922).

3. Alkaline-basalts from North-east of Pretoria.

14 Monchiquite; Zeekoegat; Shand (1921, p 81).
15 Pienaarite; Kameeldrift; (ditto).
16 + 17 Foyaiite; Leeuwkraal + Franspoort; (ditto).
18 Phonolite; Leeuwkraal; (ditto).
19 Soda-trachyte; Leeuwfontein; Shand (1921, p.232).
20, 21 Syenite; Leeuwfontein (ditto).
22 Sodalite, Aegerine foyaiite; Leeuwfontein; (ditto).
23, 24 Foyaiite; Paardefontein; Shand (1922).

*1) Ca_2SiO_4
*2) Periclase
*3) Sphene
*4) Acmite
*5) Magnetite
*6) SiO_2.

APPENDIX 29 - The Chemical analyses and molecular norms of garnet peridotite, peridotite and dunite from various parentages

A. The chemical analyses

	1	2	3	4	5	6	7	8	9	10
SiO_2	40.65	40.53	43.28	45.14	43.32	44.91	50.80	46.80	42.00	47.28
Al_2O_3	1.51	0.15	1.44	1.54	1.56	17.15	nil.	1.16	0.52	7.81
Fe_2O_3	3.73	5.14	1.09	1.01	1.19	1.68	4.40	4.62	5.64	3.36
FeO	3.41	1.68	5.26	4.70	5.15	6.45	4.90	3.02	3.56	7.41
MnO	0.07	0.05				-	0.11	0.27	0.19	0.14
MgO	40.93	39.88	42.41	41.75	42.30	14.27	36.00	27.72	37.44	12.60
CaO	0.40	0.12	2.03	1.92	2.00	11.28	0.84	10.22	3.08	15.82
Na_2O	0.07	0.07	0.16	0.14	0.15	1.01	nil	nil	nil	nil
K_2O	0.03	0.04	0.22	0.11	0.19	0.89	0.04	1.24	0.35	0.27
H_2O^+	8.91	12.46	0.18	0.20	0.16	1.52	1.97	3.72	6.86	2.31
H_2O^-	-	-	3.76	2.92	3.69	0.26	0.08	0.24	nil	nil
TiO_2	0.23	0.12	0.01	0.01	0.01	0.46	0.40	0.66	0.45	0.20
Cr_2O_3	0.22	0.16				-	0.62	0.51	nil	0.25
NiO	0.25	0.27				-	0.27	0.17	0.18	0.11
Other							0.20	0.25	0.29	2.41
Total	100.41	100.67	99.84	99.44	99.72	99.88	100.43	100.63	100.56	100.07
B. The Kata-Molecular norms										
Ab	0.5	1.1	2.3	1.5	2.1	13.2	0.3	8.4	1.9	0.9
An	1.9		2.9	3.1	2.9	36.3			0.4	21.9
Cal										
Ne										
Di		0.3	5.1	4.6	5.3	6.0	2.9	40.5	11.8	50.0
Ol	65.8	70.5	74.3	63.8	67.4	36.3	23.0	36.0	59.6	
En	28.5	22.2	14.6	26.2	21.4	6.5	69.9	10.7	22.2	24.1
Ru	0.3	0.2	0.1	0.1	0.1	0.6	0.3	0.5	0.3	0.2
Cr	0.5	0.2				0.0	0.7	0.7		0.4
Hm	2.6	5.5	0.7	0.7	0.8	1.1	2.9	3.2	3.8	2.5
Total	100.0	100.0	100.0	100.0	100.0	100.0	100.0	100.0	100.0	100.0

	11	12	13	14	15	16	17	18	19	20
SiO_2	51.25	49.04	48.40	45.00	46.40	42.44	31.16	46.00	44.77	45.57
Al_2O_3	nil	0.89	0.76	-	nil	21.40	5.63	2.78	0.84	1.43
Fe_2O_3	2.70	4.70	2.16	3.28	4.48	0.97	7.32	1.91	1.70	1.30
FeO	1.44	3.31	4.17	4.24	3.52	7.62	9.04	5.07	3.99	4.42
MnO	0.24	0.08	0.22	0.25	0.11	0.35	0.27	0.12	0.10	0.09
MgO	18.42	34.00	39.16	41.14	39.60	20.31	20.18	38.86	40.03	42.75
CaO	21.80	1.12	0.98	1.12	0.98	4.75	17.09	1.88	1.76	0.02
Na_2O	tr	2.14	nil	nil	nil	-	2.12	0.19	0.12	-
K_2O	tr	nil	nil	nil	nil	-	1.52	0.34	0.94	0.04
H_2O^+	1.10	4.33	3.25	4.50	3.95	-	1.45	2.28	4.07	3.53
H_2O^-	0.14	0.40	0.72	0.44	0.68	-	0.15	0.31	0.56	0.40
TiO_2	0.45	0.35	0.10	0.25	0.15	0.26	3.44	0.06	0.55	0.03
Cr_2O_3	1.01	0.28	0.32	0.21	0.30	2.07	-	0.31	0.14	0.14
NiO	tr	0.18	0.23	0.08	0.25	-	-	0.24	0.27	0.28
Other	0.89	0.06	0.06	0.06	0.08	-	0.90	0.09	0.15	0.09
Total	99.71	100.88	100.53	100.57	100.50	100.17	100.27	100.51	100.17	100.16
Ab		4.9						3.1	6.3	0.2
An			1.9			26.2	1.5	5.0		
Cal										
Ne							15.9			
Di	86.9	4.4	2.3	4.2	3.8		47.4	3.2	6.5	
Ol	2.9	23.8	39.4	58.9	43.8	13.0	26.4	59.7	64.1	57.6
En	5.9	63.1	54.7	35.3	49.0	57.4		27.5	21.4	41.2
Ru	0.3	0.3		0.2	0.1	0.2	2.3		0.4	
Cr	1.1	0.3	0.3	0.3	0.3	2.5		0.3	0.2	0.2
Hm	1.9	3.2	1.4	2.1	3.0	0.7	4.8	1.3	1.1	0.8
Total	100.0	100.0	100.0	100.0	100.0	100.0	100.0	100.0	100.0	100.0

	21	22	23	24	25	26	27	28	29	30	31	32	33	34
SiO_2	45.15	42.30	37.46	39.33	37.57	41.12	39.16	38.32	45.07	40.65	41.10	39.68	39.90	40.49
Al_2O_3	2.27	2.87	2.13	3.04	4.52	2.24	1.73	2.16	5.75	1.25	1.00	0.80	1.20	0.86
Fe_2O_3	0.27	2.46	0.63	5.67	7.73	2.59	4.20	5.53	3.43	2.53	6.50	7.10	8.01	2.84
FeO	6.35	5.25	7.59	2.25	0.26	3.21	1.82	3.41	9.53	6.15	2.02	2.45	1.50	5.54
MnO	0.12	0.12	0.04	0.05	0.07	0.06	0.08	0.07	0.26	0.18	0.08	0.04	0.10	-
MgO	42.21	40.01	33.79	34.36	33.16	38.52	34.30	34.15	22.88	42.35	43.50	44.21	43.00	46.32
CaO	2.08	1.75	2.92	1.27	1.45	1.40	5.13	1.51	7.48	1.29	1.21	1.00	0.76	0.70
Na_2O	0.24	0.18	1.05	0.30	0.06	0.20	0.77	0.32	1.14	0.29	0.10	0.08	0.12	0.10
K_2O	0.00	0.06	0.06	0.18	0.11	0.10			0.57	0.13				0.04
H_2O^+	0.65	4.49	3.37	2.65	3.05	1.63	1.58	1.00	-	-	0.50	1.00	1.64	0.05
H_2O^-	0.12	4.44	7.92	10.00	12.02	7.77	10.15	2.10	3.10	5.02	3.50	4.00	3.50	2.88
TiO_2	0.15	0.18	0.20	0.30	0.22	0.53	0.69	0.20	0.64	0.11	0.01	tr	0.02	0.02
Cr_2O_3	0.21	-	0.234	0.35	0.14	0.50	0.56	0.55	-	-	0.65	tr	0.005	-
NiO	-	-	0.42	0.37	nd	0.53	0.20	0.51	-	-	nd	nd	1.10	-
Other	0.03	0.04	0.11	0.03	0.06	0.04	1.63	0.78	0.15	0.04	-	-	-	-
Total	99.85	100.15	100.364	100.15	100.42	100.44	99.82	100.61	100.00	100.00	100.17	100.36	99.85	100.00
Ab	1.5	1.8	11.0	4.1	1.2	2.2		2.9	15.1	3.4	0.8	0.5	1.1	1.0
An	4.6	6.6	0.6	6.7	7.9	5.0	1.3	4.7	8.1	1.6	2.2	1.8	2.7	1.7
Cal							4.4							
Ne														
Di	3.8	1.3	2.8			1.6	20.4	2.6	23.2	3.6	2.5	2.3	0.6	1.0
Ol	70.5	69.5	67.8	55.0	48.4	63.7	69.6	58.7	45.7	83.4	72.5	78.6	72.6	88.6
En	20.0	19.0	11.8	29.4	36.2	24.6	-	26.1	4.4	6.3	17.8	12.2	17.7	5.9
Ru	0.1	0.2	0.2	0.2	0.2	0.4	0.5	0.2	0.5					
Cr	0.3		0.2	0.5	0.2	0.7	0.7	0.7						
Hm	0.2	1.6	5.6	4.1	5.9	1.8	3.1	4.1	2.4	1.7	4.2	4.6	5.3	1.8
Total	100.0	100.0	100.0	100.0	100.0	100.0	100.0	100.0	100.0	100.0	100.0	100.0	100.0	100.0

	35	36	37	38	39	40	41	42	43	44	45	46	47	48
SiO_2	35.76	35.88	37.45	35.64	36.05	34.89	45.85	38.58	40.38	44.35	42.42	44.44	46.53	44.26
Al_2O_3	2.14	3.32	2.83	3.79	3.08	2.97	2.05	0.89	2.83	2.97	1.32	6.28	11.58	5.76
Fe_2O_3	4.28	5.65	5.03	3.27	4.71	5.02	0.71	3.63	3.71	0.67	4.27	2.78	3.30	2.52
FeO	1.12	2.79	1.94	1.96	2.71	2.11	6.45	3.58	4.38	7.59	6.96	11.22	8.65	10.02
MnO	0.06	0.07	0.07	0.10	0.03	0.06	0.15	0.09	0.11	0.13	nd	0.18	0.22	0.18
MgO	35.04	35.26	36.01	36.34	35.94	37.25	41.63	40.11	36.79	40.80	40.80	24.86	16.08	27.75
CaO	4.50	2.56	3.90	2.76	2.70	2.32	1.76	0.82	2.46	2.55	1.19	7.92	11.00	6.90
Na_2O	0.96	0.73	0.81	1.91	0.81	0.43	0.15	tr	0.20	0.20	0.72	0.82	1.01	0.79
K_2O					0.12	0.09	0.08	-	-	0.01	0.45	0.02	0.02	0.01
H_2O^+	1.81	2.49	2.00	1.97	2.09	1.27	nd.	10.13	7.86	0.09	0.70	0.38	0.36	0.48
H_2O^-	14.85	13.03	9.00	11.06	10.00	12.01	nd	0.71	0.50			-	-	-
TiO_2	0.44	0.22	0.31	0.47	0.37	0.51	0.41	tr	tr	0.14	0.30	0.48	0.64	0.38
Cr_2O_3	0.55	0.66	0.48	1.20	0.54	0.51	0.48	0.63	0.57	0.41	0.40	0.24	0.12	0.35
NiO	0.22	0.30	0.26	0.48	0.49	0.40	0.26	0.12	0.10	0.31	-	0.18	0.06	0.21
Other	0.11	0.04	0.10	0.25	0.08	0.09	0.03	0.67	0.14	0.02	0.14	-	-	-
Total	100.03	100.51	100.19	100.19	99.72	99.93	100.01	99.96	100.03	100.24	99.67	99.80	99.57	99.61
Ab		5.8	4.0		4.0	5.0	1.5		1.7	1.5	6.7	7.3	7.3	6.6
An	1.6	5.8	4.2	2.0	4.8	6.6	4.3	2.5	6.9	6.6		13.1	22.4	10.4
Cal	5.4	0.7	2.0	10.6	2.4									
Ne														
Di	17.5	6.0	12.4	8.9	7.4	5.0	2.8	1.1	4.2	4.0	4.1	10.0	9.0	9.0
Ol	71.3	76.0	73.0	74.5	77.0	68.6	66.7	72.6	63.3	71.2	76.8	48.8	35.2	71.1
En	0.0		0.0			9.9	24.0	20.6	20.1	15.7	9.0	18.1	23.4	0.0
Ru	0.3	0.2	0.2	0.3	0.3	0.4	0.3			0.1	0.2	0.5	0.7	0.6
Cr	0.7	0.8	0.6	1.4	0.7	0.7	0.4	0.7	0.7	0.4	0.4	0.3	0.1	0.5
Hm	3.2	4.1	3.6	2.3	3.4	3.8	0.5	2.5	3.1	0.5	2.8	1.9	1.9	1.8
Total	100.0	100.0	100.0	100.0	100.0	100.0	100.0	100.0	100.0	100.0	100.0	100.0	100.0	100.0

	49	50	51	52	53	54	55	56	57	58	59	60	61	62
SiO_2	46.45	45.95	48.02	42.94	42.70	41.56	42.20	43.70	42.12	45.12	42.66	44.96	42.30	44.60
Al_2O_3	7.95	6.44	4.88	1.04	0.17	0.62	1.50	6.58	0.00	2.96	0.00	1.66	1.98	0.18
Fe_2O_3	2.43	2.20	1.94	9.37	7.73	7.23	2.30	6.09	8.34	5.14	9.87	5.23	2.65	6.48
FeO	8.66	10.07	8.15	0.50	3.16	2.80	5.80	3.24	1.58	4.16	0.36	3.94	5.90	2.58
MnO	0.18	0.18	0.14	0.04	0.05	0.05	0.10	0.06	0.04	0.05	0.05	0.04	0.10	0.04
MgO	22.89	29.10	32.35	37.67	40.42	42.97	43.40	33.80	43.42	36.07	44.08	39.89	45.00	39.94
CaO	9.06	4.48	2.97	3.47	3.37	2.29	2.50	4.58	1.67	3.72	1.49	2.40	1.46	3.75
Na_2O	0.88	0.59	0.66	0.28	0.44	0.22	1.30	0.47	1.47	0.38	0.22	0.34	0.25	0.31
K_2O	0.02	0.03	0.07	0.19	0.08	0.05	0.30	0.03	0.19	0.16	0.19	0.16	0.03	0.11
H_2O^+	0.29	0.52	0.79	3.54	0.38	0.22	0.87	0.34	0.0	0.0	0.04	0.00	0.30	0.64
H_2O^-	-	-	0.32	0.70	0.16	0.04	0.05	0.06	0.60	0.44	0.42	0.56	0.00	0.00
TiO_2	0.53	0.22	0.22	0.17	0.25	0.25	0.07	0.42	0.11	0.25	0.08	0.17	0.10	0.11
Cr_2O_3	0.18	0.29	0.25	0.58	1.11	0.91	0.50	0.02	0.59	0.86	0.50	0.51	0.50	1.70
NiO	0.13	0.17	-	-	-	-	-	-	-	-	-	-	-	-
Other	-	-	0.07	-	-	-	-	-	-	-	-	-	-	-
Total	99.65	100.24	100.83	100.49	100.02	99.21	100.89	99.39	100.13	99.31	99.96	99.86	100.57	100.33
Ab	8.1	5.4	4.6	3.7	1.0	2.0	10.1	3.8		4.4		3.8	1.2	0.6
An	18.5	15.5	9.8	1.0		0.5		14.9		5.3		2.1	5.2	
Cal														
Ne														
Di	11.1	2.9	3.4	12.4	12.4	7.9	3.2	5.2	6.2	9.6	5.5	7.1		13.8
Ol	59.5	74.0	43.1	52.2	62.0	71.7	81.5	53.3	66.7	52.7	62.6	61.3	79.7	51.4
En			37.3	23.5	18.3	12.1	3.2	18.6	21.1	24.1	25.0	21.7	11.1	28.3
Ru	0.8	0.3	0.2	0.1	0.2	0.2		0.3		0.2		0.1	0.5 *1)	
Cr	0.3	0.3	0.3	0.6	1.1	1.0	0.6		0.6	0.5	0.6	0.6	0.6	1.7
Hm	1.7	1.6	1.3	6.5	5.0	4.6	1.4	3.9	5.4	3.3	6.3	3.3	1.7	4.2
Total	100.0	100.0	100.0	100.0	100.0	100.0	100.0	100.0	100.0	100.0	100.0	100.0	100.0	100.0

	63	64	65	66	67	68	69	70	71	72	73	74	75	76
SiO_2	43.14	44.84	42.50	42.22	41.80	43.45	42.70	42.50	42.90	42.86	43.80	44.50	44.27	44.14
Al_2O_3	0.16	0.16	0.43	1.56	1.40	1.15	2.10	0.40	1.20	0.23	0.50	3.24	2.97	2.78
Fe_2O_3	6.86	7.16	6.89	4.05	5.40	2.45	3.40	3.50	6.59	7.25	4.45	1.68	0.67	1.02
FeO	3.28	2.21	2.82	4.44	4.10	6.12	5.10	6.50	2.57	2.57	4.95	6.83	7.59	7.33
MnO	0.04	0.04	0.04	-	0.14	0.13	0.12	0.17	0.05	0.05	0.35	0.17	0.13	0.12
MgO	40.87	42.23	40.87	45.04	44.40	45.35	41.10	44.50	40.23	42.48	43.00	41.02	40.73	41.65
CaO	1.66	1.73	2.63	1.92	2.01	0.65	2.60	1.20	2.80	2.06	1.40	2.22	2.55	2.15
Na_2O	0.15	0.19	0.19	0.11	0.21	0.30	1.20	0.70	0.38	0.19	0.65	0.22	0.20	0.19
K_2O	0.11	0.14	0.00	0.09	0.12	0.25	0.30	0.15	0.13	0.03	0.40	0.05	0.01	0.01
H_2O^+	0.00	0.88	2.40	0.11	0.60	0.15	1.00	0.85	0.00	-	0.25	-	-	-
H_2O^-	0.00	0.00	0.00	0.02	0.36	0.0	0.08	0.85	0.14	-	0.01	-	-	-
TiO_2	0.11	0.14	0.17	-	0.05	-	0.09	0.05	0.14	0.06	-	0.06	0.14	0.12
Cr_2O_3	3.06	0.58	1.40	-	0.06	0.20	0.57	0.30	1.90	1.43	0.90	-	0.41	0.25
NiO	-	-	-	-	-	-	-	-	-	-	-	-	0.31	0.23
Other	-	-	-	-	-	-	-	-	-	-	-	0.01	0.02	-
Total	99.33	100.16	100.34	100.16	100.65	100.20	100.36	100.87	99.03	99.21	100.66	100.0	100.0	100.0
Ab	0.8	1.3	1.6	1.3	2.3	3.7	7.0	6.4	3.9	1.8	2.5	2.0	1.5	1.5
An			0.2	2.5	2.3	1.0			1.1			7.0	6.6	6.2
Cal														
Ne														
Di	6.0	5.1	9.6	4.4	5.4	1.6	9.4	4.2	9.5	7.5	5.1	2.2	4.0	2.6
Ol	54.9	65.9	62.1	78.7	80.2	88.8	80.9	86.9	62.8	64.8	69.5	70.4	71.2	72.7
En	30.9	23.3	20.5	10.8	6.2	10.7			16.4	19.8	19.2	17.4	15.7	16.1
Ru		0.1	0.1		0.1				0.1				0.1	
Cr	3.1	0.5	1.4		0.1	0.2	0.6	0.3	1.9	1.5	0.9		0.4	0.3
Hm	4.4	3.8	4.5	2.6	3.4	1.5	2.1	2.2	4.3	4.6	2.8	1.1	0.5	0.6
Total	100.0	100.0	100.0	100.0	100.0	100.0	100.0	100.0	100.0	100.0	100.0	100.0	100.0	100.0

	77	78	79	80	81	82	83	84	85	86	87	88	89	90
SiO_2	38.78	39.33	40.03	45.10	44.82	44.02	44.59	44.39	43.29	44.08	42.57	41.56	40.66	39.23
Al_2O_3	0.91	0.85	2.11	3.92	8.21	1.03	2.98	3.26	2.36	0.47	0.28	1.66	0.48	1.48
Fe_2O_3	3.00	1.05	0.75	1.00	2.07	0.83	1.68	2.02	1.23	1.29	2.44	2.28	3.40	1.52
FeO	11.48	12.96	7.38	7.29	7.91	7.06	6.83	7.06	7.20	7.25	4.44	5.27	3.00	13.73
MnO	0.19	0.19	0.12	0.14	0.19	0.11	0.17	0.13	0.14	0.13	0.10	0.12	0.09	0.12
MgO	43.46	44.90	42.84	38.81	26.53	46.99	41.10	40.79	40.91	45.32	47.85	44.86	46.48	42.30
CaO	0.05	0.18	1.57	2.66	8.12	tr	2.22	0.94	2.84	0.76	0.10	1.36	0.09	0.89
Na_2O	0.10	0.04	0.28	0.27	0.89	0.05	0.22	0.35	0.33	0.14	0.03	0.10	0.04	0.30
K_2O	-	0.01	0.01	0.02	0.03	tr	0.05	0.04	0.05	0.05	0.01	0.03	0.03	0.02
H_2O^+	nd	0	0	0.07	0.11	0.09	0.09	0.13	0.93	0.65	1.72	2.41	5.51	*
H_2O^-	0.14	0.03	0.10	0.17	0.25	0.00	0.00	0.08	0.07	0.10	-	-	-	*
TiO_2	0.08	0.05	0.07	0.13	0.52	tr	0.06	0.13	0.20	0.06	0.01	0.04	0.01	0.13
Cr_2O_3	1.00	0.38	0.48	0.31	0.20	0.42	0.26	nd	0.27	0.32	0.36	0.37	0.28	0.28
NiO	nd.	0.29	0.29	0.25	0.20	-	-	-	-	-	0.38	0.34	0.36	-
Other						-	0.01	0.15	0.03	0.05	-	-	-	*
Total	99.19	100.26	100.03	100.14	100.05	100.60	100.26	99.47	99.85	100.57	100.29	100.40	100.43	100.00
Ab	0.8	0.2	2.3	2.0	7.2	0.5	1.9	4.1	3.6	1.2		0.7	0.5	2.6 *2)
An	0.2	1.0	5.3	8.7	16.0		5.9	4.4	4.1	0.5	0.6	3.6	0.5	2.6
Cal														1.4
Ne														0.1 *1)
Di	-	-	1.4	2.7	27.2		1.3		3.5	1.1		1.0		0.9
Ol	92.8	97.6	76.4	63.7	42.2	80.5	70.1	68.2	76.0	77.8	80.6	72.7	72.3	91.7
En	4.1		14.0	22.1	6.0	18.1	19.3	22.8	11.4	18.2	17.4	20.2	24.2	
Ru	0.1	0.1	0.1	0.1	0.2		0.1	0.2	0.3	0.1				0.3
Cr		0.4				0.4	0.3		0.3	0.3	0.4	0.4	0.3	0.4
Hm	2.0	0.7	0.5	0.7	1.2	0.5	1.1	1.3	0.8	0.8	1.0	1.4	2.2	0.1
Total	100.0	100.0	100.0	100.0	100.0	100.0	100.0	100.0	100.0	100.0	100.0	100.0	100.0	100.0

	91	92	93	94	95	96	97	98	99	100	101	102	103	104
SiO_2	47.55	40.65	41.75	44.93	44.77	43.91	44.93	44.69	42.38	43.82	42.55	43.40	47.6	49.2
Al_2O_3	4.77	1.90	4.80	6.40	4.16	2.65	3.21	3.19	1.98	5.04	2.10	1.76	4.8	2.4
Fe_2O_3	2.93	5.00	1.25	3.10	-	1.44	0.09	0.09	5.21	1.31	1.33	2.01	2.9	2.0
FeO	5.58	6.62	5.90	10.25	8.21	7.23	7.58	7.54	6.90	6.20	6.76	6.35	5.6	6.8
MnO	0.03	0.26	0.17	0.16	0.11	0.15	0.14	0.14	0.27	0.18	0.11	0.13	0.0	0.2
MgO	18.46	38.55	37.10	25.57	39.22	42.01	40.03	39.80	40.13	38.92	44.06	43.15	18.5	19.1
CaO	18.66	2.50	3.70	7.36	2.42	2.02	2.99	2.97	2.60	3.88	2.36	2.45	18.7	18.9
Na_2O	0.45	0.37	0.50	0.75	0.22	0.13	0.18	0.18	0.39	0.52	0.14	0.19	0.5	0.2
K_2O	0.03	-	-	0.03	0.05	0.00	0.02	0.02	-	-	0.04	0.03	0.0	0.1
H_2O^+	0.70	6.13	6.12	0.48	-	-	-	0.38	-	-	-	-	0.7	0.6
H_2O^-	0.20	3.40	4.20	-	-	-	-	-	-	-	-	--	0.2	0.2
TiO_2	0.52	-	-	0.44	0.19	0.06	0.08	0.08	-	-	0.04	0.03	0.5	0.2
Cr_2O_3	0.23	0.31	0.12	0.30	0.40	0.41	0.45	0.45	tr	tr	0.24	0.25	0.2	-
NiO	-	-	-	0.19	0.24	-	0.26	0.26	tr	tr	0.27	0.25	-	-
Other	0.04	0.38	0.34	-	0.01	0.01	0.04	0.04	0.14	0.13	tr	-	-	-
Total	100.15	100.07	99.95	99.96	100.00	100.00	100.00	99.83	100.00	100.00	100.00	100.00	100.2	99.9
Ab	0.7	3.2	4.2	7.6	1.8	1.0	1.6	1.6	3.4	4.6	1.3	1.5	4.4	2.3
An	11.0	3.3	10.2	13.4	9.4	6.1	7.2	7.3	0.9	10.1	4.4	3.5	10.7	5.4
Cal	1.8													
Ne														
Di	57.6	6.8	5.7	17.4	1.2	2.4	2.4	2.3	4.4	3.0	2.4	3.0	32.3	26.4
Ol	15.9	73.9	68.9	44.9	66.5	72.1	68.0	67.8	75.7	74.0	81.5	76.9	25.6	1.5 *3)
En	4.3 *2	9.2	10.1	13.9	20.5	17.1	20.1	20.4	12.2	7.5	8.1	13.5	24.0	62.7
Ru	1.0			0.2	0.2		0.1	0.1					0.7	0.3
Cr	0.3	0.3	0.1	0.5	0.4	0.4	0.5	0.5			0.3	0.3	0.3	
Hm	7.2	3.3	0.8	2.1		0.9	0.1		3.4	0.8	2.1	1.3	2.0	1.4
Total	100.0	100.0	100.0	100.0	100.0	100.0	100.0	100.0	100.0	100.0	100.0	100.0	100.0	100.0

APPENDIX 37 (Continued)

	105	106	107	108	109	110	111	112	113	114	115	116	117	118
SiO_2	48.3	50.7	49.5	44.57	44.24	43.56	43.10	40.50	41.2	36.55	46.20	42.50	43.70	41.40
Al_2O_3	3.0	1.6	2.0	4.10	2.91	2.36	0.71	0.22	1.2	1.7	3.49	4.56	1.04	3.16
Fe_2O_3	3.1	1.6	3.1	1.17	1.04	1.00	1.42	2.03	4.0	1.8	2.30	5.64	1.74	0.60
FeO	6.0	3.9	2.2	6.85	7.00	7.77	6.69	4.92	8.2	16.85	6.85	6.03	11.60	6.63
MnO	0.2	0.1	0.1	0.13	0.13	0.10	nd	0.10	0.1	0.15	.09	0.10	0.17	0.10
MgO	18.1	20.2	19.2	39.07	41.36	41.53	45.71	49.34	34.4	37.95	36.50	31.80	38.50	42.50
CaO	20.2	20.9	20.2	2.87	2.37	2.51	0.69	0.02	1.35	1.0	2.04	2.53	1.66	0.88
Na_2O	-	-	0.2	0.32	0.07	0.32	0.06	0.08	0.20	tr	0.42	0.04	0.06	0.22
K_2O	-	-	0.1	0.07	0.00	0.005			0.30	tr	0.25	0.03	0.01	0.11
H_2O^+	0.2	0.3	2.4	-	-	-	0.32	2.05	5.2	2.6	-	-	-	_
H_2O^-	0.3	0.2	0.3	-	-	-	0.08	0.15	0.25	0.4	-	-	-	-
TiO_2	0.4	0.3	0.2	0.12	0.17	0.04	tr	-	0.25	0.1	0.17	0.09	0.12	0.07
Cr_2O_3	0.2	0.5	0.4	0.46	0.50	0.40	0.66	0.40	3.2	0.4	0.63	0.40	0.41	0.66
NiO	-	-	-	0.25	0.21	0.34	-	-	-	tr	0.13	-	-	-
Other	-	-	-	0.02	-	0.07	0.20	-	0.05	0.65	-	-	-	-
Total	100.0	99.3	99.3	100.00	100.00	100.00	99.64	99.81	100.25	100.15	98.98	93.72	99.01	96.33
Ab			2.3	3.1	0.5	2.8	0.5	0.5	3.2		4.8	0.6	0.5	1.7
An	8.1	4.2	4.3	8.8	6.9	4.4	1.8	0.1	1.6	4.3	5.1	9.8	2.5	4.0
Cal														
Ne														
Di	36.3	38.8	38.5	5.5	3.0	5.7	1.5		3.8	0.4	2.2	0.2	4.5	
Ol	19.2	15.5	13.1	62.0	70.7	76.6	76.4	78.8	52.8	93.7	41.7	36.2	67.6	76.4
En	32.6	39.1	38.7	16.4	17.9	9.4	15.9	5.7	28.7		44.6	49.3	23.8	12.5
Ru	0.6	0.4	0.3		0.1				0.4		0.1			
Cr		0.3	0.6	0.4	0.6	0.4	0.9	0.7	6.8	0.4				
Hm	3.2	1.7	2.2	0.8	0.7	0.7	2.1 *2)	3.0 *2)	2.7	1.2	1.5	3.9	1.1	0.4
Total	100.0	100.0	100.0	100.0	100.0	100.0	100.0	100.0	100.0	100.0	100.0	100.0	100.0	100.0

	119	120	121	122	123	124	125	126	127	128	129	130	131	132
SiO_2	41.50	38.31	51.31	55.16	55.14	37.11	46.37	43.25	40.06	40.64	47.73	37.62	42.36	38.55
Al_2O_3	1.16	1.68	1.88	2.04	2.58	2.17	10.82	5.84	1.67	1.25	4.82	1.72	3.36	2.04
Fe_2O_3	2.19	3.42	1.08	0.25	8.52	4.74	1.60	5.92	6.05	7.10	2.94	5.45	5.55	7.23
FeO	6.13	8.82	8.48	7.60	-	4.06	7.85	4.67	7.52	6.03	6.54	1.44	3.07	1.76
MnO	0.53	0.19	0.12	0.17	0.05	0.16	0.16	0.08	0.19	0.18	0.17	0.05	0.10	0.41
MgO	45.50	32.91	19.58	32.05	32.01	43.53	20.78	28.87	35.55	36.03	28.98	37.80	36.48	35.88
CaO	0.53	3.03	15.80	1.54	1.48	nil	7.94	1.92	2.34	1.49	2.44	0.50	2.24	0.37
Na_2O	0.22	0.37	1.30	0.20	0.18	0.42	0.99	0.58	0.32	0.48	0.19	0.16	0.62	0.42
K_2O	0.012	0.26	0.03	0.12	0.15	0.23	0.57	0.27	0.12	0.05	0.02	0.02	0.03	0.05
H_2O^+	-	4.58	0.11	0.22	0.35	5.84	1.97	2.22	6.01	6.53	4.91	13.62	4.62	11.55
H_2O^-	-	0.75	0.14	0.22		0.60	0.82	6.01	0.28	0.31	0.49	0.96	0.50	1.01
TiO_2	0.08	0.13	0.20	nil	0.14	nil	0.13	0.38	0.06	0.03	0.12	0.03	0.10	0.04
Cr_2O_3	0.69	4.28	0.12	0.49	0.20	0.36	0.07	0.20	0.21	0.21	0.48	0.39	0.39	0.46
NiO	-	0.22	-	-	-	0.31	0.07	-	-	-	-	0.26	0.26	0.21
Other	-	0.86	0.44	0.08	-	0.78	-	-	-	tr	0.16	-	-	tr
Total	98.50	99.81	100.70	100.14	100.80	100.31	100.14	100.21	100.38	100.33	99.99	99.46	99.68	99.98
Ab	1.8	4.7	7.7	2.4	2.1	4.2	11.8	6.6	3.6	4.6	1.7	1.5	5.4	4.4
An	2.0	4.5		4.0	5.6		23.2	10.8	2.6	0.9	12.2	2.6	6.2	1.8
Cal						0.5								
Ne					2.6 *3									
Di	0.4	8.3	61.8	2.7	1.5		12.6		7.3	5.2			3.6	
Ol	85.3	66.0	23.3	8.1	0.0	91.7	34.6	33.7	67.3	65.8	19.8	64.5	59.5	59.7
En	9.1	9.3	4.1	82.0	82.3		16.5	44.1	14.7	18.4	63.5	26.8	21.1	28.4
Ru		0.1	0.2		0.1		0.1	0.3						
Cr		4.7	0.1	0.6	0.3	0.4	0.1	0.3	0.3	0.3	0.7	0.5	0.4	0.5
Hm	1.4	2.4	0.8	0.2	5.5	3.2	1.1	4.2	4.2	4.8	2.1	4.1	3.8	5.2
Total	100.0	100.0	100.0	100.0	100.0	100.0	100.0	100.0	100.0	100.0	100.0	100.0	100.0	100.0

****

Appendix 39:

The chemical analyses and molecular norms of garnet peridotite, peridotite and dunite from various parentages.

I. Ultramafic nodules in kimberlite.

1 Garnet peridotite; Premier Mine; (New analysis).
2 Spinel peridotite; ditto
3 - 5 Garnet-lherzolites; Wesselton; (New analysis).
6 -11 Ultramafic nodules; Jagersfontein; Visser (1954, 365-369).
12-15 Ultramafic nodules; Bultfontein; Visser (1964, 357-360).
16-17 Ultramafic nodules; Annual Rept. Univ. Leeds (1962-63).
18-20 Ultramafic nodules; Holmes (1936).
21-22 Ultramafic nodules; Nixon et al. (1963).
23-40 Ultramafic nodules from Russia; Bobrievich et al., (1959).
41 Ultramafic nodule; Kennedy (1968).
42-43 Ultramafic xenoliths from Chechoslovakia; Kopecky (1962).
44-45 Ultramafic nodules from Lesotho; Nixon et al.,(1963).

II. Ultramafic rocks from regional peridotites.

46-51 Ultramafic rocks from Karlskaret.

III. Ultramafic nodules in alkaline basalts.

52-73 Ultramafic nodules from France; Brousse (1968).
74 Ultramafic nodule; Wilshire and Binns (1961).
75 ditto ; Hess (1960).
76 ditto ; Kuno (1967).
77-81 Ultramafic nodules from the Nephelinites at Hawaii; Jackson et al., (1969).
82-91 Ultramafic nodules from Japan; Kuno (1967, p 338).

IV. Alpinotype dunites and peridotites and high temperature differentiates.

92-93; Ultramafic rocks from Marocco; MacGreggor et al., (1963).
94-96; Ultramafic rocks from Venezuela; Lapham (1964).

97-102; High temperature ultramafic rocks; Green (1967, p 216).
103-107; Zoned ultramafic complexes; Alaska; Taylor (1967, p 102).
109-110; ultramafic rocks from Venezuela; Lapham (1964).
111-112; ultramafic rocks from Norway; Rietz (1935).
113-114; ultramafic rocks from the Bushveld Complex; Hall (1938).
115-119: ultramafic rocks from the Bushveld Complex; Liebenberg (1957).
120-126; ultramafic rocks from South Africa; Hall (1938).
127-129; Stilwater; Hess (1960).
130-132; Mid Atlantic Ridge Peridotite; Bonatti (1968).

*1 *Kyanite*

*2 *Magnetite*

*3 *Quartz*

*4 *Other oxides, unspecified.*

ADDENDUM TO APPENDIX 29

	1.	2.	3.	4.	5.	6.
SiO_2	37.70	34.87	43.99	43.47	37.67	42.95
TiO_2	tr	0.03	0.01	0.03	tr.	0.01
Al_2O_3	0.28	0.37	0.59	0.61	1.51	1.09
Fe_2O_3	2.64	5.87	1.11	1.23	4.69	6.52
FeO	4.63	2.54	6.97	6.63	2.50	4.17
MnO	0.10	0.09	0.12	0.12	0.09	0.17
MgO	48.09	44.48	46.09	45.62	39.65	31.50
CaO	0.04	0.04	0.49	0.60	0.68	5.15
Na_2O	0.17	0.13	0.14	0.56	0.09	0.05
K_2O	0.15	0.23	0.10	0.14	0.09	0.10
Cr_2O_3	0.27	0.51	0.40	0.40	0.23	0.48
NiO	0.35	0.34	0.28	00.29	0.27	0.12
P_2O_5	1.24	0.83	0.11	0.30	1.40	0.74
CO_2	.	.	.	.	.	.
H_2O+	2.45	8.63	0.38	0.75	7.53	4.52
H_2O^-	2.49	2.57	0.21	0.48	4.01	2.39
Total	100.60	99.51	100.48	100.63	100.61	99.96

1 to 6 Ultramafic rocks from the Vourinos Ophiolitic Complex, Moore, Spec. Paper of Geol. Soc. Amer., 1969,116.

	1	2	3	4	5	6	7	8	9	10	11	12	13	14	15
SiO_2	43.56	43.32	45.36	48.70	47.16	47.20	43.64	46.20	45.04	45.40	45.68	45.80	50.60	46.60	50.28
Al_2O_3	12.80	18.22	7.49	10.87	7.29	8.49	16.48	9.89	13.13	16.51	19.17	23.86	20.68	11.87	19.94
Fe_2O_3	8.720	5.84	5.20	3.64	7.00	5.04	8.24	7.05	6.96	5.20	3.80	nil	0.96	4.56	1.04
FeO	9.43	6.26	9.72	3.55	11.34	8.42	8.42	8.78	8.13	6.48	8.10	7.22	3.09	7.41	6.26
MnO	0.21	0.21	0.31	0.08	0.29	0.03	0.10	0.29	0.11	0.33	0.29	0.07	0.16	0.21	0.11
MgO	14.40	8.42	15.55	18.36	13.60	13.68	10.80	14.04	15.33	8.64	11.52	8.28	6.62	11.88	7.20
CaO	8.68	11.48	10.92	11.90	8.54	9.94	7.84	8.40	6.86	11.20	8.69	11.34	11.48	10.36	7.84
Na_2O	nil	2.34	2.66	tr	1.13	3.89	0.86	1.01	0.56	0.54	0.20	0.33	3.29	3.78	3.86
K_2O	nil	0.18	nil	0.90	0.31	0.76	0.82	0.95	0.33	0.80	nil	nil	0.58	0.83	0.76
H_2O^+	1.30	1.91	1.25	0.25	2.43	1.82	1.77	1.63	2.06	2.38	1.98	1.34	1.38	1.68	1.48
H_2O^-	nil	0.28	0.32	0.24	-	nil	nil	0.12	nil	nil	0.16	0.12	0.16	nil	0.28
P_2O_5	0.09	0.09	0.09	0.06	0.08	0.08	0.16	0.07	0.06	0.11	0.09	0.07	0.06	0.07	0.05
Cr_2O_3	-	-	0.47	0.24	0.14	nil	nil	nil	nil	nil	nil	tr	nil	nil	nil
TiO_2	0.70	0.80	0.75	0.75	1.00	1.00	0·66	0.95	0.70	1.65	0.45	0.40	0.30	0.45	0.30
NiO	tr	-	0.12	0.10	-	tr	tr	0.11	tr	-	tr	tr	0.02	0.04	tr
Other *3)	0.16	0.19	0.26	0.64	0.04	0.12	0.09	0.16	0.17	0.34	0.21	0.44	0.21	0.15	0.14
Total	100.05	99.42	100.55	100.28	100.35	100.47	99.88	99.65	99.44	99.58	100.61	99.27	99.59	99.89	99.54

B. Molecular norms

Ab		15.2	14.3		10.1	15.8	8.1	9.2	5.2	5.0	0.7	1.9	29.2	21.8	34.6
Ne		3.8	5.9			11.3								3.8	
Or		1.1		5.2	1.6	4.4	4.9	5.7	2.0	5.0			3.6	5.0	3.5
An	36.2	39.9	8.7	26.6	13.8	3.5	40.4	20.6	33.0	42.4	43.3	57.4	40.3	13.2	34.5
Lc															
Cal															
Di	6.7	15.1	36.5	24.8	22.3	36.5		17.9	1.6	12.9			13.6	30.8	3.5
Ol	9.6	20.1	29.9	7.1	23.9	24.2	12.8	14.4	9.8		4.9	2.3	12.4	21.9	19.7
Hy	40.2			33.1	22.5		27.4	26.4	42.9	29.7	38.4	32.1			3.3
Ru	1.0	0.6	0.5	0.5	0.7	0.7	0.5	0.7	0.5	1.2	0.3	0.3	0.2	0.3	0.2
Ch			0.5	0.3	0.2										
Hm	6.3	4.2	3.7	2.5	4.8	3.5	5.9	5.1	5.0	3.8	2.7		0.7	3.2	0.7
Qz															
Ky											6.7	6.0			
Total	100.0	100.0	100.0	100.0	100.0	100.0	100.0	100.0	100.0	100.0	100.0	100.0	100.0	100.0	100.0

APPENDIX 30 (Continued)

	16	17	18	19	20	21	22	23	24	25	26	27	28	29	30
SiO_2	47.68	46.26	42.50	46.60	45.67	45.63	47.24	47.73	47.26	49.49	42.31	47.60	47.36	49.20	42.00
Al_2O_3	21.16	12.70	17.72	7.15	17.85	16.64	15.05	11.97	10.45	8.46	22.89	13.40	15.12	15.08	17.66
Fe_2O_3	1.52	7.48	2.84	0.95	2.88	2.60	2.25	3.79	2.75	3.20	1.72	0.80	3.44	6.72	3.12
FeO	4.75	10.91	7.52	4.30	8.46	9.25	8.21	9.56	8.69	5.80	4.81	8.35	4.82	5.11	4.39
MnO	0.14	0.37	0.36	0.10	0.17	0.31	0.28	0.33	0.45	0.24	0.16	0.05	0.15	0.08	0.24
MgO	5.04	9.57	13.03	16.50	11.90	13.44	13.39	13.28	15.06	16.23	13.24	15.00	12.81	10.80	13.53
CaO	10.78	9.94	9.76	19.65	7.35	7.46	8.68	8.76	8.46	10.60	7.54	10.55	13.30	9.80	10.22
Na_2O	5.62	tr	2.19	0.90	2.01	1.51	1.74	2.18	1.72	1.67	1.81	2.30	1.64	1.66	0.161
K_2O	0.58	0.66	0.58	0.10	0.39	0.68	0.22	0.40	1.96	1.12	0.66	0.65	0.42	0.18	0.37
H_2O^+	2.40	2.48	3.07	-	2.01	1.34	1.38	1.28	1.68	1.43	4.23	0.30	0.91	0.90	3.27
H_2O^-	0.08	nil	0.28	0.40	1.07	0.29	0.68	0.33	0.48	0.64	-	0.50	nil	nil	0.40
P_2O_5	0.08	0.05	0.05	0.05	0.04	0.06	0.06	0.01	0.05	0.04	0.15	0.15	0.07	0.04	0.09
Cr_2O_3	0.02	0.08	0.07	0.50	0.07	0.08	0.09	0.12	0.19	0.24	0.02	0.15	nil	nil	0.26
TiO_2	0.60	nil	0.60	0.15	0.42	0.43	0.49	0.61	0.75	0.52	tr	0.40	0.45	0.60	0.55
NiO	0.26	0.10	0.19	-	-	-	-	-	-	-	-	-	0.03	0.33	0.17
Other *3)	0.05	0.90	0.04	3.30	-	-	-	-	-	-	-	0.40	0.11	0.15	0.14
Total	100.76	100.69	100.80	100.65	100.29	99.72	99.76	100.34	99.95	99.68	99.54	100.60	100.63	100.65	99.02
Ab	31.7		12.7		18.4	13.4	15.6	19.9	15.6	15.1	6.1	16.2	16.3	15.1	1.5
Ne	6.1		2.3	4.9							6.0	3.6	-		
Or	2.6	4.1	3.3		2.3	4.2	1.1	2.2	11.8	6.4	3.9	4.2	2.5	0.1	2.1
An	30.3	34.8	37.0	10.0	37.0	36.9	32.8	21.6	14.9	13.8	37.6	15.7	25.0	33.9	50.8
Lc				0.4											
Cal				3.3											
Di	18.0	13.8	9.2	65.5	-	0.1	4.2	8.8	11.0	31.1		24.3	28.3	12.1	1.8
Ol	9.5		33.1	14.3	24.9	25.7	18.9	22.6	33.7	21.2	33.3	34.9	24.9		17.3
Hy		39.5			12.9	17.2	25.0	21.2	9.6	9.4				32.4	23.3
Ru	0.4		0.4	0.1	0.6	0.6	0.7	0.9	1.1	0.5		0.3	0.4	0.4	0.4
Ch		0.1	0.1	0.8	0.1	0.1	0.1	0.1	0.3	0.2					0.5
Hm	1.4	5.5	1.9	0.7	2.0	0.6	1.6	2.7	2.0	2.2	1.2	0.6	2.6	4.7	2.3
Qz		2.2												0.3	
Ky					1.8						11.9				
Total	100.0	100.0	100.0	100.0	100.0	100.0	100.0	100.0	100.0	100.0	100.0	100.0	100.0	100.0	100.0

APPENDIX 3Ø (Continued)

	31	32	33	34	35	36	37	38	39	40	41	42	43	44	45
SiO_2	50.60	46.20	38.52	48.61	46.65	42.72	43.04	44.00	43.25	45.15	46.98	50.24	38.18	40.36	41.42
Al_2O_3	8.03	17.49	6.94	13.61	11.70	16.62	24.09	11.80	17.50	2.39	15.26	7.71	1.88	13.68	14.58
Fe_2O_3	5.16	3.96	4.36	4.15	4.09	11.48	2.64	8.44	7.52	0.27	1.42	1.02	3.49	8.48	8.15
FeO	5.43	8.67	6.87	4.53	8.02	2.99	5.18	7.88	5.35	6.35	9.76	4.64	1.93	1.50	4.06
MnO	0.05	0.14	0.08	0.18	0.27	0.66	0.35	0.40	0.47	0.12	0.18	0.11	0.17	1.86	0.32
MgO	15.76	15.12	16.92	17.09	14.34	11.00	5.76	14.50	8.75	42.21	11.51	17.79	20.53	17.63	18.55
CaO	10.78	6.02	14.14	9.83	9.92	12.46	13.58	14.98	13.67	2.08	11.34	16.66	16.42	8.39	5.70
Na_2O	0.92	nil	0.82	1.31	1.34	nil	3.28	tr	3.28	0.24	2.30	0.97	0.12	0.38	0.29
K_2O	0.20	0.31	0.31	0.12	1.16	nil	nil	tr	-	-	0.03	0.11	0.06	0.36	0.25
H_2O^+	1.49	1.49	2.97	0.61	0.66	nil	0.58	1.36	0.89	0.65	-	-	13.14	5.51	4.07
H_2O^-	0.76	nil	0.08	0.08	0.51	0.74	0.28	0.12	0.13	0.12	-	-	3.10	0.70	1.02
P_2O_5	0.05	0.05	0.06	-	0.04	0.06	0.02	0.02	0.03	0.03	-	0.05	0.06	0.24	0.20
Cr_2O_3	0.02	0.07	0.12	0.05	0.28	nil	0.14	0.03	0.06	0.09	0.00	0.54	0.91	0.014	0.025
TiO_2	0.65	0.45	0.80	0.15	0.49	0.66	tr	0.75	0.47	0.15	1.22	0.16	0.37	1.16	1.64
NiO	0.11	0.18	0.13	0.04	0.03	0.03	0.23	0.10	0.12	-	-	-	nd	nd	nd
Other *3)	0.22	0.39	6.32	0.05	0.34	0.19	0.54	nil	0.24	-	-	-	-	-	-
Total	100.23	100.54	99.44	100.44	100.04	99.61	99.71	99.38	99.57	99.85	100.00	100.00	100.36	100.26	100.27
Ab	8.4			11.2	9.3					1.1	14.5	8.2		3.4	2.8
An			4.9		1.4		16.7			Or	3.0	0.5		2.0	1.4
Or	1.3	1.3		0.5	6.4				31.8	An 6.0	29.3	16.2		35.2	29.5
An	17.2	29.8	6.7	34.4	21.7	45.4	48.6	31	21.1	Nc	3.6		0.8		
Ac		10.9 *1	1.5										0.2		
Cal			5.8						4.8				3.6		
Di	29.7		48.4	8.9	20.4	13.2	12.5	36	33.4	2.6	20.8	51.4	57.8	5.7	
Ol		3.7	28.6	26.2	37.5	9.5	18.6	15	23.2	69.7	27.0	19.6	33.6 *2	15.8	24.7
Hy	37.0	51.0		16.0		23.4	-			20.3		2.8		31.0	26.8
Ru	0.5	0.4	0.6	0.1	0.3	0.5			0.4		0.8	0.1	0.3	0.9	1.2
Ch		0.1	0.2		0.2		0.1			0.3		0.5	1.0		
Hm	3.7	2.8	3.3	2.7	2.7	8.0	3.5	2	6.3		1.0	0.7	2.7	6.0	5.9
Qz	1.2														
Ky															7.8
Total	100.0	100.0	100.0	100.0	100.0	100.0	100.0	1	100.0	100.0	100.0	100.0	100.0	100.0	100.0

APPENDIX 30 (Continued)

	46	47	48	49	50	51	52	53	54	55	56	57	58	59	60
SiO_2	43.50	44.76	46.23	45.28	43.00	49.58	46.65	44.18	44.96	47.26	44.44	46.45	46.80	45.46	41.86
Al_2O_3	15.51	13.61	12.34	18.36	20.69	17.41	11.70	24.07	23.20	24.92	14.56	19.18	17.34	17.87	21.19
Fe_2O_3	10.97	10.37	8.79	3.24	3.84	3.20	4.09	4.84	3.14	5.24	6.01	11.79	5.69	6.69	1.92
FeO	3.59	2.43	7.69	5.11	5.21	3.62	8.02	1.76	3.30	0.84	8.95	3.94	8.95	7.73	7.77
MnO	0.23	0.27	0.20	0.15	0.12	0.13	0.27	0.03	0.05	0.06	0.36	0.27	0.15	0.23	0.29
MgO	12.67	11.67	11.11	10.42	10.84	12.93	14.34	6.11	6.42	4.00	9.34	5.23	8.07	8.15	11.38
CaO	8.32	10.38	8.12	11.77	12.41	10.78	9.92	15.06	15.47	11.04	11.30	7.02	8.54	10.27	9.67
Na_2O	0.92	1.16	1.62	1.68	1.02	0.81	1.34	1.22	1.71	3.11	1.12	1.18	1.63	0.74	1.88
K_2O	0.34	0.67	0.83	0.39	0.40	0.20	1.16	0.85	0.26	0.24	0.51	0.61	1.25	0.36	0.36
H_2O^+	2.35	1.81	1.09	1.50	2.10	0.79	0.66	0.70	0.33	0.17	1.12	1.65	0.66	0.95	3.03
H_2O^-	0.38	0.63	0.51	0.75	0.08	0.31	0.51	-	-	-	tr	0.98	0.04	0.30	
P_2O_5	0.07	0.25	0.14	0.08	0.004	-	0.04	0.14	0.11	0.14	0.16	0.18	0.08	0.06	0.15
Cr_2O_3	tr	0.008	0.01	nd	nd	0.06	0.28	0.014	0.014	0.027	0.02	0.028	tr	0.023	0.02
TiO_2	1.40	1.63	1.39	0.91	0.27	0.23	0.49	0.32	0.35	0.30	1.30	1.66	1.42	1.16	0.40
NiO	nd	nd	tr	tr	tr	tr	0.03	-	-	-	tr	nd	tr	tr	-
Other *3)	-	-	-	-	-	-	0.34	0.96	0.85	0.81	1.00	-	-	-	-
Total	100.25	99.65	100.27	99.94	99.98	100.05	100.04	100.25	100.17	99.69	100.19	100.17	100.62	99.99	99.92
Ab	8.0	10.7	14.9	15.1	9.1	7.2	12.0	11.2	3.7	28.4	9.5	11.6	15.0	6.9	9.2
Or	1.8	4.6	5.2	1.9	2.3	1.1	6.7	5.0	1.3	1.4	3.2	3.9	7.4	2.0	2.2
An	35.6	31.1	24.7	40.9	51.5	43.5	22.8	57.8	52.9	54.2	34.7	37.1	36.9	46.3	48.8
Ne									6.6						
Lc															
Cal															
Di	3.0	18.0	13.3	13.4	8.6	8.2	21.4		16.6	1.4	18.7	-	4.9	5.5	
Ol	5.7	5.0	9.7	20.2	25.6		26.5	11.4	16.5	5.9	13.9	-	11.5		33.2
Hy	30.2	22.1	24.9	2.8		37.4	7.2	4.5		4.8	13.8	22.4	19.3	33.2	
Ru	1.0	1.2	1.0	1.2	0.2	0.2	0.3	0.2	0.3	0.2	0.9	1.2	1.0	0.9	0.6
Ch							0.3					-			
Hm	14.7	7.4	6.3	4.5	2.7	2.2	2.8	3.4	2.1	3.7	4.3	8.8	4.0	4.8	1.4
Qz						0.2						6.2		0.4	
Ky								6.5				8.8			
Total	100.0	100.0	100.0	100.0	100.0	100.0	100.0	100.0	100.0	100.0	100.0	100.0	100.0	100.0	100.0

	61	62	63	64	65	66	67	68	69	70	71	72	73	74	75
SiO_2	43.46	42.91	42.46	44.32	44.48	45.31	42.83	41.99	42.00	42.75	44.45	44.96	44.18	44.48	40.26
Al_2O_3	24.11	26.27	27.08	27.79	28.69	28.70	28.85	29.10	31.04	31.40	21.93	23.20	24.07	29.70	29.43
Fe_2O_3	1.99	1.59	1.48	0.95	1.03	0.95	1.09	0.87	1.40	0.95	1.42	3.14	4.84	1.41	0.23
FeO	4.82	4.13	5.36	3.66	2.23	2.55	3.07	2.22	2.49	2.19	4.18	3.30	1.76	1.29	2.50
MnO	0.17	0.12	0.15	0.11	0.08	0.08	0.10	0.10	0.07	0.10	0.15	0.05	0.03	0.06	0.06
MgO	9.05	10.53	8.87	8.06	7.05	5.71	6.94	8.33	9.54	7.12	9.97	6.42	6.11	5.15	9.48
CaO	10.55	10.72	7.30	11.46	11.61	13.17	13.36	11.22	7.98	8.94	13.14	15.47	15.06	12.29	14.02
Na_2O	1.87	1.47	1.93	1.65	1.52	2.37	1.38	0.79	1.22	1.66	1.81	1.71	1.22	1.44	1.63
K_2O	0.53	0.47	0.54	0.69	0.79	0.47	0.27	1.22	0.30	1.26	0.45	0.26	0.85	1.04	0.18
H_2O^+ / H_2O^-	2.65	1.87	3.52	1.88	2.33	0.86	2.03	3.62	3.77	3.75	2.09	1.04	1.42	3.11	1.55
P_2O_5	0.11	0.06	0.16	0.07	0.09	0.09	0.07	0.06	0.12	0.05	0.09	0.11	0.14	0.05	0.05
Cr_2O_3	0.02	0.02	0.01	0.02	0.01	0.01	0.01	0.01	0.01	0.01	0.05	0.01	0.01	0.01	0.04
TiO_2	0.35	tr	0.57	tr	tr	tr	tr	tr	tr	tr	tr	0.35	0.32	tr	0.18
NiO	-	-	-	-	-	-	-	-	-	-	-	-	-	-	-
Other *3)	-	-	-	-	-	-	-	-	-	-	-	-	-	-	0.28
Total	99.68	100.16	99.43	100.66	99.91	100.27	100.00	99.53	99.94	100.18	99.73	100.02	100.01	100.03	99.61
Ab	9.7	2.5		5.5	5.6	9.9	4.2				11.4	14.8	11.3	7.2	
Or	3.3	2.8	4.5	4.1	4.7	2.8	1.7	1.1			2.8	1.4	5.1	6.3	
An	52.3	52.5	36.6	56.4	57.6	64.6	66.2	56.9	18.6	43.3	50.3	55.1	58.3	62.8	2.6
Ne	4.3	6.3	10.5	5.6	4.8	6.6	4.8	4.4	6.4	9.1	2.8	0.3		3.1	8.7
Lc								3.7	1.0	4.5					0.7
Cal									11.6	0.7					63.9
Di											5.9	8.8	6.9		
Ol	24.6	26.3	24.5	20.4	17.2	14.5	17.8	19.7	21.5	17.4	25.6	16.7	14.5	10.5	21.1
Hy															
Ru	0.6		0.8									0.6	0.5		0.3
Ch					0.1	0.1	0.1	0.1	0.1	0.1	0.2	0.1		0.1	0.1
Hm	1.4	1.1	1.1	0.7	0.7	0.7	0.8	0.6	1.0	0.7	1.0	2.2	3.4	1.0	0.2
Qz															
Ky	3.8	8.5	22.0	7.0	9.3	0.8	4.4	13.8	39.8	24.2				9.0	2.3
Total	100.0	100.0	100.0	100.0	100.0	100.0	100.0	100.0	100.0	100.0	100.0	100.0	100.0	100.0	100.0

APPENDIX 30 (Concluded)

	76	77	78	79	80	81	82	83	84	85	86	87	88	89
SiO_2	48.41	43.74	45.02	44.15	43.04	44.57	45.58	48.42	49.52	50.20	47.56	48.02	47.41	46.25
Al_2O_3	10.41	13.17	12.88	16.21	4.77	13.61	13.69	9.46	9.31	8.37	12.41	16.47	14.81	15.79
Fe_2O_3	2.58	6.18	3.52	1.34	2.60	4.17	3.76	3.14	2.26	1.58	5.29	2.43	3.88	1.06
FeO	5.61	5.60	6.71	9.75	11.39	8.49	5.85	7.27	5.44	5.72	8.68	8.47	8.48	9.60
MnO	0.18	0.25	0.19	0.23	0.14	0.21	0.16	0.17	0.16	0.16	0.23	0.16	0.32	
MgO	17.78	16.86	17.11	16.46	32.60	13.34	16.09	16.85	17.97	19.00	6.69	8.35	12.54	14.36
CaO	12.17	10.21	11.72	10.13	4.62	11.42	11.78	12.15	12.90	13.28	10.98	11.49	9.51	9.12
Na_2O	1.24	2.34	1.65	0.77	0.47	1.69	1.27	1.41	1.17	0.87	3.71	2.26	1.97	2.10
K_2O	0.11	0.49	0.16	0.05	0.04	0.02	0.02	0.01	0.04	0.02	0.49	0.46	0.38	0.30
H_2O^+	0.43	0.82	0.67	0.33	0.21	0.29	0.35	0.09	0.17	0.05	1.29	0.60	0.75	0.18
H_2O^-		0.00	0.05	0.14	0.12	0.14	0.32	0.10	0.16	0.04				0.83
P_2O_5	0.04	0.09	0.06	0.08	0.05	0.02	0.03	0.03	0.03	0.02	0.28	0.10		
Cr_2O_3	0.43	0.22	0.19	-	-	1.76	0.80	0.70	0.42	0.51	-	-	0.11	
TiO_2	0.62	0.66	0.44	0.75	0.30	0.06	0.12	0.22	0.35	0.24	2.56	1.22	0.47	0.47
NiO	-	-	-	-	-							-	0.06	
Other *3)	0.28	-	-	-	-	0.08	0.21	0.16	0.24	0.21	0.09	0.22		
Total	100.29	100.63	100.37	100.39	100.35	99.87	100.03	100.18	100.15	100.27	100.26	100.25	100.69	100.06
Ab	11.2	7.4	9.5	7.5	3.9	15.3	11.3	5.5	10.6	7.5	24.6	20.0	17.7	17.7
~~Ne~~ Or	0.5	3.0	0.8	0.3	0.3						3.2	2.4	2.2	1.6
~~Or~~ An	22.1	23.2	26.7	39.6	10.2	29.5	31.2	19.3	19.4	19.5	16.3	33.8	30.1	30.6
~~An~~ Ne	..	7.9	3.1					4.1			5.7			
Lc														
Cal														
Di	30.1	20.9	24.2	7.7	9.0	21.6	21.2	37.8	34.5	36.6	31.8	18.7	6.6	9.1
Ol	25.9	32.9	32.7	35.7	66.1	29.4	28.0	30.6	20.6	16.6	12.8	17.8	21.9	19.2
Hy	7.5			8.2	8.6		5.2		13.0	18.7		4.7	17.9	20.8
Ru	0.4	0.5	0.3	0.5	0.2	1.2	0.5	0.5	0.3	0.3	1.8	0.8	0.7	0.3
Ch	0.5		0.3			0.1							0.2	
Hm	1.8	4.2	2.4	0.9	1.7	2.9	2.6	2.2	1.6	1.1	3.8	1.8	2.7	0.7
Qz														
Ky														
Total	100.0	100.0	100.0	100.0	100.0	100.0	100.0	100.0	100.0	100.0	100.0	100.0	100.0	100.0

****

Appendix 30:

The chemical analyses and molecular norms of eclogite.

I. Eclogite from kimberlite.

1 Eclogite from Roberts Victor:- Hall (1938, No 113).
2 Kyanite eclogite Roberts Victor:- Hall (1938, 114).
3-10 Eclogite from Roberts Victor; Hall (1938, 115-122).
11-16 Kyanite Eclogite from Roberts Victor; Hall (1938).
17-19 Eclogite from Roberts Victor; Hall (1938).
20-26 Eclogite from Roberts Victor; Aoki and Kushiro (1968).
27-33 Eclogite from Jagersfontein; Hall (1938, 1133-1139).
34 Eclogite from Jagersfontein; Holmes (1936).
35 Eclogite from Roberts Victor; Holmes (1936).
36-39 Eclogite from Tanzania; Hall (1938, No 4137-4140).
40-42 Eclogite from Lesotho; Nixon et. al. (1963).
43 Eclogite from Mir; Bobrievich et. al. (1959).
44 Plagioclase eclogite from Udachnaya; (ditto).
45-47 eclogite from Udachnaya; (ditto).
48 plagioclase eclogite from Udachnaya; (ditto).
49 eclogite from Udachnaya; (ditto).
50-51 kyanite eclogite from Udachnaya; (ditto).
52-53 eclogite from Udachnaya and Zagodachnaya; (ditto).
54 kyanite eclogite from Zagodachnaya; (ditto).
55-59 eclogite from Zarnitsa; (ditto).
60-75 kyanite eclogite (6) and grospydite; Sobolev (1968).

II. Eclogite from alkaline basalts.

76-80 Eclogite from East Africa; Saggerson (1968).
81-85 Eclogite from Hawaii; Jackson et. al., (1969).
86 Average of alpinotype eclogite; Smulikowski, (1968).
87 Average of regional eclogite; (ditto).

III. New Analyses.

88-89 Eclogite from Roberts Victor; new analyses.

*1) Al_2O_3

*2) Ca_2SiO_4

*3) Other oxides, unspecified.

PROFILE 1 ALONG THE 18 TUNNEL (BB ON MAP 2)

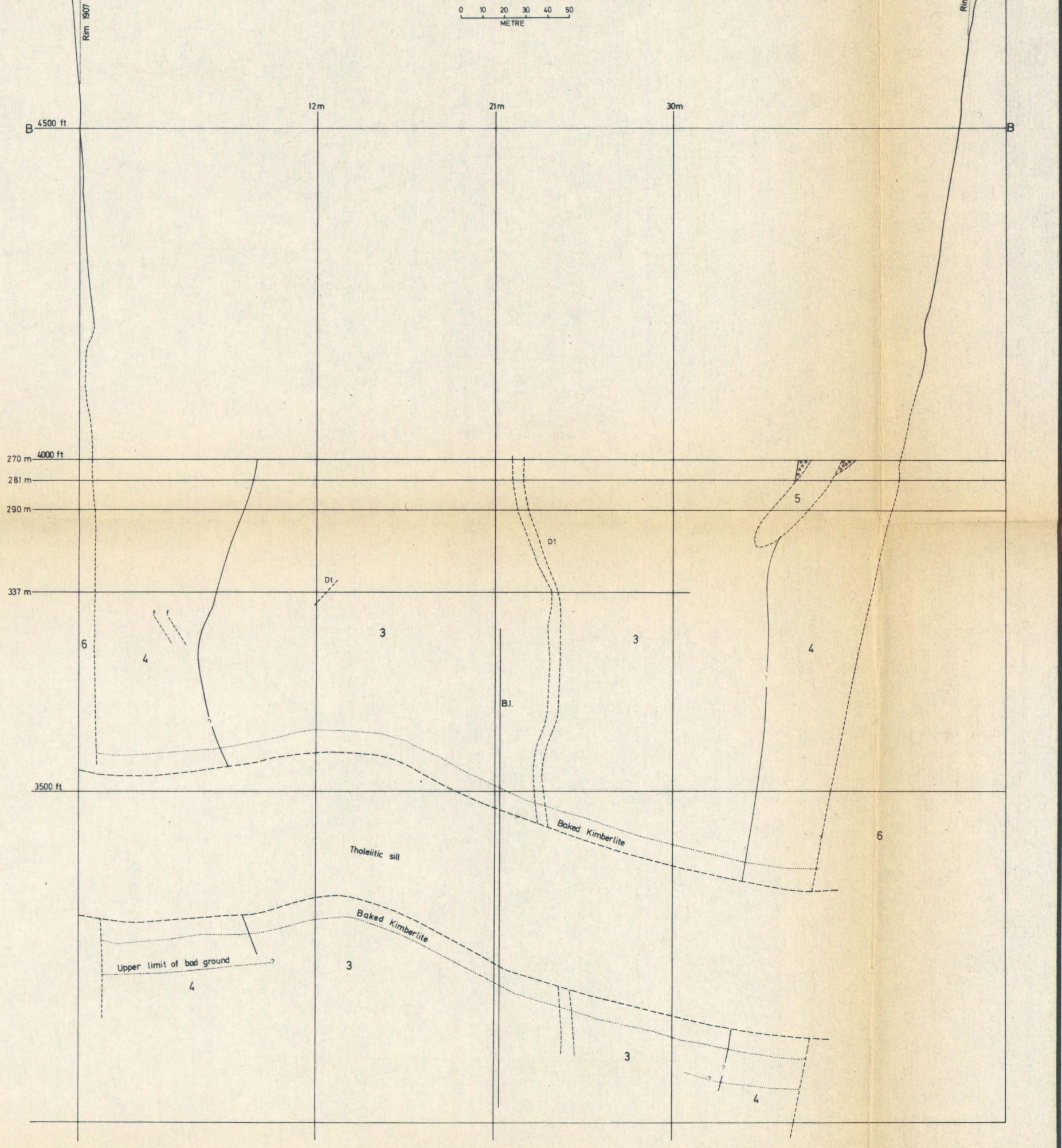

MAP 2 A GENERALIZED MAP OF THE GEOLOGY OF PREMIER MINE ON THE 337 METER LEVEL

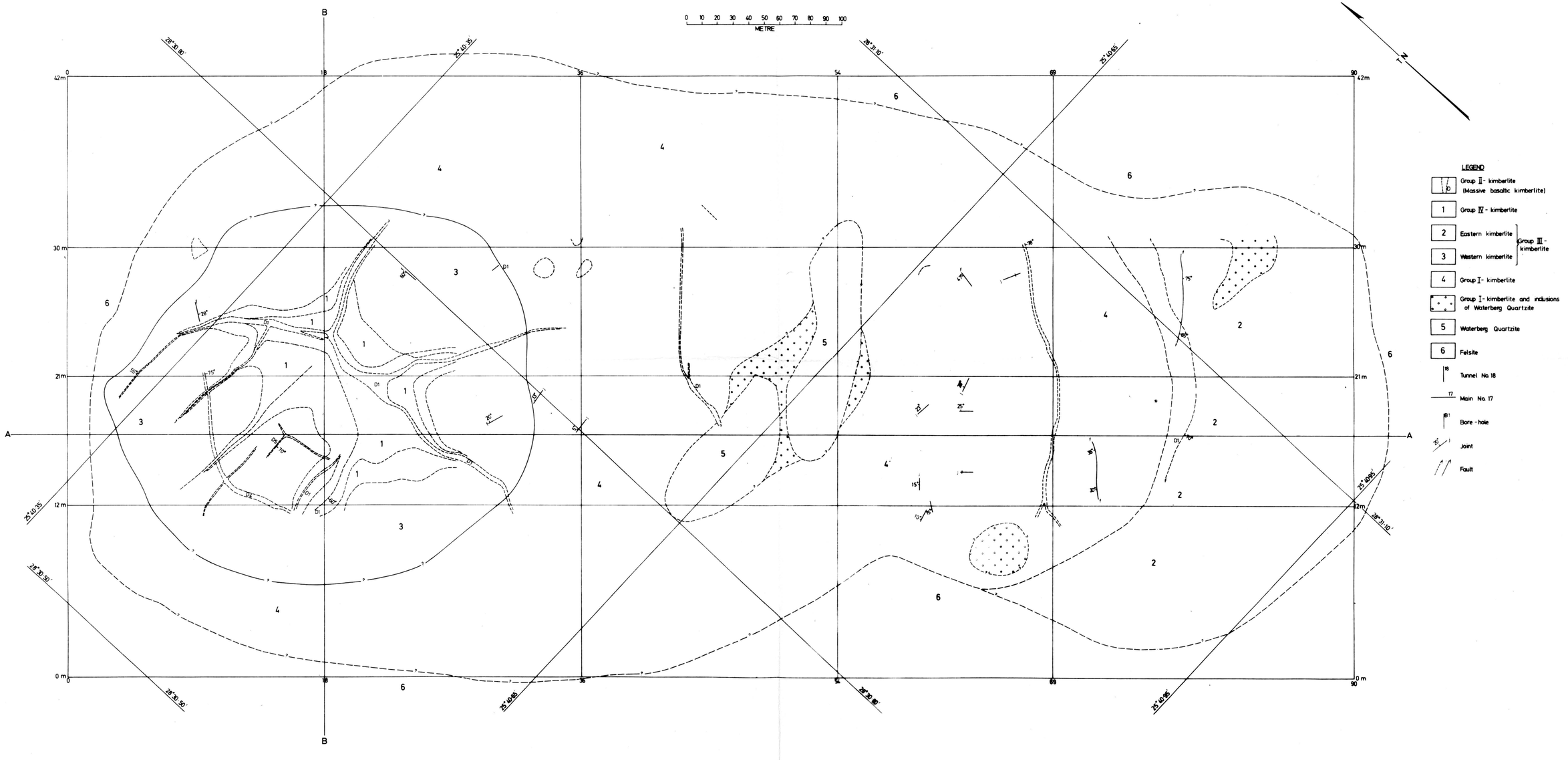

MAP I THE STRUCTURAL GEOLOGY OF THE VICINITY OF PRETORIA

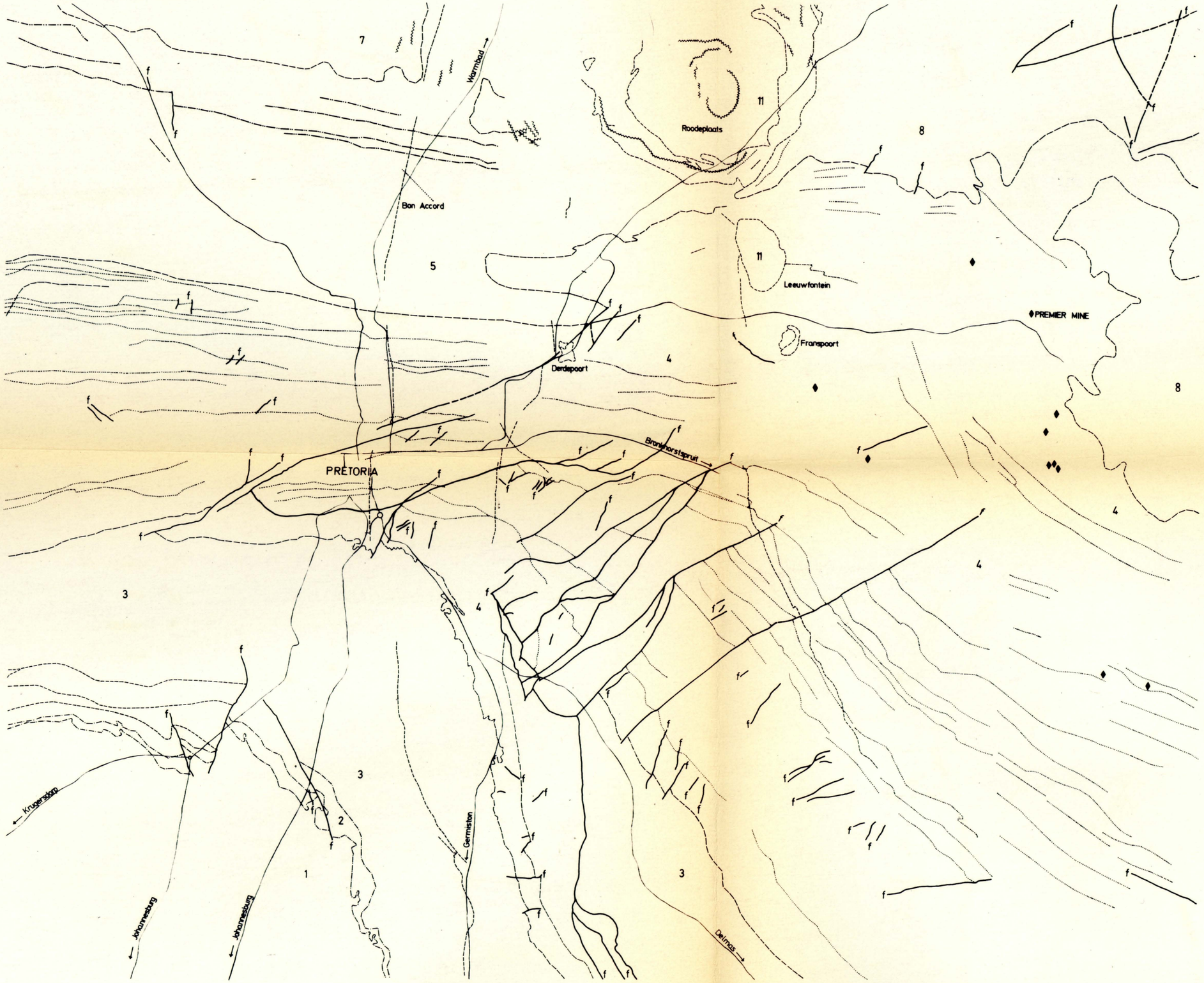

PROFILE 2 ALONG THE 17 TUNNEL (AA ON MAP 2)

0 10 20 30 40 50
METRE